FAULT TOLERANT OPTIMAL CONTROL

by

Howard Jay Chizeck

B.S. Case Western Reserve University
(1974)

M.S. Case Western Reserve University
(1976)

SUBMITTED TO THE DEPARTMENT OF
ELECTRICAL ENGINEERING AND COMPUTER SCIENCE
IN PARTIAL FULFILLMENT OF THE
REQUIREMENTS OF THE DEGREE OF

DOCTOR OF SCIENCE

at the
MASSACHUSETTS INSTITUTE OF TECHNOLOGY

August 1982

Signature of Author_____
Department of Electrical Engineering
and Computer Science
August 23, 1982

Certified by_____
Alan S. Willsky
Thesis Supervisor

Accepted by_____
Arthur C. Smith
Chairman, Departmental Graduate Committee

FAULT TOLERANT OPTIMAL CONTROL

by

Howard Jay Chizeck

Submitted to the Department of Electrical Engineering and Computer Science on August 23, 1982 in partial fulfillment of the requirements for the Degree of Doctor of Science

ABSTRACT

The control of dynamic systems subject to abrupt, state-dependent structural changes such as component failures, at random times, is considered. This investigation is motivated by the need for design techniques that yield fault-tolerant systems, in the sense that they can perform satisfactorily despite untoward events. This work concentrates on the tradeoffs between good performance and reliability requirements.

The approach used is to formulate discrete-time nonlinear stochastic control problems that capture some of the issues of fault tolerant control, and to analyze the behavior of the controllers obtained by solving these problems.

These problems are approached using dynamic programming methods. A preliminary result is the derivation for discrete-time noiseless problems with Markovian structure, results analogous to existing results in continuous time. In addition necessary and sufficient conditions for the existence of a steady-state controller yielding finite expected cost are obtained.

This preliminary result is then used to attack the harder problems of state-dependent structure changes. The basic method used is to convert the state-dependent problems into the comparison of a set of constrained (in the state) problems that have state-independent transition probabilities. First systems where the structure transition probabilities depend upon the state in a piecewise--constant way are considered. For scalar problems with no input noise an algorithm is obtained that determines the optimal controller off line, in advance of system operation. For problems with additional structure this algorithm collapses into the simultaneous solution of a set of coupled difference equations that are similar to Riccati equations.

Two examples of such problems are considered in detail; one involves performance and reliability goals that are conflicting and in the other case they are commensurate. Both cases are analyzed to see how the optimal controller handles the tradeoff between these goals. One controller action is to drive the state to the low cost

goals. Then additive input noise, more general costs structures and more general functional dependence of transition probabilities on the state are considered. The additve noise changes the problem in a fundamental way since the controller cannot position the state with certainty. However an algorithm that yileds the optimal controller can be obtained and qualitative properties of the controller can be analyzed.

Finally several extensions of these problems are considered.

Thesis Supervisor: Alan S. Willsky

Title: Associate Professor of Electrical Engineering and Computer Science.

ACKNOWLEDGEMENTS

I am grateful to Professor Alan S. Willsky for teaching me how to attack problems. His insights, questions, observations and suggestions have contributed greatly to the work reported here.

I wish to thank my thesis readers Professor Michael Athans, Dr. David Castanon and Professor Robert Tenney for their valuable suggestions and discussions during the course of this research.

I also wish to express my gratitude and deepest respect to Professor Sanjoy K. Mitter for his quiet guidance by example.

I am especially grateful to Dr.Marcel Coderch for his friendship and for may valuable and enjoyable conversations regarding matters technical and political. Many thanks also go to my fellow graduate students Jim Lewis, Dr. Charlie Rohrs, Ricky Lee and Dr. Peter Thompson. They were an extraordinary group to work among and I benefited greatly from my interaction with them.

Mr. Norman Darling, Mr. Arthur Giordani and my wife Holly Glaser are to be thanked for their fine art work. I am also grateful to Ms. Fifa Monserrate, Ms. Frantiska Frolik and Mrs. Naomi Glaser Alpern for their diligent and excellent typing. In the latter case, this is performance beyond the call of duty for any mother-in-law!

I would like to express my deep appreciation to Ms. Marilyn Pierce for cutting through departmental red tape and bureaucratic impediments.

I would also like to thank all of the people at the Laboratory for Information and Decision Systems that made my time at MIT interesting and enjoyable. In particular I wish to thank Larry George, Barbara Peacock-Coady, Margret Flaherty and Richard Osborne.

I wish to express my sincere thanks to my dear friends Henri Holekamp and Harry Swift for their advice and friendship, and for graciously extending their hospitality to us when the roof collapsed and our apartment was condemned. They made a very frightening and frustrating set of events seem almost funny.

I am deeply grateful for the encouragement and support offered to our household during this very trying time by my mother and my in-laws. Without their unselfish aid this effort would not have been possible. I also wish that I could thank my father for his encouragement and enthusiasm that led me to an interest in science and engineering. To his memory I dedicate this effort.

Finally I would like to express my deepest gratitude to my wife Holly, for encouraging me when I was discouraged and for working very hard to releive me of many of my responsibilities to allow me more time for this task; for doing far more than her share in the raising of our daughter, Rebecca----without her love this thesis would never have been completed.

TABLE OF CONTENTS

PART II: JLQ PROBLEMS WITH X-INDEPENDENT FORMS

PART III: THE SCALAR X-DEPENDENT JLQ CONTROL PROBLEM

PART IV: EXTENSIONS TO THE SCALAR X-DEPENDENT NOISELESS JLQ PROBLEM

LIST OF EXAMPLES

LIST OF FIGURES

LIST OF PROPOSITIONS, COROLLARIES, LEMMAS AND FACTS

LIST OF TABLES

PART I

INTRODUCTION AND BACKGROUND

1. INTRODUCTION

This thesis considers the control of dynamic systems that experience abrupt, structural changes at random times. These changes are caused by phenomena such as component failures and repairs, and large environmental disturbances.

This document is divided into five parts. Part I contains introductory, motivational and background material. It also presents the perspective and conceptual basis of the work. A different class of problems is considered in each of the next four parts. Part V closes the thesis with a summary of results, concluding comments and suggestions for further research.

1.1 Fault-Tolerant Systems

This thesis is motivated by the need for design techniques that yield automatic systems that are fault-tolerant; that is, systems which are are able to survive and adequately function despite the occurrence of component failures and other disruptions.[1,2]

Some examples of situations where there is need for fault-tolerant system designs are when:

---

[1] The term fault-tolerance comes from digital computer design, where fault refers to any disruption in the specified behavior of a system. For example, see [5].

[2] In (English translations of) Russian reliability theory literature, a fault-tolerant system is any system having components that can be repaired. For example, see [33].

- failures can jeopardize human lives, such as in
  - life support systems,
  - medical prosthetics,
  - air traffic control systems,
  - automated military systems,
  - systems for handling hazardous material,
  - electric power plants (especially nuclear),
  - aircraft, manned spacecraft, trains, automobiles, elevators and other mechanized conveyances.
- failures have high monetary costs, such as in
  - electric power distribution,
  - automated manufacturing processes,
  - communications systems.
- repair or maintenance by humans is inadvisable or impossible, such as in
  - deep-space vehicles,
  - deep-water systems,
  - systems operating in extreme temperature, radioactive, biohazardous or toxic environments.

We can identify three basic issues that must be taken into account in the design of fault-tolerant systems. They are

- the type and level of redundancy used,
- the effects of failure-related uncertainties,

and

- conflicting system performance and reliability goals.

These design issues will be briefly discussed here.

REDUNDANCY

Engineering systems have traditionally been made reliable through the use of redundant components, so that individual failures need not be catastrophic to the entire system (and by the use of highly reliable components and assembly procedures so that failures are unlikely). Redundant components are used to detect failures and to compensate for them. There are essentially two kinds of redundancy that can be used:

- direct redundancy - Multiple copies of the same component are used, in 'voting' schemes for failure detection and as 'backups' for failure compensation.
- functional redundancy - The system is designed so that components and subsystems have overlapping capabilities.

FAILURE- RELATED UNCERTAINTIES

Failure event uncertainties that must be addressed in fault-tolerant system designs include:

- plant uncertainties - Failure events change the system state or dynamics in ways and at times that are not known in advance.
- detection uncertainties - The ability to detect, isolate and estimate failures is usually imperfect. The possibilities of incorrect failure detections and decisions must be taken into account in the system design.

CONFLICTING GOALS

The goals of reliability and fault-tolerance may conflict with other system performance objectives. Here are three classes of costs associated with the attainment of fault-tolerance:

- Fixed costs - Fault-tolerant designs usually require additional or different hardware that is not needed during fault-free operation. This extra equipment may involve not only purchase costs but also degraded system performance (e.g., extra weight in aircraft).
- Hedging costs - The operation of a system so that it is fault-tolerant may conflict with the optimal way to operate the system in fault-free circumstances. A cost, in terms of performance loss before failure, is paid to improve the expected performance when failures occur or to reduce the probability of failure.
- Maintenance costs - Preventive maintenance (and inspection) results in direct costs (for parts, labor, etc.) as well as performance losses while maintenance activities are undertaken.

FOCUS OF THIS WORK

This thesis concentrates on the second fault-tolerance issue listed above - the tradeoffs and conflicts between reliability goals and system performance. Specifically, we consider the attainment of fault-tolerance through control strategies, rather than by direct redundancy.

We seek control problem formulations that yield controller designs which endow systems with fault-tolerance. An optimal fault-tolerant controller should utilize all system capabilities and take into account all known system limitations and failure likelihoods, so as to achieve the best tradeoff between reliability and system performance. We believe this to be an important step in the ongoing development of theories and methods for fault-tolerant system design.

1.2 Fault-Tolerant Control

Fault-tolerant control is the use of control strategies to make failure-prone systems responsive to untoward events. This requires the 'building in' of fault-tolerance, by modelling how failures can happen and what can be done to avoid or overcome them. In general, fault-tolerant controllers will trade some degradation of performance quality before failures occur for system 'survival' afterwards. This may involve component repair, maintenance, or reconfiguration of the control system.

From an examination of common engineering practices and consideration of fault-tolerance needs of engineering systems, some attributes that fault-tolerant controllers should possess can be identified. We call them:

- Passive Hedging
- Active Hedging (Risk Reduction)
- Adaptability

- Robustness
- Implementability.

These properties of fault-tolerant controllers are discussed in this section.

Passive and active hedging require the balancing of conflicts between system performance and reliability goals. Adaptability involves the use of redundancy, probabilistic descriptions of failure occurrences, and the ability to detect them. Robustness and implementability are necessary for successful operation of any fault-tolerant controller.

PASSIVE HEDGING

This is simply taking into account the possibility of failures (and associated costs) in the choice of control. For example, an automobile driver speeding around a curve might avoid the outer edge of the road, so that if a tire blowout occurs the system can still recover. Passive hedging does not involve using controls to affect the probability of future failure event occurrences.

ACTIVE HEDGING (RISK REDUCTION)

Probabilistic knowledge of failures may be used to alter their likelihoods. Preventive maintenance (replacement before failure) is an example of this. If failure probabilities depend upon control inputs (directly, or indirectly as a function of the system state)

then controls can be used to actively hedge as well as to minimize operating costs. For example, voltages and currents in an electrical system might be kept below levels that cause components to burn out.

ADAPTABILITY

In general, some kind of on-line, real-time system testing and failure detection process must take place. When a failure is known to have occurred, 'contingency' controls are used. The primary system goal may then become, for example

- degraded recovery - 'graceful degradation', 'fail-soft' operation
- safe shutdown - ('fail-safe' operation) so as to avoid further system damage by continued operation.

The system must detect its failures and reorganize itself to compensate for them.

ROBUSTNESS AND IMPLEMENTABILITY

Fault-tolerant controller designs should be robust in the sense that they are insensitive to small disturbances and modelling inaccuracies. Fault-tolerant control strategies must be implementable in real-time if they are to be useful. This restricts the complexity of controller designs.

The controller designs that are obtained using any proposed fault-tolerant control theory must be evaluated in terms of these five attributes, to determine if the theory is meaningful. The task at hand is to develop objective problem formulations that capture these subjective fault-tolerance attributes. In particular, since we are concerned here with the balancing of conflicting system performance and reliability goals, we will focus on the hedging properties of fault-tolerant controllers.

1.3 Modelling Fault-Prone Systems

A key step in the development of any theory for system design and analysis is the abstraction of physical reality by approximate but representative mathematical models. To study fault-tolerant controllers we must first develop models that adequately capture the salient characteristics of fault-prone systems. We need models that are sufficiently realistic for the design of good fault-tolerant controllers and are mathematically amenable to detailed analysis. We also require tractable problems in order to gain insight into fault-tolerant structures.

A characterizing attribute of fault-prone systems is their operation in different forms or modes. Fault-prone systems experience abrupt changes in their structure and state from phenomena such as component failures and repairs, changing subsystem interconnections, changes in operating points and abrupt environmental disturbances.

Each system form corresponds to some combination of these events.[1]

The state of a fault-prone system can thus be decomposed into two parts: a form process, which indicates the operational status of the system, and the rest of the state which we call the x process. A logical structure for modelling this kind of arrangement depicted in figure 1.1. It is a feedback connection of two subsystems: a form subsystem that describes abrupt structural changes in the system and an x-subsystem that represents the dynamic evolution of the system between form transitions.

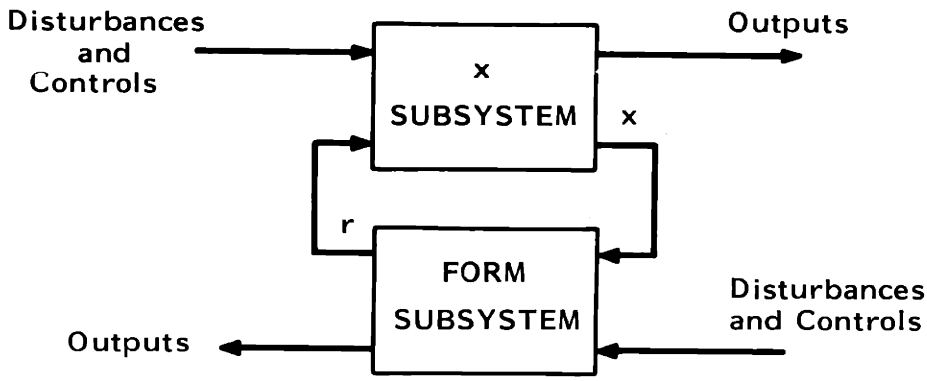

Figure 1.1: General Hybrid System Structure.

[1] In reliability theory the structural conditions of a system are usually called modes (eg., normal mode, failure modes, etc.). In control theory the term mode has a different meaning, and a third definition pertains to statistical analysis. Since the problems we are investigating draw from reliability theory, control theory and stochastic processes, we have elected to avoid the term mode. Instead, form is used to denote the operational status or structure of the system.

The form is a stochastic process taking values in a finite set. Its transition probabilities are dependent, in general, on the x-subsystem state and control inputs. The x-subsystem is modelled by deterministic or stochastic finite-dimensional vector differential or difference equations. The parameters of these equations depend on the form, which feeds into the x-subsystem.

The use of this kind of continuous-plus-discrete-state structure to model fault-prone systems is not new. For example, some applications are surveyed in [67]. These systems have been called stochastic hybrid models by Willsky, et al [75] in the analysis of electric power systems.

The use of stochastic models when representing fault-prone systems is essential. As in other control analysis applications, the system model used must successfully deal with sources of uncertainty such as

- sensor errors, measurement noise
- parameter errors and other modelling errors in the mathematical representation of the physical system
- external random disturbances (driving noises) that effect the time evolution of the system.

For fault-prone systems an additional source of uncertainty comes from random disturbances that alter the system structure. Deterministic system models just cannot adequately represent these fundamental system characteristics.

In this thesis we restrict our attention to the fault-tolerant control of discrete-time systems. There are several reasons for doing this. The increasingly digital nature of control technology and the inexpensive availability of microprocessors for components in 'smart' controllers make discrete-time models appropriate for controller design and analysis. Since implementability is a required attribute of fault-tolerant controllers, it seems preferable to avoid problems arising from the discrete approximation of continuous-time designs, by obtaining discrete-time designs directly.

In addition the discrete-time formulations of these problems are more easily analyzed than continuous-time ones. When dynamic programming is used to solve discrete-time trajectory control problems there is no partial differential equation that must be solved. Thus we can sidestep the inability to solve the Bellman equation for control problems with x-dependent form transition probabilities.[1] This allows us to gain considerable conceptual insight into the structure of fault-tolerant control systems.

This research considers discrete-time systems that are special cases of the following model:

$$\bar{x}_{k+1} = A(r_k)x_k + B(r_k)u_k + \Xi(r_k)v_k \tag{1.1}$$

$$\Pr\{r_{k+1}=j \,|\, r_k=i,\ \bar{x}_{k+1}=x,\ u_k=u,\ q_k=q\} = p(i,j;x,u,q) \tag{1.2}$$

$$x_{k+1} = Rs[r_k,\ r_{k+1},\ \bar{x}_{k+1}] \tag{1.3}$$

---

[1] See, for example, [70].

$$y_k = C(r_k)x_k + D(r_k)u_k + \Lambda(r_k)w_k \qquad (1.4)$$

The 'order of operations' is as follows:

(1) at time k the system is in state (x_k, r_k)

(2) controls u_k and q_k are chosen

(3) during time interval (k,k+1), $\bar{x}_{k+1}$ is generated via (1.1)

(4) then r_{k+1} is generated according to (1.2), based on $\bar{x}_{k+1}$, u_k, q_k and r_k

(5) when the form changes from r_k to r_{k+1}, $\bar{x}_{k+1}$ may be "reset" to x_{k+1}. This resetting is generally nonlinear.

(6) The output of the x-subsystem, y_k, is produced by (1.4).

This convention allows for a failure or other form change to be modelled as occurring at the final time K=N (when $N<\infty$).

In the above

. time index k takes integer values

$$k \in \{k_0, k_0+1, \ldots, N-1, N\}$$

. $x_k \in R^n$ x-process

. $u_k \in R^m$ x-controls

. $v_k \in R^{\bar{m}}$ x-driving noise

- $y_k \in R^p$ x-subsystem output
- $w_k \in R^{\bar{p}}$ x-observation noise

The form process $\{r_k: k=k_0,\ldots,N\}$ takes values in a finite set

$$r_k \in \underline{M} \equiv \{1,2,\ldots,M\} \qquad M<\infty .$$

The <u>form controls</u> $\{q_0,q_1,\ldots,q_{N-1}\}$ take values in a finite set

$$q_k \in \underline{L} \equiv \{1,2,\ldots,L\} \qquad L<\infty .$$

$A(r_k)$, $B(r_k)$, $C(r_k)$, $D(r_k)$, $\Xi(r_k)$ and $\Lambda(r_k)$ are appropriately-dimensioned matrices where:

$A(r)$ = open-loop x dynamics given the current form r

$B(r)$ = x-process input gain in form r

$\Xi(r)$ = x-process driving noise gain in form r

$C(r)$ = x-process sensor gain in form r

$D(r)$ = input-output direct link in form r

$\Lambda(r)$ = x-process observation noise gain in form r.

Thus the model (1.1)-(1.4) is sufficiently general to allow representation of form-dependence in dynamics, actuators, sensors and noise.

The form transition probabilities $p(i,j;x,u,q)$ in (1.2) must obey

$$p(i,j;x,u,q) \geq 0 \qquad \text{for all } i,j \in \underline{M} \text{ and all } x,u,q$$

$$\sum_{j=1}^{M} p(i,j;x,u,q)=1 \qquad \text{for each } i \in \underline{M} \text{ and all } x,u,q \quad .$$

The noise processes $\{v_k\}$ and $\{w_k\}$ are assumed to be 'white', in that

$$E\{[v_k-E(v_k)]'[v_s-E(v_s)]\} = 0 \qquad s\neq k$$

$$E\{[w_k-E(w_k)]'[w_s-E(w_s)]\} = 0 \qquad s\neq k$$

with unity variance matrices and

- all elements of v_k and w_s are independent (for all times k,s)
- all elements of v_k and x_s, and of w_k and x_s, are independent for all $k\geq s$
- all elements of v_k and w_k are independent of r_s for all $k\geq s$.

A crucial consideration in the modelling of fault-prone systems is the realistic representation of form transitions. There are two basic kinds of transitions:

- <u>independent of x</u>
- <u>x-dependent</u>

The x-independent form transitions occur as though no x-to-r feedback link exists in figure 1.1. They may be <u>uncontrolled</u>, or

controlled by form controls $\{q_0,\ldots,q_{N-1}\}$ that are not chosen in response to $\{x_0,\ldots,x_{N-1}\}$. Example of x-independent form shifts are random 'no wearout' component failures and lightning-induced failures in electrical power distribution systems.

The x-dependent form transitions are always controllable in some sense, either by form controls q_k (which <u>can</u> be based on x_k) or through <u>active hedging</u> (by $\{u_k\}$ and the resulting x-process). Examples of x-dependent form shifts in electrical power distribution systems include the restructuring of a system when generator-protecting relays and circuit-breakers trip, human operator control actions based on observation of x-dynamics (such as switching on auxilary generators) and transmission-line failures due to current overloads. Thus form shifts can be <u>totally unpredictable</u> (as in random 'no wearout' component failures), <u>totally predictable</u> (as in scheduled, deterministic actions) or <u>partially predictable</u> (as in the switching of relays precisely (or approximately) when a random quantity reaches a given threshold).

Suppose that the "reset" operation in (1.3) is linear. Then the x-subsystem dynamics are linear in x and control u if the form process $\{r_k\}$ does not depend on x. For such systems with x-dependent forms, the only source of x-dynamics nonlinearity is through the form transition probabilities.

In this thesis we will consider x-dependent form transition probabilities that are <u>piecewise-constant</u> in x (or which can be

approximated as such). This yields a kind of dynamics model that is amenable to detailed analysis, since it consists of linear 'pieces'.

1.4 Formulating Fault-Tolerant Optimal Control Problems

A general fault-tolerant control system structure is shown in figure 1.2. Both the x-controls $\{u_0,\ldots,u_{N-1}\}$ and the form controls $\{q_0,\ldots,q_{N-1}\}$ can depend upon possibly noisy observations of current (or past) values of the hybrid system state (x,r). If these quantities are not perfectly observable then the design of x and r estimators is an integral part of the overall fault-tolerant optimal control problem.

When form transitions are x-dependent, imperfect knowledge of x causes uncertainty about future form shifts even if r is perfectly observed. When r is not perfectly observed, failure detection and isolation (hence form estimation) usually involves some combination of hypothesis testing ideas and dynamic stochastic estimators (such as the Kalman filter). A thorough survey of failure detection and isolation methods appears in the survey paper [74].

When the form is not perfectly observed, the control serves a 'dual' purpose. It can be used both to control the state and to probe for information about it. Tradeoffs between control costs, the costs resulting from incorrect form detection and the expected benefits of probing must be considered in these cases. A general discussion of

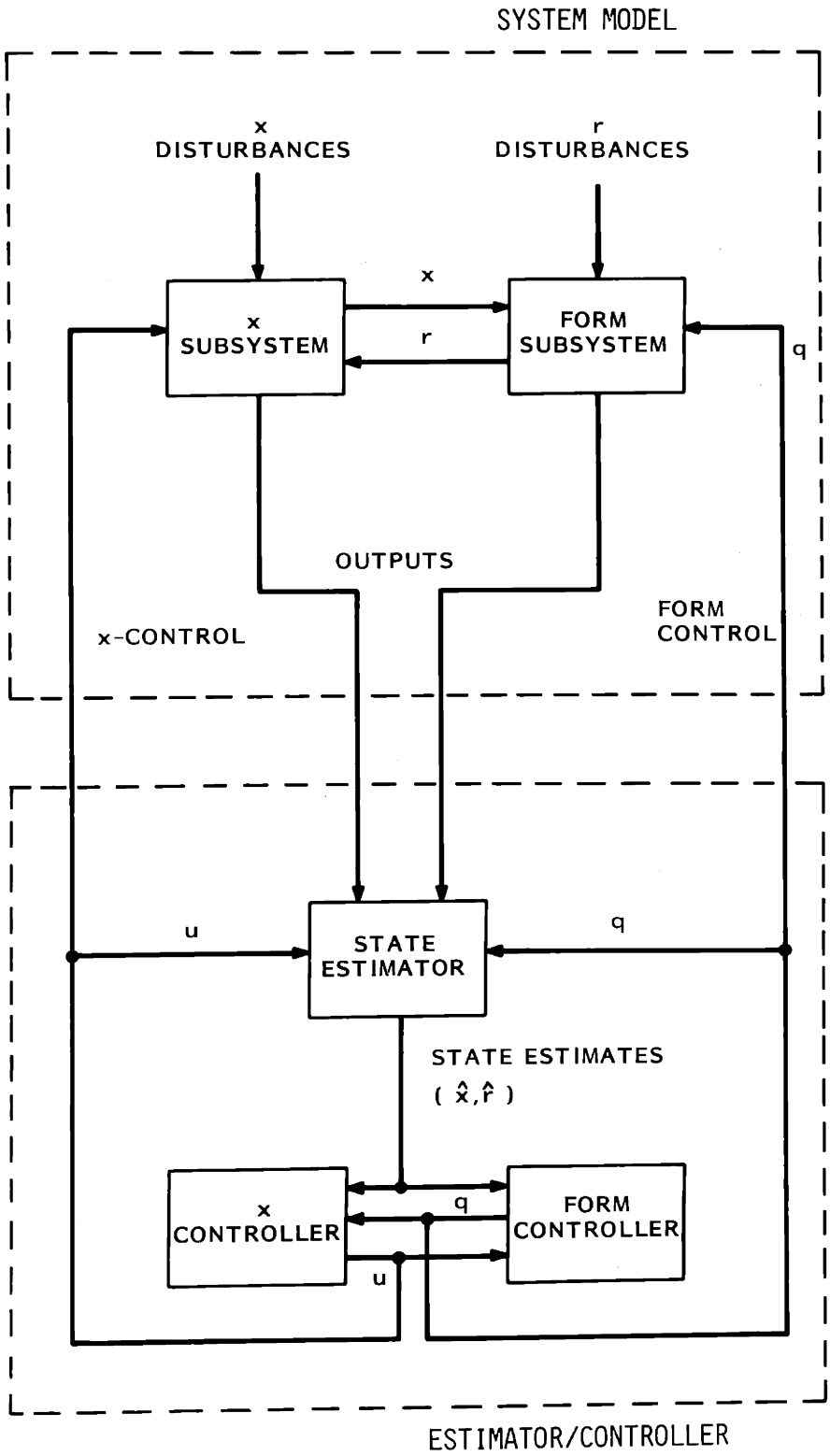

Figure 1.2: Fault-Tolerant Control System Structure

this 'dual control' phenomenon first appeared in 1960 in the work of Fel'dbaum [24].

Two types of form control actions are possible:

- indirect form control - This is the control of the probabilities of form transitions.
- direct form control - This involves control actions that immediately, deterministically change r.

An example of indirect form control is preventive maintenance, which improves failures probabilities (at some incurred cost). Switching to backup systems in anticipation of (or response to) failures is an example of direct form control.

Embedded in any fault-tolerant control problem is an implicit criterion of system reliability. The problem formulation incorporates models of failure occurrences, and reflects the relative importance of various form-dependent costs.

In this thesis we propose extensions of the well-known linear quadratic Gaussian (LQG) control methodology to systems having randomly jumping structures and parameters that are described by reliability-theoretic models. We call this the jump linear quadratic (JLQ) control problem.

The cost function to be minimized is quadratic in the x-control, u_k. If the system is in state (x_i, r_i) at time i, we want to minimize

$$J_i(x_i, r_i) = E\left\{ \sum_{k=i}^{N-1} u_k' R(r_k, q_k) u_k + Q[x_{k+1}, r_k, r_{k+1}, q_k] + Q_N[x_N, r_N] \;\middle|\; \begin{matrix} x_i \\ r_i \end{matrix} \right\} \quad (1.5)$$

where the expectation is with regards to $\{v_k\}$, $\{w_k\}$ and $\{r_k\}$.

$R: \underline{M} \times \underline{L} \rightarrow R^{mxm}$ is a bounded positive-definite symmetric matrix-valued function

$$R(r,q) = R'(r,q) > 0 \qquad \text{all } r,q \tag{1.6}$$

and $Q: R^n \times \underline{M} \times \underline{M} \times \underline{L} \rightarrow R$ is a bounded nonnegative scalar-valued function

$$Q(x,r_1,r_2,q) \geq 0. \qquad \text{all } x,r_1,r_2,q\,. \tag{1.7}$$

The optimal expected cost-to-go from state (x_k,r_k) at time k is

$$V_k(x_k,r_k) = \min_{\{u_i,q_i : k \leq i \leq N-1\}} J_k(x_k,r_k)\,. \tag{1.8}$$

Thus the optimal controls are found by minimizing the expected value of a cost functional which may include:

- operating costs that penalize control energy expenditure and system performance differently in each form.
- jump costs that are charged if and when the form changes. These might represent start-up or shut-down costs of equipment, or undesirable transient phenomena; load shedding costs in electric power systems are examples.
- terminal costs dependent upon the final state (including form) of the system.

The control costs $u_k'R(r_k,q_k)u_k$ (and usually the x-cost $Q[x_{k+1},r_k, r_{k+1},q_k]$) are chosen to be quadratic because of the

wide applicability and good robustness properties of linear quadratic control problem formulations (see, for example, [3]). The q_k-dependence of these costs models the penalties incurred in applying form controls. The Q cost depends, in general, on the current and prior form (r_{k+1} and r_k) so that jump costs can be included. The control sequences $\{u_k\}$, $\{q_k\}$ are constrained to be <u>feedback controls</u> of the form

$$u_k = f_k[\{y_s : k_0 \leq s \leq k\}, \{u_s, q_s : k_0 \leq s \leq k-1\}, \{r_s : k_0 \leq s \leq k\}] \tag{1.9}$$

$$q_k = g_k[\{y_s : k_0 \leq s \leq k\}, \{u_s, q_s : k_0 \leq s \leq k-1\}, \{r_s : k_0 \leq s \leq k\}] \tag{1.10}$$

That is, the <u>x-control</u> and form control at time k are determined from past outputs, past (known) controls, and <u>perfectly observed</u> form observations.

Control problems for continuous-time stochastic hybrid systems with x-indpendent r have been extensively studied in the literature. The stochastic hybrid models used are usually special cases of those analyzed by Gihman and Skorohod [26]. Under the assumption of perfect observations, continuous-time optimal control problems for a large class of system dynamics, form transition models and cost functionals can be reduced to the search for solutions of nonlinear partial differential equations using 'verification' theorems of dynamic programming.

Krasovskii and Lidskii [34] obtained most of the results that are currently available in the literature for stochastic hybrid system control (with x-independent form processes and perfect state observations). The problem was studied later by Wonham [76]. He obtained conditions for the existence and uniqueness of solutions in the JLQ case, and also derived a separation theorem under Gaussian noise assumptions for JLQ control problems with Markovian forms and noisy x (but perfect r) observations. Sworder [63] obtains similar results using a stochastic maximum principle.

Discrete-time versions of the JLQ x-control problems for stochastic hybrid systems have not been thoroughly investigated in the literature. A special case[1] of the x-independent JLQ discrete-time problem is considered in Birdwell [12] and [13]-[14].

A great deal of work has recently been done concerning the modelling and analysis of jump processes like those describing the form subsystems here. References of particular note include [16-18,20, 25,42,62,71]. An excellent discussion of martingale methods for optimal control problems is contained in [21].

This thesis focuses on systems where the form observations are <u>not</u> noisy. This has not been done because the noisy observation case is unimportant. The reason for this problem restriction is that, even when the form is perfectly observed, the solution of control problems of this

---

[1] Only the actuator gain is form dependent.

kind for the x- and u-dependent form transition probability cases is very difficult, previously unsolved, important, and useful in terms of the insight which it provides us regarding the trade-offs between reliability and system performance goals in fault-tolerant controller designs.

1.5 Problems Addressed and Results Obtained

Using dynamic programming, several classes of the discrete-time jump linear quadratic (JLQ) control problem formulation of the last section have been solved. In this section these problems and results are surveyed.

PART II: JLQ Problems with x-independent forms

In part II of this theses the 'easiest' class of JLQ problems is examined. These involve systems with x-independent, Markovian form processes.

The noiseless case is addressed in chapter 3. The control laws that are obtained are linear in x, with a different law for each form. The expected costs-to-go are quadratic in x (for each form). All of the control gains and costs are obtained by solving off-line a set of M precomputable Riccati-like difference equations (one for each form).

The continuous-time version of this problem was first solved by Krasovskii and Lidskii [34], and later by Wonham [76] and Sworder [67]. A special case of the discrete-time result presented in chapter 3 appears in Birdwell [12].

For infinite time-horizon problems, steady-state results similar to those obtained in the standard LQG problem are accessible. An interesting (but, in retrospect, obvious) fact is that the controlled, closed-loop dynamics in every form need not be stabilizing so long as the probability of entering and remaining in these stable forms is not "too large." A similar but less inclusive sufficient condition for the continuous-time version of the problem was developed by Wonham [76].

These controllers exhibit the desired adaptability property in that different laws are used in each form. That is, the system reorganizes itself when a failure occurs so as to best use available direct and functional redundancy. The controllers derive robustness and implementability from the linear quadratic nature of the problem. Passive hedging is used to minimize the expected costs. That is, potential failures and other form changes are taken into account (via the cost functional) in the choice of the optimal control. But no active hedging (controlled modification of failure probabilities) is possible because of the independent, uncontrollable nature of the failures.

In chapter 4 several extensions of the x-independent JLQ problem are considered. These include the addition of jump costs, linear resets of x, and additive white input and x-observation noises.

The presence of additive (usually Gaussian) white observation and input noise does not complicate these problems. Since the form is perfectly observed (with delay), a separation theorem like that of the standard LQG problem follows. In each form, a Kalman filter estimates x, and this estimate is then used by the control law for that form.

PART III: Scalar JLQ Problems with x-dependent forms

In part III we consider JLQ control problems that involve state-dependent structural changes. These problems possess

- perfect observations of the state (x_k, r_k) at time k
- quadratic costs in scalar x_k and u_k, for each form,
- no driving or observation noises,
- x dynamics that would be linear, if not for randomly jumping parameters,
- jump probabilities that depend upon x in a piecewise-constant way (with finitely many pieces) or are approximated as such.

For finite time-horizon problems in the x-dependent case we have obtained a recursive algorithm that determines the optimal

expected costs-to-go and control laws off-line, in advance of system operation.

The optimal control laws are piecewise-linear in x (with x^1, x^0 terms) and the optimal expected costs-to-go are piecewise-quadratic in x (with x^2, x^1, x^0 terms). The gains and costs are obtained from a set of precomputable Riccati-like equations (not the same as in the x-independent failure case). The number of "pieces" grows only additively (going backwards in time from a finite terminal time). The additive increase depends upon the number of different forms that the system can change to (from its current one), and the number of pieces in the relevant piecewise-constant-in-x transition probabilities. Thus there is a tradeoff between the accuracy of the modelling of failure probability state-dependence versus the computational burden of control law determination (and the complexity of the controller.

The optimal controller attempts to minimize the cost incurred both by the usual LQ regulator action, and by driving the system state to regions where the likelihood of undesirable form shifts is reduced. The different "pieces" of the optimal expected cost-to-go and control law correspond to using the control alter form transition probabilities at various future times. That is, to actively hedge.

In general, for infinite time horizon problems the number of pieces becomes infinite. Fortunately, for a large class of problems

this is not an obstacle to implementation because most of the control law and cost pieces converge. That is, although the true optimal control law involves a (countably) infinite number of pieces, each valid over a different range of the x variable, most of these pieces are "almost the same."

Thus there is a tradeoff between closeness to optimality and controller complexity. Nearly optimal, steady-state controllers can be obtained to within any specified deviation from optimal, but with a corresponding level of complexity (number of separate-interval control laws).

PART IV: Extensions to the Scalar x-dependent JLQ Problem

In this part of the thesis we extend the results of chapters 5-7 to more general JLQ problems. In chapter 8 we consider a modification of the solution algorithm of Part III that lets us solve approximately problems involving:

- x operating costs and terminal costs that are piecewise-quadratic in x (with x^2, x^1 and x^o terms)
- cost pieces that are concave-up as well as concave-down.

This jump linear piecewise quadratic (JLPQ) control problem is solved using a recursive algorithm that determines the optimal control law and expected costs-to-go off-line. As in the JLQ case, the optimal JLPQ control laws are piecewise-linear in x_k, in each form. The optimal expected costs-to-go are piecewise-quadratic. Unlike the JLQ case, the number of pieces of

the optimal JLPQ controller may grow at a faster-than-linear rate as the number of stages from the finite terminal time increases. The piecewise structure of the optimal controller is caused by both the piecewise-constant nature of the form transition probabilities (as in chapters 5-7) and by the piecewise-quadratic nature of the x-operating and terminal costs.

In chapter 9 we extend the solution methodology of chapters 5-8 to address a larger class of scalar jump linear control problems, possessing additive input noise and a more general class of x-dependent form transition probabilities, x-operating costs and x-terminal costs. Specifically we consider scalar jump linear control problems with quadratic control penalties and

- input noise densities that are twice continuously differentiable except at a finite number of points,
- x-operating costs $Q(x,r)$, x-terminal costs $Q_T(x,r)$ and form transition probabilities $p(i,j=x)$ consist of a finite number of convex or concave (in x) pieces.

We call this the jump linear piecewise convex (JLPC) control problem. Our study of this class of problems is motivated by a desire to make the solution approach of chapters 5-8 applicable to more realistic control problems. The major extension of chapter 9 is the inclusion of additive input noise in the x-process dynamics. Additive input noise profoundly changes the nature of the optimal controller. The piecewise-quadratic structure of the optimal cost and piecewise-linear structure of the optimal control laws is lost due to the "blurring" effect of the noise. In chapter 9 we show how JLPC control problems with additive input noise can be reformulated (at each time stage) as different but equivalent JLPC problems that do not possess input noise. These reformulated problems can be

solved using the approach of chapters 5-8. The optimal controller for noisy JLPC problems can be obtained following the steps of an algorithm (presented in flowchart form) which generates, off-line, the optimal control laws and expected costs at each time k and from each form j. Since the optimal control laws are not piecewise-linear in x_k, we don't have the nice inductive controller structure of the JLQ and JLPQ problems. We therefore propose a suboptimal approximation of the JLPC controller that is easier to determine and implement than the optimal controller. The suboptimal control laws are piecewise-linear in x_k at all times k (and from each form j).

In chapter 10 we examine further extensions of the solution methodology of Part III. We first consider jump linear control problems where the x process is not scalar. This class of problems is far more complicated than the scalar case. However we can obtain approximate (suboptimal) controllers for these problems using an algorithm based upon the suboptimal controller approximation of the JLPC problem (of chapter 9).

We next consider jump linear control problems involving u-dependent form transition probabilities. This class of problems is of practical importance since it captures the issue of actuator-dependent failures and it allows us to examine conflicts between system performance goals and reliability requirements. The control problems (for scalar x and u) can be solved using a modified version of the solution algorithm of Part III. At each time stage the optimal expected cost is piecewise-quadratic in x.

In chapter 10 we also consider JLQ problems where the form process can be controlled on the basis of observed x_k and r_k values. This allows us to study controllers that use strategies such as preventive maintenance,

switching to backup systems in anticipation of failures and the like. Both direct form control (deterministically switching between forms) and indirect form control (altering form transition probabilities) are considered. For scalar-x versions of these problems with x-independent form transition probabilities (if no form controls are applied), after one time stage (backwards from a finite terminal time) the optimal control problem resembles the x-dependent JLPQ problems of chapter 8. The optimal expected costs-to-go are piecewise-quadratic in x and are indexed by the choice of form control q_k as well as the current form r_k, at each time k. The optimal controller must determine the best form control option on-line, given observations of (x_k, r_k). These choices are based upon parameters that are computed (off-line) by Riccati-like difference equations, in a modification of the algorithms of chapters 7-9.

PART V: Conclusions and Suggestions for Future Research

In chapter 11 we summarize the results of this thesis and we identify a number of specific and more general directions for future research.

In conclusion, this thesis considers the control of dynamic systems subject to abrupt structural changes at random times. It is motivated by the need for design techniques that yield fault-tolerant systems. This thesis concentrates on the tradeoffs and conflicts between system reliability and performance goals. Specifically, we consider the attainment of fault-tolerance through control strategies rather than by direct redundancy. This is, of

course, only part of the overall fault-tolerant design problem. However the problem formulations here capture many important issues. We believe that the problems that are addressed and the results obtained in this thesis provide an important step in the development of a general theory of fault-tolerant control.

2. BACKGROUND AND RELATED LITERATURE

The design of fault tolerant, failure-resistant dynamically-reliable control systems is a problem that falls within the scope of both automatic control theory and reliability theory. The purpose of this chapter is to provide background for this investigation from both of these fields, and to survey results relating to the design of fault-tolerant control systems.

In section 2.1 we consider the relationship between the fault-tolerant control problem and reliability theory. In section 2.2 we will describe approaches to the design of fault-tolerant control systems that are distinctly different from the methods we are considering. More closely related work on the control of jumping parameter systems is discussed in section 2.3.

2.1 Relations to Reliability Theory

Reliability engineering is primarily concerned with the design and analysis of systems that can perform their missions with high probability despite component failures.

Reliability developed as an engineering discipline in response to the military requirements of World War II. The first formal reliability study reportedly (see [23]) sought to explain why German V1 and V2 missles performed so poorly despite their construction from highly reliable components.

Following the war, complex system design problems in the electronic, nuclear, aircraft and space industries gave impetus to the field. Most of this early work involved the modelling of failure phenomena and the collection of component failure data.

Early theoretical considerations of reliability in the context of automata theory (Von Neumann [73]) and reliable circuit synthesis (Moore and Shannon [43]) concerned achieving overall reliability through the "proper" use of unreliable components.

The first book on reliability (by Bazovsky) did not appear until 1961 [8]. It was followed by a number of texts in the early 1960's, such as [6], [19], [28], [46], [52], [54], [72] and [81]. Three more recent texts are [29], [43] and [23]. The works of Gnedenko, et.al [27] and Barlow and Proschan [7] provide more mathematically rigorous treatments of reliability theory.

Current activity in reliability theory consists, in large part, in the development of mathematical theories and associated computerized algorithms for the analysis of reliability characteristics for systems composed of highly reliable components. In most contemporary engineering applications, many (or all) of a system's component parts must be extremely reliable if strict system reliability standards are to be met. One motivation for the development of a dynamic control approach to reliability engineering is the existence of problems (for example, electric power systems) in which the system's dynamics and its

reliability are intrinsically intertwined. Also the use of controls to achieve reliability may, in some applications, facilitate the use of fewer and less reliable (that is, less expensive) components in the design of reliable systems.

There are two basic approaches that are currently used for the reliability analysis of complex systems (or proposed designs). One approach might be called the 'static' consideration of system reliability. This kind of analysis seeks to determine the probability that a given system will not fail (or will achieve various degraded modes of operation) after some fixed time interval, based on a priori information about the components, their connections, etc. Some examples of this static approach, which involves fault-trees, cut sets, graph theory and the like are in [39],[44].

A second approach to system reliability analysis focuses on the dynamic behavior of system failure probabilities. It involves the use of queueing theory models of complex systems. Queueing systems might be thought of as combinations of sequences of elementary operations such as single component failures, repairs or replacements, maintenance, fault searches and detections, successful component operation prior to failure, etc. These elementary operations overlap in time, in general. They are usually considered to be independent of each other; depending only on the operational status of the overall system.

The outlook of this thesis is in the spirit of this second approach to reliability analysis. However, we are particularly concerned with the dynamic performance of systems and the evolution of (continuous-state space) physical quantities as well as the failure status of the components that manipulate these quantities. We want to formulate control problems that achieve good system performance and high reliability. It is important to realize that the goals of reliability and performance may be conflicting. For example, the use of a large control to quickly drive the system into a safe region of the state space, so as to reduce the probability of a failure, may entail a large control cost. On the other hand the use of control to maximize performance may result in a loss of system reliability. Reliability considerations often limit the performance that can be obtained from a system; electric power systems are an example of this.

The motivation for our work is a desire to obtain a systematic, objective means for designing systems that take into account the need for both high reliability and performance and also account for possible intrinsic conflicts between these goals. Consequently such systems should use available system redundancy in a quantifiably efficient manner.

2.2 Other Approaches to Fault-Tolerant Control

A number of approaches to the design of fault-tolerant control systems that are distinctly different from the methods used here have been considered previously. We will survey them here. In the next

section we will then consider previous work that is more closely related to ours, and we will indicate how previous efforts differ from the work of this thesis.

A mathematical framework for building reliable control systems through the use of redundant, less reliable controllers is presented in the work of Siljak [61]. This approach is a direct extension, in spirit, of the work of van Neumann [73] for automata, Moore and Shannon [43] in synthesizing reliable circuits, and Barlow and Proschan [7] in constructing reliable system from unreliable comments. In [61], control reliability is defined to be the probability that a given control structure will insure stability of the controlled system under a specified class of failures which occur with known probabilities. Experimental observations indicate high reliability of decentralized control schemes for large systems with respect to structural perturbations of interconnections and nonlinearities of subsystem couplings [59],[60],[22] and low reliability of these same decentralized strategies when the system is subject to structural perturbations in feedback interconnections and controller failures. The main reason is that, in reliability-theoretic terms, decentralized controllers are generally series connections of controllers; hence any one controller failure can cause total system failure. The natural solution suggested by reliability theory is to introduce a kind of parallel controller action, through multiple control systems

that have "functional" redundancy (i.e., overlap of capabilities). This is explored in [61]. This kind of overlapping decentralized control system decomposition has been used for the modelling and control of a string of high-speed vehicles [4] and in freeway traffic flow regulation [32].

Another approach to the analysis of reliable systems appears in the work of Beard [9]. He examines 'self-reorganizing' linear systems which restructure themselves to compensate for actuator and sensor failures, using the functional redundancy of their components. Beard's approach is to identify any change (from a set of known possibilities) and then to attempt to alter the system's feedback control law so as to achieve closed-loop stability. He obtains bounds on the number of actuators and sensors needed (that is, the level of component redundancy) using controllability and observability criteria.

A third method for achieving fault-tolerant designs makes no explicit reference to reliability theory. This approach is to try to obtain a kind of "passive" fault-tolerance through the design of non-adapting, robust controllers that attempt to provide satisfactory control in all forms. The fundamental work on the robustness of feedback systems is that of Bode [15]. These results were extended by Horowitz [30], [31], Kriendler [35] and others, and by Kwakernank and Sivan ([38], p.427) in the discrete-time case. Geometric approaches to the analysis of robustness properties of feedback controllers have been

used by Wong [77], [78], Zames [79], [80] and Safonov and Athans [55], [56], [57]. In particular, Safonov [56] has obtained conditions characterizing the robustness of controllers when parameter variations result from a change of operating points in a nonlinear system. The recent thesis of Lehtomaki [41] provides a common framework for these and new robustness tests.

An alternative approach to the design of fault-tolerant controllers is the use of actively adapting controllers that respond to changes in the operating environment. There are a large number of diverse problem approaches and formulations that go by the name 'adaptive control', some of which are relevant to fault-tolerant control. We will not review these here since general excellent surveys exist (see, for example [3], [1], and [40]).

2.3 Control of Jumping Parameter Systems

In this thesis we consider control problem formulations that explicitly include the possibility of system failures and structural changes. We propose extension of the well known linear quadratic (LQ) control problem to include systems having randomly jumping parameters, and costs that reflect these changes in system structure. As discussed in Section 1.4, in this way we hope to capture some of the reliability and performance tradeoffs in the fault tolerant control problem. We call this the jump linear quadratic (JLQ) control problem.

Control problems involving systems having jumping parameters are not new. For example, some applications are surveyed in [67]. These continuous-plus-discrete-state models have been called stochastic hybrid models by Willsky, et.al [75] in the analysis of electric power systems. Control problems for continuous-time stochastic hybrid systems having state and control-independent discrete-state parts (i.e., x-independent form processes in the terminology of section 1.3) have been extensively studied in the literature.

The stochastic hybrid models used are usually special cases of those analyzed by Gihman and Skorohod [26]. Under the assumption of perfect observations, continuous-time optimal control problems for a large class of system dynamics, form transition models and cost functionals can be reduced to the search for solutions of nonlinear partial differential equations using 'verification' theorems of dynamic programming. Krasovskii and Lidskii [34] obtained most of these results that are currently available in the literature for stochastic hybrid system control (with x-independent form processes and perfect state observations). The problem was studied later by Wonham [76]. He obtained conditions for the existence and uniqueness of solutions in the JLQ case, and also derived a separation theorem under Gaussian noise assumptions for JLQ control problems with Markovian forms and noisy x (but perfect r) observations. Sworder [63] obtains similar results using a stochastic maximum principle and has published a number of

extensions with his co-workers, including [45], [64], [65], [66], [68], [69]. Stochastic minimum principle formulations for continuous time problems involving jump process have also been considered by Rishel ([48],[49],[50],[51]), Kushner [36], and others.

Robinson and Sworder [53], [70] have derived the appropriate nonlinear partial differential equation for continuous-time jump parameter systems having state and control-dependent rates. A similar result appears in the work of Kushner [36] and an approximation method for the solution of such problems has been developed by Kushner and DiMasi [37]. This is important work but technical issues, such as the lack of existence of closed form solutions, make it difficult to expose how the optimal controller effects the tradeoff between performance and reliability.

The major focus of this thesis (i.e., part III) is on systems subject to structural form changes that can be implicitly controlled, through the dependence of form transition probabilities on the continuous part of the state. This dependence allows for the modelling of conflicts between performance and reliability goals. We choose to consider discrete-time versions of the jump linear quadratic (JLQ) control problem, rather than extend the continuous-time x-dependent results of Sworder [53], [70] because the discrete-time formulation is amenable to detailed analysis. In discrete time we can get insight into how the optimal controller balances reliability and performance goals. Qualitative fault-tolerance concepts such as active hedging can be quantified in the discrete-time setting.

The control of jumping parameter systems in discrete time have not been as thoroughly investigated as in continuous time. The only results available in the literature are for x-independent JLQ problems where the actuator is form-dependent. These are considered in the thesis of Birdwell [12] and in [13], [14].

As a preliminary step in our investigation we also consider discrete-time JLQ problems with x-independent forms. The derivation of the basic result is straightforward and analogous to the continuous time problem for finite time horizons. We obtain some interesting results regarding infinite time horizon problems, including necessary and sufficient conditions for the existence of steady-state optimal controllers. These results are stronger than the corresponding continuous-time sufficient conditions obtained by Wonham [76], and they provide significant insight into the different types of behavior that can be exhibited by JLQ systems.

2.4 Summary

In this thesis we consider the design of fault-tolerant control systems through the jump linear quadratic control problem formulation that was introduced in Chapter 1. These problems involve the control of continuous-plus-discrete state, stochastic hybrid systems.

Continuous time control problems for such systems have been extensively studied in the x-independent form case (with perfect form

observations). The continuous-time x-dependent case leads to nonlinear partial differential equations that are analytically intractible, although approximation techniques have been proposed. The results available for the continuous-time case don't expose how the tradeoff between reliability and performance is effected by the optimal controller.

We consider discrete time problems in order to obtain some understanding of the control tradeoffs involved between system performance and reliability goals, when structural changes and failures depend upon the continuous part of the state. The main focus of this thesis is on problems involving x-dependent form transitions since this dependence allows for the modelling of conflicts between performance and reliability. To the best of our knowledge, discrete-time problems with this x-dependence have not been studied previously in detail.

PART II

JLQ PROBLEMS WITH X-INDEPENDENT FORMS

3. NOISELESS MARKOVIAN-FORM JUMP LINEAR QUADRATIC OPTIMAL CONTROL PROBLEMS

3.1 Introduction

In this chapter we consider a special class of the jump linear quadratic (JLQ) control problem formulation in chapter 1. We examine the optimal control of jump linear systems having

- x-independent Markovian form processes
- perfect state observations and no noises
- purely quadratic operating and terminal costs
- no 'resets' of x when the form changes.

This class of problems is formulated and solved in sections 3.2-3.3. The optimal control laws are linear in x_k (a different law for each form) and the optimal expected costs-to-go are quadratic in x_k. These control laws and costs can be computed off-line, in advance of system operation, by solving M coupled Riccati-like matrix difference equations.

The continuous-time version of this problem was first formulated and solved by Krasovskii and Lidskii [34], and later by Wonham [70] and Sworder [63]. A special case of the discrete-time result presented here appears in Birdwell [12-14].

The solution of the discrete-time JLQ problem that is developed here is a necessary logical first step in the study of more general control problems for systems with abruptly changing structure which will be used in later chapters. The controller derivation presented here is

conceptually straightforward. However study of the optimal controller provides valuable insights into the qualitative behavior and stability properties of jump linear systems. Several of these properties are highlighted by example problems in section 3.4.

In section 3.5 the steady-state control problem is considered. Necessary and sufficient conditions are derived for the existence of a set of steady-state constant expected cost-to-go functions. It is shown that the corresponding set of time-invariant steady-state control laws stabilizes the controlled system, in that $E\{x_k' x_k\} \to 0$ as $(k-k_0) \to \infty$ and that the steady-state control laws minimize the limiting expected cost-to-go as $(N-k_0) \to \infty$, with finite optimal expected cost.

A more restrictive sufficient condition for the continuous-time version was developed by Wonham [76]. To the best of our knowledge, the discrete time steady-state results are new.

3.2 Problem Formulation

Consider the discrete-time jump linear system

$$x_{k+1} = A_k(r_k)x_k + B_k(r_k)u_k \tag{3.1}$$

$$Pr\{r_{k+1}=j \mid r_k=i\} = p_{k+1}(i,j) \tag{3.2}$$

where

$$x(k_0) = x_0 \ , r(k_0) = r_0 \quad .$$

In the above we have

- time index k takes integer values

  $$k \in \{k_0, k_0+1, \ldots, N-1, N\}$$

- $x_k \in R^n$ x-process

- $u_k \in R^m$ x-control .

The form process $\{r_k: k=k_0,\ldots,N\}$ is a finite-state Markov chain taking values in

$$r_k \in \underline{M} \equiv \{1,2,\ldots,M\} \qquad M<\infty .$$

That is,

$$\Pr\{r_{k+1}=j \,|\, r_0, r_1, \ldots, r_k\} = \Pr\{r_{k+1}=j \,|\, r_k\}, \quad \forall j \in \underline{M} \text{ and } k \tag{3.3}$$

where the <u>form transition probabilities</u> $p_k(i,j)$ in (3.2) must satisfy

$$p_k(i,j) \geq 0 \qquad \forall i,j \in \underline{M} \text{ and } k$$

$$\sum_{j=1}^{M} p_k(i,j) = 1 \qquad \forall i \in \underline{M} \text{ and } k \cdot$$

Here $A(\cdot)$ and $B(\cdot)$ are appropriately -dimensioned matrices where, for $i \in \underline{M}$

$A(i)$ = open-loop x dynamics in form i

$B(i)$ = x-process input gain in form i.

The cost criterion to be minimized is

$$J_{K_0}(x_0,r_0) = E\left\{\begin{array}{l}\sum_{k=k_0}^{N-1}\left[u_k'R_k(r_k)u_k + x_{k+1}'Q_{k+1}(r_{k+1})x_{k+1}\right] \\ \\ + x_N'K_T(r_N)x_N\end{array}\right\} \quad . \tag{3.4}$$

The $R_K(j)$, $Q_{k+1}(j)$ (for each k=0,...,N-1) and $K_T(j)$ are positive-semidefinite symmetric matrices for each $j \in \underline{M}$ where

$$R_k(j) + B_k'(j)\left[\sum_{i=1}^{M} p_{k+1}(j,i)Q_{k+1}(i)\right]B_k(j) > 0 \quad . \tag{3.5}$$

In particular, (3.5) is satisfied if

$$\begin{array}{l} R_k(j) > 0 \\ \\ Q_k(j) \geq 0 \end{array} \qquad \text{for all } j \in \underline{M} \text{ and times } k \ .$$

The $x_N'K_T(r_N)x_N$ term is a terminal cost in addition to $x_N'Q_N(r_N)x_N$.

3.3 Problem Solution

The optimal control law can be derived using dynamic programming [10]. Let $V_k(x_k,r_k)$ be the expected cost-to-go from state (x_k,r_k) at time k:

$$V_N[x_N, r_N] = x_N' K_T(r_N) x_N$$

$$V_k[x_k, r_k] = \min_{u_k} E\left\{ \begin{array}{l} u_k' R_k(r_k) u_k + x_{k+1}' Q_{k+1}(r_{k+1}) x_{k+1} \\ \\ + V_{k+1}(x_{k+1}, r_{k+1}) \end{array} \middle| \begin{array}{l} r_k \\ \\ x_k \end{array} \right\} . \tag{3.6}$$

Thus $V_k[x_k, r_k]$ is the minimal value of the cost criterion (3.4), computed over time interval $\{k, k+1, \ldots, N\}$. Hence

$$V_{k_0}(x_{k_0}, r_{k_0}) = \min_{u_{k_0}, u_{k_0+1}, \ldots, u_{N-1}} J_{k_0}(x_{k_0}, r_{k_0}) .$$

The iterative relationship (3.6) can be recursively solved for $V_k(x_k, r_k)$ and $u_k(x_k, r_k)$, going backwards in time from finite time N.

Proposition 3.1: Consider the discrete-time noiseless Markovian-form jump linear quadratic optimal control problem (3.1)-(3.5). The optimal control law is given by

$$u_{k-1} = -L_{k-1}(j) x_{k-1} \qquad \text{for } r_{k-1} = j \in \underline{M}, \quad k = k_0+1, \ldots, N$$

and the optimal expected cost-to-go by

$$V_k[x_k, r_k = j] = x_k' K_k(j) x_k \qquad r_k = j \in \underline{M}, \quad k = k_0, k_0+1, \ldots, N$$

where the optimal gains $L_{k-1}(j)$ are given by

$$L_{k-1}(j) = \begin{bmatrix} \left\{ R_{k-1}(j) + B'_{k-1}(j) \left[\sum_{i=1}^{M} p_k(j,i) \begin{bmatrix} Q_k(i) \\ + \\ K_k(i) \end{bmatrix} \right] B_{k-1}(j) \right\}^{-1} \cdot \\ \left\{ B'_{k-1}(j) \left[\sum_{i=1}^{M} p_k(j,i) \begin{bmatrix} Q_k(i) \\ + \\ K_k(i) \end{bmatrix} \right] A_{k-1}(j) \right\} \end{bmatrix} . \tag{3.7}$$

for each $j \in \underline{M}$, and the sequence of sets of positive semi-definite symmetric matrices $\{K_{k-1}(j): j \in \underline{M}\}$ satisfies the set of M coupled matrix difference equations

$$K_{k-1}(j) = A'_{k-1}(j) \left[\sum_{i=1}^{m} p_k(j,i) \begin{bmatrix} Q_k(i) \\ + \\ K_k(i) \end{bmatrix} \right] \begin{bmatrix} A_{k-1}(j) \\ -B_{k-1}(j) L_{k-1}(j) \end{bmatrix} \tag{3.8}$$

$$j \in \underline{M}$$

with terminal conditions

$$K_N(j) = K_T(j) \ .$$

The value of the optimal expected criterion (3.4) that is achieved with these control laws is given by

$$x'_0 \, K_{k_0}(r_0) x_0 \ .$$

The proof of this Proposition is contained in Appendix B.1.

Note that the $\{K_k(j): j \in \underline{M}\}$ and optimal gains $\{L_k(j): j \in \underline{M}\}$ can be recursively computed off-line, using the M coupled difference equations (3.7)-(3.8). The M coupled Riccati-like matrix difference equations cannot be written as a single nM-dimensional Riccati-equation, because of the inverse terms. Proposition 3.1 essentially[1] appears in Birdwell's thesis [12], where it is called the switching gain solution.

3.4 Examples and Discussions

In this section some qualitative aspects of the JLQ controller given in Proposition 3.1 are illustrated via example systems. For convenience, the examples considered here are time-invariant and scalar in x with M=2 forms. That is,

$$x_{k+1} = a_1 x_k + b_1 u_k \qquad \text{if} \quad r_k=1$$

$$x_{k+1} = a_2 x_k + b_2 u_k \qquad \text{if} \quad r_k=2$$

$$\min E\left\{ \sum_{k=0}^{N-1} \left[x_{k+1}^2 Q(r_k) + u_k^2 R(r_k) \right] + x_N^2 K_T(r_N) \right\}$$

with form transition probabilities as shown in Figure 3.1.

---

[1] Time-invariant parameters with A, R, Q independent of the form r.

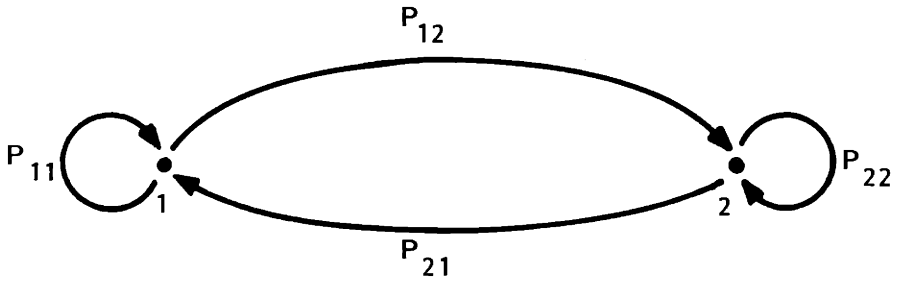

Figure 3.1: Example System Form Structure

From Proposition 3.1 we see that the optimal expected costs-to-go and control laws are

$$V_K(x_k, r_k=j) = x_k^2 K_k(j) \qquad j=1,2$$

$$u_k(x_k, r_k=j) = -L_k(j)x_k \qquad j=1,2$$

where

$$L_{K-1}(j) = \frac{b_j a_j \left\{ p_{j1} \left[\begin{matrix} Q_1 \\ + \\ K_k(1) \end{matrix} \right] + p_{j2} \left[\begin{matrix} Q_2 \\ + \\ K_k(2) \end{matrix} \right] \right\}}{R_j + b_j^2 \left\{ p_{j1} \left[\begin{matrix} Q_1 \\ + \\ K_k(1) \end{matrix} \right] + p_{j2} \left[\begin{matrix} Q_2 \\ + \\ K_k(2) \end{matrix} \right] \right\}} \tag{3.9}$$

and

$$K_{k-1}(j) = a_j \left\{ p_{j1} \left[\begin{matrix} Q_1 \\ + \\ K_k \end{matrix} \right] + p_{j2} \left[\begin{matrix} Q_2 \\ + \\ K_k(2) \end{matrix} \right] \right\} \left[a_j - b_j L_{K-1}(j) \right] \tag{3.10}$$

for j=1,2 and K=N,N-1,...,0.

The closed-loop optimal system thus obeys

$$x_{k+1} = \frac{a_j R_j}{R_j + b_j^2 \left\{ p_{j1}\left(Q_1 + K_{k+1}(1) \right) + p_{j2}\left(Q_2 + K_{k+1}(2) \right) \right\}} x_k \qquad (3.11)$$

for $k=0,1,\ldots,N-1$ and $r_k=j$.

The $\left\{K_k(j),\ j \in \underline{M}\right\}$ may or may not converge as k decreases from N, and x_k may or may not be driven to zero, as shown in the following examples.

Example 3.1: Here is an example in which the $\left\{K_k(j)\right\}$ converge quickly and x is driven to zero. Let

$$x_{k+1} = x_k + u_k \qquad \text{if} \quad r_k=1$$

$$x_{k+1} = 2x_k + 2u_k \qquad \text{if} \quad r_k=2$$

with

$$p_{ij} = 1/2$$

$$K_T(j) = 0$$

$$Q(j) = 1 \qquad i,j=1,2$$

$$R(j) = 1$$

The optimal costs, control gains and closed-loop dynamics (computed using (3.9)-(3.11)) are given in Tables 3.1 and 3.2, for four iterations:

	$K_k(1)=L_k(1)$	$K_k(2)=L_k(2)$
k=N-1	.5	.8
k=N-2	.6226415	.868421
k=N-3	.6357717	.87472
k=N-4	.6370559	.875327

Table 3.1: Optimal Gains and Costs of Example 3.1.

	$a_1-b_1L_k(1)$	$a_2-b_2L_k(2)$
k=N-1	.5	.4
k=N-2	.3773585	.263158
k=N-3	.3642283	.25056
k=N-4	.3629441	.249346

Table 3.2: Closed-Loop Dynamics of Example 3.1.

The expected cost parameters $K_k(j)$ and optimal gains $L_k(j)$ are converging as (N-k) increases. The same is true for the closed-loop systems, which are stable

$$|a_j - b_j K_k(j)| < 1$$

for all times k=N-1, N-2,...,0 and $j \in \underline{M}$. Conditions for convergence will be addressed in the next section.

In the 'worst case' of $r_k=2$ for all times k=0,1,...,

$$\lim_{N\to\infty} |x_N| \leq \lim_{N\to\infty} (.5)^{N-1}|x_0| = 0.$$

Thus x is driven to zero by the optimal controller.

This example demonstrates the passive hedging behavior of the optimal controller. That is, possible future form changes and their associated costs are taken into account. To see this, consider the usual LQ regulator gains and cost parameters (as if $p_{11}=p_{22}=1$ and $p_{12}=p_{21}=0$), which are listed in Table 3.3

	$K_k(1) = L_k(1)$ (with $p_{11}=1$)	$K_k(2) = L_k(2)$ (with $p_{22}=1$)
k=N-1	.5	.8
k=N-2	.6	.8780487
k=N-3	.6153846	.8825214
k=N-4	.617647	.8827678

Table 3.3: Standard LQ Solution for Example 3.1.

Comparing Tables 3.1 and 3.3, note that for $k \leq N-2$ the gains of the Proposition 3.1 JLQ controller are modified (relative to LQ controller) to reflect future form changes and costs. The JLQ controller has higher r=1 gains to compensate for the possibility that the system might shift to the more expensive form r=2. Similarly, the r=2 gains are lower in the JLQ controller.

Example 3.2: Here is an example where the optimal closed-loop systems in different forms are not all stable, although the expected value of x is driven to zero. Let

$$x_{k+1} = x_k + u_k \qquad \text{if } r_k=1$$

$$x_{k+1} = 2x_k + u_k \qquad \text{if } r_k=2$$

$$p_{11} = p_{21} = .9 \qquad p_{12} = p_{22} = .1$$

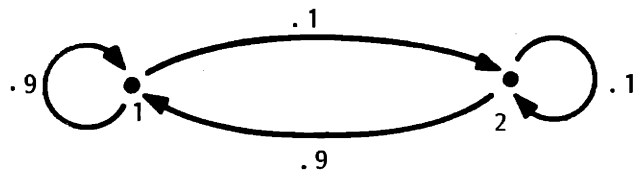

where

$$K_T(j) = 0 \qquad j=1,2$$

$$Q(j) = 1$$

and

$$R(1) = 1$$

$$R(2) = 1000.$$

Thus there is a high penalty on control in form 2.

This system is nine times more likely to be in r=1 than in r=2 at any time. We might expect that the optimal control strategy may tolerate instability while in the expensive-to-control form r=2, since the system is likely to return soon to the form r=1 where control costs are much less. Computation of (3.8)-(3.11) for four iterations demonstrates this, as shown in Tables 3.4 and 3.5.

	$K_k(1)$	$K_k(2)$	$L_K(1)$	$L_K(2)$
k=N	0	0		
k=N-1	.5	3.996004	.5	1.998×10^{-3}
k=N-2	.6490736	7.384818	.6490736	3.67203×10^{-3}
k=N-3	.6990352	9.2692147	.6990352	4.60253×10^{-3}
k=N-4	.7187893	10.198343	.7187893	5.06036×10^{-3}

Table 3.4: Optimal Gains and Costs of Example 3.2.

	$a_1-b_1L_K(1)$	$a_2-b_2L_K(2)$
k=N-1	.5	1.998002
k=N-2	.3590264	1.996328
k=N-3	.3009648	1.9953975
k=N-4	.2812107	1.9949396

Table 3.5: Closed-Loop Optimal Dynamics of Example 3.2.

These quantities are converging as $(N-k)\to\infty$. Note that the closed-loop system is unstable while in r=2.

Direct calculation of the expected value of x_k, given x_0 and r_0, shows that $E|x_k|$ decreases as k increases. This is shown in Table 3.6.

	if r_0=1	if r_0=2
x_0	1.0	1.0
x_1	.28121	1.99494
$E\{x_2\}$	.13228	.93844
$E\{x_3\}$	.06915	.49057
$E\{x_4\}$	.04493	.31877

Table 3.6: $E\{x_k\}$ for Example 3.2.

In four time steps, $E\{x\}$ is reduced by over 95% in form 1 and 68% in form 2. Note that if the system starts in the expensive-to-control form r=2, x is allowed to increase for one time step (until control while in r=1 is likely to reduce it).

Example 3.3: This example illustrates how 'small' errors in the modelling of transition probabilities near zero or one can cause large differences in the JLQ optimal controller. Let

$$x_{k+1} = x_k + u_k \qquad \text{if} \quad r_k=1$$

$$x_{k+1} = x_k \qquad \text{if} \quad r_k=2$$

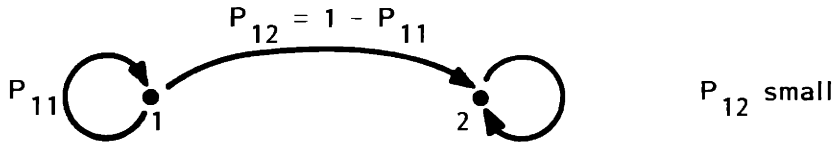

---

where $N=4$

$Q_1=1$

$Q_2=0$

$R_1=100$

$R_2=0$

$K_T(1)=0$

$K_T(2)=10^8$

The system starts in form $r_0=1$. If a failure occurs at time k (that is, $r_k=2$) then a cost

$$V_K(x_k,r_k=2) = x_k^2 K_k(2)$$

is charged. But since no control is possible in the failed form (i.e, $b(2)=0$),

$$V_K(x_k,r_k=2) = x_k^2 K_T(2) \quad .$$

We will consider three values of the failure probability p_{12} here:

Case A: No failures possible $p_{12}=0$

Case B: $p_{12}=.001$

Case C: $p_{12}=.002$

in order to examine the effects of small errors in the modelling of p_{12}.

If there is no chance of failure (Case A) then the optimal LQ control slowly drives x towards zero (less than 4% reduction in 4 time intervals). The optimal costs, control gains and closed loop dynamics (for r=1) in this case are given by Table 3.7.

	$K_k(1)$	$L_K(1)$	$a_1-b_1L_K(1)$
k=N-1	.99099	.00990099	.99099
k=N-2	1.951267	.0195126	.9804874
k=N-3	2.8666641	.028666	.971334
k=N-4	3.7227191	.0372271	.9627729

Table 3.7: Example 3.3 JLQ controller in form r=1, under Case A ($p_{12}=0$).

If there is a small nonzero failure probability (Case B p_{12}=.001, Case C p_{12}=.002) then the optimal JLQ controller drives x_k to zero almost completely in the first time step, as shown in Table 3.8. Thus a small difference in the value of p_{12} here makes a large difference in the optimal controller only if the difference changes the form transition structure of the system ((Case A vs. Case B) but not (Case B vs. Case C)).

	$K_k(1)$	$L_k(1)$	$a_1-b_1L_k(1)$
k=N-1	99.990001	.9999	$9.999\text{x}10^{-5}$
k=N-2	99.990002	.9999	$9.99801\text{x}10^{-5}$
k=N-3	99.990002	.9999	$9.99801\text{x}10^{-5}$
k=N-4	99.990002	.9999	$9.99801\text{x}10^{-5}$

(a) Case B: p_{12}=.001 , b(2)=0

	$K_k(1)$	$L_k(1)$	$a_1-b_1L_k(1)$
k=N-1	99.995	.99995	$4.999975\text{x}10^{-5}$
k=N-2	99.995	.99995	$4.99951\text{x}10^{-5}$
k=N-3	99.995	.99995	$4.99951\text{x}10^{-5}$
k=N-4	99.995	.99995	$4.99951\text{x}10^{-5}$

(b) Case C: p_{12}=.002 , b(2)=0

Table 3.8: Example 3.3 JLQ controller in form r=1 with b(2)=0 and (a) p_{12}=.001 (b) p_{12}=.002.

Now consider what happens when the wrong controller is used in the above cases, where $x_0=1$ and $r_0=1$.

If the true value is $p_{12}=0$ and the $p_{12}=.001$ controller is used then

$$u_0 = .999002$$

$$x_1 = 9.98\text{x}10^{-4}$$

and the achieved cost-to-go is around 99.801, or about twenty-six times greater than the cost with the correct ($p_{12}=0$) controller.

If the time $p_{12}=.001$ but the $p_{12}=0$ controller is mistakenly used, then

$$x_1 = .9627729$$

$$E\{x_2\} = .9352016$$

$$E\{x_3\} = .9188873$$

$$E\{x_4\} = .9087535$$

and the expected cost-to-go is

346290.67

which is around 3400 times greater than what the correct controller obtains.

In general, sensitivity to small parameters can be expected if the closed-loop costs are very different in the different forms and if a small change in the form transition probabilities alters

the form chain structure (probabilities very near zero and one). Changes in the controllability structure are reasonable in models of failure-prone systems. Different cost structures for failed and unfailed forms are also appropriate; for example, a system may use expensive back-up equipment when failures occur. The example system above is an extreme case which illustrates some of the issues that arise in deriving general theoretical results concerning JLQ systems.

3.5 The Steady-State Problem

In this section we consider the JLQ Markovian form control problem (3.1)-(3.5) when all parameters are time-invariant and the time horizon $(N-k_0)$ becomes infinite.

We wish to minimize

$$\lim_{(N-k_0)\to\infty} E\left\{ \sum_{k=k_0}^{N-1} \left[u_k' R(r_k) u_k + x_{k+1}' Q(r_{k+1}) x_{k+1} \right] + x_N' K_T(r_N) x_N \;\middle|\; \begin{matrix} x_{k_0} \\ r_0 \end{matrix} \right\} \tag{3.12}$$

subject to

$$x_{k+1} = A(r_k)x_k + B(r_k)u_k \tag{3.13}$$

$$\Pr\left\{ r_{k+1}=j \,\middle|\, r_k=i \right\} = p(i,j) \tag{3.14}$$

$$x(k_0)=x_0 \qquad r(k_0)=r_0 \ .$$

From Proposition 3.1 we have that the optimal control laws are

$$u_{k-1}(x_{k-1}, r_{k-1}=j) = -L_{k-1}(j)x_{k-1}$$

with optimal expected costs-to-go

$$V_k(x_k, r_k=j) = x_k' K_k(j) x_k$$

where for each $j \in \underline{M}$, and $k=N-1,N-2,\ldots,k_0$

$$L_K(j) = \left[\left\{ R(j) + B'(j) \left[\sum_{i=1}^{M} p(j,i) \left[\begin{matrix} Q(i) \\ + \\ K_{k+1}(j) \end{matrix} \right] B(j) \right\}^{-1} \cdot \right. \\ \left. \cdot B'(j) \left[\sum_{i=1}^{M} p(j,i) \left[\begin{matrix} Q(i) \\ + \\ K_{k+1}(i) \end{matrix} \right] A(j) \right] \right] \tag{3.15}$$

and

$$K_k(j) = A'(j) \left[\sum_{i=1}^{M} p(j,i) \begin{pmatrix} Q(i) \\ + \\ K_{k+1}(i) \end{pmatrix} \right] \begin{pmatrix} A(j) \\ -B(j)L_k(j) \end{pmatrix} \tag{3.16}$$

with

$$K_N(j) = K_T(j) \quad .$$

The optimal closed-loop dynamics in each form $j \in \underline{M}$ are thus

$$x_{k+1} = D_k(j) x_k$$

where

$$D_k(j) = \left[I - B_j \left\{ \begin{matrix} R_j \\ + \\ B'_j \left[\sum_{i=1}^{M} p_{ji} \begin{pmatrix} Q_i \\ + \\ K_{k+1}(i) \end{pmatrix} \right] B_j \end{matrix} \right\}^{-1} B'_j \left[\sum_{i=1}^{M} p_{ji} \begin{pmatrix} Q_i \\ + \\ K_{k+1}(1) \end{pmatrix} \right] \right] A_j \, . \tag{3.17}$$

Before stating the main result of this section, we recall the following terminology pertaining to finite-state Markov chains:

- A state is <u>transient</u> if a return to it is not guaranteed.
- A state i is <u>recurrent</u> if an eventual return to i is guaranteed. If the state set is finite, the mean time until return is finite.
- state i is <u>accessible</u> from state j if it is possible to begin in j and arrive in i in some finite number of steps.
- states i and j are said to <u>communicate</u> if each is accessible from the other.
- A <u>communicating class</u> is <u>closed</u> if there are no possible transitions from inside the class to any state outside of it.
- A closed communicating class containing only one member, j, is an <u>absorbing state</u>. That is, $p_{jj}=1$.

- A Markov chain state set can be divided into disjoint sets $\underline{T}$, $C_1,\ldots,C_s$, where all of the states in $\underline{T}$ are transient, and each C_j is a closed communicating class (of recurrent states).[1]

Define the cover c_j of a form $j \in \underline{M}$ to be the set of all forms accessible from j in one time step. That is,

$$c_j = \{i \in \underline{M}: p(j,i) \neq 0\} \quad .$$

The main result of this section is the following:

Proposition 3.2

Consider the time-invariant Markovian JLQ problem (3.12)-(3.14). Suppose that there exist feedback control laws

$$u_k = -F_i x_k \qquad \text{for each} \quad i \in \underline{M}$$

such that the following conditions hold:

(1) For each absorbing form i (ie: $p_{ii}=1$) the (deterministic) cost-to-go from $(x_k=x, r_k=i)$ at time k remains finite (for any finite x) as $(N-k)\to\infty$. This is true if and only if

$$\sum_{t=0}^{\infty} (A_i-B_iF_i)'^t (Q_i+F_i'R_iF_i)(A_i-B_iF_i)^t < \infty \qquad (3.18)$$

(each element finite).

---

[1] See [36], p.53.

(2) For each closed communicating class C_j (having two or more members) the expected cost-to-go from $(x_k=x,\ r_k=j \in C_j)$ at time k remains finite (for any finite x and each $i \in C_j$) as $(N-K)\to\infty$. This will be true if and only if for each such class C_j there exists a set of finite positive-definite nxn matrices $\{z_1,\ldots,z_{|C_j|}\}$ satisfying (3.19):

$$Z_i = (1-p_{ii}) \sum_{t=1}^{\infty} p_{ii}^{t-1} (A_i-B_iF_i)'^t \left[Q_i+F_i'R_iF_i + \sum_{\substack{\ell\in C_j \\ \ell\neq i}} \frac{p_{i\ell}}{1-p_{ii}} Z_\ell \right] (A_i-B_iF_i)^t \tag{3.19}$$

for all $i \in C_j$.

(3) For each transient form $i \in T \subset M$, the expected cost-to-go until the form process leaves T (that is, until a closed communicating class is entered) is finite. This is true if and only if there exist finite positive-definite nxn matrices $\{G_1,\ldots,G_T\}$ satisfying (3.20):

$$G_i = (1-p_{ii}) \sum_{t=1}^{\infty} p_{ii}^{t-1} (A_i-B_iF_i)'^t \left[Q_i+F_i'R_iF_i + \sum_{\substack{\ell\in T \\ \ell\neq i}} \frac{p_{i\ell}}{1-p_{ii}} G_\ell \right] (A_i-B_iF_i)^t \tag{3.20}$$

for all $i \in T$.

The existence of feedback laws F_i satisfying these conditions is necessary and sufficient for the solution of the set of coupled matrix difference equations (3.15)-(3.16) to converge to a unique constant steady-state set

$$\{K(j) \geq 0;\ j \in \underline{M}\} \tag{3.21}$$

as $(N-k_0) \to \infty$, given by the M coupled equations

$$K(j) = \left[\begin{array}{l} A_j' \left[\sum_{i=1}^{M} p_{ji} \left(\begin{array}{c} Q_i \\ + \\ K(i) \end{array} \right) \right] A_j \\ \\ -A_j' \left[\sum_{i=1}^{M} p_{ji} \left(\begin{array}{c} Q_i \\ + \\ K(i) \end{array} \right) \right] B_j \left\{ \begin{array}{c} R_j \\ + \\ B_j' \left[\sum_{i=1}^{M} p_{ji} \left(\begin{array}{c} Q_i \\ + \\ K(i) \end{array} \right) \right] B_j \end{array} \right\}^{-1} B_j' \left[\sum_{i=1}^{M} p_{ji} \left(\begin{array}{c} Q_i \\ + \\ K(i) \end{array} \right) \right] A_j \end{array} \right] \tag{3.22}$$

for $j \in \underline{M}$. The steady-state optimal control laws

$$u_k = -L_j x_k \qquad j \in \underline{M}$$

have time-invariant gains $\{L_j:\ j \in \underline{M}\}$ given by

$$L_j = \left\{ \begin{array}{c} R_j \\ + \\ B_j' \left[\sum_{i=1}^{M} p_{ji} \left(\begin{array}{c} Q_i \\ + \\ K(i) \end{array} \right) \right] B_j \end{array} \right\}^{-1} B_j' \left[\sum_{i=1}^{M} p_{ji} \left(\begin{array}{c} Q_i \\ + \\ K(i) \end{array} \right) \right] A_j \tag{3.23}$$

and minimize (3.12)-(3.14) with

$$V_{k_0}(x_0, r_0) = x_0' K(r_0) x_0 < \infty \tag{3.24}$$

for $x_0' x_0 < \infty$.

When the steady-state optimal control laws (3.23)-(3.24) exist, they stabilize the system in the sense that

$$E\{x_k' x_k\} \to 0$$

as $(k-k_0) \to \infty$, and $K(j) > 0$ for each $j \in \underline{M}$ if

(4) for at least one form i in each closed communicating subset of $\underline{M}$, the null spaces

$$\eta(Q_i^{1/2}) \cap \eta(L_i) = \{0\} \quad . \tag{3.25}$$

□

The conditions (2)-(3) take into account

- the probability of being in forms that have unstable closed loop dynamics
- the relative expansion and contraction effects of unstable and stable form dynamics, and how the eigenvectors of accessible forms are "aligned." That is, it is not necessary or sufficient for all forms to be stable, since the interaction of different expected form dynamics determines the behavior of $E\{x_k' x_k\}$.

This will be illustrated in the examples of this section. The conditions in Proposition 3.2 differ from those of the usual discrete-time linear quadratic regulator problem[1] in that:

- necessary and sufficient conditions (1)-(3) replace the sufficient condition that the (single form) system is stabilizable

[1] See, for example [38], p. 497.

- condition (4) replaces the assumption that the (single form) pair $(A, Q^{1/2})$ is <u>detectable</u>.

Unfortunately conditions (1)-(4) are not easily verified. There is no evident algebraic test for (3.18)-(3.21) like the controllability and observability tests in the LQ problem. The use of the conditions in Proposition 3.2 will be demonstrated in examples later in this section.

The proof of Proposition 3.2 has the same basic outline as in the LQ problem:

(i) First show that conditions (1)-(3) guarantee that with zero terminal costs $\{K_N(j)=0;\ j \in \underline{M}\}$, the sequence of positive semidefinite symmetric matrices $\{K_{k_0}(j)\}$ (for each $j \in \underline{M}$) in (3.16) is increasing and bounded above as $(N-k_0)$ increases and hence the $K_{k_0}(j)$ converge element by element to bounded matrices

$$\lim_{(N-k_0)\to\infty} K_{k_0}(j) = K(j)$$

Then (3.15)-(3.16) yield the steady-state values (3.22)-(3.23) and the costs

$$x_0' K(j) x_0 \qquad r_0 = j \in \underline{M}$$

are finite for finite x_0.

(ii) Condition (4) is then shown to guarantee that $E\{x_k' x_k\}$ goes to zero as $(k-k_0)$ becomes large, and that $K(j)>0$ for each $j \in \underline{M}$.

(iii) Next it is shown that these results hold for arbitrary finite symmetric terminal cost matrices

$$\{K_T(j) \geq 0 , \qquad j \in \underline{M}\} \quad .$$

(iv) Finally it is easily shown (by contradiction) that the $\{K(j),\ j \in \underline{M}\}$ are the unique positive definite solutions of (3.18).

Once (i)-(ii) are proved then (iii)-(iv) are easily established.[1] Step (ii) is proved in Appendix B.2. Note that:

Corollary 3.3: The null-space requirement in condition (4) of proposition 3.2 is satisfied if, for at least one form i in each closed communicating subset of M,

$$Q_i > 0 \ . \qquad \square$$

The difficult part of proving Proposition 3.2 is establishing that conditions (1)-(3) have the desired effect. Equations (3.18)-(3.20) follow by a direct application of dynamic programming. The cost-to-go from $(x_k,\ r_k=i)$ if i is an absorbing form is

$$x_k' \left(\sum_{t=0}^{\infty} (A_i - B_i F_i)'^t (Q_i + F_i' R_i F_i)(A_i - B_i F_i)^t \right) x_k$$

(where control law gain $-F_i$ is used), hence (3.18). For a closed communicating class C_j, the expected costs-to-go from $(x_k, r_k=i)$ for each

---

[1] As in [11], pp. 76-79.

$i \in C_j$ are

$$x_k' Z_i x_k \qquad \left(i \in C_j\right)$$

as given in (3.19), if these Z_i are all positive-definite and finite. Similar arguments yields (3.20). Details of this are given in Appendix B.3.

In the remainder of this section conditions (1)-(3) are examined and illustrated via examples.

Consider the following simple scalar example problem that shows how the conditions of Proposition 3.2 can be tested.

Example 3.4

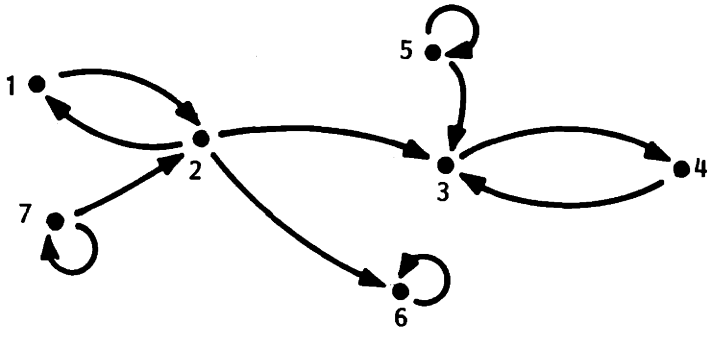

$$x_{k+1} = a(r)x_k \qquad r\varepsilon\{1,2,3,4,5,6,7\}$$

$$Q(r) > 0$$

Here

6 is an absorbing form

$\{3,4\}$ is a closed communicating class

$\underline{T} = \{1,2,5,7\}$ are transient forms

For the absorbing form r=6, (3.18) yields

$$\sum_{t=0}^{\infty} a(6)^t Q(6) a(6)^t < \infty \quad .$$

Hence

$$Q(6) \sum_{t=0}^{\infty} \left(a^2(6)\right)^t < \infty \quad .$$

Thus we have condition

(i) $\quad a^2(6) < 1 \quad .$

For the closed communicating class {3,4}, (3.19) gives coupled equations

$$Z_3 = a(3)[Q_3 + Z_4]\, a(3)$$

$$Z_4 = a(4)[Q_4 + Z_3]\, a(4)$$

Plugging in for Z_4 in the first equation yields

$$Z_3 = \frac{a^2(3)}{1 - a^2(3)a^2(4)} [Q(3) + a^2(4)Q(4)]$$

$$Z_4 = \frac{a^2(4)}{1 - a^2(3)a^2(4)} [Q(4) + a^2(3)Q(3)] \quad .$$

Thus for Z_3, Z_4 positive we have condition

(ii) $\quad a^2(3)a^2(4) < 1 \quad .$

For the transient forms {1,2,5,7}, (3.20) yields

$$G_1 = a(1)[Q(1) + G_2\ ]\ a(1)$$

$$G_2 = a(2)[Q(2) + p_{21}G_1]\ a(2)$$

$$G_7 = (1-p_{77}) \sum_{t=1}^{\infty} p_{77}^{t-1}\ a^{2t}(7)\left[Q(7) + \frac{p_{72}}{1-p_{77}}\right]G_2$$

$$G_5 = (1-p_{55}) \sum_{t=1}^{\infty} p_{55}^{t-1}\ a^{2t}(5)Q(5) \quad .$$

Now for $0 < G_5 < \infty$ we have the condition

(iii) $p_{55}\ a^2(5) < 1$

with the resulting

$$G_5 = \frac{Q(5)a^2(5)(1-p_{55})}{1-p_{55}a^2(5)} \quad .$$

We find from the G_1 and G_2 equations above that

$$G_1 = \frac{a^2(1)[Q(1)+ a^2(1)Q(2)]}{1-a^2(1)a^2(2)p_{21}}$$

$$G_2 = \frac{a^2(2)[Q(2)+ a^2(1)p_{21}Q(1)]}{1-a^2(1)a^2(2)p_{21}}$$

so for $0 < G_1, G_2 < \infty$ we have conditions

$$\text{(iv)} \quad a^2(1)a^2(2)p_{21} < 1 \quad .$$

Finally we find

$$G_7 = a^2(7)(1-p_{77}) \left[Q(7) + \frac{p_{72}G_2}{1-p_{77}} \right] \sum_{t=1}^{\infty} \left(a^2(7)p_{77} \right)^t$$

so for $0 < G_7 < \infty$ we have condition

$$\text{(v)} \quad a^2(7)p_{77} < 1$$

and

$$G_7 = \frac{a^2(7)(1-p_{77})}{1-a^2(7)p_{77}} \left[Q(7) + \frac{p_{72}a^2(2)[Q(2)+a^2(1)p_{21}Q(1)]}{(1-p_{77})(1-a^2(1)a^2(2)p_{21})} \right] .$$

Thus (i)-(v) are the necessary and sufficient conditions of Proposition 3.2. For this example we see that

- The absorbing form r=6 must have stable system dynamics (i)
- one of the forms in the closed communicating class {3,4} can be unstable as long as the other form's dynamics make up for the instability (ii)
- transient forms r=5,7 can have unstable dynamics as long as the probability of staying in them for any length of time is low enough (iii), (v)

- some instability of the dynamics of form r=1,2 is okay so long as the probability of repeating a
  $$2 \to 1 \to 2$$
  cycle is low enough (iv).

From (3.15)-(3.16) it is clear that each $\{K_k(j)\}$ sequence is increasing as (N-K) increases.

In the proof of the LQ problem, the existence of an upper bound can be guaranteed by assuming the stabilizability of the system. This does not suffice here (except for scalar x), as shown in the following example.

Example 3.5: Stabilizability not sufficient for finite cost

Let M=2 where

$$A_1 = \begin{pmatrix} 1/2 & 10 \\ 0 & 1/2 \end{pmatrix} \qquad B_1 = \begin{pmatrix} 0 \\ 0 \end{pmatrix}$$

$$A_2 = \begin{pmatrix} 1/2 & 0 \\ 10 & 1/2 \end{pmatrix} \qquad B_2 = \begin{pmatrix} 0 \\ 0 \end{pmatrix}$$

with $p_{12}=p_{21}=1$, $p_{11}=p_{22}=0$ (a "flip-flop" system).

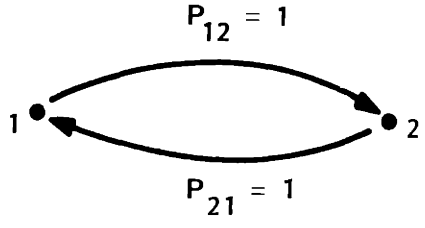

Both forms have stable systems (eigenvalues 1/2, 1/2) and hence are stabilizable. However

$$x_{k+2} = \begin{pmatrix} 100.25 & 5 \\ 5 & .25 \end{pmatrix} x_k \qquad \text{if} \quad r_k=1$$

$$x_{k+2} = \begin{pmatrix} .25 & 5 \\ 5 & 100.25 \end{pmatrix} x_k \qquad \text{if} \quad r_k=2$$

which is clearly unstable. Thus x_k and the expected cost (3.12) become infinite as $(N-k_0)$ goes to infinity.

In fact, controllability in each form is not sufficient, as demonstrated below.

Example 3.6; Controllability not sufficient for finite cost

Let M=2 where

$$A_1 = \begin{pmatrix} 0 & 2 \\ 0 & 0 \end{pmatrix} \qquad B_1 = \begin{pmatrix} 0 \\ 1 \end{pmatrix}$$

$$A_2 = \begin{pmatrix} 0 & 0 \\ 2 & 0 \end{pmatrix} \qquad B_2 = \begin{pmatrix} 1 \\ 0 \end{pmatrix} .$$

Thus in each form (r=1,2) the system is controllable, and the closed-loop systems have dynamics

$$x_{k+1} = D_j x_k \qquad r_k=j$$

where

$$D_1 = \begin{pmatrix} 0 & 2 \\ f_1 & f_2 \end{pmatrix}$$

$$D_2 = \begin{pmatrix} f_3 & f_4 \\ 2 & 0 \end{pmatrix}$$

where f_1, f_2, f_3, f_4 are determined by the feedback laws chosen. Now suppose that we have a "flip-flop" system as in the previous example:

$$p_{11} = p_{22} = 0$$

$$p_{21} = p_{12} = 1$$

Then

$$x_{2k} = (D_2D_1)^k x_0 \qquad \text{if} \quad r_0=1$$

$$x_{2k} = (D_1D_2)^k x_0 \qquad \text{if} \quad r_0=2$$

where

$$D_2D_1 = \begin{pmatrix} f_1f_4 & 2f_3+f_2f_4 \\ 0 & 4 \end{pmatrix}$$

$$D_1D_2 = \begin{pmatrix} 4 & 0 \\ f_1f_3+2f_2 & f_1f_4 \end{pmatrix} .$$

Both D_1D_2 and D_2D_1 have 4 as an eigenvalue. Thus x_k grows without bound for $x_0 \neq 0$ as k increases.[1] Controllability in each form allows us to place the eigenvalues of each form's closed loop dynamics matrix (D_i) as we choose, but we cannot place the eigenvectors. In this example, there is no choice of feedback laws that can align the eigenstructures of each of the closed loop systems so that the overall dynamics are stable. The following example demonstrates that (for $n \geq 2$) stabilizability of even one form is not necessary for the costs to be bounded above.

Example 3.7

Let M=2 with

$$A_1 = \begin{pmatrix} 1 & -1 \\ 0 & 1/2 \end{pmatrix} \qquad B_1 = \begin{pmatrix} 0 \\ 0 \end{pmatrix}$$

$$A_2 = \begin{pmatrix} 1/2 & 1 \\ 0 & 1 \end{pmatrix} \qquad B_2 = \begin{pmatrix} 0 \\ 0 \end{pmatrix} .$$

Both forms are unstable, uncontrollable systems so neither is stabilizable. We again take

---

[1] The closed-loop systems are stable if and only if the moduli of each eigenvalue is less than one. See, for example, [38] p. 454.

$$p_{11} = p_{22} = 0$$

$$p_{12} = p_{21} = 1$$

Then

$$x_{2k} = (A_2A_1)^k x_0 \qquad \text{if} \quad r_0=1$$

$$x_{2k} = (A_1A_2)^k x_0 \qquad \text{if} \quad r_0=2$$

where

$$A_2A_1 = A_1A_2 = \begin{pmatrix} 1/2 & 0 \\ 0 & 1/2 \end{pmatrix} .$$

Thus x_{2k} goes to zero geometrically as k increases and hence the cost (for any finite Q_j, $R_j \geq 0$ j=1,2) is finite. We next show that this example does satisfy condition (2) of Proposition 3.2. From (3.19),

$$Z_1 = A_1'[Q_1 + Z_2]A_1$$

$$Z_2 = A_2'[Q_2 + Z_1]A_2 \quad .$$

Suppose, for convenience, that $Q_1 = Q_2 = I$. Then we obtain from the first equation above that

$$\begin{pmatrix} Z_{11}(1) & Z_{12}(1) \\ Z_{21}(1) & Z_{22}(1) \end{pmatrix} = \begin{pmatrix} 1+Z_{11}(2) & -1-Z_{11}(2)+\frac{1}{2}Z_{12}(2) \\ -1-Z_{11}(2)+\frac{1}{2}Z_{21}(2) & \begin{pmatrix} 1+Z_{11}(2)-\frac{1}{2}Z_{21}(2) \\ -\frac{1}{2}Z_{12}(2)+\frac{1}{4}+\frac{1}{4}Z_{22}(2) \end{pmatrix} \end{pmatrix}$$

and plugging this into the second equation:

$$\begin{pmatrix} Z_{11}(2) & Z_{12}(2) \\ Z_{21}(2) & Z_{22}(2) \end{pmatrix} = \begin{pmatrix} \frac{1}{2} + \frac{1}{4} Z_{11}(2) & \frac{1}{2} + \frac{1}{4} Z_{12}(2) \\ \frac{1}{2} + \frac{1}{4} Z_{21}(2) & 2\frac{1}{4} + \frac{1}{4} Z_{22}(2) \end{pmatrix}.$$

This yields four equations in four unknowns. Solving, we find

$$\begin{pmatrix} Z_{11}(2) & Z_{12}(2) \\ Z_{21}(2) & Z_{22}(2) \end{pmatrix} = \begin{pmatrix} 2/3 & 2/3 \\ 2/3 & 3 \end{pmatrix}$$

and thus

$$\begin{pmatrix} Z_{11}(1) & Z_{12}(1) \\ Z_{21}(1) & Z_{22}(1) \end{pmatrix} = \begin{pmatrix} 5/3 & -4/3 \\ -4/3 & 5/3 \end{pmatrix},$$

which are both positive definite. Thus Z_1 and Z_2 satisfy (2) of Proposition 3.2. □

We can obtain <u>sufficient conditions</u>

that replace the necessary and sufficient conditions (1)-(3) in Proposition 3.2, and are somewhat easier to compute, in terms of the singular values of certain matrices. For any matrix A,

$$\begin{aligned} ||A|| &= [\text{max eigenvalue } A'A]^{1/2} \\ &= \text{max singular value of } A \\ &\triangleq \bar{\sigma}(A). \end{aligned} \tag{3.26}$$

Note: In the above, $||A||$ is the spectral norm of A, defined as

$$||A|| \triangleq \max_{||u||=1} \{||Au||\} \tag{3.27}$$

over all vectors u of unit length where $||\cdots||$ on the right in (3.27) designates the ordinary euclidean norm of a vector

$$||x|| = \left[\sum_{i=1}^{n} x_i^2 \right]^{1/2} .$$

Corollary 3.4: Consider the problem of Proposition 3.2. Sufficient conditions for the existence of the steady-state control law (and finite expected costs-to-go), replacing (1)-(3), are:

there exist feedback control laws

$$u_k = -F_i x_k \qquad i \in \underline{M}$$

such that

(1) for each absorbing form i ($p_{ii}=1$),

$$\sum_{t=0}^{\infty} ||(A_i - B_i F_i)^t||^2 < \infty \tag{3.28}$$

(2) for each recurrent, nonabsorbing form i

$$(1-p_{ii}) \sum_{t=1}^{\infty} p_{ii}^{t-1} ||(A_i - B_i F_i)^t||^2 < c < 1 \tag{3.29}$$

(3) for each transient form $i \in T$ that is accessible from a form $j \in \mathcal{C}_i$ in its cover ($j \neq i$)

$$(1-p_{ii}) \sum_{t=1}^{\infty} p_{ii}^{t-1} \left|\left|(A_i-B_iF_i)^t\right|\right|^2 < c < 1 \qquad (3.30)$$

and for each transient form $i \in T$ that is not accessible from any form $j \in \mathcal{C}_i$ in its cover (except itself):

$$(1-p_{ii}) \sum_{t=1}^{\infty} p_{ii}^{t-1} \left|\left|(A_i-B_iF_i)^t\right|\right|^2 < \infty . \qquad (3.31) \quad \square$$

The proof of this Corollary is given in Appendix B.3. A similar result for continuous-time systems is obtained by Wonham[1] [76], except that stabilizability and observability of each form is required, and a condition (3.29)=(3.30) is required for all nonabsorbing forms.

Condition (3) is motivated as follows. The cost incurred while in a particular transient form is finite with probability one since, eventually, the form process leaves the transient class T and enters a closed communicating class. If a particular transient form $i \in T$ can be repeatedly re-entered, however, the expected cost incurred while in i may be infinite; (3.30) excludes such cases. Note that the sufficient conditions of Corollary 3.4 are violated in example 3.7 (in both forms). This demonstrates that they are restrictive, in that they ignore

[1] Theorem 6.1, p.195 of [76].

the relative "directions" of x growth in the different forms (i.e. the eigenvector structure). We consider next a sufficient condition that is easier to verify than (1)-(3) of Corollary 3,4, but more restrictive.

Corollary 3.5: Sufficient conditions (1)-(3) in Proposition 3.2 can be replaced by the following:

For each form $i \in \underline{M}$, there exist feedback control laws

$$u_k = -F_i x_k$$

such that

$$||A_i - B_i F_i|| < c < 1 \quad . \tag{3.32}$$

Proof: If this condition holds, then with these F_i we have (with x_0 finite)

$$E\left\{ \sum_{k=0}^{\infty} x_k' Q(r_k) x_k + u_k' R(r_k) u_k \right\}$$

$$\leq ||x_0||^2 \left(\max_j ||Q_j + F_j' R_j F_j|| \right) \max_i \sum_{k=0}^{\infty} ||A_i - B_i F_i||^{2k}$$

$$\leq \text{(constant)} \sum_{k=0}^{\infty} c^{2k} < \infty$$

since $c < 1$. □

Note that if (3.32) holds then conditions (1)-(3) do. Note also that we are guaranteed that $||x_k|| \to 0$ with probability one, if (3.32) holds only for recurrent forms. However this is not enough to have finite expected cost, as demonstrated in the following examples.

Example 3.8:

Let

$$A_1 = \begin{pmatrix} a & 0 \\ 0 & a \end{pmatrix} \qquad B_1 = \begin{pmatrix} 0 \\ 0 \end{pmatrix}$$

$$A_2 = \begin{pmatrix} 0 & 0 \\ 0 & 0 \end{pmatrix} \qquad B_2 = \begin{pmatrix} 0 \\ 0 \end{pmatrix}$$

$$Q_1 = \begin{pmatrix} 1 & 0 \\ 0 & 1 \end{pmatrix} \qquad Q_2 = \begin{pmatrix} 0 & 0 \\ 0 & 0 \end{pmatrix}$$

$$R_i = \begin{pmatrix} 0 & 0 \\ 0 & 0 \end{pmatrix} \qquad i=1,2$$

with

$$p_{11} = p \qquad p_{22} = 1$$

$$p_{12} = 1-p \qquad p_{21} = 0$$

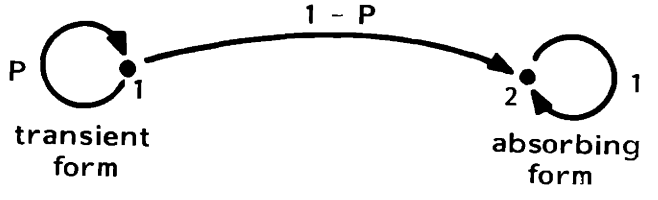

Thus

$$\min_{F_1} ||A_1 - B_1 F_1|| = \left|\left| \begin{pmatrix} a & 0 \\ 0 & a \end{pmatrix} \right|\right| = a > 1$$

$$\min_{F_2} ||A_2 - B_2 F_2|| = 0$$

and for $r_0 = 1$ and $||x_0||$ finite

$$E\left\{ \sum_{k=0}^{\infty} x_k' Q(r_k) x_k + u_k' R(r_k) u_k \right\}$$

$$= \sum_{k=0}^{\infty} p^k a^{2k} ||x_0||^2$$

$$= ||x_0||^2 \sum_{k=0}^{\infty} (a^2 p)^k \quad .$$

If

$$a^2 p < 1$$

then the expected cost is

$$\frac{||x_0||^2}{1 - a^2 p} < \infty$$

but if $a^2 p \geq 1$ then the expected cost-to-go is infinite. This demonstrates that (3.32) holding only for nontransient forms is not sufficient. □

Example 3.9: Let

$$x_{k+1} = \begin{pmatrix} 1 & 1 \\ -1 & -1 \end{pmatrix} x_k \qquad \text{if} \quad r_k = 1,3$$

$$x_{k+1} = \begin{pmatrix} a & 0 \\ 0 & a \end{pmatrix} x_k \qquad \text{if} \quad r_k = 2 \quad (a \neq 0)$$

where

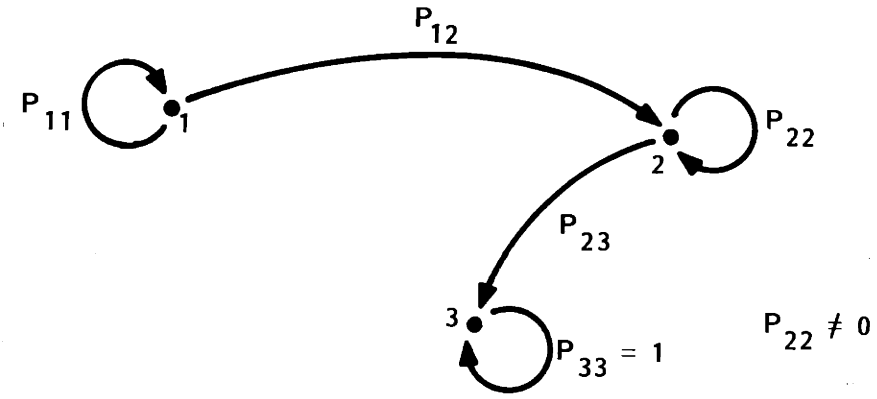

If the system is in form 1 for three successive times ($r_k = r_{k+1} = r_{k+2} = 1$), then $x'_{k+2} = (0\ 0)$ for any x_k. The same is true for three successive times in the absorbing form $r=3$.

In form $r=2$, the expected cost incurred until the system leaves (at time T) given that the state at time k is $(x_k, r_k=2)$ is

$$E\left\{\sum_{t=k}^{\tau-1} x_t' Q_2 x_t\right\} = x_k' \left[(1-p_{22}) \sum_{t=1}^{\infty} p_{22}^{t-1} (A_t')^t Q_2 A_2^t\right] x_k \ .$$

For this cost to be finite we must have

$$(1-p_{22}) \sum_{t=1}^{\infty} p_{22}^{t-1} (A_2')^t Q_2 A_2^t$$

$$= Q_2 a^2 (1-p_{22}) \sum_{t=0}^{\infty} (p_{22} a^2)^t < \infty$$

which is true (for Q_2 finite) if and only if

$$a^2 p_{22} < 1.$$

Thus we would expect that the optimal expected costs-to-go in Proposition 3.2 will be finite if and only if

$$a^2 p_{22} < 1 \ .$$

Let us verify that the necessary and sufficient conditions of Proposition 3.2 say this.

From (3.18), for absorbing form r=3

$$\sum_{t=0}^{\infty} A_3^t (Q_3) A_3^t < \infty$$

but

$$A_3^t = \begin{pmatrix} 0 & 0 \\ 0 & 0 \end{pmatrix} \quad \text{for} \quad t \geq 2 \ ,$$

so this condition is met.

For transient forms {1,2} we must have $0 \leq G_1, G_2 < \infty$

where

$$G_1 = (1-p_{11}) \sum_{t=1}^{\infty} p_{11}^{t-1} (A_1')^t \left[Q_1 + \frac{p_{12}}{1-p_{11}} G_2 \right] A_1^t$$

$$G_2 = (1-p_{22}) \sum_{t=1}^{\infty} p_{22}^{t-1} (A_2')^t Q_2 A_2^t$$

Now

$$(A_2')^t = A_2^t = \begin{pmatrix} a^t & 0 \\ 0 & a^t \end{pmatrix}$$

thus

$$G_2 = Q_2(1-p_{22})a^2 \sum_{t=0}^{\infty} (p_{22}a^2)^t$$

hence we have condition

$$\text{(i)} \quad a^2 p_{22} < 1$$

and $G_2 = Q_2 a^2 (1-p_{22})/(1-p_{22}a^2)$. Finally since

$$(A_1)^t = \begin{pmatrix} 0 & 0 \\ 0 & 0 \end{pmatrix} \quad \text{for} \quad t \geq 2,$$

we have

$$G_1 = (1-p_{11})\left[A_1'\left[Q_1 + \frac{p_{12}}{1-p_{11}} G_2\right]A_1\right]$$

$$= (1-p_{11})\left[A_1'\left(Q_1 + \frac{p_{12}a^2(1-p_{22})}{(1-p_{11})(1-p_{22}a^2)} Q_2\right)A_1\right],$$

which is positive-definite since Q_1, $Q_2 > 0$. Thus the necessary and sufficient conditions of Proposition 3.2 here reduce to (i), as we deduced earlier. Note that the sufficient condition (3.32) of Corollary 3.5 is <u>never</u> met for r=1, r=3

$$||A_1|| = ||A_3|| = \left[\lambda_{max}\begin{pmatrix} 2 & 2 \\ 2 & 2 \end{pmatrix}\right]^{1/2} = 2 > 1.$$

and to meet (3.32) for r=2 requires

$$||A_2|| = |\sqrt{a^2}| < 1 \Rightarrow a^2 < 1 .$$

However the sufficient conditions for Corollary 3.4 are met because forms {1,2} are 'non-re-enterable' transient forms satisfying (3.31) (if $a^2p_{22} < 1$ for r=2).

3.6 Summary

Let us consider the JLQ controller here in terms of the fault-tolerance criteria of section 1.2. We note that the controller (3.7)-(3.8) is clearly adaptable (in the terminology of section 1.2), since a different control law is used in each form. That is, when a failure or other structural change occurs it is instantaneously detected (by assumption) and this information is used to reorganize the controller.

Passive hedging (the taking into account of possible future form changes and associated costs) is accomplished via the

$$\sum_{i=1}^{M} p_k(j,i)[Q_k(i)+K_k(i)]$$

terms in (3.7)-(3.8). There is no active hedging possible in this problem formulation because the form transition probabilities cannot be controlled. With regards to the implementability attribute of fault-tolerant controllers of section 1.2, the precomputable nature of (3.7)-(3.8) should facilitate the use of this controller if $M(N-k_0)$ (the number of gains that must be computed and stored) is not too large. When the steady-state controller of Proposition 3.2 exists, a set of M optimal steady-state gains that can be used in place of the $M(N-k_0)$ gains; this certainly should simplify implementation.

While in each form, the optimal JLQ controller of Proposition 3.1 is endowed with robustness properties derived from the linear quadratic problem. However the JLQ controller may be extremely sensitive to small errors in the modelling of form transition probabilities, if the probability in question is close to zero or one and if the controllability of the dynamics changes between forms, as illustrated in example 3.3.

Proposition 3.2 provides necessary and sufficient conditions for existence of the optimal steady-state JLQ controller. These conditions are not easily tested for nonscalar-x problems, however since they require the simultaneous solution of coupled matrix equations containing infinite sums. In Corollaries 3.4 and 3.5 sufficient conditions that are based upon singular values are presented that are somewhat more testable for some problems. However the derivation of easily calculable conditions for the JLQ steady state problem (like the controllability and observability conditions of the LQ problem) remains an open question.

4. EXTENSIONS OF THE X-INDEPENDENT JLQ PROBLEM

In this chapter we develop two extensions of the JLQ problem formulation. Our purpose is to indicate how the ideas and results of Chapter 3 can be applied to more general problems. We will consider here only problems with form processes that are not explicitly x-dependent. The more difficult cases of x and u dependent forms are the subject of Parts III and IV of the thesis.

In section 4.1 we consider JLQ problems with additive input noise to and noisy observations of the x subsystem (but perfect observations of the form). As in the LQ problem, a separation result holds. The only complication is that the parameters of the estimator of x_k (from noisy observations) depend upon r_k, and thus cannot be computed off-line.

In section 4.2 we widen the range of physical situations that can be captured by the JLQ control problem by including in the problem formulation jump costs and x-resets when the form changes.

4.1 The JLQ Problem with additive input and x-observation noise

In this section we extend the JLQ problem of Chapter 3 to include additive white input noise, and we assume that a linear function of x_k is observed at each time k in the presence of additive white noise. Under the crucial assumption that the form process is perfectly observed

at each time k, the optimal control law is the same as in the noiseless case but it acts upon an estimate of the x process. This estimate is obtained by a Kalman filter, where the update parameters are determined at each time by the observed form value.

We are considering the discrete-time jump linear system with additive driving noise:

$$x_{k+1} = A(r_k)x_k + B(r_k)u_k + \Xi(r_k)v_k \tag{4.1}$$

$$\Pr\{r_{k+1}=j \,|\, r_k=i\} = p_{ij} \qquad i,j \in \underline{M}$$

where

$$x(k_0) = x_0$$

$$r(k_0) = r_0$$

$$p_{ij} \geq 0$$

$$\sum_{j=1}^{M} p_{ij}=1 \qquad \forall i,j \in \underline{M}$$

$$\underline{M} = \{1,2,\ldots,M\}$$

$$x_k \in R^n \qquad u_k \in R^n$$

$$k=k_0,\ k_0+1,\ldots,N \quad .$$

At each time we observe r_k perfectly and a linear function of x_k contaminated by white observation noise:

$$y_k = C(r_k)x_k + D(r_k)u_k + \Lambda(r_k)w_k \quad . \tag{4.2}$$

In (4.1)-(4.3), $v_k \in R^{\bar{m}}$ and $w_k \in R^{\bar{p}}$. The input noise sequence $\{v_k\}$ and observation noise sequence $\{w_k\}$ are white, Gaussian with

$$E\{v_k\}=0 \qquad \forall k$$

$$E\{v_k\, v_\ell'\} = \begin{cases} 0 & \ell \neq k \\ I & \ell = k \end{cases} \qquad \forall \ell, k$$

$$E\{w_k\}=0 \qquad \forall k$$

$$E\{w_k\, w_\ell'\} = \begin{cases} 0 & \ell \neq k \\ I & \ell = k \end{cases} \qquad \forall k, \ell$$

and are independent of each other, of the form sequence $\{r_k\}$ and the initial condition x_0. Here

$$E\{x_0\} = \bar{x}_0$$

$$E\{[x_0-\bar{x}_0][x_0-\bar{x}_0]'\} = \Psi_0$$

and x_0 is independent of the (deterministic) r_0.

We seek to minimize the cost criterion

$$J_{k_0}(x_0,r_0) = E\left\{ \begin{array}{l} \sum_{k=k_0}^{N-1} \left[\begin{array}{l} u_k' R(r_k) u_k + x_{k+1}' Q(r_{k+1}) x_{k+1} \\ \quad + S(r_{k+1}) x_{k+1} + P(r_{k+1}) \end{array} \right] \\ \quad + x_N' K_T(r_N) x_N + H_T(r_N) x_N + G_T(r_N) \end{array} \middle| x_0, r_0 \right\} . \tag{4.3}$$

Note that we have x_k^1 and x_k^o terms in (4.3). These are included here for later comparison with the x-dependent form problems in Part III of this thesis. In (4.1)-(4.3) we take, for each $i \in \underline{M}$,

$$
\begin{aligned}
&R(i) > 0 \\
&\begin{pmatrix} Q(i) & S'(i)/2 \\ S(i)/2 & P(i) \end{pmatrix} \geq 0 \\
&\begin{pmatrix} K_T(i) & H_T'(i)/2 \\ H_T(i)/2 & G_T(i) \end{pmatrix} \geq 0 \\
&\Psi_0 \geq 0 \qquad .
\end{aligned}
\tag{4.4}
$$

The term

$$x_N' K_T(r_N) x_N + H_T(r_N) x_N + G_T(r_N)$$

in (4.3) is a terminal cost charged in addition to the time-invariant cost

$$x_N' Q(r_N) x_N + S(r_N) x_N + P(r_N) \ .$$

The control problem is then to find the control law

$$u_k = \tilde{\phi}_k(y(k_0),\ldots,y(k);\ r(k_0),\ldots,r(k)) \tag{4.5}$$

that minimizes (4.3). As in the linear quadratic Gaussian (LQG) problem the optimal solution to this problem satisfies a separation principle. In particular we have the following:

Proposition 4.1

The stochastic JLQ problem with incomplete and noisy measurements, as in (4.1)-(4.5) has the following solution. The optimal control law is given by

$$u_{k-1}(x_{k-1}, r_{k-1}=j) = -L_{k-1}(j)\hat{x}_{k-1} + F_{k-1}(j) \quad . \tag{4.6}$$

The control law parameters in (4.6) are

$$L_k(j) = \left[\begin{array}{c} R(j) \\ + \\ B'(j)\hat{K}_{k+1}(j)B(j) \end{array} \right]^{-1} B'(j)\hat{K}_{k+1}(j)A(j) \tag{4.7}$$

$$F_k(j) = -\frac{1}{2} \left[\begin{array}{c} R(j) \\ + \\ B'(j)\hat{K}_{k+1}(j)B(j) \end{array} \right]^{-1} B'(j)\hat{H}_{k+1}(j) \tag{4.8}$$

for $k=N-1, N-2, \ldots, k_0$ and $j \in \underline{M}$ where $\{L_k(j), F_k(j)\}$ are computed recursively, backwards in time from $k=N$, by the following sets of M coupled matrix difference equations:

$$K_k(j) = A'(j)\hat{K}_{k+1}(j)\left[I - B(j)\left[\begin{array}{c} R(j) \\ + \\ B'(j)\hat{K}_{k+1}(j)B(j) \end{array} \right]^{-1} B'(j)\hat{K}_{k+1}(j) \right] A(j) \tag{4.9}$$

$$H_k(j) = \hat{H}_{k+1}(j)\left[I - B(j)\left[\begin{array}{c} R(j) \\ + \\ B'(j)\hat{K}_{k+1}(j)B(j) \end{array} \right]^{-1} B'(j)\hat{K}_{k+1}(j) \right] A(j) \tag{4.10}$$

where

$$\hat{K}_{k+1}(j) = \sum_{i=1}^{M} p(j,i)[K_{k+1}(i)+Q(i)] \tag{4.11}$$

$$\hat{H}_{k+1}(j) = \sum_{i=1}^{M} p(j,i)[H_{k+1}(i)+S(i)] \tag{4.12}$$

with terminal conditions

$$K_N(j) = K_T(j) \tag{4.13}$$

$$H_N(j) = H_T(j) \tag{4.14}$$

The optimal (minimum mean square error) estimate $\hat{x}_k$ in (4.6) is given by the following form-dependent Kalman filter:

x-estimate extrapolation

$$\hat{x}_k(-) = A(r_{k-1})\hat{x}_{k-1}+B(r_{k-1})u_{k-1} \tag{4.15}$$

error covariance extrapolation

$$\Psi_k(-) = A(r_{k-1})\Psi_{k-1}(r_{k-1})A'(r_{k-1}) + \Xi(r_{k-1})\Xi'(r_{k-1}) \tag{4.16}$$

x-estimate update

$$\hat{x}_k = \hat{x}_k(-) + \Gamma_k(r_k)\begin{bmatrix} y_k - C(r_k)\hat{x}_k(-) \\ -D(r_k)u_{k-1} \end{bmatrix} \tag{4.17}$$

error covariance update

$$\Psi_k(r_k) = [I-\Gamma_k(r_k)C(r_k)]\Psi_k(-) \tag{4.18}$$

filter gain matrix

$$\Gamma_k(r_k) = \Psi_k(-)C'(r_k)\begin{bmatrix} C(r_k)\Psi_k(-)C'(r_k) \\ + \\ \Lambda(r_k)\Lambda'(r_k) \end{bmatrix}^{-1} \tag{4.19}$$

with initial conditions

$$\hat{x}_{k_0}(-) = \bar{x}_0 \tag{4.20}$$

$$\Psi_{k_0}(-) = \Psi_0 \quad . \tag{4.21}$$

The optimal expected cost-to-go is

$$\begin{aligned} V_{k_0}(x_0, r_0) = {} & \bar{x}_0' K_{k_0}(r_0)\bar{x}_0 + H_{k_0}(r_0)\bar{x}_0 \\ & + G_{k_0}(r_0) + \mathrm{tr}[K_{k_0}(r_0)\Psi_0] \\ & + \sum_{k=k_0}^{N-1} \mathrm{tr}\left\{\Psi_k(r_k)L_k'(r_k)\hat{K}_{k+1}(r_k)B(r_k)L_k(r_k)\right\} \end{aligned} \tag{4.22}$$

where

$$\begin{aligned} G_k(j) = {} & \hat{G}_{k+1}(j) + \sum_{k=1}^{M} p(j,i)\,\mathrm{tr}\left\{\Xi'(i)\begin{bmatrix} K_{k+1}(i) \\ + \\ Q(i) \end{bmatrix}\Xi(i)\right\} \\ & - \frac{1}{4}\hat{H}_{k+1}(j)B(j)\begin{bmatrix} R(j) \\ + \\ B'(j)\hat{K}_{k+1}(j)B(j) \end{bmatrix}^{-1} B'(j)\hat{H}_{k+1}'(j) \end{aligned} \tag{4.23}$$

with

$$\hat{G}_{k+1}(j) = \sum_{i=1}^{M} p(j,i)[G_{k+1}(i) + P(i)] \tag{4.24}$$

and terminal condition

$$G_N(j) = G_T(j) \qquad j \in \underline{M} \ . \tag{4.25}$$

At each time $k=N,N-1,\ldots,k_0$

$$\begin{pmatrix} K_k(j) & H_k'(j)/2 \\ H_k(j)/2 & G_k(j) \end{pmatrix} \geq 0 \tag{4.26}$$

This is proved in Appendix B.4. □

Note that the control law is unchanged if there is no observation or driving noise (ie., $\Xi(j)=0$, $\Lambda(j)=0$, $\forall j \in \underline{M}$). That is, the certainty equivalence principle applies here.

4.2 Jump Costs and Resets

In this section we extend the range of problems that can be captured by the JLQ problem formulation. Specifically we consider problems where

- jump costs are incurred when the form changes from r_{k-1} to r_k at time k

- the value of the x process may be <u>reset</u> to an affine function of its current value when the form changes.

Jump costs might represent start-up or shut-down costs of equipment when the system form changes. They might also model undesirable transient phenomena such as load shedding costs in electrical power systems, or the cost of equipment destroyed by the form change.

The resetting of x allows us to model failures that result from abrupt changes to the dynamic state of the system. For example, phenomena such as failure-caused biases in communication equipment or rapid voltage jumps due to changing interconnections in electronic devices can be modelled by resets of x. In addition we can use resets to represent nonlinear systems as a collection of linear systems, each associated with a different operating point. The x process might represent the deviation of the state from the current nominal value. If we assume that changes in the operating point are caused by external events (and are not x-dependent) then the results of this section can be applied. The x-dependent case is treated in Part III.

Consider the following class of jump linear systems with <u>affine</u> resets:

$$\bar{x}_{k+1} = A(r_k)x_k + B(r_k)u_k + \Xi(r_k)v_k \tag{4.27}$$

$$\Pr\{r_{k+1}=j \mid r_k=i\} = p_{ij} \qquad i,j \in \underline{M} \tag{4.28}$$

$$x_{k+1} = \bar{A}(r_k, r_{k+1})\bar{x}_{k+1} + Z(r_k, r_{k+1}) \tag{4.29}$$

We will assume in this section that the state process (x_k, r_k) is perfectly observed at each time k. The problem is to find the optimal control laws

$$u_k = \phi_k(x_0, \ldots, x_k;\ r_0, \ldots, r_k) \tag{4.30}$$

that minimize

$$J_{k_0}(x, r_0) = E\left\{ \sum_{k=k_0}^{N-1} \left[u_k' R(r_k) u_k + x_{k+1}' Q(r_k, r_{k+1}) x_{k+1} + S(r_k, r_{k+1}) x_{k+1} + P(r_k, r_{k+1}) \right] + x_N' K_T(r_{N-1}, r_N) x_N + H_T(r_{N-1}, r_N) x_N + G_T(r_{N-1}, r_N) \,\middle|\, x_0, r_0 \right\}. \tag{4.31}$$

Jump costs enter into this cost function through the dependence of Q, S, P, K_T, H_T and G_T on both the "old" and "new" values of the form. That is, we can assign a different x-cost to each form <u>transition</u> as well as to each form, if desired. Here the time-invariant parameters

$$R(j) > 0 \tag{4.32}$$

$$\begin{pmatrix} Q(i,j) & S'(i,j)/2 \\ S(i,j)/2 & P(i,j) \end{pmatrix} \geq 0 \tag{4.33}$$

and

$$\begin{pmatrix} K_T(i,j) & H_T'(i,j)/2 \\ H_T(i,j)/2 & G_T(i,j) \end{pmatrix} \geq 0 \tag{4.34}$$

for all $i,j \in \underline{M}$.

To find the optimal control law we apply dynamic programming. We have

$$V_N[x_N, r_{N-1}, r_N] = x_N' K_T(r_{N-1}, r_N) x_N + H_T(r_{N-1}, r_N) x_N + G_T(r_{N-1}, r_N) \tag{4.35}$$

$$V_{N-1}[x_{N-1}, r_{N-1}=j] = \min_{u_{N-1}} \left\{ \begin{array}{l} u_{N-1}' R(j) u_{N-1} \\ \quad + \\ E\left\{ \begin{array}{l} x_N' Q(j, r_N) x_N \\ \quad + \\ S(j, r_N) x_N + P(j, r_N) \\ \quad + \\ V_N[x_N, r_{N-1}=j, r_N] \end{array} \middle| \begin{array}{l} x_{N-1} \\ r_{N-1}=j \end{array} \right\} \end{array} \right\} \tag{4.36}$$

and for $k=N-2,\ldots,k_0$

$$V_k(x_k, r_k=j) = \min_{u_k} \left\{ \begin{array}{l} u_k' R(j) u_k \\ \quad + \\ E\left\{ \begin{array}{l} x_{k+1}' Q(j, r_{k+1}) x_{k+1} \\ \quad + \\ S(j, r_{k+1}) x_{k+1} + P(j, r_{k+1}) \\ \quad + \\ V_{k+1}(x_{k+1}, r_{k+1}) \end{array} \middle| \begin{array}{l} x_k \\ r_k=j \end{array} \right\} \end{array} \right\} . \tag{4.37}$$

Using (4.29) (4.31) we can rewrite (4.37) as $V_k(x_k, r_k=j) =$

$$\min_{u_k} \left\{ \sum_{i=1}^{M} p(j,i) E \left\{ \begin{aligned} & u_k' R(j) u_k \\ & + \\ & \left[\bar{A}(j,i) \left[\begin{matrix} A(j)x_k \\ + \\ B(j)u_k \\ + \\ \Xi(j)v_k \end{matrix} \right] + Z(j,i) \right]' Q(j,i) \left[\bar{A}(j,i) \left[\begin{matrix} A(j)x_k \\ + \\ B(j)u_k \\ + \\ \Xi(j)v_k \end{matrix} \right] + Z(j,i) \right] \\ & + \\ & S(j,i)[\bar{A}(j,i)\{A(j)x_k + B(j)u_k + \Xi(j)v_k\} + Z(j,i)] \\ & + \\ & P(j,i) \\ & + \\ & V_{k+1}[\bar{A}(j,i)\{A(j)x_k + B(j)u_k + \Xi(j)v_k\} + Z(j,i), i] \end{aligned} \middle| \begin{matrix} x_k \\ r_k=j \end{matrix} \right\} \tag{4.38}$$

Solving (4.38) recursively for the optimal control sequence then yields the following:

Proposition 4.2: For the problem (4.27)-(4.34) the optimal control law is given by

$$u_{k-1}(x_{k-1}, r_{k-1}=j) = -L_{k-1}(j)x_{k-1} + F_{k-1}(j) \tag{4.39}$$

for $k=N, N-1, \ldots, k_0+1$ and the optimal expected cost-to-go is

$$V_k(x_k, r_k=j) = x_k' K_k(j) x_k + H_k(j) x_k + G_k(j) \tag{4.40}$$

for $k=N-1, N-2, \ldots, k_0$ for each $j \in \underline{M}$, where the parameters in (4.39)-(4.40) are computed recursively, backwards in time, by

$$K_k(j) = A'(j)\hat{K}_{k+1}(j)\left[I-B(j)\left[\begin{matrix}R(j)\\ +\\ B'(j)\hat{K}_{k+1}(j)B(j)\end{matrix}\right]^{-1}B'(j)\hat{K}_{k+1}(j)\right]A(j) \quad (4.41)$$

$$H_k(j) = \hat{H}_{k+1}(j)\left[I-B(j)\left[\begin{matrix}R(j)\\ +\\ B'(j)\hat{K}_{k+1}(j)B(j)\end{matrix}\right]^{-1}B'(j)\hat{K}_{k+1}(j)\right]A(j) \quad (4.42)$$

$$G_k(j) = \hat{G}_{k+1}(j) - \frac{1}{4}\hat{H}_{k+1}(j)B(j)\left[\begin{matrix}R(j)\\ +\\ B'(j)\hat{K}_{k+1}(j)B(j)\end{matrix}\right]^{-1}B'(j)\hat{H}'_{k+1}(j)$$

$$+\sum_{i=1}^{M} p(j,i)\mathrm{tr}\left\{\Xi'(j)\bar{A}'(j,i)\left[\begin{matrix}Q(j,i)\\ +\\ K_{k+1}(i)\end{matrix}\right]\bar{A}(j,i)\Xi(j)\right\} \quad (4.43)$$

$$L_k(j) = \left[\begin{matrix}R(j)\\ +\\ B'(j)\hat{K}_{k+1}(j)B(j)\end{matrix}\right]^{-1}B'(j)\hat{K}_{k+1}(j)A(j) \quad (4.44)$$

$$F_k(j) = -\frac{1}{2}\left[\begin{matrix}R(j)\\ +\\ B'(j)K_{k+1}(j)B(j)\end{matrix}\right]^{-1}B'(j)\hat{H}'_{k+1}(j) \quad (4.45)$$

as in Proposition 4.1, but with

$$\hat{K}_{k+1}(j) = \sum_{i=1}^{M} p(j,i)\bar{A}'(j,i)\left[\begin{matrix}K_{k+1}(i)\\ +\\ Q(j,i)\end{matrix}\right]\bar{A}(j,i) \quad (4.46)$$

$$\hat{H}_{k+1}(j) = \sum_{i=1}^{M} p(j,i) \left[\left\{ 2Z'(j,i) \begin{bmatrix} K_{k+1}(i) \\ + \\ Q(j,i) \end{bmatrix} + \begin{bmatrix} H_{k+1}(i) \\ + \\ S(j,i) \end{bmatrix} \right\} \bar{A}(j,i) \right] \quad (4.47)$$

$$\hat{G}_{k+1}(j) = \sum_{i=1}^{M} p(j,i) \begin{bmatrix} Z'(j,i) \begin{bmatrix} K_{k+1}(i) \\ + \\ Q(j,i) \end{bmatrix} \bar{Z}(j,i) \\ + \\ [H_{k+1}(i) + S(j,i)]Z(j,i) \\ + \\ [G_{k+1}(i) + P(j,i)] \end{bmatrix} \quad (4.48)$$

and terminal conditons

$$\hat{K}_N(j) = \sum_{i=1}^{M} p(j,i) \bar{A}'(j,i) \begin{bmatrix} K_T(j,i) \\ + \\ Q(j,i) \end{bmatrix} \bar{A}(j,i) \quad (4.49)$$

$$\hat{H}_N(j) = \sum_{i=1}^{M} p(j,i) \left[\left\{ 2Z'(j,i) \begin{bmatrix} K_T(j,i) \\ + \\ Q(j,i) \end{bmatrix} + \begin{bmatrix} H_T(j,i) \\ + \\ S(j,i) \end{bmatrix} \right\} \bar{A}(j,i) \right] \quad (4.50)$$

$$\hat{G}_N(j) = \sum_{i=1}^{M} p(j,i) \begin{bmatrix} Z'(j,i) \begin{bmatrix} K_T(j,i) \\ + \\ Q(j,i) \end{bmatrix} Z(j,i) \\ + \\ [H_T(j,i) + S(j,i)]Z(j,i) \\ + \\ [G_T(j,i) + P(j,i)] \end{bmatrix} . \quad (4.51)$$

At each time $k=N-1,\ldots,k_0$,

$$\begin{pmatrix} K_k(j) & H_k'(j)/2 \\ H_k(j)/2 & G_k(j) \end{pmatrix} \geq 0 \quad . \tag{4.52}$$

□

Comparing this result with Proposition 4.1 in the noiseless case (ie, $\Xi(j)=0$, $\Lambda(j)=0$, $\forall j \in \underline{M}$) we see that the cost and control laws are the same[1] but the definitions of $\hat{K}_{k+1}(j)$, $\hat{H}_{k+1}(j)$ and $\hat{G}_{k+1}(j)$ are different. Note that

- the $\bar{A}(j,i)$ (linear reset) parameters enter into <u>all</u> of the cost and control law terms (as do the $Q(j,i)$'s)
- the $Z(j,i)$ (constant reset) parameters do not affect the linear gain of the optimal control law.

The following example illustrates some of the qualitative effects of jump costs on the controlled system's behavior.

<u>Example 4.1</u>:

Consider the following problem:

$$x_{k+1} = x_k + u_k \qquad \text{if} \quad r_k=1$$

$$x_{k+1} = 2x_k + u_k \qquad \text{if} \quad r_k=2$$

---

[1] For deterministic x_{k_0}.

$p(1,1) = .9 \qquad p(1,2) = .1$

$p(2,1) = .9 \qquad p(2,2) = .1$

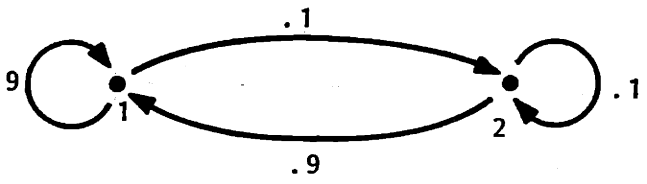

with

$$\min E\left\{\sum_{k=k_0}^{N-1} u_k^2 R(r_k) + x_{k+1}^2 Q(r_k, r_{k+1})\right\}$$

where

$R(1) = 1$ cheap to control when $r_k=1$

$R(2) = 1000$ expensive to control when $r_k=2$.

If we take

$Q(1,1) = Q(1,2)=1 \qquad Q(2,1) = Q(2,2)=1$

(ie, no jump costs) then we have the same problem as example 3.2. The optimal JLQ controller parameters and the closed-loop dynamics for this case are listed for four time stages in Tables 4.1 and 4.2, respectively.

	$K_k(1)$	$K_k(2)$	$L_k(1)$	$L_k(2)$
K=N	0	0		
K=N-1	.5	3.996004	.5	1.998×10^{-3}
K=N-2	.6490736	7.384818	.6490736	3.67203×10^{-3}
K=N-3	.6990352	9.2692147	.6990352	4.60253×10^{-3}
K=N-4	.7187893	10.198343	.7187893	5.06036×10^{-3}

Table 4.1: Optimal Gains and Costs of Example 4.1

	$a(1)-b(1)L_k(1)$	$a(2)-b(2)L_k(2)$
K=N-1	.5	1.998002
K=N-2	.3590264	1.996328
K=N-3	.3009648	1.9953975
K=N-4	.2812107	1.9949396

Table 4.2: Closed-Loop Optimal Dynamics of Example 4.1.

Now suppose that there is a jump cost charged when the form changes from r=1 to r=2. Take

$$Q(1,2) = 2$$

$$Q(1,1) = Q(2,1) = Q(2,2) = 1 .$$

The optimal controller parameter and closed-loop dynamics for this case are listed in Tables 4.3 and 4.4, respectively. Note that the additional expected cost-to-go caused by this penalty is slight: about 1.25% greater from $r_{N-4}=1$ and 0.70% greater from $r_{N-4}=2$. Comparing Tables 4.2 and 4.4 we see that in form 1, the closed loop optimal system drives x to zero a little more quickly when this jump cost is present.

k	$K_k(1)$	$K_k(2)$	$L_k(1)$	$L_k(2)$
N-1	.5238095	3.996004	.5238095	$1.998\text{x}10^{-3}$
N-2	.6634162	7.4701392	.6634162	$3.73506\text{x}10^{-3}$
N-3	.7096495	9.3545273	.7096495	$4.67726\text{x}10^{-3}$
N-4	.7278253	10.270011	.7278253	$5.135\text{x}10^{-3}$

Table 4.3: Example 4.1 with Q(1,2)=2.

k	$a(1)-b(1)L_k(1)$	$a(2)-b(2)L_k(2)$
N-1	.4761905	1.998002
N-2	.3365838	1.9962649
N-3	.2903505	1.9953227
N-4	.2721747	1.9949865

Table 4.4: Closed-Loop Optimal Dynamics when Q(1,2)=2.

Now suppose that the jump cost is high. Take

$$Q(1,2) = 1000$$

$$Q(1,1) = Q(2,1) = Q(2,2) = 1 .$$

Then the optimal strategy in form 1 is to drive x almost completely to zero in one time step (incurring a cost of about $u^2R(1)=1$). The optimal strategy in form 2 remains the same; almost no control is used. The optimal cost and control law parameters for this high jump cost case are listed in Table 4.5, and the closed-loop dynamics are in Table 4.6.

k	$K_k(1)$	$K_k(2)$	$L_k(1)$	$L_k(2)$
N-1	.9901864	3.996004	.9901864	$1.998\text{x}10^{-3}$
N-2	.9903092	9.1421301	.9903092	$4.57196\text{x}10^{-3}$
N-3	.9903573	11.190689	.9903573	$5.594534\text{x}10^{-3}$
N-4	.9903763	12.005421	.9903763	$6.00271\text{x}10^{-3}$

Table 4.5: Example 4.1 with Q(1,2)=1000.

k	$a(1)-b(1)L_k(1)$	$a(2)-b(2)L_k(2)$
N-1	$9.8136\text{x}10^{-3}$	1.998002
N-2	$9.6908\text{x}10^{-3}$	1.995428
N-3	$9.6427\text{x}10^{-3}$	1.9944055
N-4	$9.6237\text{x}10^{-3}$	1.9939973

Table 4.6: Closed-Loop Optimal Dynamics when $Q(1,2)=1000$.

4.3 Summary

This chapter completes our study of JLQ problems with x-independent forms. As we have shown in this chapter and in chapter 3, the linear quadratic optimal control problem formulation can be extended to jump linear systems in a straightforward way, provided that the jumps are x-independent and perfectly observed.

In parts III and IV of the thesis we will consider JLQ problems that involve form changes that are x-dependent, either explicitly or through controls. As we shall see, the structure and behavior of the optimal JLQ controller becomes much more complex in these cases and displays features not captured by the problems studied to this point.

PART III

THE SCALAR X-DEPENDENT NOISELESS JLQ CONTROL PROBLEM

5. SCALAR JLQ PROBLEMS WITH X-DEPENDENT FORMS

5.1 Introduction

In this chapter we examine a class of nonlinear stochastic control problems that capture the active hedging issue of fault-tolerant optimal control. The problems under consideration are scalar-in-x JLQ problems with form transition probabilities that depend on x. Specifically, we consider

- form transition probabilities that are (or can be approximated as being) piecewise-constant in x.

For this class of problems we develop a recursive procedure for the determination of the optimal expected costs-to-go and control laws "off-line," in advance of system operation. We also establish a number of qualitative properties of the optimal controller.

The optimal expected costs-to-go are piecewise-quadratic and the control laws are piecewise-linear in x_k, in each form. That is, the real line is partitioned into a number of intervals of x values (pieces), and over each such interval $V_k(x_k,r_k=j)$ is quadratic[1] in x_k and $u_k(x_k,r_k=j)$ is linear, for each form $j \in \underline{M}$.

For each $j \in \underline{M}$ at time k the expected cost-to-go $V_k(x_k,r_k=j)$ and control law $u_k(x_k,r_k=j)$ have the same number of pieces, $m_k(j)$. In general this number grows as (N-k) increases. A typical expected cost-to-go and control law are shown in figure 5.1.

---

[1] In this chapter the term quadratic in x_k is used for functions of the form $a_0+a_1x_k+a_2x_k^2$; the term linear is used for functions of the form $a_0+a_1x_k$.

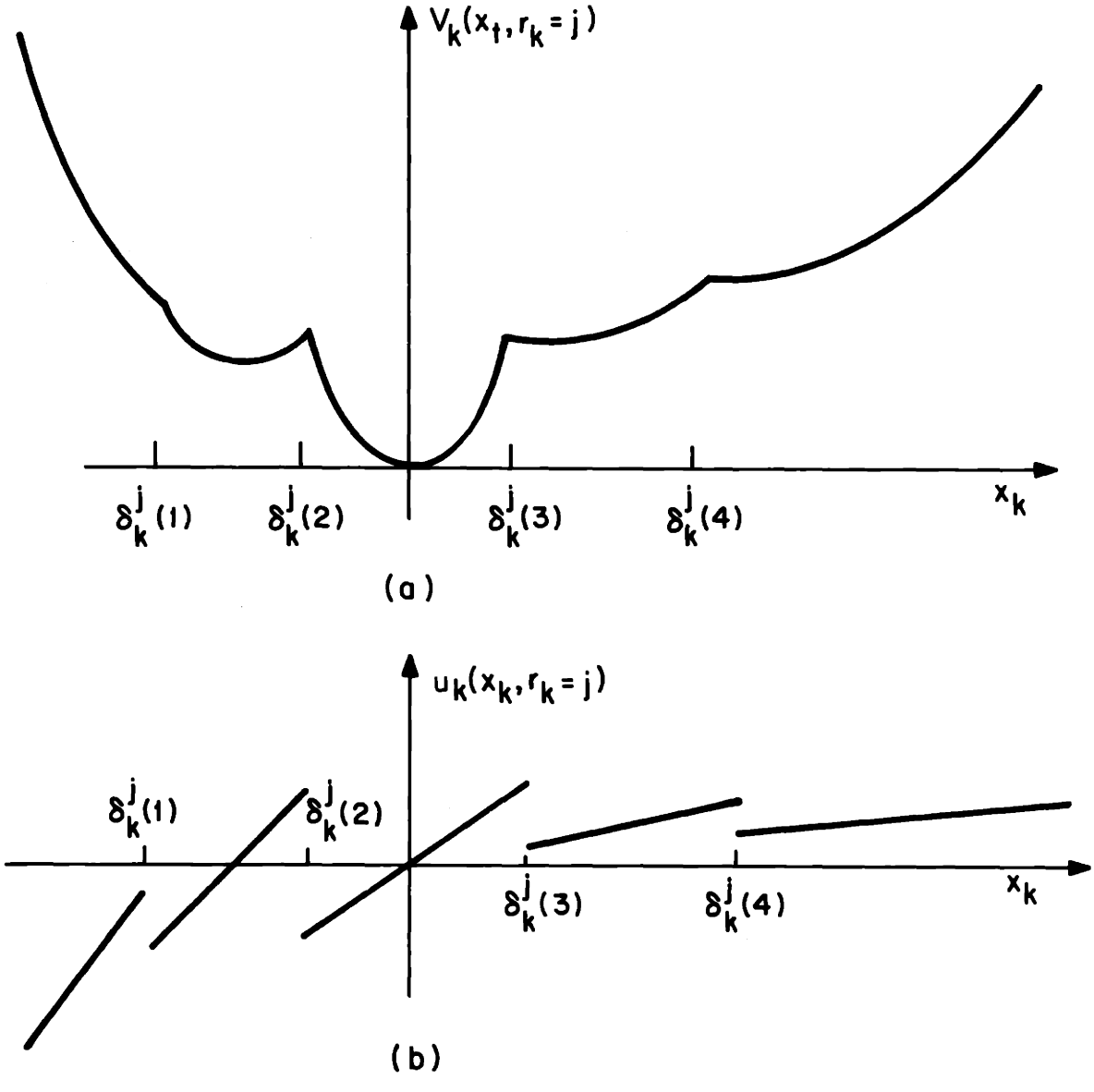

FIGURE 5.1: Typical curves of (a) $V_k(x_k, r_k=j)$ and (b) $u_k(x_k, r_k=j)$ with $m_k(j)=5$ pieces.

The different pieces of $V_k(x_k, r_k=j)$ and $u_k(x_k, r_k=j)$ arise from using the control to actively hedge. Intuitively, at each stage the optimal controller must take into account what the expected cost of driving x into different regions will be, where different values of the form transition probabilities apply. As the control problem is solved backwards in time from a finite terminal time (using dynamic programming), the controller must take into account what the effects of active hedging will be at the intervening times.

The procedure that is developed here for computing the optimal $m_k(j)$, $V_k(x_k, r_k=j)$ and $u_k(x_k, r_k=j)$ (inductively, backwards in time for finite time-horizon problems) involves the computation and comparison of a growing number of quadratic functions at each stage and for each $j \in \underline{M}$. These quadratic functions are computed via Riccati-like difference equations. All of these computations can be done off-line, as in the x-independent JLQ problem.

The basic idea of this solution procedure is simple; essentially the nonlinearity of the system dynamics (due to the x-dependence of the form transition probabilities) is converted into computational complexity in the determination of $V_k(x_k, r_k=j)$. It is the piecewise-constant structure of the form transition probabilities that allows us to do this.

At each time stage k, the control problem involving the determination of $V_k(x_k, r_k=j)$ for a system having the full hybrid structure (as pictured on the left of figure 5.2) is transformed into the comparison of many

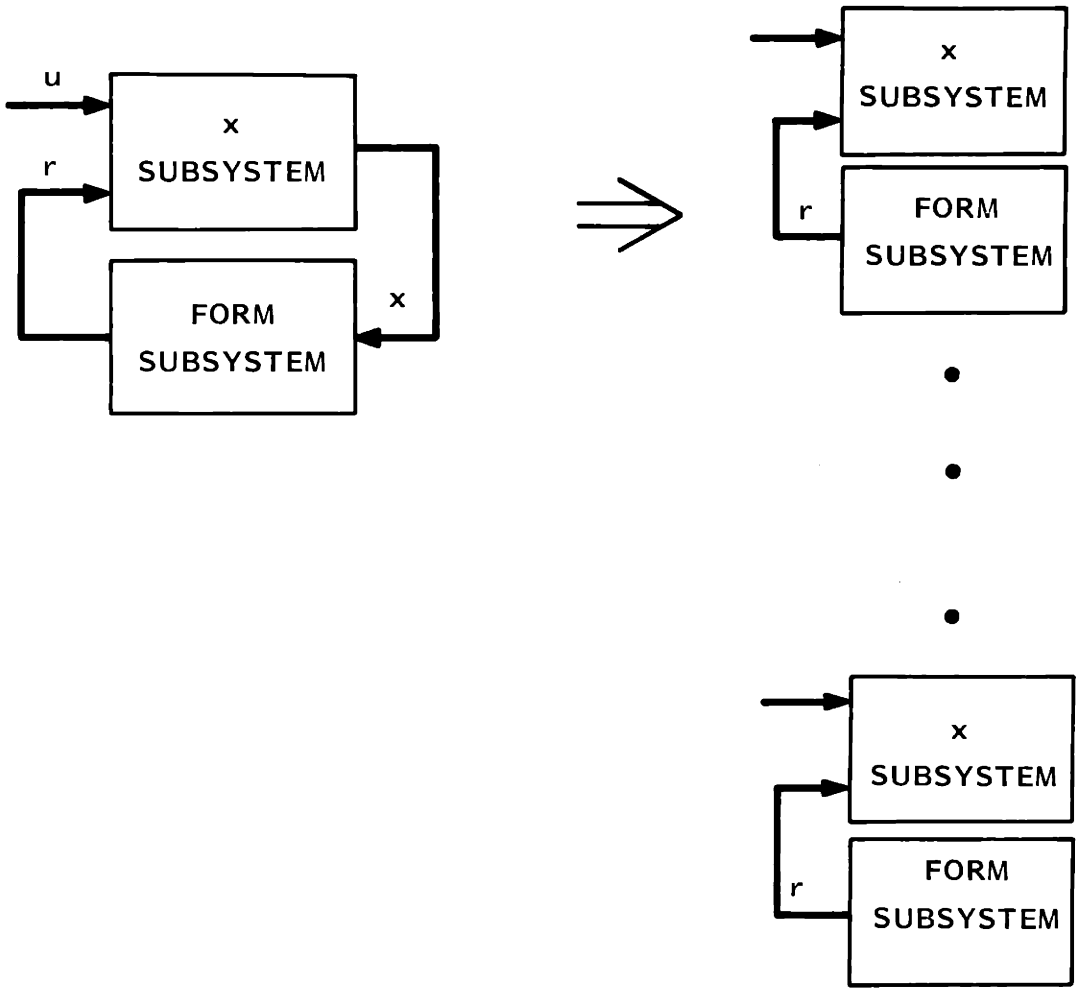

FIGURE 5.2: Conversion of nonlinearity into computational complexity.

constrained-in- x_{k+1} JLQ control problem costs with x-independent form transitions (as pictured on the right in figure 5.2). One constrained problem arises for each region of x_{k+1} values having different

- form transition probabilities out of j (p_{ji}, $i \in c_j$)
- different pieces in the expected costs-to-go at the succeeding time (i.e., $V_{k+1}(x_{k+1}, r_{k+1}=i)$), for each form in the cover of j (i.e., $i \in c_j$).

The number of costs-to-go that must be compared at each stage, and the number of pieces, $m_k(j)$, in $V_k(x_k, r_k=j)$ grows

- at most <u>linearly</u> with the number of transition probability pieces
- at most <u>geometrically</u> with the number of forms that are accessible from form j in one time step.

The "piecewise" structure of the optimal expected costs-to-go and control laws is caused by the piecewise-constant structure of the form transition probabilities.

The solution procedure developed in this chapter provides an "approximately optimal" controller for problems where the true x-dependent form transition probabilities have been approximated in a piecewise-constant way. Clearly this approximation can be made

arbitrarily close to the true controller by using a fine enough piecewise-constant approximation. Thus there is a tradeoff between

> accuracy of the form-transition probability approximations (and the resulting optimal controller)

vs.

> computational complexity in the off-line determination of the optimal controller and in the number of controller pieces $m_k(j)$ that must be implemented on-line.

Although the basic idea of this chapter is simple, the derivation and presentation of the general result involves unavoidably complicated notation and "bookkeeping" problems. For this reason, this chapter has been organized as follows:

1. In section 5.2 the general problem is formulated.
2. In section 5.3 one-stage of a simple problem is solved from first principles .
3. Guided by intuition gained from this example, a general solution procedure is developed in section 5.4 and certain qualitative properties of the optimal controller are established.
4. In section 5.5 this solution procedure is used to solve the next stage of the example problem.
5. In section 5.6 a number of combinatoric properties (i.e., concerning the number of pieces of the optimal

solutions, etc.) and qualitative properties of the optimal controller are established. These results are motivated by the example problem.

From the study of the optimal controllers developed here we can gain insight into the structures of controllers that use active hedging, and into the qualitative effects of their control actions.

In chapters 6 and 7 the results of this chapter are used to investigate a number of additional qualitative properties of the controller; in particular, steady-state behaviors are examined. In addition, an algorithm flowchart that efficiently performs the calculations specified in section 5.3 is presented. In Part IV this algorithm is extended to include more general jump linear control problems.

5.2 General Problem Formulation

In this section we present the general problem formulation that is addressed in this chapter. We restrict our attention to the time-invariant case so as to simplify notation somewhat. All of the results of this chapter can be directly extended to the time-varying case.

Consider the discrete-time jump linear system

$$x_{k+1}=a(r_k)x_k + b(r_k)u_k \tag{5.1}$$

$$P_r\{r_{k+1}=j \mid r_k=i,\ x_{k+1}=x\} = p(i,j;x) \tag{5.2}$$

$$x(k_0) = x_0 \qquad r(k_0) = r_0 \quad .$$

Each transition probability $p(i,j;x)$ of the form process is assumed to be piecewise-constant in x, having a finite number of pieces $\bar{\nu}_{ij}$. That is, the real line is partitioned into $\bar{\nu}_{ij}$ disjoint intervals with the transition probabilities taking constant values over each interval:

$$p(i,j;x) = \lambda_{ij}(s) \tag{5.3}$$

if

$$\nu_{ij}(s-1) < x < \nu_{ij}(s)$$

where

$$s = 1,2,\ldots,\bar{\nu}_{ij}$$

$$-\infty \triangleq \nu_{ij}(0) < \nu_{ij}(1) < \ldots < \nu_{ij}(\bar{\nu}_{ij}-1) < \nu_{ij}(\bar{\nu}_{ij}) \triangleq \infty \quad . \tag{5.4}$$

These grid points $\nu_{ij}(s)$ may be different for each pair $(i,j) \in \underline{M} \times \underline{M}$. For all $s=1,2,\ldots,\bar{\nu}_{ij}$

$$\lambda_{ij}(s) \geq 0 \qquad \text{for each } i,j \in \underline{M}$$

$$\sum_{j=1}^{M} \lambda_{ij}(s) = 1 \qquad \text{for each } i \in \underline{M} \quad .$$

A typical $p(i,j;x)$ is illustrated in figure 5.3.

The form process is not Markovian because of its dependence on x. However the joint state process $\{x_k, r_k : k=k_0,\ldots,N\}$ is Markov. It is assumed that the state (x_k, r_k) is perfectly observed at each time. The problem is to find the optimal control laws

$$u_k = \phi_k(x_0,\ldots,x_k;\ r_0,\ldots,r_k)$$

that minimize the cost criterion (5.5) below:

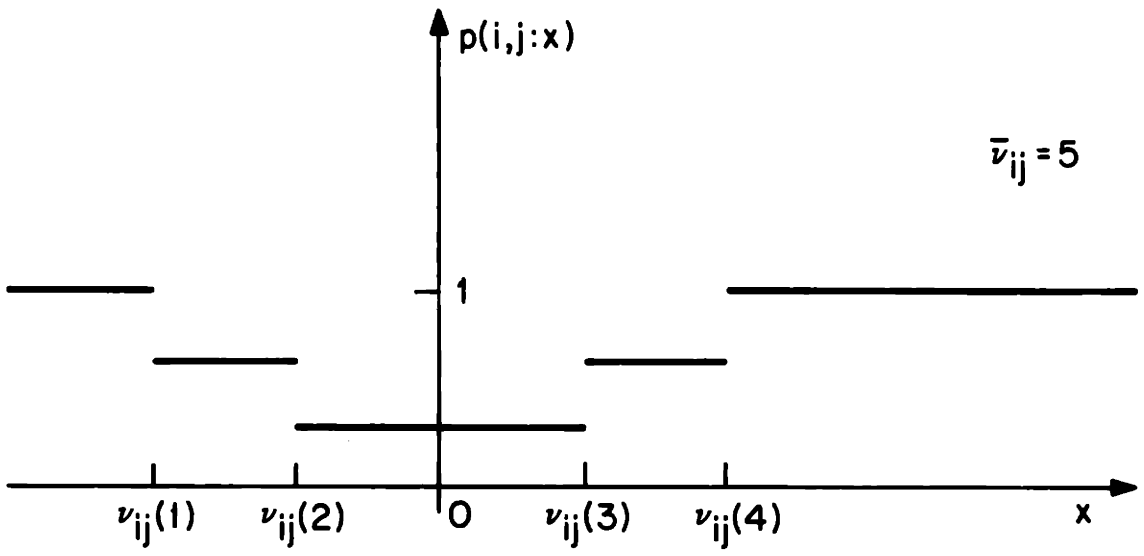

FIGURE 5.3: Typical piecewise-constant transition probability.

$$J_{k_0}(x_0,r_0) = E\left\{\sum_{k=k_0}^{N-1}\left[u_k^2 R(r_k) + x_{k+1}^2 Q(r_{k+1}) + S(r_{k+1})x_{k+1} + P(r_{k+1})\right] + x_N^2 K_T(r_N) + H_T(r_N)x_N + G_T(r_N)\right\} \quad (5.5)$$

where the expectation is over $\{r_{k_0},\ldots,r_N\}$. Since $\{(x_k,r_k): k=k_0,\ldots,N\}$ is a Markov process we need only consider feedback laws of the form

$$u_k = \phi_k(x_k,r_k) .$$

Here

$$R(i) > 0$$

$$\begin{pmatrix} Q(i) & S'(i)/2 \\ S(i)/2 & P(i) \end{pmatrix} \geq 0 \quad (5.6)$$

$$\begin{pmatrix} K_T(i) & H_T'(i)/2 \\ H_T(i)/2 & G_T(i) \end{pmatrix} \geq 0$$

for each $i \in \underline{M}$. We will assume here[1] that $b(j) \neq 0$ for each $j \in \underline{M}$.

---

[1] The result for forms where $b(j)=0$ (that is, the system just "coasts" in form j) is presented at the end of Appendix C.2. This result is used in some of the examples in chapter 6 and 7.

The term

$$x_N^2 K_T(r_N) + x_N H_T(r_N) + G_T(r_N)$$

in (5.5) is a terminal cost charged in addition to the time-invariant cost

$$x_N^2 Q(r_N) + x_N S(r_N) + P(r_N) \quad .$$

The x_k^1 and x_k^o terms ($x_k S(r_k)$, $P(r_k)$, $x_N H_T(r_N)$ and $G_T(r_N)$) are included in (5.5) because they naturally arise in the computation of the expected costs-to-go. Even if the x-costs in (5.5) are simple quadratics (i.e., $S(i) = P(i) = H_T(i) = G_T(i)=0$), some of the quadratic pieces of the optimal expected costs-to-go will have x_k^1 and x_k^o terms.

5.3 One Stage of an Example Problem

In this section we solve one time stage of a simple example problem satisfying (5.1)-(5.6). This is done to illustrate the basic solution idea alluded to in section 5.1, and to gain insight into the qualitative properties of this class of problems. A number of observations and claims inspired by this example are listed at the end of this section for later consideration.

Example 5.1: Consider the following system having M=2 forms:

$$x_{k+1} = x_k + u_k \qquad \text{if } r_k=1$$

$$x_{k+1} = 2x_k + u_k \qquad \text{if } r_k=2$$

$$p(1,2:x) = \begin{cases} 1/4 & |x|<1 \\ 3/4 & |x|>1 \end{cases}$$

$$p(1,1:x) = 1-p(1,2:x) \qquad p(2,2)=1 \qquad p(2,1)=0 \quad .$$

We seek to minimize

$$\min_{u_0,..,u_{N-1}} E\left\{\sum_{k=0}^{N-1} (u_k^2 + x_{k+1}^2) + x_N^2 K_T(r_N)\right\}$$

where $K_T(1)=0$, $K_T(2)=3$. The form structure and form transition probability $p(1,2:x)$ for this example are shown in figure 5.4.

The values r=1 and r=2 might denote, respectively, "normal" and "failure mode" operation. The $K_T(2)$ parameter represents a penalty charged for failure of the system. The probability of failure $p(1,2:x)$ is low for small magnitude x, and larger if $|x|>1$.

Once the system fails (attains form r=2), it stays there. In this form the usual LQ solution applies. The optimal (deterministic) cost-to-go is

$$V_k(x_k, r_k=2) = x_k^2 K_k(2)$$

for k=N,N-1,...,0 where

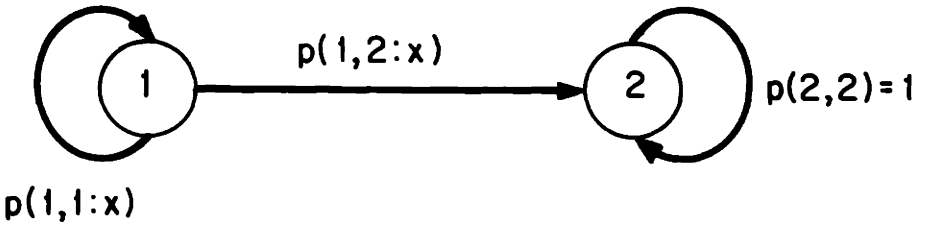

(a)

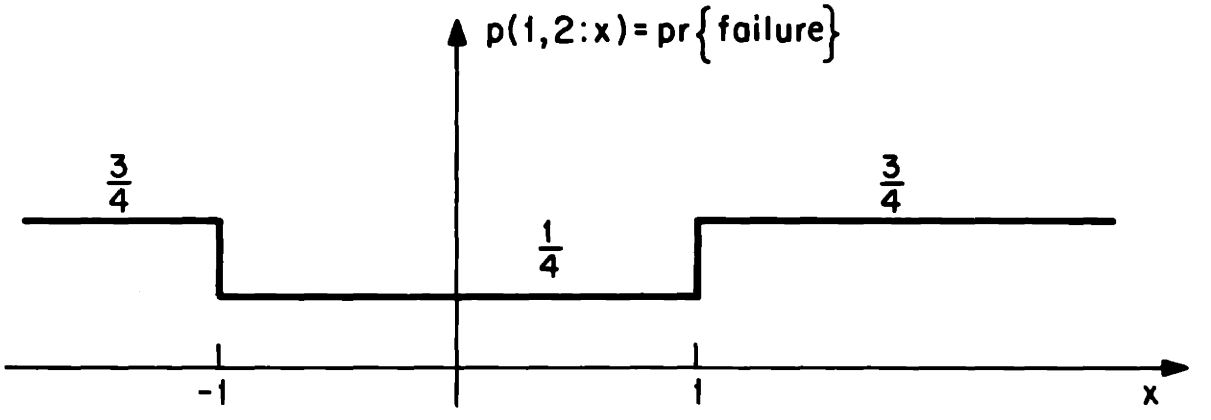

(b)

FIGURE 5.4: Example 5.1: (a) form structure, and (b) transition probability p(1,2:x).

$$K_N(2) = K_T(2) = 3$$

$$K_k(2) = \frac{a^2(2)R(2)[K_{k+1}(2)+Q(2)]}{R(2)+b^2(2)[K_{k+1}(2)+Q(2)]} = \frac{4(K_{k+1}(2)+1)}{2+K_{k+1}(2)}$$

and the optimal control law in form r=2 is given by

$$u_k(x_k, r_k=2) = -L_k(2)x_k$$

where

$$L_k(2) = \frac{a(2)b(2)[K_{k+1}(2)+Q(2)]}{R(2)+b^2(2)[K_{k+1}(2)+Q(2)]} = \frac{2(K_{k+1}(2)+1)}{2+K_{k+1}(2)} \quad .$$

Here we have quick convergence as (N-k) decreases, to

$$K_k(2) \longrightarrow 1 + \sqrt{5} \qquad = 3.236068$$

$$L_k(2) \longrightarrow \frac{1+\sqrt{5}}{2} \qquad = 1.618034$$

as seen in Table 5.1, below.

k	$K_k(2)$	$L_K(2)$
N	3	-
N-1	3.2	1.6
N-2	3.2307692	1.6153846
N-3	3.2352941	1.6176471

Table 5.1: $K_k(2)$ and $L_k(2)$ for example 5.1.

Now we examine what happens when $r_{N-1}=1$. We are given that

$$V_N(x_N, r_N=1) = x_N^2 K_T(1)=0.$$

Now consider the situation one stage back in time. With probability $p(1,2:x_N)$ the system will switch to form 2 at time N, and we will be charged

$$x_N^2\begin{pmatrix} K_N(2) \\ + \\ Q(2) \end{pmatrix} = 4x_N^2 \quad .$$

With probability $[1-p(1,2:x_N)]$ the system will stay in form 1 and we will be charged

$$x_N^2\begin{pmatrix} K_T(1) \\ + \\ Q(1) \end{pmatrix} = x_N^2 \quad .$$

In addition we will be charged a control cost

$$u_{N-1}^2 R(1) = u_{N-1}^2 \ ,$$

for whatever control we choose. That is,

$$V_{N-1}(x_{N-1}, r_{N-1}=1) = \min_{u_{N-1}} \left\{ \begin{array}{l} u_{N-1}^2 \\ + \\ p(1,1;x_N)\,[x_N^2 + V_N(x_N, r_N=1)] \\ + \\ p(1,2;x_N)\,[x_N^2 + V_N(x_N, r_N=2)] \end{array} \right\}$$

$$= \min_{u_{N-1}} \left\{ \begin{array}{l} u_{N-1}^2 \\ + \\ p(1,1;x_N)\,x_N^2 \\ + \\ p(1,2;x_N)\,4x_N^2 \end{array} \right\} \quad .$$

Note that we can control the failure probability $p(1,2;x_N)$, and thus the cost incurred at time N, by our choice of x_N (through the choice of u_{N-1}). It is this point that makes $V_{N-1}(x_{N-1}, r_{N-1}=1)$ a non-quadratic function of x_{N-1}. However, as we have indicated, it is piecewise quadratic and this is a direct consequence of the piecewise constant nature of $p(i,j;x_N)$. The basic reason for this is actually quite simple and by going through it we can obtain an initial understanding of the nature of the problem.

Suppose that x_{N-1} has a given value. Then, by applying our optimal control, one of three things will happen: either $x_N \leq -l^-$, or $-l^+ \leq x_N \leq l^-$ or $x_N \geq l^+$. In each of these cases the cost

$$p(1,1;x_N)x_N^2 + p(1,2;x_N)4x_N^2$$

is a quadratic function of x_N. Consequently this suggests the following strategy for computing $V_{N-1}(x_{N-1}, r_{N-1}=1)$ and the associated optimal control law:

> For each of the 3 possible regions, solve the constrained optimization problem assuming that x_N is in the specified region. As indicated above, each such constrained problem is quadratic. Once we have the solutions to these problems, we compare them and obtain the optimal solution by choosing the smallest of these for each value of x_{N-1}. As we will see the result is a piecewise quadratic cost-to-go and a piecewise linear optimal control law.

As we have indicated, in this example there are three x_N regions:

(1) $x_N \leq -1^-$ where $p(1,2:x_N)=3/4$

(2) $-1^+ \leq x_N \leq +1^-$ where $p(1,2:x_N)=1/4$

(3) $1^+ \leq x_N$ where $p(1,2:x_N)=3/4$.

The three corresponding constrained control problems are

$$V_{N-1}(x_{N-1}, r_{N-1}=1 \mid 1) = \min_{\substack{u_{N-1} \text{ st.} \\ x_{N-1} \leq -1^-}} \left\{ u_{N-1}^2 + \frac{13}{4} x_N^2 \right\} \tag{5.7}$$

$$V_{N-1}(x_{N-1}, r_{N-1}=1|2) = \min_{\substack{u_{N-1} \text{ st.} \\ -1^+ \leq x_{N-1} \leq 1^-}} \left\{ u_{N-1}^2 + \frac{7}{4} x_N^2 \right\} \tag{5.8}$$

$$V_{N-1}(x_{N-1}, r_{N-1}=1|3) = \min_{\substack{u_{N-1} \text{ st.} \\ 1^+ \leq x_{N-1}}} \left\{ u_{N-1}^2 + \frac{13}{4} x_N^2 \right\} . \tag{5.9}$$

Note that the costs in the first and third regions of x_N values are the same, because of the symmetry of $p(1,2:x)$ about zero.

Consider the second x_N region:

$$-1^+ < x_N < 1^- \quad .$$

Differentiating $V_{N-1}(x_{N-1}, r_{N-1}=1|2)$ in (5.8) with respect to u_{N-1} and setting the derivative to zero, we find that

$$u_{N-1}(x_{N-1}) = -.6363636\ x_{N-1} \tag{5.10}$$

with the resulting cost

$$V_{N-1}(x_{N-1}) = .6363636\ x_{N-1}^2 \quad . \tag{5.11}$$

But this u_{N-1} only solves (5.8) if the x_N that results from it obeys the constraint

$$-1^+ < x_N < 1^- \quad .$$

That is, we must have[1]

$$-1^{+} < x_N = x_{N-1} - .6364\ x_{N-1} < 1^{-}$$

which holds if and only if

$$-2.75 < x_{N-1} < 2.75$$

For $x_{N-1} > 2.75$ the best value of x_N in the interval (-1,1) is $x_N = 1^{-}$. This is achieved if

$$u_{N-1}(x_{N-1}) = \frac{x_N - a(1)x_{N-1}}{b(1)} = 1^{-} - x_{N-1}$$

and the resulting cost is

$$V_{N-1}(x_{N-1}) = x_{N-1}^2 - 2x_{N-1} + 2.75 \qquad (5.12)$$

Similarly, for $x_{N-1} < -2.75$, the best value of x_N in the interval (-1,1) is at $x_N = -1^{+}$. This is achieved with

$$u_{N-1}(x_{N-1}) = -1^{+} - x_{N-1}$$

and the resulting cost is

$$V_{N-1}(x_{N-1}) = x_{N-1}^2 + 2x_{N-1} + 2.75 \qquad (5.13)$$

---

[1]Rounding numbers to four significant digits.

Thus the optimal cost-to-go of (5.8) (where x_N is constrained to be in (-1,1) has the three-piece quadratic form of figure 5.5.

The unconstrained cost of (5.11), as a function of x_{N-1}, is indicated by the dashed line. It applies for $x_{N-1} \in (-2.75, 2.75)$; this is indicated by the solid over-line.

The constrained cost (5.12), corresponding to making $x_N = 1^-$ is depicted by the dot-dash line. It applies for $x_{N-1} > 2.75$, as indicated by the solid line.

The constrained cost (5.13), which results from $x_N = -1^+$, is represented (as a function of x_{N-1}) by the dotted line. It applies for $x_{N-1} < -2.75$.

Note that the constrained costs ((5.12),(5.13)) are greater than the unconstrained cost (5.11) except at a single point. At this point their <u>values</u> and their <u>slopes</u> match. This fact will be of interest later in this chapter.

The other two constrained control problems (5.7),(5.9) can be solved as we have done above for (5.8). Their solutions have only two quadratic parts because x_N is not constrained in one direction.

The optimal expected costs-to-go for all three problems ((5.7)-(5.9)) are:

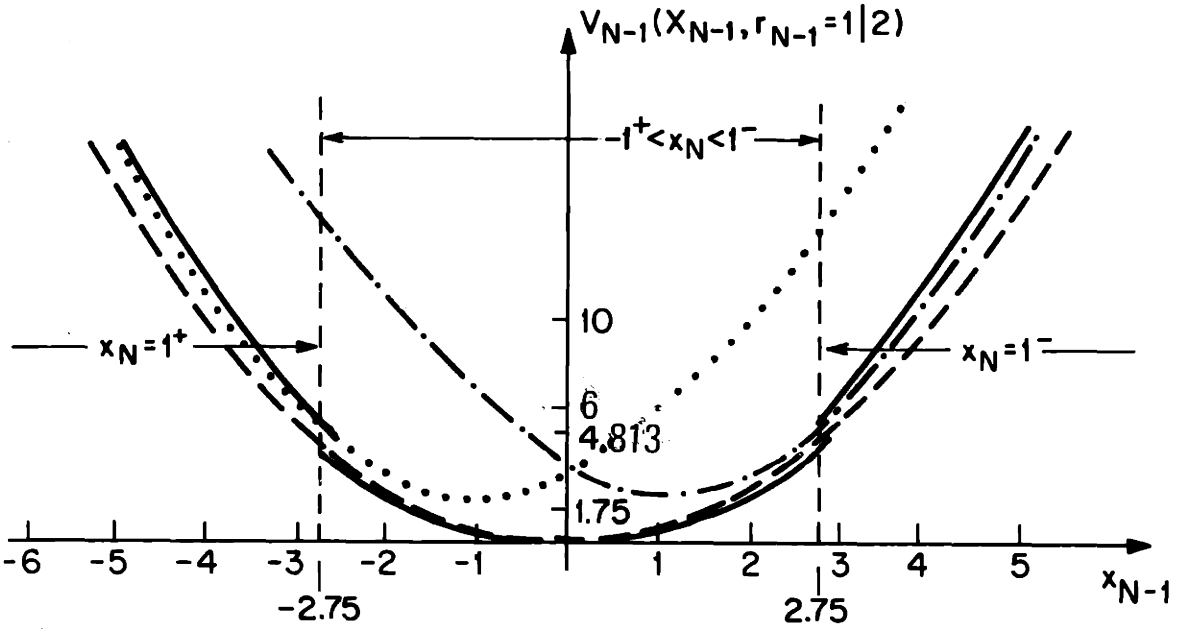

FIGURE 5.5: $V_{N-1}(x_{N-1}, r_{N-1}=1|2)$ of example 5.1 is indicated by the solid overline, where the dotted line represents the cost of driving to $x_N=-1^+$, the dot-dash line represents the cost of driving to $x_N=1^-$ and the dashed line indicates the unconstrained solution of (5.8).

$$V_{N-1}(x_{N-1},1|1) = \begin{cases} .7647058\ x_{N-1}^2 & \text{if } x_{N-1} \leq -4.25 \\ x_{N-1}^2+2x_{N-1}+4.2499985 & \text{if } x_{N-1} \geq -4.25 \end{cases} \tag{5.14}$$

$$V_{N-1}(x_{N-1},1|2) = \begin{cases} x_{N-1}^2+2x_{N-1}+2.75 & \text{if } x_{N-1} \leq -2.75 \\ .6364\ x_{N-1}^2 & \text{if } -2.75 \leq x_{N-1} \leq 2.75 \\ x_{N-1}^2-2x_{N-1}+2.75 & \text{if } x_{N-1} \geq 2.75 \end{cases} \tag{5.15}$$

$$V_{N-1}(x_{N-1},1|3) = \begin{cases} x_{N-1}^2-2x_{N-1}+4.25 & \text{if } x_{N-1} \leq 4.25 \\ .7647\ x_{N-1}^2 & \text{if } x_{N-1} \geq 4.25 \end{cases} \tag{5.16}$$

These costs are shown in figures 5.6, 5.5, and 5.7, respectively.

Having solved the constrained problems (5.7)-(5.9), we are now ready to compare them:

$$V_{N-1}(x_{N-1},r_{N-1}=1) = \min_{t=1,2,3} V_{N-1}(x_{N-1},r_{N-1}=1|t) \quad .$$

This is done graphically in figure 5.8.

Choosing the lowest of the three constrained costs at each x_{N-1} value, we see that:

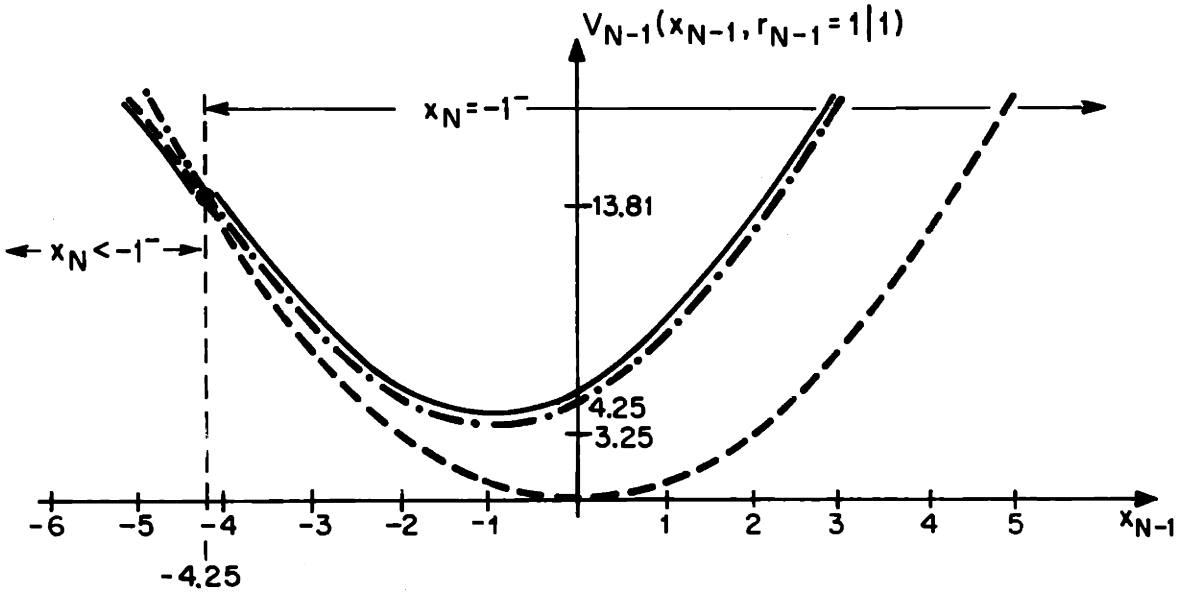

FIGURE 5.6: $V_{N-1}(x_{N-1}, r_{N-1}=1|1)$ of example 5.1 is indicated by the solid overline, where the dot-dash line represents the cost of driving to $x_N=-1^-$ and the dashed line indicates the unconstrained solution of (5.7).

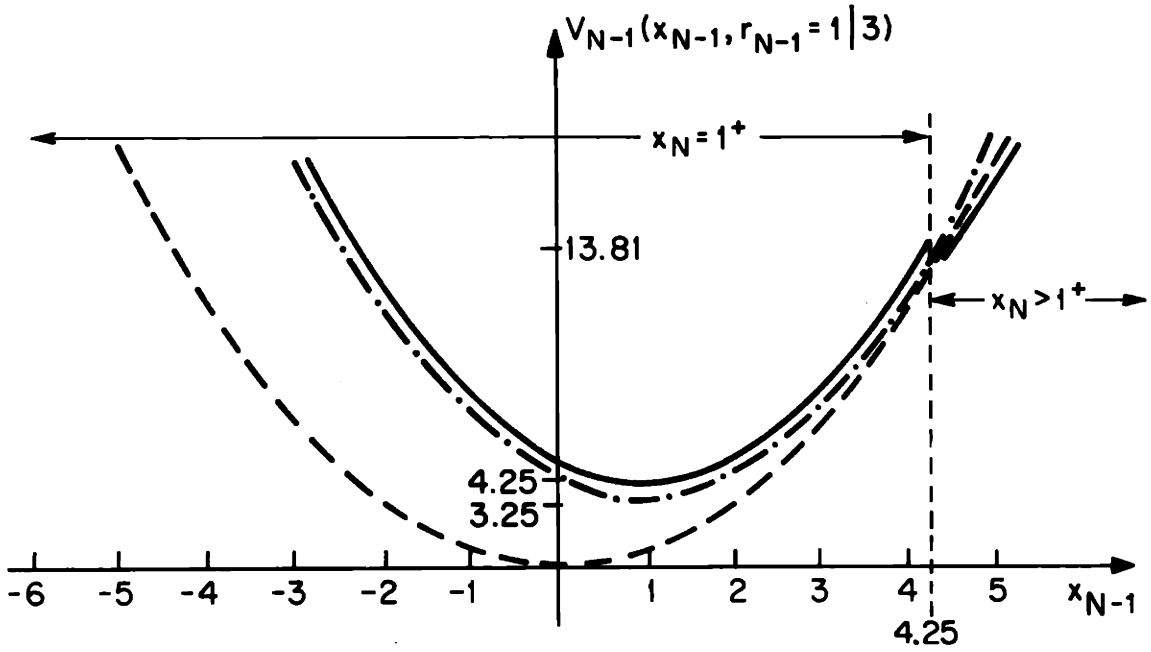

FIGURE 5.7: $V_{N-1}(x_{N-1}, r_{N-1}=1|3)$ of example 5.1 is indicated by the solid overline, where the dot-dash line represents the cost of driving to $x_N=1^+$ and the dashed line indicates the unconstrained solution of (5.9).

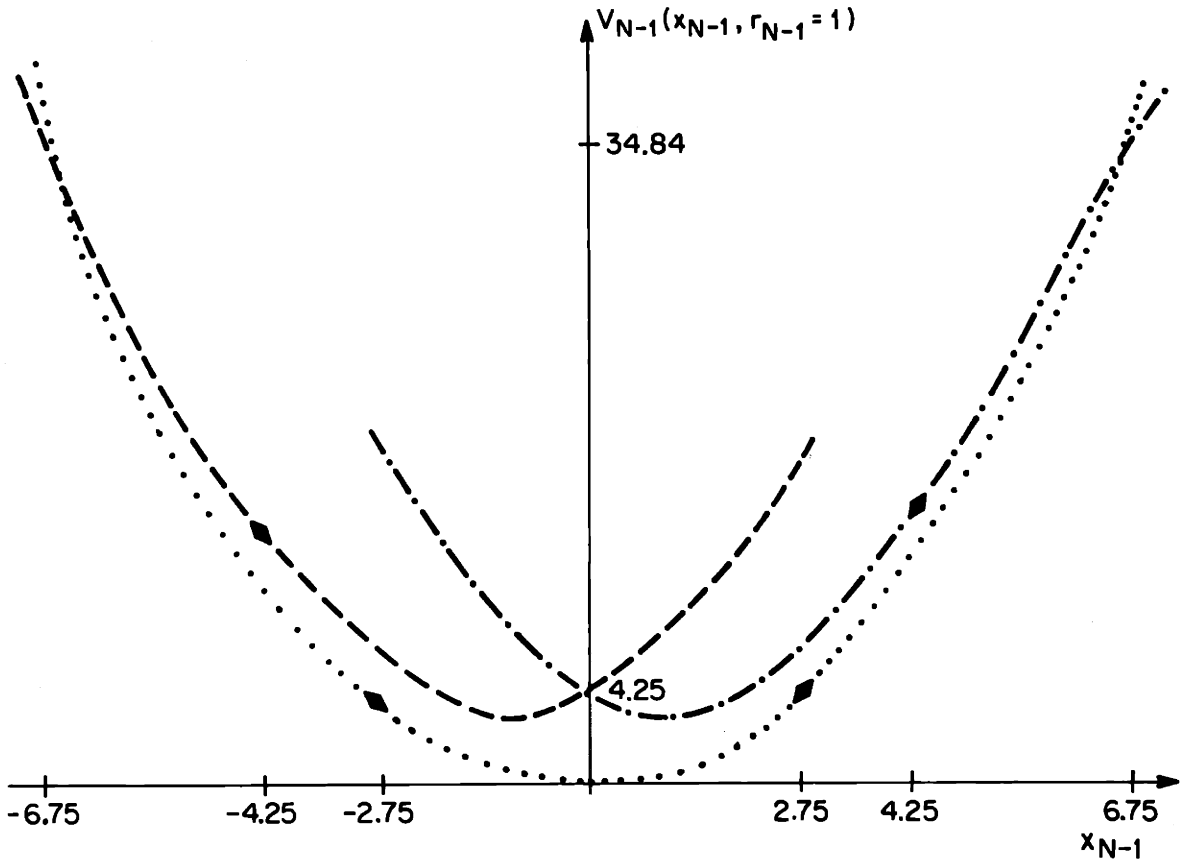

FIGURE 5.8: Determining $V_{N-1}(x_{N-1}, r_{N-1}=1)$ in example 5.1 by minimizing the constrained subproblem costs. $V_{N-1}(x_{N-1}, 1|1)$ is indicated by the dashed line, $V_{N-1}(x_{N-1}, 1|2)$ by the dotted line and $V_{N-1}(x_{N-1}, 1|3)$ by the dot-dash line.

(1) $V_{N-1}(x_{N-1}, r_{N-1}=1|1)$ is optimal from $x_{N-1}=-\infty$ until it crosses $V_{N-1}(x_{N-1}, r_{N-1}=1|2)$, at

$x_{N-1} = -6.7684932.$

(2) $V_{N-1}(x_{N-1}, r_{N-1}=1|2)$ is then optimal until it crosses $V_{N-1}(x_{N-1}, r_{N-1}=1|3)$ at $x_{N-1} = 6.7684932.$

(3) Then $V_{N-1}(x_{N-1}, r_{N-1}=1|3)$ is optimal for all larger x_{N-1}.

From (5.14)-(5.16), we find the values of the costs at their intersections is 38.84.

Collecting the above information we have that the optimal expected cost-to-go from $(x_{N-1}, r_{N-1}=1)$ is

$$V_{N-1}(x_{N-1}, r_{N-1}=1) = \begin{cases} .7647058\, x_{N-1}^2 & \text{if } x_{N-1} \leq \delta_{N-1}(1) \\ x_{N-1}^2 + 2x_{N-1} + 2.7499997 & \text{if } \delta_{N-1}(1) \leq x_{N-1} \leq \delta_{N-1}(2) \\ .6363636\, x_{N-1}^2 & \text{if } \delta_{N-1}(2) \leq x_{N-1} \leq \delta_{N-1}(3) \\ x_{N-1}^2 - 2x_{N-1} + 2.7499997 & \text{if } \delta_{N-1}(3) \leq x_{N-1} \leq \delta_{N-1}(4) \\ .7647058\, x_{N-1}^2 & \text{if } \delta_{N-1}(4) \leq x_{N-1}. \end{cases} \tag{5.17}$$

The optimal control laws are

$$u_{N-1}(x_{N-1}, r_{N-1}=1) = \begin{cases} -.7647058\ x_{N-1} & \text{if } x_{N-1} \leq \delta_{N-1}(1) \\ -x_{N-1}^{-1} & \text{if } \delta_{N-1}(1) \leq x_{N-1} \leq \delta_{N-1}(2) \\ -.6363636\ x_{N-1} & \text{if } \delta_{N-1}(2) \leq x_{N-1} \leq \delta_{N-1}(3) \\ -x_{N-1}^{+1} & \text{if } \delta_{N-1}(3) \leq x_{N-1} \leq \delta_{N-1}(4) \\ -.7647058\ x_{N-1} & \text{if } \delta_{N-1}(4) \leq x_{N-1} \end{cases} \tag{5.18}$$

and the value of x_N obtained by application of the optimal control law is

$$x_N(x_{N-1}, r_{N-1}=1) = \begin{cases} .2352942\ x_{N-1} & \text{if } x_{N-1} \leq \delta_{N-1}(1) \\ -1^{+} & \text{if } \delta_{N-1}(1) \leq x_{N-1} \leq \delta_{N-1}(2) \\ .3636364\ x_{N-1} & \text{if } \delta_{N-1}(2) \leq x_{N-1} \leq \delta_{N-1}(3) \\ 1^{-} & \text{if } \delta_{N-1}(3) \leq x_{N-1} \leq \delta_{N-1}(4) \\ .2352942\ x_{N-1} & \text{if } \delta_{N-1}(4) \leq x_{N-1} \end{cases} \tag{5.19}$$

where we denote the "joining points" (where these quantities change) by

$$\delta_{N-1}(1) = -6.77 = -\delta_{N-1}(4)$$

$$\delta_{N-1}(2) = -2.75 = -\delta_{N-1}(3) \quad .$$

The notation $x_N(x_{N-1},r_{N-1})$ in (5.19) is used for the optimal value of x_N that is obtained in form r_{N-1}, as a function of x_{N-1}. This notation will be used in the remainder of the thesis. The optimal expected costs-to-go, control laws and obtained x_N values are illustrated in figures 5.9, 5.10 and 5.11, respectively. Figure 5.9 ($V_{N-1}(x_{N-1},r_{N-1}=1)$ has purposely <u>not</u> been drawn to scale so that the behavior at the joining points can be clearly seen.

In light of the solution of this last-stage example problem we make the following observations and claims:

1. From (5.17)-(5.18) we see that in this example the optimal expected cost $V_{N-1}(x_{N-1},r_{N-1}=1)$ is piecewise-quadratic in x_{N-1} and the optimal control law is piecewise-linear. When we go back another stage in time, the optimal cost $V_{N-2}(x_{N-2},r_{N-2}=1)$ can be obtained using a similar approach. Things become more complicated, however.

Specifically, one step further back we will confronted with another optimization problem to compute the optimal cost-to-go. Following the same procedure, we can break the real line into regions in which the function to be optimized <u>is</u> quadratic. In doing this we must take into account into what x_{N-1} piece of $V_{N-1}(x_{N-1},r_{N-1}=1)$ we are driving the system as well as into what probability piece.

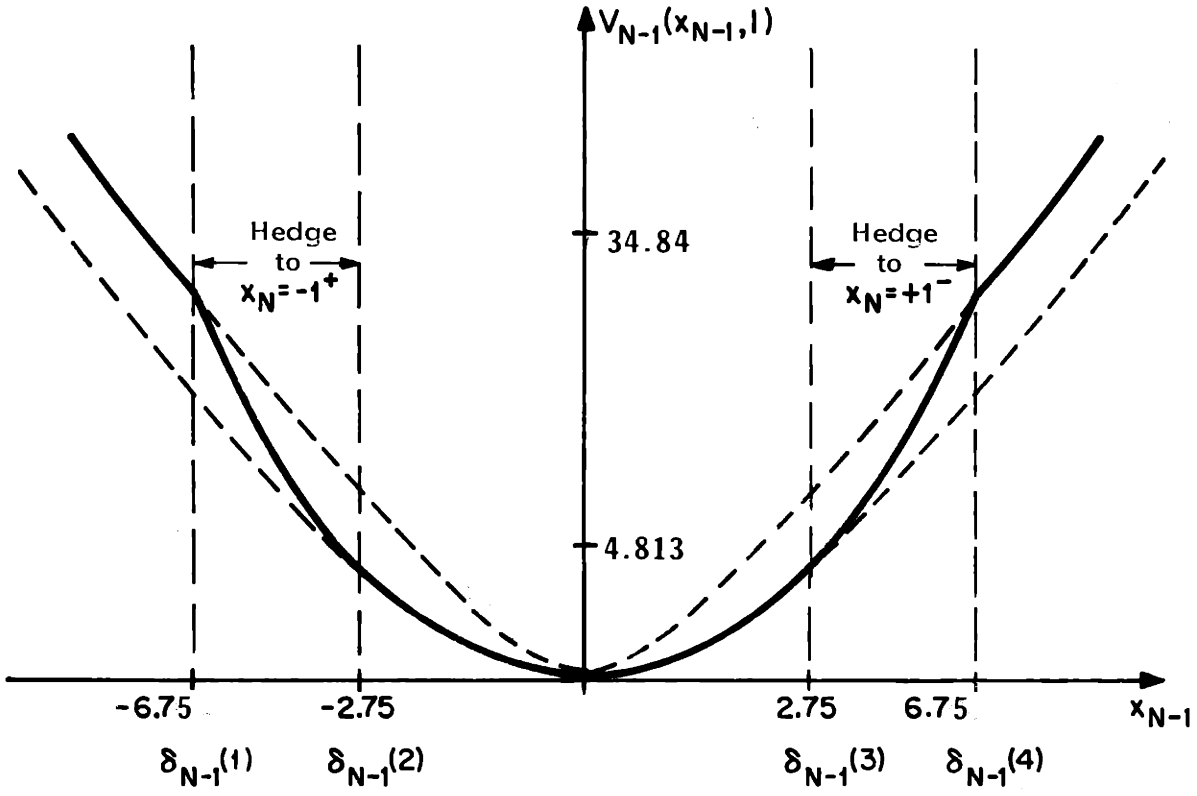

FIGURE 5.9: The optimal expected cost-to-go from $(x_{N-1}, r_{N-1}=1)$ in example 5.1 (not drawn to scale).

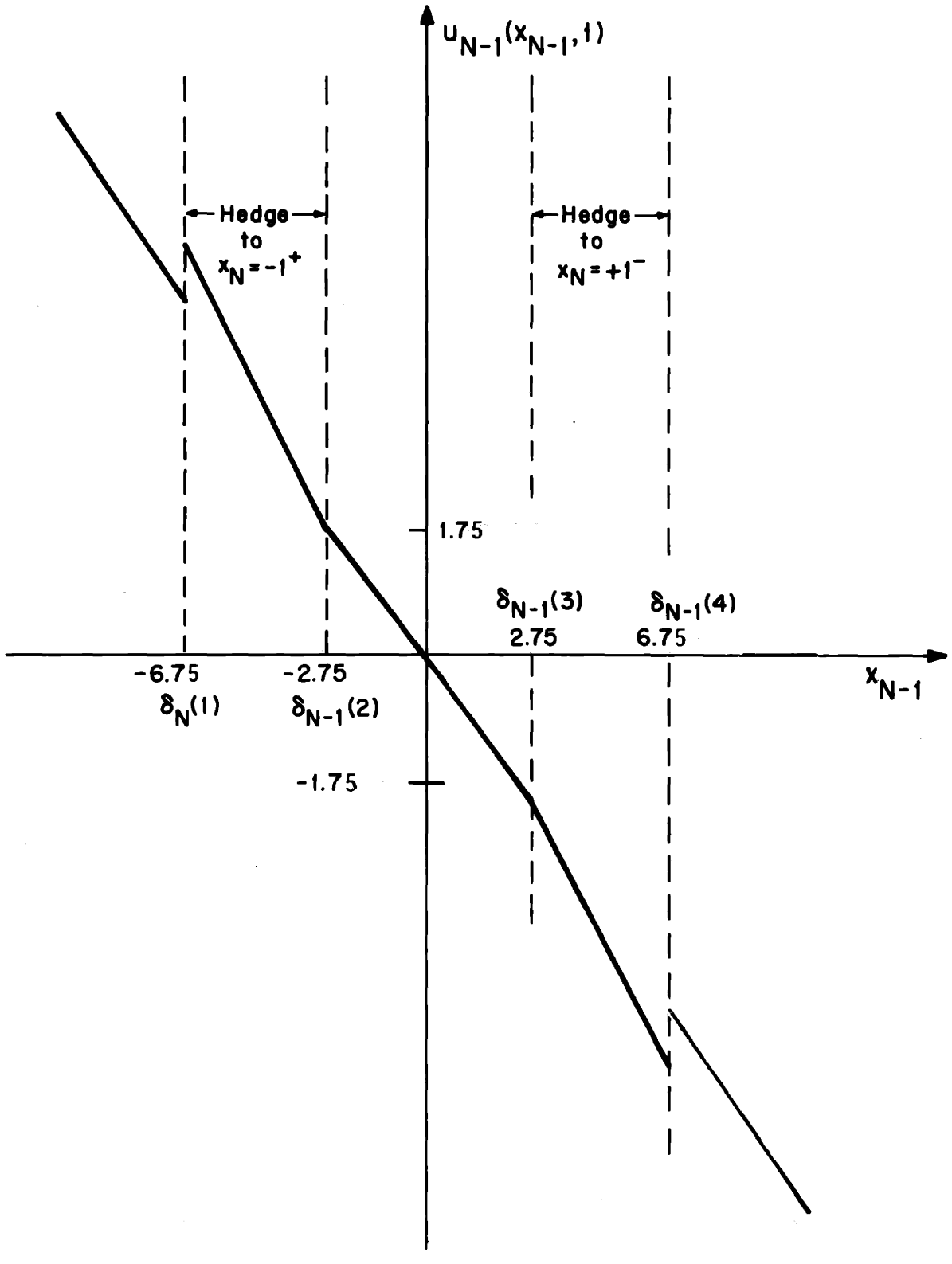

FIGURE 5.10: Optimal control laws from $(x_{N-1}, r_{N-1}=1)$ in example 5.1.

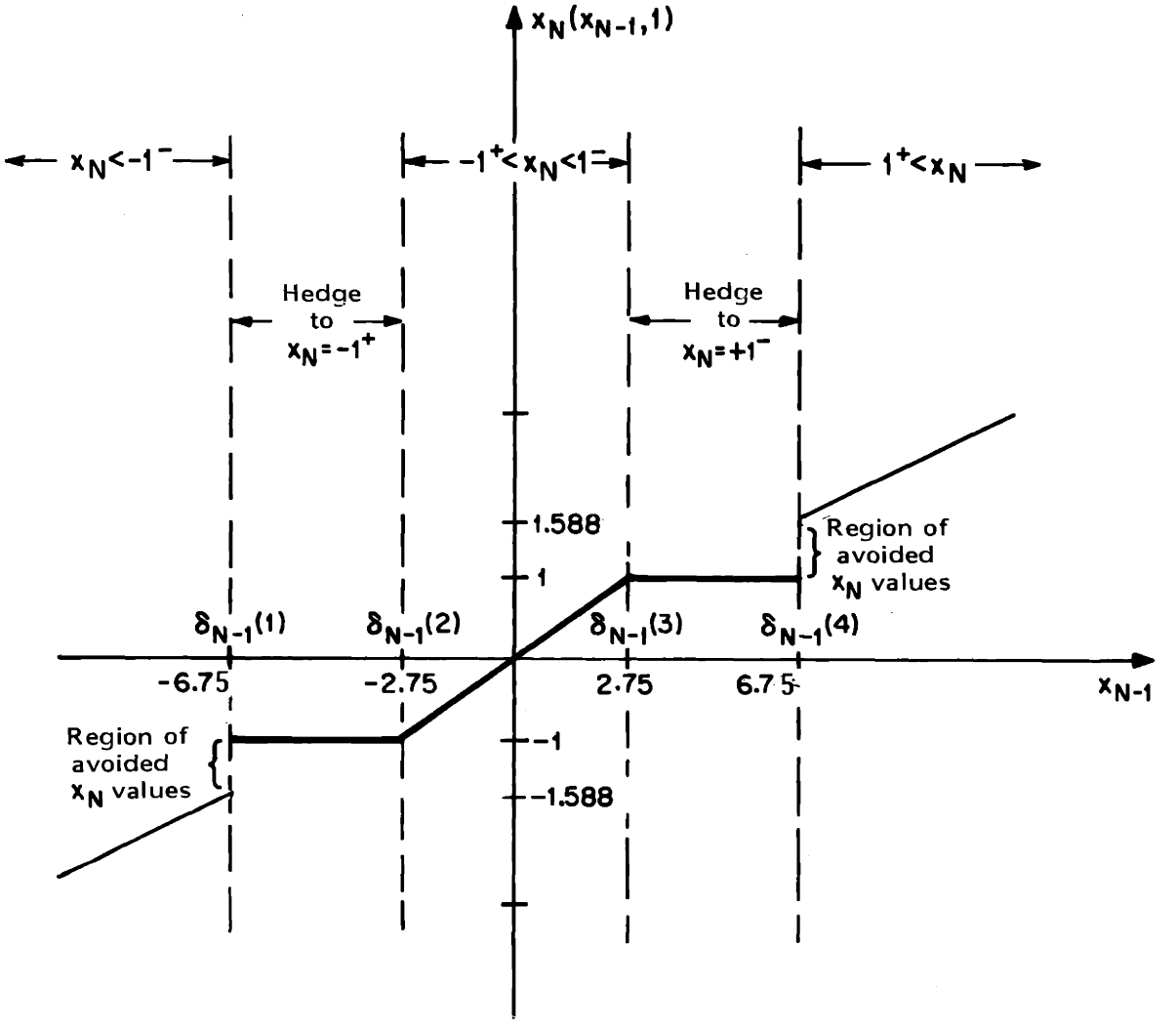

FIGURE 5.11: x_N values obtained from $(x_{N-1}, r_{N-1}=1)$ using the optimal controls, in example 5.1.

It is intuitively obvious that the optimal expected cost-to-go $V_k(x_k, r_k=j)$ will be piecewise-quadratic in x_k (and the controls piecewise linear) at each time stage k. The bookkeeping details of this will be taken care of in Section 5.4.

2. In figure 5.9 we see that at $\delta_{N-1}(2)$ and $\delta_{N-1}(3)$, the optimal expected cost has continuous slope. At $\delta_{N-1}(2)$ and $\delta_{N-1}(3)$, the slope decreases discontinuously. This illustrates a general property: at its "joining points" $\{\delta_k^j(t)\colon t=1,\ldots,M_k(j)-1\}$ the slope of the optimal expected cost-to-go $V_k(x_k, r_k=j)$ is either <u>continuous</u> or it decreases discontinuously. (see Proposition 5.1).

3. In figure 5.10 we see that at $\delta_{N-1}(1)$ and $\delta_{N-1}(4)$, the optimal controls are <u>discontinuous</u> in x_{N-1}. However at $\delta_{N-1}(2)$ and $\delta_{N-1}(3)$, the controller is continuous (and the optimal cost is differentiable).

   In general, at each of its joining points $\delta_k^j(t)$ the optimal control law $u_k(x_k, r_k=j)$ is discontinuous if and only if the slope of $V_k(x_k, r_k=j)$ decreases there, and $u_k(x_k, r_k=j)$ is continuous but not differentiable if and only if $V_k(x_k, r_k=j)$ is differentiable there. (see Proposition 5.3 in Section 5.6).

4. Note that for x_{N-1} negative enough, the optimal controller (in one time step) does not drive x_N

into a different probability piece. That is, for $x_{N-1} < \delta_{N-1}(1)$, the optimal controller keeps $x_N < -1$. Similarly for x_{N-1} large enough, the optimal controller keeps x_N in the same probability piece; for $x_{N-1} > \delta_{N-1}(4)$, we get $x_N > 1$.

In general $V_k(x_k, r_k=j)$ and $u_k(x_k, r_k=j)$ have extreme regions of x_k values (left endpieces for $x_k < \delta_k^j(1)$ and right endpieces for $x_k > \delta_k^j(m_k(j)-1)$) from which the optimal controller will never (through the terminal time N) drive the system into a different piece of the form transition probabilities p_{ji} (for any form i accessible form j). The properties of these endpieces will be addressed in detail in Chapter 6.

5. Let

$$\hat{V}_{k+1}(x_{k+1}|r_k=j) \triangleq E\left\{\begin{array}{l} x_{k+1}^2 Q(r_{k+1}) + S(r_{k+1})x_{k+1} + P(r_{k+1}) \\ + V_{k+1}(x_{k+1}, r_{k+1}) \end{array}\right| r_k = j\Bigg\}$$

denote the conditional expected cost-to-go from (x_{k+1}, r_{k+1}) given that $r_k=j$. This is a function of x_{k+1}. For this example, the conditional expected cost $\hat{V}_N(x_N|r_{N-1}=1)$ is shown in figure 5.12, and is given by

$$\hat{V}_N(x_N|r_{N-1}=1) = \begin{cases} \frac{13}{4} x_N^2 & \text{if } |x_N| > 1 \\ \frac{7}{4} x_N^2 & \text{if } |x_N| < 1 \end{cases}.$$

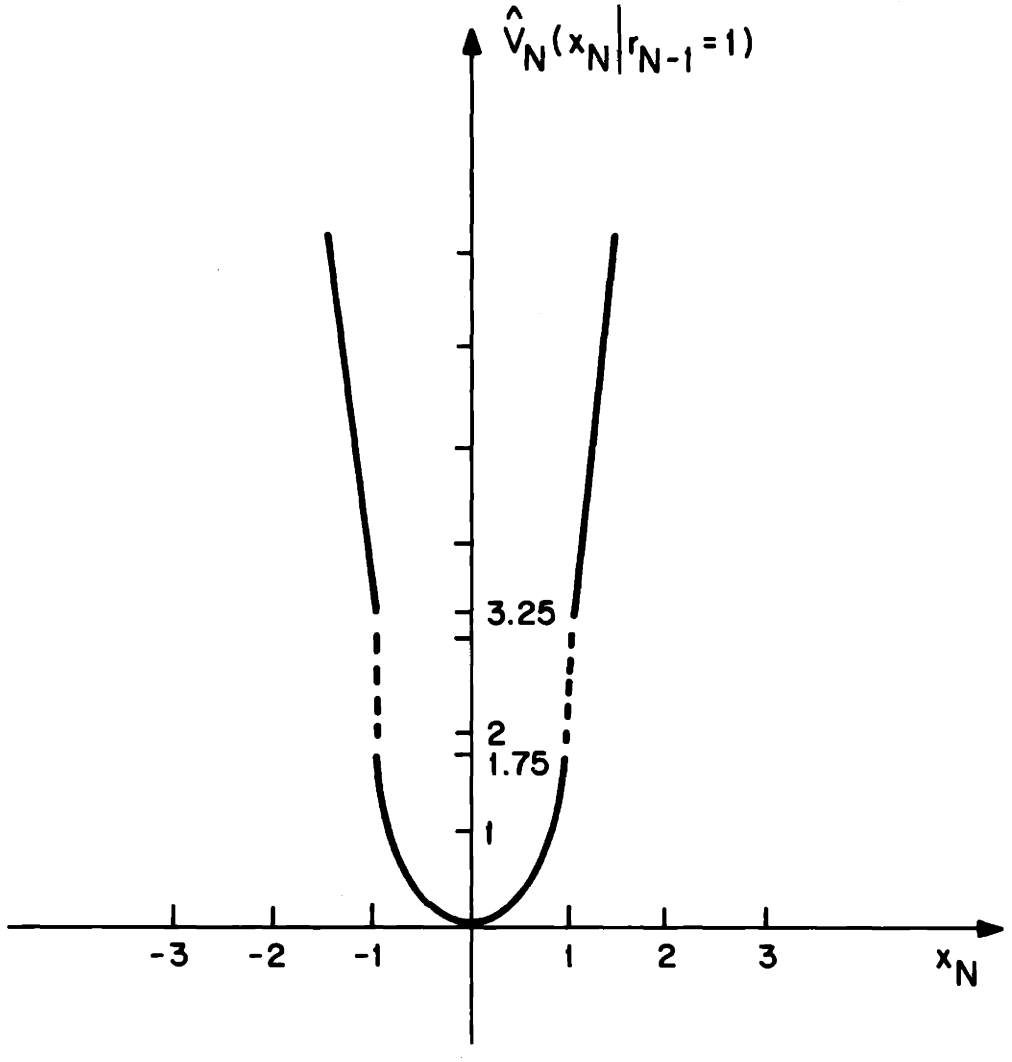

FIGURE 5.12: $\hat{V}_N(x_N|r_{N-1}=1)$ for example 5.1.

As we shall see in later sections of this chapter, the behavior of this conditional expected cost function is intimately related to qualitative properties of the optimal controller and combinatoric properties of the solution.

One relationship is apparent from example 5.1: active hedging to a point from $(x_k, r_k=j)$ occurs only to points x_{k+1} where the conditional expected cost $\hat{V}_{k+1}(x_{k+1}|r_k=j)$ is discontinuous; these points can only arise from form transition probability discontinuities. This will be proved in section 5.6.

For x_{N-1} values between $\delta_{N-1}(1) = -6.77$ and $\delta_{N-1}(2) = -2.75$, the optimal strategy is to drive x_N into $(-1,1)$, where the conditional expected cost-to-go $\hat{V}_N(x_N|r_{N-1}=1)$ is lower. Thus we have $x_N=-1^+$ here. Similarly for x_{N-1} values between $\delta_{N-1}(3)$ and $\delta_{N-1}(4)$ we get $x_N=1^-$. In these two regions of x_{N-1} values, the optimal controller actively hedges to a point. That is, it uses control u_{N-1} to alter the probability of failure $p(1,2;x_N)$ value. In this example the system actively hedges only to points x_N that are transition probability discontinuities.

6. For $\delta_{N-1}(2) \leq x_{N-1} \leq \delta_{N-1}(3)$, the optimal controller doesn't have to actively hedge since the system is driven into $(-1,1)$ by (5.10) anyway.

This is true in general for systems with purely quadratic costs (i.e., $S(i) = P(i) = H_T(i) = G_T(i)=0$, all $i \in \underline{M}$). For such systems, $V_k(x_k,r_k=j)$ and $u_k(x_k,r_k=j)$ have <u>middle pieces</u> containing $x_k=0$, from which the optimal controller never (through terminal time N) drives the system into a different piece of the form transition probabilities p_{ji} (for any form i accessible from j). The existence and properties of <u>middle pieces</u> will be addressed in chapter 6.

7. In figure 5.11 we can see that certain x_N values are never obtained by the optimal controller. In particular, we have

$$x_N \notin (-1.589,-1), \; x_N \notin (1, 1.589).$$

These <u>regions of x_N avoidance</u> are state values that the system must avoid if it is to be optimally controlled. Note that these regions of x_N avoidance correspond to x_{N-1} values where $V_{N-1}(x_{N-1},r_{N-1}=1)$ is not differentiable (ie., $\delta_{N-1}(1)$ and $\delta_{N-1}(2)$).

In general, there is a region of x_{k+1} values that is avoided from $(x_k,r_k=j)$ corresponding to each nondifferentiable point of the optimal expected cost $V_k(x_k,r_k=j)$. This is shown in Proposition 5.3 (in section 5.6).

In the next section we will develop a procedure for the solution of one stage of the general problem formulation of section 5.2, and we will verify the first two of the seven claims above.

5.4 One Stage of the General Problem

In this section we use intuition gained from the example problem of the last section to solve the optimal control problem of section 5.2 for one time stage. As we indicated earlier, the notation and "book-keeping" becomes quite complex, but the basic idea is the same as illustrated in the previous section. Inductive application of the one stage solution (backwards in time from finite terminal time N) then establishes that the solution of problem (5.1)-(5.6) yields optimal expected costs-to-go that are piecewise-quadratic in x and optimal control laws that are piecewise-linear, for all forms $j \in \underline{M}$:

$$V_k(x_k, r_k=j) = x_k^2 K_k(t:j) + x_k H_k(t:j) + G_k(t:j) \tag{5.20}$$

$$u_k(x_k, r_k=j) = -L_k(t:j)x_k + F_k(t:j) \tag{5.21}$$

when

$$\delta_k^j(t-1) < x_k < \delta_k^j(t) \ , \tag{5.22}$$

where

$$\{\delta_k^j(1) < \delta_k^j(2) < \ldots < \delta_k^j(m_k(j)-1)\}$$

are the points where the pieces of $V_k(x_k, j)$ are joined together (the boundaries of the x_k -intervals) and

$$\delta_k^j(0) \triangleq -\infty, \qquad \delta_k^j(m_k(j)) \triangleq \infty \ .$$

The proof of the one-stage optimal controller result is constructive. It suggests an algorithm for the recursive determination of the optimal expected costs-to-go and control laws for this problem.

The one-stage solution result is as follows:

Proposition 5.1: (One stage solution)

Consider the problem of section 5.2. If at time k+1, for each $r_{k+1} = j \in \underline{M}$ we have

(i) $V_{k+1}(x_{k+1}, r_{k+1}=j)$ is piecewise-quadratic with $m_{k+1}(j)$ pieces joined continuously at

$$\{\delta^j_{k+1}(1) < \delta^j_{k+1}(2) < \ldots < \delta^j_{k+1}(m_{k+1}(j)-1)\}$$

(ii) $$\begin{pmatrix} K_{k+1}(t:1) & H_{k+1}(t:1)/2 \\ H_{k+1}(t:1)/2 & G_{k+1}(t:1) \end{pmatrix} \geq 0$$

for $t=1,\ldots,m_{k+1}(j)$

(iii) $\dfrac{\partial V_{k+1}(x_{k+1}, r_{k+1}=j)}{\partial x_{k+1}}$ is continuous or decreases discontinuously at the joining points $\{\delta^j_{k+1}(1),\ldots,\delta^j_{k+1}(m_{k+1}(j)-1)\}$,

then for each $r_k = j \in \underline{M}$

(1) $V_k(x_k, r_k=j)$ is piecewise-quadratic and $u_k(x_k, r_k=j)$ is piecewise-linear (as in (5.20)-(5.22)),each having $m_k(j)$ pieces joined continuously at

$$\{\delta^j_k(1) < \delta^j_k(2) < \ldots < \delta^j_k(m_k(j)-1)\}$$

(2) $\begin{pmatrix} K_k(t:j) & H_k(t:j)/2 \\ H_k(t:j)/2 & G_k(t:j) \end{pmatrix} \geq 0 \qquad t=1,2,\ldots,m_k(j)$

(3) $\dfrac{\partial V_k(x_k, r_k=j)}{\partial x_k}$ is continuous or decreases discontinuously at the joining points $\{\delta_k^j(1),\ldots,\delta_k^j(m_k(j)-1)\}$. □

At time k=N, conditions (i-iii) are clearly satisfied. Thus this proposition can be applied inductively, backwards in time from k=N. Equations for the iterative computation of the quantities $m_k(j)$, $K_k(t:j)$, $H_k(t:j)$, $G_k(t:j)$ and $\{\delta_k^j(\ell): \ell=1,\ldots,m_k(j)-1\}$ for each $i, j \in \underline{M}$ are listed in appendix C.1. These equations are developed in the proof of Proposition 5.1, which constitutes the remainder of this section (with some details in appendix C.1).

Proof of Proposition 5.1:

For each form $r_k = j \in \underline{M}$, the minimization in (5.5) subject to (5.1)-(5.2) is converted into the comparison of a finite set of constrained-in-x_{k+1} JLQ problems, each with x-independent forms. This is done conceptually via the following four steps:

Step 1: Obtaining a Composite Partition of x_{k+1} values from the partitions associated with the form transition probabilities p(j,i;x) and the expected costs-to-go

$V_{k+1}(x_{k+1}, r_{k+1}=i)$ for each $i \in C_j$. Note that the partitions are of x_{k+1} values for each different form at time k (not at k+1).

Step 2: Formulating a set of constrained (in x_{k+1}) JLQ problems having x-independent form transition probabilities and quadratic costs; one problem for each region of x_{k+1} values in the composite partition of Step 1.

Step 3: Solving the constrained subproblems that are formulated in Step 2. These problem solutions represent the optimal expected costs-to-go from $(x_k, r_k=j)$ if x_{k+1} is constrained to be in one of the specific regions of values defined in Step 1.

Step 4: Comparing the constrained costs. The optimal expected cost-to-go $V_k(x_k, r_k=j)$ from any x_k value is the minimum of the constrained expected costs-to-go that are obtained in Step 3. This minimization involves the comparison of piecewise-quadratic functions in x_k.

We will describe each of these conceptual steps in sequence so as to demonstrate the validity of Proposition 5.1. The actual solution algorithm (as described in chapter 7) mixes these steps and uses the combinatoric results of section 5.6 to solve the control problem efficiently (i.e., with fewer calculations.)

Step 1: Obtaining a Composite Partition of x_{k+1}. For each form $j \in \underline{M}$ we construct a composite partition of the real line (i.e. for x_{k+1} values) by superimposing the grids associated with each $p(j,i;x)$ and $V_{k+1}(x_{k+1}, r_{k+1}=i)$, for all $i \in c_j$. The construction of these composite grids is first illustrated for an example system below. The general procedure is then specified.

Example 5.2:

Consider a system whose form structure is as shown in figure 5.13. This system might represent the following situation:

$r_k = 1$	normal operation
$r_k = 2$	degraded operation (repairable failure)
$r_k = 3$	nonrepairable failure
$p(1,2:x)$	one-step probability of repairable failure occurrence (x-dependent)
$p(2,1)$	one-step probability of repair
$p(1,3:x)$	one-step probability of nonrepairable system failure occurrence.

The form transition probabilities from $r_k=1$ are piecewise constant in x (but $p(2,1)$, $p(2,2)$ and $p(3,3)$ are x-independent).

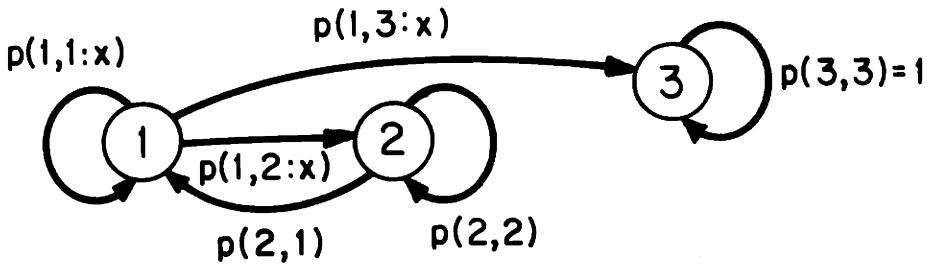

FIGURE 5.13: Form structure for example 5.2. Form 3 is an absorbing form. Here $c_1=\{1,2,3\}$, $c_2=\{1,2\}$, $c_3=\{3\}$.

$$(p(1,1;x)\ p(1,2:x)\ p(1,3:x)) = \begin{cases} (.89 \quad .1 \quad .01) \text{ if } |x| < 1 \\ (.7 \quad .2 \quad .1\ ) \text{ if } 1<|x| < 2 \\ (\ 0 \quad .2 \quad .8\ ) \text{ if } |x| > 2 \end{cases}.$$

$$p(2,1) = p(2,2) = .5$$

Thus the numbers of pieces in each of the form transition probabilites are

$$\bar{\nu}_{11} = \bar{\nu}_{12} = 5$$

$$\bar{\nu}_{12} = 3$$

$$\bar{\nu}_{21} = \bar{\nu}_{22} = \bar{\nu}_{23} = \bar{\nu}_{31} = \bar{\nu}_{32} = \bar{\nu}_{33} = 1.$$

The x-dependent transition probabilities are shown in figure 5.14.

Suppose that at time k+1, the number of pieces in each expected cost-to-go $V_{k+1}(x_{k+1}, r_{k+1}=i)$ is

$$m_{k+1}(1)=5 \quad m_{k+1}(2)=5 \quad m_{k+1}(3)=1$$

as illustrated in figure 5.15. Superimposing the appropriate partitions for each form $r_k=j \in \underline{M}$, we obtain the composite partitions of x_{k+1} values shown in figure 5.16. The number of pieces in each partition, denoted by ψ^j_{k+1} are

$$\psi^1_{k+1}=9 \quad \psi^2_{k+1}=7 \quad \psi^3_{k+1}=1.$$

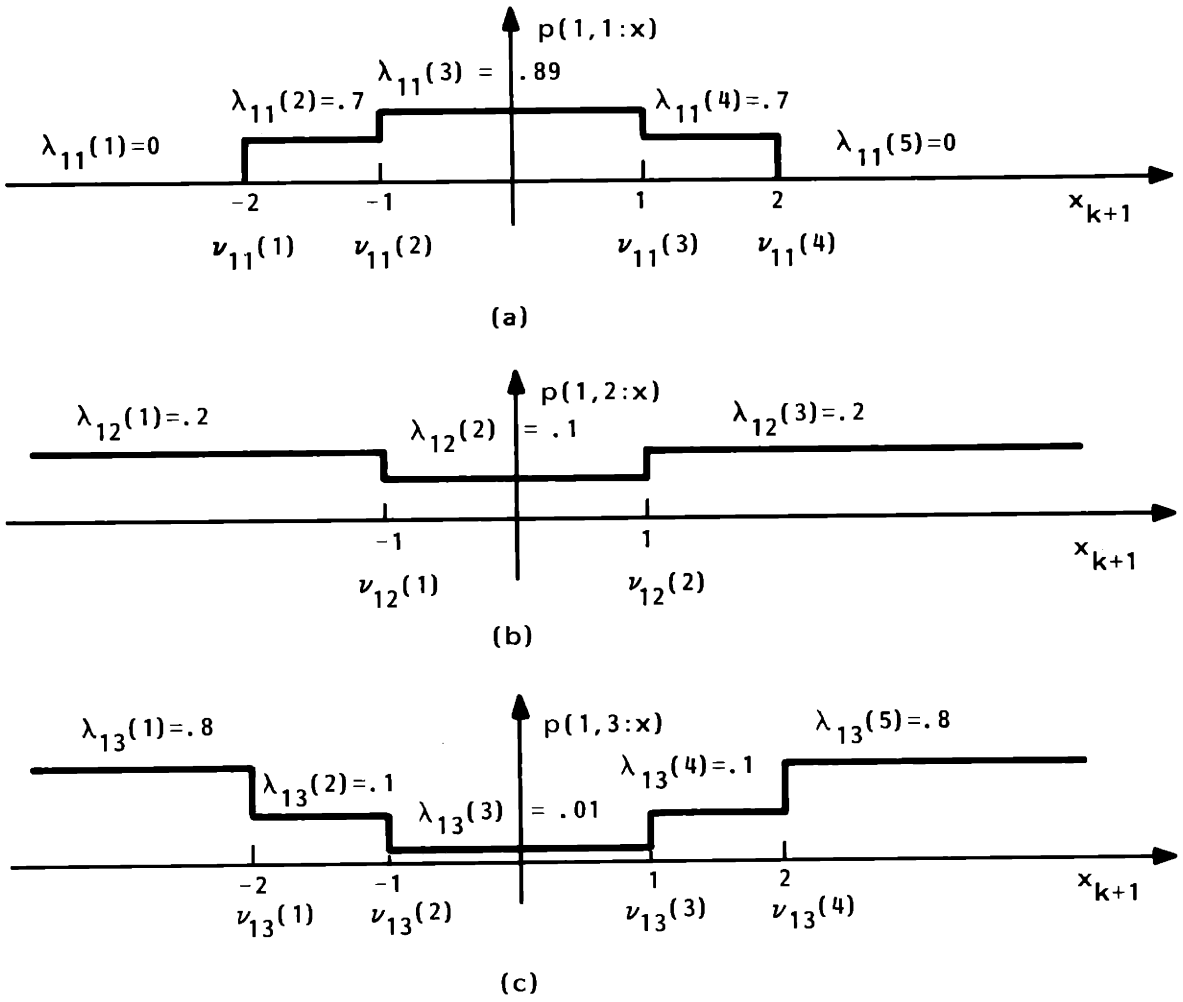

FIGURE 5.14: Piecewise-constant form transition probabilities from form r_k=1 in example 5.2; (a) p(1,1:x) with $\overline{\nu}_{11}$=5 pieces, (b) p(1,2:x) with $\overline{\nu}_{12}$=3 pieces, (c) p(1,3:x) with $\overline{\nu}_{13}$=5 pieces.

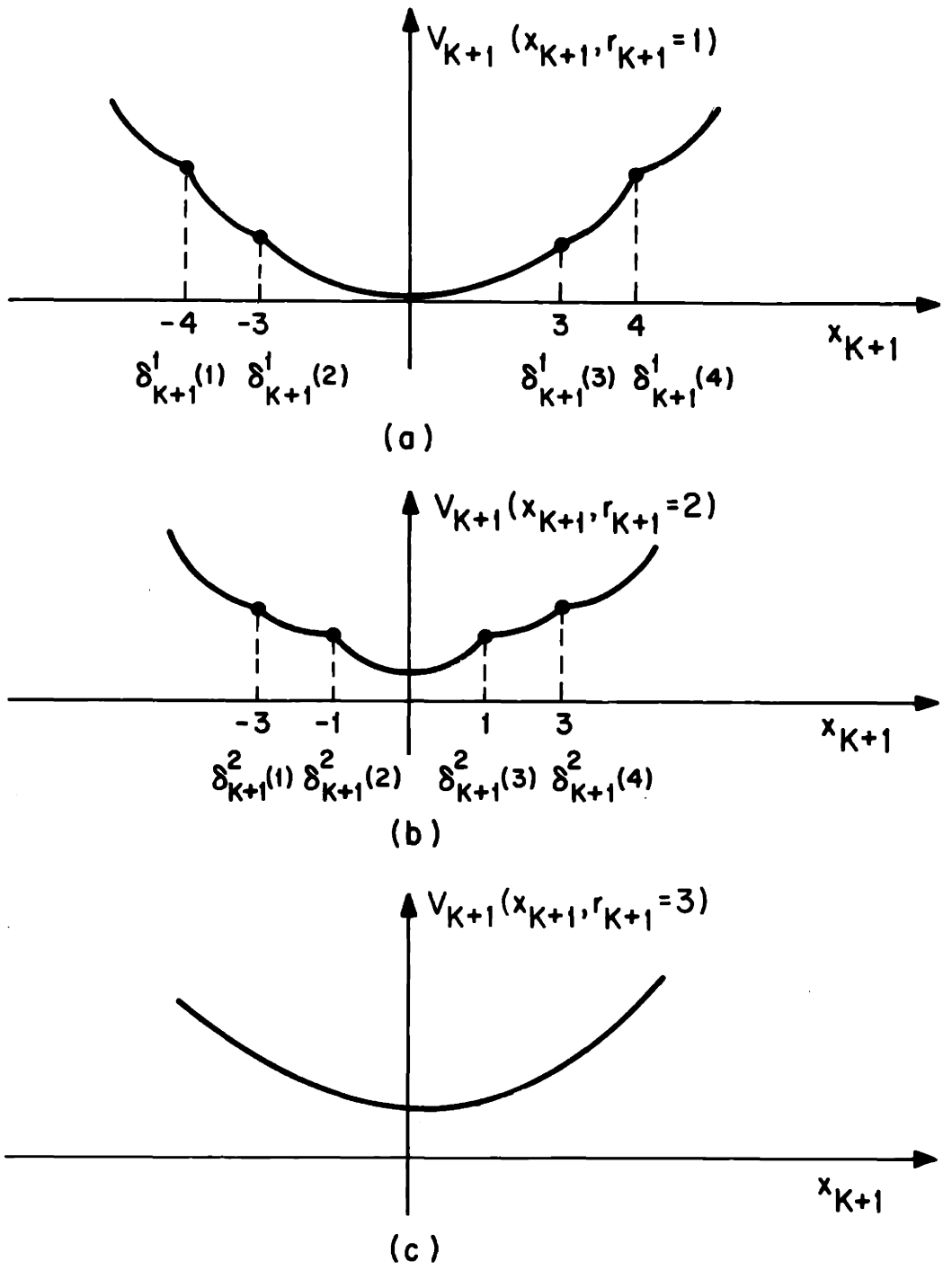

FIGURE 5.15: Piecewise-quadratic expected costs-to-go from (x_{k+1}, r_{k+1}) in example 5.2; (a) $V_{k+1}(x_{k+1}, r_{k+1}=1)$ has $m_{k+1}(1)=5$ pieces, (b) $V_{k+1}(x_{k+1}, r_{k+1}=2)$ has $m_{k+1}(2)=5$ pieces, (c) $V_{k+1}(x_{k+1}, r_{k+1}=3)$ has $m_{k+1}(3)=1$ piece.

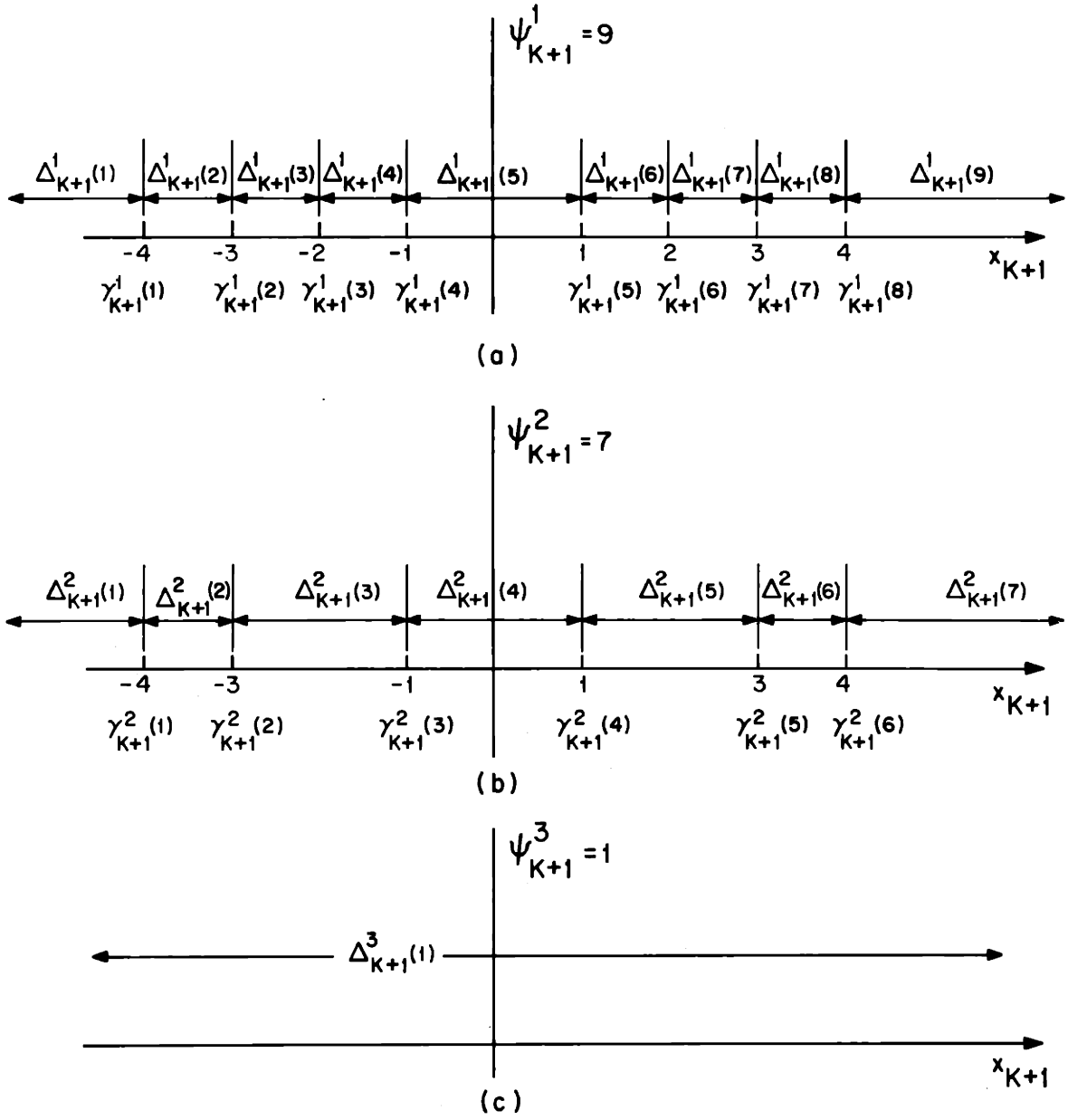

FIGURE 5.16: Composite x_{k+1} partitions for example 5.1; (a) for $r_k=1$ the partition has $\psi^1_{k+1}=9$ pieces, (b) for $r_k=2$ the partition has $\psi^2_{k+1}=7$ pieces, (c) for $r_k=3$ the partition has $\psi^3_{k+1}=1$ pieces.

The x_{k+1} intervals are denoted by

$$\Delta^j_{k+1}(t) \qquad t=1,\ldots,\psi^j_{k+1}$$

with boundary values (grid points)

$$\gamma^j_{k+1}(t-1) \quad \text{and} \quad \gamma^j_{k+1}(t) \ .$$

□

The general procedure for obtaining the composite partitions is as follows:

For each $r_k=j \in \underline{M}$ the real line can be divided into a finite number of intervals of x_{k+1} values by superimposing the grids

$$\{\delta^i_{k+1}(t): \quad t=1,2,\ldots,m_{k+1}(i)-1\}$$

$$\{\nu_{ji}(t): \quad t=1,\ldots,\bar{\nu}_{ji}-1\}$$

$$\text{for each } i \in C_j \ ,$$

obtaining the composite partition

$$-\infty \triangleq \gamma^j_{k+1}(0) < \gamma^j_{k+1}(1) < \gamma^j_{k+1}(2) < \ldots < \gamma^j_{k+1}(\psi^j_{k+1}-1) < \gamma^j_{k+1}(\psi^j_{k+1}) \triangleq \infty$$

of unique grid points. As in example 5.2, we define

$$\psi^j_{k+1} \triangleq \text{the (finite) number of such nonempty } x_{k+1} \text{ intervals}$$

where the t^{th} such interval is

$$\Delta^j_{k+1}(t) \triangleq \{x_{k+1}: \gamma^j_{k+1}(t-1) < x_{k+1} < \gamma^j_{k+1}(t)\} \ .$$

$$t=1,\ldots,\psi^j_{k+1}-1$$

Note that

$$\psi_{k+1}^{j} = 1 + \left| \bigcup_{i \in c_j} \left[\left\{ \nu_{ji}(\ell) : \ell = 1, \ldots, \bar{\nu}_{ji} - 1 \right\} \cup \left\{ \delta_{k+1}^{i}(\ell) : \ell = 1, \ldots, m_{k+1}(i) - 1 \right\} \right] \right| \tag{5.23}$$

where $|A|$ denotes the cardinality of a set A (the number of elements). An upper bound on ψ_{k+1}^{j} is given by

$$\psi_{k+1}^{j} \leq 1 + \sum_{i \in c_j} [\bar{\nu}_{ji} + m_{k+1}(i) - 2] \tag{5.24}$$

where the equality in (5.24) holds if

$$\nu_{ji}(\ell) \neq \nu_{jn}(\rho) \qquad \nu_{ji}(\ell) \neq \delta_{k+1}^{i}(t)$$

for all i, $n \in c_j$, $\ell = 1, 2, \ldots, \bar{\nu}_{ji} - 1$ $t = 1, 2, \ldots, m_{k+1}(i) - 1$ and $\rho = 1, \ldots, \bar{\nu}_{jn} - 1$.

Note that in example 5.2, the bounds of (5.23) are not tight because of the overlapping values:

$$-3 = \delta_{k+1}^{1}(2) = \delta_{k+1}^{2}(1) \qquad 3 = \delta_{k+1}^{1}(3) = \delta_{k+1}^{2}(4)$$

$$-2 = \nu_{11}(1) = \nu_{13}(1) \qquad 2 = \nu_{11}(4) = \nu_{13}(4)$$

$$-1 = \nu_{11}(2) = \nu_{12}(1) = \nu_{13}(2) = \delta_{k+1}^{2}(2) \qquad 1 = \nu_{11}(3) = \nu_{12}(2) = \nu_{13}(3) = \delta_{k+1}^{2}(3). \tag{5.25}$$

Step 2: Formulating the Constrained Subproblems

In Step 1 we obtained for each $r_k=j \in \underline{M}$ a composite partition of x_{k+1} values into ψ_{k+1}^j intervals. We can formulate for each $r_k=j \in \underline{M}$ a set of ψ_{k+1}^j constrained JLQ problems having x_{k+1} -independent form transition probabilities and quadratic (not piecewise-quadratic) expected costs---one corresponding to each region of x_{k+1} values. To see this note that over each such region $\Delta_{k+1}^j(t)$,

$V_{k+1}(x_{k+1}, r_{k+1}=i)$ is quadratic and

$p(j,i;x_{k+1})$ is constant in x_{k+1}, for all $i \in c_j$. These constrained problems are

$$V_k[x_k, r_k=j \,|\, x_{k+1} \in \Delta_{k+1}^j(t)] \triangleq V_k[x_k, j|t] =$$

$$= \min_{\substack{u_k \text{ s.t.} \\ x_{k+1} \in \Delta_{k+1}^j(t)}} E\left\{\begin{array}{l} u_k^2 R(j) + x_{k+1}^2 Q(r_{k+1}) \\ + S(r_{k+1})x_{k+1} + P(r_{k+1}) \\ + V_{k+1}(x_{k+1}, r_{k+1}) \end{array}\right\} \tag{5.26}$$

$$= \min_{\substack{u_k \text{ s.t.} \\ x_{k+1} \in \Delta_{k+1}^j(t)}} \left\{ u_k^2 R(j) + \sum_{i=1}^{M} p(j,i,x_{k+1}) \left[\begin{array}{l} x_{k+1}^2 Q(i) + x_{k+1} S(i) \\ + P(i) \\ + V_{k+1}(x_{k+1}, i) \end{array} \right] \right\} \tag{5.27}$$

$$= \min_{\substack{u_k \text{ s.t.} \\ x_{k+1} \in \Delta^j_{k+1}(t)}} \left\{ u_k^2 R(j) + \hat{V}_{k+1}(x_{k+1} | r_k = j) \right\} \tag{5.28}$$

subject to (5.1)-(5.3) for each $t=1,2,\ldots,\psi^j_{k+1}$.

Step 3: Solving the constrained subproblems

The third step in this constructive proof of Proposition 5.1 is to solve the constrained JLQ problems of (5.26). As in example 5.1, for each $r_k=j \in \underline{M}$ the solutions of these ψ^j_{k+1} constrained optimization problems involve optimal expected costs-to-go that are piecewise-quadratic in x_k with three parts (except for t=1 and $t = \psi^j_{k+1}$ which have only two parts):

$$V_k[x_k, r_k=j | x_{k+1} \in \Delta^j_{k+1}(t)] = \begin{cases} V_k^{t,L}(x_k, j) & \text{if } a(j)x_k \leq \theta^j_k(t) \\ V_k^{t,U}(x_k, j) & \text{if } \theta^j_k(t) \leq a(j)x_k \leq \Theta^j_k(t) \\ V_k^{t,R}(x_k, j) & \text{if } \Theta^j_k(t) \leq a(j)x_k \end{cases} \tag{5.29}$$

with corresponding optimal control laws

$$u_k[x_k, r_k=j \,|\, x_{k+1} \in \Delta_{k+1}^j(t)] = \begin{cases} u_k^{t,L}(x_k,j) & \text{if } a(j)x_k < \theta_k^j(t) \\ u_k^{t,U}(x_k,j) & \text{if } \theta_k^j(t) < a(j)x_k < \Theta_k^j(t) \\ u_k^{t,R}(x_k,j) & \text{if } \Theta_k^j(t) < a(j)x_k \end{cases} . \tag{5.30}$$

The derivation of expressions for these control law and expected cost pieces involves straightforward (but tedious) algebraic manipulations that are described in Appendix C.2. Formulae for the quantities in (5.29)-(5.30) are listed for reference in Appendix C.1.

As in example 5.1, one piece of each expected cost-to-go in (5.29) and control law in (5.30), denoted by $V_k^{t,U}(x_k,j)$ and $u_k^{t,U}(x_k,j)$, corresponds to performing the minimization in (5.26) without the $x_{k+1} \in \Delta_{k+1}^j(t)$ constraint. The functions $V_k^{t,U}(x_k,j)$ and $u_k^{t,U}(x_k,j)$ solve (5.26) only for those x_k values for which the constraint $x_{k+1} \in \Delta_{k+1}^j(t)$ is inactive; that is, where application of the control that minimizes (5.26) results in an x_{k+1} value in the interior of $\Delta_{k+1}^j(t)$. We define $\theta_k^j(t)$ and $\Theta_k^j(t)$ so that these x_k values (where $V_k^{t,U}(x_k,j)$ applies) satisfy $\theta_k^j(t) < a(j)x_k < \Theta_k^j(t)$.

For $t=2,3,\ldots,\psi_{k+1}^j$ another piece of $V_k(x_k, j\,|\,t)$ in (5.26), denoted by by $V_k^{t,L}(x_k,j)$, corresponds to driving x_{k+1} to the left boundary of constraint region $\Delta_{k+1}^j(t)$. That is, $x_{k+1} = [\gamma_{k+1}^j(t-1)]^+$. The functions $V_k^{t,L}(x_k,j)$ and $u_k^{t,L}(x_k,j)$ solve (5.26) for those x_k values where the constraint $x_k \in \Delta_{k+1}^j(t)$ is active, and where $u_k^{t,U}(x_k,j)$ results in $x_{k+1} < \gamma_{k+1}^j(t-1)$. That is, $V_k^{t,L}(x_k,j)$ and $u_k^{t,L}(x_k,j)$ solve (5.26) for $a(j)x_k < \theta_k^j(t)$.

For $t=1,2,..,\ \psi_{k+1}^{j}-1$ another piece of $V_k(x_k,j|t)$ in (5.26), denoted by $V_k^{t,R}(x_k,j)$, corresponds to driving x_{k+1} to the <u>right boundary</u> of constraint region $\Delta_{k+1}^{j}(t)$. That is, $x_{k+1} = [\gamma_{k+1}^{j}(t)]^{-}$. The functions $V_k^{t,R}(x_k,j)$ and $u_k^{t,R}(x_k,j)$ solve (5.26) for those x_k values where the constraint $\Delta_{k+1}^{j}(t)$ is <u>active</u>, and where $u_k^{t,U}(x_k,j)$ results in $x_{k+1} > \gamma_{k+1}^{j}(t)$. That is, $V_k^{t,R}(x_k,j)$ and $u_k^{t,R}(x_k,j)$ solve (5.26) for

$$a(j)x_k > \Theta_k^{j}(t) \ .$$

For $t=\psi_{k+1}^{j}$ there is no finite right boundary of $\Delta_{k+1}^{j}(\psi_{k+1}^{j})$ (i.e., $\gamma_{k+1}(\psi_{k+1}^{j}) \triangleq \infty$), so there is no $V_k^{\psi_{k+1}^{j},L}(x_k,j)$ piece; thus $\Theta_k^{j}(\psi_{k+1}^{j}) = +\infty$ in (5.29)-(5.30). We summarize the solution to (5.26) in table 5.2.

For $t=2,3,..,\psi_{k+1}^{j}-1$ a typical three-part $V_k(x_k, r_k=j | x_{k+1} \in \Delta_{k+1}^{j}(t))$ looks like either (a),(b) or (c) of figure 5.17. Here the quadratic (in x_k) function

$V_k^{t,L}(x_k,j)$ is denoted by the dotted line

$V_k^{t,U}(x_k,j)$ is denoted by the dashed line

$V_k^{t,R}(x_k,j)$ is denoted by the dot-dash line

Pieces of $V_k(x_k, r_k=j \mid x_{k+1} \in \Delta_{k+1}^j(t))$ and $u_k(x_k, r_k=j \mid x_{k+1} \in \Delta_{k+1}^j(t))$	valid for values of x_k such that	the optimal solution of (5.26) results in x_{k+1} such that
$V_k^{t,L}(x_k, j)$ $u_k^{t,L}(x_k, j)$ $t=2,\ldots,\psi_{k+1}^j$	$a(j)x_k < \theta_k^j(t)$	$x_{k+1} = [\gamma_{k+1}^j(t-1)]^+$ on the left boundary of $\Delta_{k+1}^j(t)$
$V_k^{t,U}(x_k, j)$ $u_k^{t,U}(x_k, j)$ $t=1,\ldots,\psi_{k+1}^j$	$\theta_k^j(t) < a(j)x_k < \Theta_k^j(t)$	$\gamma_{k+1}^j(t-1) < x_{k+1} < \gamma_{k+1}^j(t)$ in the interior of $\Delta_{k+1}^j(t)$
$V_k^{t,R}(x_k, j)$ $u_k^{t,R}(x_k, j)$ $t=1,\ldots,\psi_{k+1}^j-1$	$\Theta_k^j(t) \leq a(j)x_k$	$x_{k+1} = [\gamma_{k+1}^j(t)]^-$ on the right boundary of $\Delta_{k+1}^j(t)$

Table 5.2: Pieces of $V_k(x_k, r_k=j \mid t)$ and $u_k(x_k, r_k=j \mid t)$

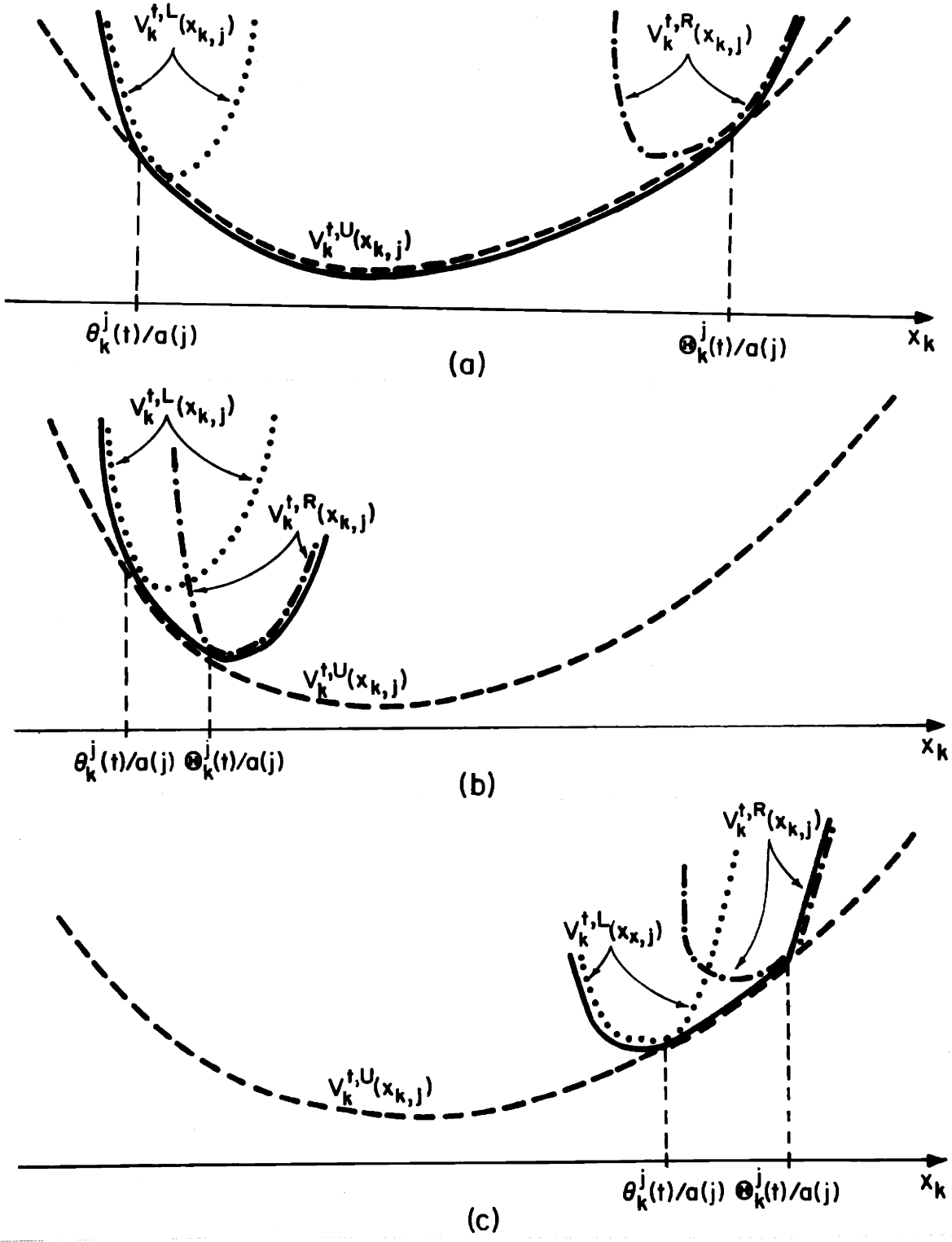

FIGURE 5.17: Typical optimal expected costs-to-go $V_k(x_k, r_k=j \mid x_{k+1} \in \Delta_{k+1}^j(t))$ where $a(j)>0$.

The solid line in each figure indicates which of these three cost functions applies over various x_k values.

The three different possible shapes of $V_k(x_k,j|t)$ shown in figure 5.17 arise from the relative values of the minimal points of $V_k^{t,L}(x_k,j)$, $V_k^{t,U}(x_k,j)$ and $V_k^{t,R}(x_k,j)$. At $x_k = \theta_k^j(t)/a(j)$ the values and slopes of $V_k^{t,L}(x_k,j)$ and $V_k^{t,U}(x_k,j)$ are the same. At $x_k = \Theta_k^j(t)/a(j)$, the <u>values</u> and <u>slopes</u> of $V_k^{t,R}(x_k,j)$ and $V_k^{t,U}(x_k,j)$ are the same. At all other x_k values, the constrained costs are greater than the unconstrained costs. That is, for $t=2,\ldots,\psi_{k+1}^j$:

$$V_k^{t,L}(x_k,j) > V_k^{t,U}(x_k,j) \qquad x_k \neq \theta_k^j(t)/a(j)$$

$$V_k^{t,L}(x_k,j)\Big|_{x_k = \frac{\theta_k^t(t)}{a(j)}} = V_k^{t,U}(x_k,j)\Big|_{x_k = \frac{\theta_k^j(t)}{a(j)}} \tag{5.31}$$

$$\frac{\partial V_k^{t,L}(x_k,j)}{\partial x_k}\Bigg|_{x_k = \frac{\theta_k^j(t)}{a(j)}} = \frac{\partial V_k^{t,U}(x_k,j)}{\partial x_k}\Bigg|_{x_k = \frac{\theta_k^j(t)}{a(j)}} \tag{5.32}$$

and for $t=1,\ldots,\psi_{k+1}^j - 1$:

$$V_k^{t,R}(x_k,j) > V_k^{t,U}(x_k,j) \qquad x_k \neq \frac{\Theta_k^j(t)}{a(t)}$$

$$V_k^{t,R}(x_k,j)\Big|_{x_k=\frac{\Theta_k^j(t)}{a(j)}} = V_k^{t,U}(x_k,j)\Big|_{x_k=\frac{\Theta_k^j(t)}{a(j)}} \tag{5.33}$$

$$\frac{\partial V_k^{t,R}(x_k,j)}{\partial x_k}\Big|_{x_k=\frac{\Theta_k^j(t)}{a(j)}} = \frac{\partial V_k^{t,U}(x_k,j)}{\partial x_k}\Big|_{x_k=\frac{\Theta_k^j(t)}{a(j)}} \cdot \tag{5.34}$$

As is evident in figure 5.17, since $V_k^{t,R}(x_k,j)$ and $V_k^{t,L}(x_k,j)$ have the same curvature it follows that:

$$V_k^{t,R}(x_k,j) < V_k^{t,L}(x_k,j) \text{ if } a(j)x_k > \Theta_k^j(t) \tag{5.35}$$

$$V_k^{t,L}(x_k,j) < V_k^{t,R}(x_k,j) \text{ if } a(j)\ x_k < \theta_k^j(t) \quad , \tag{5.36}$$

Step 4: Comparing the Constrained Costs.

The fourth step in this proof of Proposition 5.1 is to compare the solutions of the ψ_{k+1}^j constrained JLQ problems specified by (5.26). For each $r_k = j \in \underline{M}$, $V_k(x_k,r_k=j)$ at each x_k value is the smallest of the constrained costs in (5.29). That is,

$$V_k(x_k,r_k=j) = \min_{t=1,\ldots,\psi_{k+1}^j} \left\{ V_k(x_k,r_k=j \,|\, x_{k+1} \in \Delta_{k+1}^j(t)) \right\} \cdot \tag{5.37}$$

This minimization involves the comparison of piecewise-quadratic functions in x_k.

In principle we can use (5.37) to find $V_k(x_k, r_k=j)$ and $u_k(x_k, r_k=j)$ (that is, the quantities $K_k(t:j)$, $H_k(t:j)$, $G_k(t:j)$, $L_k(t:j)$, $F_k(t:j)$, $\{\delta_k^j(t): t=1,\ldots,m_k(j)-1\}$ and $m_k(j)$ as in (5.20)-(5.22)). This minimization was done graphically for example 5.1. In general, we must accomplish the minimization of (5.37) by finding the intersections of the $(3\psi_{k+1}^j-2)$ quadratic functions

$$\left\{ \begin{array}{l} V_k^{1,U}(x_k,j),\ V_k^{1,R}(x_k,j),\ V_k^{2,L}(x_k,j),\ V_k^{2,U}(x_k,j),\ V_k^{2,R}(x_k,j),\ldots, \\ V_k^{\psi_{k+1}^j-1,L}(x_k,j), V_k^{\psi_{k+1}^j-1,U}(x_k,j), V_k^{\psi_{k+1}^j-1,R}(x_k,j), V_k^{\psi_{k+1}^j L}(x_k,j), V_k^{\psi_{k+1}^j,U}(x_k,j) \end{array} \right\} \tag{5.38}$$

and choosing $V_k[x_k, r_k=j]$ at each value of x_k to be the one having the lowest value there (for those costs that are valid at x_k). Thus $V_k[x_k, r_k=j]$ is piecewise-quadratic in x_k and $u_k(x_k, r_k=j)$ is piecewise-linear, as claimed in (1) of Proposition 5.1. The verification of (2) in the proposition is straightforward.

The fact that

$$\frac{\partial V_k(x_k, r_k=j)}{\partial x_k} \quad \text{is continuous or decreases discontinuously}$$

at the joining points $\{\delta_k^j(1),\ldots,\delta_k^j(m_k(j)-1)\}$ follows directly from the comparison in (5.37): a particular joining point $\delta_k^j(\ell)$ can arise in two ways:

(1) two (or more) of the constrained costs-to-go in (5.37) may cross at $\delta_k^j(\ell)$. Since $V_k(x_k, r_k=j)$ is the smallest candidate cost at each x_k value, the slope of $V_k(x_k, r_k=j)$ must decrease discontinuously at such a $\delta_k^j(\ell)$. This is illustrated in figure 5.18.

(2) $\delta_k^j(\ell)$ may be an x_k value where the optimal candidate cost in (5.37) changes from a constrained piece to an unconstrained piece (or vice versa). That is, $\delta_k^j(\ell)$ corresponds to either

- $x_k = \theta_k^j(t)/a(j)$ where $V_k(x_k, j|t)$ changes from $V_k^{t,L}(x_k, j)$ to $V_k^{t,U}(x_k, j)$ and $\partial V_k(x_k, j|t)/\partial x_k$ is continuous or
- $x_k = \theta_k^j(t)/a(j)$ where $V_k(x_k, j|t)$ changes from $V_k^{t,U}(x_k, j)$ $V_k^{t,R}(x_k, j)$ and $\partial V_k(x_k, j|t)/\partial x_k$ is continuous.

This concludes the proof of the one-stage solution given by Proposition 5.1. Certain qualitative properties of the optimal controller that are developed later in this chapter and in chapters 6,7 will be used to simplify the procedure that is described above. The actual solution algorithm is presented in chapter 7. In the next section we will demonstrate the application of steps 1-4 in the next stage (k=N-2) of example 5.1.

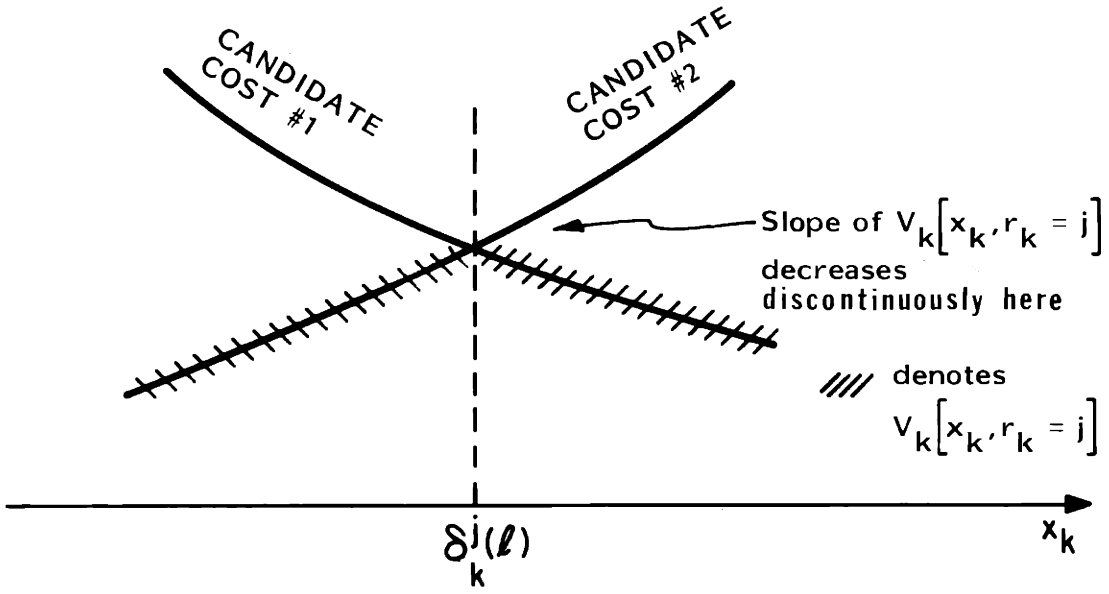

FIGURE 5.18: Crossing candidate costs and $x_k = \delta_k^j(\ell)$.

5.5 The Next Stage of Example 5.1

In this section we demonstrate the application of the four steps detailed in section 5.4, by solving the next stage of example 5.1. From this example we can gain further intuition about the qualitative and combinatoric properties of the optimal controller which will be exploited in section 5.6 and chapters 6 and 7.

First we note that the last stage solution of example 5.1 that was carried out in section 5.3, in terms of the notation of section 5.4, involved the partitioning of the real line (of x_N values) into $\psi_N=3$ regions

$$\Delta_N(1) \triangleq (\gamma_N(0),\gamma_N(1)) = (-\infty,-1)$$

$$\Delta_N(2) \triangleq (\gamma_N(1),\gamma_N(2)) = (-1, 1)$$

$$\Delta_N(3) \triangleq (\gamma_N(2),\gamma_N(3)) = (1, \infty)$$

and

$$\theta_{N-1}(1) = -\infty \quad = -\Theta_{N-1}(2)$$

$$\Theta_{N-1}(1) = -4.25 \quad = -\theta_{N-1}(3)$$

$$\theta_{N-1}(2) = -2.75 \quad = -\Theta_{N-1}(3) \quad .$$

---

[1] The superscript "1" in ψ_N^1, $\Delta_N^1(t)$, $\gamma_N^1(t)$, $\theta_{N-1}^1(t)$, $\Theta_{N-1}^1(t)$, $\delta_{N-1}^1(t)$, etc. is suppressed in this section since we only consider r=1.

From (5.17)-(5.18), the solution at stage k=N-1 is

$$V_{N-1}(x_{N-1},r_{N-1}=1) = x_{N-1}^2 K_{N-1}(t:1) + x_{N-1} H_{N-1}(t:1) + G_{N-1}(t:1)$$

$$u_{N-1}(x_{N-1},r_{N-1}=1) = -L_{N-1}(t:1)x_{N-1} + F_{N-1}(t:1)$$

$$\text{for} \quad \delta_{N-1}(t-1) < x_{N-1} < \delta_{N-1} < \delta_{N-1}(t)$$

where

$$m_{N-1}(1)=5$$

$\delta_{N-1}(0) = -\infty$ $\qquad$ $\delta_{N-1}(3) = 2.75$

$\delta_{N-1}(1) = -6.77$ $\qquad$ $\delta_{N-1}(4) = 6.77$

$\delta_{N-1}(2) = -2.75$ $\qquad$ $\delta_{N-1}(5) = \infty$

and

$K_{N-1}(1:1) = .7647 = K_{N-1}(5:1)$

$K_{N-1}(2:1) = 1 = K_{N-1}(4:1)$

$K_{N-1}(3:1) = .6364$

$H_{N-1}(2:1) = 2 = -H_{N-1}(4:1)$

$H_{N-1}(1:1) = H_{N-1}(3:1) = H_{N-1}(5:1) = 0$

$G_{N-1}(2:1) = 2.75 = G_{N-1}(4:1)$

$G_{N-1}(1:1) = G_{N-1}(3:1) = G_{N-1}(5:1) = 0$

$$L_{N-1}(1:1) = .7647 = L_{N-1}(5:1)$$

$$L_{N-1}(2:1) = 1 = L_{N-1}(4:1)$$

$$L_{N-1}(3:1) = .6364$$

$$F_{N-1}(2:1) = -1 = -F_{N-1}(4:1)$$

$$F_{N-1}(1:1) = F_{N-1}(3:1) = F_{N-1}(5:1) = 0$$

as shown in figures 5.9, 5.10.

Now we proceed to the next stage, following the four solution steps of solution 5.4.

Step 1:

Given $\{\delta_{N-1}(1), \delta_{N-1}(2), \delta_{N-1}(3), \delta_{N-1}(4)\}$ from section 5.2 and the form transition probability discontinuities

$$\nu_{12}(1) = -1$$

$$\nu_{12}(2) = +1$$

we can obtain the composite partition of x_{N-1}. From (C.1.1)-(C.1.3) and (C.1.6) we can compute the conditional expected cost-to-go $V_{N-1}(x_{N-1}|r_{N-2}=1)$ as well. We find that $V_{N-1}(x_{N-1}|r_{N-2}=1)$ has $\psi_{N-1}=7$ pieces with boundaries

$$\gamma_{N-1}(1) = \delta_{N-1}(1) = -6.77$$

$$\gamma_{N-1}(2) = \delta_{N-1}(2) = -2.75$$

$$\gamma_{N-1}(3) = \nu_{12}(1) = -1$$

$$\gamma_{N-1}(4) = \nu_{12}(2) = 1$$

$$\gamma_{N-1}(5) = \delta_{N-1}(3) = 2.75$$

$$\gamma_{N-1}(6) = \delta_{N-1}(4) = 6.77$$

and that

$$\hat{V}_{N-1}(x_{N-1}|r_{N-2}=1) = x_{N-1}^2\hat{K}_{N-1}(t) + x_{N-1}\hat{H}_{N-1}(t) + \hat{G}_{N-1}(t)$$

$$\text{if } x_{N-1} \in \Delta_{N-1}(t)$$

$$\text{for } t=1,\ldots,\psi_{N-1}(7)$$

with

$$\hat{K}_{N-1}(1) = \hat{K}_{N-1}(7) = 3.591$$

$$\hat{K}_{N-1}(2) = \hat{K}_{N-1}(6) = 3.65$$

$$\hat{H}_{N-1}(2) = .5$$

$$\hat{H}_{N-1}(6) = -.5$$

$$\hat{G}_{N-1}(2) = \hat{G}_{N-1}(6) = .6875$$

$$\hat{K}_{N-1}(3) = \hat{K}_{N-1}(5) = 3.559$$

$$\hat{K}_{N-1}(4) = 2.277$$

$\hat{V}_{N-1}(x_{N-1}|r_{N-2}=1)$ is shown in figure 5.19.

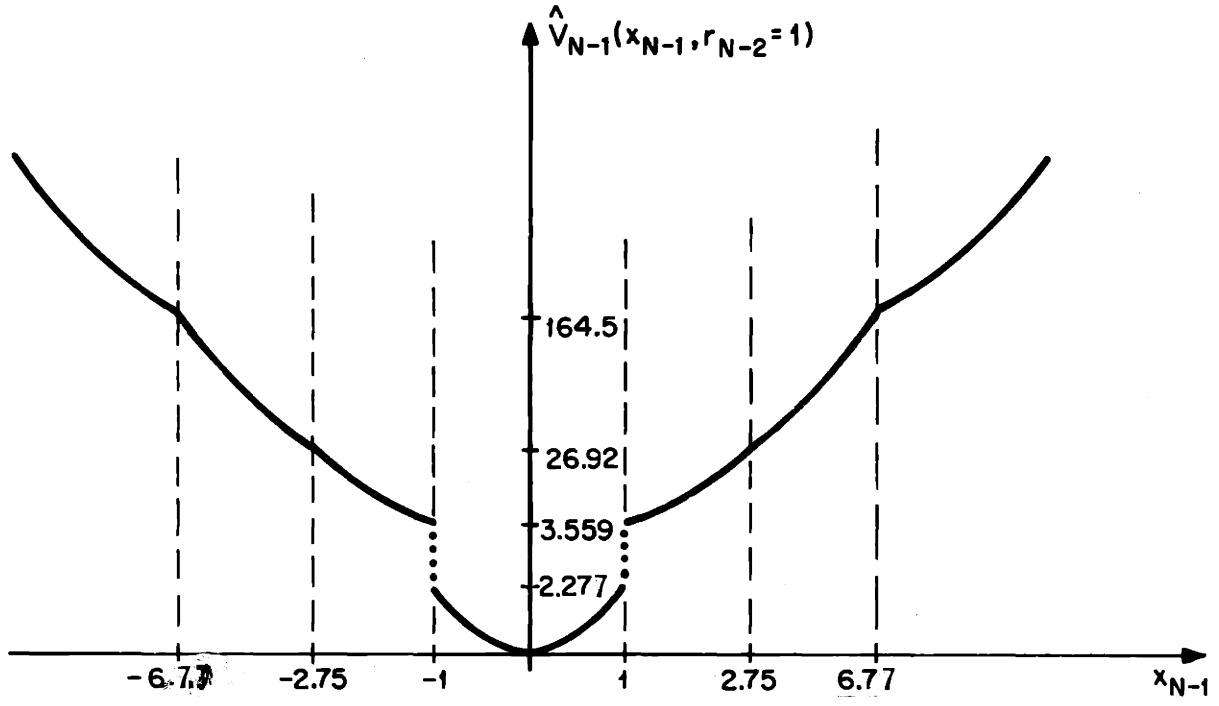

FIGURE 5.19: $\hat{V}_{N-1}(x_{N-1}|r_{N-2}=1)$ for example 5.1. (Not drawn to scale).

Step 2: The $\psi_{N-1}=7$ constrained JLQ problems, as in (5.28) are thus

$$V_{N-2}(x_{N-2}, r_{N-2}=1|1) = \min_{\substack{u_{N-2} \text{ s.t.} \\ x_{N-1} \in \Delta_{N-1}(1)}} \left\{ u_{N-2}^2 + (3.5911765) x_{N-1}^2 \right\}$$

$$V_{N-2}(x_{N-2}, r_{N-2}=1|2) = \min_{\substack{u_{N-2} \text{ s.t.} \\ x_{N-1} \in \Delta_{N-1}(2)}} \left\{ u_{N-2}^2 + 3.65\, x_{N-1}^2 + \frac{1}{2} x_{N-1} + .6875 \right\}$$

$$V_{N-2}(x_{N-2}, r_{N-2}=1|3) = \min_{\substack{u_{N-2} \text{ s.t.} \\ x_{N-1} \in \Delta_{N-1}(3)}} \left\{ u_{N-2}^2 + (3.5590909) x_{N-1}^2 \right\}$$

$$V_{N-2}(x_{N-2}, r_{N-2}=1|4) = \min_{\substack{u_{N-2} \text{ s.t.} \\ x_{N-1} \in \Delta_{N-1}(4)}} \left\{ u_{N-2}^2 + 2.2772727\, x_{N-1}^2 \right\}$$

$$V_{N-2}(x_{N-2}, r_{N-2}=1|5) = \min_{\substack{u_{N-2} \text{ s.t.} \\ x_{N-1} \in \Delta_{N-1}(5)}} \left\{ u_{N-2}^2 + (3.5590909) x_{N-1}^2 \right\}$$

$$V_{N-2}(x_{N-2}, r_{N-2}=1|6) = \min_{\substack{u_{N-2} \text{ s.t.} \\ x_{N-1} \in \Delta_{N-1}(6)}} \left\{ \begin{matrix} u_{N-2}^2 + 3.65\, x_{N-1}^2 \\ -\frac{1}{2} x_{N-1} + .6874999 \end{matrix} \right\}$$

$$V_{N-2}(x_{N-2}, r_{N-2}=1|7) = \min_{\substack{u_{N-2} \text{ s.t.} \\ x_{N-1} \in \Delta_{N-1}(7)}} \left\{ u_{N-2}^2 + (3.5911765) x_{N-1}^2 \right\}.$$

Step 3: Solving these constrained problems (using the formulae of appendix C.1) we find that

$$V_{N-2}(x_{N-2}, 1|1) = \begin{cases} V_{N-2}^{1,U} = .78219\, x_{N-2}^2 & \text{if } x_{N-2} \leq -30.975976 \\ V_{N-2}^{1,R} = \left[\begin{matrix} x_{N-2}^2 + 13.537586\, x_{N-2} \\ + 210.33327 \end{matrix} \right] & \text{if } x_{N-2} \geq -30.975976 \end{cases}$$

$$V_{N-2}(x_{N-2}, 1|2) = \begin{cases} V_{N-2}^{2,L} = \left[\begin{matrix} x_{N-2}^2 + 13.537586\, x_{N-2} \\ + 210.33327 \end{matrix} \right] & \text{if } x_{N-2} \leq -31.223493 \\ V_{N-2}^{2,U} = \left[\begin{matrix} .7849462\, x_{N-2}^2 \\ +.1075268\, x_{N-2} \\ +.674059 \end{matrix} \right] & \text{if } -31.223493 \leq x_{N-2} \leq -12.53749 \\ V_{N-2}^{2,R} = \left[\begin{matrix} x_{N-2}^2 + 5.4999994\, x_{N-2} \\ + 34.478117 \end{matrix} \right] & \text{if } -12.537499 \leq x_{N-2} \end{cases}$$

$$V_{N-2}(x_{N-2},1|3) = \begin{cases} V_{N-2}^{3,L} = \left[x_{N-2}^2 + 5.4999994x_{N-2} + 34.478117\right] & \text{if } x_{N-2} \leq -12.537499 \\ V_{N-2}^{3,U} = .780658x_{N-2}^2 & \text{if } -12.537499 \leq x_{N-2} \leq 4.5590909 \\ V_{N-2}^{3,R} = \left[x_{N-2}^2 + 2x_{N-2} + 4.5590909\right] & \text{if } x_{N-2} \geq -4.5590909 \end{cases}$$

$$V_{N-2}(x_{N-2},1|4) = \begin{cases} V_{N-2}^{4,L} = x_{N-2}^2 + \left[2x_{N-2} + 3.2772727\right] & \text{if } x_{N-2} \leq -3.2772727 \\ V_{N-2}^{4,U} = .6948682x_{N-2}^2 & \text{if } -3.2772727 \leq x_{N-2} \leq 3.2772727 \\ V_{N-2}^{4,R} = \left[x_{N-2}^2 - 2x_{N-2} + 3.2772727\right] & \text{if } x_{N-2} \geq 3.2772727 \end{cases}$$

$$V_{N-2}(x_{N-2},1|5) = \begin{cases} V_{N-2}^{5,L} = \left[x_{N-2}^2 - 2x_{N-2} + 4.5590909\right] & \text{if } x_{N-2} \leq 4.5590909 \\ V_{N-2}^{5,U} = .780658\, x_{N-2}^2 & \text{if } 4.5590909 \leq x_{N-2} \leq 12.537499 \\ V_{N-2}^{5,R} = \left[x_{N-2}^2 - 5.4999994x_{N-2} + 34.478117\right] & \text{if } x_{N-2} \geq 12.537499 \end{cases}$$

$$V_{N-2}(x_{N-2},1|6) = \begin{cases} V_{N-2}^{6,L} = \left[x_{N-2}^2 - 5.4999994\, x_{N-2} + 34.478117\right] & \text{if } x_{N-2} \leq 12.5374999 \\ V_{N-2}^{6,U} = \left[.7849462\, x_{N-2}^2 - .1075268\, x_{N-2} + .674059\right] & \text{if } 12.537499 \leq x_{N-2} \leq 31.223493 \\ V_{N-2}^{6,R} = \left[x_{N-2}^2 - 13.537586x_{N-2} + 210.33327\right] & \text{if } x_{N-2} \geq 31.223493 \end{cases}$$

$$V_{N-2}(x_{N-2},1|7) = \begin{cases} V_{N-2}^{7,L} = \left[x_{N-2}^2 - 13.537586 x_{N-2} + 210.33327\right] & \text{if } x_{N-2} \leq 30.975476 \\ V_{N-2}^{7,v} = .7821909\, x_{N-2}^2 & \text{if } x_{N-2} \geq 30.975976 \end{cases} .$$

That is,

$$\theta_{N-2}(2) = -31.22 = -\Theta_{N-2}(6)$$

$$\Theta_{N-2}(1) = -30.98 = -\theta_{N-2}(7)$$

$$\Theta_{N-2}(2) = \theta_{N-2}(3) = -12.54 = -\Theta_{N-2}(5) = -\theta_{N-2}(6)$$

$$\Theta_{N-2}(3) = -4.559 = -\theta_{N-2}(5)$$

$$\theta_{N-2}(4) = -3.277 = -\Theta_{N-2}(4)$$

Step 4:

Now we are ready to compare the constrained problem costs, so as to solve

$$V_{N-2}(x_{N-2}, r_{N-2}=1) = \min_{t=1,\ldots,\psi_{N-1}=7} \left\{ V_{N-2}(x_{N-2},1|t) \right\} , \qquad (5.39)$$

as in (5.37).

In figure 5.20 the values $\{\theta_{N-2}(t+1), \Theta_{N-2}(t): t=1,\ldots,6\}$ are plotted (on the x_{N-2} axis) and the regions of x_{N-2} values where each candidate cost applies are indicated. For example, when x_{N-2} is in the interval $(\Theta_{N-3}(3), \theta_{N-2}(4))$, the eligible candidates are $\{V^{1,R}, V^{2,R}, V^{3,R}, V^{4,L}, V^{5,L}, V^{6,L}, V^{7,L}\}$; note that all of the eligible costs over this interval correspond to active hedging to some point.

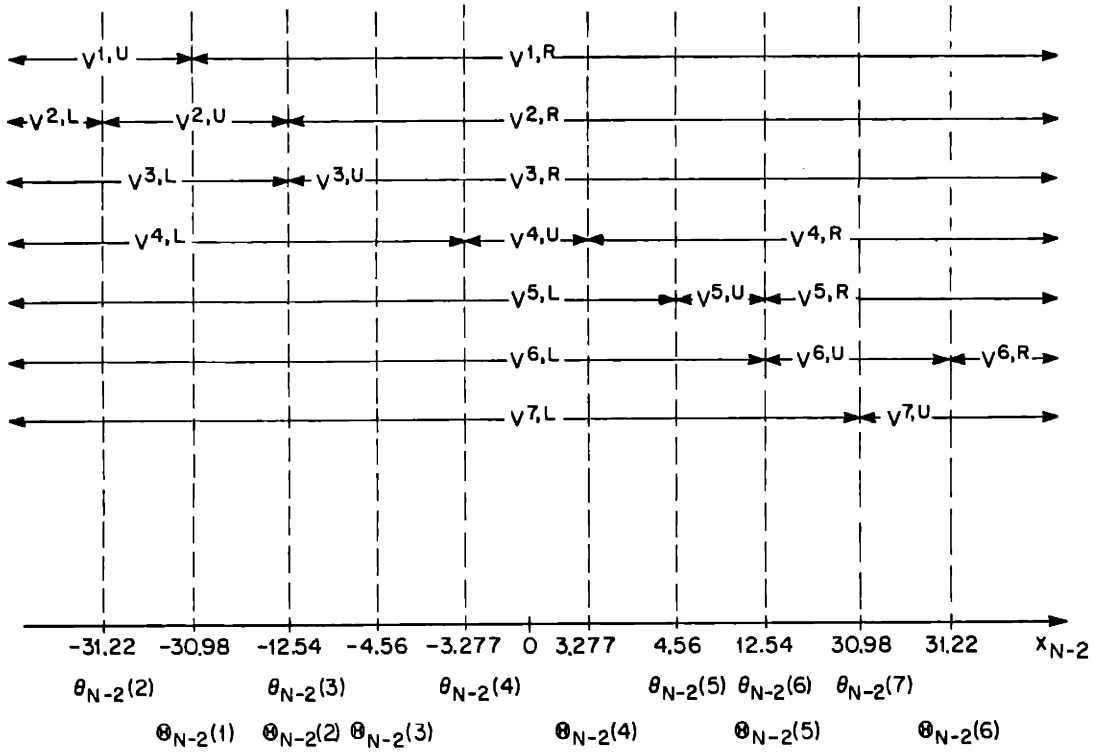

Figure 5.20: Eligible Regions of x_{N-2} values for candidate costs-to-go in example 5.1.

A "brute force" approach to solving (5.39) would be to compute all 19 functions of x_{N-2} shown in figure 5.20, and then to compare those that are eligible over each of the indicated x_{N-2} intervals so as to determine which is optimal.

Fortunately we can avoid many of these calculations and computations from a consideration of the shape of the conditional expected cost-to-go $\hat{V}_{N-1}(x_{N-1}|r_{N-2}=1)$ in figure 5.19, and by using facts (5.31)-(5.36) that were developed in the proof of Proposition 5.1.

Consider $V_{N-2}^{1,R}(x_{N-2},1)$ and $V_{N-2}^{2,L}(x_{N-2},1)$ as functions of x_{N-2}. Each corresponds to driving x_{N-1} to the value $\gamma_{N-1}(1) = -6.750$ (from the right or from the left). But the conditional expected cost-to-go $\hat{V}_{N-1}(x_{N-1}|r_{N-2}=1)$ is continuous at $\gamma_{N-1}(1)$ (and equals 164.5, as shown in figure 5.19). Thus $V_{N-2}^{1,R}(x_{N-2},1)$ equals $V_{N-2}^{2,L}(x_{N-2},1)$ <u>as a function of</u> x_{N-2}. The same is true for each pair of functions $V_{N-2}^{t,R}$, $V_{N-2}^{t+1,L}$ that correspond to driving x_{N-1} to a point $\gamma_{N-1}(t+1)$ where $\hat{V}_{N-1}(x_{N-1}|1)$ is continuous. That is,

$$V_{N-2}^{1,R}(x_{N-2},1) \equiv V_{N-2}^{2,L}(x_{N-2},1) \qquad \text{(driving } x_{N-1} \text{ to } \gamma_{N-1}(1)\text{)}$$

$$V_{N-2}^{2,R}(x_{N-2},1) \equiv V_{N-2}^{3,L}(x_{N-2},1) \qquad \text{(driving } x_{N-1} \text{ to } \gamma_{N-1}(2)\text{)}$$

$$V_{N-2}^{5,R}(x_{N-2},1) \equiv V_{N-2}^{6,L}(x_{N-2},1) \qquad \text{(driving } x_{N-1} \text{ to } \gamma_{N-1}(5)\text{)}$$

$$V_{N-2}^{6,R}(x_{N-2},1) \equiv V_{N-2}^{7,L}(x_{N-2},1) \qquad \text{(driving } x_{N-1} \text{ to } \gamma_{N-1}(6)\text{)} .$$

At a point $x_{N-1}=\gamma$ where $V_{N-1}(x_{N-1}|1)$ is discontinuous, the cost-to-go that corresponds to driving to the side of $x_{N-1}=\gamma$ where $\hat{V}_{N-1}(x_{N-1}|1)$ is <u>less</u> is obviously lower than the cost of driving to the more expensive side of $x_{N-1}=\gamma$. Thus as functions of x_{N-2},

$$V_{N-2}^{4,L}(x_{N-2},1) < V_{N-2}^{3,R}(x_{N-2},1) \qquad \text{(best side is to } \gamma_{N-1}(3)^{+} = -1^{+}\text{)}$$

$$V_{N-2}^{4,R}(x_{N-2},1) < V_{N-2}^{5,L}(x_{N-2},1) \qquad \text{(best side is to } \gamma_{N-1}(4)^{-} = 1^{-}\text{)}$$

Using the above relationships and (5.31)-(5.36) we can eliminate $\{V_{N-2}^{1,R}, V_{N-2}^{2,L}, V_{N-2}^{3,R}, V_{N-2}^{5,L}, V_{N-2}^{5,R}, V_{N-2}^{6,L}, V_{N-2}^{6,R}, V_{N-2}^{7,L}\}$ from consideration by the following steps (each of which is indicated on figure 5.21):

1. As functions of x_{N-2},

   $V_{N-2}^{1,R}(x_{N-2},1) \equiv V_{N-2}^{2,L}(x_{N-2},1) > V_{N-2}^{2,U}(x_{N-2},1)$ (equality at $x_{N-2} = \theta_{N-2}(2)$). Thus

   $V_{N-2}^{1,R}$ cannot be optimal for $x_{N-2} \in (\theta_{N-2}(1), \theta_{N-2}(2))$.

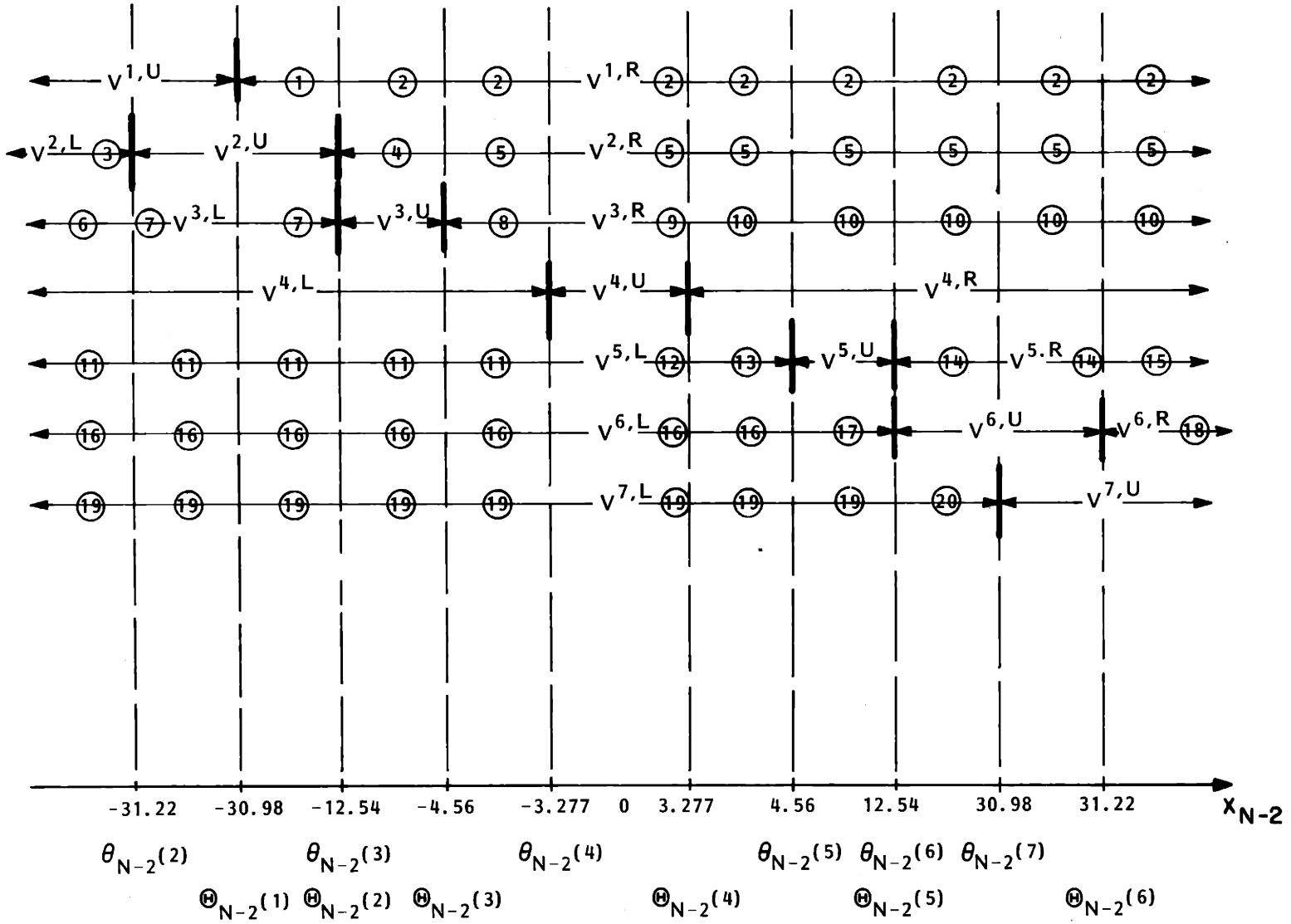

FIGURE 5.21: Eliminating candidate costs; (n) indicates that the specified costs is eliminated over this interval of x_{N-2} values by step 1 in the text.

2. $V_{N-2}^{1,R}$ cannot be optimal for $x_{N-2} > \Theta_{N-2}(2)$ because

$V_{N-2}^{1,R}(x_{N-2},1) \equiv V_{N-2}^{2,L}(x_{N-2},1) > V_{N-2}^{2,R}(x_{N-2},1)$.

3. $V_{N-2}^{2,L}$ cannot be optimal for $x_{N-2} < \theta_{N-2}(2)$ because

$V_{N-2}^{2,L} \equiv V_{N-2}^{1,R} > V_{N-2}^{1,U}$.

4. $V_{N-2}^{2,R}$ cannot be optimal for $x_{N-2} \in (\theta_{N-2}(3), \Theta_{N-2}(3))$

because $V_{N-2}^{2,R} \equiv V_{N-2}^{3,L} > V_{N-2}^{3,U}$.

5. $V_{N-2}^{2,R}$ cannot be optimal for $x_{N-2} > \Theta_{N-2}(3)$ because

$V_{N-2}^{2,R} \equiv V_{N-2}^{3,L} > V_{N-2}^{3,R}$ for $x_{N-2} > \Theta_{N-2}(3)$.

6. $V_{N-2}^{3,L}$ cannot be optimal over $x_{N-2} < \theta_{N-2}(2)$ because

$V_{N-2}^{3,L} \equiv V_{N-2}^{2,R} > V_{N-2}^{2,L}$ for $x_{N-2} < \theta_{N-2}(2)$.

7. $V_{N-2}^{3,L}$ cannot be optimal for $x_{N-2} \in (\theta_{N-2}(2), \Theta_{N-2}(2))$

$V_{N-2}^{3,L} \equiv V_{N-2}^{2,R} > V_{N-2}^{2,U}$.

8. $V_{N-2}^{3,R}$ cannot be optimal for $x_{N-2} \in (\Theta_{N-2}(3), \theta_{N-2}(4))$

because $V_{N-2}^{3,R} > V_{N-2}^{4,L}$.

9. $V_{N-2}^{3,R}$ cannot be optimal for $x_{N-2} \in (\theta_{N-2}(4), \Theta_{N-2}(4))$

because $V_{N-2}^{3,R} > V_{N-2}^{4,L} > V_{N-2}^{4,U}$.

10. $V_{N-2}^{3,R}$ cannot be optimal for $x_{N-2} > \Theta_{N-2}(4)$

because $V_{N-2}^{3,R} > V_{N-2}^{4,L}$ and $V_{N-2}^{4,L} > V_{N-2}^{4,R}$ for $x_{N-2} > \Theta_{N-2}(4)$.

11. $V_{N-2}^{5,L}$ cannot be optimal for $x_{N-2} < \theta_{N-2}(4)$ because

$V_{N-2}^{5,L} > V_{N-2}^{4,R}$ and $V_{N-2}^{4,R} > V_{N-2}^{4,L}$ for $x_{N-2} < \theta_{N-2}(4)$.

12. $V_{N-2}^{5,L}$ cannot be optimal for $x_{N-2} \in (\theta_{N-2}(4), \Theta_{N-2}(4))$

because $V_{N-2}^{5,L} > V_{N-2}^{4,R} > V_{N-2}^{4,U}$.

13. $V_{N-2}^{5,L}$ cannot be optimal for $x_{N-2} \in (\Theta_{N-2}(4), \theta_{N-2}(5))$

because $V_{N-2}^{5,L} > V_{N-2}^{4,R}$.

14. $V_{N-2}^{5,R}$ cannot be optimal for $x_{N-2} \in (\theta_{N-2}(6), \Theta_{N-2}(6))$

because $V_{N-2}^{5,R} \equiv V_{N-2}^{6,L} > V_{N-2}^{6,U}$.

15. $V_{N-2}^{5,R}$ cannot be optimal for $x_{N-2} > \Theta_{N-2}(6)$ because

$V_{N-2}^{5,R} = V_{N-2}^{6,L} > V_{N-2}^{6,R}$ for $x_{N-2} > \Theta_{N-2}(6)$.

16. $V_{N-2}^{6,L}$ cannot be optimal for $x_{N-2} < \theta_{N-2}(5)$ because

$$V_{N-2}^{6,L} \equiv V_{N-2}^{5,R} > V_{N-2}^{5,L} \quad \text{for} \quad x_{N-2} < \theta_{N-2}(5).$$

17. $V_{N-2}^{6,L}$ cannot be optimal for $x_{N-2} \in (\theta_{N-2}(5), \Theta_{N-2}(5))$

because $V_{N-2}^{6,L} \equiv V_{N-2}^{5,R} > V_{N-2}^{5,U}$.

18. $V_{N-2}^{6,R}$ cannot be optimal for $x_{N-2} > \Theta_{N-2}(6)$ because

$$V_{N-2}^{6,R} \equiv V_{N-2}^{7,L} > V_{N-2}^{7,U} .$$

19. $V_{N-2}^{7,L}$ cannot be optimal for $x_{N-2} < \theta_{N-2}(6)$ because

$$V_{N-2}^{7,L} \equiv V_{N-2}^{6,R} > V_{N-2}^{6,L} \quad \text{for} \quad x_{N-2} < \theta_{N-2}(6).$$

20. $V_{N-2}^{7,L}$ cannot be optimal for $x_{N-2} \in (\theta_{N-2}(6), \theta_{N-2}(7))$

because $V_{N-2}^{7,L} \equiv V_{N-2}^{6,R} > V_{N-2}^{6,U}$.

Thus the only constrained costs left in consideration are $V_{N-2}^{4,L}$ and $V_{N-2}^{4,R}$. For this problem, active hedging to a point can occur only to

$$x_{N-1} = \gamma_{N-1}(3)^{+} = \nu_{12}(1)^{+} = -1^{+}$$

or

$$x_{N-1} = \gamma_{N-1}(4)^{-} = \nu_{12}(2)^{-} = 1^{-} \quad .$$

We see from figure 5.21 that

- $V_{N-2}^{4,U}$ is optimal for $\theta_{N-2}(4) \leq x_{N-2} \leq \Theta_{N-2}(4)$
- $V_{N-2}^{4,L}$ is optimal for $\Theta_{N-2}(3) \leq x_{N-2} \leq \theta_{N-2}(4)$
- $V_{N-2}^{4,R}$ is optimal for $\Theta_{N-2}(4) \leq \gamma_{N-2} \leq \theta_{N-2}(5)$.

To complete the minimization of (5.39), we first solve for the intersections of $V_{N-2}^{4,L}(x_{N-2},1)$ and $V_{N-2}^{3,U}(x_{N-2},1)$. We find that they intersect at

$$x_{N-2} = -6.977, -2.1414$$

and that for $x_{N-2} < -6.977$ $V_{N-2}^{4,L} > V_{N-2}^{3,U}$. Thus

- $V_{N-2}^{3,U}$ is optimal for

  $\theta_{N-2}(3) \leq x_{N-2} \leq -6.977$

- $V_{N-2}^{4,L}$ is optimal for

  $-6.977 \leq x_{N-2} \leq \theta_{N-2}(4)$.

In addition,

- $V_{N-2}^{4,L}$ doesn't interesect $V_{N-2}^{2,U}$ in $(\theta_{N-2}(2), \Theta_{N-2}(2))$

and

- $V_{N-2}^{4,L}$ doesn't intersect $V_{N-2}^{1,U}$

  in $(-\infty, \theta_{N-2}(1))$.

Thus to complete the determination of $V_{N-2}(x_{N-2}, r_{N-2}=1)$ for $x_{N-2} \leq 0$, we need only to find the intersections of $V_{N-2}^{2,U}$ and $V_{N-2}^{1,U}$.

These occur at

$$x_{N-2} = -31.18,\ -7.846$$

and for $x_{N-2} < -31.18$, $V_{N-2}^{1,U} < V_{N-2}^{2,U}$.

Thus from figure 5.21 we see that

- $V_{N-2}^{1,U}$ is optimal for

  $$x_{N-2} \leq -31.18$$

- $V_{N-2}^{2,U}$ is optimal for

  $$-31.18 \leq x_{N-2} \leq -12.54 = \theta_{N-2}(3).$$

From the symmetry of this problem we need only consider $x_{N-2} \leq 0$ or $x_{N-2} \geq 0$ (this is easily verified from the $V_{N-2}(x_{N-2}, 1|t)$ computed above). Collecting all of the above information we thus have the following:

The optimal expected cost-to-go $V_{N-2}(x_{N-2},r_{N-2}=1)$ and control law $u_{N-2}(x_{N-2},r_{N-2}=1)$ have

$$m_{N-2}(1) = 9$$

pieces, with joining points

$$\begin{aligned}
\delta_{N-2}(1) &= -31.18 \\
\delta_{N-2}(2) &= -12.54 \\
\delta_{N-2}(3) &= -6.977 \\
\delta_{N-2}(4) &= -3.277 \\
\delta_{N-2}(5) &= 3.277 \\
\delta_{N-2}(6) &= 6.977 \\
\delta_{N-2}(7) &= 12.54 \\
\delta_{N-2}(8) &= 31.18
\end{aligned} \tag{5.40}$$

$$V_{N-2}(x_{N-2},r_{N-2}=1) = \begin{cases} V_{N-2}^{1,U} & \text{if} \quad x_{N-2} \leq \delta_{N-2}(1) \\ V_{N-2}^{2,U} & \text{if} \quad \delta_{N-2}(1) \leq x_{N-2} \leq \delta_{N-2}(2) \\ V_{N-2}^{3,U} & \text{if} \quad \delta_{N-2}(2) \leq x_{N-2} \leq \delta_{N-2}(3) \\ V_{N-2}^{4,L} & \text{if} \quad \delta_{N-2}(3) \leq x_{N-2} \leq \delta_{N-2}(4) \\ V_{N-2}^{4,U} & \text{if} \quad \delta_{N-2}(4) \leq x_{N-2} \leq \delta_{N-2}(5) \\ V_{N-2}^{4,R} & \text{if} \quad \delta_{N-2}(5) \leq x_{N-2} \leq \delta_{N-2}(6) \\ V_{N-2}^{5,U} & \text{if} \quad \delta_{N-2}(6) \leq x_{N-2} \leq \delta_{N-2}(7) \\ V_{N-2}^{6,U} & \text{if} \quad \delta_{N-2}(7) \leq x_{N-2} \leq \delta_{N-2}(8) \\ V_{N-2}^{7,U} & \text{if} \quad \delta_{N-2}(8) \leq x_{N-2} \end{cases} \tag{5.41}$$

That is,

$$\begin{aligned} K_{N-2}(1{:}1) &= .7821909 = K_{N-2}(9{:}1) \\ K_{N-2}(2{:}1) &= .7849462 = K_{N-2}(8{:}1) \\ K_{N-2}(3{:}1) &= .780658 = K_{N-2}(7{:}1) \\ K_{N-2}(4{:}1) &= 1 = K_{N-2}(6{:}1) \\ K_{N-2}(5{:}1) &= .6948682 \end{aligned} \tag{5.42}$$

$$\begin{aligned} H_{N-2}(2{:}1) &= .1075268 = -H_{N-2}(8{:}1) \\ H_{N-2}(4{:}1) &= 2 = -H_{N}(6{:}1) \\ H_{N-2}(1{:}1) &= H_{N-2}(3{:}1) = H_{N-2}(5{:}1) = H_{N-2}(7{:}1) = H_{N-2}(9{:}1) = 0 \end{aligned}$$

$$G_{N-2}(2:1) = .674059 = G_{N-2}(8:1)$$

$$G_{N-2}(4:1) = 3.2772727 = G_{N-2}(6:1)$$

$$G_{N-2}(1:1) = G_{N-2}(3:1) = G_{N-2}(5:1) = G_{N-2}(7:1) = G_{N-2}(9:1) = 0$$

$$L_{N-2}(1:1) = .7821909 \qquad L_{N-2}(9:1)$$

$$L_{N-2}(2:1) = .7849462 \qquad L_{N-2}(8:1)$$

$$L_{N-2}(3:1) = .780658 = L_{N-2}(7:1)$$

$$L_{N-2}(4:1) = 1 = L_{N-2}(6:1)$$

$$L_{N-2}(5:1) = .6948682$$

$$F_{N-2}(2:1) = -.0537634 = -F_{N-2}(8:1)$$

$$F_{N-2}(4:1) = -1 = -F_{N-2}(6:1)$$

$$F_{N-2}(1:1) = F_{N-2}(3:1) = F_{N-2}(5:1) = F_{N-2}(7:1) = F_{N-2}(9:1) = 0 \ .$$

The value of the x_{N-1} obtained by application of the optimal control laws is given by

$$x_{N-1}(x_{N-2}, r_{N-2}=1) = \begin{cases} .2178091\, x_{N-2} & \text{if } x_{N-2} \leq \delta_{N-2}(1) \\ .2150538 x_{N-2} - .0537634 & \text{if } \delta_{N-2}(1) \leq x_{N-2} \leq \delta_{N-2}(2) \\ .219342\, x_{N-2} & \text{if } \delta_{N-2}(2) \leq x_{N-2} \leq \delta_{N-2}(3) \\ -1^{+} & \text{if } \delta_{N-2}(3) \leq x_{N-2} \leq \delta_{N-2}(4) \\ .305138\, x_{N-2} & \text{if } \delta_{N-2}(4) \leq x_{N-2} \leq \delta_{N-2}(5) \\ +1^{-} & \text{if } \delta_{N-2}(5) \leq x_{N-2} \leq \delta_{N-2}(6) \\ .219342\, x_{N-2} & \text{if } \delta_{N-2}(6) \leq x_{N-2} \leq \delta_{N-2}(7) \\ .2150538 x_{N-2} + .0537634 & \text{if } \delta_{N-2}(7) \leq x_{N-2} \leq \delta_{N-2}(8) \\ .2178091\, x_{N-2} & \text{if } \delta_{N-2}(8) \leq x_{N-2} \end{cases}$$

(5.43)

The optimal expected cost-to-go, control law and obtained x_{N-1} values are shown in figures 5.22, 5.23 and 5.24, respectively.

From the solution of this stage of the example problem we can make the following observations:

1. As in the last stage solution, the optimal control law is discontinuous at (and only at) x_{N-2} values where $V_{N-2}(x_{N-2}, r_{N-2}=1)$ decreases discontinuously; that is at $\delta_{N-2}(1)$, $\delta_{N-2}(3)$, $\delta_{N-2}(5)$, $\delta_{N-2}(8)$.

2. At time k=N-2 (as at time k=N-1), active hedging occurs only to discontinuous points of the form transition probabilities:

   $\nu_{12}(1)=-1 \quad \nu_{12}(2)=1$.

3. We see that for this example system:

   $m_N(1)=1$

   $m_{N-1}(1)=5$

   $m_{N-2}(1)=9$

   That is, as (N-k) increases the number of pieces is increasing <u>linearly</u>, by

   2·(number of probability pieces, $\bar{\nu}_{12}=2$) = 4

   at each time.

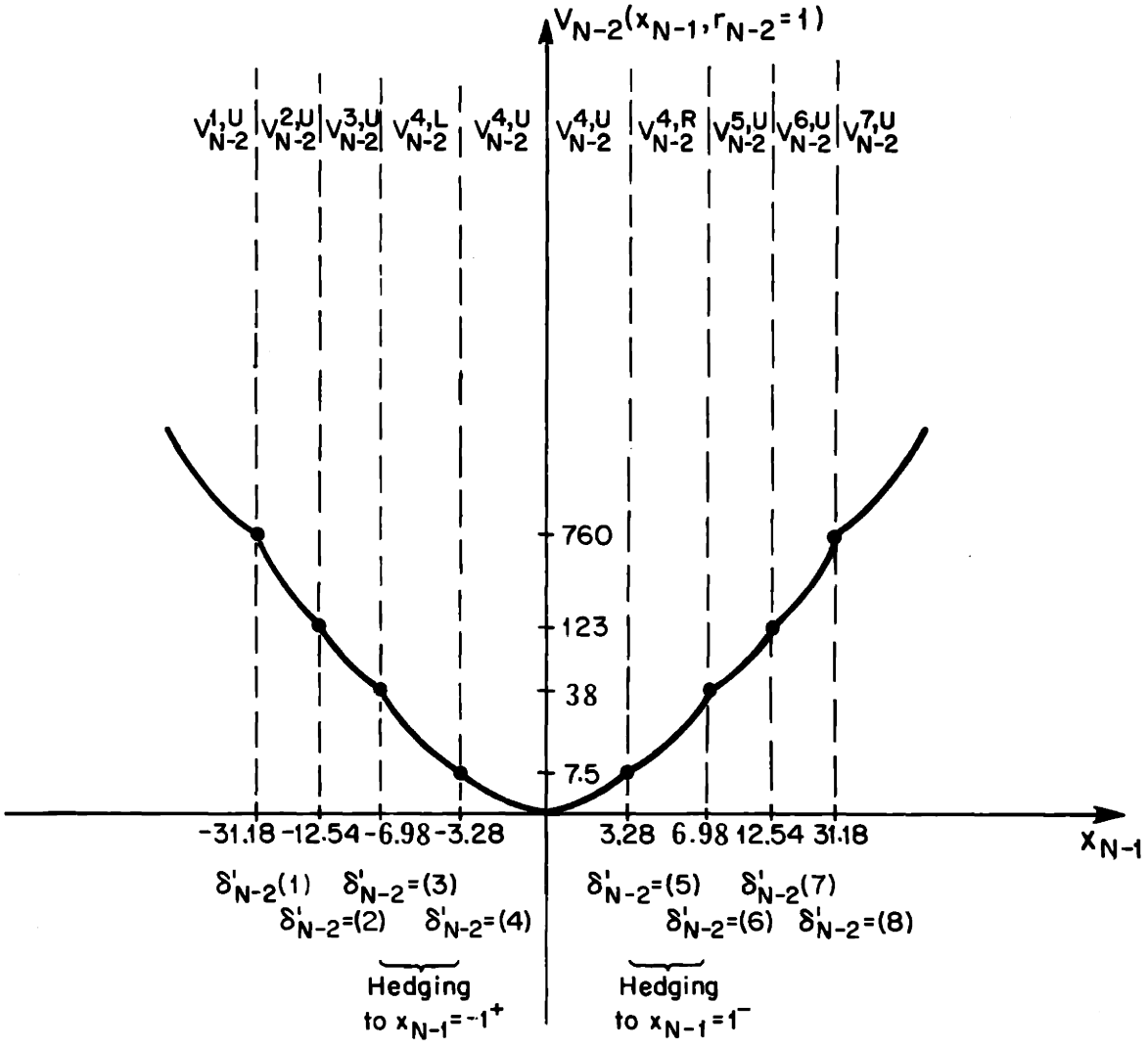

FIGURE 5.22: Optimal expected cost-to-go from $(x_{N-2}, r_{N-2}=1)$ in example 5.1. (not drawn to scale).

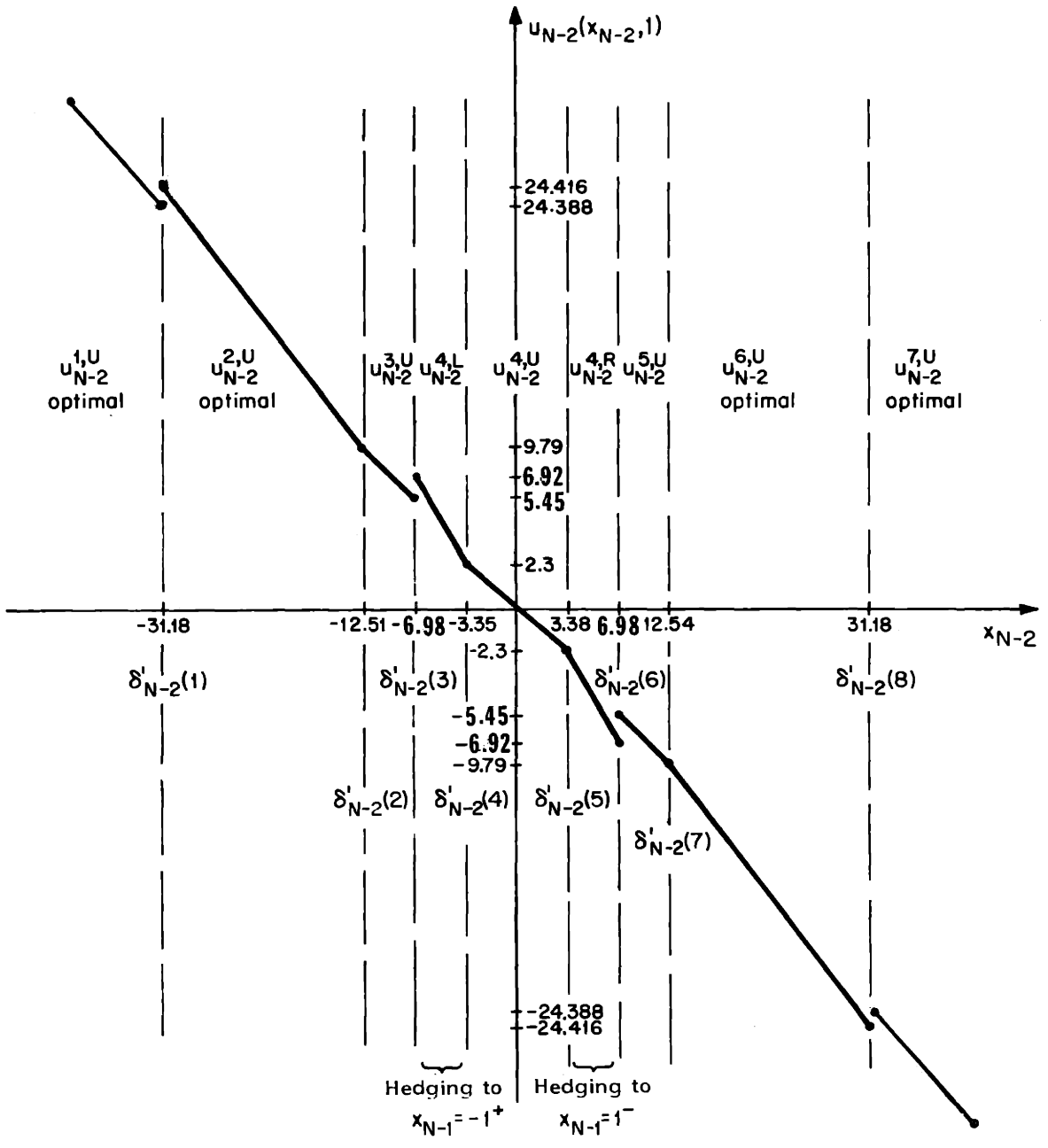

FIGURE 5.23: Optimal control law from $(x_{N-2}, r_{N-2}=1)$ in example 5.1. (not drawn to scale).

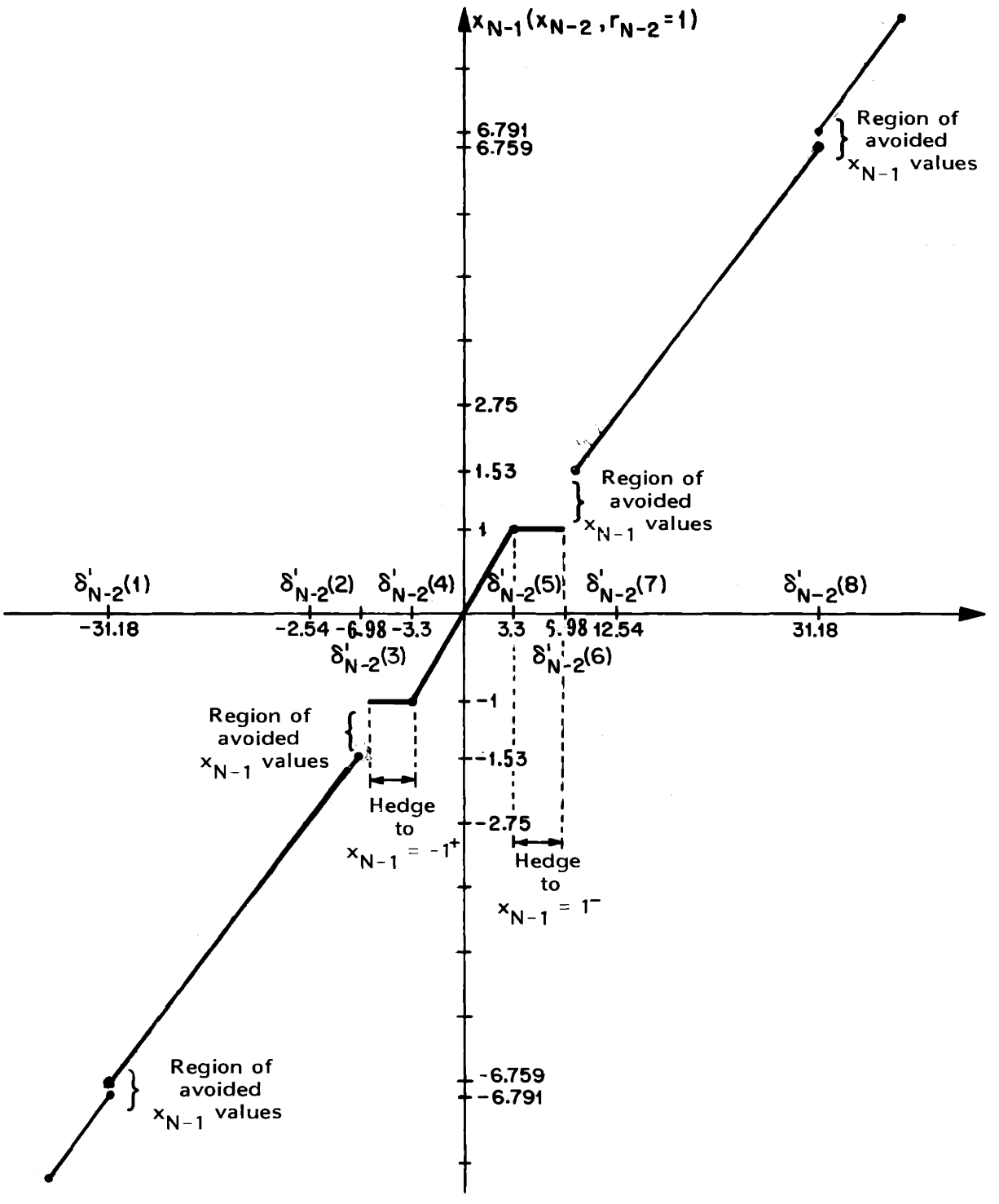

FIGURE 5.24: x_{N-1} values obtained using the optimal control from $(x_{N-2}, r_{N-2}=1)$ in example 5.1. (not drawn to scale).

4. There are four regions of x_{N-1} avoidance:

$$x_{N-1} \notin (-6.759, -6.791) \qquad x_{N-1} \notin (1, 1.53)$$

$$x_{N-1} \notin (-1.53, -1) \qquad x_{N-1} \notin (+6.759, 6.791)$$

As the previous stage, these regions of avoidance correspond to x_{N-2} values where $V_{N-2}(x_{N-2}, r_{N-2}=1)$ is not differentiable. That is, to

$$\{(\delta_{N-2}(1), \delta_{N-2}(3), \delta_{N-2}(5), \delta_{N-2}(7)\}$$

Note that there is no hedging-to-a-point (from time N-2) associated with $\delta_{N-2}(1)$ and $\delta_{N-2}(7)$.

5. In the determination of $V_{N-2}(x_{N-2}, r_{N-2}=1)$ above, we did not have to compute and compare many of the quadratic functions listed in (5.38).

The five phenomena listed above are examined for the general problem in the next section, and are characterized by Propositions 5.2, 5.3 and Corollary 5.4. From consideration of both stages of this example, we can make the following additional observations and claims that are addressed in the next chapters:

6. The boundaries of the left and right endpieces are much further from zero at time N-2 than at time N-1:

$$\delta_{N-2}(1) = -6.75 = -\delta_{N-1}(4)$$

$$\delta_{N-2}(1) = -31.2 = -\delta_{N-2}(8)$$

This is an example of a general property: except for pathological problems, the range of x_k values for which the optimal controller involves changing the probability piece that the state will be in (at some time $\{k+1, k+2,\ldots,N-1,N\}$) monotonely increases as (N-k) increases. That is, the endpieces move "further out" from zero as (N-k) increases.

7. The size of the middle piece, where active hedging serves no useful purpose, also grows between k=N-1 and k=N-2, but more slowly than the distance to the end pieces:

   - at time k=N-1, the middle piece is
     $(\delta_{N-1}(2), \delta_{N-1}(3) = (-2.75, 2.75)$
   - at time k=N-2, the middle piece is
     $(\delta_{N-2}(4), \delta_{N-2}(5) = (-3.3, 3.3)$.

This suggests a general property: as (N-k) increases, the sizes of the middle pieces converge monotonely (increasing or decreasing) to steady-state values.

8. Note that the curves

$$V_{N-2}^{1,U} = V_{N-2}^{7,U} \quad \text{and} \quad V_{N-2}^{3,U} = V_{N-2}^{5,U}$$

are very close together (see (5.41)); in fact, they are so close that figure 5.22 could not be drawn to scale and still show the behavior of $V_{N-2}(x_{N-2}, r_{N-2}=1)$ at its joining points. This suggests that even though the number of pieces $m_k(j)$ of $V_k(x_k, r_k=j)$ increases as (N-k) increases, many of them may be "almost the same." This phenomena is the basis of a "finite look-ahead" approximation to the optimal steady-state (infinite time horizon) solution of the general problem, which is developed in chapter 7.

Setting aside for now the steady-state phenomena (6)-(8) above, we proceed to clarify the combinatoric properties (1)-(5), in the following section.

5.6 Some Combinatoric and Qualitative Issues

In this section we examine several combinatoric and qualitative issues related to the (off-line) determination of the optimal control laws and costs of Proposition 5.1. Aspects of the problem that are addressed here include:

- the nature of active hedging; examining what values of x an optimal controller will hedge to and why, and what values of x will be avoided and why,
- determining how many of the candidate costs (and control laws) in (5.38) must actually be computed and compared,
- characterizing the number of pieces, $m_k(j)$ of the optimal expected cost $V_k(x_k, r_k=j)$ and control law $u_k(x_k, r_k=j)$.

The topics studied here are useful in the specification of an efficient way to carry out the algorithm steps that are indicated in the proof of Proposition 5.1.

A "brute force" way of determining $V_k(x_k, r_k=j)$ in (5.37) is to compute and compare all of the

$$3\psi_{k+1}^{j} - 2 = 1 + 3\left|\bigcup_{i \in \mathcal{C}_j} [\{\nu_{ji}(t): t=1,\ldots,\bar{\nu}_{ji}-1\} \cup \{\delta_{k+1}^{j}(t): t=1,\ldots,m_{k+1}(i)-1\}\right| \tag{5.44}$$

candidate quadratic cost functions listed in (5.38) (the right hand side of (5.44) follows from (5.23)). Thus

---

[1] As done in example 5.2.

$$3\psi^{j}_{k+1} - 2 \leq 1 + 3 \sum_{i=1}^{M} \left[\nu_{ji} + m_{k+1}(i) - 2 \right] \qquad (5.45)$$

where equality in (5.45) corresponds to the "worst case"

$|c_j| = M$ all forms are accessible to each other in one step

and all the $\nu_{ji}(\ell)$ $\ell = 1, \ldots, \bar{\nu}_{ji} - 1$

$\delta^{j}_{k+1}(t)$ $t = 1, \ldots, m_{k+1}(i) - 1$ $i = 1, \ldots, M$

values are different.

This suggests that the number of pieces, $m_k(j)$, of each $V_k[x_k, r_k = j]$ might be growing geometrically (with powers of 3) as N-k increases. Fortunately, this is <u>not</u> the case, as suggested in the previous section. The underlying reason that many of the candidate costs in (5.38) can be discarded is the nonincreasing-slope condition (3) of Proposition 5.1. In particular, the optimal controller only actively hedges to x values that are discontinuous points of form transition probabilities (ie, to ν's). There is no active hedging to joining points of the (next-stage forward) expected costs (ie, to δ's) precisely because the slope of these costs is nonincreasing at such points.

These facts will be established as we pursue the following:

(1) first we show that many of the candidate costs in (5.38) cannot be optimal (for any x_k value) and hence they need not be computed (Proposition 5.2),

(2) Next we show that each candidate cost in (5.38) can be optimal over, at most, a single interval of x_k values. This bounds the number of pieces $m_k(j)$ of $V_k(x_k, r_k=j)$. (Proposition 5.3 and Corollary 5.4).

The following proposition relates values of x_{k+1} that are hedged to with discontinuities of the expected cost-to-go $\hat{V}_{k+1}(x_{k+1}|r_k=j)$, and it eliminates many of the candidate costs in (5.38) from consideration.

Proposition 5.2

The optimal control law $u_k(x_k, r_k=j)$ can only hedge to points that are discontinuities of the conditional expected cost-to-go $\hat{V}_{k+1}(x_{k+1}; r_k=j)$. That is

$$\begin{pmatrix} \text{hedging} \\ \text{to some} \\ \text{point x from} \\ (x_k, r_k=j) \end{pmatrix} \Rightarrow \begin{pmatrix} \text{x is a discontinuous point} \\ \text{of form transition probability} \\ \quad p(j,i;x) \\ \text{for some } i \in C_j \end{pmatrix} .$$

Only

$$\zeta^j_{k+1} = \psi^j_{k+1} + \left| \bigcup_{i \in C_j} \{\nu_{ji}(\ell): \ell=1,\ldots,\bar{\nu}_{ji}-1\} \right| \tag{5.46}$$

of the candidate costs listed in (5.38) must actually be computed and compared in (5.37) so as to determine $V_k(x_k, r_k=j)$.

These costs are:

(i) for each x_{k+1} region $\Delta^j_{k+1}(t)$, $t=1,\ldots,\psi^j_{k+1}$, the "unconstrained" cost $V^{t,U}_k(x_k,j)$

(ii) for each form transition probability discontinuity $\nu_{ji}(\ell)$ (for $i\in c_j$, $\ell=1,\ldots,\bar{\nu}_{ji}-1$), which is denoted by $\gamma^j_{k+1}(t)$ for some $t\in\{1,\ldots,\psi^j_{k+1}-1\}$, we must consider

- the "left constrained" cost $V^{t+1,L}_k(x_k,j)$ if
$$\hat{V}_{k+1}([\gamma^j_{k+1}(t)]^-;j) \geq \hat{V}_{k+1}([\gamma^j_{k+1}(t)]^+;j)$$
- the "right constrained" cost $V^{t,R}_k(x_k,j)$. is
$$\hat{V}_{k+1}([\gamma^j_{k+1}(t)]^+;j) > \hat{V}_{k+1}([\gamma^j_{k+1}(t)]^-;j).$$

□

This proposition is proved in Appendix C.3. The proof follows from certain relationships between the relative values of $\theta^j_k(t)$ and $\Theta^j_k(t)$.

From Proposition 5.2 we know that the mapping

$$x_k \mapsto x_{k+1}(x_k, r_k=j)$$

need not be one-to-one, in that hedging to points may occur.

The following proposition lists a number of general qualitative properties of the optimal controller that are suggested by example 5.1. In particular, it characterizes the behavior of the $x_k \mapsto x_{k+1}(x_k, r_k=j)$ mapping.

Proposition 5.3:

The optimal controller of Proposition 5.1 has the following properties:

(1) At each time k and in each form $j \in M$, between joining points $\{\delta_k^j(t): t=1,\ldots,m_k(j)-1\}$ of $V_k(x_k, r_k=j)$:

$$u_k(x_k, r_k=j) = \frac{-b(j)}{2a(j)R(j)} \frac{\partial V_k(x_k, r_k=j)}{\partial x_k} \tag{5.47}$$

$$x_{k+1}(x_k, r_k=j) = a(j)x_k - \frac{b^2(j)}{2a(j)R(j)} \frac{\partial V_k(x_k, r_k=j)}{\partial x_k} \tag{5.48}$$

(here $a(j)R(j)\neq 0$, $b(j)\neq 0$).

(2) At those joining points δ where the slope of $V_k(x_k, r_k=j)$ does not change $\left(\text{ie, } \left.\frac{\partial V_k(x_k, r_k=j)}{\partial x_k}\right|_{x_k=\delta} \text{ exists}\right)$, $u_k(x_k, r_k=j)$ and $x_{k+1}(x_k, r_k=j)$ are continuous functions of x_k.

(3) At those joining points $\delta_k^j(t)$ where the slope of $V_k(x_k, r_k=j)$ decreases discontinuously $\left(\text{ie } \left.\frac{\partial V_k(x_k, r_k=j)}{\partial x_k}\right|_{x_k=\delta^+} < \left.\frac{\partial V_k(x_k, r_k=j)}{\partial x_k}\right|_{x_k=\delta^-}\right)$,

(i) $u_k(x_k, r_k=i)$ increases discontinuously at δ when $\frac{b(j)}{a(j)} > 0$ (and decreases discontinuously at δ when $\frac{b(j)}{a(j)} < 0$)

(ii) the mapping $x_k \longmapsto x_{k+1}(x_k, r_k=j)$ <u>increases</u>

discontinuously at δ when $a(j) > 0$) (and decreases discontinuously at δ when $a(j) < 0$),

(4) The mapping

$$x_k \longmapsto x_{k+1}(x_k, r_k=j)$$

has the following properties:

(i) the mapping is <u>monotonely nondecreasing</u> if

$a(j) > 0$ (and monotonely nonincreasing if

$a(j) < 0$) for each $j \in \underline{M}$

(ii) it consists of $m_k(j)$ line segments:

- one line segment with positive slope if

  $a(j) > 0$ (negative slope if $a(j) < 0$) for

  each x_k region where an "unconstrained cost"

  $V_k^{t,U}(x_k, r_k=1)$ is optimal

$$V_k(x_k, r_k=j) = V_k^{t,U}(x_k, r_k=j) \qquad t \in \{1, \ldots, \psi_{k+1}^j\}$$

$$x_{k+1} = \left[\frac{a(j)R(j)}{R(j)+b^2(j)\hat{K}_{k+1}^j(t)}\right] x_k - \frac{b^2(j)\hat{H}_{k+1}^j(t)}{2[R(j)+b^2(j)\hat{K}_{k+1}^j(t)]} \tag{5.49}$$

- a <u>constant</u> line segment for each x_k region

  where there is active hedging-to-a-point:

$$x_{k+1} = \gamma_{k+1}^j(t) \qquad t \in \{1, \ldots, \psi_{k+1}^j - 1\}$$

(iii) there are regions of x_{k+1} avoidance associated with (and only with) each $x_k=\delta$ value where the slope of $V_k(x_k,r_k=j)$ decreases discontinuously.

(5) Each candidate linear control law (associated with the costs listed in (5.38)) can be optimal over, at most, a single interval of x_k values.

□

The proof of this appears in Appendix C.4, and it will be verified at the end of this section for example 5.1.

Proposition 5.2 restricts the number of candidate costs that must be considered in (5.37), and fact (5) of Proposition 5.3 says that each candidate can be optimal over at most one x_k interval. Thus we immediately have :

Corollary 5.4:

The number of pieces of the optimal expected costs-to-go $V_k(x_k,r_k=j)$ and their associated control laws are bounded above by

$$m_k(j) \leq \zeta_{k+1}^j = \psi_{k+1}^j + \left| \bigcup_{i \in c_j} \{\nu_{ji}(\ell): \ell=1,\ldots,\bar{\nu}_{ji}-1\} \right| . \qquad (5.50)$$

A weaker bound which follows from (5.24) is

$$m_k(j) \leq \zeta_{k+1}^j \leq 1 + \sum_{i \in c_j} (m_{k+1}(i)-1) + 2\left| \bigcup_{i \in c_j} \{\nu_{ji}(\ell): \ell=1,\ldots,\bar{\nu}_{ji}-1\} \right| . \qquad (5.51)$$

□

Note that in (5.50) the factor of 3 in (5.45) is eliminated. Corollary 5.4 says that the number of pieces in each optimal expected cost $V_k(x_k, r_k=j)$, grows

- at most linearly with the number of transition probability pieces
- at most geometrically with the number of elements of $\mathcal{C}_j$; that is, the number of forms accessible from j in one time step.

Suppose that the piecewise-constant form transition probabilities in (5.3) are <u>approximations</u> of the true probabilities. From (5.50)-(5.51) we see that there is a tradeoff between

- the accuracy of p(j,i:x) approximations (in terms of the number of pieces $\overline{\nu}_{ji}$ that are used)

versus

- the complexity of
  - the algorithm computations (in terms of ζ_{k+1}^{j})

  and
  - the resulting controller (in terms of the number of $V_k(x_k, r_k=j)$ and $u_k(x_k, r_k=j)$ pieces, $m_k(j)$).

We conclude this section by applying the Propositions and Corollaries developed here to example 5.1.

Example 5.1, continued:

We have already seen that hedging-to-a-point from $(x_{N-1}, r_{N-1}=1)$ and from $(x_{N-2}, r_{N-2}=1)$ is only to the discontinuities of the form transition probabilities $\nu_{12}(1) = -1$ and $\nu_{12}(2) = +1$ (see (5.19) and (5.43)).

Since for this example

$$\left| \bigcup_{i \in \mathcal{C}} \{\nu_{1i}(\ell): \ell=1,2\} \right| = 2,$$

and $\psi_N = 3$, $\psi_{N-1} = 7$,

the number of candidate costs that actually had to be computed and compared (according to (5.46) of Proposition 5.2) was

$$\zeta_N = 5$$

$$\zeta_{N-1} = 9 \quad .$$

From the shapes of $\hat{V}_N(x_N | r_{N-1}=1)$ (figure 5.12) and $\hat{V}_{N-1}(x_{N-1} | r_{N-2}=1)$ (figure 5.19), Proposition 5.2 specifies that these candidates are:

for $V_{N-1}(x_{N-1}, r_{N-1}=1)$:

$$\left\{ V_{N-1}^{1,U},\ V_{N-1}^{2,L},\ V_{N-1}^{2,U},\ V_{N-1}^{2,R},\ V_{N-1}^{3,U} \right\} \tag{5.52}$$

for $V_{N-2}(x_{N-2}, r_{N-2}=1)$:

$$\left\{ \begin{array}{lll} V_{N-2}^{1,U}, & V_{N-2}^{2,U}, & V_{N-2}^{3,U}, \\ V_{N-2}^{4,U}, & V_{N-2}^{5,U}, & V_{N-2}^{6,U}, \\ V_{N-2}^{7,U}, & V_{N-2}^{4,R}, & V_{N-2}^{4,L} \end{array} \right\} \tag{5.53}$$

.

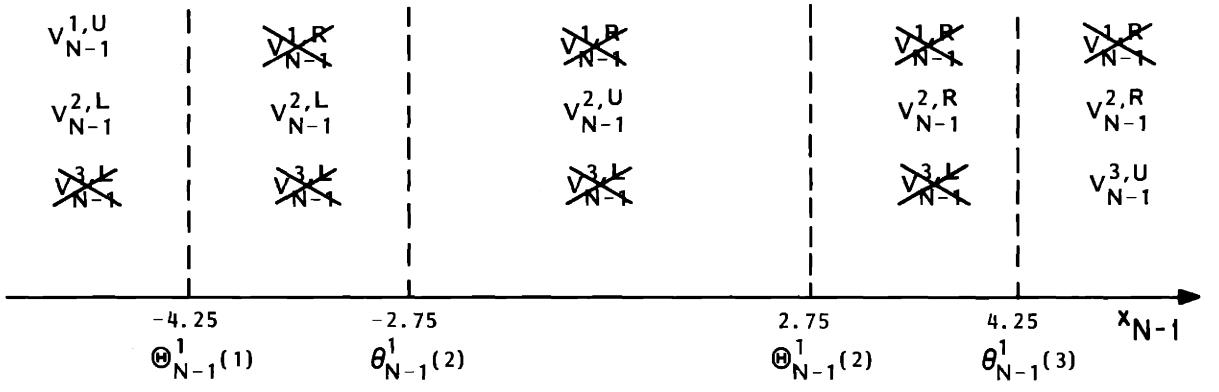

FIGURE 5.25: Eligible costs for $V_{N-1}(x_{N-1}, r_{N-1}=1)$ in example 5.1.

The x's in the figure indicate candidate costs that are eliminated from consideration in (5.37) by Proposition 5.2.

Thus we see that we did not have to compute $V_{N-1}^{1,R}$ and $V_{N-1}^{3,L}$ in Section 5.3. The application of Proposition 5.2 for $V_{N-1}(x_{N-1}, r_{N-1}=1)$ is shown pictorially in figure 5.25. The candidate costs listed in (5.53) are precisely those that we found we had to compute in section 5.5. We have already shown[1] that Proposition 3.2, 3.3 and Corollary 3.4 hold for this problem at k=N-1, k=N-2. Note that the bound (5.50) in Corollary 5.4 holds with equality, and

$$m_{N-k}(1) \leq 1 + 4k$$

follows directly.

5.7 Summary

In this chapter we have considered a class of nonlinear stochastic JLQ control problems and have developed a procedure for their solution. The basic idea of this solution procedure is simple and the solution form is conceptually straightforward (although the notation required becomes quite complex).

We have identified some basic properties of the problem that reduce the combinatorics involved in the solution procedure. These facts (and others to be developed) will be exploited in the construction of an efficient solution algorithm in chapter 7.

---

[1] In the previous section.

We have also identified some basic qualitative properties of the optimal controller. These include hedging-to-a-point, regions of avoidances, and endpieces and middlepieces of the expected costs-to-go and control laws.

From analysis of the optimal controllers developed here we can gain insight into the structure and nature of controllers that use active hedging. In chapters 6 and 7 we will continue our examination of the qualitative properties of these controllers. In particular, the steady-state behavior of the infinite time horizon problem is examined.

6. QUALITATIVE PROPERTIES OF THE SCALAR x-DEPENDENT JLQ CONTROLLER

6.1 Introduction

In this chapter we consider certain qualitative properties of the optimal JLQ controller of chapter 5, as the number of stages (N-k) from the terminal time increases. We will restrict our attention to JLQ problems like those of chapter 5, but for simplicity we make the additional assumptions that

$$(1) \quad P(j) = G_T(j)=0 \tag{6.1}$$

$$(2) \quad S(j) = H_T(j)=0 \tag{6.2}$$

$$(3) \quad a(j)> 0 \tag{6.3}$$

$$(4) \quad Q(j)> 0 \tag{6.4}$$

for all $j \in \underline{M}$.

We begin in sections 6.2 and 6.3 by examining the behavior of the optimal control laws and expected costs-to-go when x is far from zero ("endpieces") and when x is near zero ("middlepieces"). Over these regions of x values, $V_k(x_k,r_k=j)$ can be computed from sets of recursive difference equations without carrying out all of the steps of section 5.4. The equations specifying these endpieces and middlepieces of the optimal controller are the same as those that solve certain corresponding x-independent JLQ problems (as in chapter 3).

In section 6.4 we obtain upper and lower bounds on the costs $V_k(x_k,r_k=j)$ when x_k is between these endpiece and middlepiece regions. When the system is stabilizable in each form $j \in \underline{M}$, the difference equations

describing these bounds converge to steady-state values. These bounds can themselves be bounded by certain x-independent JLQ problems (of chapter 3). From this fact we obtain sufficient (but not necessary) conditions for the upper and lower bounds on $V_k(x_k, r_k=j)$ to converge to steady-state values when not all of the forms have stabilizable dynamics.

In sections 6.5 and 6.6 we illustrate certain fundamental qualitative properties of the optimal JLQ controller. We do this by exploring a particular class of problems in greater detail. Specifically we examine the parametric dependence of

- hedging regions: these are intervals of x values from which the optimal controller hedges to a point; specifically, the best strategy from such an x is to use the control to drive the system into a different piece of the form transition probabilities.
- regions of avoidance: these are x values that the optimal controller keeps the system away from.
- the stability properties of the closed loop optimally controlled system over different pieces (of x values).
- the existence of local minima in the expected costs-to-go.

In chapter 7 we will present a solution algorithm that uses the results of this chapter and chapter 5 to eliminate many of the computations specified by the section 5.4 solution procedure. We will also use the problem class discussed in sections 6.5-6.6 as a vehicle for exploring additional qualitative properties of the controller.

6.2 Endpieces of the JLQ Optimal Controller

In this section we study the endpieces[1] of $V_k(x_k, r_k=i)$ and $u_k(x_k, r_k=j)$:

$$V_k^{Le}(x_k, j), \quad u_k^{Le}(x_k, j) \quad \text{for} \quad x_k \leq \delta_k^j(1) \tag{6.5}$$

$$V_k^{Re}(x_k, j), \quad u_k^{Re}(x_k, j) \quad \text{for} \quad x_k \geq \delta_k^j(m_k(j)-1) \tag{6.6}$$

(for each $j \in \underline{M}$).

The basic results of this section are as follows:

(1) for finite time horizon problems, if x_k is negative enough or positive enough the optimal strategy is to keep x in the same extreme x-pieces of the form transition probabilities $p(j,i:x)$ for all $i \in \underline{i}_j$ (from each $j \in \underline{M}$) for all future times.

That is, the controls

$$u_k, u_{k+1}, \ldots, u_{N-1}$$

[1] 'Le' denotes "left endpiece" and 'Re' denotes "right endpiece."

keep $x_{k+1},\ldots,x_N$ in the same extreme (i.e., far from zero) piece of the form transition probability.

For these extreme x_k values the x-dependent JLQ control problem of chapter 5 reduces to an x-independent one. The optimal expected costs-to-go and control laws (in each $j \in \underline{M}$) for these endpieces can be computed off-line via a set of M coupled recursive difference equations (one set for the left endpieces and one for the right endpieces). Thus the endpiece functions can be computed without following all of the steps of section 5.4.

(2) For infinite time-horizon problems, as $(N-k)\to\infty$ these endpieces of the costs-to-go and control laws converge to steady-state (constant parameter) functions of x if the dynamics in each form are <u>stabilizable</u> (i.e., $b(j) \neq 0$ or $|a(j)|<1$).

(3) In general the range of x_k values between these endpieces becomes infinite as $(N-k)\to\infty$. The width of x_k between the endpieces of $V_k(x_k, r_k = j)$ remains finite if, once the system is in form j, it cannot be in any[1] form having x-dependent form transition (exit) probabilities for <u>more than one</u> time step.

Fact (2) is well known from the LQ case. Facts (1) and (3) are proved in Proposition 6.1 and Proposition 6.3 respectively.

[1] Including (possibly) j itself.

The following proposition lists the equations for the left and right endpieces. It is stated for the general JLQ controller of Proposition 5.1 (with $P(j)$, $G_T(j)$, $S(j)$, $H_T(j)$ not necessarily zero). However to simplify notation we assume that

$$a(j) > 0 \qquad j \in \underline{M} \tag{6.7}$$

and we will exclude problems where the system "just coasts" in some form j with $u_k(x_k, r_k) \equiv 0$ by requiring

$$\begin{pmatrix} Q(j) & S(j)/2 \\ S(j)/2 & P(j) \end{pmatrix} + \begin{pmatrix} K_T(j) & H_T(j)/2 \\ H_T(j)/2 & G_T(j) \end{pmatrix} > 0 \quad . \qquad \forall\, j \in \underline{M}. \tag{6.8}$$

Proposition 6.1 (Endpieces)

Consider the JLQ problem of Proposition 5.1, where (6.7)-(6.8) hold.

(1) For $x_k \leq \delta_k^j(1)$, the optimal control laws and expected costs-to-go are

$$V_k(x_k, r_k=j) = V_k^{1,U}(x_k, j)$$

$$\triangleq V_k^{Le}(x_k, j) = x_k^2 K_k^{Le}(j) + x_k H_k^{Le}(j) + G_k^{Le}(j) \tag{6.9}$$

$$u_k(x_k, r_k=j) = u_k^{1,U}(x_k, j)$$

$$\triangleq u_k^{Le}(x_k, j) = -L_k^{Le}(j) x_k + F_k^{Le}(j) \tag{6.10}$$

(2) For $x_k \geq \delta_k^j(m_k(j)-1)$, the optimal expected costs-to-go and control laws are

$$V_k(x_k, r_k=j) = V_k^{\psi_{k+1}^{j,U}}(x_k, j)$$

$$\triangleq V_k^{Re}(x_k, j) = x_k^2 K_k^{Re}(j) + x_k H_k^{Re}(j) + G_k^{Re}(j) \qquad (6.11)$$

$$u_k(x_k, r_k=j) = u_k^{\psi_{k+1}^{j,U}}(x_k, j)$$

$$\triangleq u_k^{Re}(x_k, j) = -L_k^{Re}(j)x_k + F_k^{Re}(j) \qquad (6.12)$$

(3) The parameters in (6.9)-(6.12) are computed recursively, backwards in time from N by

$$K_k^{Le}(j) = \frac{a^2(j)R(j)\hat{K}_{k+1}^{Le}(j)}{R(j)+b^2(j)\hat{K}_{k+1}^{Le}(j)} \qquad (6.13)$$

$$H_k^{Le}(j) = \frac{a(j)R(j)\hat{H}_{k+1}^{Le}(j)}{R(j)+b^2(j)\hat{K}_{k+1}^{Le}(j)} \qquad (6.14)$$

$$G_k^{Le}(j) = \hat{G}_{k+1}^{Le}(j) - \frac{b^2(j)[\hat{H}_{k+1}^{Le}(j)]^2}{4[R(j)+b^2(j)\hat{K}_{k+1}^{Le}(j)]} \qquad (6.15)$$

where

$$\hat{K}_{k+1}^{Le}(j) = \sum_{i \in c_j} \lambda_{ji}(1)[K_{k+1}^{Le}(i)+Q(i)] \qquad (6.16)$$

$$\hat{H}^{Le}_{k+1}(j) = \sum_{i \in c_j} \lambda_{ji}(1)\,[H^{Le}_{k+1}(i)+S(i)] \tag{6.17}$$

$$\hat{G}^{Le}_{k+1}(j) = \sum_{i \in c_j} \lambda_{ji}(1)\,[G^{Le}_{k+1}(i)+P(i)] \tag{6.18}$$

and

$$K^{Re}_{k}(j) = \frac{a^2(j)R(j)\hat{K}^{Re}_{k+1}(j)}{R(j)+b^2(j)\hat{K}^{Re}_{k+1}(j)} \tag{6.19}$$

$$H^{Re}_{k}(j) = \frac{a(j)R(j)\hat{H}^{Re}_{k+1}(j)}{R(j)+b^2(j)\hat{K}^{Re}_{k+1}(j)} \tag{6.20}$$

$$G^{Re}_{k}(j) = \hat{G}^{Re}_{k+1}(j) - \frac{b^2(j)\,[\hat{H}^{Re}_{k+1}(j)]^2}{4[R(j)+b^2(j)\hat{K}^{Re}_{k+1}(j)]} \tag{6.21}$$

where

$$\hat{K}^{Re}_{k+1}(j) = \sum_{i \in c_j} \lambda_{ji}(\bar{\nu}_{ji})\,[K^{Re}_{k+1}(i)+Q(i)] \tag{6.22}$$

$$\hat{H}^{Re}_{k+1}(j) = \sum_{i \in c_j} \lambda_{ji}(\bar{\nu}_{ji})\,[H^{Re}_{k+1}(i)+S(i)] \tag{6.23}$$

$$\hat{G}^{Re}_{k+1}(j) = \sum_{i \in c_j} \lambda_{ji}(\bar{\nu}_{ji})\,[G^{Re}_{k+1}(i)+P(i)] \tag{6.24}$$

with terminal conditions

$$K_N^{Le}(j) = K_N^{Re}(j) = K_T(j) \tag{6.25}$$

$$H_N^{Le}(j) = H_N^{Re}(j) = H_T(j) \tag{6.26}$$

$$G_N^{Le}(j) = G_N^{Re}(j) = G_T(j) \quad . \tag{6.27}$$

The control law gains are

$$L_K^{Le}(j) = \frac{a(j)b(j)\hat{K}_{k+1}^{Le}(j)}{R(j)+b^2(j)\hat{K}_{k+1}^{Le}(j)} \tag{6.28}$$

$$F_k^{Le}(j) = \frac{-b(j)\hat{H}_{k+1}^{Le}(j)}{2[R(j)+b^2(j)\hat{K}_{k+1}^{Le}(j)]} \tag{6.29}$$

$$L_k^{Re}(j) = \frac{a(j)b(j)\hat{K}_{k+1}^{Re}(j)}{R(j)+b^2(j)\hat{K}_{k+1}^{Re}(j)} \tag{6.30}$$

$$F_k^{Re}(j) = \frac{-b(j)\hat{H}_{k+1}^{Re}(j)}{2[R(j)+b^2(j)\hat{K}_{k+1}^{Re}(j)]} \qquad \square \tag{6.31}$$

Proof (sketch): Recall that each form transition probability $p(j,i)$ is piecewise-constant in x with $\bar{\nu}_{ji}$ pieces:

$$x \in (\nu_{ji}(i-1),\ \nu_{ji}(i))$$

$$i=1,\ldots,\bar{\nu}_{ji}-1$$

where $\nu_{ji}(0) \stackrel{\Delta}{=} -\infty$, $\nu_{ji}(\bar{\nu}_{ji}) = +\infty$.

It is clear that for x_k negative enough we will have

$$x_{k+\ell} < \nu_{ji}(1) \qquad \forall i,j \in \underline{M} \tag{6.32}$$

and for x_k positive enough we will have

$$x_{k+\ell} > \nu_{ji}(\bar{\nu}_{ji}-1) \qquad \forall i,j \in \underline{M} \tag{6.33}$$

for $\ell=1,..,N-k$ (here $N<\infty$). This is verified in Appendix C.5. Thus Proposition 6.1 is just a restatement of the x-independent JLQ solution (Prop. 3.1), where we make the identifications

for left endpieces: $p_{ji} = \lambda_{ji}(1)$

for right endpieces: $p_{ji} = \lambda_{ji}(\bar{\nu}_{ji})$ $\qquad \forall i,j \in \underline{M}$.

Recall that the optimal expected cost-to-go $V_k(x_k, r_k=j)$ has $m_k(j)$ pieces, with joining points $\delta_k^j(1) < \delta_k^j(2) < \ldots < \delta_k^j(m_k(j)-1)$.

For $x_k < \delta_k^j(1)$ and $x_k > \delta_k^j(m_k(j)-1)$, the form transition probabilities <u>will not</u> change from time k+1 until time N, (ie, we will stay in an extreme piece of each p(j,i:x)) because the optimal

controller will not drive x past $\nu_{\ell i}(1)$ or $\nu_{\ell i}(\bar{\nu}_{\ell i}-1)$, respectively (for any i, ℓ accessible from j) at any future time.

Between $\delta_k^j(1)$ and $\delta_k^j(m_k(j)-1)$, the optimal controller will drive x into a different probability piece[1] at some time k+2,...,N. We define the switching region S_k^j of the controller from $r_k=j$ to be these x_k values

$$S_k^j \triangleq \{x_k: \delta_k^j(1) < x_k < \delta_k^j(m_k(j)-1)\} , \tag{6.34}$$

as shown in figure 6.1.

As we will see, the behavior of the optimal controller and corresponding state trajectories stating from $x_n \in S_k^j$ can involve one of several phenomena. Specifically, for x_k values close to zero the optimal controller will keep future x's in the same probability piece as it drives to zero. No active hedging is involved in these "middle pieces" on either side of zero, as we will see in the next section. Outside of this region (but in δ_k^j) the state will switch probability regions. However this can occur in distinctly different ways (involving hedging to points, regions of avoidance and other types of behavior). We will characterize these types of controller behaviors later in this chapter.

Clearly for finite times (N-k)< ∞, the switching region S_k^j has finite width, for each j $\in$ M:

$$|S_k^j| = \delta_k^j(m_k(j)-1)-\delta_k^j(1) < \infty \quad . \tag{6.35}$$

---

[1] From the piece that x_{k+1} is in.

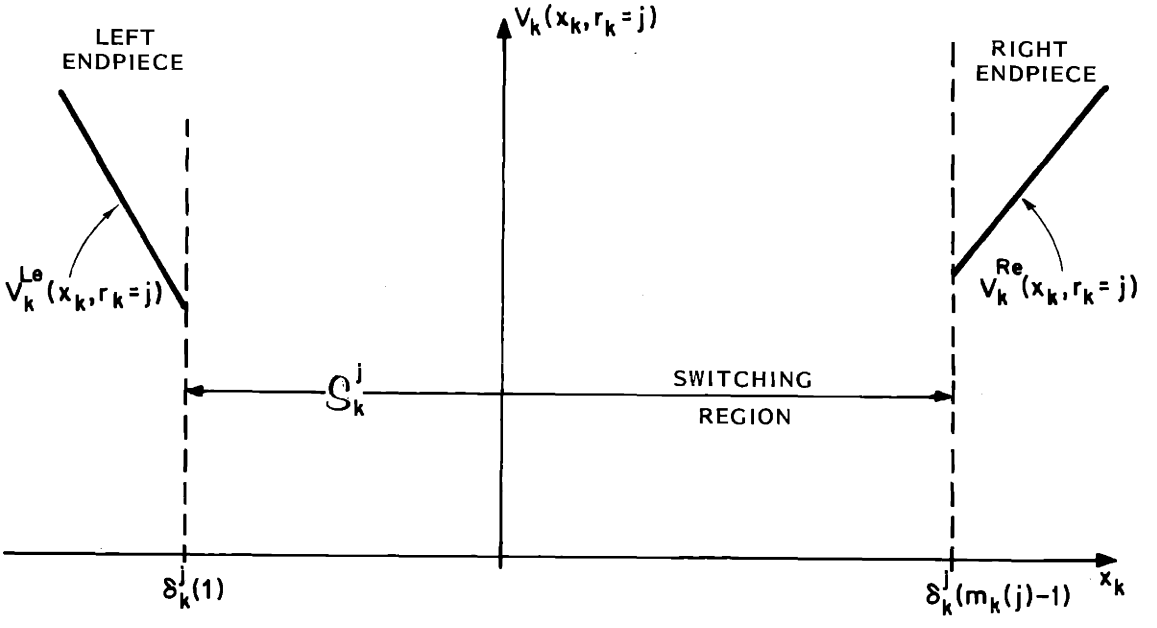

FIGURE 6.1: Endpieces and Switching Region for $V_k(x_k, r_k=j)$.

Note that we have not yet characterized the values of $\delta_k^j(1)$ and $\delta_k^j(m_k(j)-1)$.

Now consider the infinite time version of the problem, where we wish to minimize

$$\lim_{(N-k_0)\to\infty} E\left\{\sum_{k=k_0}^{N-1} [u_k^2 R(r_k)+x_{k+1}^2 Q(r_{k+1})]+ x_N^2 K_T(r_N)\right\} \tag{6.36}$$

subject to (5.1)-(5.4) and (5.6).

We consider the existence of the limiting functions

$$V_\infty^{Le}(x,j) \triangleq \lim_{(N-k)\to\infty} V_k^{Le}(x_k=x,r_k=j)$$

$$V_\infty^{Re}(x,j) \triangleq \lim_{(N-k)\to\infty} V_K^{Re}(x_k=x,r_k=j) \ .$$

Since the endpiece costs-to-go are obtained in Proposition 6.1 by equations which correspond to x-independent JLQ problems, Proposition 3.2 gives necessary and sufficient conditions for there to exist steady-state endpieces to the expected costs-to-go and control laws in Proposition 6.1, as (N-k) grows large. We have directly the following:

Proposition 6.2: Consider the JLQ problem of Proposition 5.1 where (6.1)-(6.4) hold. Then if we take

$$p_{ji} = \lambda_{ji}(1) \qquad \forall i,j\in\underline{M},$$

then conditions (1)-(3) of Proposition 3.2 are necessary and sufficient for the solution of the coupled difference equations (6.13)-(6.18), (6.25)-(6.27) to converge to a unique constant set of nonnegative steady-state values $\{K_\infty^{Le}(j) \geq 0,\ j \in \underline{M}\}$ as $(N-k)\to\infty$, given by the M coupled algebraic equations

$$K_\infty^{Le}(j) = \frac{a^2(j)R(j)\left[\sum_{i\in c_j} \lambda_{ji}(1)\left[K_\infty^{Le}(i)+Q(i)\right]\right]}{R(j)+b^2(j)\left[\sum_{i\in c_j} \lambda_{ji}(1)\left[K_\infty^{Le}(i)+Q(i)\right]\right]} \tag{6.37}$$

for $j \in \underline{M}$, with the optimal steady-state left endpieces

$$V_\infty^{Le}(x,j) = x^2 K_\infty^{Le}(j) \quad . \tag{6.38}$$

The steady-state left endpiece control laws are

$$u_\infty^{Le}(x,j) = -L_\infty^{Le}(j)x \qquad\qquad j \in \underline{M} \tag{6.39}$$

where the time invariant gains are given by

$$L_\infty^{Le}(j) = K_\infty^{Le}(j)\,\frac{b(j)}{a(j)R(j)} \quad . \tag{6.40}$$

Similarly, if we take

$$p_{ji} = \lambda_{ji}(\bar{\nu}_{ji}) \qquad\qquad \text{for all } i,j \in \underline{M},$$

then conditions (1)-(3) of Proposition 3.2 are necessary and sufficient for the solution of (6.19)-(6.27) to converge to a set of unique finite constant nonnegative steady-state values $\{K_\infty^{Re}(j) \geq 0,\ j \in \underline{M}\}$ as $(N-k) \to \infty$ given by the M coupled algebraic equations

$$K_\infty^{Re}(j) = \frac{a^2(j)R(j)\left[\sum_{i \in c_j} \lambda_{ji}(\bar{\nu}_{ji})[K_\infty^{Re}(i)+Q(i)]\right]}{R(j)+b^2(j)\left[\sum_{i \in c_j} \lambda_{ji}(\bar{\nu}_{ji})[K_\infty^{Re}(i)+Q(i)]\right]} \tag{6.41}$$

for $j \in \underline{M}$, with the optimal steady-state right endpieces

$$V_\infty^{Re}(x,j) = x^2 K_\infty^{Re}(j) \tag{6.42}$$

$$u_\infty^{Re}(x,j) = -L_\infty^{Re}(j)x \tag{6.43}$$

where

$$L_\infty^{Re}(j) = K_\infty^{Re}(j)\,\frac{b(j)}{a(j)R(j)} \quad . \tag{6.44}$$

□

Since we are considering a scalar x problem, if the dynamics in each form are stabilizable then the expected costs-to-go (from each form) will remain finite as $(N-k) \to \infty$. Stabilizability is trivial to check for scalar systems: $b(j) \neq 0$ or $|a(j)| < 1$ is required, for each $j \in \underline{M}$. If any absorbing form j (ie., $p_{jj}=1$) is not stabilizable then the expected costs-to-go becomes infinite for all forms from which j is accessible.

If any nonabsorbing form j (ie., $P_{jj}<1$) is not stabilizable then the existence of steady-state endpieces (and costs-to-go) depends upon the dynamics of, and transition probabilities to, all forms accessible from j. The existence of unstabilizable nonabsorbing forms is not out of the realm of possibility in failure prone systems. For example such a form might represent the temporary loss of an actuator until it is repaired. The existence of finite steady-state endpieces for systems having these forms is characterized by the necessary and sufficient conditions of Proposition 3.2, which reduce to the following:

There exist constants F_i for all $i \in \underline{M}$ such that:

(1) For <u>each</u> closed communicating class C_j (having two or more members), there exists a set of <u>finite</u>, <u>positive</u> scalars $\{z_1,\ldots,z_{|C_j|}\}$ satisfying the coupled equations

$$z_i = (1-p_{ii}) \sum_{t=1}^{\infty} p_{ii}^{t-1} (a_i - b_i F_i)^{2t} \left(Q_i + F_i^2 R_i + \sum_{\substack{\ell \in C_j \\ \ell \neq i}} \frac{p_{i\ell}}{1-p_{ii}} z_\ell \right)$$

for all $i \in C_j$.

(2) There exists a set of finite positive scalars $\{G_1,\ldots,G_T\}$ satisfying the coupled equations

$$G_i = (1-p_{ii}) \sum_{t=1}^{\infty} p_{ii}^{t-1} (a_i - b_i F_i)^{2t} \left(\begin{array}{c} Q_i + F_i^2 R_i \\ + \\ \sum\limits_{\substack{\ell \in \underline{T} \\ \ell \neq i}} \frac{p_{i\ell}}{1-p_{ii}} G_\ell \end{array} \right)$$

(for all $i \in \underline{T} \subset \underline{M}$; $\underline{T}$ is the subset of transient forms in $\underline{M}$).

(3) all absorbing forms are stabilizable.

The reason that these conditions are so complex is that the controller must account for an extremely wide range of possible behaviors. For example, it is <u>not</u> enough that the system will eventually enter a stabilizable state with probability one, as we will see in example 6.2. When the only unstabilizable forms are transient forms $(i \in \underline{T})$ that are not accessible from any form in their covers $i \in C_j$ except themselves (that is, once we leave i we can't return), then corollary 3.4 yields a sufficient condition for the existence of steady-state endpiece cost functions that is easier to test than (1)-(2) above:

$$p_{ii}\, a_i^2 < 1 \quad .$$

Let us now consider the growth of the switching regions

$$|S_k^j| = \delta_k^j(m_k(j)-1) - \delta_k^j(1) \tag{6.45}$$

as (N-k) grows large. If this quantity were to converge to a finite value as $(N-k)\to\infty$ it would mean that for x_k negative enough (or positive enough), the optimal controller <u>does not</u> make use of the knowledge that the p(j,i) can be changed by <u>active hedging.</u> This situation will obviously arise if none of the form transitions that the system can make once it is in j are x-dependent (since active hedging will be of no use). Finite switching regions also arise when the system cannot be susceptible to any x-dependent $p(i,\ell)$ more than once, after it has entered j. In general however, the switching regions grow in width without bound as $(N-k)\to\infty$.

<u>Proposition 6.3</u> <u>(Growth of Switching Regions)</u>

Consider the JLQ problem of Proposition 5.1. For each form j:

(i) If, once the system is in form $r_k = j$, <u>all</u> of the form transitions that the system can make are <u>x-independent</u> then $V_k(x_k, r_k = j)$ has one piece

$$m_k(j) = 1 \qquad \text{all } k$$

(ii) If, once the system is in form $r_k = j$, all of the form transitions that the system can make are x-independent except for (at least) one that has a single transition probability discontinuity at $x = 0$, then $V_k(x_k, r_k = j)$ has two pieces

$$m_k(j) = z$$

with

$$\delta_k(j) = 0 \qquad \text{(joined at zero)}$$

and

$$|S_k^j| = 0$$

as $(N-k) \to \infty$.

(iii) Assume that each form has stabilizable dynamics. If, for $r_k = j$, the system cannot (from time k+1 to N) be in any form having x-dependent exit probabilities for more than one time step then

$|S_k^j|$ will remain finite as $(N-k) \to \infty$.

Note that the system must have $p(j,j) = 0$ if $p(j,i)$ is x-dependent for any $i \in \mathcal{C}_j$.

If one or more of the form accessible from j is not stabilizable then $|S_k^j| \to \infty$ as $(N-k) \to \infty$.

(iv) if for $r_k = j$ it is possible to repeat an x-dependent from transition (from j or from any i accessible form j, including possibly p(j,j)) with transition probability discontinuities not all at zero, then $|S_k^j| \to \infty$ as $(N-k) \to \infty$.

Proof: (Sketch) :

Parts (i) and (ii) are obvious. For part (iii), since there are only finitely many forms then after a finite number of times (say $\bar{m}$) the system will have entered a stabilizable form i that satisfies part (i) or part (ii). Thus as $(N-k) \to \infty$, since $|S_k^i| = 0$ we have $|S_{k-\bar{m}}^j|$ finite. For parts (iii) and (iv), if one or more of the forms accessible from j is not stabilizable then $|S_k^j| \to \infty$ since the expected cost-to-go in this form becomes infinite as $(N-k) \to \infty$.

In (iv) if all of the forms are stabilizable then the ability to repeat an x-dependent transition makes $|S_k^j|$ grow without bound. The basic idea is as follows: Since each form j is stabilizable we have by Proposition 6.2 that the steady-state endpieces exist. The closed-loop optimal gain in the left endpiece becomes arbitrarily close to:

$$\left(a(j) - \frac{b^2(j)}{a(j)R(j)} \; K_\infty^{Le}(j)\right) \tag{6.46}$$

$$= \quad a(j)\left(\frac{1}{1+\frac{b^2(j)}{R(j)} \; \hat{K}_\infty^{Le}(j)}\right) \tag{6.47}$$

as $(N-k)\to\infty$. This limiting value of the closed loop optimal gain must be stable if the steady-state endpiece cost functions of Proposition 6.2 are to be finite. That is, we must have

$$a(j) < 1 + \frac{b^2(j)}{R(j)} \; \hat{K}_\infty^{Le}(j) \tag{6.48}$$

In appendix C.6 we show that the condition in (iv) and (6.48) make $|S_k^j| \to \infty$ as $(N-k)\to\infty$.

The steady-state endpiece functions $V_\infty^{Le}(x,j)$ and $V_\infty^{Re}(x,j)$ are useful in describing the asymptotic behavior of the optimal JLQ controller even though the switching region between the endpieces becomes arbitrarily large (in general) as $(N-k)\to\infty$. In particular, they are useful in "finite-look ahead" approximations of the steady-state controller which will be discussed in Chapter 7.

This completes on discussion the endpieces of $V_k(x_k, r_k=1)$ and $u_k(x_k, r_k=j)$. Several examples will be presented at the end of the next section of this chapter.

6.3 Middlepieces of the JLQ Optimal Controller

In this section we consider the behavior of the optimal JLQ controller of Proposition 5.1 near the origin, when the x-costs are simple quadratics (i.e., when (6.1)-(6.4) hold). That is, we examine here the middle pieces[1] of $V_k(x_k,r_k=j)$ and $u_k(x_k,r_k=j)$ for each $j \in \underline{M}$:

$$\left.\begin{matrix} V_k^{LM}(x_k,j) \\ u_k^{LM}(x_k,j) \end{matrix}\right\} \quad \text{for} \quad \underline{\delta}_k^j \leq x_k \leq 0 \tag{6.50}$$

$$\left.\begin{matrix} V_k^{RM}(x_k,j) \\ u_k^{RM}(x_k,j) \end{matrix}\right\} \quad \text{for} \quad x_k \; 0 \leq x_k \leq \overline{\delta}_k^j \tag{6.51}$$

where

$$\underline{\delta}_k^j \triangleq \max \{\delta_k^j(\ell) < 0\} \tag{6.52}$$

$$\overline{\delta}_k^j \triangleq \min \{\delta_k^j(\ell) > 0\} \tag{6.53}$$

where $\ell=0,1,\ldots,m_k(j)$.

As we will see, if there are no form transition probability discontinuities at zero

$$\nu_{ji}(t)\neq 0 \qquad t=1,\ldots,\overline{\nu}_{ji}-1 \quad \text{for} \quad i,j \in \underline{M}$$

---

[1] The superscript "LM" and "RM" denote "left middlepiece" and "right middlepiece", respectively.

then the left and right middle pieces in Proposition 6.6 are given by the same equations. That is, there is a single middlepiece valid in

$$\underline{\delta}_k^j < x_k < \overline{\delta}_k^j$$

given by

$$V_k^{RM}(x_k,j) \equiv V_k^{LM}(x_k,j)$$

at each time k and in each form j. The basic results of this section are as follows:

(1) for finite time horizon problems, if x_k is close enough to zero the optimal controller keeps $x_{k+1},\ldots,x_N$ in the same close-to-zero pieces of the transition probabilities p (j,i:x) (and x is driven to zero).

The controls

$$u_{k+1},\ldots,u_{N-1}$$

<u>do not actively hedge</u> (i.e., don't change form probability pieces) from the close-to-zero piece that x_{k+1} is in) because there is no advantage in doing so. The best strategy for these x close to zero is just to go to zero.

As with the endpieces, the middlepieces correspond to x-independent JLQ control problems. The middle pieces of $V_k(x_k,r_k=j)$ and $u_k(x_k,r_k=j)$ can be computed via sets of M coupled recursive difference equations.

---

(2) For infinite time-horizon problems, as $(N-k)\to\infty$ these middlepieces converge to steady-state (constant parameter) functions of x if the dynamics are stabilizable.

(3) At all times, the widths of the middlepieces are finite (except when a middlepiece and endpiece are the same at all times for some form j, because there are no form transition probability discontinuities on one side of zero for any form accessible from j).

The above results are obtained in Propositions 6.4, 6.6 and 6.5, respectively. We first have the following:

Proposition 6.4: (Middlepieces)

Consider the JLQ problem of Proposition 5.1, where (6.1)-(6.4) hold.

(1) For $\underline{\delta}_k^j \leq x_k \leq 0$ the optimal expected costs-to-go and control laws are

$$V_k(x_k, r_k=j) = V_k^{LM}(x_k, j)$$

$$\triangleq x_k^2 K_k^{LM}(j) \tag{6.54}$$

$$u_k(x_k, r_k=j) = u_k^{LM}(x_k, j)$$

$$\triangleq -L_k^{LM}(j)x_k \tag{6.55}$$

(2) For $0 \leq x_k \leq \bar{\delta}_k^j$ the optimal expected costs-to-go and control laws are

$$V_k(x_k, r_k=j) = V_k^{RM}(x_k, j)$$

$$\triangleq x_k^2 K_k^{RM}(j) \tag{6.56}$$

$$u_k(x_k, r_k=j) = u_k^{RM}(x_k, j)$$

$$\triangleq -L_k^{RM}(j) x_k \tag{6.57}$$

(3) The parameters in (6.54)-(6.57) are computed recursively, backwards in time from N by (6.13)-(6.31) where, for each $i,j \in \underline{M}$ we make the substitutions

LM replaces Le

$\lambda_{ji}(i)$ is replaced by $\lambda_{ji}(LM)$, the value of

$p(j,i,x)$ valid for $x \in (\max\{\nu_{ji}<0\}, 0)$

RM replaces Re

$\lambda_{ji}(\bar{\nu}_{ji})$ is replaced by $\lambda_{ji}(RM)$, the value of

$p(j,i,x)$ valid for $x \in (0, \min\{\nu_{ji}>0\})$.

Proof (sketch):

This proposition is a restatement of Proposition 3.1, where

for left middlepieces: $p_{ji} = \lambda_{ji}$ valid in $(\underline{\nu}_{ji}, 0]$

for right middlepieces: $p_{ji} = \lambda_{ji}$ valid in $[0, \underline{\nu}_{ji})$

where

$$\underline{\nu}_{ji} \triangleq \max\{\nu_{ji}(\ell)<0\} \tag{6.58}$$

$$\overline{\nu}_{ji} \triangleq \min\{\nu_{ji}(\ell)>0\} \quad , \quad \text{for all } x,j \in \underline{M} \, . \tag{6.59}$$

We have only the x_k^2 turn in (6.54), (6.56) because of (6.1) - (6.2).

Consider figure 6.2. We see that there are two switching regions

- left switching region S_k^{jL}
- right switching region S_k^{jk}

which, together with the middle pieces, constitute the switching region S_k^j of figure 6.1.

For $x_k \in (\underline{\delta}_k^j \, , \, 0)$ and $x_k \in (0, \, \overline{\delta}_k^j)$ the form transition probabilities will <u>not</u> change from time k+1 until N because the optimal controller is (at x_{k+1}) in the probability piece that contains (or is bounded by) zero. That is, for these x_k values the controller does not actively hedge with $u_{k+1},..,u_{N-1}$. The following proposition characterizes the values of $\underline{\delta}_k^j$ and $\overline{\delta}_k^j$.

<u>Proposition 6.5:</u> Consider the middlepieces of Proposition 6.4.

(1) If there is <u>no</u> form transition probability <u>discontinuity</u> to the right of zero for any p(j,i) ($\forall i \in C_j$) and for any p(ℓ,t) ($\forall \ell$ accessible from j) then

$V_k(x_k, r_k = j)$ has only one piece for $x_k \geq 0$.

That is, right middlepiece $V_k^{RM}(j)$ extends to $+\infty$;

$\overline{\delta}_k^j = \infty$ by (6.53).

(2) Similarly if there is no form transition probability discontinuity to the left of zero for any $p(j,i)$ ($\forall\, i \in \mathcal{C}_j$) and for any $p(\ell,t)$ ($\forall \ell$ accessible from j) then

$V_k(x_k, r_k = j)$ has only one piece for $x_k \leq 0$.

That is, left middlepiece $V_k^{LM}(j)$ extends to $-\infty$;

$\underline{\delta}_k^j = -\infty$ by (6.52).

(3) Now suppose (1) does not hold. Let

$$\beta_j \triangleq \min\left\{ \nu_{ji}(t) > 0 \;\middle|\; \begin{array}{l} i \in \mathcal{C}_j \\ t = 1,\ldots, \overline{\nu}_{ji} - 1 \end{array} \right\}$$

Then at each time $k = N-1, N-2, \ldots, k_o$:

$$0 \leq \overline{\delta}_k^j \leq \frac{\beta_j}{a(j)} \left[1 + \frac{b^2(j)}{R(j)} \hat{K}_{k+1}^{RM}(j) \right] . \tag{6.60}$$

In addition the $\{\delta_k^j \mid k = N-1, N-2, \ldots\}$ are related as follows if $j \in \mathcal{C}_j$:

$$0 \leq \overline{\delta}_k^j \leq \frac{\overline{\delta}_{k+1}^j}{a(j)} \left[1 + \frac{b^2(j)}{R(j)} \hat{K}_{k+1}^{RM}(j) \right] . \tag{6.61}$$

(4) Now suppose (2) doesn't hold. Let

$$\alpha_j \triangleq \max\left\{ \nu_{ji}(t) < 0 \;\middle|\; \begin{array}{l} i \in C_j \\ t = 1,\ldots,\bar{\nu}_{ji}-1 \end{array} \right\}.$$

Then at each time $k = N-1, N-2, \ldots, k_o$:

$$\frac{\alpha_j}{a(j)}\left[1 + \frac{b^2(j)}{R(j)}\hat{K}^{LM}_{k+1}(j)\right] \leq \underline{\delta}^j_k \leq 0 \quad . \tag{6.62}$$

In addition the $[\underline{\delta}^j_k \mid k = N-1, N-2, ..]$ are related as follows, if $j \in C_j$:

$$\frac{\underline{\delta}^j_{k+1}}{a(j)}\left[1 + \frac{b^2(j)}{R(j)}\hat{K}^{LM}_{k+1}(j)\right] \leq \underline{\delta}^j_k \leq 0 \quad . \qquad \square \tag{6.63}$$

The proof of this proposition appears in appendix C.7. It is obtained by direct calculation from the optimal closed loop dynamics in the middlepieces, as specified by (6.55), (6.57).

We now consider the existence of steady-state middle pieces

$$V^{LM}_{\infty}(x,j) = \lim_{(N-k)\to\infty} V^{LM}_k(x_k=x,\ r_k=j)$$

$$V^{RM}_{\infty}(x,j) = \lim_{(N-k)\to\infty} V^{RM}_k(x_k=x,\ r_k=j)$$

for the infinite time horizon problem.

As in Proposition 6.2, we have directly the following:

Proposition 6.6: For the problem of Proposition 5.1 where (6.1)-(6.4) hold, if we take

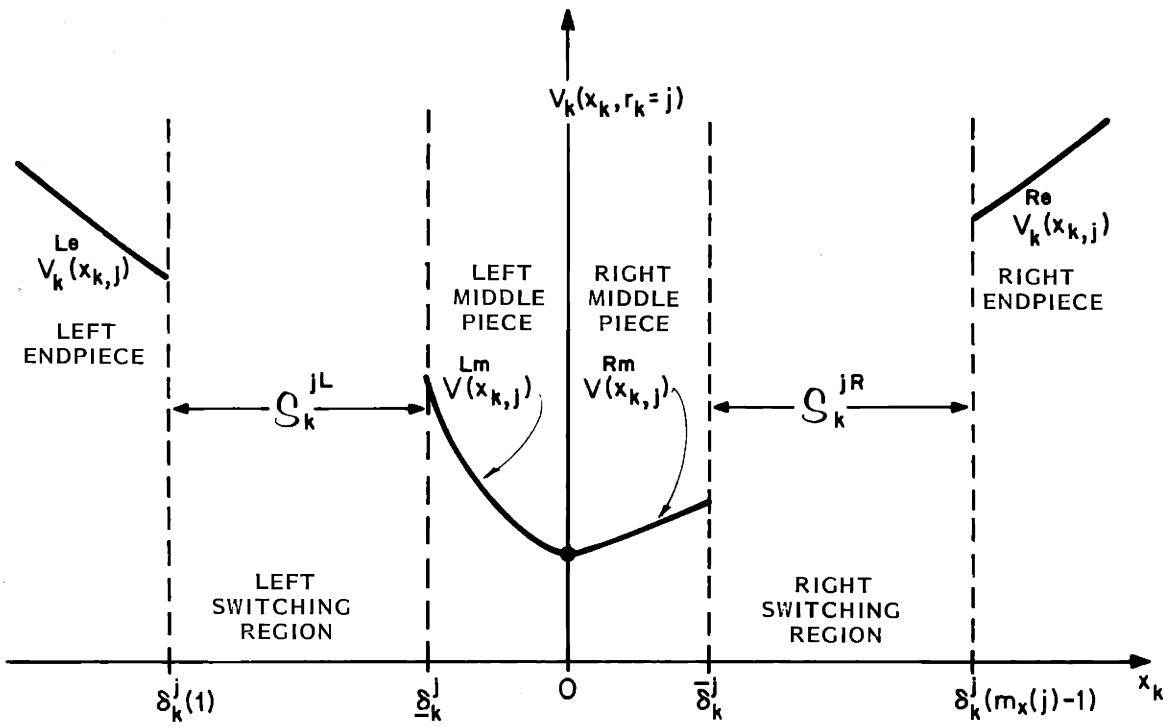

FIGURE 6.2: Switching regions, endpieces and middlepieces of $V_k(x_k, r_k=j)$.

$$p_{ji} = \lambda_{ji}(LM) \qquad \text{for all } i,j \in \underline{M}$$

or

$$p_{ji} = \lambda_{ji}(RM)$$

then conditions (1)-(3) of Proposition 3.2 are necessary and sufficient for the solution of the coupled difference equations of Proposition 6.4 to converge to the unique constant sets of steady-state values :

$$\{K_\infty^{LM}(j) \geq 0 , \quad j \in \underline{M}\} \qquad \text{for left middlepieces}$$

$$\{K_\infty^{RM}(j) \geq 0 , \quad j \in \underline{M}\} \qquad \text{for right middlepieces}$$

as $(N-k) \to \infty$, given by the solutions of the sets of M coupled algebraic equations

$$K_\infty^{LM}(j) = \frac{a^2(j)R(j)\left[\sum_{i \in c_j} \lambda_{ji}(LM)\left[K_\infty^{LM}(i)+Q(i)\right]\right]}{R(j)+b^2(j)\left[\sum_{i \in c_j} \lambda_{ji}(LM)\left[K_\infty^{LM}(i)+Q(i)\right]\right]} \tag{6.64}$$

$$K^{RM}(j) = \frac{a^2(j)R(j)\left[\sum_{i \in c_j} \lambda_{ji}(RM)\left[K_\infty^{RM}(i)+Q(i)\right]\right]}{R(j)+b^2(j)\left[\sum_{i \in c_j} \lambda_{ji}(RM)\left[K_\infty^{RM}(i)+Q(i)\right]\right]} \tag{6.65}$$

with

$$V_\infty^{LM}(x,j) = x^2 K_\infty^{LM}(j)$$

$$V_\infty^{RM}(x,j) = x^2 K_\infty^{RM}(j) \qquad j \in \underline{M}. \tag{6.66}$$

The steady-state middlepieces of the optimal control laws are

$$u_\infty^{LM}(x,j) = -L_\infty^{LM}(j)x$$

$$u_\infty^{RM}(x,j) = -L_\infty^{RM}(j)x \tag{6.67}$$

where

$$L_{\infty}^{LM}(j) = K_{\infty}^{LM}(j)/a(j)$$
$$L_{\infty}^{RM}(j) = K_{\infty}^{RM}(j)/a(j) \ . \tag{6.68}$$

These middlepieces are valid

for $V_{\infty}^{RM}(j)$: $0 \leq x \leq \bar{\delta}_{\infty}^{j}$ (6.69)

for $V_{\infty}^{LM}(j)$: $\underline{\delta}_{\infty}^{j} \leq x \leq 0$

where, if (6.60), (6.62) hold:

$$0 \leq \bar{\delta}_{\infty}^{j} \leq \frac{\beta_j}{a(j)} \left(1 + \frac{b^2(j)}{R(j)} \hat{K}_{\infty}^{RM}(j)\right) < \infty \tag{6.70}$$

$$-\infty < \frac{\alpha_j}{a(j)} \left(1 + \frac{b^2(j)}{R(j)} \hat{K}_{\infty}^{LM}(j)\right) \leq \underline{\delta}_{\infty}^{j} \leq 0 \ . \tag{6.71}$$

□

As with the endpieces we have that if each form is stabilizable then (by Corollary 3.5) these conditions are satisfied and the steady-state middle pieces exist. And for transient forms that the system does not return to after leaving, we can relax this stabilizability requirement to

$$p_{ii} \ a_i^{\ 2} < 1$$

by Corollary 3.4.

Example 6.1 (Example 5.1 Revisited)

From proposition 6.1 we can compute the endpieces of $V_k(x_k, r_k=1)$ and $u_k(x_k, r_k=1)$ recursively. We find that

$$V_k^{Le}(x_k, r_k=1) = V_k^{Re}(x_k, r_k=1) = x_k^2 K_k^{Le}(1)$$

$$u_k^{Le}(x_k, r_k=1) = u_k^{Re}(x_k, r_k=1) = -L_k^{Le}(1)x_k$$

where

$$K_N^{Le}(1) = K_N^{Re}(1)=0$$

$$K_k^{Le}(1) = K_k^{Re}(1) = \frac{1 + \frac{1}{4} K_{k+1}^{Le}(1) + \frac{3}{4} K_{k+1}(2)}{2 + \frac{1}{4} K_{k+1}^{Le}(1) + \frac{3}{4} K_{k+1}(2)}$$

$$= L_k^{Le}(1) = L_k^{Re}(1) \quad .$$

$V_k^{Le}(x_k, r_k=1)$ and $V_k^{Ke}(x_k, r_k=1)$ are the same in this example because of the symmetry (about zero) of the form transition probabilities.

From Proposition 6.6 we get the middlepieces

$$V_k^{LM}(x_k, 1) = V_k^{RM}(x_k, 1) = x_k^2 K_k^{LM}(1)$$

$$u_k^{LM}(x_k, 1) = u_k^{RM}(x_k, 1) = -L_k^{LM}(1)x_k$$

where

$$K_N^{LM}(1) = K_N^{RM}(1) = 0$$

$$K_k^{LM}(1) = K_k^{RM}(1) = \frac{1 + \frac{3}{4} K_{k+1}^{LM}(1) + \frac{1}{4} K_{k+1}(2)}{2 + \frac{3}{4} K_{k+1}^{LM}(1) + \frac{1}{4} K_{k+1}(2)}$$

$$= L_k^{LM}(1) = L_k^{RM}(1)$$

The values of these endpiece and middlepiece parameters are listed for several time stages in table 6.1.

k	Endpieces $K_k^{LM}(1)=K_k^{RM}(1)=L_k^{LM}(1)=L_k^{RM}(1)$	Middlepieces $K_k^{Le}(1)=K_k^{Re}(1)=L_k^{Le}(1)=K_k^{Re}(1)$
N	-	-
N-1	.7647058	.636363
N-2	.7821909	.694868
N-3	.7834843	.6995943
	↓	↓
	.7836889	.7000659

TABLE 6.1: Middlepiece and endpieces for Example 6.1

Since $b(1) \neq 0$, these parameters quickly converge as (N-k) increases to the steady-state values

$$K_\infty^{RM}(1) \equiv K_\infty^{LM}(1) \approx .7836889$$

$$K_\infty^{Le}(1) \equiv K_\infty^{Re}(1) \approx .7000659$$

□

The following two examples further illustrate the qualitative properties of these middlepiece and endpiece cost functions. In particular, example 6.3 demonstrates that the endpiece and middlepiece functions can become infinite as $(N-k)\to\infty$ even though the cost-to-go is, in fact, finite with probability one.

Example 6.2:

We consider the following system:

$$x_{k+1} = 2x_k \qquad \text{if } r_k=1$$

$$x_{k+1} = \frac{1}{2}x_k + u_k \qquad \text{if } r_k=2$$

$$p(1,2:x) = \begin{cases} 0 & \text{if } |x|<1 \\ \lambda=1/2 & \text{if } |x|>1 \end{cases}$$

$$p(2,1:x) = \begin{cases} 1 & \text{if } |x|<1 \\ 1/2 & \text{if } |x|>1 \end{cases}$$

The form structure and transition probabilities $p(1,2:x)$ and $p(2,1:x)$ are illustrated in Figure 6.3.

We seek to minimize

$$\min_{u_{k_0},\ldots,u_{N-1}} \sum_{k=k_0}^{N-1} (x_{k+1}^2 + u_k^2) + x_N^2 \quad .$$

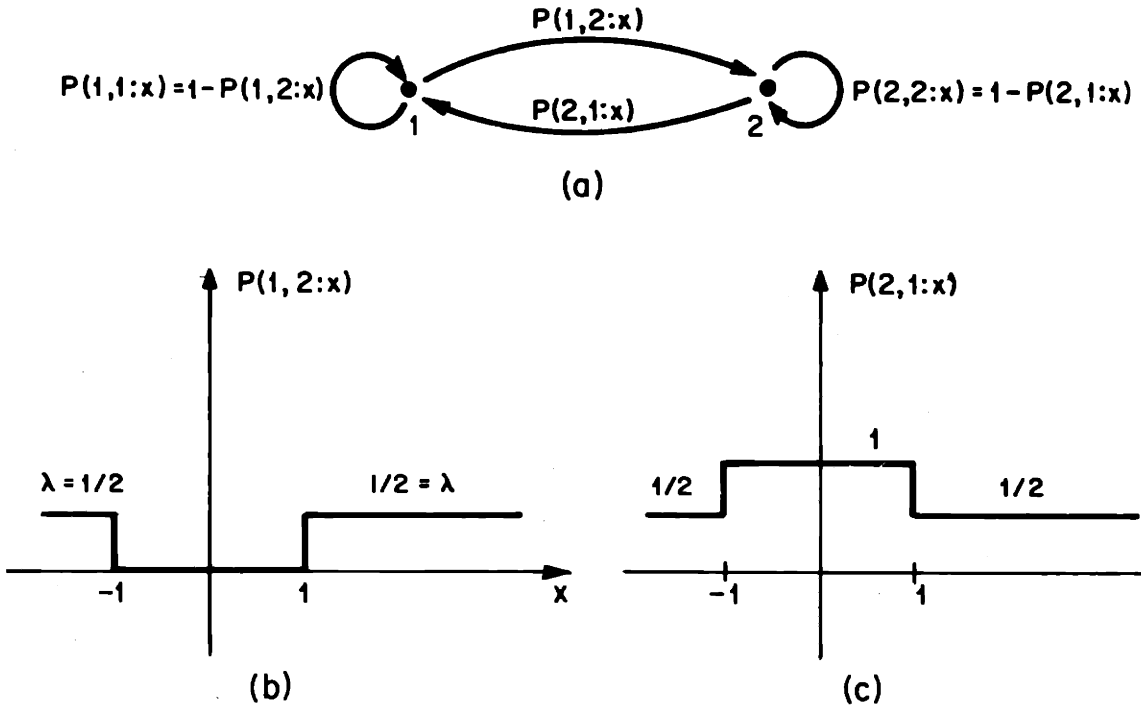

Figure 6.3: (a) Form structure and probabilities (b) p(1,2:x) and (c) p(2,1:x) for examples 6.2 and 6.3.

Let us consider some qualitative properties of the optimal expected costs-to-go $V_k(x_k, r_k=1)$ and $V_k(x_k, r_k=2)$. In form $r=2$ the system is controllable. Thus we know that $V_k(x_k, r_k=2)$ is bounded (for any finite x) since the control

$$u_k = \frac{-a(2)}{b(2)} x_k$$

will drive x_{k+1} to zero with a (nonoptimal) cost of

$$\frac{a^2(2)}{b^2(2)} x_k^2 .$$

Note that the system is not stabilizable in form 1. Thus the value of $|x|$ will double and a cost of x_{k+1}^2 will be changed at each succeding time, until the system jumps into form $r=2$. Once it get into $r=2$, the expected cost-to-go is finite.

Since $p(1,2) > 0$ for $|x|>1$ it is clear that the optimal cost will be finite with probability one as $(N-k)\to\infty$. As we will see, this does not guarantee that the expected cost-to-go $V_k(x_k, r_k=1)$ will remain finite, however. That is, the convergence of the cost-to-go with probability one does not imply that the controlled system is moment stable.

From Proposition 6.1 we have that

$$K_k^{Le}(1) = K_k^{Re}(1) = 4\left[1 + \frac{1}{2} K_{k+1}^{Le}(1) + \frac{1}{2} K_{k+1}^{Le}(2)\right]$$

$$K_k^{Le}(2) = K_k^{Re}(2) = \frac{\frac{1}{4}\left[1+ \frac{1}{2} K_{k+1}^{Le}(1)+ \frac{1}{2} K_{k+1}^{Le}(2)\right]}{1+\left[1+ \frac{1}{2} K_{k+1}^{Le}(1)+ \frac{1}{2} K_{k+1}^{Le}(2)\right]}$$

$$K_N^{Le}(1) = K_N^{Le}(2) = 1 \quad .$$

From the first of these equations we can verify that there is no finite positive steady-state value $K_\infty^{Le}(1)$. If the steady-state values $K_\infty^{Le}(1)$, $K_\infty^{Le}(2)$ were to both exist then they would have to satisfy

$$K_\infty^{Le}(1) = 4 + 2K_\infty^{Le}(1) + 2K_\infty^{Le}(2)$$

hence

$$K_\infty^{Le}(1) = -4-2K_\infty^{Le}(2) \quad .$$

For any $K_\infty^{Le}(2) \geq 0$ (which must be the case), $K_\infty^{Le}(1) < -4$. Thus we see that $K_\infty^{Le}(1)$ grows without bound as $(N-k)\to\infty$.

However,

$$K_\infty^{Le}(2) = \frac{\frac{1}{4}\left[\frac{1}{K_{k+1}^{Le}(1)} + \frac{1}{2} + \frac{1}{2}\left(K_{k+1}^{Le}(2)/K_{k+1}^{Le}(1)\right)\right]}{\left(\frac{2}{K_{k+1}^{Le}(1)}\right) + \frac{1}{2} + \frac{1}{2}\left(K_{k+1}^{Le}(2)/K_{k+1}^{Le}(1)\right)} \quad .$$

Therefore as $(N-k)\to\infty$ and $K_{k+1}^{Le}(1)\to\infty$ we have

$$\lim_{(N-k)\to\infty} K_k^L(2) = \frac{\frac{1}{4}(\frac{1}{2})}{\frac{1}{2}} = 1/4 \quad .$$

That is,

$$K_\infty^{Le}(2) = K_\infty^{Re}(2) = 1/4 \ .$$

From Proposition 6.4 we have

$$K_k^{LM}(1) = K_k^{RM}(1) = 4[1+K_{k+1}^{LM}(1)]$$

$$K_k^{LM}(2) = K_k^{RM}(2) = \frac{\frac{1}{4}[1+K_{k+1}^{LM}(1)]}{1+[1+K_{k+1}^{LM}(1)]}$$

where

$$K_k^{LM}(1) = K_k^{LM}(2) = 1 \ .$$

Note that these middle piece costs are not coupled. This is because the middlepieces are valid only in a region contained inside the interval (-1,1), in which form r=1 is an absorbing form.

From the above we see that as $(N-k)\to\infty$,

$$K_k^{LM}(1) \equiv K_k^{RM}(1)$$

become infinite and

$$K_k^{LM}(2) = K_k^{RM}(2) \longrightarrow 1/4 = K_\infty^{LM}(2) = K_\infty^{RM}(2) \ .$$

The values of the quantities described above are computed for four time steps in Table 6.2.

k	$K_k^{Le}(1)=K_k^{Re}(1)$	$K_k^{Le}(2)=K_k^{Re}(2)$	$K_k^{LM}(1)=K_k^{RM}(1)$	$K_k^{LM}(2)=K_k^{RM}(2)$
N	1	1	1	1
N-1	8	.1666666	8	.166666
N-2	20.333333	.2089041	36	.225
N-3	45.084474	.229269	148	.243421
N-4	94.628202	.2398609	596	.248333
	$\downarrow$ ∞	$\downarrow$ 1/4	$\downarrow$ ∞	$\downarrow$ 1/4

TABLE 6.2: Middlepiece and Endpieces for Example 6.2

Note that for both the middlepieces and endpieces in form 1, the sufficient condition for finite steady-state costs of Corollary 3.4 is not met. That is,

$$p_{11}a^2(1) > 1 \ .$$

This is illustrated in figure 6.4. However the cost-to-go $V_k(x_k, r_k=1)$ is finite with probability one.

□

In the next example we let $p(1,2:x)$ for $|x|>1$ be a parameter. If the probability of switching from $r=1$ to $r=2$ is high enough, the endpieces of $V_k(x_k, r_k=1)$ remain finite as $(N-k)$ increases but the middlepiece of $V_k(x_k, r_k=1)$ still blows up.

Example 6.3: We generalize the previous example by considering arbitrary λ values:

$$p(1,2:x) = \begin{cases} \lambda & |x|> 1 \\ 0 & |x|< 1 \end{cases} .$$

Then

$$K_k^{Le}(1) = K_k^{Re}(1) = 4[1+(1-\lambda)K_{k+1}^{Le}(1)+ \lambda K_{k+1}^{Le}(2)]$$

$$K_k^{Le}(2) = K_k^{Re}(2) = \frac{\frac{1}{4}\,[1+ \frac{1}{2}\, K_{k+1}^{Le}(1)+ \frac{1}{2}\, K_{k+1}^{Le}(2)]}{1+[1+ \frac{1}{2}\, K_{k+1}^{Le}(1)+ \frac{1}{2}\, K_{k+1}^{Le}(2)]}$$

with $K_k^{LM}(1) \equiv K_k^{RM}(1)$ and $K_k^{LM}(2) \equiv K_k^{RM}(2)$ taking the same values as in example 6.2.

for middle pieces:

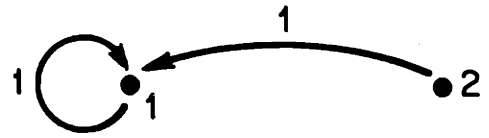

$P_{11}\, a_1^2 = 4$ $\qquad$ $b(2) = 1 \neq 0$

$b(1) = 0$

for end pieces:

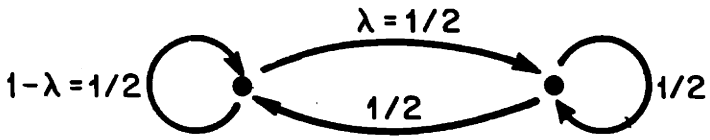

$P_{11}\, a_1^2 = 2$ $\qquad$ $b(2) = 1 \neq 0$

$b(1) = 0$

Figure 6.4: Form structures applicable for endpieces and middlepieces in examples 6.2 and 6.3.

From Figure 6.4 we see that the sufficient conditions for the existence of steady-state middlepieces are not satisfied in form 1 since $p_{11}a_1^2 = 4>1$. But if $3/4 < \lambda \leq 1$ then the sufficient condition for the existence of steady-state endpieces in Corollary 3.4 is satisfied:

$$p_{11}a_1^2 = (1-\lambda)4<1 \qquad 3/4 < \lambda \leq 1 \ .$$

When this holds we find that for the endpieces, $K_k^{Le}(1) \equiv K_k^{Re}(1)$ converge to a finite positive steady-state value (as do $K_k^{Le}(2) \equiv K_k^{Re}(2)$ and $K_k^{LM}(2) \equiv K_k^{RM}(2)$) even though the middlepiece in r=1 has infinite steady-state cost. The steady-state values of the endpieces of $V_\infty(x,r=j)$ are given by

$$K_\infty^{Le}(2) = K_\infty^{Re}(2) = \frac{-(56\lambda-29)+\sqrt{(56\lambda-29)^2+4(8\lambda-2)(32\lambda-12)}}{2(32\lambda-12)}$$

$$K_\infty^{Le}(1) = K_\infty^{Re}(1) = \frac{4(1+\lambda K_\infty^{Le}(2))}{4\lambda-3} \ .$$

For example, take $\lambda=7/8$. Then we can compute the values shown in Table 6.3, and from the above we have that

$$K_\infty^{Le}(2) = K_\infty^{Re}(2) = \frac{-5+\sqrt{45}}{8} = .2135254$$

$$K_\infty^{Le}(1) = K_\infty^{Re}(1) = 9.4946778 \ .$$

k	$K_k^{Le}(1)=K_k^{Re}(1)$	$K_k^{Le}(2)=K_k^{Re}(2)$
N	1	1
N-1	8	.1666666
N-2	8.5833331	.2089041
N-3	9.0228298	.2109138
N-4	9.2496132	.2122178
	↓	↓
	9.4946778	.2135254

TABLE 6.3: Endpieces for Example 6.3.

We might guess that since the middle pieces in form 1 grow without bound (in value) as $(N-k)\to\infty$, the "width" of these pieces is going to zero. That is,

$$\lim_{(N-k)\to\infty} \delta_{-k}^{1} = 0$$

$$\lim_{(N-k)\to\infty} \bar{\delta}_{k}^{1} = 0 \quad .$$

Examples 6.1-6.3 illustrate some of the diverse behaviors that the endpieces and middlepieces can exhibit as $(N-k)\to\infty$. These behaviors are directly related to the expected behavior of the controlled x-process, and to the qualitative properties of the entire expected cost-to-go $V_k(x_k,r_k)$. As we saw in example 6.2, for very simple examples we can get phenomena such as finite cost-to-go w.p.1 but infinite expected cost.

This concludes our discussion of the middlepieces of $V_k(x_k,r_k=j)$ and $u_k(x_k,r_k=j)$ for the JLQ control problems of section 6.1. We have thus far characterized the behavior of $V_k(x_k,r_k=j)$ and $u_k(x_k,r_k=j)$ over extreme values of x (far from zero) and for x near zero. In particular, we have obtained a description of the steady-state behavior of these endpieces and middlepieces in turns of corresponding x-independent JLQ problems of Chapter 3. In the next section we consider the behavior of the controller over the switching regions of Figure 6.2, between the endpieces and middlepieces.

6.4 Bounds on the expected costs-to-go

In this section we continue or examination of the steady-state properties of the scalar, x-dependent JLQ controller. We are concerned with the nature of the expected costs-to-go $V_k(x_k,r_k)$ between the endpieces and middlepiece (ie,in the switching regions of fig. 6.2). We

develop upper and lower bounds on $V_k(x_k, r_k)$ here that correspond to x-independent JLQ problems. Thus bounds can be computed off line via recursive difference equations and, using the results of Chapter 3, we have necessary and sufficient conditions for these bounds to converge to finite values as the time horizon becomes infinite.

We motivate our derivation of these bounds by the following example which demonstrates that the cost-to-go, if we stay with certainty in the "most expensive form", is <u>not</u> always an upper bound on $V_k(x_k, r_k=j)$ and the cost-to-go, if we stay with certainty in the "least expensive form", is <u>not</u> necessarily a lower bound on $V_k(x_k, r_k=j)$.

<u>Example 6.4</u>: Consider the problem

$$x_{k+1} = x_k + u_k \qquad \text{for} \quad r_k=1,2$$

where we minimize

$$\min E\left\{ \sum_{k=0}^{N-1} [x_{k+1}^2 Q(r_{k+1}) + u_k^2 R(r_k)] \right\} ,$$

and the form structure is a "flip-flop" system:

$$p(1,2)=1 \qquad p(2,1)=1$$

$$p(1,1)=0 \qquad p(2,2)=0 \quad .$$

Let

$$Q(1)=1 \qquad R(1)=100$$

$$Q(2)=100 \qquad R(2)=1 \quad .$$

That is, the dynamics in each form are the same, and

- in form 1 the control cost is high
- in form 2 the control cost is low.

The solution to the LQ problem corresponding to staying in form 1 for all times (that is, with Q=1, R=100) yields

$$V_k^{(1)} = x_k^2 \, K_k^{(1)}$$

where $K_N^{(1)} = 0$

$$K_k^{(1)} = \frac{100(K_{k+1}^{(1)}+1)}{100+(K_{k+1}^{(1)}+1)} = \frac{100\,K_{k+1}^{(1)}+100}{101+K_{k+1}^{(1)}} \quad .$$

The solution to the LQ problem corresponding to staying in form 2 for all times (that is, with Q=100, R=1) yields

$$V_k^{(2)} = x_k^2 \, K_k^{(2)}$$

where

$$K_N^{(2)} = 0$$

$$K_k^{(2)} = \frac{K_{k+1}^{(2)}+100}{1+(K_{k+1}^{(2)}+100)} = \frac{K_{k+1}^{(2)}+100}{101+K_{k+1}^{(2)}} \quad .$$

The solution to the x-independent JLQ problem (by Proposition 3.1) yields

$$V_k(x_k, r_k=i) = x_k^2 K_k(i) \qquad i=1,2$$

where

$$K_N(1) = K_N(2) = 0$$

$$K_k(1) = \frac{100(100 + K_{k+1}(2))}{100+(100 + K_{k+1}(2))} = \frac{10^4+100\, K_{k+1}(2)}{200+K_{k+1}(2)}$$

$$K_k(2) = \frac{1+K_{k+1}(1)}{1+(1+K_{k+1}(1))} = \frac{1+K_{k+1}(1)}{2+K_{k+1}(1)} \quad .$$

All of the above costs are listed for four time steps in Table 6.4.

time k	always in "cheap" form Q(2)=100 R(2)=1 $K_k(2)$	always in "expensive" form Q(1)=1 R(1)=100 $K_k(1)$	optimal solutions to flip-flop problem $K_k(1)$	$K_k(2)$
N-1	.990099	.990099	50	5
N-2	.9901951	1.9512669	50.124688	.9807692
N-3	.9901951	2.866664	50.243994	.9808152
N-4	.9901951	3.7227189	50.244006	.980859

TABLE 6.4: Costs for example 6.4.

From Table 6.4 we see that the optimal costs-to-go in the flip-flop JLQ problem are <u>not</u> bounded by the cheap and expensive LQ problems. That is

$$V_k(x_k, r_k=1) > V_k^{(1)}(x_k) \geq V_k^{(2)}(x_k)$$

$$V_k(x_k, r_k=2) < V_k^{(2)}(x_k) \leq V_k^{(1)}(x_k) \quad .$$

The reasons for this can be summarized as follows:

1. $V_k^{(2)}$ is not a lower bound on $V_k(x_k, r_k)$ because

   - in the "cheap form" problem the optimal LQ controller (assuming $r_k=2$, $\forall k$) spends a lot of control energy (since R(2) is only 1) to avoid the relatively expensive (Q(2)=100) cost on x_{k+1}^2 .
   - in the flip-flop problem when $r_k=2$ the controller does not have to spend as much energy since r_{k+1} will be 1, and thus the lower cost

     $$x_{k+1}^2 Q(1) = x_{k+1}^2$$

     will be charged instead of $x_{k+1}^2 Q(2) = 100\, x_{k+1}^2$.

2. $V_k^{(1)}$ is not an upper bound on $V_k(x_k, r_k)$ because

- in the "expensive form" problem the optimal LQ controller (assuming $r_k=1$, $\forall k$) keeps u_k small to avoid the relatively expensive control cost $u_k^2 R(1) = 100\, u_k^2$.

- in the flip-flop problem with $r_k=1$, the optimal JLQ controller must spend more control energy than this since, at the next time step, $x_{k+1}^2 Q(2) = 100\, x_{k+1}^2$ will be charged instead of $x_{k+1}^2 Q(1) = x_{k+1}^2$.

□

From this example it is clear that upper and lower bounds on $V_k(x_k, r_k=j)$ must take into account the form transition probability structures. The following proposition develops these bounds.

Proposition 6.7: (Bounds on $V_k(x_k, r_k)$)

Consider the JLQ problem of Proposition 5.1, where (6.1)-(6.4) hold. Then for each $j \in \underline{M}$, the expected cost-to-go $V_k(x_k, r_k=j)$ is bounded by

$$V_k^{LB}(x_k, j) \leq V_k(x_k, r_k=j) \leq V_k^{UB}(x_k, j) \tag{6.72}$$

for each x_k, where

$$V_k^{LB}(x_k,j) \triangleq x_k^2 K_k^{LB}(j) \qquad \text{lower bound} \qquad (6.73)$$

$$V_k^{UB}(x_k,j) \triangleq x_k^2 K_k^{UB}(j) \qquad \text{upper bound} \qquad (6.74)$$

with the parameters in (6.72)-(6.74) computed recursively, backwards in time by

$$K_k^{LB}(j) = \frac{a^2(j)R(j)\hat{K}_{k+1}^{LB}(j)}{R(j)+b^2(j)\hat{K}_{k+1}^{LB}(j)} \qquad (6.75)$$

$$K_k^{UB}(j) = \frac{a^2(j)R(j)\hat{K}_{k+1}^{UB}(j)}{R(j)+b^2(j)\hat{K}_{k+1}^{UB}(j)} \qquad (6.76)$$

where

$$\hat{K}_{k+1}^{LB}(j) = \min_{t=1,..,\psi_{k+1}^j} \sum_{i\in c_j} \lambda_{ji}(\ell_t^{ji})[K_{k+1}^{LB}(i)+Q(i)] \qquad (6.77)$$

$$\hat{K}_{k+1}^{UB}(j) = \max_{t=1,..,\psi_{k+1}^j} \sum_{i\in c_j} \lambda_{ji}(\ell_t^{ji})[K_{k+1}^{UB}(i)+Q(i)] \qquad (6.78)$$

with

$$K_N^{UB}(j) = K_N^{LB}(j) = K_T(j) \ . \qquad (6.79)$$

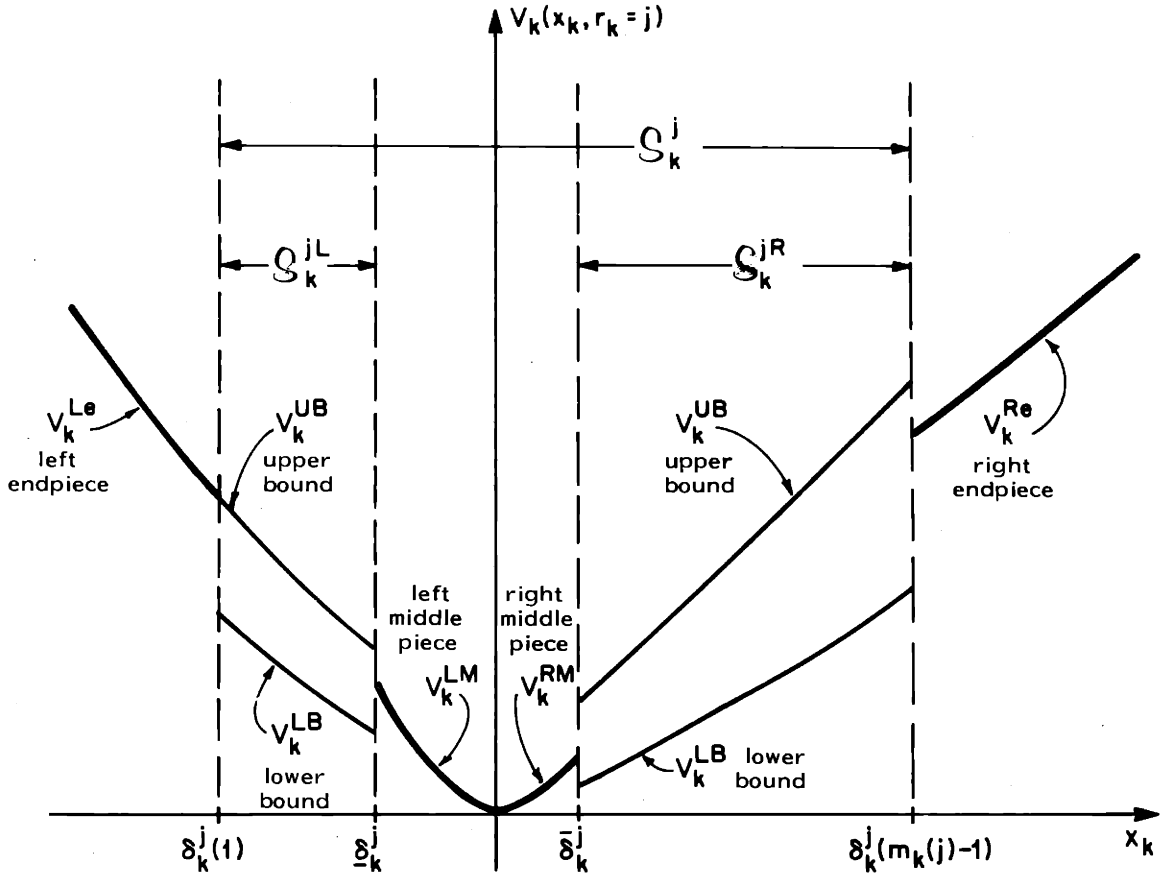

Figure 6.5: Upper and lower bounds, endpieces, middlepieces and switching regions of $V_k(x_k, r_k=j)$.

Here ℓ_t^{ji} is the index[1] of the $p(j,i:x)$ piece that is valid for $x \in \Delta_{k+1}^{j}(t)$. □

The proof of this proposition is given in Appendix C.8. Basically these bounds arise by taking the worst case and best case transition probability pieces in (6.78), (6.77) at each time (for each $j \in \underline{M}$). Thus the bounds are quadratic (not piecewise quadratic) in x_k. In Figure 6.5 this upper and lower bound is illustrated for an example problem. Note that for this particular example, the upper bound and left endpiece are the same. That is, $V_k^{Le}(x_k,j) = V^{UB}(x_k,j)$. In general the endpieces need not be the same as either the upper or lower bound.

We now consider the existence of steady-state upper and lower bounds on the steady-state expected cost-to-go:

$$V_\infty^{LB}(x,j) \triangleq \lim_{(N-k)\to\infty} V_k^{LB}(x_k=x,r_k=j)$$

$$V_\infty^{UB}(x,j) \triangleq \lim_{(N-k)\to\infty} V_k^{UB}(x_k=x,r_k=j)$$

for the infinite time horizon problem where (if all of these quantities exist):

$$V_\infty^{LB}(x,j) \leq \lim_{(N-k)\to\infty} V_k(x_k=x,r_k=1) \leq V_\infty^{UB}(x,j).$$

[1] As defined in Appendix C.1.

We cannot directly apply the conditions of Proposition 3.2 to Proposition 6.7 (as we did for steady-state endpieces in Proposition 6.2 and middlepieces in Proposition 6.6) because the upper and lower bound calculations in (6.75)-(6.79) do not directly correspond to time-invariant x-independent problems. The choice of index (t) in (6.77)-(6.78) may change with k, as (N-k) increases. However we can find weaker upper and lower bounds on the expected costs-to-go that do correspond to x-independent JLQ problems and that do converge as $(N-k) \rightarrow \infty$.

Proposition 6.8: (Steady-state Bounds)

With

$$P_{ji} = \max_{t=1,..,\bar{\nu}_{ji}} \lambda_{ji}(t) \qquad \text{all } i,j \in \underline{M} \tag{6.80}$$

conditions (1)-(3) of Proposition 3.2 are sufficient for the existence of a set of nonnegative scalars

$$\{\bar{K}(j) \geq 0,\ j \in \underline{M}\}$$

such that, as $(N-k) \rightarrow \infty$ we have for each $j \in \underline{M}$

$$K_k^{UB}(j) \leq \bar{K}(j). \tag{6.81}$$

Here $\{\bar{K}(j): j \in \underline{M}\}$ are the nonnegative solutions of the set of M coupled equations

$$\bar{K}(j) = \frac{a^2(j)R(j)\left[\sum_{i\epsilon c_j} p_{ji}(\bar{K}(i)+Q(i))\right]}{R(j)+b^2(j)\left[\sum_{i\epsilon c_i} p_{ji}(\bar{K}(i)+Q(i))\right]} \tag{6.82}$$

with the p_{ji} in (6.82) given by (6.80). Similarly with

$$p_{ji} = \min_{t=1,..,\bar{\nu}_{ji}} \lambda_{ji}(t) \qquad \text{all} \quad i,j \in \underline{M} \tag{6.83}$$

conditions (1)-(3) of Proposition 3.2 are <u>sufficient</u> for the existence of a set of nonnegative scalars

$$\underline{K}(j) \geq 0 \quad j\epsilon\underline{M}$$

such that, as $(N-k) \longrightarrow \infty$ for each $j \in \underline{M}$

$$\underline{K}(j) - K_k^{LB}(j) \tag{6.84}$$

where $\{\underline{K}(j): j \in \underline{M}\}$ are the nonnegative solutions of the set of M coupled equations

$$\underline{K}(j) = \frac{a^2(j)R(j)\left[\sum_{i\in C_j} p_{ji}(\underline{K}(i)+Q(i))\right]}{R(j)+b^2(j)\left[\sum_{i\in C_j} p_{ji}(\underline{K}(i)+Q(i))\right]} \tag{6.85}$$

with the p_{ji} in (6.85) given by (6.83). Thus as $(N-k)\longrightarrow\infty$ we have

$$V_K^{UB}(x,j) = x^2 K_K^{UB}(j) \qquad \leq x^2\bar{K}(j) \tag{6.86}$$

$$V_K^{LB}(x,j) = x^2 K_K^{LB}(j) \qquad \geq x^2\underline{K}(j) \tag{6.87}$$

respectively, for each $j \in \underline{M}$. □

The proof of this proposition appears in Appendix C.9. These bounds correspond to the highest and lowest possible cost parameters at each time stage. Note that for problems with each form stabilizable, the above conditions are immediately met.

To summarize, in this section we have obtained upper and lower bounds on $V_k(x_k,r_k=j)$ that are recursively computed with an embedded comparison of scalar quantities at each time step (in (6.77)-(6.78)).

We then obtained sufficient conditions for weaker bounds to converge to steady-state values as $(N-k)\to\infty$. In Chapter 6

(i.e., when (6.1)-(6.4) hold) the stabilizability of each form is then sufficient for the existence of steady-state endpieces, middle-pieces and overall bounds on the costs-to-go. Example 6.3 shows that this is not a necessary condition.

6.5 A Single Form-Transition Problem

In this section we formulate a special class of JLQ problems that will be used in the remainder of this chapter and chapter 7 to illustrate various qualitative properties of the x-dependent JLQ controller.

We consider systems with M=2 forms:

$$x_{k+1} = a(r_k)x_k + b(r_k)u_k \qquad r_k \in \{1,2\} \tag{6.88}$$

$$p(1,2:x) = \begin{cases} \omega_1 & \text{if } |x| < \alpha \\ \omega_2 & \text{if } |x| > \alpha \end{cases}$$

$$p(1,1:x) = 1-p(1,2:x) \qquad p(2,1)=0 \quad p(2,2)=1 \tag{6.90}$$

The form structure and possible shapes of p(1,2:x) are shown in Figure 6.6. There is only one possible form change here (from r=1 to r=2) and the form transition probabilities are symmetric about zero.

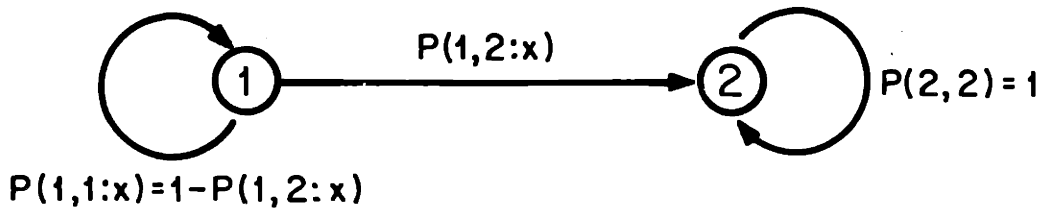

(a)

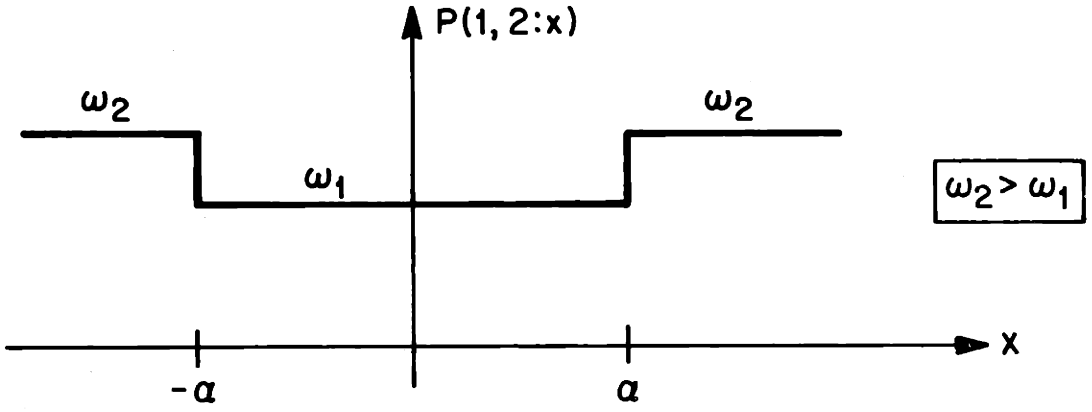

(b)

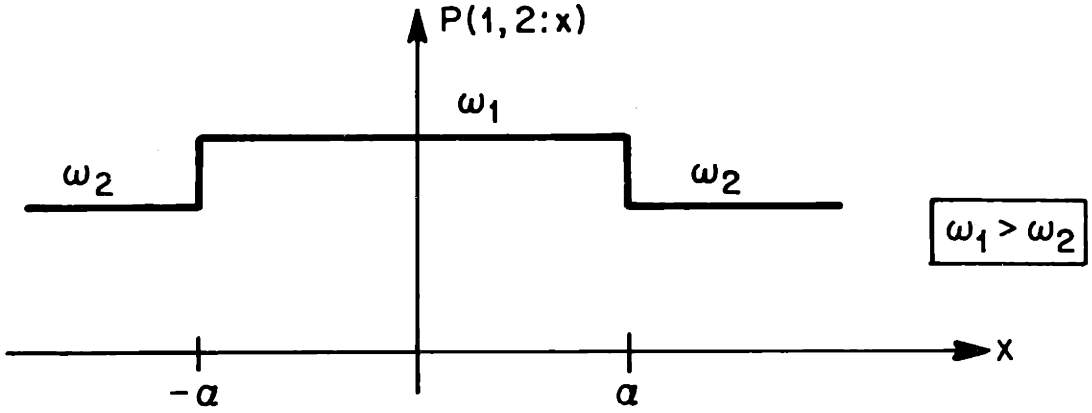

(c)

Figure 6.6: Form structure (a), and p(1,2:x) for (6.1)-(6.2) where (b) $\omega_2 > \omega_1$, and (c) $\omega_1 > \omega_2$.

We seek to minimize

$$\min_{u_0,\ldots,u_{N-1}} E\left\{\sum_{k=k_0}^{N-1} [u_k^2 R(r_k)+x_{k+1}^2 Q(r_{k+1})]+ x_N^2 K_T(r_N)\right\} . \qquad (6.91)$$

Here for each j=1,2, the following parameters are all finite

$$\begin{aligned} &Q(1)> 0 \\ &Q(2)\geq 0 \\ &K_T(j)\geq 0 \\ &R(j)> 0 \\ &b(j)\neq 0 \\ &a(j)> 0 \\ &\alpha > 0 \end{aligned} \qquad (6.92)$$

and

$$\begin{aligned} &0 < \omega_1 < 1 \\ &0 < \omega_2 < 1 \end{aligned} \qquad (6.93)$$

From the symmetry of the form transition probabilities (6.88)-(6.90) and costs (6.91) about x=zero, it is clear that the expected costs-to-go $V_k(x_k,r_k)$ will be symmetric about zero.

Note that this class of example problems includes example 5.1 as a special case.

Note that once the system enters form r=2, it stays there. Thus the usual LQ theory yields the following:

$$V_k(x_k, r_k=2) = x_k^2 K_k(1:2) \qquad k=N,N-1,\ldots,0 \tag{6.94}$$

$$u_k(x_k, r_k=2) = L_k(1:2)x_k \qquad k=N-1,\ldots,0 \tag{6.95}$$

where

$$K_N(1:2) = K_T(2)$$

$$K_k(1:2) = \frac{a^2(2)R(2)[K_{k+1}(1:2)+Q(2)]}{R(2)+b^2(2)[K_{k+1}(1:2)+Q(2)]} \tag{6.96}$$

$$L_k(1:2) = \frac{-b(2)a(2)[K_{k+1}(1:2)+Q(2)]}{R(2)+b^2(2)[K_{k+1}(1:2)+Q(2)]} \quad . \tag{6.97}$$

Since $b(2)\neq 0$, $K_k(1:2)$ converges monotonely as (N-k) increases, to

$$K_\infty(1:2) = \left[\begin{matrix} R(2)[a^2(2)-1] \\ -b^2(2)Q(2) \end{matrix}\right] + \frac{\sqrt{\left(\begin{matrix} R(2)[a^2(2)-1] \\ -b^2(2)Q(2) \end{matrix}\right)^2 + 4b^2(2)a^2(2)R(2)Q(2)}}{2b^2(2)} \tag{6.98}$$

where $K_k(1:2)$ decreases as (N-k) increases if $K_T(2) > K_\infty(1:2)$ and increases if $K_T(2) < K_\infty(1:2)$.

Now consider what happens when $r_{N-1}=1$. We are given that at time k=N,

$$V_N(x_N, r_N=1) = x_N^2 K_T(1) \quad . \tag{6.99}$$

From sections 6.2 and 6.3, the endpieces and middlepiece of $V_k(x_k, r_k=1)$ and $u_k(x_k, r_k=1)$ are given by

$$V_k^{Re}(x_k,1) = V_k^{Le}(x_k,1) = x_k^2 K_k^{Le}(1) \tag{6.100}$$

$$u_k^{Re}(x_k,1) = u_k^{Le}(x_k,1) = -L_k^{Le}(1)x_k \tag{6.101}$$

and

$$V_k^{RM}(x_k,1) = V_k^{LM}(x_k,1) = x_k^2 K_k^{LM}(1) \tag{6.102}$$

$$u_k^{RM}(x_k,1) = u_k^{LM}(x_k,1) = -L_k^{LM}(1)x_k \tag{6.103}$$

where

$$K_N^{Re}(1) = K_N^{Le}(1) = K_N^{LM}(1) = K_N^{RM}(1) = K_T(1)$$

and

$K_k^{Le}(1) \equiv K_k^{Re}(1)$, $K_k^{LM}(1) \equiv K_k^{RM}(1)$ are given by

$$K_k^{Re}(1) = K_k^{Le}(1) = \frac{a^2(1)R(1)\hat{K}_{k+1}^{Le}(1)}{R(1)+b^2(1)\hat{K}_{k+1}^{Le}(1)} \tag{6.104}$$

$$L_k^{Re}(1) = L_k^{Le}(1) = \frac{-b(1)}{a(1)R(1)} K_k^{Le}(1)$$

where

$$\hat{K}_{k+1}^{Le}(1) = (1-\omega_2)(K_{k+1}^{Le}(1)+Q(1)) + \omega_2(K_{k+1}(1:2)+Q(2))$$

and

$$K_k^{RM}(1) \equiv K_k^{LM}(1) = \frac{a^2(1)R(1)\hat{K}_{k+1}^{LM}(1)}{R(1)+b^2(1)\hat{K}_{k+1}^{LM}(1)} \tag{6.105}$$

$$L_k^{RM}(1) = L_k^{LM}(1) = \frac{-b(1)}{a(1)R(1)} K_k^{LM}(1)$$

where

$$\hat{K}_{k+1}^{LM}(1) = (1-\omega_1)(K_{k+1}^{LM}(1)+Q(1)) + \omega_1(K_{k+1}(1:2)+Q(2)).$$

Since $b(1)\neq 0$, the steady-state quantities $K_\infty^{Le}(1) \equiv K_\infty^{Re}(1)$ and $K_\infty^{LM}(1) \equiv K_\infty^{RM}(1)$ are finite and positive, satisfying

$$K_\infty^{Re}(1) = K_\infty^{Le}(1) = \frac{a^2(1)R(1)\left[(1-\omega_2)\begin{pmatrix} K_\infty^{Le}(1) \\ + \\ Q(1)\end{pmatrix} + \omega_2\begin{pmatrix} K_\infty(1:2) \\ + \\ Q(2)\end{pmatrix}\right]}{R(1)+b^2(1)\left[(1-\omega_2)\begin{pmatrix} K_\infty^{Le}(1) \\ + \\ Q(1)\end{pmatrix} + \omega_2\begin{pmatrix} K_\infty(1:2) \\ + \\ Q(2)\end{pmatrix}\right]} \tag{6.106}$$

$$K_{\infty}^{RM}(1) = K_{\infty}^{LM}(1) = \frac{a^2(1)R(1)\left[(1-\omega_1)\begin{pmatrix}K_{\infty}^{LM}(1)\\+\\Q(1)\end{pmatrix} + \omega_1\begin{pmatrix}K_{\infty}(1:2)\\+\\Q(2)\end{pmatrix}\right]}{R(1)+b^2(1)\left[(1-\omega_1)\begin{pmatrix}K_{\infty}^{LM}(1)\\+\\Q(1)\end{pmatrix} + \omega_1\begin{pmatrix}K_{\infty}(1:2)\\+\\Q(2)\end{pmatrix}\right]} \quad . \tag{6.107}$$

The partition of x_N values specified in step 1 of Section 5.4 is

$$\Delta_N(1) = (\gamma_N(0),\gamma_N(1)) = (-\infty,-\alpha)$$

$$\Delta_N(2) = (\gamma_N(1),\gamma_N(2)) = (-\alpha,\alpha)$$

$$\Delta_N(3) = (\gamma_N(2),\gamma_N(3)) = (\alpha,\infty)$$

as shown[1] in Figure 6.7.

The conditional expected cost-to-go

$$\hat{V}_N(x_N|r_{N-1}=1) = x_N^2\hat{K}_N(t) + x_N\hat{H}_N(t) + \hat{G}_N(t)$$

$$\text{for } x_N \in \Delta_N(t)$$

$$\hat{K}_N(1) \equiv \hat{K}_N(3) = (1-\omega_2)(K_T(1)+Q(1)) + \omega_2\,(K_T(2)+Q(2))$$

$$\hat{K}_N(2) = (1-\omega_1)(K_T(1)+Q(1)) + \omega_1(K_T(2)+Q(2))$$

---

[1] The superscript "1" is not used in $\Delta_N^1(t)$, $\hat{K}_N^1(t)$, etc., in this section since we are only considering form 1.

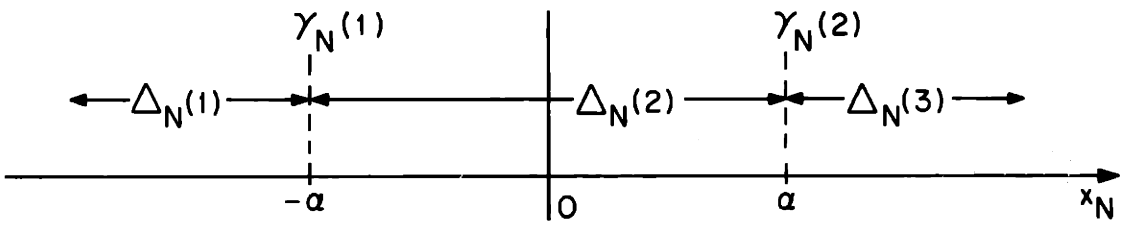

Figure 6.7: x_N partition for (6.1)-(6.4) example problem.

can take the two possible shapes shown in Figure 6.8, depending upon the values of ω_1, ω_2, $Q(1)$, $Q(2)$, $K_T(1)$ and $K_T(2)$. We will consider each case in turn.

Case 1: If

$$(\omega_2-\omega_1)[(K_T(2)+Q(2))-(K_T(1)+Q(1))]>0 \tag{6.108}$$

hence

$$\hat{K}_N(1) > \hat{K}_N(2) \tag{6.109}$$

then $\hat{V}_N(x_N|r_{N-1}=1)$ is as shown in Figure 6.8(a). The conditions (6.108), (6.109) are met when

- $\omega_2 > \omega_1$ the probability of the form change is greater away from zero than near it
- $K_T(2)+Q(2) > K_T(1)+Q(1)$ the cost charged at time N is greater in form 2 than in form 1.

This corresponds to regulation problems in failure prove systems. The system is operating normally when r=1 and has failed when r=2. A higher cost is charged in the failed mode than in normal operation, and the probability of failure is greater away from the regulator goal of zero than near it.

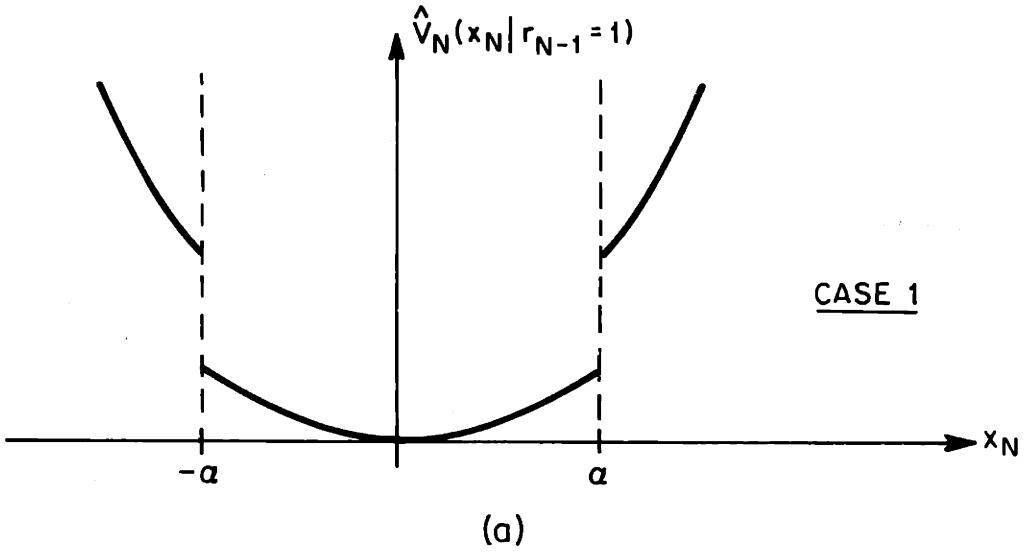

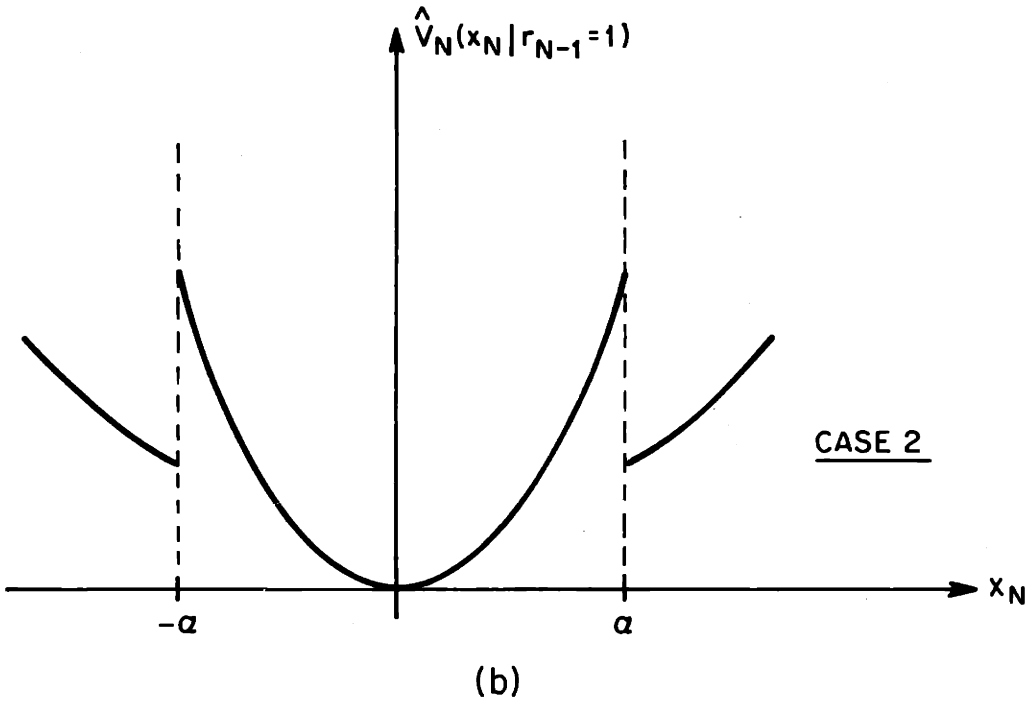

Figure 6.8: $\hat{V}_N(x_N|r_{N-1}=1)$ when (a) $\hat{K}_N(1) \equiv \hat{K}_N(3) > \hat{K}_N(2)$ (case 1) and when (b) $\hat{K}_N(2) > \hat{K}_N(1) \equiv \hat{K}_N(3)$ (case 2).

Example 5.1 illustrates this situation. Conditions (6.108)-(6.109) are also met when

- $\omega_1 > \omega_2$ the probability of the form change is greater <u>near</u> zero than away from it
- $K_T(1)+Q(1) > K_T(2)+Q(2)$ the cost charged at time N is greater in form 1 than in form 2.

<u>Case 2</u>: If

$$(\omega_1-\omega_2)[(K_T(2)+Q(2))-(K_T(1)+Q(1))] > 0 \tag{6.110}$$

hence

$$\hat{K}_N(2) > \hat{K}_N(1) \tag{6.111}$$

then we have the situation shown in Figure 6.8(b). Conditions (6.110)-(6.111) are met in problems where the probability of transition form r=1 to r=2 is at "cross purposes" with the cost structure. The case

$$\omega_1 > \omega_2$$

$$K_T(2)+Q(2) > K_T(1)+Q(1)$$

corresponds to the probability of "failure" (i.e., changing to the higher cost form) being <u>higher</u> near the regulator goal of zero than

away from it. The case

$$\omega_2 > \omega_1$$

$$K_T(1)+Q(1) > K_T(2)+Q(2)$$

corresponds to the probability of "success" being lower near the regulator goal than away from it. As we will see in the next section, the "cross purposes" of the form transition probabilities and costs can lead to local minima of the expected costs-to-go.

6.6 Last Stage Solution

In this section we develop the last-stage solution for the two cases of the last section. The solutions of these one-stage problems illustrate certain basic qualitative properties of x-dependent JLQ controllers.

Using Appendix C.1 we find that for both cases of the last section,

$$\theta_{N-1}(2) = -\alpha\left(1+ \frac{b^2(1)\hat{K}_N(2)}{R(1)}\right) \tag{6.112}$$

$$\Theta_{N-1}(2) = \alpha\left(1+ \frac{b^2(1)\hat{K}_N(2)}{R(1)}\right) \tag{6.113}$$

$$\theta_{N-1}(3) = \alpha\left(1+ \frac{b^2(1)\hat{K}_N(3)}{R(1)}\right) \tag{6.114}$$

$$\Theta_{N-1}(1) = -\alpha\left(1+ \frac{b^2(1)\hat{K}_N(1)}{R(1)}\right) \tag{6.115}$$

and from Proposition 5.2 we find that

$$\zeta_N = 5 \tag{6.116}$$

candidate costs-to-go must be considered. For Case 1 ($\hat{K}_N(1) \equiv \hat{K}_N(3) > \hat{K}_N(2)$) these candidates are

$$\bullet\ V_{N-1}^{1,U},\ V_{N-1}^{2,U},\ V_{N-1}^{3,U},\ V_{N-1}^{2,L},\ U_{N-1}^{2,R} \tag{6.117}$$

if $\hat{K}_N(1) \equiv \hat{K}_N(3) > \hat{K}_N(2)$

(i.e., $V_{N-1}^{1,R}$ and $V_{N-1}^{3,L}$ eliminated)

and the θ's and Θ's in (6.112)-(6.116) satisfy

$$\Theta_{N-1}(1) < \theta_{N-1}(2) < \Theta_{N-1}(2) < \theta_{N-1}(3) \quad \bullet \tag{6.118}$$

For Case 2 ($\hat{K}_N(1) \equiv \hat{K}_N(3) < \hat{K}_N(2)$) the candidate costs are

$$\bullet\ V_{N-1}^{1,U},\ V_{N-1}^{2,U},\ V_{N-1}^{3,U},\ V_{N-1}^{3,L},\ V_{N-1}^{1,R} \tag{6.119}$$

if $\hat{K}_N(2) > \hat{K}_N(1) \equiv \hat{K}_N(3)$

(i.e., $V_{N-1}^{2,L}$ and $V_{N-1}^{2,R}$ eliminated)

and

$$\theta_{N-1}(2) < \Theta_{N-1}(1) < \theta_{N-1}(3) < \Theta_{N-1}(2) \quad \bullet \tag{6.120}$$

The eligible costs for $V_{N-1}(x_{N-1},r_{N-1}=1)$ over various x_{N-1} values are shown for each case in Figure 6.9.

From Figure 6.9(a) it is evident in Case 1 there are intervals of x_{N-1} values over which the optimal controller must involve hedging to a point. These are

$$x_{N-1} \in \left(\frac{\theta_{N-1}(1)}{a(1)}, \frac{\theta_{N-1}(2)}{a(1)}\right), \left(\frac{\theta_{N-1}(2)}{a(1)}, \frac{\theta_{N-1}(3)}{a(1)}\right) .$$

We will now determine $V_{N-1}(x_{N-1},r_{N-1}=1)$ for these case 1 problems where the costs and form transition probabilities are not at "cross purposes". That is, where

$$\hat{K}_N(1) \equiv \hat{K}_N(3) > \hat{K}_N(2) .$$

We have already computed $V_{N-1}(x_{N-1},r_{N-1}=1)$, $u_{N-1}(x_{N-1},r_{N-1}=1)$ and $x_N(x_{N-1},r_{N-1}=1)$ for an example problem of this type in Section 5.3. The same steps detailed there (with the shortcuts described in Section 5.6) yield the following:

Fact 6.9: When $\hat{K}_N(1) = \hat{K}_N(3) > \hat{K}_N(2)$ (Case 1), the optimal cost-to-go and control laws have

$$m_{N-1}(1) = 5 \qquad (6.121)$$

pieces, joined at x_{N-1} values

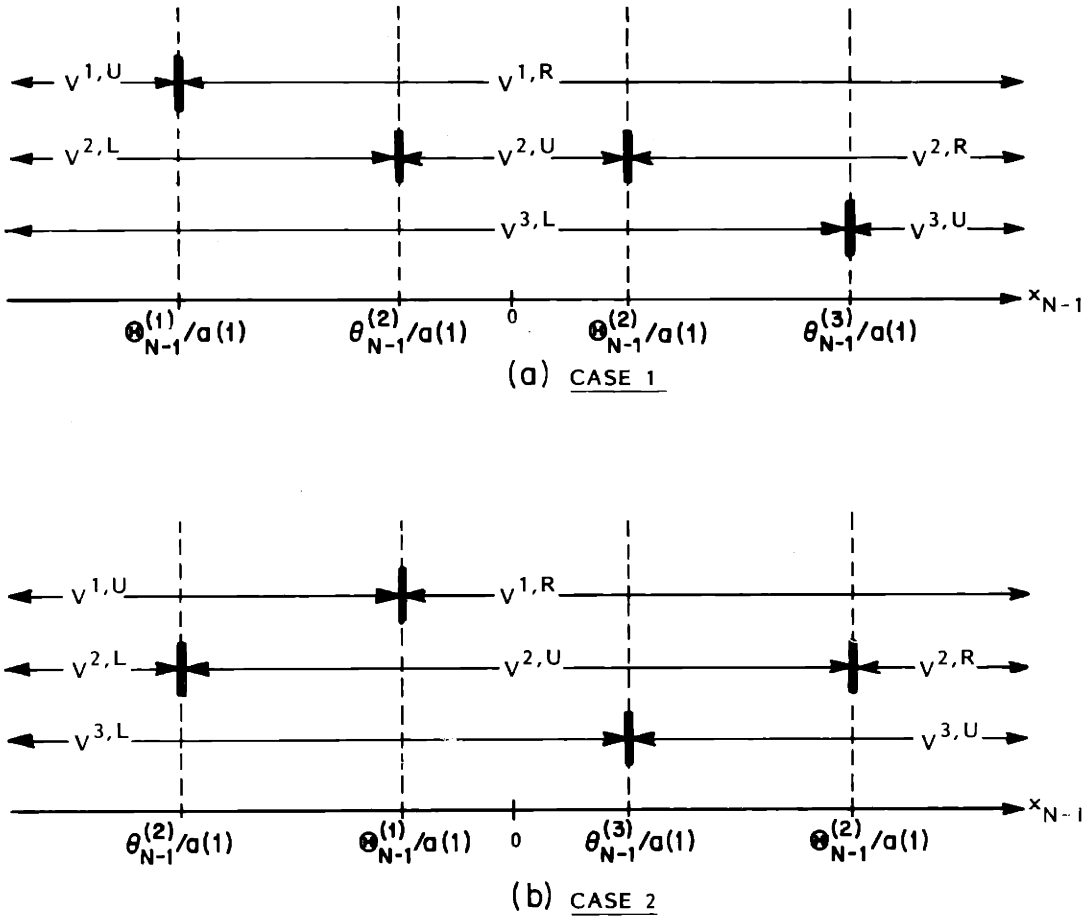

Figure 6.9: Eligible costs for $V_{N-1}(x_{N-1}, r_{N-1}=1)$ when
(a) $\hat{K}_N(1) \equiv \hat{K}_N(3) > \hat{K}_N(2)$ (case 1) and
(b) $\hat{K}_N(2) > \hat{K}_N(1) \equiv \hat{K}_N(3)$ (case 2).

$$\delta_{N-1}(1) = \frac{\Theta_{N-1}(1)}{a(1)}\left[1+\sqrt{1-\frac{\theta_{N-1}(2)}{\Theta_{N-1}(1)}}\right]$$

$$= \frac{-\alpha}{a(1)R(1)}\left[R(1)+b^2(1)\hat{K}_N(1)\right]\left[1+\sqrt{1-\frac{R(1)+b^2(1)\hat{K}_N(2)}{R(1)+b^2(1)\hat{K}_N(1)}}\right] \tag{6.122}$$

$$\delta_{N-1}(2) = \frac{\theta_{N-1}(2)}{a(1)} = \frac{-\alpha}{a(1)R(1)}\left[R(1)+b^2(1)\hat{K}_N(2)\right] \tag{6.123}$$

$$\delta_{N-1}(3) = -\delta_{N-1}(2) \tag{6.124}$$

$$\delta_{N-1}(4) = -\delta_{N-1}(1) \tag{6.125}$$

The optimal candidate costs-to-go are

$$V_{N-1}(x_{N-1}, r_{N-1}=1) = \begin{cases} V_{N-1}^{1,U}(x_{N-1},1) & \text{if } x_{N-1} \le \delta_{N-1}(1) \\ V_{N-1}^{2,L}(x_{N-1},1) & \text{if } \delta_{N-1}(1) \le x_{N-1} \le \delta_{N-1}(2) \\ V_{N-1}^{2,U}(x_{N-1},1) & \text{if } \delta_{N-1}(2) \le x_{N-1} \le \delta_{N-1}(3) \\ V_{N-1}^{2,R}(x_{N-1},1) & \text{if } \delta_{N-1}(3) \le x_{N-1} \le \delta_{N-1}(4) \\ V_{N-1}^{3,U}(x_{N-1},1) & \text{if } \delta_{N-1}(4) \le x_{N-1} \end{cases} \tag{6.126}$$

Thus the optimal expected cost-to-go is given by

$$V_{N-1}(x_{N-1}, r_{N-1}=1) = \begin{cases} x_{N-1}^2 K_{N-1}(t:1) + x_{N-1} H_{N-1}(t:1) + G_{N-1}(t:1) \\ \quad \text{for} \quad \delta_{N-1}(t-1) \le x_{N-1} \le \delta_{N-1}(t) \end{cases} \tag{6.127}$$

where $t=1,\ldots,m_{N-1}(1)=5$ and $\delta_{N-1}(0)\triangleq-\infty$, $\delta_{N-1}(5)\triangleq+\infty$ with

$$K_{N-1}(1:1) = \frac{a^2(1)R(1)\hat{K}_N(1)}{R(1)+b^2(1)\hat{K}_N(1)} = K_{N-1}(5:1) \tag{6.128}$$

$$K_{N-1}(2:1) = \frac{a^2(1)R(1)}{b^2(1)} = K_{N-1}(4:1) \tag{6.129}$$

$$K_{N-1}(3:1) = \frac{a^2(1)R(1)\hat{K}_N(2)}{R(1)+b^2(1)\hat{K}_N(2)} \tag{6.130}$$

$$H_{N-1}(2:1) = \frac{2a(1)R(1)\alpha}{b^2(1)} = -H_{N-1}(4:1) \tag{6.131}$$

$$H_{N-1}(1:1) = H_{N-1}(3:1) = H_{N-1}(5:1) = 0 \tag{6.132}$$

$$G_{N-1}(2:1) = \frac{\alpha^2}{b^2(1)}\left(R(1)+b^2(1)\hat{K}_N(2)\right) = G_{N-1}(4:1) \tag{6.133}$$

$$G_{N-1}(1:1) = G_{N-1}(3:1) = G_{N-1}(5:1) = 0 \tag{6.134}$$

The optimal control law is

$$u_{N-1}(x_{N-1},r_{N-1}=1) = \begin{cases} -L_{N-1}(t:1)x_{N-1}+F_{N-1}(t:1) \\ \text{for} \quad \delta_{N-1}(t-1)<x_{N-1}<\delta_{N-1}(t) \end{cases} \tag{6.135}$$

with

$$L_{N-1}(1:1) = \frac{a(1)b(1)\hat{K}_N(1)}{R(1)+b^2(1)\hat{K}_N(1)} = L_{N-1}(5:1) \tag{6.136}$$

$$L_{N-1}(2:1) = \frac{a(1)}{b(1)} = L_{N-1}(4:1) \tag{6.137}$$

$$L_{N-1}(3:1) = \frac{a(1)b(1)\hat{K}_N(2)}{R(1)+b^2(1)\hat{K}_N(2)} \tag{6.138}$$

$$F_{N-1}(2:1) = \frac{-\alpha^+}{b(1)} = -F_{N-1}(4:1) \tag{6.139}$$

$$F_{N-1}(1:1) = F_{N-1}(3:1) = F_{N-1}(5:1) = 0 \quad . \tag{6.140}$$

The x_N value obtained by application of the optimal control law, as a function of x_{N-1} is

$$x_N(x_{N-1}, r_{N-1}=1) = \begin{cases} [a(1)-L_{N-1}(t:1)]x_{N-1}+F_{N-1}(t:1) \\ \text{for} \quad \delta_{N-1}(t-1)<x_{N-1}<\delta_{N-1}(t) \end{cases} \tag{6.141}$$

hence

$$x_N(x_{N-1}, r_{N-1}=1) = \begin{cases} \dfrac{a(1)R(1)}{R(1)+b^2(1)\hat{K}_N(1)}\, x_{N-1} \\ \\ -\alpha^+ \\ \\ \dfrac{a(1)R(1)}{R(1)+b^2(1)\hat{K}_N(2)}\, x_{N-1} \\ \\ \alpha^- \\ \\ \dfrac{a(1)R(1)}{R(1)+b^2(1)\hat{K}_N(3)}\, x_{N-1} \end{cases} \tag{6.142}$$

□

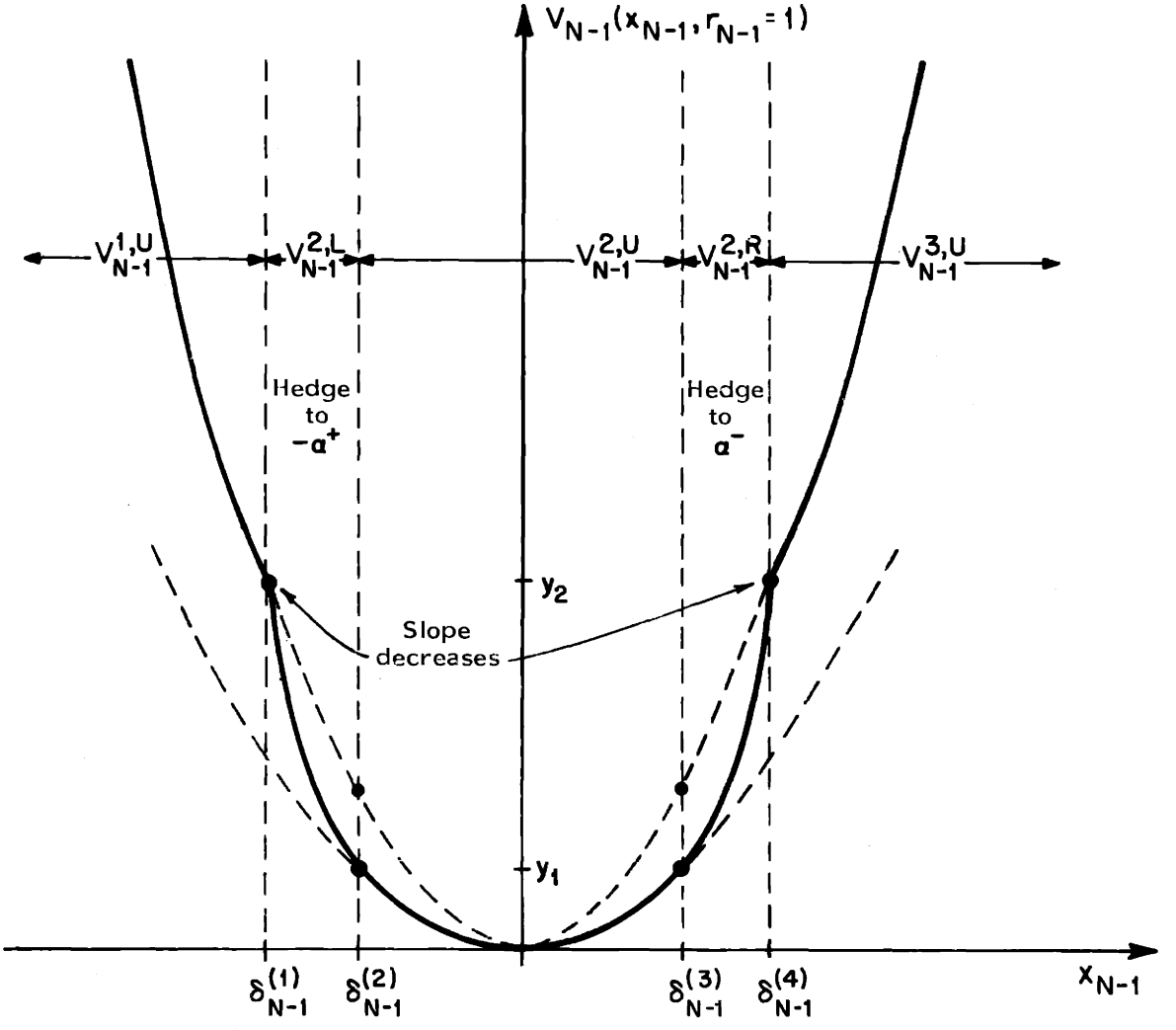

$$y_1 = \frac{\alpha^2 \hat{k}_N(2)}{R(1)} \left[R(1) + b^2 (U \hat{k}_N(2)\right]$$

$$y_2 = \frac{\alpha^2 \hat{k}_N(1)}{R(1)} \left[R(1) + b^2(1)\hat{k}_N(1)\right] \left[1 + \sqrt{1 - \frac{R(1) + b^2(1)\hat{k}_N(2)}{R(1) + b^2(1)\hat{k}_N(1)}}\right]^2$$

Figure 6.10: $V_{N-1}(x_{N-1}, r_{N-1}=1)$ when $\hat{K}_N(1) \equiv \hat{K}_N(3) > \hat{K}_N(2)$. (case 1). The optimal candidate cost function over each region of x_{N-1} values is indicated by the solid line.

In Figure 6.10 $V_{N-1}(x_{N-1}, r_{N-1}=1)$ is shown for this case. The slope of $V_{N-1}(x_{N-1}, r_{N-1}=1)$ decreases discontinuously at $\delta_{N-1}(1)$ and $\delta_{N-1}(4)$, and is continuous elsewhere. For $x_{N-1} \in (\delta_{N-1}(1), \delta_{N-1}(2))$ the optimal controller <u>actively hedges</u> to $x_N = -\alpha^+$ and, as is evident in Figure 6.10, the resulting optimal expected cost-to-go is a quadratic interpolation between $V_{N-1}^{1,U}$ and $V_{N-1}^{2,U}$. Similarly, the optimal expected cost-to-go over $x_{N-1} \in (\delta_{N-1}(3), \delta_{N-1}(4))$ is a quadratic interpolation between $V_{N-1}^{2,U}$ and $V_{N-1}^{3,U}$. The width of these one-step hedging regions is

$$\left(\begin{matrix}\text{width of one-}\\ \text{step hedging}\\ \text{regions}\end{matrix}\right) = \left(\frac{\alpha}{a(1)}\right)\left(\frac{b^2(1)}{R(1)}\right)\left[\left(\hat{K}_N(1)-\hat{K}_N(2)\right) + \sqrt{\left(\hat{K}_N(1)-\hat{K}_N(2)\right)\left(\frac{R(1)}{b^2(1)}+\hat{K}_N(1)\right)}\right]. \tag{6.143}$$

Thus we see that the widths of these regions:

- increase as the "control effectiveness" $\frac{b^2(1)}{R(1)}$ in form 1 increases. (Thus we have more hedging to a point when the control cost is low then when it is high and we have more hedging when the input gain is large than when it is small).
- are linearly related to the ratio of
$$\frac{\left(\begin{matrix}\text{the distance of the point we are}\\ \text{hedging to from zero}\end{matrix}\right)}{\left(\begin{matrix}\text{the open loop dynamics in form 1}\\ a(1)\end{matrix}\right)} .$$

In other words the more stable the open loop system is, the smaller the range of x_{N-1} values where hedging to a point is optimal.

- increase as the difference in costs between the "good" and "bad" sides of the $\hat{V}_N(x_N|r_{N-1}=1)$ discontinuities, $\hat{K}_N(1)-\hat{K}_N(2)$, increases. Thus if the savings obtained by hedging are very small ($\hat{K}_N(1)\approx\hat{K}_N(2)$), the range of x_{N-1} values where hedging to a point is optimal also becomes small.

In figure 6.11, $u_{N-1}(x_{N-1},r_{N-1}=1)$ is shown for $b(1)>0$ (if $b(1)<0$, the graph is flipped around the x_{N-1} axis). The control law increases discontinuously at $x_{N-1} = \delta_{N-1}(1)$, where the optimal strategy changes from driving x_N into $\Delta_N(1)$, to hedging to point $-\alpha^+ \in \Delta_N(2)$. Similarly, $u_{N-1}(x_{N-1},r_{N-1}=1)$ increases discontinuously at $x_{N-1}=\delta_{N-1}(4)$. At all other values of x_{N-1} it is continuous.

In Figure 6.12 the values of x_N obtained by application of the optimal control law is plotted (as a function of x_{N-1}). From (6.142) and Figure 6.12 we can deduce that

- the optimal closed loop system is more stable than the open loop system in form 1 for case 1 problems.

That is, the optimal controller "brakes" the open loop system dynamics. To see this note that over the regions of x_{N-1} values that do not

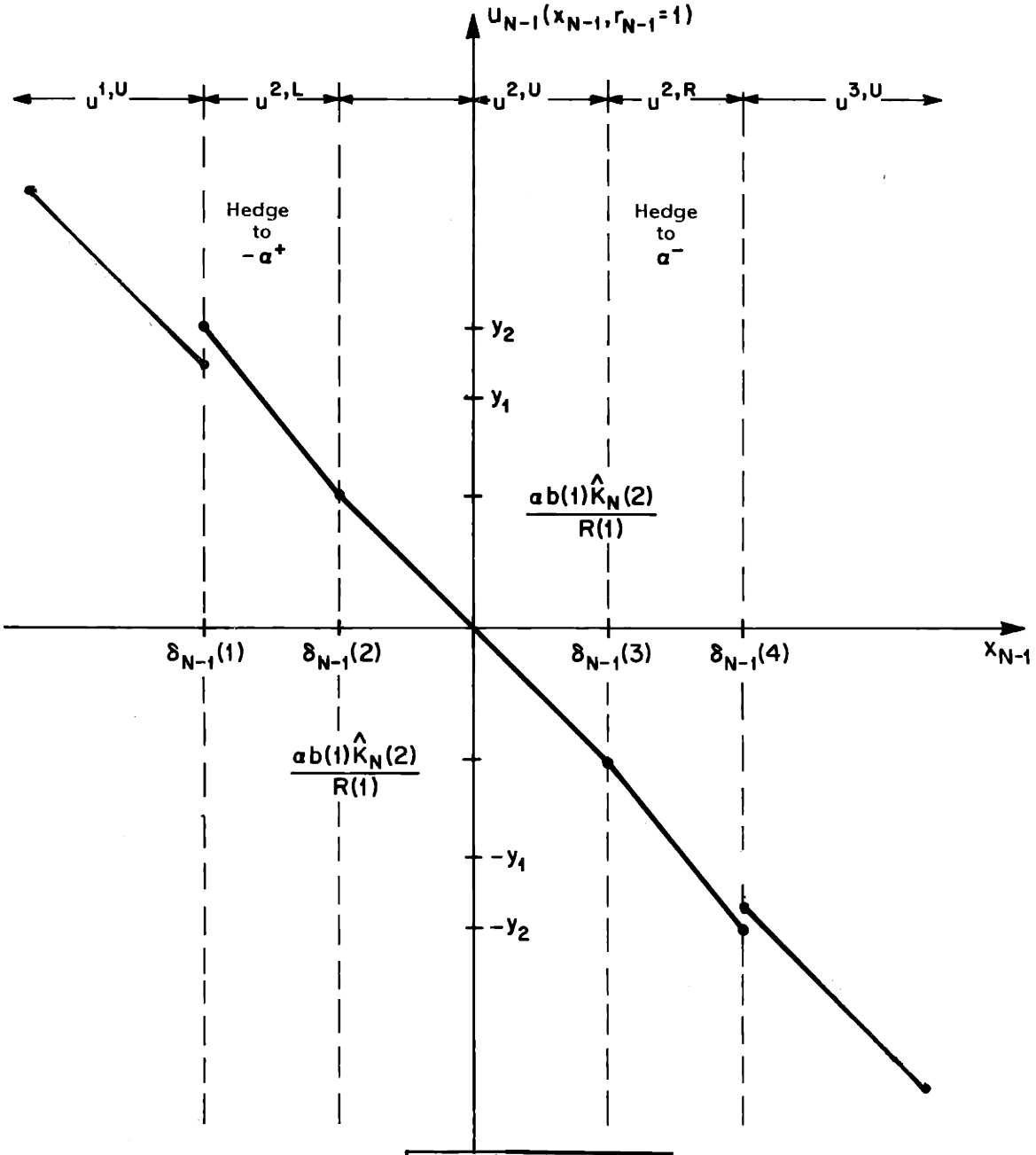

$$y_1 = \frac{\alpha b(1)}{R(1)} \hat{K}_N(1)\left[1+\sqrt{1- \frac{R(1)+b^2(1)\hat{K}_N(2)}{R(1)+b^2(1)\hat{K}_N(1)}}\right]$$

$$y_2 = \frac{\alpha b(1)}{R(1)} \left[\left(\hat{K}_N(1)+ \frac{R(1)}{b^2(1)}\right)\sqrt{1- \frac{R(1)+b^2(1)\hat{K}_N(2)}{R(1)+b^2(1)\hat{K}_N(1)}} + \hat{K}_N(1)\right]$$

Figure 6.11: Control law $u_{N-1}[x_{N-1}, r_{N-1}=1]$ when $\hat{K}_N(1) \equiv \hat{K}_N(3) > \hat{K}_N(2)$ and $b(1)>0$. The optimal control over each region of x_{N-1} values is indicated.

correspond to hedging to a point (i.e., where the slope in Figure 6.12 is positive), the closed loop dynamics are

$$a(1)\left[\frac{1}{1+\frac{b^2(1)}{R(1)}\hat{K}_N(i)}\right] < a(1) \qquad i=1,2,3 \quad .$$

In the hedging regions $x_{N-1} \epsilon (\delta_{N-1}(1), \delta_{N-1}(2))$ and $x_{N-1} \epsilon (\delta_{N-1}(3), \delta_{N-1}(4)$, the optimal controller will be

- more stable than the open loop system (in form 1) if

$$a(1)|x_{N-1}| > \alpha$$

- less stable than the open loop system (in form 1) if

$$a(1)|x_{N-1}| < \alpha \quad .$$

But from (6.112)-(6.116) we see that

$$\left.\begin{array}{l} x_{N-1} \epsilon (\delta_{N-1}(1), \delta_{N-1}(2)) \\ x_{N-1} \epsilon (\delta_{N-1}(3), \delta_{N-1}(4)) \end{array}\right\} \Longrightarrow |x_{N-1}| > \frac{\alpha}{a(1)}\left(1+\frac{b^2(1)}{R(1)}\hat{K}_N(2)\right)$$

hence

$$a(1)|x_{N-1}| > \alpha \quad .$$

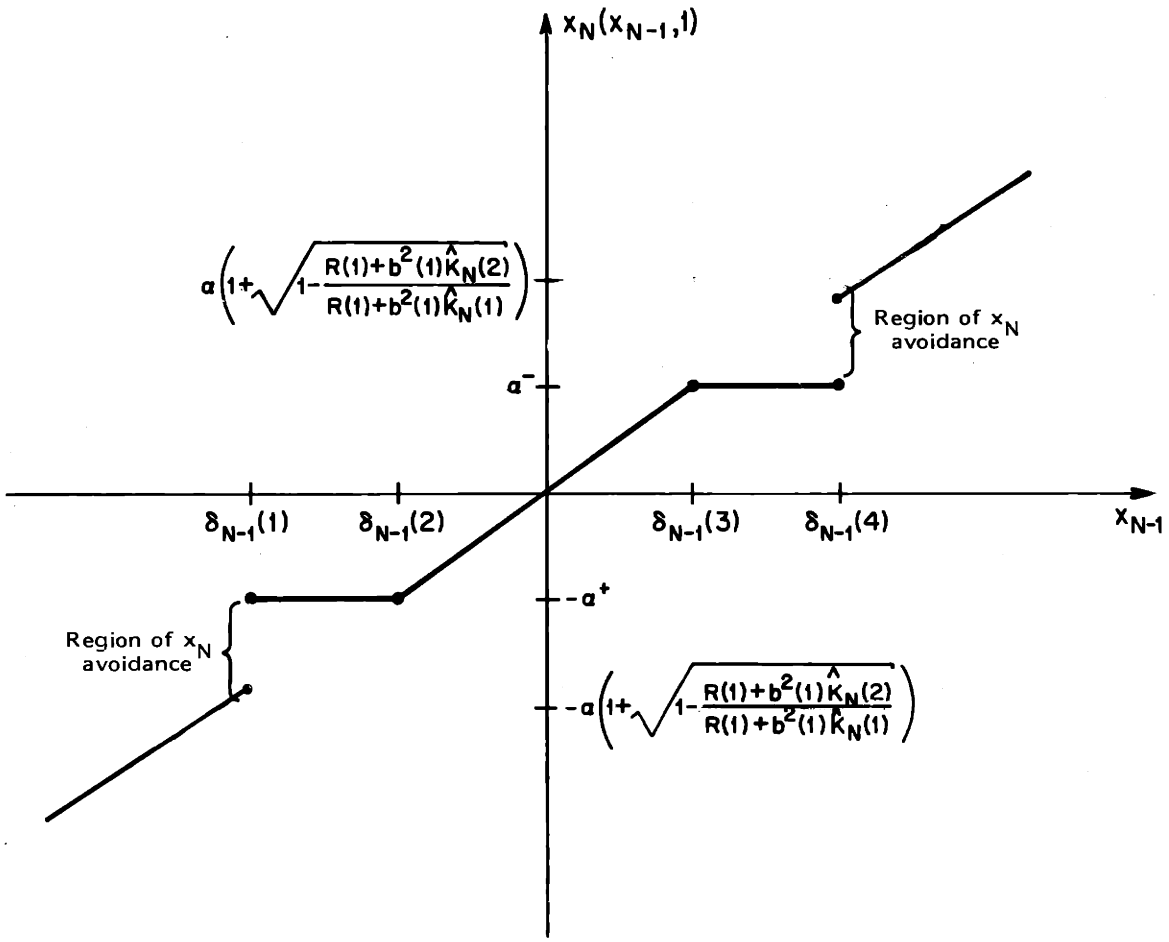

Figure 6.12: $x_N(x_{N-1}, r_{N-1}=1)$ when $\hat{K}_N(1) \equiv \hat{K}_N(3) > \hat{K}_N(2)$ (case 1).

Thus the closed loop system is more stable than the unforced system.

Note that there are two regions of x_N values that are avoided by the optimal controller:

$$x_N \notin \left[\alpha,\ \alpha\ \ 1\left(+\sqrt{1-\frac{R(1)+b^2(1)\hat{K}_N(2)}{R(1)+b^2(1)\hat{K}_N(1)}}\right)\right]$$

$$x_N \notin \left(-\alpha\left(1+\sqrt{1-\frac{R(1)+b^2(1)\hat{K}_N(2)}{R(1)+b^2(1)\hat{K}_N(1)}}\right),\ -\alpha\right] . \tag{6.144}$$

The width of each of these regions of x_N avoidance is

$$\alpha < \alpha\left(\sqrt{1-\frac{R(1)+b^2(1)\hat{K}_N(2)}{R(1)+b^2(1)\hat{K}_N(1)}}\right) < 2\alpha \quad . \tag{6.145}$$

Thus the widths of these regions of avoidance are

- linearly related to the distance of the point we are hedging to from zero (i.e., α)
- increase as the savings from hedging increases.
- increase as the control effectiveness $\frac{b^2(1)}{R(1)}$ in form 1 increases.

Each region of avoidance here is associated with a joining point where the slope of $V_{N-1}(x_{N-1}, r_{N-1}=1)$ decreases discontinuously (i.e., with $\delta_{N-1}(1)$ and $\delta_{N-1}(4)$). These are the x_{N-1} values where two candidates costs cross.

We now examine Case 2 problems where the x-costs and form transition probabilities are at "cross purposes." That is, where

$$\hat{K}_N(2) > \hat{K}_N(1) \equiv \hat{K}_N(3)$$

as in Figures 6.8(b), 6.9(b).

The eligible costs for $V_{N-1}(x_{N-1}, r_{N-1}=1)$ for this case are shown in Figure 6.13 (as in Figure 6.9(b)). By the following arguments (each indicated on Figure 6.13), we can eliminate many of these candidate costs from consideration over certain x_{N-1} regions:

1. As noted earlier (in 6.117), Proposition 5.2 eliminates $V_{N-1}^{2,L}$ and $V_{N-1}^{2,R}$ from consideration (costs corresponding to hedging to the "wrong" sides of $\hat{V}_N(x_N | r_{N-1}=1)$ discontinuities).

2. $\hat{K}_N(2) > \hat{K}_N(1)$ implies that $K_{N-1}(1) < K_{N-1}(2)$ hence $V_{N-1}^{1,U} < V_{N-1}^{2,U}$ (as functions of x_{N-1}). So $V_{N-1}^{2,U}$ is not optimal over $x_N \in (\theta_{N-1}(2)/a(1), \Theta_{N-1}(2)/a(1))$. Similarly,

$V_{N-1}^{2,U}$ is not optimal over $(\theta_{N-1}(3)/a(1),$ $\Theta_{N-1}(2)/a(1))$ since $V_{N-1}^{1,U} \equiv V_{N-1}^{3,U}$ (as functions of x_{N-1}).

3. $V_{N-1}^{3,L} > V_{N-1}^{3,U} \equiv V_{N-1}^{1,U}$ for $x_{N-2} < \theta_{N-1}(2)/a(1)$, so $V_{N-1}^{3,L}$ is not optimal here. Similarly, for $V_{N-1}^{1,R}$ over $x_N > \theta_{N-1}(3)/a(1)$.

Thus we see from Figure 6.13 that

- $V_{N-1}^{1,U}$ is optimal for $x_{N-1} < \Theta_{N-1}(1)/a(1)$
- $V_{N-1}^{3,U}$ is optimal for $x_{N-1} > \theta_{N-1}(3)/a(1)$

and for $x_{N-1} \in (\Theta_{N-1}(1)/a(1), \theta_{N-1}(3)/a(1))$ the three candidates $V_{N-1}^{1,R}$, $V_{N-1}^{2,U}$, $V_{N-1}^{3,R}$ are still eligible.

Solving for the intersections of $V_{N-1}^{1,R}$ and $V_{N-1}^{2,U}$ we find that $V_{N-1}^{1,R} - V_{N-1}^{2,U} = 0$ at

$$x_{N-1} = \frac{\theta_{N-1}(2)}{a(1)}\left[1 \pm \sqrt{1 - \frac{\Theta_{N-1}(1)}{\theta_{N-1}(2)}}\right] \tag{6.146}$$

$$= \frac{1}{a(1)}\left[\theta_{N-1}(2) \mp \sqrt{(\theta_{N-1}(2) - \Theta_{N-1}(1))\theta_{N-1}(2)}\right] .$$

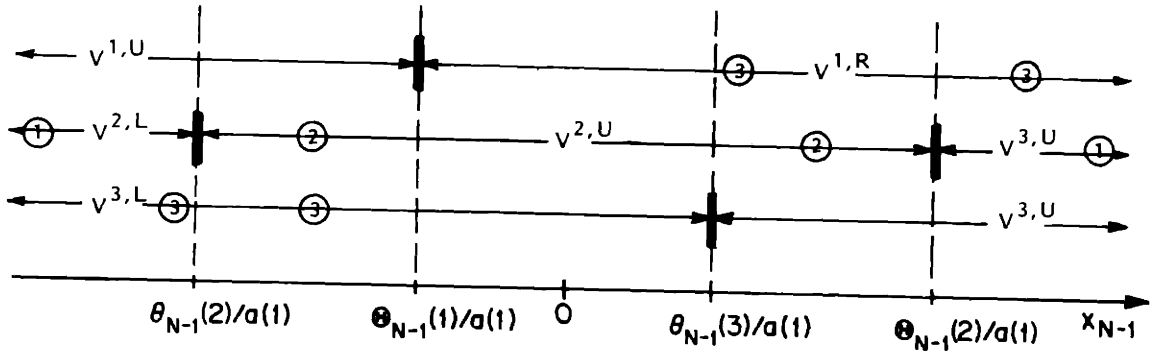

Figure 6.13: Eliminating candidate cost-to-go functions over different regions of x_{N-1} values when $\hat{K}_N(2) > \hat{K}_N(1) \equiv \hat{K}_N(3)$ (case 2); (n) indicates that the specified candidate is eliminated over this interval of x_{N-1} values by step n in the text.

The intersection in (6.146) that is greater than $\theta_{N-1}(2)/a(1)$

$$x_{N-1} = \frac{\theta_{N-1}(2)}{a(1)}\left[1-\sqrt{1-\frac{\Theta_{N-1}(1)}{\theta_{N-1}(2)}}\right] .$$

This is the point at which the optimal candidate cost changes from $V_{N-1}^{1,R}$ to $V_{N-1}^{2,U}$. Similarly, the optimal candidate cost changes from $V_{N-1}^{2,U}$ to $V_{N-1}^{3,L}$ at

$$x_{N-1} = \frac{\Theta_{N-1}(2)}{a(1)}\left[1-\sqrt{1-\frac{\theta_{N-1}(3)}{\Theta_{N-1}(2)}}\right] .$$

Collecting all of this information yields the following:

Fact 6.10: When $\hat{K}_N(2) < \hat{K}_N(1) \equiv \hat{K}_N(3)$ (Case 2), the optimal cost-to-go and control laws have

$$m_{N-1}(1)=5 \tag{6.147}$$

pieces joined at x_{N-1} values

$$\delta_{N-1}(1) = \frac{\Theta_{N-1}(1)}{a(1)} = \frac{-\alpha}{a(1)R(1)}\left[R(1)+b^2(1)\hat{K}_N(1)\right]$$

$$\delta_{N-1}(2) = \frac{\theta_{N-1}(2)}{a(1)}\left[1-\sqrt{1-\frac{\Theta_{N-1}(1)}{\theta_{N-1}(2)}}\right] \tag{6.148}$$

$$= \frac{-\alpha}{a(1)R(1)}\left(R(1)+b^2(1)\hat{K}_N(2)\right)\left[1-\sqrt{1-\frac{R(1)+b^2(1)\hat{K}_N(1)}{R(1)+b^2(1)\hat{K}_N(2)}}\right] \tag{6.149}$$

$$\delta_{N-1}(3) = -\delta_{N-1}(2) \tag{6.150}$$

$$\delta_{N-1}(4) = -\delta_{N-1}(1) \quad . \tag{6.151}$$

The optimal candidate costs-to-go are

$$V_{N-1}(x_{N-1}, r_{N-1}=1) = \begin{cases} V_{N-1}^{1,U}(x_{N-1},1) & \text{if } x_{N-1} \leq \delta_{N-1}(1) \\ V_{N-1}^{1,R}(x_{N-1},1) & \text{if } \delta_{N-1}(1) \leq x_{N-1} \leq \delta_{N-1}(2) \\ V_{N-1}^{2,U}(x_{N-1},1) & \text{if } \delta_{N-1}(2) \leq x_{N-1} \leq \delta_{N-1}(3) \\ V_{N-1}^{3,L}(x_{N-1},1) & \text{if } \delta_{N-1}(3) \leq x_{N-1} \leq \delta_{N-1}(4) \\ V_{N-1}^{3,U}(x_{N-1},1) & \text{if } \delta_{N-1}(4) \leq x_{N-1} \end{cases} \quad . \tag{6.152}$$

Thus the optimal expected cost-to-go is given by (6.127) where $\{K_{N-1}(t:1),\ H_{N-1}(t:1):\ t=1,\ldots,m_{N-1}(1)=5\}$ are the same as for the earlier case (as in 6.128)-(6.152)) except that

$$G_{N-1}(2:1) = \frac{\alpha^2}{b^2(1)}\left(R(1)+b^2(1)\hat{K}_N(1)\right) = G_{N-1}(4:1) \tag{6.153}$$

$$G_{N-1}(1:1) = G_{N-1}(3:1) = G_{N-1}(5:1)=0 \quad .$$

The optimal control law is given by (6.135) where $\{L_{N-1}(t:1):\ t=1,\ldots,m_{N-1}(1)=5\}$ is the same as for the earlier case (as in (6.136)-(6.138)) except that

$$F_{N-1}(2:1) = \frac{-\alpha^-}{b(1)} = -F_{N-1}(4:1)$$
$$F_{N-1}(1:1) = F_{N-1}(3:1) = F_{N-1}(5:1) = 0 \quad . \tag{6.153}$$

The x_N value obtained by the application of the optimal control law, as a function of x_{N-1}, is given by (6.141). Hence

$$x_N(x_{N-1}, r_{N-1}=1) = \begin{cases} \dfrac{a(1)R(1)}{R(1)+b^2(1)\hat{K}_N(1)}\, x_{N-1} \\ -\alpha^- \\ \dfrac{a(1)R(1)}{R(1)+b^2(1)\hat{K}_N(2)}\, x_{N-1} \\ \alpha^+ \\ \dfrac{a(1)R(1)}{R(1)+b^2(1)\hat{K}_N(3)}\, x_{N-1} \end{cases} \quad . \tag{6.154}$$

□

We see that for this case, hedging is to the other side of $-\alpha$ and $+\alpha$ (since $V_N(x_N|r_{N-1}=1)$ is now less on the opposite side of these x_N values). In Figure 6.14, $u_{N-1}(x_{N-1}, r_{N-1}=1)$ is shown for $b(1) > 0$. The control law increases discontinuously at $x_{N-1}=\delta_{N-1}(2)$, where the optimal strategy changes from hedging to the point $-\alpha^- \in \Delta_N(1)$ to driving x_N into $\Delta_N(2)$. Similarly, $u_{N-1}(x_{N-1}, r_{N-1}=1)$ increases at $x_{N-1}=\delta_{N-1}(3)$. Elsewhere it is continuous.

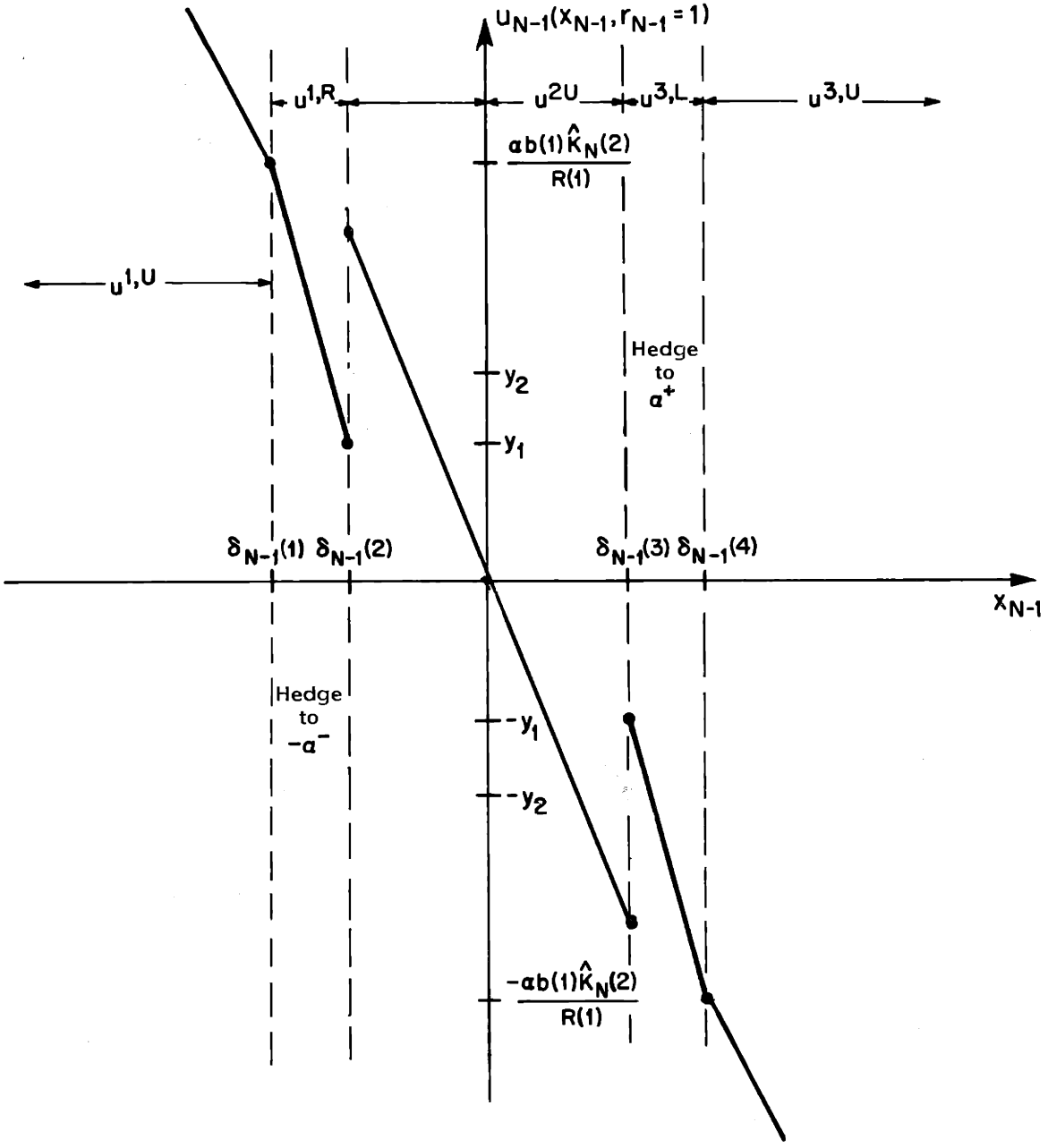

$$y_2 = \frac{\alpha b(1)\hat{K}_N(2)}{R(1)}\left(1-\sqrt{1-\frac{R(1)+b^2(1)\hat{K}_N(1)}{R(1)+b^2(1)\hat{K}_N(2)}}\right)$$

$$y_1 = \frac{\alpha b(1)}{R(1)}\left[\hat{K}_N(2)-\left(\frac{R(1)}{b^2(1)}+\hat{K}_N(2)\right)\sqrt{1-\frac{R(1)+b^2(1)\hat{K}_N(1)}{R(1)+b^2(1)\hat{K}_N(2)}}\right]$$

Figure 6.14: Control law $u_{N-1}(x_{N-1}, r_{N-1}=1)$ when $\hat{K}_N(1)\equiv\hat{K}_N(3)<\hat{K}_N(2)$ (Case 2) and $b(1)>0$.

The value of x_N obtained by application of the optimal control law to x_{N-1} is shown in figure 6.15. Recall that in the earlier case (where $\hat{K}_N(2) < \hat{K}_N(1) \equiv \hat{K}_N(3)$) we saw that the optimal closed loop system was more stable than the open loop system in form 1. This need not be true when $\hat{K}_N(2) > \hat{K}_N(1) \equiv \hat{K}_N(3)$. In particular, the optimal controller in form r=1

- is more stable than the open loop system for x_{N-1} values from which we do not hedge to a point.
- may be more stable or less stable than the open loop system over x_{N-1} values from which we hedge to a point, depending upon the values of the quantities

$$\frac{b^2(1)}{R(1)} \quad \text{and} \quad (\hat{K}_N(2), -\hat{K}_N(1)) \quad .$$

To see this we note that (as in the earlier case) for x_{N-1} regions where the slope in Figure 6.15 is positive, the closed loop dynamics are

$$a(1)\left[\frac{1}{1+\frac{b^2(1)}{R(1)}\hat{K}_N(i)}\right] < a(1) \qquad i=1,2,3 \ .$$

But in the hedging regions $x_{N-1} \in (\delta_{N-1}(1), \delta_{N-1}(2))$ and $x_{N-1} \in (\delta_{N-1}(3), \delta_{N-1}(4))$ the optimal controller is more stable

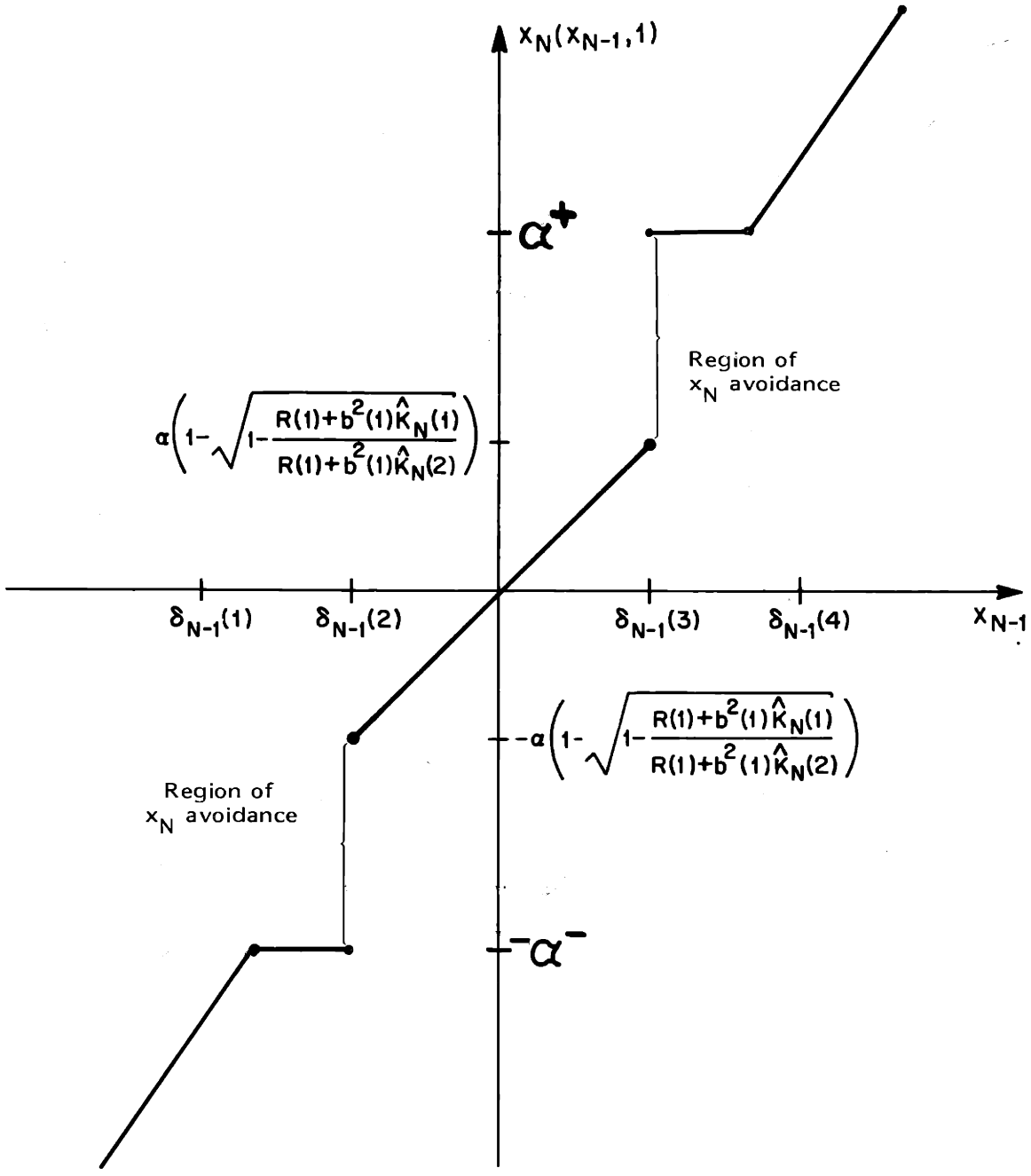

Figure 6.15: $x_N(x_{N-1}, r_{N-1}=1)$ when $\hat{K}_N(2) > \hat{K}_N(1) \equiv \hat{K}_N(3)$. (Case 2).

if $a(1)|x_{N-1}| > \alpha$ and less stable if $a(1)|x_{N-1}| < \alpha$. In these hedging regions

$$|\delta_{N-1}(2)| < |x_{N-1}| < |\delta_{N-1}(1)|$$

hence from (6.148)-(6.151),

$$\alpha\left(1 + \frac{b^2(1)}{R(1)}\hat{K}_N(2)\right)\left(1-\sqrt{1-\frac{R(1)+b^2(1)\hat{K}_N(1)}{R(1)+b^2(1)\hat{K}_N(2)}}\right) < |x_{N-1}|a(1) < \alpha\left(1+\frac{b^2(1)}{R(1)}\hat{K}_N(1)\right) . \tag{6.155}$$

Thus, we have $a(1)|x_{N-1}| > \alpha$ for all x_{N-1} in the hedging regions unless

$$\left(1 + \frac{b^2(1)}{R(1)}\hat{K}_N(2)\right)\left(1-\sqrt{1-\frac{R(1)+b^2(1)\hat{K}_N(1)}{R(1)+b^2(1)\hat{K}_N(2)}}\right) < 1 . \tag{6.156}$$

This can happen if and only if

$$\frac{\hat{K}_N(1)-\hat{K}_N(1)}{\hat{K}_N(1)\hat{K}_N(2)} > \frac{b^2(1)}{R(1)} . \tag{6.157}$$

That is, the optimal closed loop system will be less stable than the open loop system in form 1 for some x_{N-1} values where the optimal strategy is to hedge to a point, if and only if

(1) The excess cost $\hat{K}_N(2)-\hat{K}_N(1)$ of being on the wrong side of the hedging point is <u>large enough</u>

(2) the control effectiveness $\frac{b^2(1)}{R(1)}$ is small enough.

Note that there are two regions of avoided x_N values in Figure 6.15 (as in the earlier case). They are

$$x_N \notin \left[-\alpha,-\alpha\left(1-\sqrt{1-\frac{R(1)+b^2(1)\hat{K}_N(1)}{R(1)+b^2(1)\hat{K}_N(2)}}\right)\right]$$
$$x_N \notin \left(\alpha\left(1-\sqrt{1-\frac{R(1)+b^2(1)+\hat{K}_N(1)}{R(1)+b^2(1)\hat{K}_N(2)}}\right),\ \alpha\right] \quad . \tag{6.158}$$

The width of each of these regions of x_N avoidance is

$$\alpha < \alpha\left(\sqrt{1-\frac{R(1)+b^2(1)\hat{K}_N(2)}{R(1)+b^2(1)\hat{K}_N(1)}}\right) < 2\,\alpha \quad . \tag{6.159}$$

Comparing (6.159) with (6.145) we see that the width of these regions of avoidance varies with α, $b^2(1)/R(1)$ and the savings from hedging (here $\hat{K}_N(2)-\hat{K}_N(1)$), as in the previous case.

Each region of avoidance is again associated with a joining point where the slope of $V_{N-1}(x_{N-1},r_{N-1}=1)$ discontinuously decreases (i.e., $\delta_{N-1}(2)$ and $\delta_{N-1}(3)$ in this case).

There are two different shapes that the expected cost-to-go $V_{N-1}(x_{N-1}, r_{N-1}=1)$ can taken when $\hat{K}_N(2) > \hat{K}_N(1) \equiv \hat{K}_N(3)$. These are shown in Figure 6.16. In both Figures 6.16(a) and 6.16(b), the slope of $V_{N-1}(x_{N-1}, r_{N-1}=1)$ has a negative discontinuity at $\delta_{N-1}(2)$ and $\delta_{N-1}(3)$, and is continuous elsewhere. For $x_{N-1} \in (\delta_{N-1}(1), \delta_{N-1}(2))$ the optimal controller actively hedges to $x_N = -\alpha^-$. The resulting optimal expected cost-to-go is a quadratic interpolation between $V_{N-1}^{1,U}$ and $V_{N-1}^{2,U}$. Similarly for $x_{N-1} \in (\delta_{N-1}(3), \delta_{N-1}(4))$. In this case (as opposed to Figure 6.10), the $V_{N-1}^{1,U}$ curve is below the $V_{N-1}^{2,U}$ curve.

The width of the one-step hedging regions for this case is

$$\begin{pmatrix}\text{width of one-}\\ \text{step hedging}\\ \text{regions}\end{pmatrix} = \left(\frac{\alpha}{a(1)}\right)\left(\frac{b^2(1)}{R(1)}\right)\left[\left(\hat{K}_N(2)-\hat{K}_N(1)\right)-\sqrt{\begin{pmatrix}\hat{K}_N(2)\\ -\hat{K}_N(1)\end{pmatrix}\begin{pmatrix}\hat{K}_N(2)\\ +\\ R(1)/b^2(1)\end{pmatrix}}\right] \tag{6.160}$$

(compare to (6.143)). The comments following (6.143) regarding the width of these hedging regions apply for this case as well. Thus when $\alpha \neq 0$, the optimal expected cost-to-go $V_{N-1}(x_{N-1}, r_{N-1}=1)$ for <u>all</u> problems of the class formulated in Section 6.5 involves active hedging to a point.

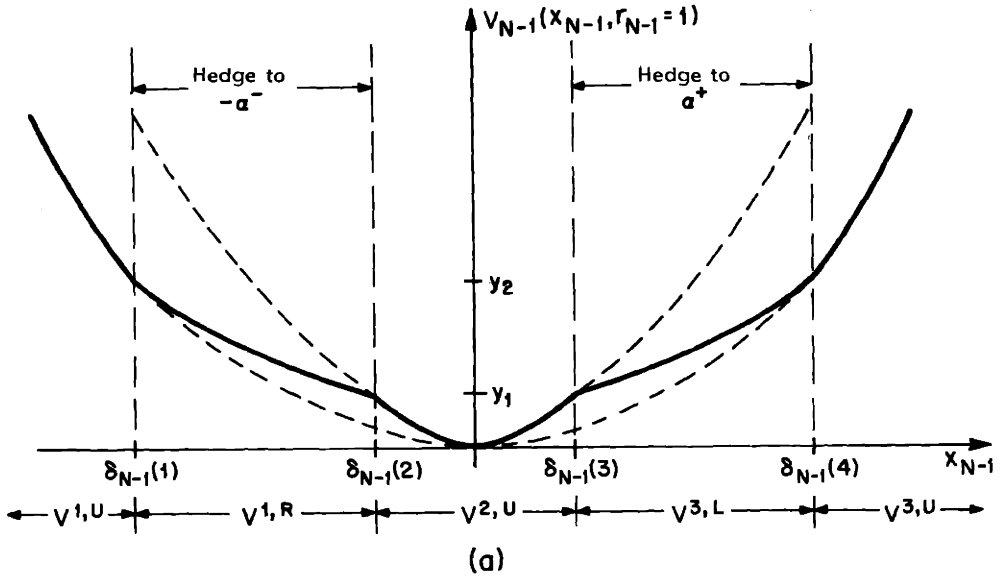

(a)

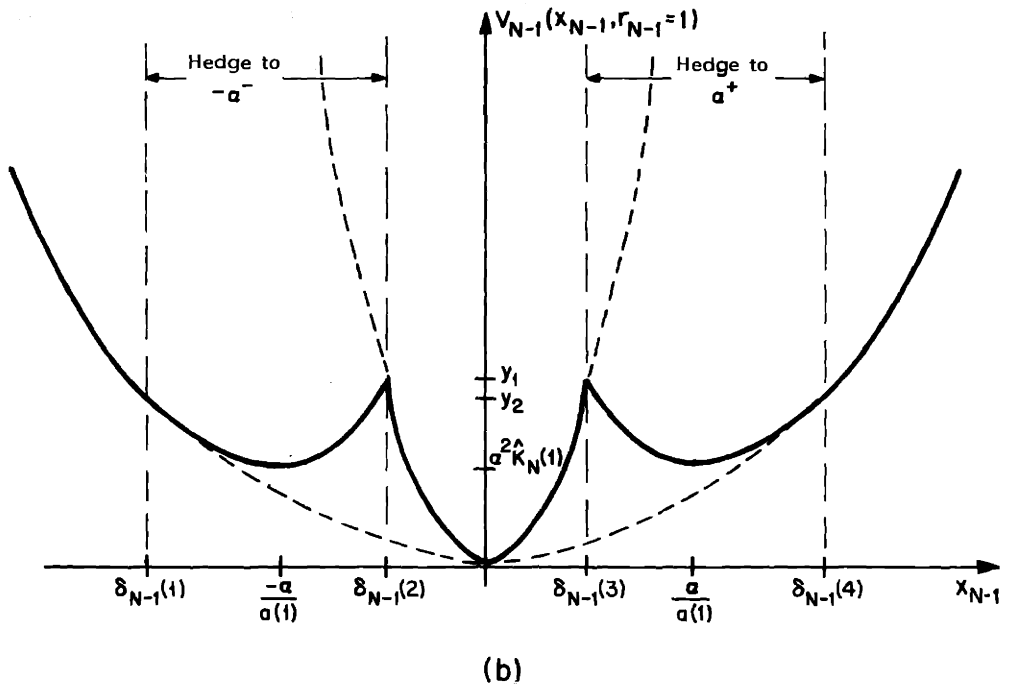

(b)

$$y_1 = \frac{a^2\hat{K}_N(2)}{R(1)} \begin{bmatrix} R(1) \\ + \\ b^2(1)\hat{K}_N(2) \end{bmatrix} \left[1 - \sqrt{1 - \frac{R(1)+b^2(1)\hat{K}_N(1)}{R(1)+b^2(1)\hat{K}_N(2)}} \right]^2$$

$$y_2 = \frac{a^2\hat{K}_N(1)}{R(1)} \begin{bmatrix} R(1) \\ + \\ b^2(1)\hat{K}_N(1) \end{bmatrix}$$

Figure 6.16: $V_{N-1}(x_{N-1}, r_{N-1}=1)$ when $\hat{K}_N(2) > \hat{K}_N(1) \equiv \hat{K}_N(3)$ with (a) single minimum and (b) local minima as well.

When Figure 6.16(a) applies $V_{N-1}(x_{N-1}, r_{N-1}=1)$ has a single local minimum at $x_{N-1}=0$, as in Case 1. But when Figure 6.16(b) applies $V_{N-1}(x_{N-1}, r_{N-1}=1)$ has <u>two</u> additional <u>local</u> minima as well as the global minimum at $x_{N-1}=0$. In this situation $V_{N-1}(x_{N-1}, r_{N-1}=1)$ is <u>not</u> montone for $x_{N-1} \leq 0$ and $x_{N-1} \geq 0$ (Note: in Figure 6.16(a) $y_2 > y_1$ but in Figure 6.16(b) we can have $y_2 \geq y_1$ or $y_1 \geq y_2$).

The following proposition states necessary and sufficient conditions for $V_{N-1}(x_{N-1}, r_{N-1}=1)$ to have local minima (for the problem of Section 6.5):

<u>Proposition 6.11</u> (Local minima)

Consider the problem of Section 6.5. $V_{N-1}(x_{N-1}, r_{N-1}=1)$ has a single local minimum at zero if and only if the following condition holds:

$$\frac{\hat{K}_N(2)-\hat{K}_N(1)}{\hat{K}_N(1)\hat{K}_N(2)} \leq \frac{b^2(1)}{R(1)} \quad . \tag{6.161}$$

If (6.161) does not hold then $V_{N-1}(x_{N-1}, r_{N-1}=1)$ has two local minima as well, at

$$x_{N-1} = \frac{-\alpha}{a(1)} \quad , \quad \frac{\alpha}{a(1)} \tag{6.162}$$

each with value

$$V_{N-1}\left(\frac{-\alpha}{a(1)}\ ,\ r_{N-1}=1\right) = V_{N-1}\left(\frac{\alpha}{a(1)}\ ,\ r_{N-1}=1\right) = \alpha^2\hat{K}_N(1). \tag{6.163}$$

The proof of this is straightforward, and appears in Appendix C.10. □

This proposition can be explained as follows:

$V_{N-1}(x_{N-1}, r_{N-1}=1)$ has local minima if and only if the following conditions both hold:

(1) $\hat{K}_N(2) > \hat{K}_N(1) \equiv \hat{K}_N(3)$

(the costs are at "cross purposes")

and

(2) the control effectiveness

$\frac{b^2(1)}{R(1)}$ is small enough.

Thus the form transition probability discontinuity locations, $\pm\alpha$, do not bear upon the existence of these local minima (and at time k=N-1; a(1) does not effect them either).

Note that the condition (6.161) for local minima is the same condition (6.157) for the optimal closed loop system to be <u>less</u> stable than the open loop system (for some x_{N-1} values). In particular, we can derive a relationship between the existence of local minima and

the values of $a(1)$ and α in terms of the joining points where the slope of $V_{N-1}(x_{N-1}, r_{N-1}=1)$ decreases. Clearly the local minima exist if and only if

$$\begin{aligned} &\min_{x_{N-1}} \; V_{N-1}^{1,R} = \frac{-\alpha}{a(1)} < \delta_{N-1}(2) \\ &\min_{x_{N-1}} \; V_{N-1}^{3,L} = \frac{\alpha}{a(1)} > \delta_{N-1}(3) \quad . \end{aligned} \tag{6.164}$$

Thus they exist if and only if

$$\begin{aligned} &a(1)\delta_{N-1}(2) > -\alpha \\ &a(1)\delta_{N-1}(3) < \alpha \end{aligned} \tag{6.165}$$

which means that the open loop drift $a(1)$ would drive

$$x_{N-1} = \delta_{N-1}(2), \quad x_{N-1} = \delta_{N-1}(3)$$

to the more costly sides of $x_N=-\alpha$ and $x_N=\alpha$, respectively. But (6.165) holds if and only if

$$\left(1 + \frac{b^2(1)}{R(1)} \hat{K}_N(2)\right)\left(1-\sqrt{1- \frac{R(1)+b^2(1)\hat{K}_N(1)}{R(1)+b^2(1)\hat{K}_N(2)}}\right) < 1$$

which illustrates the α independence of the existence of these local minima.

We can extend these ideas to more general x-dependent JLQ problems. A necessary condition for the existence of local minima in $V_k(x_k, r_k=j)$ can be stated in terms of the conditional expected cost-to-go $\hat{V}_k(x_{k+1}|r_k=j)$ as follows:

Proposition 6.12: Consider the problem of Proposition 5.1, where all of the x costs have only quadratic terms (i.e., $S(j) = \underline{P}(j) = H_T(j) = G_T(j)=0$, $j \in \underline{M}$). If $\hat{V}_{k+1}(x_{k+1}|r_k=j)$ is monotonely nonincreasing for $x_{k+1} \leq 0$ and monotonely nondecreasing for $x_{k+1} \geq 0$, then $V_k(x_k, r_k=j)$ has a single minimum.

Thus V_{k+1} $r_k=j)$ must be nonmonotone if $V_k(x_k, r_k=j)$ has a local minimum. This proposition follows direction from proposition 5.3 (part 4). Note that Proposition 6.12 does not provide necessary conditions for the existence of additional local minima. For example, in case 2 problems where

$$\frac{b^2(1)}{R(1)} \leq \frac{\hat{K}_N(2)-\hat{K}_N(1)}{\hat{K}_N(1)\hat{K}_N(2)}$$

we have $\hat{V}_N(x_N|r_{N-1}=1)$ nonmonotone for $x_N>0$ and $x_N<0$ (as in Figure 6.8(b)) but, by Proposition 6.11, $V_{N-1}(x_{N-1}, r_{N-1}=1)$ has a single minimum at zero (as in Figure 6.16(a)).

This concludes our consideration of the last-stage solution for the class of problems that are formulated in Section 6.5. We have shown that :

1. With the exception of problems having $\alpha=0$, there are <u>always</u> regions of x_{N-1} values from which the optimal controller <u>hedges to a point</u>.

2. The width of these hedging regions increases with increasing

$$\frac{\alpha}{a(1)} \ , \ \frac{b^2(1)}{R(1)} \quad \text{and} \quad \left|\hat{K}_N(1)-\hat{K}_N(2)\right| \ .$$

3. Except when $\alpha=0$, there are <u>always</u> regions of avoided x_N values. Each is associated with a joining point where the slope of $V_{N-1}(x_{N-1},r_{N-1}=1)$ decreases discontinuously.

4. The width of these regions of x_N avoidance increases with increasing

$$\alpha, \quad \frac{b^2(1)}{R(1)} \quad \text{and} \quad \left|\hat{K}_N(1)-\hat{K}_N(2)\right| \ .$$

5. When $\hat{K}_N(2) < \hat{K}_N(1) \equiv \hat{K}_N(3)$ (Case 1), the optimal closed loop system is <u>more stable</u> than the open loop dynamics in form 1, for all x_{N-1}.

6. When $\hat{K}_N(2) > \hat{K}_N(1) \equiv \hat{K}_N(3)$ (Case 2), the optimal closed loop system is <u>less stable</u> for some of the x_{N-1} values from which the controller hedges to a point if

$$\frac{\hat{K}_N(2)-\hat{K}_N(1)}{\hat{K}_N(1)\hat{K}_N(2)} > \frac{b^2(1)}{R(1)} \ .$$

7. This same condition is necessary and sufficient for the existence of local minima in $V_{N-1}(x_{N-1}, r_{N-1}=1)$.

6.7 Summary

We have now characterized the time-varying and steady-state behavior of the endpieces and middlepieces of the optimal JLQ controller (when (6.1)-(6.4)) hold and we have obtained bounds on the expected costs-to-go that afford some description between these pieces. For a special class of problems we have explored all of the possible behaviors of the last time stage solution and have given some indication of the issues which arise at the next time stage.

In the next chapter we will examine further the two problem cases of sections 6.5-6.6. Under certain conditions these problems have easily computable solutions that will enable us to gain insight into the general steady-state behavior of JLQ problems with x-dependent forms. An algorithm for solving the general scalar JLQ problem of Chapter 5 will also be presented and illustrated by numerical examples. In addition, we will consider "finite look-ahead" approximations of the optimal steady-state controller.

7. COMPUTATION AND TIME-VARYING BEHAVIOR OF THE JLQ CONTROLLER

7.1 Introduction

In this chapter we conclude our examination of the noiseless, scalar x-dependent JLQ control problem of chapters 5 and 6 with a study of two topics in detail. These are

- the efficient computation of the optimal JLQ controller of Proposition 5.1, using the qualitative and combinatoric results established in chapters 5 and 6.
- the time varying behavior of the optimal controller (as the number of stages from the terminal time increases).

In section 7.2 we develop a solution algorithm for the general problem of Proposition 5.1. It is presented in flowchart form and described in detail. The basic idea is to compute the optimal cost function $V_k(x_k, r_k=j)$ at time stage k (and in each form j) one piece at a time, starting on the left (with the left endpiece). Using Propositions 5.2 and 5.3, the number of calculations and computations that this solution algorithm must make is greatly reduced from those of the "brute force" solution technique in chapter 5.

The solution algorithm developed in section 7.2 is applicable to all problems satisfying the requirements of Proposition 5.1. This

class of problems is extremely rich. The resulting optimal controllers can exhibit a wide variety of qualitative behaviors. Analytical characterizations of these JLQ controllers that are sufficiently general to encompass the entire problem class tend to be uninformative, since so many diverse behaviors must be simultaneously accounted for.

We have chosen in sections 7.3-7.6 to focus on problems that lend insight into the kinds of qualitative JLQ controller behaviors that are appropriate in fault-tolerant control applications. Our vehicle for doing this is the single form-transition problem that was developed in sections 6.5 and 6.6. We are particularly interested in comparing and contrasting the qualitative behaviors of the optimal JLQ controllers in two archetypical classes of problems. In one of these classes the twin goals of high performance and high reliability are commensurate. In the other class they are at cross purposes.

In sections 7.3 and 7.4 we illustrate the wide range of parametrically determined, qualitatively different cases that can arise even in the single form-transition problem of section 6.5. In particular we find conditions which imply that the middlepiece and/or endpieces of the optimal expected cost-to-go $V_k(x_k, v_k=1)$ coincide with the upper and lower bounds of chapter 6 (that is, they are described by the same function of x_k).

The facts established in sections 7.3 and 7.4 are used in sections 7.5 and 7.6 to obtain and study in detail classes of problems (mentioned above) that are representative of fault-tolerant control problem applic ations. For these problems the algorithm of section 7.2 reduces to the solution of (increasingly many) sets of difference equations (as (N-k)

increases). This makes these problems amenable to further detailed analysis and it lets us illustrate some of the controller properties and qualitative issues that arise from the use of control to achieve both reliability and performance goals. We can analyze the infinite time horizon behavior of JLQ problems in these two classes and obtain the optimal steady-state controllers as $(N-k)\to\infty$ since the optimal controller at cach time can be obtained from the solution of increasingly many difference equations without making the comparisons and tests in the solution algorithm that are needed in general.

The steady-state solutions that are obtained for these two problem classes exhibit a structure that suggests a "natural" approximation to the steady-state optimal controller (both for these problems and the general class of problems in chapter 5 that can be made arbitrarily close to optimal. These approximations correspond to finite look-ahead controllers which ignore eventualities that occur beyond some fixed planning time. By ignoring the far future optimality is lost in these controllers but the computational burden of determining them and the complexity and cost of implementing them is reduced. This approximation idea is developed in section 7.7. Finally in section 7.8 we summarize the results of Part III of the thesis.

7.2 An Algorithm for the Off-line Determination of the Optimal Controller

In this section we develop an algorithm that enables us to solve the general scalar-x JLQ problem of Chapter 5. This algorithm is based upon

application of the one-stage solution of Proposition 5.1 recursively, backwards in time, for each form $j \in \underline{M}$ that the system can take.

The solution of Proposition 5.1 at a specific time k and from a specific form j involves the computation and comparison of many quadratic cost functions. These cost functions correspond to single time steps of constrained in x and unconstrained JLQ problems with x-independent transition probabilities, as described in chapter 5. Fortunately many of the candidate cost computations and comparisons that are indicated in the constructive proof of Proposition 5.1 (in section 5.4) can be avoided, due to the qualitative properties and facts that we have established in chapters 5 and 6. Our algorithm takes advantage of these results.

The basic ideas of the algorithm can be summarized as follows:

1. For each form $j \in \underline{M}$ at time k, we can compute $V_k(x_k, r_k = j)$ and $u_k(x_k, r_k = j)$ one piece at a time, sweeping from left to right along the axis of $a(j)x_k$ values. We start with the endpiece of $V_k(x_k, r_k = j)$ that corresponds to large negative values of $a(j)x_k$ (i.e., $V_k^{Le}(x_k, j)$ for $a(j) > 0$ and $V_k^{Re}(x_k, j)$ for $a(j) < 0$), since we know that this endpiece is optimal for sufficiently negative $a(j)x_k$ (from Proposition 6.1).

2. As we sweep rightwards along the $a(j)x_k$ axis, we compare the solutions of each of the constrained-in-x_{k+1}, x-independent JLQ control problems of step 3 in section 5.4. The optimal cost $V_k(x_k, r_k = j)$ at each x_k value is the minimal value of these constrained problem solutions, evaluated at x_k. We will say

that a quadratic cost function is valid over a specific interval of $a(j)x_k$ values if it solves a constrained problem of step 3 section 5.4 over this interval. That is

$V_k^{t,L}$ is valid for $x_k \leq \frac{\theta_k^j(t)}{a(j)}$

$V_k^{t,U}$ is valid for $\frac{\theta_k^j(t)}{a(j)} \leq x_k \leq \frac{\theta_k^j(t)}{a(j)}$

$V_k^{t,R}$ is valid for $x_k \geq \theta_k^j(t)/a(j)$.

Thus the list of valid costs changes as we sweep rightwards along the $a(j)x_k$ axis. In each successive region of $a(j)x_k$ values we need only look at those quadratic cost functions that are valid.

3. At each point we have a prevailing optimal cost which is the optimal cost for points immediately to the left. As we proceed from left to right along the $a(j)x_k$ axis we must decide when this prevailing cost ceases to be optimal, and which valid candidate cost-to-go function becomes the new prevailing optimal. The old prevailing cost can cease to be optimal if it is crossed by another valid candidate cost (which thereafter becomes the prevailing optimal cost as we continue the rightward sweep of the algorithm), or if it ceases to be valid. In the latter case, the newly valid cost function (that replaces the former prevailing optimal cost function as the solution of one of the

constrained JLQ problems of step 3 in section 5.4) becomes the new prevailing cost. Thus, as we sweep rightwards along the axis of $a(j)x_k$ values we only need to compare valid candidate cost functions to the prevailing one.

4. Furthermore, from Propositions 5.2 and 5.3 we know that not all of the valid cost functions in a given region of $a(j)x_k$ values are eligible for optimality. By eligible we mean that the candidate cost function (of x_k) in question has not been ruled out by Proposition 5.2 (at the beginning) or by Proposition 5.3 (as the algorithm progresses). Recall that Proposition 5.2 disqualifies from optimality (for any x_k) all candidate cost functions except the unconstrained $V_k^{t,U}(x_k,j)$ costs and those constrained $V_k^{t,L}(x_k,j)$, $V_k^{t,R}(x_k,j)$ costs that correspond to driving x_{k+1} to the less expensive side of a $V_{k+1}(r_k = j)$ discontinuity. Also recall that the mapping from x_k to the optimal choice of x_{k+1} :

$$x_k \longmapsto x_{k+1}(x_k, r_k = j)$$

is monotone (see Proposition 5.3). As we sweep from left to right along the axis of $a(j)x_k$ values, this fact can also be used to remove candidate cost functions from eligibility. We can exclude from further consideration those candidate cost-to-go functions that correspond to driving x_{k+1} to the left (in $a(j) > 0$; to the right in $a(j) < 0$) of where the prevailing controller does. In this way, Proposition 5.3 is used to reduce

the list of eligible candidate cost functions as we sweep rightwards.

Thus the algorithm proceeds, for each form $j \in \underline{M}$ and at each time k, by sweeping rightwards along the $a(j)x_k$ axis, comparing valid, eligible candidate cost functions to the prevailing one. This process begins with the appropriate endpiece ($V_k^{Le}(x_{k'i})$) if $a(j) > 0$, $V_k^{Re}(x_{k'i})$) if $a(j) < 0$) and ends when the other endpiece becomes the prevailing optimal. If the problem is completely symmetric about zero (i.e., all costs and form transition probabilities) then the sweep need only proceed until the middle piece is reached.

An overview of the solution algorithm is shown [1] in figure 7.1. The algorithm is initialized with the terminal time ($k = N$) cost parameter (block 1). Then for successively decreasing times through $k = k_o$ (block 2), the one-stage solution of Proposition 5.1 is obtained for each form $j \in M$ (block 3).

---

[1] The symbol := in figure 7.1 denotes replacement. For example, $j := 2j + i + 1$ means that the value of variable j is replaced by the value of the expression $2j + i + 1$.

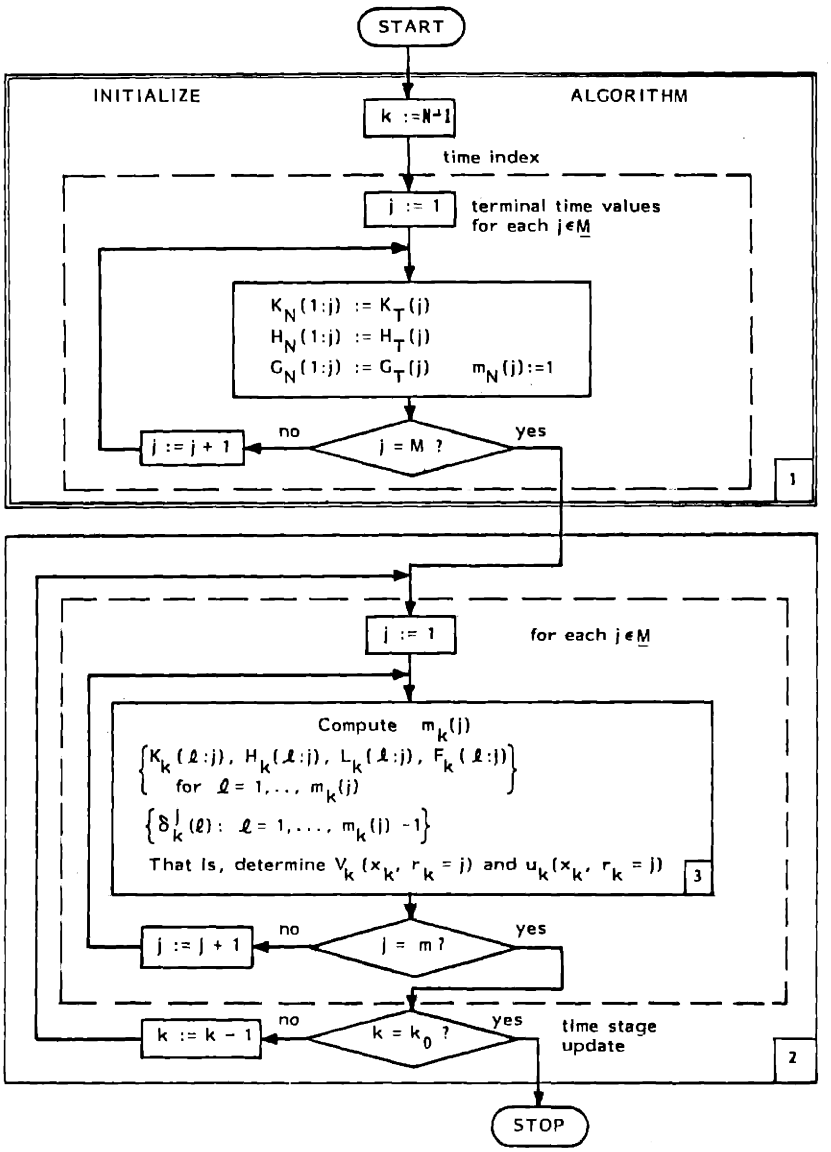

Figure 7.1: Algorithm Overview

Before discussion how the solution algorithm accomplishes this determination of $V_k(x_k, r_k=j)$ and $u_k(x_k, r_k=j)$ let us recall the steps for doing this that were specified in section 5.4. We will then indicate how these tasks can be simplified. The steps in section 5.4 were:

Step 1: A composite partition of the real line (of x_{k+1} values) is obtained, consisting of

$$\psi^j_{k+1} \qquad \text{nonoverlapping intervals}$$

$$\Delta^j_{k+1}(t) = (\gamma^j_{k+1}(t-1), \gamma^j_{k+1}(t)) \qquad t = 1,.., \psi^j_{k+1}$$

where $\gamma^j_{k+1}(0) \triangleq -\infty$, $\gamma^j_{k+1}(\psi^j_{k+1}) \triangleq \infty$

and the grid points $\{\gamma^j_{k+1}(t) : t = 1,..., \psi^j_{k+1} - 1\}$.

This is done by superimposing the grids of the next-time expected costs-to-go $V_{k+1}(x_{k+1}, r_{k+1} = i)$ joining points :

$$\{\delta^i_{k+1}(\ell) : \ell = 1,...,m_{k+1},(i)-1\}$$

and from the transition probability discontinuity locations

$$\{\nu_{ji}(\ell) : \ell = 1,...,\bar{\nu}_{ji} -1 \}$$

for all i in the cover of j ($i \in C_j$)).

Step 2: For each of these ψ^j_{k+1} intervals ($t=1,..., \psi^j_{k+1}$) a constrained-in x_{k+1} JLQ problem is formulated:

$$V_k(x_k, r_k=j \,|\, x_{k+1} \in \Delta^j_{k+1}(t)) = \min_{\substack{u_k \\ \text{s.t.} \\ x_{k+1} \in \Delta^j_{k+1}(t)}} \left\{ u_k^2 R(j) + \hat{V}_{k+1}(x_{k+1} \,|\, r_k=j) \right\}$$

Step 3: These constrained problems are then each solved. Their solutions are piecewise-quadratic in x_k with three pieces

$$V_k(x_k, r_k=j \,|\, x_{k+1} \in \Delta^j_{k+1}(t)) = \begin{cases} V_k^{t,L} & x_k \leq \dfrac{\theta^j_k(t)}{a(j)} \\ V_k^{t,U} & \dfrac{\theta^j_k(t)}{a(j)} \leq x \leq \dfrac{\theta^j_k(t)}{a(j)} \\ V_k^{t,R} & x \geq \dfrac{\theta^j_k(t)}{a(j)} \end{cases}$$

except for $t = 1$ and $t = \psi^j_{k+1}$ which have only two pieces ($\theta^j_k(1)/a(j) = -\infty$, $\theta^j_k(\psi^j_{k+1})/a(j) = +\infty$).

Step 4: The optimal expected cost-to-go $V_k(x_k, r_k = j)$ at each x_k is the lowest of the constrained cost solutions (of steps) at that x_k.

A "brute force" implementation of step 4 would be to compute and find the intersections of the $(3\psi^j_{k+1} - 2)$ quadratic functions of x_k:

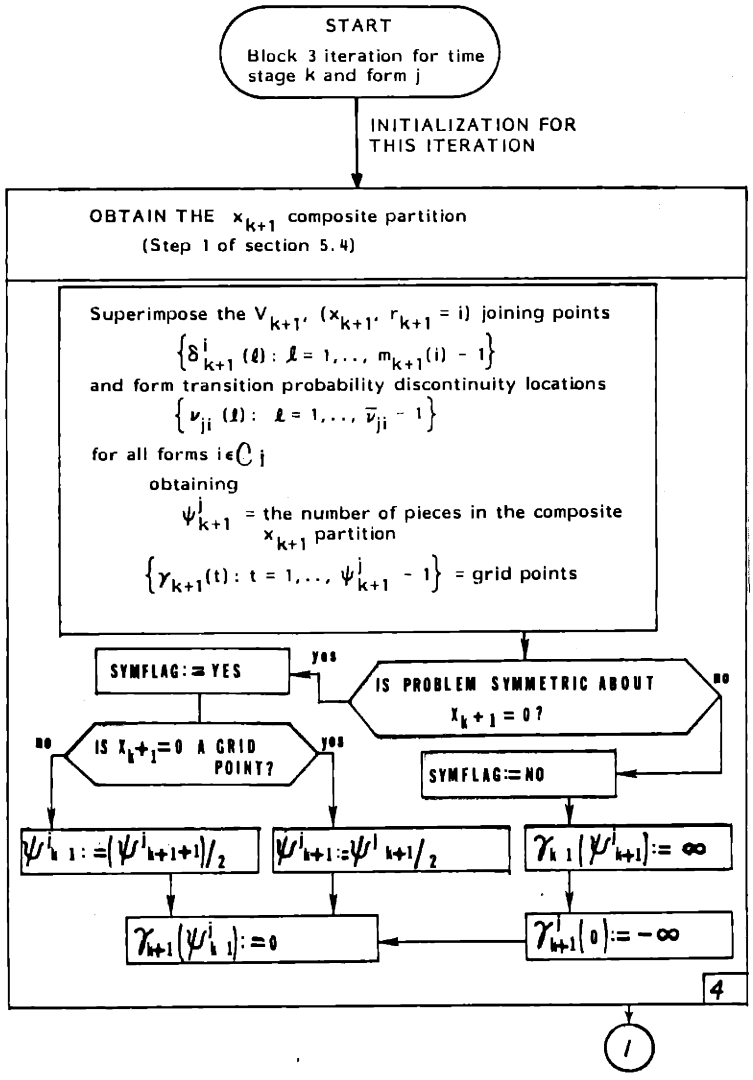

Figure 7.2: One Stage Solution Flowchart - Part II

$$\left\{ V_k^{1,U}(x_k,j), V^{1,R}(x_k,j),\ V^{2,L}(x_k,j),\ V^{2,U}(x_k,j),\ V^{2,R}(x_k,j),\ldots \right.$$

$$\ldots, V_k^{\psi^j_{k+1}-1,L}(x_k,j) V_k^{\psi^j_{k+1}-1,U}(x_k,j),\ V_k^{\psi^j_{k+1}-1,R}(x_k,j),\ V_k^{\psi^j_{k+1}}(x_k,j),$$

$$\left. \ldots\ldots,\ V_k^{\psi^j_{k+1},U}(x_k,j) \right\}. \tag{7.1}$$

At each x_k value, V_k (x_k r_k=j) is then chosen to be the candiate having the least cost, among those that are valid at this x_k.

Now we will develop a sequence of tasks that carries out these four steps in a more efficient manner. In the following discussion we will refer to a flowchart of the algorithm that is shown in figures 7.2 -7.6. All of the steps indicated in this flowchart together constitute one iteration of block 3 in figure 7.1. That is, they determine the one-stage JLQ solution that is specified by Proposition 5.1 for some time stage k and form j.

A macroscopic overview of the algorithm specified by figures 7.2 - 7.6 is as follows:

1. The algorithm first performs step 1 (above) in block 4 (of figure 7.2). The composite x_{k+1} partition is obtained from quantities that were computed at the previous time stage (i.e. at time k+1), and from known parameters of the problem. If the entire problem is symmetric about zero then we need only consider this partition for $x_{k+1} \leq 0$.

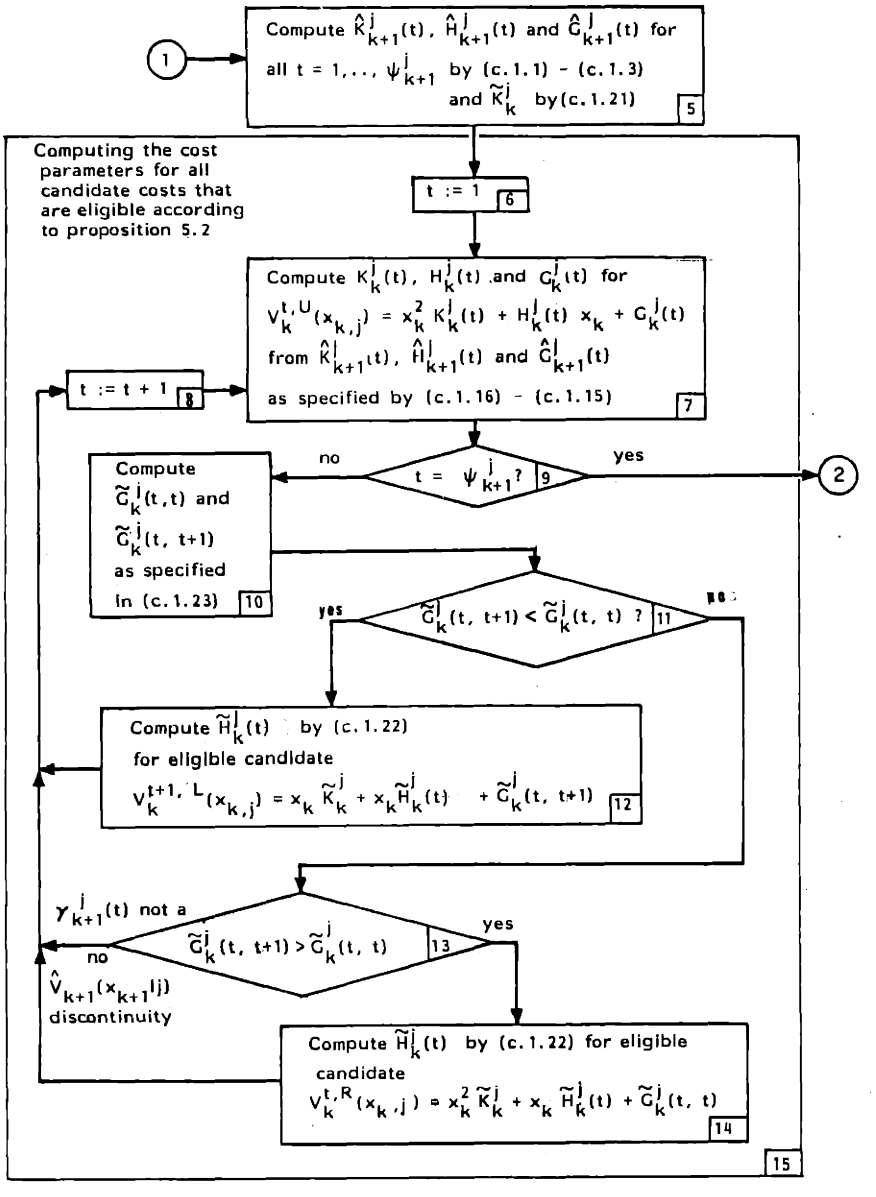

Figure 7.3: Flowchart, Part III: Using Proposition 5.2

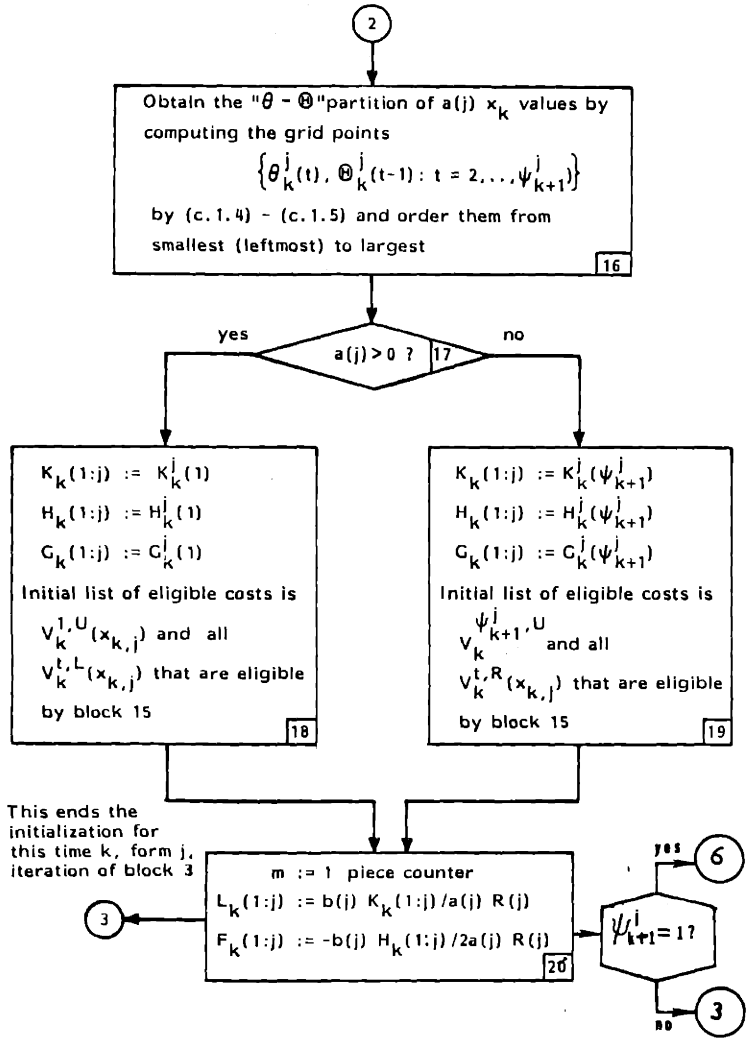

Figure 7.4: Flowchart, Part IV: End of Initialization

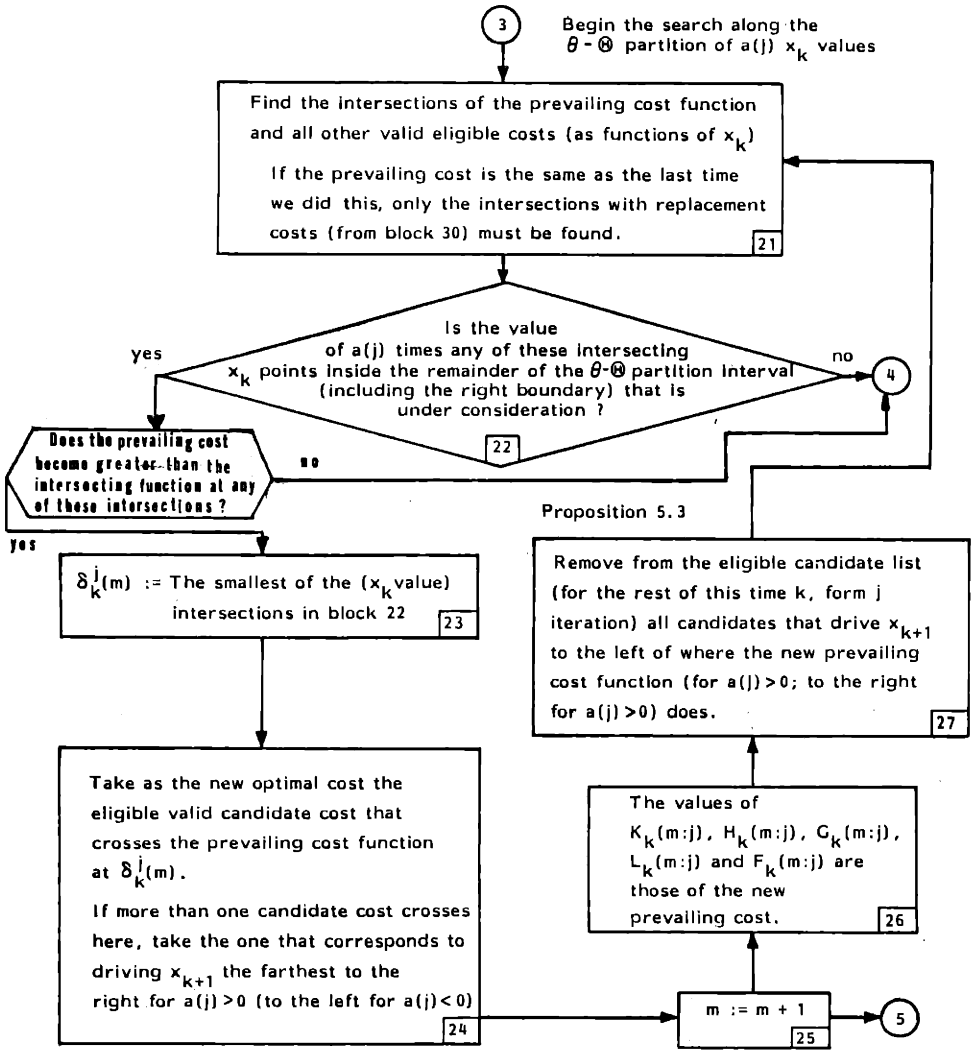

Figure 7.5: Flowchart, Part V: Comparisons within a θ - ⊗ Interval

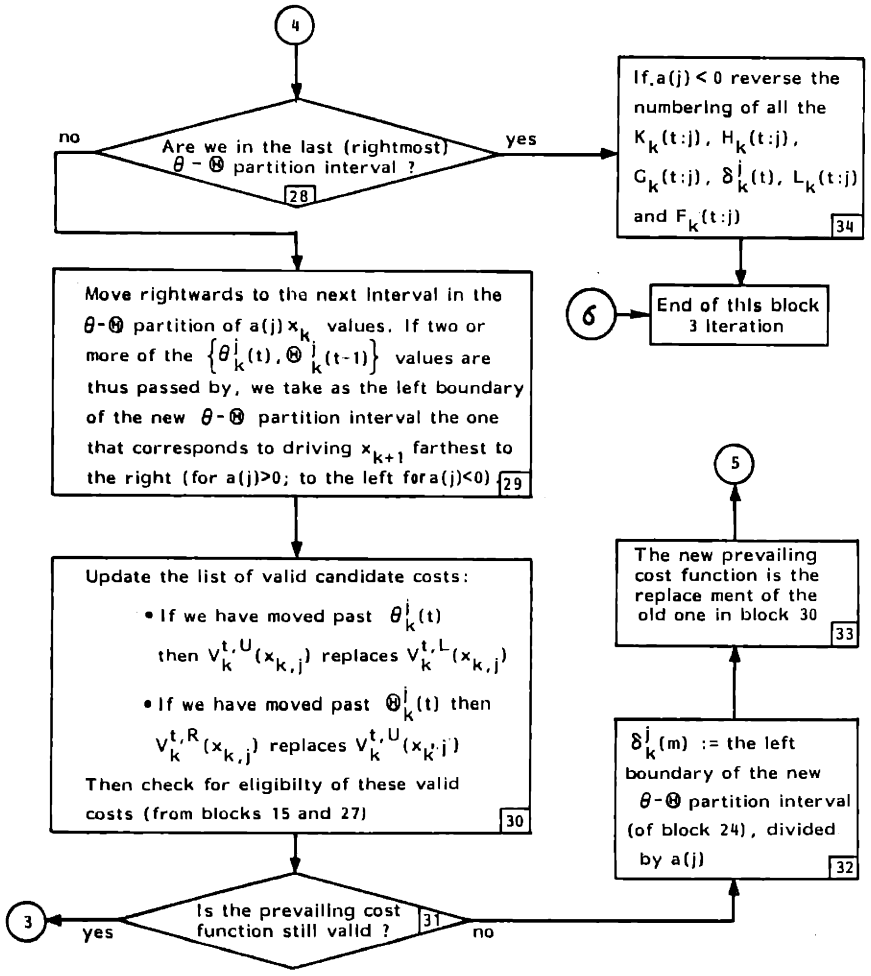

Figure 7.6: Flowchart, Part VI: Moving Rightwards

2. The next task is to determine which candidate cost-to-go functions are eligible for optimality with respect to Proposition 5.2, and to compute the parameters for these eligible functions. Recall that Proposition 5.2 excludes from eligibility all cost functions that correspond to actively hedging to a point that is <u>not</u> a discontinuity of the conditional expected cost-to-go $\hat{V}_{k+1}(x_{k+1}|r_k=j)$.

In block 5 the parameters of $\hat{V}_{k+1}(x_{k+1}|r_k=j)$ are computed. Using these quantities the parameters are computed for all candidate expected cost-to-go functions that are eligible for optimality according to Proposition 5.2. This is done in block 15, as follows:

- for each x_{k+1} interval $\Delta^j_{k+1}(t) \quad t = 1,\ldots,\psi^j_{k+1}$ we compute the parameters for the "unconstrained" cost function $V^{t,U}_k$ (block 3)
- then at each grid point $\{\gamma^j_{k+1}(t) \quad t = 1,\ldots,\psi^j_{k+1} - 1\}$ we test to see if $\hat{V}_{k+1}(X_{k+1}|r_k=j)$ is discontinuous (blocks 10,11,13). If $\gamma^j_{k+1}(t)$ is a discontinuous point of the conditional expected cost-to-go, then the parameters of the eligible candidate cost (corresponding to driving to the low cost side of $\gamma^j_{k+1}(t)$) are computed (blocks 12,14).

3. Then we prepare for the rightward sweep along the $a(j)x_k$ axis by obtaining(in block 16, figure 7.4) the partition of the real line (of $a(j)x_k$ values) that is caused by the points

$$\{\theta_k^j(t),\ \Theta_k^j(t-1) \quad : t = 2\ldots,\ \psi_{k+1}^j\}$$

These quantities are computed using the values obtained in block 7.

4. Finally, the algorithm determines the optimal cost (and control law) over each interval of $a(j)x_k$ values in this $\theta - \Theta$ partition, starting on the left. The algorithm sequentially finds

$$V_k(j:j) = x_k^2 K_k(i:j) + x_k H_k(i:j) + G_k(i:j)$$

for $1,2,\ldots,m_k(1)$ when $a(j) > 0$. When $a(j) < 0$ these pieces are found in reverse order. The same flowchart applies for both $a(j) > 0$ and $a(j) < 0$; if $a(j) < 0$ then we start with the right endpiece instead of the left endpiece as the initial prevailing cost function (block 19), and we revise all indices at the end of the sweep (block 34).

The fourth task above constitutes the main body of the solution algorithm. We will describe it in detail below. Before doing so, however, let us consider the $\theta - \Theta$ partition that was obtained for example 5.1 at time k = N-2. We will use this example throughout this section to demonstrate the algorithm's steps.

Example 7.1 (example 5.1 & 6.1 revisited)

The candidate cost-to-go functions for $V_{N-2}(x_{N-2}, r_{N-2} = 1)$ that are valid and eligible at the start of the left-to-right sweep are shown in figure 7.7. The seven rows correspond to the constrained-in-x_{N-1} optimal costs

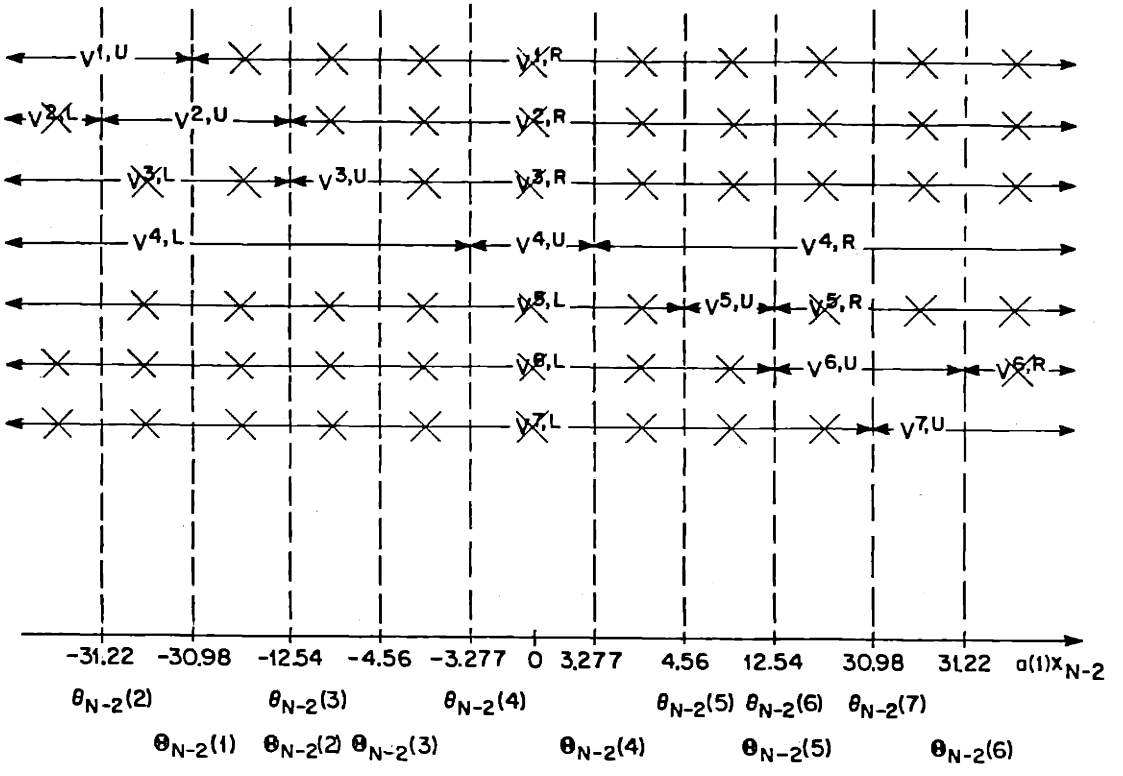

Figure 7.7: Valid, Eligible Regions of $V_{N-2}(x_{N-2}, r_{N-2}=1)$ Candidate Cost Functions in Example 5.1, 6.1

$$V_{N-2}(x_{N-2}, r_{N-2}=1 \mid x_{N-1} \in \Delta_{N-1}(t))$$

for $t = 1,2,..,\psi_{N-1} = 7$. The regions of $a(1)x_{N-2}$ values[1] where the various pieces of these $V_{N-2}(x_{N-2}=1 \mid x_{N-1} \in \Delta_{N-1}(t))$ costs-to-go are valid are labelled between the arrows in this figure, and candidate cost functions that are ineligible (due to Proposition 5.2) at the start of the (j=1, k=N-2) alogorithm iteration are x'd out. Thus at the start of the left-to-right sweep the eligible, valid candidate cost-to-go functions for $V_{N-2}(x_{N-2}, r_{N-2}=1)$ are as listed in table 7.1.

We now resume our description of the solution algorithm with a detailed description of the left-to-right sweep. The list of initially eligible candidate cost functions is determined in block 15, and is updated in block 27 as each new piece of $V_k(x_k, r_k = j)$ is determined. In the leftmost interval of $a(j)x_k$ values (that is, at the start of the left-to-right sweep), the valid and eligible candidate cost-to-go functions are

- for $a(j) > 0$:

  $V_k^{1,U}(x_k, j)$ and those

  $V_k^{t,L}(x_k, j)$ $t = 2,\ldots, \psi_{k+1}^{j}$ that are eligible according to Proposition 5.2 (block 15)

[1] In this example, $a(1) = 1$.

Candidate cost-to-go Function for $V_{N-2}(x_{N-2}, r_{N-2}=1)$	Region of a(1) x_{N-2} Values where Valid	Eligible from Proposition 5.2 ?
$v^{1,U}$	$(-\infty, \Theta_{N-2}(1))$	yes
$v^{1,R}$	$(\Theta_{N-2}(1), \infty)$	no
$v^{2,L}$	$(-\infty, \theta_{N-2}(2))$	no
$v^{2,U}$	$(\theta_{N-2}(2), \Theta_{N-2}(2))$	yes
$v^{2,R}$	$(\Theta_{N-2}(2), \infty)$	no
$v^{3,L}$	$(-\infty, \theta_{N-2}(3))$	no
$v^{3,U}$	$(\theta_{N-2}(3), \Theta_{N-2}(3))$	yes
$v^{3,R}$	$(\Theta_{N-2}(3), \infty)$	no
$v^{4,L}$	$(-\infty, \theta_{N-2}(4))$	yes
$v^{4,U}$	$(\theta_{N-2}(4), \Theta_{N-2}(4))$	yes
$v^{4,R}$	$(\Theta_{N-2}(4) \infty)$	yes
$v^{5,L}$	$(-\infty, \theta_{N-2}(5))$	no
$v^{5,U}$	$(\theta_{N-2}(5), \Theta_{N-2}(5))$	yes
$v^{5,R}$	$(\Theta_{N-2}(5), \infty)$	no
$v^{6,L}$	$(-\infty, \theta_{N-2}(6))$	no
$v^{6,U}$	$(\theta_{N-2}(6), \Theta_{N-2}(6))$	yes
$v^{6,R}$	$(\Theta_{N-2}(6), \infty)$	no
$v^{7,L}$	$(-\infty, \theta_{N-2}(7))$	no
$v^{7,U}$	$(\theta_{N-2}(7) \infty)$	ves

Table 7.1: Candidate cost-to-go Functions for $V_{N-2}(x_{N-2}, r_{N-2}=1)$; Regions of Validity and Eligibility due to Proposition 5.2

- for $a(j) < 0$:

  $V_k^{\psi_{k+1}^j,U}(x_k,j)$ and those

  $V_k^{t,R}(x_k,j)$ $\quad t = 1,\ldots,\psi_{k+1}^j - 1$ that are

  eligible according to Proposition 5.2.

From Proposition 6.1 we know that for sufficiently negative values of $a(j)x_k$, the optimal candidate cost is

- the left end piece $V_k^{Le}(x_k,j) \equiv V_k^{1,U}(x_k,j)$ if $a(j) > 0$

- the right end piece $V_k^{Re}(x_k,j) \equiv V_k^{\psi_{k+1}^j,U}(x_k,j)$ if $a(j) < 0$.

This provides starting values for the algorithm. In blocks 17, 18 and 19 the first piece cost parameters $K_k(1{:}j)$, $H_k(1{:}j)$ and $G_k(1{:}j)$ are assigned the appropriate endpiece values, and the appropriate current list of valid eligible candidates is designated. In block 20 the piece counter (m) is set to one and the control law parameters for the first piece are assigned. The rightward search (along the axis of $a(j)x_k$ values) for the pieces of the optimal cost function $V_k(x_k, r_k = j)$ begins in this leftmost interval of the $\theta - \Theta$ partition, as indicated in figure 7.5.

Either the prevailing optimal cost (the endpiece function) is

optimal over this entire first interval of $a(j)x_k$ values or it is crossed by one of the other valid eligible candidates. The intersections of the prevailing optimal cost (at the start of the $\theta - \Theta$ partition interval) with all other valid eligible candidate cost functions (in this $\theta - \Theta$ interval) are computed in block 21. We then test (in block 22) to see if any of these intersections are inside the interval of $a(j)x_k$ values that is under consideration. If the answer to this question (block 22) is "no", then we know that the prevailing optimal cost is optimal over the remainder of this $\theta - \Theta$ partition interval, and we proceed to the next interval (to the right).

If instead the answer in block 22 is "yes" then the leftmost of these intersections determines the next joining point $\delta_k^j(m)$ of $V_k(x_k, r_k = j)$, as indicated in block 23.

The assignments of values for the next optimal piece of $V_k(x_k, r_k = j)$ and $u_k(x_k, r_k = j)$ in this "yes" case are made in blocks 24, 25 and 26. If only one of the candidate cost functions crosses the prevailing optimal cost function at $\delta_k^j(m)$ then this cost becomes the new prevailing optimal. If two or more of the candidate costs intersect the prevailing optimal cost[1] at $\delta_k^j(m)$ then we take as the next piece of $V_k(x_k, r_k = j)$ the intersecting candidate cost which corresponds to driving x_{k+1}

- the furthest to the right if $a(j) > 0$
- the furthest to the left if $a(j) < 0$.

This choice is made because we know from the monotonicity of the

[1] An unlikely but possible occurrence.

optimal $x_k \rightarrow x_{k+1}(x_k, r_k = j)$ mapping (in Proposition 5.3) that the other costs intersecting at $\delta_k^j(m)$ can be optimal only at this single intersecting point.

We can use this monotonicity (in block 27) to remove from further consideration during the remainder of this leftward sweep[1] all candidate costs that drive x_{k+1}

- to the left (for $a(j) > 0$)

or

- to the right (for $a(j) < 0$)

of where the new prevailing optimal cost does. In particular, the candidate cost that ceased to be optimal at $\delta_k^j(m)$ cannot be optimal again (as we move rightward along the $a(j)x_k$ line).

This process is continued until $V_k(x_k, r_k = j)$ has been determined over the entire interval in the $\theta - \Theta$ partition (that is, until the answer to block 22's question is "no").

Then the next interval in the $\theta - \Theta$ partition of $a(j)x_k$ values (to the right) is considered. Because we have moved past one[2] of the $\{\theta_k^j(t), \Theta_k^k(t-1)\}$ values in entering this next interval, the set of valid candidate cost functions changes:

- if we have moved past a $\theta_k^j(t)$ value then $V_k^{t,L}(x_k, j)$ ceases to be a valid cost; it is replaced by $V_k^{t,U}(x_k, j)$ in the list of valid costs

---

[1] For a specific value of j at time k.

[2] Or more than one if they have the same value.

- if we have moved past a $\Theta_k^j(t)$ values then $V_k^{t,U}(x_k,j)$ ceases to be a valid cost; it is replaced by $V_k^{t,R}(x_k,j)$ in the list of valid costs.

This updating is done in block 30. These replacements may or may not be eligible candidates for optimality with respect to the criterion of Proposition 5.2 (block 15) and the monotonicity property of the $x_k \rightarrow x_{k+1}(x_k, r_k = j)$ mapping of Proposition 5.3.

Once the new list of valid costs that are eligible for optimality has been determined, the algorithm must check to see if the prevailing optimal cost is still valid (block 31). If it is, then the procedure described above is carried out for this new interval in the $\theta - \Theta$ proposition (starting in block 21).

If the prevailing optimal cost ceases to be valid in the new $\theta - \Theta$ interval (that is, the answer in block 31 is "no") then the next joining point, $\delta_k^j(m)$, of $V_k(x_k, r_k = j)$ and $u_k(x_k, r_k = j)$ corresponds to this $\theta - \Theta$ interval boundary (as in block 32). In this situation the replacement in block 29 of the former (now invalid) prevailing cost becomes the new prevailing cost if it is eligible. If this replacement cost is not eligible, then at least one of the other newly valid costs will be eligible.[1] The newly valid eligible cost that corresponds to driving x_{k+1} farthest to the right (for $a(j) > 0$; to the left for $a(j) < 0$) is the new prevailing optimal cost (see block 33).

[1] Either the replacement of the now not valid former prevailing cost is eligible for optimality (w.r.to Propositions 5.2 5.3) or another eligible valid cost must intersect the former prevailing optimal cost at the left boundary of the new $a(j)x_k$ interval, since $V_k(x_k, r_k=j)$ must be continous in x_k (by Proposition 5.1).

The algorithm proceeds through each interval in the θ - Θ partition until the last partition interval has been completed[1] (block 28). Then if a(j) < 0, the indexing of the solution parameters is reversed (in block 34). This completes the one-stage solution (as in Prop. 5.1, and block 3) for time stage k in form j.

Example 7.1 (= 5.1,6.1) continued

Let us now illustrate the algorithm for the k = N-2, j = 1 iteration of example 5.1. Since a(1) = 1 >0 (in block 17), the left-to-right sweep of the algorithm begins with the left-endpiece cost function $V^{Ie}_{N-2}(1) = V^{1,U}$ initially prevailing, and the first θ-Θ interval to be considered is $(-\infty, \theta_{N-2}(2))$. The values of the first piece of $V_{N-2}(x_{N-2},1)$ and $u_{N-2}(x_{N-2},1)$ are assigned as specified by blocks 18 and 20. We list below these assignments and all successive ones at the left-to-right sweep progresses.

1. Searching interval $(-\infty, \theta_{N-2}(2) = -31.22)$
   Eligible valid candidates: $V^{1,U}$, $V^{4,L}$

- $V^{1,U}$ initially prevailing since a(1) > 0 — block 17
- $K_{N-2}(1:1) = K^{1,U}_{N-2}$ — block 18
  $H_{N-2}(1:1) = G_{N-2}(1:1) = 0$
- m = 1 — block 19
  $L_{N-2}(1:1) = b(1)\ K_{N-2}(1:1)/a(1)R(1)$ — block 19
  $F_{N-2}(1:1) = 0$

[1] If the problem is completely symmetric about zero, then the sweep can be halted when the middle piece cost function becomes optimal.

- prevailing cost function $V^{1,U}$ does not intersect the (only) eligible valid candidate $V^{4,L}$ before $\theta_{N-2}(1)$ — blocks 21,22
- move rightwards to $(\theta_{N-2}(2), \theta_{N-2}(1))$ — block 29

2. Searching interval $(-31.22 = \theta_{N-2}(2), \theta_{N-2}(1) = -30.98)$

   Eligible valid candidates: $V^{1,U}$, $V^{2,U}$, $V^{4,L}$ — block 30
   ($V^{2,U}$ replaces $V^{2,L}$ as valid cost since we have passed $\theta_{N-2}(2)$ and it is eligible)

- Prevailing cost $V^{1,U}$ is still valid — block 31
- Prevailing cost function $V^{1,U}$ intersects $V^{2,U}$ at $x_{N-2} = -31.179, -7.847$; intersections of $V^{1,U}$ and $V^{4,L}$ were computed above — block 21
- Since

  -31.179 is inside the search interval — block 22

  we have

  $\delta_{N-2}(1) = -31.179$ — block 23

  and

  $V^{2,U}$ is the new prevailing cost — block 24

- Thus $m = 2$ — block 25

  and

  $K_{N-2}(2:1) = K^{2,U}_{N-2}$ — block 26

  $H_{N-2}(2:1) = H^{2,U}_{N-2}$

  $G_{N-2}(2:1) = G^{2,U}_{N-2}$

  $L_{N-2}(2:1) = L^{2,U}_{N-2}$

  $F_{N-2}(2:1) = F^{2,U}_{N-2}$

- Remove $V^{1,U}$ and $V^{1,R}$ from future eligibility (due to Proposition 5.3) — block 27

3. Searching interval $(-31.179 = \delta_{N-2}(1), \Theta_{N-2}(1) = -30.98)$

   Eligible valid candidates remaining: $V^{2,U}$, $V^{4,L}$

   - Prevailing cost $V^{2,U}$ does not intersect the (only) eligible valid candidate $V^{4,L}$ inside the search interval — blocks 21, 22
   - move rightwards to $(\Theta_{N-2}(1), \Theta_{N-2}(2) = \theta_{N-2}(3)) =$ $= (-30.98, -12.54)$ — block 29

4. Searching interval $(\Theta_{N-2}(1), \Theta_{N-2}(2) = \theta_{N-2}(3)) = (-30.98, -12.54)$

   Eligible valid candidates: $V^{2,U}$, $V^{4,L}$

   ($V^{1,R}$ replaces $V^{1,U}$ in list of valid candidate costs since we have passed $\Theta_{N-2}(1)$, but $V^{1,R}$ is not eligible). — block 30

   - prevailing cost $V^{2,U}$ is still valid — block 31
   - intersections of $V^{2,U}$ and $V^{4,L}$ are known from above and they are not in this interval — blocks 21, 22
   - move rightwards to $(\theta_{N-2}(3) = \Theta_{N-2}(2), \Theta_{N-2}(3)) =$ $= (-12.54, -4.56)$ — block 29

5. Searching interval $(\theta_{N-2}(3) = \Theta_{N-2}(2), \Theta_{N-2}(3)) = (-12.54, -4.56)$

   Eligible candidates: $V^{3,U}$, $V^{4,L}$

   ($V^{2,R}$ replaces $V^{2,U}$ and $V^{3,U}$ replaces — block 30

$V^{3,R}$ since we have passed $\theta_{N-2}(3) = \Theta_{N-2}(2)$).

$V^{3,U}$ is eligible but $V^{2,R}$ is not, by Proposition 5.2).

- The prevailing cost $V^{2,U}$ is no longer valid. block 31
- $\delta_{N-2}(2) = \theta_{N-2}(3)$ $(= \Theta_{N-2}(2) = -12.54)$ block 32
- since

  the old prevailing cost is replaced by block 33

  $V^{2,R}$ <u>which is not eligible</u>,

  $V^{3,U}$ is the new prevailing cost.

- Thus

  $m = 3$ block 25

  and

  $K_{N-2}(3:1) = K_{N-2}^{3,U}$ block 26

  $H_{N-2}(3:1) = 0$

  $G_{N-2}(3:1) = 0$

  $L_{N-2}(3:1) = L_{N-2}^{3,U}$

  $F_{N-2}(3:1) = 0$

- $V^{2,U}$ is removed from future eligibility block 27
- The intersection of the new prevailing cost block 21

  $V^{3,U}$ and the (only other) eligible valid cost

  $V^{4,L}$ are at

  $$x_{N-2} = -6.977,\ -2.1417$$

- Since -6.977 is <u>inside</u> the search interval we have

  $\delta_{N-2}(3) = -6.977$ block 23

and

$V^{4,L}$ is the new prevailing cost — block 24

- Thus

m=4 — block 25

and

$K_{N-2}(4:1) = K^{4,L}_{N-2}$

$H_{N-2}(4:1) = H^{4,L}_{N-2}$ — block 26

$G_{N-2}(4:1) = G^{4,L}_{N-2}$

$L_{N-2}(4:1) = L^{4,L}_{N-2}$

$F_{N-2}(4:1) = F^{4,L}_{N-2}$

- Remove $V^{3,U}$ from future eligibility — block 27
- The only valid eligible candidate cost in the remainder of this search interval is the prevailing cost $V^{4,L}$ — blocks 21, 22
- Move rightwards to search the interval

$(\theta_{N-2}(3), \theta_{N-2}(4))$ — block 29

6. Searching interval $(\theta_{N-2}(3), \theta_{N-2}(4)) = (-4.56, -3.277)$

Eligible valid candidates: $V^{4,L}$ only — block 30

($V^{3,R}$ replaces $V^{3,U}$ since we have passed $\theta_{N-2}(3)$, but $V^{3,R}$ isn't eligible).

- Since only $V^{4,L}$ is valid and eligible. move rightwards to the interval $(\theta_{N-2}(4), 0)$. — blocks 30,31,21, 22,29

7. Searching interval $(\theta_{N-2}(4),0) = (-3.277, 0)$

Eligible valid candiates: $V^{4,U}$

($V^{4,U}$ replaces $V^{4,L}$ as a valid candidate since we have passed $\theta_{N-2}(4)$, and $V^{4,L}$ is eligible) block 30

- The prevailing cost $V^{4,L}$ is no longer valid. block 31
- $\delta_{N-2}(4) = \theta_{N-2}(4) = -3.277$ block 32
- Since $V^{4,U}$ is eligible it is the new prevailing cost block 33
- Thus

  $m = 5$ block 25

  and

  $K_{N-2}(5:1) = K^{4,U}_{N-2}$ block 26

  $H_{N-2}(5:1) = G_{N-2}(5:1) = 0$

  $L_{N-2}(5:1) = L^{4,U}_{N-2}$

  $F_{N-2}(5;L) = 0$

- Remove $V^{4,L}$ from future eligibility block 27
- $V^{4,U}$ is the only eligible valid cost blocks 21, 22

- We are in the <u>rightmost</u> partition since this example is a symmetric problem (see block 4) block 28

8. This completes the left-to-right search for $j=1$, $k=N-2$. The optimal cost-to-go $V_{N-2}(x_{N-2}, r_{N-2} = 1)$ and control law $u_{N-2}(x_{N-2}, r_{N-2} = 1)$ parameters have been determined for $x_{N-2} < 0$ and can be obtained for $x_{N-2} > 0$ directly by symmetry. □

The algorithm presented in this section computes, off-line, the optimal control laws and expected cost-to-go parameters in each form $j \in \underline{M}$ and at each time, for the general class of finite time horizon JLQ problems formulated in chapter 5. This algorithm can also be used to obtain approximations of the optimal steady-state solutions of infinite time horizon problems (provided such steady-state solutions exist) as we will see in Section 7.7.

7.3 Qualitative Behavior of the Optimal Controller in the Single Form-Transition Problem: $\hat{V}_{N-1}(x_{N-1} | r_{N-2} = 1)$ Shapes

Using the algorithm that was described in the previous section we can compute the optimal controller for any JLQ problem (of chapter 5) with form transition probabilities that are piecewise constant in x. The remainder of this chapter contains a further examination of the qualitative properties of these controllers.

The class of control problems that is solvable using the algorithm of section 7.2 is extremely rich. A wide range of optimal controllers exhibiting myriad possible qualitative behaviors can be obtained, depending upon the choice of problem parameters. Some of these controllers are relevant to fault-tolerant control applications and some are not. Consequently, it is impossible to make further meaningful

qualitative statements about the piecewise constant-in-x JLQ control problem in general - there are just too many parametric cases to account for.

We have chosen therefore to focus our attention in the remainder of this chapter on subclasses of JLQ problems that enable us to gain insight into the kinds of parametrically determined qualitative behaviors that are appropriate to fault-tolerant controllers. In particular we will study in further detail the single form-transition problem of section 6.5 (i.e.:(6.88) - (6.93). This problem is a useful tool for study because the iterative algorithm procedures of section 7.2 can be described by recursive difference equations that are amenable to detailed analysis[1], but this problem is still sufficiently general to expose the tradeoffs between controller performance and reliability goals that are the essence of fault-tolerant control.

In this section we will examine the shape of the conditional expected cost-to-go $\hat{V}_{N-1}(x_{N-1}|r_{N-2}-1)$ for the entire class of single form transition problems. The purpose of this is to demonstrate the tremendous diversity of $\hat{V}_{N-1}$ shapes (and hence the broad range of optimal controllers) that can arise at k = N-2 in this problem, leading to the wide variety of controllers as (N-k) increases. In later sections we will examine certain subclasses of the single form-transition problem that possess special structures that facilitate analysis in greater detail.

---

[1] Under certain reasonable assumptions about parameter values.

Recall that the single form-transition problem is as follows: we have the system

$$x_{k+1} = a(r_k)x_k + b(r_k)u_k \tag{7.2}$$

$$r_k \in \{1,2\}$$

$$p(1,2:x) = \begin{cases} \omega_1 & \text{if } |x| < \alpha \\ \omega_2 & \text{if } |x| > \alpha \end{cases} \tag{7.3}$$

$$p(1,1:x) = 1 - p(1,2:x) \qquad p(2,1) = 0 \qquad p(2,2) = 1$$

where we wish to minimize

$$\min_{u_o,\ldots,u_{N-1}} \quad E\left\{ \sum_{k=k_o}^{N-1} [u_k^2 R(r_k) + x^2_{k+1} Q(r_{k+1})] + x^2_N K_T(r_N) \right\} \tag{7.4}$$

with the following finite parameters:

$$Q(1) > 0 \qquad Q(2) \geq 0 \qquad \alpha > 0$$

$$0 < \omega_1 < 1 \qquad 0 < \omega_2 < 1 \tag{7.5}$$

$$K_T(j) \geq 0$$

$$R(j) > 0 \qquad j = 1,2$$

$$b(j) \neq 0$$

$$a(j) > 0$$

In sections 6.5 and 6.6 we solved for the last stage solution $V_{N-1}(x_{N-1}, r_{N-1}=1)$ for all parametric cases of (7.2) - (7.5). We did this by first examining the conditional expected cost-to-go $\hat{V}_N(x_N | r_{N-1}=1)$. Recall that there are two parametric cases of interest:

$$\underline{\text{Case 1:}} \quad \hat{K}_N(2) > \hat{K}_N(1) \equiv \hat{K}_N(3) \tag{7.6}$$

$$\underline{\text{Case 2:}} \quad \hat{K}_N(2) > \hat{K}_N(1) \equiv \hat{K}_N(3) \tag{7.7}$$

Case 1 problems occur when

$$(\omega_2 - \omega_1)\ [K_T(2) + Q(2) - (K_T(1) + Q(1))] > 0 \tag{7.8}$$

This situation arises when the system performance goals and reliability goals are commensurate. For example, suppose that

- $\omega_2 > \omega_1$ — the probability of the form change is greater away from zero than near it
- $K_T(2) + Q(2) > K_T(1) + Q(1)$ — the cost charged at time N is greater in form 2 than in form 1

This would correspond to a system when entry into form 2 represents the occurrence of a costly failure, with the probability of failure $p(1,2:x)$ increasing away from the regulator goal of x=0. The performance goal (of keeping a weighted sum of $x_N^2 + u_{N-1}^2$ small) is met by making x_N^2 small without using too much control (i.e., without making u_{N-1}^2 too large). This performance goal is consistent with keeping x_N small so as to reduce the probability of failure.

Case 1 problems also arise when

- $\omega_1 > \omega_2$
- $K_T(2) + Q(2) < K_T(1) + Q(1)$.

Here the transition to form 2 results in a lower cost charged at time N and the probability of making this desirable transition is greater near zero than away from it. So again, the performance goal (keeping x_N^2 small with small u_{N-1}^2) and the reliability goal (increasing the probability of the favorable transition) are commensurate.

Case 1 problems possess a conditional expected cost-to-go $\hat{V}_N(x_N|r_{N-1}=1)$ at time k = N like that of figure 7.8(a). The conditional cost is discontinuous at $x_N = \pm\alpha$ and the "good" (low cost) sides of these discontinuities are the sides nearer zero.

Case 2 problems occur when

$$(\omega_1 - \omega_2)\,[K_T(2) + Q(2) - (K_T(1) - Q(1)] > 0 \qquad (7.9)$$

This situation arises when the system performance goals and reliability goals are conflicting. That is, the best strategy to reduce the instantaneous cost (a weighted sum of $x_N^2 + u_{N-1}^2$) is at cross-purposes with reducing the probability of being in the more costly form at time N. Case 2 problems occur when either

$$\omega_1 > \omega_2$$

$$K_T(2) + Q(2) > K_T(1) + Q(1)$$

or

$$\omega_2 > \omega_1$$

$$K_T(1) + Q(1) > K_T(2) + Q(2) \quad .$$

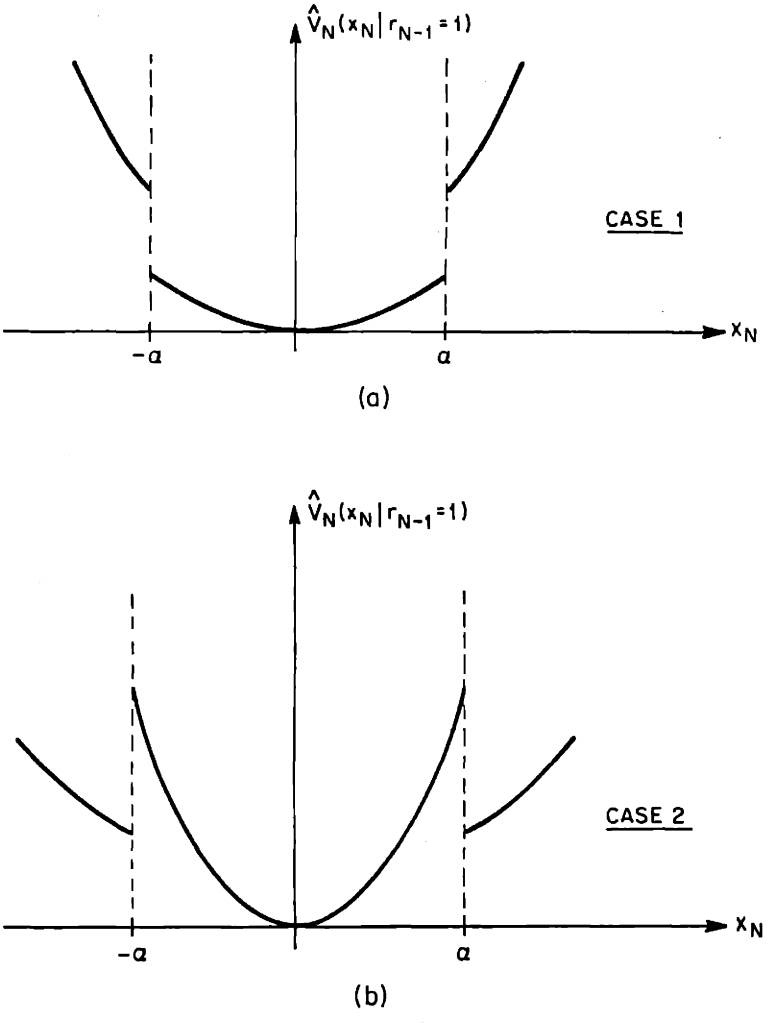

Figure 7.8: $\hat{V}_N(x_N|r_{N-1}=1)$ when (a) $\hat{K}_N(1) = \hat{K}_N(3) > \hat{K}_N(2)$ (Case 1) and when (b) $\hat{K}_N(2) > \hat{K}_N(3) = \hat{K}_N(1)$ (Case 2).

They have a conditional expected cost-to-go $\hat{V}_N(x_N|r_{N-1}=1)$ like that shown in figure 7.8(b). This conditional cost is discontinuous at $x_N = -\alpha$ but the "good" sides of the discontinuities are away from zero.

As shown in section 6.6, there are three possible shapes for the optimal expected cost-to-go $V_{N-1}(x_{N-1},r_{N-1}=1)$. These are repeated here in figure 7.9. For Case 1 problems, $V_{N-1}(x_{N-1},r_{N-1}=1)$ has a single minimum at zero (shown in figure 7.9(a)). For Case 2 problems $V_{N-1}(x_{N-1},r_{N-1}=1)$ can have two additional local minima at $x_{N-1} = \pm\alpha/a(1)$ if and only if

$$\frac{b^2(1)}{R(1)} \qquad \frac{\hat{K}_N(2) - \hat{K}_N(1)}{\hat{K}_N(1)\ \hat{K}_N(2)} \quad . \tag{7.10}$$

Each of these three $V_{N-1}(x_{N-1},r_{N-1}=1)$ shapes can lead to several different shapes of the next stage conditional expected cost-to-go, $\hat{V}_{N-1}(x_{N-1}|r_{N-2}=1)$, depending upon the ordering of the grid points in the composite partition of x_{N-1} (that is, depending on the relative values of $\pm\alpha$, $\delta_{N-1}(1)$, $\delta_{N-1}(2)$, $\delta_{N-1}(3)$ and $\delta_{N-1}(4)$).

Each of the different shapes of the <u>conditional</u> expected cost-to-go $\hat{V}_{N-1}(x_{N-1}|r_{N-2}=1)$ will in turn result in one (or more) qualitatively different shapes for the optimal expected cost-to-go at time k = N-2, $V_{N-2}(x_{N-2},r_{N-2}=1)$. This diversity of possible controllers increases geometrically as (N-k) increases even for the relatively simple problem (7.2) - (7.5). It is this diversity of parametric cases that makes it difficult to make further descriptive qualitative statements about optimal JLQ controllers that have generality (even though we <u>can</u> solve for the controller in each specific case via section 7.2).

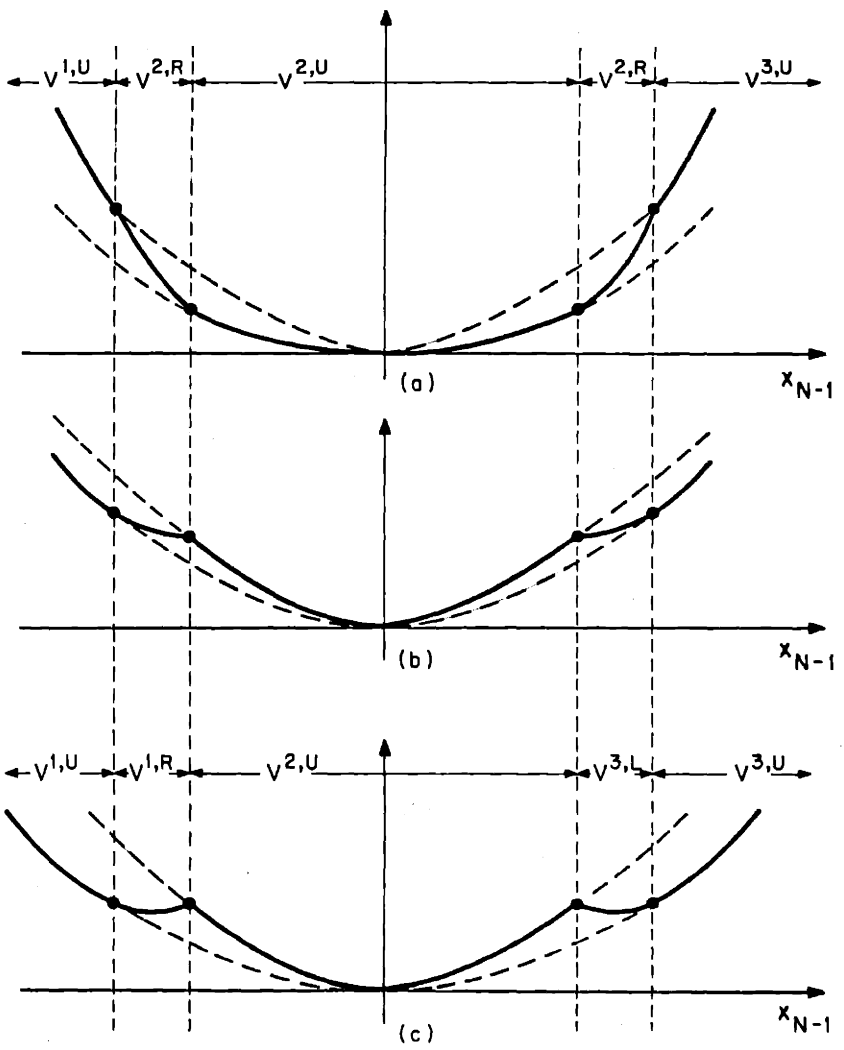

Figure 7.9: Shape of $V_{N-1}(x_{N-1}, r_{N-1} = 1)$ for (a) Case 1 as in (7.6);
(b) Case 2 as in (7.7) with (7.10) not holding;
(c) Case 2 as in (7.7) with (7.10) holding.

Let us now consider the possible shapes of the next stage conditional expected cost-to-go $\hat{V}_{N-1}(x_{N-1}|r_{N-2}=1)$. Recall that $\hat{V}_{N-1}(x_{N-1}|r_{N-2}=1)$ is a piecewise-quadratic function of x_{N-1}:

$$\hat{V}_{N-1}(x_{N-1}|r_{N-2}=1) = \begin{cases} x_{N-1}^2 \hat{K}_{N-1}(i) + x_{N-1} \hat{H}_{N-1}(i) + \hat{G}_{N-1}(i) \\ \text{for} \quad x_{N-1} \in \Delta_{N-1}(i) \\ \quad i = 1,\ldots,\psi_{N-1} \end{cases} \tag{7.11}$$

where the regions $\{\Delta_{N-1}(i)\}$ of x_{N-1} values in (7.21) are those specified by the composite partition in step 1 of section 5.4. This partition (as described in section 5.4) is constructed by superimposing the grids due to the joining points $\{\delta_{N-1}(i):i = 1,2,3,4)\}$ of $V_{N-1}(x_{N-1},r_{N-1}=1)$ and the form transition probability discontinuities $\{\nu_{12}(1) = -\alpha\ ,\ \nu_{12}(2) = \alpha\}$. The number of regions of x_{N-1} values induced by this partition is $\psi_{N-1} = 7$, except for the degenerate cases of $\delta_{N-1}(1) = -\alpha$ or $\delta_{N-1}(2) = -\alpha$. There are three different non-degenerate situations that can occur, as listed in table 7.2.

	$\gamma_{N-1}(1)$	$< \gamma_{N-1}(2)$	$< \gamma_{N-1}(3)$	$< \gamma_{N-1}(4)$	$< \gamma_{N-1}(5)$	$< \gamma_{N-1}(6)$
(1)	$\delta_{N-1}(1)$	$\delta_{N-1}(2)$	$-\alpha$	α	$\delta_{N-1}(3)$	$\delta_{N-1}(4)$
(2)	$\delta_{N-1}(1)$	$-\alpha$	$\delta_{N-1}(2)$	$\delta_{N-1}(3)$	α	$\delta_{N-1}(4)$
(3)	$-\alpha$	$\delta_{N-1}(1)$	$\delta_{N-1}(2)$	$\delta_{N-1}(3)$	$\delta_{N-1}(4)$	α

Table 7.2 Nondegenerate Partitions of x_{N-1} Values

The value of the open loop dynamics (a(i) in form 1 determines which of the situations in table 7.2 applies. From the equations for the $\delta_{N-1}(i)$ we obtain the following directly:

For <u>case 1</u> problems (where $\hat{K}_N(2) < \hat{K}_N(1) \equiv \hat{K}_N(3)$

$$(1) \Longleftrightarrow a(1) < 1 + \frac{b^2(1)}{R(1)} \hat{K}_N(2) \tag{7.12}$$

$$(3) \Longleftrightarrow a(1) > \left(1 + \frac{b^2(1)}{R(1)} \hat{K}_N(1)\right) \left(1 + \sqrt{1 - \frac{R(1) + b^2(1)\, \hat{K}_N(2)}{R(1) + b^2(1)\, \hat{K}_N(1)}}\right) \tag{7.13}$$

with (2) in table 7.2 corresponding to case 1 problems with a(1) between the two values in (7.12) - (7.13).

For <u>case 2</u> problems (where $\hat{K}_N(2) > \hat{K}_N(1) \equiv \hat{K}_N(3)$

$$(1) \Longleftrightarrow a(1) < \left(1 + \frac{b^2(1)\, \hat{K}_N(2)}{R(1)}\right) \left(1 - \sqrt{1 - \frac{R(1) + b^2(1)\, \hat{K}_N(1)}{R(1) + b^2(1)\, \hat{K}_N(2)}}\right) \tag{7.14}$$

$$(3) \Longleftrightarrow a(1) > 1 + \frac{b^2(1)}{R(1)} \hat{K}_N(1) \tag{7.15}$$

with (2) in table 7.2 corresponding to case 2 problems with a(1) between the two values in (7.14) - (7.15).

From the above we see that the partition ordering (in table 7.2) is a stability-related property by the form 1 open loop dynamics:

- for case 1 problems, all open loop stable systems in form 1 (i.e. $a(1) < 1$) satisfy (1) in table 7.2 (as do some not-too unstable open loop systems). Only unstable $a(1)$ can yield situations (2) and (3).

- for case 2 problems, only open loop unstable systems in form 1 satisfy (3) in table 7.2. If there are local minima for $V_{N-1}(x_{N-1}, r_{N-1}=1)$, which occurs if and only if (7.10) holds, then all open loop stable ($a(1) < 1$) systems satisfy situation (1) in table 7.2. Since the right-hand side of (7.14) is less one if, and only if (7.10) holds, we have that if there are no local minima in $V_{N-1}(x_{N-1}, r_{N-1}=1)$ (except for the global minimum at $x_{N-1}=0$) then only unstable $a(1)$ yield situation (2) in table 7.2.

We have now characterized the different x_{N-1} partitions that can arise in step 1 of section 5.4 (and block 4 of the algorithm of section 7.2) at time $k = N-1$. In section 6.6 we saw now how the shape of the conditional expected cost-to-go $\hat{V}_N(x_N | r_{N-1}=1)$ was directly related to the qualitative properties $V_{N-1}(x_{N-1}, r_{N-1}=1)$. Similarly the shape of $\hat{V}_{N-1}(x_{N-1} | r_{N-2}=1)$ is intimately tied to the qualitative properties of the next stage solution, $V_{N-2}(x_{N-2}, r_{N-2}=1)$. The number of qualitatively different shapes of $\hat{V}_{N-1}(x_{N-1} | r_{N-2}=1)$ that can arise for the single form-transition problem (and lead to significantly different optimal controller properties) is large. To demonstrate this we illustrate in figures 7.10 - 7.12 the six different basic shapes that $\hat{V}_{N-1}(x_{N-1} | r_{N-2}=1)$ can take for case 1

problems (even more[1] shapes arise for case 2 problems). Depending upon the relative values of the problem parameters ω_1, ω_2, $\{K_{N-1}(t:1) + Q(1) : t=1,\ldots,m_{N-1}(5)\}$ and $K_{N-1}(1:2) + Q(2)$, the conditional expected cost-to-go $\hat{V}_{N-1}(x_{N-1}|r_{N-2}=1)$ can be monotone nonincreasing for $x_{N-1} < 0$, or not, for each of the composite partition situations (1) - (3) listed in table 7.2.

In this section we have indicated how, in only two time steps, the number of parametrically determined, qualitatively different optimal JLQ controllers becomes large for the relatively simple single form-transition problem. In the remainder of this chapter we will obtain parametric conditions on (7.2) - (7.5) that specify particular subclasses of the JLQ problem which possess special structures in the composite partition of x_k (at each time k) and thus in the optimal controller as well.

---

[1] The existence of local minima makes case 2 problems more complicated.

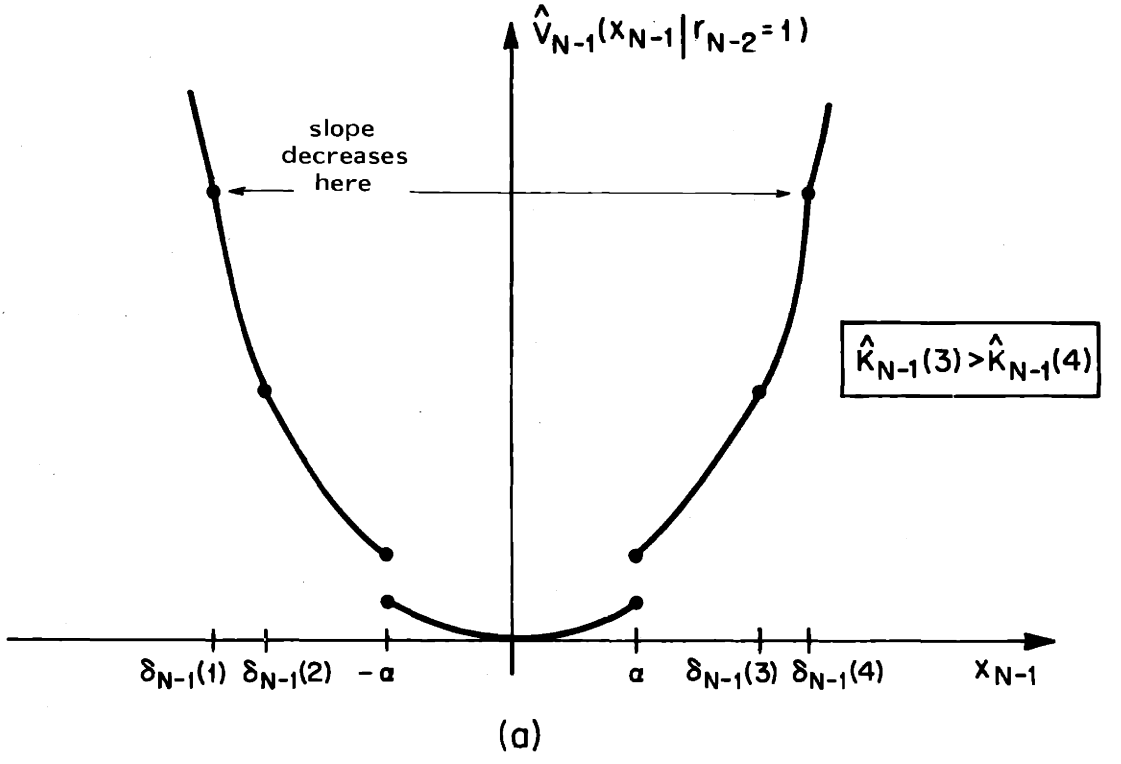

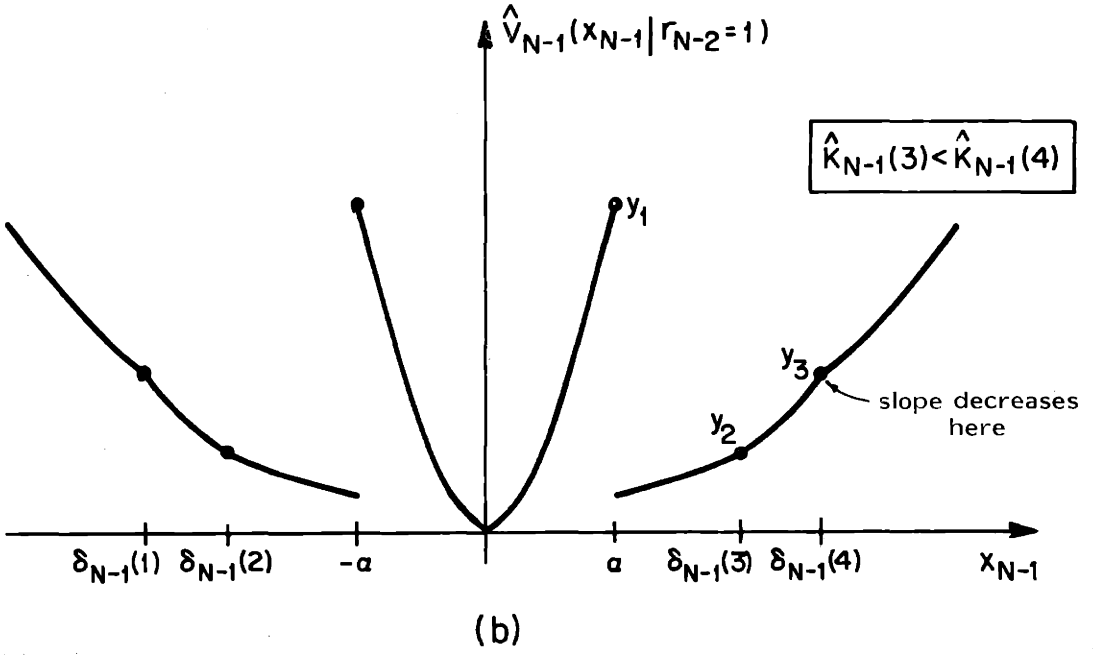

Figure 7.10: Possible $\hat{V}_{N-1}(x_{N-1}|r_{N-2}=1)$ Shapes for Case 1 in Situation 1 of Table 7.2. In (b) we can have $y_1<y_2<y_3$, $y_2<y_1<y_3$ or $y_2<y_3<y_1$.

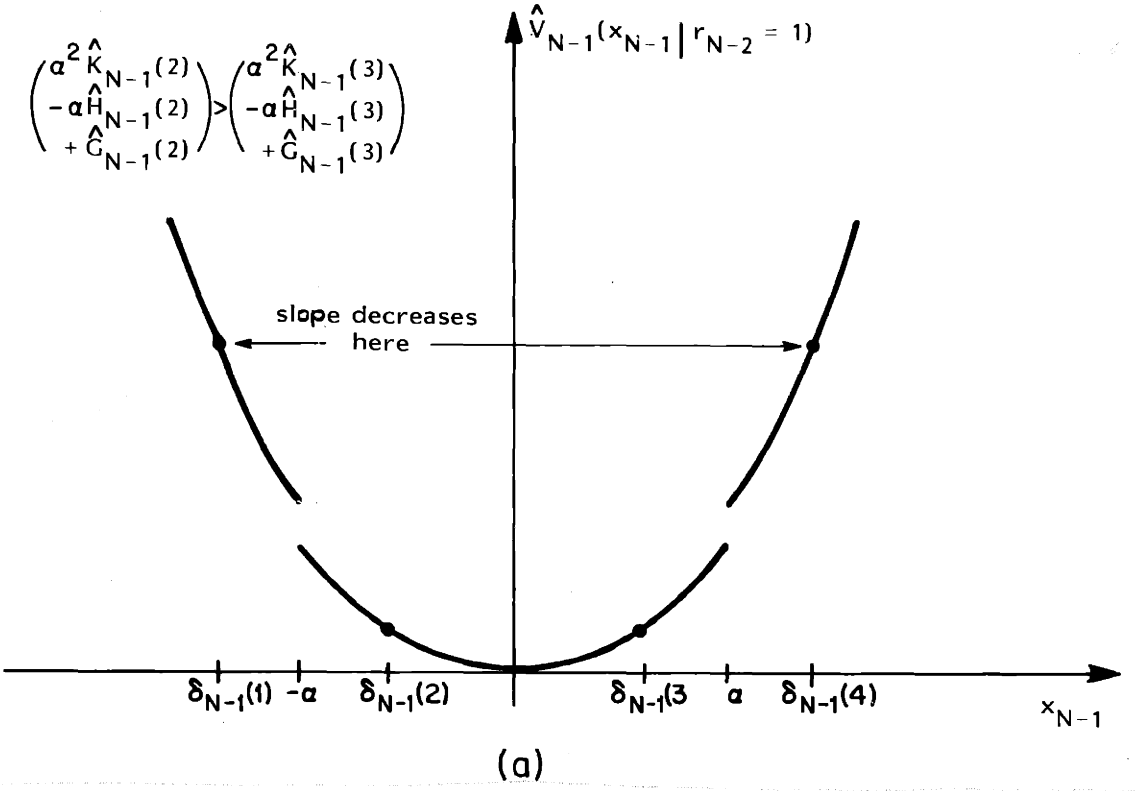

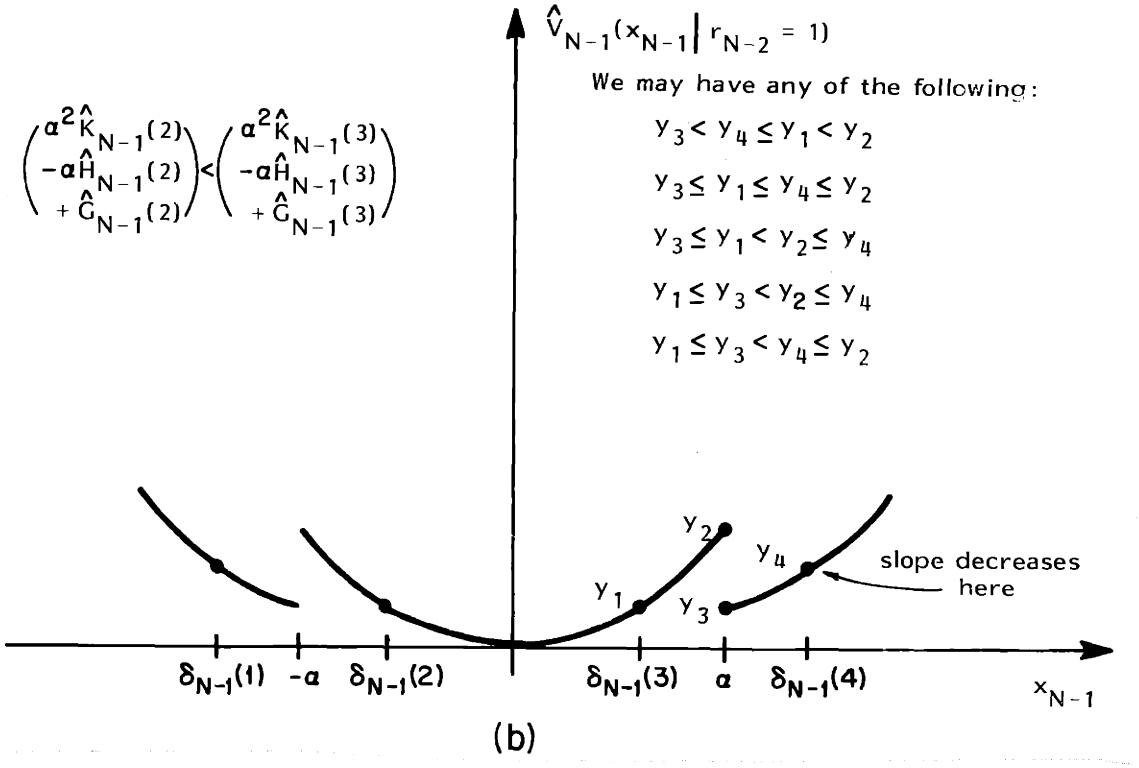

Figure 7.11: Possible $\hat{V}_{N-1}(x_{N-1} \mid r_{N-2}=1)$ Shapes for Case 1 in situation 2 of table 7.2.

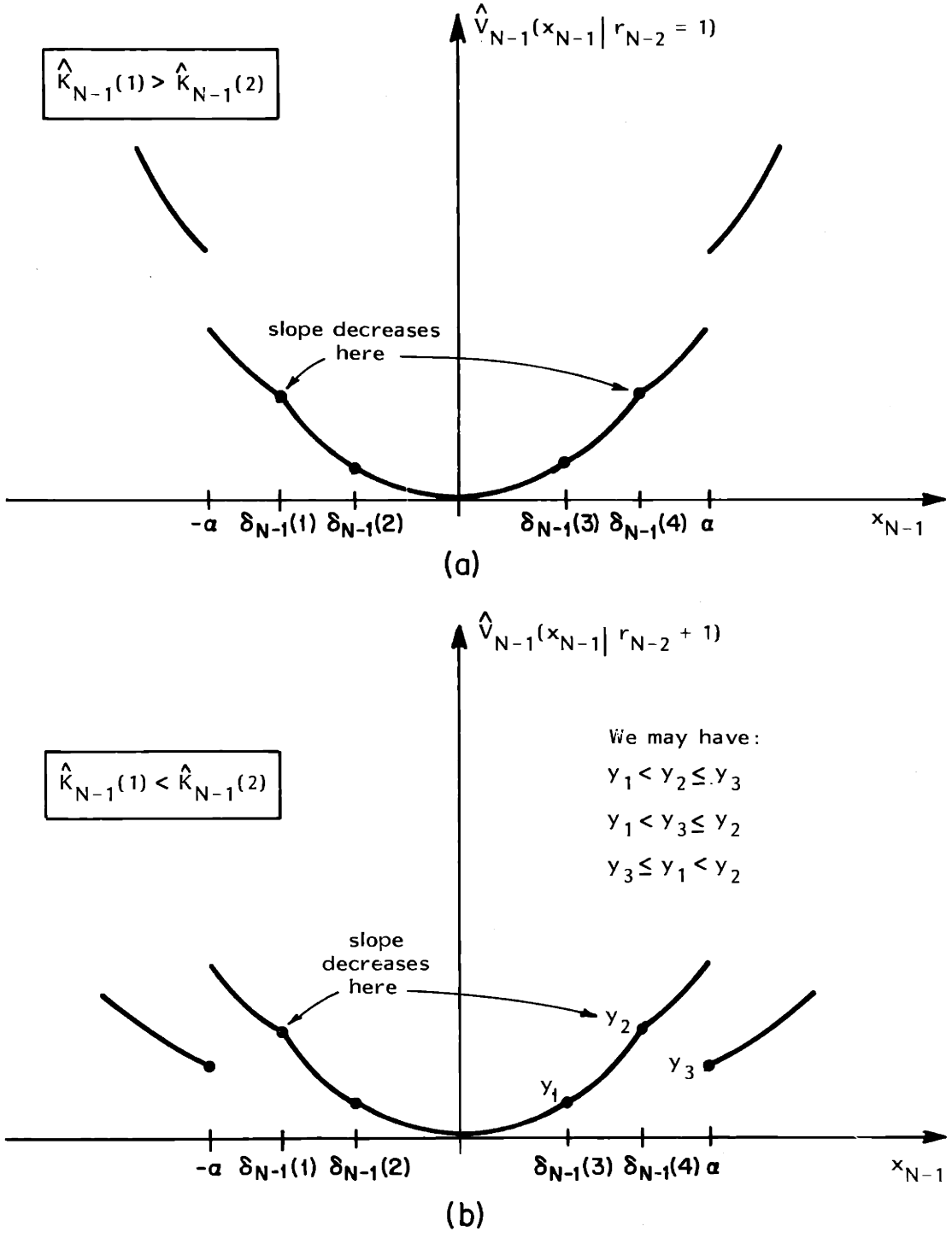

Figure 7.12: Possible $\hat{V}_{N-1}(x_{N-1} | r_{N-2}=1)$ Shapes for Case 1 in Situation (3) of Table 7.2

7.4 Qualitative Behavior of the Optimal Controller in the Single Form-Transition Problem: Bounds, Endpieces and Middlepiece

In this section we identify certain conditions on the parameters of the single form-transition problem (7.2) - (7.5) which yield example problems that have a fairly simple structure (so as to be amenable to detailed analysis) but are still sufficiently general to expose the tradeoffs between the reliability and performance goals of fault-tolerance controllers.

In chapter 6 we established certain facts about the optimal expected cost-to-go $V_k(x_k, r_k=1)$, as k decreases from N. These included the following:

(1) The endpieces of $V_k(x_k, r_k=1)$, valid for extremely negative and positive values of x_k, are described by the same finite positive quadratic cost function $V_k^{Le}(x_{k,1}) = V_k^{Re}(x_{k,1})$ of x_k, given by (6.99) - (6.104). They are the same functions due to the symmetry (about 0) of the problem.

The endpiece cost function converges as (N-k) increases, to the steady-state endpiece cost function specified by $K_\infty^{Re}(1) \equiv K_\infty^{Le}(1)$ in (6.106).

(2) The switching region S_k^j (between the endpieces) has finite width at each time k, but as $(N-k) \to \infty$ this width grows without bound (Proposition 6.3).

(3) The expected cost-to-go $V_k(x_k, r_k = 1)$ has a single middle-piece cost function, given by (6.99), (6.102), (6.105). This finite positive quadratic function of x_k converges to the steady-state middlepiece cost function specified by $K_\infty^{RM}(1) \equiv K_\infty^{LM}(1)$ in (6.107).

(4) $V_k(x_k, r_k = 1)$ lies between the upper bound function $V_k^{UB}(x_k, 1)$ and lower bound function $V_k^{LB}(x_k, 1)$ that are specified in Proposition 6.7, at each value of x_k. These bounds are quadratic (not piecewise quadratic) functions of x_k. As $(N-k) \to \infty$, these bounds converge to the steady-state bounds $V_\infty^{UB}(x,1)$ and $V_\infty^{LB}(x,1)$ given in (6.86)-(6.87).[1]

Now what else can we say, in general, about the qualitative properties of the optimal controller for the single form-transition problem?

Let us restrict our attention to single form-transition problems (7.2) - (7.5) where, at each time k, the sum of the x_k cost and the expected cost-to-go from x_k is higher in form $r_k = 2$ than it is in form $r_k = 1$. This situation is what we expect to occur when $r = 2$ denotes operation in a failed or degraded mode. Thus we are focusing here on single form-transition JLQ problems that are appropriate representations for fault-tolerant control applications. The following conditions ensure this situation:

---

[1] Since $a(1) > 0$, by Proposition 6.7.

Fact 7.1: For the single form-transition JLQ control problem of (7.2) - (7.5) if

$$Q(1) \leq Q(2) \quad \left\{ \text{same or greater x-cost} \right. \tag{7.16}$$

$$K_T(1) \leq K_T(2) \quad \left\{ \text{charged in form 2 than in form 1} \right. \tag{7.17}$$

$$0 < a(1) \leq a(2) \quad \text{form 2 not more stable than form 1} \tag{7.18}$$

$$\frac{a^2(1)}{a^2(2)} \leq \frac{[b^2(1)/R(1)]}{[b^2(2)/R(2)]} \quad \text{ratio of control effectiveness in form 1 to form 2 is greater than (or equal to) square of ratio of open loop dynamics} \tag{7.19}$$

then at each time $k = N, N-1, N-2, \ldots, k_o+1$ we have

$$\begin{pmatrix} x_k^2 Q(2) \\ + \\ V_k(x_k, r_k=2) \end{pmatrix} = x_k^2 \begin{pmatrix} Q(2) \\ + \\ K_k(1:2) \end{pmatrix} \geq x_k^2 \begin{pmatrix} Q(1) \\ + \\ K_k^{UB}(1) \end{pmatrix} = \begin{pmatrix} x_k^2 Q(1) \\ + \\ V_k^{UB}(x_k, r_k=1) \end{pmatrix} \tag{7.20}$$

Proof: Conditions (7.16)- (7.17) guarantee that (7.20) holds at time $k = N$. The additional conditions (7.18)- (7.19) and direct substitution for $V_k^{UB}(x_k, r_k=1)$ and $V_k(x_k, t_k=2)$ from (6.74), (6.86), (6.78) - (6.79) and (6.94), (6.96) yield an inductive proof of (7.20) as k decreases. □

Thus, when (7.16)-(7.19) hold then the x-cost and cost-to-go in the failure mode $r = 2$ are greater than (or equal to) that in the normal form $r = 1$, at every time k. Condition (7.16) and (7.17) are obviously appropriate if form r=2 is a failure mode of operation, and (7.18) is not

unreasonable. Condition (7.19) is not excessively restrictive. It says that for the problem (7.2) - (7.5) to have structure (7.20) we must have :

- open loop squared dynamics ratio $a^2(1)/a^2(2)$ small enough (failure Mode not too stable relative to normal operation)
- energy cost ratio R(2)/R(1) large enough (cost of energy in failure Mode not too low - in normal made, not too high)
- actuator gain squared ratio $b^2(1)/b^2(2)$ large enough (actuator gain large enough in normal operation and not too large after failure).

Note by (7.18) that (7.20) is satisfied if

$$\frac{b^2(1)}{R(1)} > \frac{b^2(2)}{R(2)} \tag{7.21}$$

We will now further restrict our attention to problems where the functions $V_k(x_k, r_k=2)$, $V_k^{LM}(x_k, r_k=1) \equiv V_k^{RM}(x_k, r_k=1)$ and $V_k^{Le}(x_k, r_k=1) \equiv V_k^{Re}(x_k, r_k=1)$ all <u>increase</u> <u>monotonically</u> as (N-K) increases. This restriction (which is made for analytical convenience), is characterized by the following:

<u>Fact 7.2</u>: For the single form-transition JLQ control problem of (7.2) - (7.5), with conditions (7.16) - (7.19) of Fact 7.1 holding,

(1) $K_k(1:2)$ (hence $V_k(x_k, r_k=2)$ for each x_k) increase monotonically as (N-K) increases if and only if

$$0 \leq K_T(2) < \frac{\begin{bmatrix} R(2)\ [a^2(2)\ -1)] \\ -b^2(2)\ Q(2) \end{bmatrix} + \sqrt{\begin{pmatrix} R(2)\ [a^2(2)\ -1] \\ -b^2(2)\ Q(2) \end{pmatrix}^2 + 4b^2(2)a^2(2)R(2)Q(2)}}{2b^2(2)} \qquad (7.22)$$

2) If, in addition to (7.22) condition (7.23) below is true for $i = 1$, then the middlepiece parameter $K_k^{LM}(1) \equiv K_k^{RM}(1)$ (and hence $V_k^{LM}(x_k,1)$ for each x_k) increases monotonically as N-k increases.

3) If, in addition to (7.22) condition (7.23) below is true for $i = 2$, then the endpiece parameters $K_k^{Re}(1) \equiv K_k^{Le}(1)$ (and hence $V_k^{Le}(x_k,1)$ and $V_k^{Re}(x_k,1)$ for each x_k) increase monotonically as N-k) increases:

$$0 \leq K_T(1) < \frac{\begin{bmatrix} -\{R(1)\ (1-a^2(1)\ (1-\omega_i)) + b^2(1)\ [Q(1) + \omega_i(K_T(2) + Q(2) - Q(1))]\} \\ + \sqrt{\{R(1)(1-a^2(1)(1-\omega_i)) + b^2(1)[Q(1) + \omega_i(K_T(2) + Q(2) - Q(1))]\}^2 + 4a^2(1)\ R(1)\ b^2(1)\ (1-\omega_i)\ [Q(1) + \omega_i(K_T(2) + Q(2) - Q(1))]} \end{bmatrix}}{2b^2(1)\ (1-\omega_i)} \qquad (7.23) \quad \square$$

Condition (1) says that $K_k(1{:}2)$ decreases as (N-k) increases if the terminal cost $K_T(2)$ is not too large. Conditions (2) and (3) require that terminal cost $K_T(1)$ is not too large. In particular, Fact 7.2 holds if $K_T(1) = K_T(2) = 0$.

The proof of Fact 7.2 is by induction. It involves straightforward but tedious algebraic manipulations that are detailed in Appendix C.11.

The parameter restrictions of Facts 7.1 and 7.2 also guarantee the following strong relationship between the functions (of x_k) that describe the middlepiece, endpiece and bounds of $V_k(x_k, r_k{=}1)$.

Fact 7.3: For the single form-transition JLQ control problem (7.2) - (7.5) with parameter values satisfying conditions of Fact 7.1 we have the following:

(1) If

$$\omega_2 > \omega_1 \tag{7.24}$$

(that is, the "failure probability" $p(1,2{:}x)$ is higher away from $x = 0$ than near it) then at all times $k = N,\ N-1,\ N-2,\ldots$

- The endpieces $V_k^{Le}(1)$, $V_k^{Re}(1)$ and upper bound $V_k^{LB}(1)$ of $V_k(x_k, r_k = 1)$ are given by the same function of x_k (that is, $K_k^{Le}(1) = K_k^{Re}(1) = K_k^{UB}(1)$ for all k)

and

- the <u>middlepiece</u> and $V_k^{LM}(1) \equiv R_k^{RM}(1)$ and <u>lower bound</u> $V_k^{LB}(1)$ of $V_k(x_k, r_k = 1)$ are given by the <u>same function</u> of x_k (that is, $K_k^{LM}(1) \quad K_k^{RM}(1) = K_k^{LB}(1)$ for all k).

(2) If

$$\omega_1 > \omega_2 \tag{7.25}$$

(that is, the "failure probability" p(1,2:x) is higher near x = 0 than away from it) then at all times k = N, N-1, N-2,...

- the <u>endpieces</u> $V_k^{Le}(1)$, $V_k^{Re}(1)$ and <u>lower bound</u> $V_k^{LB}(1)$ of $V_k(x_k, r_k = 1)$ are given by the <u>same function</u> of x_k (that is, $K_k^{Le}(1) = K_k^{Re}(1) = K_k^{LB}(1)$

and

- the middlepiece $V_k^{LM}(1) \equiv V_k^{RM}(1)$ and <u>upper bound</u> $V_k^{UB}(1)$ of $V_k(x_k, r_k = 1)$ are given by the same function of x_k (that is, $K_k^{LM}(1) \equiv K_k^{RM}(1) = K_k^{UB}(1)$.

The proof of this fact is a straightforward induction, given in Appendix C 12.

□

The two cases of $p(1,2:x)$ in (7.24) - (7.25) are shown in figure 6.6. The general shapes of $V_k(x_k,r_k = 1)$ that result from these (at any k) are illustrated in figure 7.13. Note that (7.11) and figure 7.13(a) correspond to problems where the twin goals of system performance and reliability are commensurate; driving x toward zero reduces the operating cost at k and keeps the probability of failure small. Thus far from zero $V_k(x_k,r_k=1)$ is coincident with its upper bound, and near x = 0 the lower bound function is reached since both goals are being met. Figure 7.13(b) and (7.25) pertain to fault-tolerant control problems where these goals are contradictory; driving x towards zero (inside of $(-\alpha,\alpha)$ reduces the operating cost but increases the probability of failure. Therefore, near zero $V_k(x_k,r_k=1)$ is equal to its upper bound, since the probability of failure (and higher cost, by Fact 7.1) is high; far from zero, $V_k(x_k,r_k=1)$ is equal to its lower bound since the risk of failure is kept small.

In this section we have specified certain parametric restrictions (i.e. (7.16) - (7.19), (7.22) - (7.23) for which the single form-transition problem (7.2) - (7.5) has a simplified solution structure. This reduced class is rich enough to include problems with conflicting control goals and some with commensurate ones, however. These two cases will be studied in greater detail in the next two sections.

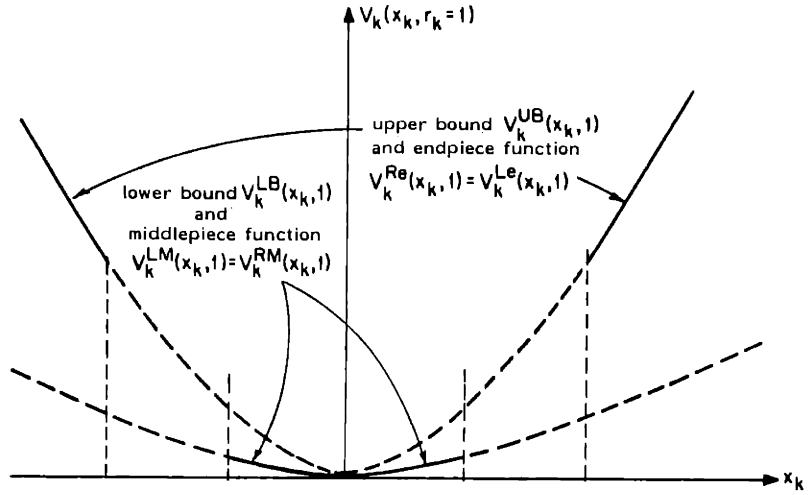

(a)

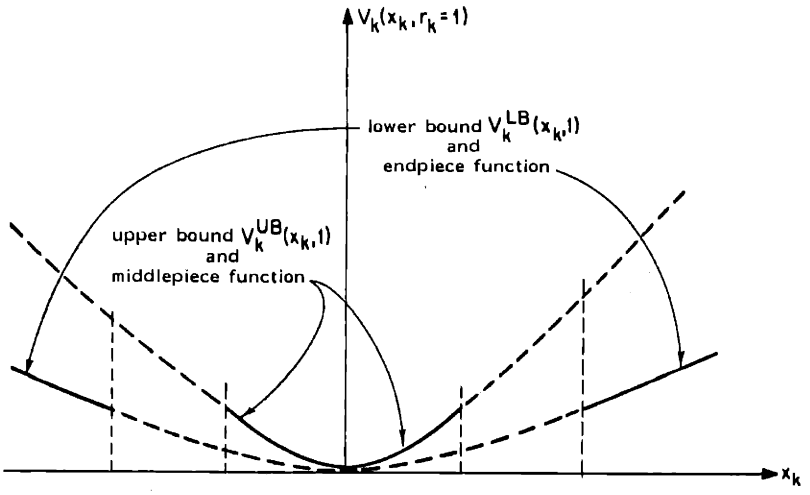

(b)

Figure 7.13: $V_k(x_k, r_k = 1)$ structure when Facts 7.1,7.2 hold for (a) $\omega_2 > \omega_1$ (commensurate goals) and (b) $\omega_1 > \omega_2$ (conflicting goals).

7.5 Active Hedging When Reliability and Performance Goals are Commensurate

As we have discussed previously, the optimal JLQ controllers for problems having x-dependent form processes (which are the subject of chapters 5-7) are qualitatively different from the JLQ controllers for Markovian form systems (as in chapter 3), in that they can use the control to change the probabilities of form transitions. That is, they actively hedge[1]. In this section we will study this active hedging behavior for a class of JLQ problems with x-dependent form transitions where the system reliability and performance goals are commensurate. Our purpose here is to illustrate how the optimal controller uses active hedging to achieve fault tolerance. In the next section we will consider the use of active hedging when the system performance and reliability goals are at cross-purposes.

We will consider here the "case 1" single form-transition problem of the last section, as (N-k) increases. Under certain additional parametric conditions (that are derived here), the optimal JLQ controller at all times $k = N, N-1,\ldots,k_o$ can be specified by recursive difference equations that is, $V_k(x_k,r_k=1)$ and $u_k(x_k,r_k=1)$ can be obtained without performing the various comparisons and tests of the general solution algorithm that is flowcharted in section 7.2. In this section we will discuss the optimal steady-state controller for this example, as (N-k) approaches infinity.

The discussion here will be carried out primarily via figures. A detailed technical development paralleling this section is contained in appendices C.13 and C.14.

---

(1) In the terminology of chapter 1.

Let us consider the scalar, single form-transition problem (7.2)-(7.5) where Facts 7.1, 7.2 and 7.3(1) hold. We also assume that (7.12) holds. That is, $\pm\alpha$ are the grid points of the x_{N-1} composite partition that are closest to zero. In figure 7.14 we collect (for convenience) the curves $V_N(x_N, r_N=1)$, $\hat{V}_N(x_N | r_{N-1}=1)$, $\dot{V}_{N-1}(x_{N-1}, r_{N-1}=1)$ and $\hat{V}_{N-1}(x_{N-1} | r_{N-2}=1)$ for this problem.

Let us consider now the candidate cost-to-go functions (of X_{N-2}) that are eligible[1] for $V_{N-2}(x_{N-2}, r_{N-2}=1)$. In figure 7.15 we show the candidate functions $V_{N-2}^{t,U}$ (i=1,...,7). Recall that these functions of x_{N-2} coincide with solutions of the constrained (in x_{N-1}) problems[2]:

$$\min_{u_{N-2}} \left\{ V_{N-2}(x_{N-2}, r_{N-2}=1) \right\}$$

s.t.

$$x_{N-1} \in \Delta_{N-1}(i) = (\gamma_{N-1}(i-1), \gamma_{N-1}(i))$$

for those x_{N-2} values where the resulting value of x_{N-1} is in the interior of $\Delta_{N-1}(i)$.

The following relationships that are pictured in figure 7.15 are verified in appendix C.13:

$$V_{N-2}^{4,U} < V_{N-2}^{3,U} \equiv V_{N-2}^{5,U} < V_{N-2}^{1,U} \equiv V_{N-2}^{7,U} \qquad \text{at all } x_{N-2} \tag{7.26}$$

$$V_{N-2}^{2,U} > V_{N-2}^{3,U} \qquad \text{for all } x_{N-2} \text{ except equality at } x_{N-2} = \theta_{N-2}(3)/a(1), \tag{7.27}$$

$$V_{N-2}^{6,U} > V_{N-2}^{5,U} \qquad \text{for all } x_{N-2} \text{ except equality at } x_{N-2} = \theta_{N-2}(6)/a(1). \tag{7.28}$$

In addition to the seven candidate cost functions that are shown in fig 7.15,

---

(1) In the sense of section 7.2

(2) Here $\gamma_{N-1}(0) \overset{\Delta}{=} -\infty$ and $\gamma_{N-1}(7) \overset{\Delta}{=} +\infty$

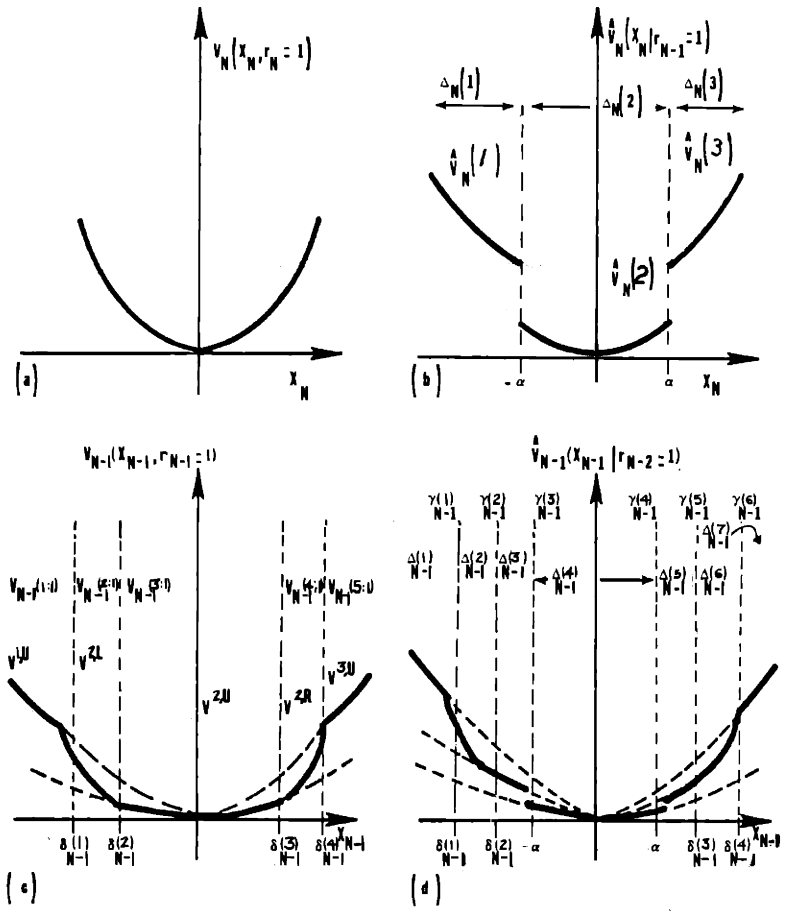

Figure 7.14: Curves for Case 1 Single Form-Transition Problem where Facts 7.1, 7.2 and 7.3(1) Hold: (a) $V_N(x_N, r_N=1)$, (b) $\hat{V}_N(x_N \mid r_{N-1}=1)$, (c) $V_{N-1}(x_{N-1}, r_{N-1}=1)$ and (d) $\hat{V}_{N-1}(x_{N-1} \mid r_{N-2}=1)$ when (7.12) Holds .

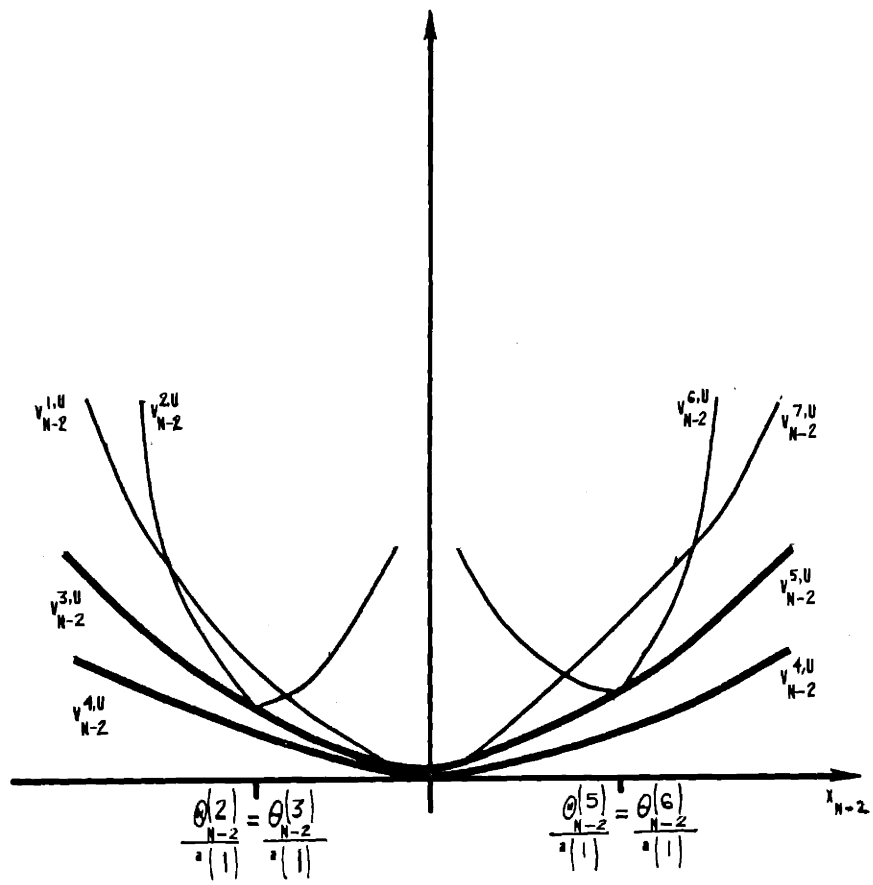

Figure 7.15: The Candidate Cost-To-Go Functions $V^{i,U}_{N-2}$ (i=1,2,..,7).

there are two other eligible candidate functions for $V_{N-2}(x_{N-2}, r_{N-2}=1)$. These are those "constrained" functions [1] which, according to Prop. 5.2 (and block 15 of the algorithm of section 7.2), correspond to hedging to the lower cost side of a $\hat{V}_{N-1}(x_{N-1} | r_{N-2}=1)$ discontinuity; that is, driving to $x_{N-1} = -\alpha^+$ or $x_{N-1} = \alpha^-$ (see figure 7.14(d)). These candidate cost functions are:

$V^{4,L}_{N-2}(x_{N-2}, r_{N-2}=1)$ driving x_{N-1} to $-\alpha^+$ (left boundary of $\Delta_{N-1}(4)$)

$V^{4,R}_{N-2}(x_{N-2}, r_{N-2}=1)$ driving x_{N-1} to α^- (right boundary of $\Delta_{N-1}(4)$).

The parameters of $V^{4,L}_{N-2}$ and $V^{4,R}_{N-2}$ are listed in appendix C.13.

If we superimpose the curves of $V^{4,L}_{N-2}$ and $V^{4,R}_{N-2}$ on figure 7.15 and compare the regions of x_{N-2} - validity of each curve [2], then we can obtain the optimal expected cost-to-go

$$V_{N-2}(x_{N-2}, r_{N-2}=1) = \min_{i=1,\ldots,7} \left\{ \min_{u_{N-2}} \left\{ V_{N-2}(x_{N-2}, r_{N-2}=1) \right\} \right\}$$
$$\text{s.t. } x_{N-1} \in (\gamma_{N-1}(i-1), \gamma_{N-1}(i))$$

(see chapter 5) for each value of x_{N-2}. However $V^{4,L}_{N-2}$ and $V^{4,R}_{N-2}$

---

(1) Corresponding to driving x_{N-1} to one of the boundary points $\gamma_{N-1}(1), \ldots, \gamma_{N-1}(6)$ of the composite partition intervals $\Delta_{N-1}(1), \ldots, \Delta_{N-1}(7)$.

(2) As in section 7.2

can be in three different graphical positions relative to the $V_{N-2}^{i,U}$., depending upon the values of the problem parameters. We will examine each of these three possibilities and analyze the relationships between the qualitative properties of the optimal controllers which they specify and the problem parameters.

We first note that, by definition:

$$V_{N-2}^{4,L} > V_{N-2}^{4,U} \qquad \text{except equality at } x_{N-2} = \theta_{N-2}(4)/a(1) \tag{7.29}$$

$$V_{N-2}^{4,R} > V_{N-2}^{4,U} \qquad \text{except equality at } x_{N-2} = \Theta_{N-2}(4)/a(1). \tag{7.30}$$

Now $V_{N-2}^{4,U}(x_{N-2},1)$ is the middlepiece cost function for $V_{N-2}(x_{N-2},r_{N-2}=1)$, thus as we have shown it is also a lower bound for this problem.[1] Consequently $V_{N-2}^{4,U}$ must be optimal over its entire valid domain; that is

$$V_{N-2}(x_{N-2},r_{N-2}=1) = V_{N-2}^{4,U}$$

$$\text{for} \qquad \frac{\theta_{N-2}(4)}{a(1)} \leq x_{N-2} \leq \frac{\Theta_{N-2}(4)}{a(1)} \cdot \tag{7.31}$$

From Proposition 6.1 we know that the optimal expected cost-to-go $V_{N-2}(x_{N-2},r_{N-2}=1)$ coincides with the endpiece cost function $V_{N-2}^{1,U}$ for x_{N-2} negative enough, and it coincides with $V_{N-2}^{7,U}$ for x_{N-2} large enough. We also know (from Proposition 5.1) that $V_{N-2}(x_{N-2},r_{N-2}=1)$ is continuous in x_{N-2}.

---

(1) See Fact 7.3

Refer now to figure 7.15. Considering the optimality of $V_{N-2}^{1,U}$ for x_{N-2} sufficiently negative, of $V_{N-2}^{4,U}$ for x_{N-2} near zero, and of $V_{N-2}^{7,U}$ for x_{N-2} sufficiently large and bearing in mind the required monotomicity[1] of the optimal mapping

$$x_{N-2} \longmapsto x_{N-1}(x_{N-2}, r_{N-2}=1),$$

the remaining question that must be resolved so as to find $V_{N-2}(x_{N-2}, r_{N-2}=1)$ for this problem is the following: how does $V_{N-2}(x_{N-2}, r_{N-2}=1)$ "get from" the $V_{N-2}^{1,U}$ curve to the $V_{N-2}^{4,U}$ curve as X_{N-2} increases (and from $V_{N-2}^{4,U}$ to $V_{N-2}^{7,U}$) ?

The three possible situations that can occur, depending upon the values of the problem parameters, are shown in figures 7.16 - 7.18 and are summarized in table 7.3. Complete details for each case appear in appendix C.13.

The first situation (shown in figure 7.16) results in $V_{N-2}(x_{N-2}, r_{N-2}=1)$ having $m_{N-2}(1) = 9$ pieces[2] . Each piece corresponds to a different active hedging strategy using u_{N-2} and u_{N-1}. In the endpieces $V_{N-2}(1{:}1)$ $V_{N-2}(9{:}1)$ the controller does <u>not</u> use controls u_{N-2}, u_{N-1} to change the p(1,2:x) piece that the x process is in. In the middlepiece $V_{N-2}(4{:}1)$ we have $|x_{N-1}|<\alpha$, $|x_N|<\alpha$. The left and right switching regions ($S_{N-2}^{1,L}$ and $S_{N-2}^{1,R}$) of x_{N-2} values are divided into three parts:

- intervals of x_{N-2} values where <u>immediate</u> hedging-to-a-point

(1) From Proposition 5.3 we know that this mapping is always monotone

(2) This is the upperbound on $m_{N-2}(1)$, according to Proposition 5.4

(to $x_{N-1} = -\alpha^+$ with cost $V_{N-2}(4:1)$ or to $x_{N-1} = \alpha^-$ with cost $V_{N-2}(6:1)$) using u_{N-2} is optimal

- intervals of x_{N-2} values where the optimal strategy uses control u_{N-1} to hedge-to-a-point (to $x_N = -\alpha^+$ with cost $V_{N-2}(2:1)$ or $x_N = \alpha^-$ with cost $V_{N-2}(8:1)$),

- intervals of x_{N-2} values where x_{N-1} and x_N are in different $p(1,2:x)$ pieces but hedging-to-a-point is not used; ($V_{N-2}(3:1)$, $V_{N-2}(7:1)$ are the optimal costs here).

The second situation (shown in figure 7.17) results in $V_{N-2}(x_{N-2}, r_{N-2}=1)$ having only $m_{N-2}(1) = 7$ pieces. Unlike the first situation of figure 7.16, there are <u>no</u> x_{N-2} values from which the optimal controller causes x_{N-1} and x_N to be in different $p(1,2:x)$ pieces without using hedging-to-a-point. Here the switching regions ($S^{1,L}_{N-2}$, $S^{1,R}_{N-2}$) are each divided into two parts:

- intervals of x_{N-2} where immediate hedging-to-a-point (to $x_{N-1} = -\alpha^+$ with cost $V_{N-2}(3:1)$ or to $x_{N-1} = \alpha^-$ with cost $V_{N-2}(5:1)$) using u_{N-2} is optimal

- intervals of x_{N-2} values where the optimal strategy keeps x_{N-1} in the same $p(1,2:x)$ piece as x_{N-2}, but then uses control u_{N-1} to hedge-to-a-point (to $x_N = -\alpha^+$

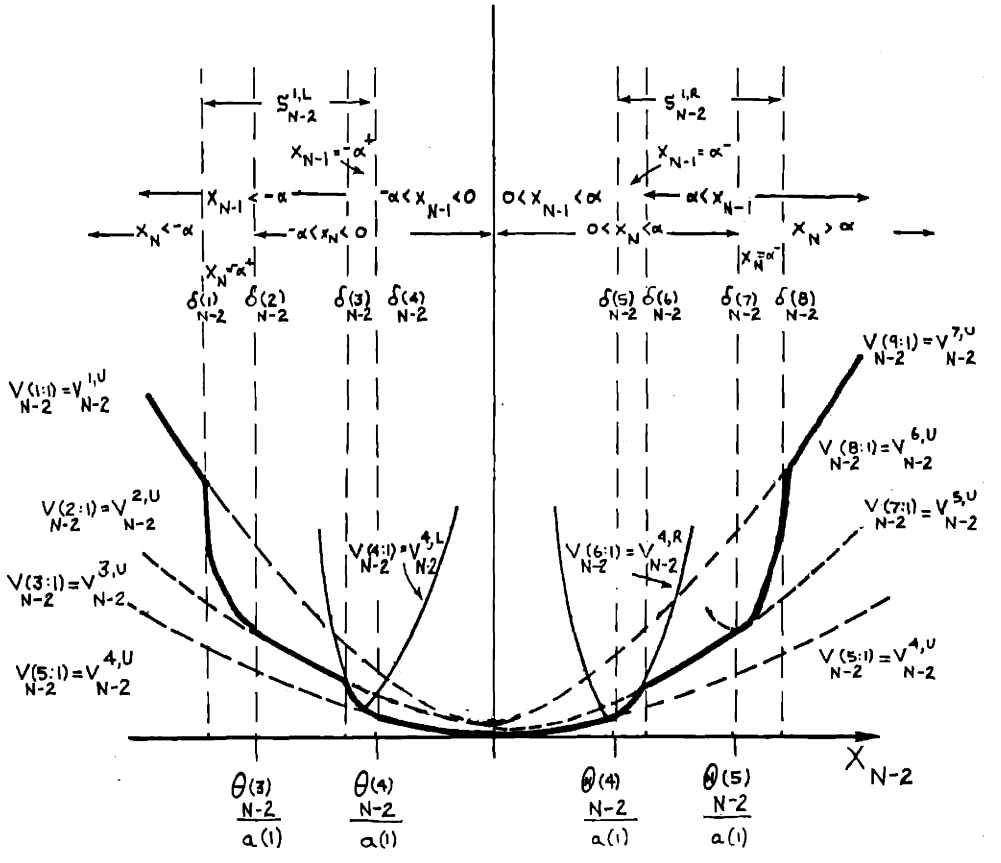

Figure 7.16: $V_{N-2}(x_{N-2}, r_{N-2}=1)$ in the first situation. The optimal is indicated by the heavier line. The resulting optimal values of x_N and x_{N-1} for each of the 9 pieces of $V_{N-2}(x_{N-2}, r_{N-2}=1)$ are also indicated; $V_{N-2}(t:1)$ denotes the t^{th} piece (from the left) of $V_{N-2}(x_{N-2}, r_{N-2}=1)$

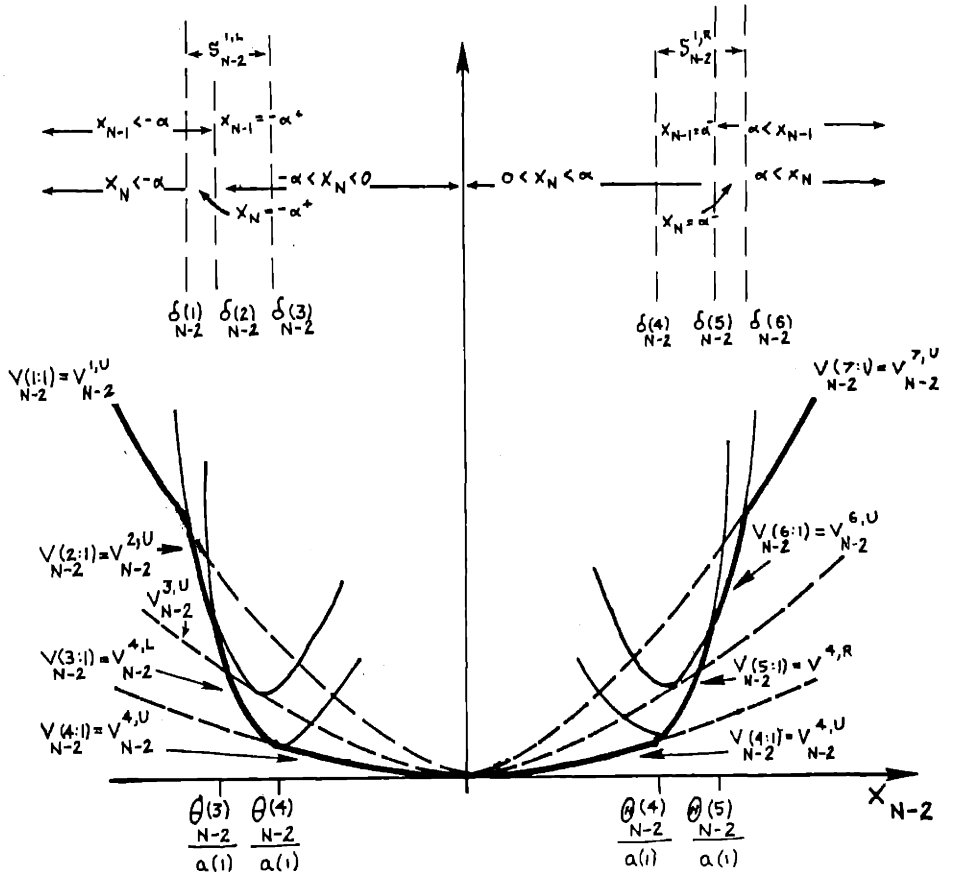

Figure 7.17: $V_{N-2}(x_{N-2}, r_{N-2}=1)$ in the second situation. The optimal is indicated by the heavier line. The resulting optimal values of x_N and x_{N-1} for each of the 7 pieces of $V_{N-2}(x_{N-2}, r_{N-2}=1)$ are also labelled.

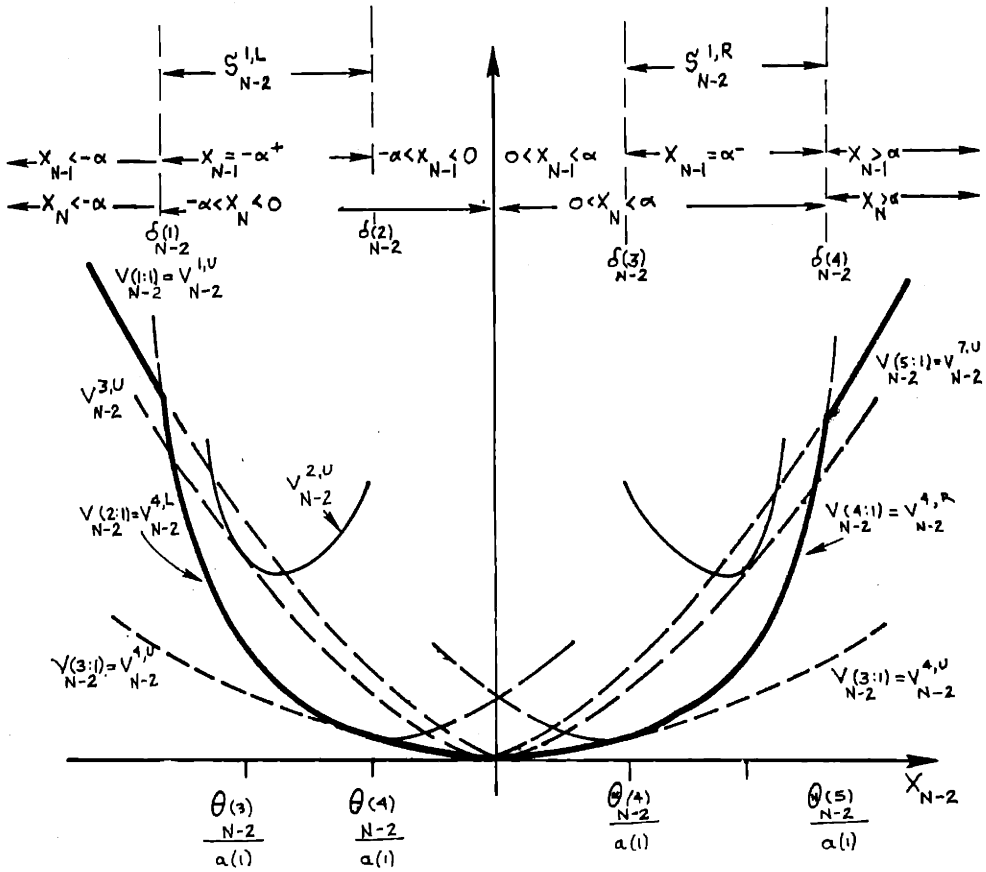

Figure 7.18: $V_{N-2}(x_{N-2}, r_{N-2}=1)$ in the third situation. The optimal is indicated by the heavier line. The resulting optimal values of x_N and x_{N-1} for each of the 5 pieces of $V_{N-2}(x_{N-2}, r_{N-2}=1)$ are also labelled.

with cost $V_{N-2}(2:1)$ or to $x_N = \alpha^-$ with cost $V_{N-2}(6:1)$).

In the third possible situation that can arise for $V_{N-2}(x_{N-2}, r_{N-2}=1)$, as shown in figure 7.18, the optimal controller has only $m_{N-2}(1) = 5$ pieces (the same number of pieces that $V_{N-1}(x_{N-1}, r_{N-1} = 1)$ has). In this situation the optimal controller drives x_{N-1} into the same $p(1,2:x)$ piece which

piece into which it drives x_N. That is, active hedging (if any) is done <u>immediately</u> (ie, at time k = N-1) using control u_{N-2}. The control u_{N-2} is used to hedge to $x_{N-2} = -\alpha^+$ (for $V_{N-2}(2:1)$ or $x_{N-1} = \alpha^-$ (for $V_{N-2}(4:1)$.

Various aspects of these three situations are summarized in table 7.3. What we would like to do is relate these various active hedging strategies to the values of the problem parameters. We first note that from figures 7.16 - 7.18 we can obtain the following graphical conditions related to these three possible situations for $V_{N-2}(x_{N-2}, r_{N-2}=1)$ in this problem. These are:

<u>Fact 7.4</u> : For the problem (7.2) - (7.5) with facts 7.1, 7.2, 7.3(1) holding and (7.12), we have the following:

(1) Situation (1), as in figure 7.16, occurs <u>if and only if</u> the leftmost intersection of the two quadratic functions $V_{N-2}^{4,L}(x_{N-2})$ and $V_{N-2}^{3,U}(x_{N-2})$ is to the right of $\theta_{N-2}(3)/a(1)$.

(2) Situation (3), as in figure 7.18, occurs <u>if and only if</u> the leftmost intersection of $V_{N-2}^{4,L}(x_{N-2})$ and $V_{N-2}^{1,U}(x_{N-2})$ is to the left of or exactly at the leftmost intersection of

	Situation 1 (Fig.7.16)	Situation 2 (Fig.7.17)	Situation 3 (Fig.7.18)
Number of pieces of $V_{N-2}(x_{N-2}, r_{N-2}=1)$ and $u_{N-2}(x_{N-2}, r_{N-2}=1) = m_{N-2}(1)$	9 (maximum possible)	7	5
Endpiece functions	$V_{N-2}(1:1)$ $V_{N-2}(9:1)$	$V_{N-2}(1:1)$ $V_{N-2}(7:1)$	$V_{N-2}(1:1)$ $V_{N-2}(5:1)$
Middlepiece function	$V_{N-2}(5:1)$	$V_{N-2}(4:1)$	$V_{N-2}(3:1)$
Other pieces that do not involve hedging-to α^- or $-\alpha^+$	$V_{N-2}(3:1)$ $V_{N-2}(7:1)$	--	--
Pieces involving hedging-to-a-point with u_{N-2}	$V_{N-2}(4:1)$ $V_{N-2}(6:1)$	$V_{N-2}(3:1)$ $V_{N-2}(5:1)$	$V_{N-2}(3:1)$ $V_{N-2}(4:1)$
Pieces involving hedging-to-a-point with u_{N-1} (but not with u_{N-2})	$V_{N-2}(2:1)$ $V_{N-2}(8:1)$	$V_{N-2}(2:1)$ $V_{N-2}(6:1)$	--

Table 7.3 Comparison of three possible situations for $V_{N-2}(x_{N-2}, r_{N-2}=1)$

$V_{N-2}^{2,U}(x_{N-2})$ and $V_{N-2}^{1,U}(x_{N-2})$

(3) Situation (2), as in figure 7.17, occurs when (1) and (2) above are both not met. A necessary condition is what $V_{N-2}^{4,L}$ and $V_{N-2}^{2,U}$ intersect. □

Proof: Immediate from figures 7.16 - 7.18.

In appendix C.13 the values of the leftmost intersections of $(V_{N-2}^{4,L}$ and $V_{N-2}^{3,U})$, $(V_{N-2}^{4,L}$ and $V_{N-2}^{1,U})$, $(V_{N-2}^{2,U}$ and $V_{N-2}^{1,U})$, $(V_{N-2}^{4,L}$ and $V_{N-2}^{2,U})$ and the value of $\theta_{N-2}(3)/a(1)$ are listed. From fact 7.4 and these values we obtain the following:

Fact 7.5: For the problems of fact 7.4,

(1) situation (1), as in figure 7.16, occurs if and only if

$$a(1) < \frac{(1 + \frac{b^2(1)}{R(1)} \hat{K}_N(2))}{\left(1 + \sqrt{1 - \frac{R(1) + b^2(1)\, \hat{K}_{N-1}(4)}{R(1) + b^2(1)\, \hat{K}_{N-1}(3)}}\right)} \quad . \tag{7.32}$$

(2) situation (3), as in figure 7.18, occurs if and only if

$$a(1) > \frac{(1 + \frac{b^2(1)}{R(1)} \hat{K}_N(1))\ ((1 + \sqrt{1 - x_1})}{1 + \sqrt{1 - \frac{R(1) + b^2(1)\, \hat{K}_{N-1}(4)}{R(1) + b^2(1)\, \hat{K}_{N-1}(1)}}} \tag{7.33}$$

where x_1 is given by (C.13.36).

(3) situation (2), as in figure 7.17 occurs if and only if (7.32) and (7.33) are <u>both</u> not true. A necessary condition is that $x_2 \leq 1$ where x_2 is given by (C.13.44).

<u>Proof</u>: These conditions are derived in appendix C.13.

Conditions (7.32) - 7.33) are implicit relationships that can be tested for any given set of problem parameters. These conditions are quite complicated, however, and it is consequently very difficult to deduce general analytical properties from them. However, we can use facts 7.1, 7.2, and 7.3(1) to obtain <u>sufficient</u> conditions that are more easily analyzed.

<u>Fact 7.6:</u> For the problem (7.2) - (7.5) with facts 7.1, 7.2, 7.3(1) and equation (7.12) holding

(1) if

$$a(1) < \left(\frac{\left[1 + \frac{b^2(1)}{R(1)} \hat{K}_N(2)\right]}{1 + \sqrt{\frac{b^2(1)}{R(1)}(\omega_2 - \omega_1)\left(K_{N-1}(1{:}2) + Q(2) - Q(1) - K_T(1)\right)}} \right)$$

$$\sqrt{1 + \frac{b^2(1)}{R(1)}\left[(1-\omega_2)(K_T(1) + Q(1)) + \omega_2(K_{N-1}(1{:}2) + Q(2))\right]}$$

then situation (1) (figure 7.16) describes $V_{N-2}(x_{N-2}, r_{N-2}=1)$.

In particular we have this situation when

$$a(1) < \frac{1}{2}\left(1 + \frac{b^2(1)}{R(1)} \hat{K}_N(2)\right). \tag{7.25}$$

(2) If

$$a(1) > \left[\left(1+\frac{b^2(1)}{R(1)}\hat{K}_N(1)\right)\left(1+\sqrt{\frac{1-\left[1+\frac{b^2(1)}{R(1)}\hat{K}_N(2)\right]\left[1+\frac{b^2(1)}{R(1)}\left[(1-\omega_2)(K_T(1)+Q(1)) + \omega_2(K_{N-1}(1:2)+Q(2))\right]\right] - (1-\omega_2)\left(1+\frac{b^2(1)}{R(1)}\hat{K}_N(2)\right)}{\left(1+\frac{b^2(1)}{R(1)}\hat{K}_N(1)\right)\left(1+\frac{b^2(1)}{R(1)}\left[K_{N-1}(1:2)+(1-\omega_2)Q(1)+\omega_2 Q(2)\right]\right)}}\right)\right] \Bigg/ \left[1+\sqrt{\frac{b^2(1)}{R(1)}\frac{(\omega_2-\omega_1)(2K_{N-1}(1:2)+Q(2)-Q(1)-K_T(1))}{R(1)+b^2(1)[K_{N-1}(1:2)+1-\omega_2)Q(1)+\omega_2 Q(2)]}}\right] \tag{7.36}$$

then situation (3) (figure 7118) describes $V_{N-2}(x_{N-2}, r_{N-2}=1)$.

(3) If

$$a(1) > \frac{\left[1 + \frac{b^2(1)}{R(1)}\ \hat{K}_N(2)\right]}{\left(1 + \sqrt{\frac{\frac{b^2(1)}{R(1)}\ (\omega_2-\omega_1)\ Q(2) - Q(1))}{1 + \frac{b^2(1)}{R(1)}\ (K_{N-1}(1:2) + (1-\omega_2)\ Q(1) + \omega_2\ (Q(2))}}\right)} \tag{7.37}$$

and

$$a(1) < \left(1+ \frac{b^2(1)}{R(1)}\ \hat{K}_N(1)\right)\left(1 + \sqrt{\frac{\left(1+ \frac{b^2(1)}{R(1)}\ \hat{K}_N(2)\right)\left(1+ \frac{b^2(1)}{R(1)}\left[K_{N-1}(1:2) + (1-\omega_2)\ Q(1)\right.\right.}{\left.\left.+ \omega_2(K_{N-1}(1:2) + Q(2))\right]\right)}{\left(1+ \frac{b^2(1)}{R(1)}\ K_N(1)\right)}}\right)$$

$$\left(1+ \frac{b^2(1)}{R(1)}\left[(1-\omega_2)(K_T(1) + Q(1))\right.\right.$$
$$\left.\left.+ \omega_2(K_{N-1}(1:2) + Q(2))\right]\right)$$

$$1 + \sqrt{\frac{b^2(1)[(\omega_2-\omega_1)\ (Q(2) - Q(1) + K_T(1)]}{+ K_{N-1}(1:2) - K_T(1))]}}$$
$$\sqrt{\frac{}{R(1) + b^2(1)}}$$
$$\sqrt{[(1-\omega_2)(K_T(1) + Q(1) + \omega_2(K_{N-1}(1:2) + Q(2))]}$$

(7.38)

Then situation (2) (figure 7.17 describes $V_{N-2}(r_{N-2}, r_{N-2}=1)$. □

Proof: See Appendix C.13.

Using (C.13.52) - (C.13.53) in appendix C.13, we can compare (7.32) with (7.34) and (7.33) with (7.38). We find that for (7.34) and (7.38) to be necessary as well as sufficient we would need either $b(1) = 0$ or $\omega_2 = \omega_1$ or $K_{N-1}(1:2) = K_T(1)$. All of these possibilities are excluded by facts 7.1 - 7.3. That is, the conditions in fact 7.6 are <u>always</u> sufficient but not necessary.

Note that conditions (7.34) - (7.38) of fact 7.6 depend upon the value of a(1) on only <u>one side</u> of each equation. This lets us interpret fact 7.6 as a set of conditions which relates values of a(1) (that is, the stability of form r=1 open loop dynamics) to the three active hedging strategies of figures 7.16 - 7.18. For sufficiently small a(1), where (7.34) is satisfied, we have the optimal controller of figure 7.16. For larger a(1) satisfying (7.37) - (7.38) the optimal controller must hedge-to-a-point with either u_{N-2} or u_{N-1} for all x_{N-2} that are not in the endpieces and middlepiece domains. For sufficiently unstable a(1) satisfying (7.36) the optimal JLQ controller cannot delay in its active hedging - for all x_{N-2} inside the switching regions it will immediately hedge-to-a-point using control u_{N-2}. Thus for this example problem with commensurate performance and reliability goals, greater instability of the normal operation dynamics (that is, larger values of a(1)) force the controller to actively hedge sooner. The optimal controller must drive x into the advantageous[1] region of p(1,2:x) sooner for large a(1) than for small a(1) because the larger value of a(1) tends to push x deeper into the disadvantageous region of p(1,2:x). Thus the cost of hedging-to-a-point (crossing into the good p(1,2=x) piece)

---

[1] where the probability p(1,2≠x) of a (costly) failure occurring is smaller (that is, $|x| < \infty$).

In the remainder of this section we will examine the optimal JLQ controller for problems satisfying (7.34) of fact 7.6. What we find is that at all times (N-k), the optimal JLQ controller follows the pattern of figure 7.16. This lets us obtain a recursive description of $V_{N-k}(X_{N-k}, r_{N-k}=1)$ and $u_{N-k}(x_{N-k}, r_{N-k}=1)$ at each time (N-k).

A typical $V_{N-k}(X_{N-k}, r_{N-k}=1)$ curve is shown in figure 7.19. It has $m_{N-k}(1) = 4k+1$ pieces:

- 2k pieces wholly to the left of zero
- 2k pieces wholly to the right of zero

and

- the middlepiece around $X_{N-k} = 0$.

The curve is symmetric about $x_{N-k} = 0$.

For x_{N-k} in the middlepiece (i.e., for $\delta_{N-k}(2k) < x_{N-k} < \delta_{N-k}(2k+1)$), the optimal controller will result in $|x_{N-k+\ell}| < \alpha$ for $\ell = 1,\ldots,k$. That is, the x process will be in the advantageous piece of p(1,2,:x) at all future times.

The first piece to the left of the middlepiece (i.e., $\delta_{N-k}(2k-1) < x_{N-k} < \delta_{N-k}(2k)$) corresponds to using u_{N-k} to achieve $x_{N-k+1} = -\alpha^+$. That is, we use the control u_{N-k} to immediately hedge to a point. Then the optimal controller will keep the x process in the middlepiece from time (N-k) + 2 through time N. Similarly the first piece to the right of the middlepiece (i.e. $\delta_{N-k}(2k+1) < x_{N-k} < \delta_{N-k}(2k + 2)$) corresponds to using u_{N-k} to immediately hedge to $x_{N-k+1}=\alpha^-$ (and to keeping $|x_{N-k+\ell}| < \alpha$ for $\ell = 2,3,\ldots,k$).

The second pieces of $V_{N-k}(x_{N-k}, r_{N-k}=1)$ to the left and right of

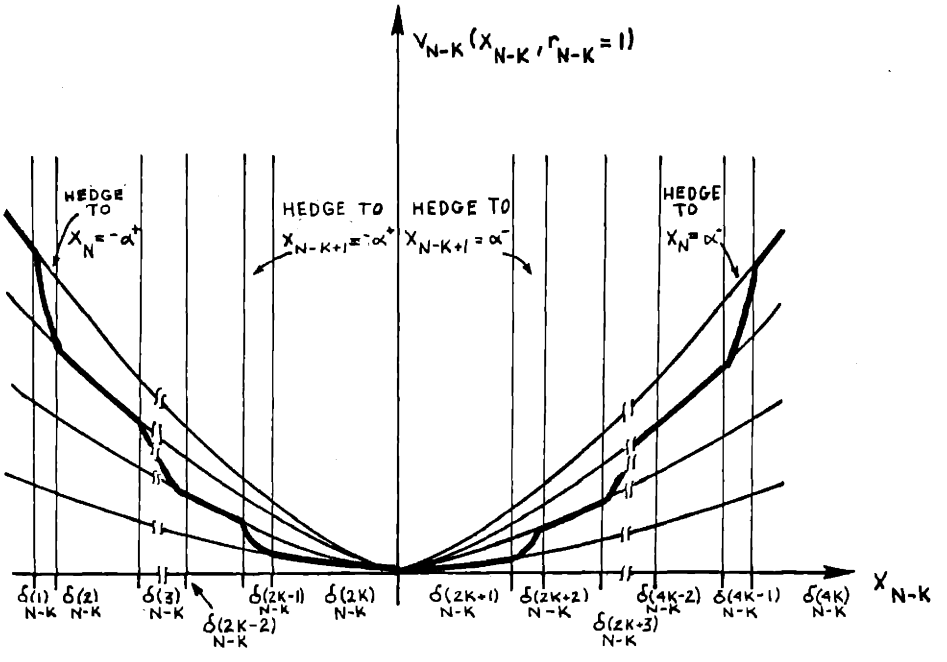

Figure 7.19: Optimal Expected Cost-To-Go $V_{N-k}(x_{N-k}, r_{N-k}=1)$ for the Problems of Proposition 7.7

the middlepiece correspond to having $|x_{N-k+1}| > \alpha$ but $|x_{N-k+\ell}| < \alpha$ for $\ell = 2,3,\ldots,k$. That is, the optimal controller for x_{N-k} in these pieces will <u>never</u> (using controls $u_{N-k},\ldots,u_{N-1}$) <u>hedge-to-a-point</u>. However, the x process will be in the advantageous piece of $p(1,2,:x)$ from time x_{N-k+2} onwards.

The third pieces of $V_{N-k}(x_{N-k},r_{N-1}=1)$ to the left and right of the middlepiece correspond to hedging-to-a-point <u>one</u> time step in the future; that is, u_{N-k+1} is used to obtain $|x_{N-k+2}| = \alpha^-$. Then the x process is kept inside $(-\alpha,\alpha)$ from time $(N-k)+3$ through N.

In general, the $2m^{th}$ pieces of $V_{N-k}(x_{N-k},r_{N-k}=1)$ to the right and left of the middlepiece correspond to <u>never</u> hedging-to-a-point. The x process will be in the disadvantageous piece of $p(1,2:x)$ for $x_{N-k+1},\ldots,x_{N-k+m}$ and then inside the advantageous piece $(-\alpha,\alpha)$ from time $(N-k) + m + 1$ through time N. Note that the $2k^{th}$ pieces of $V_{N-k}(X_{N-k},r_{N-k}=1)$ to the left and right of the middlepiece are the endpieces of the optimal cost. For $x_{N-k} < \delta_{N-k}(1)$ and $x_{N-k} > \delta_{N-k}(4k)$, the optimal controller does not drive the x process inside the advantageous piece $(-\alpha,\alpha)$ of $p(1,2:x)$.

The $(2m+1)^{th}$ pieces of $V_{N-k}(x_{N-k},r_{N-k}=1)$ correspond to using u_{N-k+m} to hedge to $x_{N-k+m+1}= \alpha^-$ or $x_{N-k+m+1}= -\alpha^+$. Then $|x_{N-k+\ell}| < \alpha$ for $\ell = m+2,\ldots,k$.

This class of problems illustrates that using control to alter failure probabilities (that is, active hedging) at future times is directly reflected in the expected cost-to-go. The optimal controller that is obtained for this example (and in the next section) suggests a natural

way of thinking about future hedging options that leads to the finite time-horizon approximation of the infinite time problem[1] that is developed in section 7.7.

Before stating the solution to problem (7.2) - (7.5) with facts 7.1,7.2,7.3(1) and 7.6(1) holding, let us recall the following shorthand notation. Let $V_{N-k}(i:1)$ and $u_{N-k}(i:1)$ denote the i^{th} piece of $V_{N-k}(x_{N-k},r_{N-k}=1)$ and $u_{N-k}(x_{N-k},r_{N-k}=1)$, respectively, counting from left to right. That is,

$$\begin{aligned} V_{N-k}(x_{N-k},r_{N-k}=1) &= V_{N-k}(i:1) \\ u_{N-k}(x_{N-k},r_{N-k}=1) &= u_{N-k}(i:1) \end{aligned} \tag{7.39}$$

$$\text{for} \quad \delta_{N-k}(i-1) \leq x_{N-k} \leq \delta_{N-k}(i)$$

$$i = 1,\ldots,(4k+1)$$

Proposition 7.7: For the problem (7.2)-(7.5) with facts 7.1,7.2,7.3(1) and 7.6(1) holding, the optimal JLQ controller can be described by:

1) The number of pieces of $V_{N-k}(x_{N-k},r_{N-k}=1)$ and $u_{N-k}(x_{N-k},r_{N-k}=1)$ at time N-k) is

$$m_{N-k}(1) = 4k + 1 \tag{7.40}$$

---

[1] For the general problem of chapter 5.

2) This is the maximum possible number of pieces. That is all eligible candidate cost-to-go functions (by Proposition 5.2) are optimal over some portion of their regions of validity. These eligible candidate costs are

$V^{t,U}_{N-k}$ $\quad t=1,\ldots,4k-1$ (driving $x_{N-k+1} = 1$ into $\Delta^{(t)}_{N-k+1}$)

$V^{2k,L}_{N-k}$ (hedging to $x_{N-k+1} = -\alpha^{+}$)

$V^{2k,R}_{N-k}$ (hedging to $x_{N-k+1} = \alpha^{-}$) .

3) $V_{N-k}(x_{N-k}, r_{N-k}=1)$ and $u_{N-k}(x_{N-k}, r_{N-k}=1)$ are symmetric about $x_{N-k} = 0$. That is,

$$V_{N-k}(i:1)\Big|_{-x_{N-K}} = V_{N-K}(4k+2-i:1)\Big|_{x_{N-k}} \tag{7.41}$$

$$u_{N-k}(i:1)\Big|_{-x_{N-k}} = u_{N-k}(4k+2-i:1)\Big|_{x_{N-k}} \tag{7.42}$$

$$\delta_{N-k}(1) = -\delta_{N-k}(4k+1-i) \tag{7.43}$$

for $i=1,2,\ldots,(2k+1)$. (Here $\delta_{N-k}(0) \triangleq -\infty$.

4) The closest grid points to zero in the composite x_{N-k+1} partition are $\pm\alpha$.

That is

$$\begin{aligned}
\gamma_{N-k+1}(i) &= \delta_{N-k+1}(i) \qquad i = 1,\ldots,2k-2 \\
\gamma_{N-k+1}(2k-1) &= -\alpha \\
\gamma_{N-k+1}(2k) &= \alpha \\
\gamma_{N-k+1}(j) &= \delta_{N-k+1}(j-2) \qquad j = 2k+1,\ldots,4k-2
\end{aligned} \tag{7.44}$$

5) The odd-numbered pieces of $V_{N-k}(x_{N-k},r_{N-k}=1)$ and $u_{N-k}(x_{N-k},r_{N-k}=1)$ are given by

$$V_{N-k}(i:1) = x_{N-k}^2 \; K_{N-k}(i:1) \tag{7.45}$$

$$u_{N-k}(i:1) = -L_{N-k}(i:1)\; x_{N-k} \tag{7.46}$$

optimal for $\delta_{N-k}(i-1) \leq x_{N-k} \leq \delta_{N-k}(i)$

$i = 1,3,5,\ldots,(4k+1)$

These costs are optimal for x_{N-k} values where the best strategy is not to use any of the controls $u_{N-k},\ldots,u_{N-1}$ to hedge-to-a-point. They include the left-endpiece

$$V_{N-k}^{Le}(1) = V_{N-k}(1:1) \quad ,$$

the middle-piece

$$V_{N-k}^{Lm}(1) \equiv V_{N-k}^{Rm}(1) = V_{N-k}(2k+1:1) \quad ,$$

and the right-endpiece

$$V_{N-k}^{Re}(1) = V_{N-k}(4k+1:1) \quad .$$

6) The even-numbered pieces of $V_{N-k}(x_{N-k},r_{N-k}=1)$ and $u_{N-k}(x_{N-k},r_{N-k}=1)$ are given by

$$V_{N-k}(i:1) = x_{N-k}^2 \; K_{N-k}(i:1) + x_{N-k}\; H_{N-k}(i:1) + G_{N-k}(i:1) \tag{7.47}$$

$$u_{N-k}(i:1) = -L_{N-k}(i:1)\; x_{N-k} + F_{N-k}(i:1) \tag{7.48}$$

optimal for $\delta_{N-k}(i-1) \leq x_{N-k} \leq \delta_{N-k}(1)$

$i = 2,4,6,\ldots,4k$

These costs correspond to actively hedging-to-a-point at one future time. Specifically, at each time $(N-k) < N$ and for each $i = 1,2,\ldots,k$:

$V_{N-k}(2i:1)$ is the cost associated with using control u_{N-i} to hedge-to-a-point. That is, it is the expected cost-to-go which results if

$$u_{N-k+\ell-1} \text{ keeps } x_{N-k+\ell} < -\alpha$$

for each $1 \leq \ell \leq k-i$ (when $k \geq 2$)

and then

$$u_{N-i} \text{ hedges to } x_{N-i+1} = -\alpha^+$$

and then

$$u_{N-k+\ell-1} \text{ keeps } -\alpha < x_{N-k+\ell} < 0 \quad \text{for } \ell = k-i+2,\ldots,k$$

(when $k \geq 2$).

So $V_{N-k}(2k:1)$ corresponds to hedging-to-a-point <u>immediately</u> (using u_{N-k}) and $V_{N-k}(2:1)$ corresponds to hedging-to-a-point at the <u>last time</u> (using u_{N-1}). Similarly, for $V_{N-k}(j:1)$ (where $j = 2k+2,\ldots,4k$) the optimal controller uses

$$u_{N-\left[\frac{4k+2-j}{2}\right]}$$

to hedge to

$$x_{N-\left[\frac{4k-j}{2}\right]} = \alpha^-$$

7) The cost parameters in (7.45)-(7.48) are given recursively by the following set of coupled difference equations:

- For k = N-1,N-2,...., the form r=2 parameters obey:

$$K_k(1:2) = \frac{a^2(2)\, R(2)\, [K_{k+1}(1:2) + Q(2)]}{R(2) + b^2(2)[K_{k+1}(1:2) + Q(2)]} \tag{7.49}$$

$$L_k(1:2) = \frac{b(2)}{a(2)R(2)}\, K_k(1:2) \tag{7.50}$$

with

$$K_N(1:2) = K_T(2) \tag{7.51}$$

- For k=1,2,...,N

$$K_{N-k}(2k+1:1) = \frac{a^2(1)\, R(1)\, \hat{K}_{N-k+1}(2k)}{R(1) + b^2(1)\, \hat{K}_{N-k+1}(2k)} \tag{7.52}$$

where

$$\hat{K}_{N-k+1}(2k) = (1-\omega_1)[K_{N-k+1}(2k-1:1) + Q(1)] + \omega_1[K_{N-k+1}(1:2) + Q(2)] \tag{7.53}$$

with

$$K_N(1) = K_T(1)$$

and

$$L_{N-k}(2k+1:1) = \frac{b(1)}{a(1)\, R(1)}\, K_{N-k}(2k+1:1) \tag{7.54}$$

(Here $K^{LM}_{N-k}(1) \equiv K^{Rm}_{N-k}(1) \equiv K^{LB}_{N-k}(1) \equiv K_{N-k}(2k+1:1)$).

- For k=1,2,...,N and i=1,2,3,...,2k-1 :

$$K_{N-k}(i:1) = \frac{a^2(1)\, R(1)\, \hat{K}_{N-k+1}(i)}{R(1) + b^2(1)\, \hat{K}_{N-k+1}(i)} \tag{7.55}$$

where

$$\hat{K}_{N-k+1}(i) = (1-\omega_2)\begin{pmatrix} K_{N-k+1}(i:1) \\ + \\ Q(1) \end{pmatrix} + \omega_2 \begin{pmatrix} K_{N-k+1}(1:2) \\ + \\ Q(2) \end{pmatrix} \tag{7.56}$$

with

$$K_N(i) = K_T(1) \tag{7.57}$$

and

$$L_{N-k}(i:1) = \frac{b(1)}{a(1)\ R(1)}\ K_{N-k}(i:1)\ , \tag{7.58}$$

- for $k = 1,2,\ldots,N$

$$K_{N-k}(2k:1) = \frac{a^2(1)\ R(1)}{b^2(1)} \tag{7.59}$$

$$H_{N-k}(2k:1) = \frac{2a(1)\ R(1)\alpha}{b^2(1)} \tag{7.60}$$

$$G_{N-k}(2k:1) = \frac{\alpha^2}{b^2(1)}\ [R(1) + b^2(1)\ \hat{K}_{N-k+1}(2k)] \tag{7.61}$$

$$L_{N-k}(2k:1) = a(1)/b(1) \tag{7.62}$$

$$F_{N-k}(2k:1) = -\alpha/b(1)\ , \tag{7.63}$$

- for $k = 2,3,\ldots,N$ and $i = 2,4,\ldots,2k-2$:

$$H_{N-k}(i:1) = \frac{a(1)R(1)(1-\omega_2)H_{N-k+1}(i:1)}{R(1) + b^2(1)\hat{K}_{N-k+1}(i)} \tag{7.64}$$

$$= \frac{2a(1)R(1)\alpha}{b^2(1)} \prod_{\ell=1}^{(k-1)/2} \left[\frac{a(1)R(1)(1-\omega_2)}{R(1) + b^2(1)\ K_{N-k+\ell(i)}}\right] \tag{7.65}$$

and

$$G_{N-k}(i:1) = \begin{bmatrix} (1-\omega_2) G_{N-k+1}(i:1) \\ \\ - \dfrac{b^2(1)\ (1-\omega_2)^2 [H_{N-k+1}(i)]^2}{4[R(1) + b^2(1)\ \hat{K}_{N-k+1}(i)]} \end{bmatrix} \tag{7.66}$$

$$F_{N-k}(i:1) = \frac{-b(1)\ (1-\omega_2)\ H_{N-k+1}(i:1)}{2[R(1) + b^2(1)\ \hat{K}_{N-k+1}(i)]} \tag{7.67}$$

- for k=1,2,...,N

$$\delta_{N-k}(2k) = \frac{-\alpha}{\alpha(1)} \left(1 + \frac{b^2(1)}{R(1)}\ \hat{K}_{N-k+1}(2k)\right) \tag{7.68}$$

- for k = 2,3,...,N and i = 1,2,...,k-1

$$\delta_{N-k}(2i) = \frac{\delta_{N-k+1}(2i)}{a^2(1)} \left(1 + \frac{b^2(1)}{R(1)}\ \hat{K}_{N-k+1}(2i+1)\right) \tag{7.69}$$

$$= \frac{-\alpha}{a(1)} \left(\left(1 + \frac{b^2(1)}{R(1)}\ \hat{K}_{N-i+1}(2i)\right) \prod_{\ell=1}^{k=i} \frac{\left(1 + \dfrac{b^2(1)}{R(1)}\ \hat{K}_{N-k+\ell}(2i+1)\right)}{a(1)}\right) \tag{7.70}$$

- for k=1,2,...,N and i = 1,2,...,k

$$\delta_{N-k}(2i-1) = \frac{-H_{N-k}(2i:1) - \sqrt{H^2_{N-k}(2i:1) - 4\left[\begin{matrix} K_{N-k}(2i:1) \\ -K_{N-k}(2i-1:1) \end{matrix}\right] G_{N-k}(2i:1)}}{2[K_{N-k}(2i:1) - K_{N-k}(2i-1:1)]} \tag{7.71}$$

8) By symmetry we have (for each k=1,2,...,N) for i=1,2,...2k;

$$K_{N-k}(i:1) = K_{N-k}(4k+2-i:1) \tag{7.72}$$

$$H_{N-k}(i:1) = -H_{N-k}(4k+2-i:1) \tag{7.73}$$

$$G_{N-k}(i:1) = G_{N-k}(4k+2-i:1) \tag{7.74}$$

$$F_{N-k}(i:1) = F_{N-k}(4k+2-i:1) \tag{7.75}$$

$$L_{N-k}(i:1) = -L_{N-k}(4k+2-i:1) \tag{7.76}$$

9) At each time k = 1,2,... we have the following relationships:

$$K_{N-k}(2k+1:1) < K_{N-k}(2k-1:1) < \ldots < K_{N-k}(3:1) < K_{N-k}(1:1) < K_{N-k}(2:1) < K_{N-k}(4:1) < \ldots < K_{N-k}(2k:1) \tag{7.77}$$

$$\delta_{N-k}(2i-1:1) < \delta_{N-k}(2i:1) < \delta_{N-k}(2i+1:1) \qquad i=1,2,\ldots,k \tag{7.78}$$

$$\hat{K}_{N-k}(2k+2) < \hat{K}_{N-k}(2k+1) < \hat{K}_{N-k}(2k-1) < \hat{K}_{N-k}(2k-3) < \ldots < \hat{K}_{N-k}(3) < \hat{K}_{N-k}(1) < \hat{K}_{N-k}(2) < \hat{K}_{N-k}(4) \quad \ldots \quad \ldots < \hat{K}_{N-k}(2k) \tag{7.79}$$

Here $K_{N-k}(2k+1:1) = K^{LB}_{N-k}(1) = K^{LM}_{N-k}(1)$ and

$K_{N-k}(1:1) = K^{Le}_{N-k}(1) = K^{UB}_{N-k}(1)$.

10) For $i = 1,\ldots,k$

$$V_{N-k}(2i:1) > V_{N-k}(2i+1:1) \quad \text{except} \tag{7.80}$$

$$\text{equality at } x_{N-k} = \delta_{N-k}(2i)$$

and

$\delta_{N-k}(2i-1)$ is at the leftmost intersection of

$V_{N-k}(2i:1)$ and $V_{N-k}(2i-1:1)$.

Proof: The proof of this theorem involves an induction on (N-k), starting with k=2. The proof is developed in appendix C.14 □

The remarkable thing about this problem is that the optimal control law and expected cost-to-go at each time $k=k_o,\ldots,N$ (for any finite time horizon problem) can be computed recursively from a (growing) number of difference equations running backwards in time. We need not follow all the flowchart comparisons and tests of section 7.2 for this class of problems. Thus this problem lends itself to detailed analysis and interpretation.

In particular, for this problem we can clearly see what each piece of the controller is trying to accomplish. Refer again to fig. 7.19, where a typical $V_{N-k}(x_{N-k}, r_{N-k}=1)$ is shown. The middlepiece is the lower bound cost associated with not having to hedge-to-a-point, because x_{N-k+1} will be in the p(1,2:x) region that is best according to both the system performance and reliability goals. The endpieces are highest

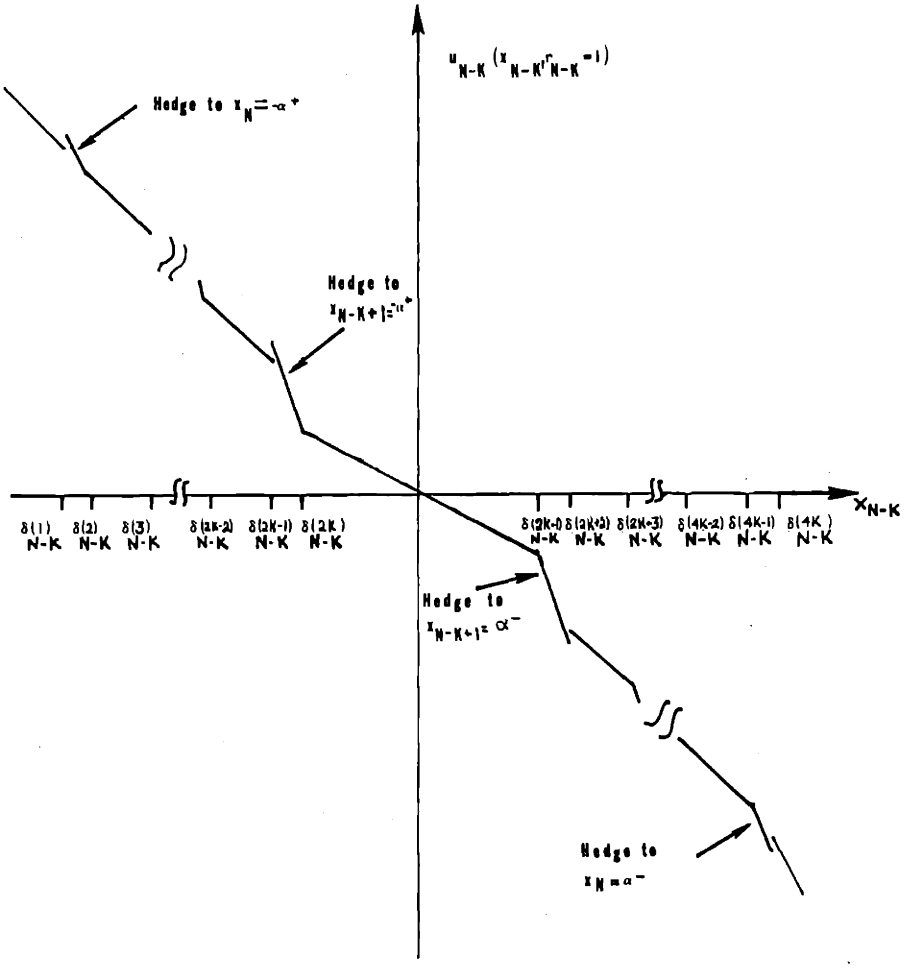

Figure 7.20: Optimal control law $u_{N-k}(x_{N-k}, r_{N-k}=1)$ for the problems of Proposition 7.7.

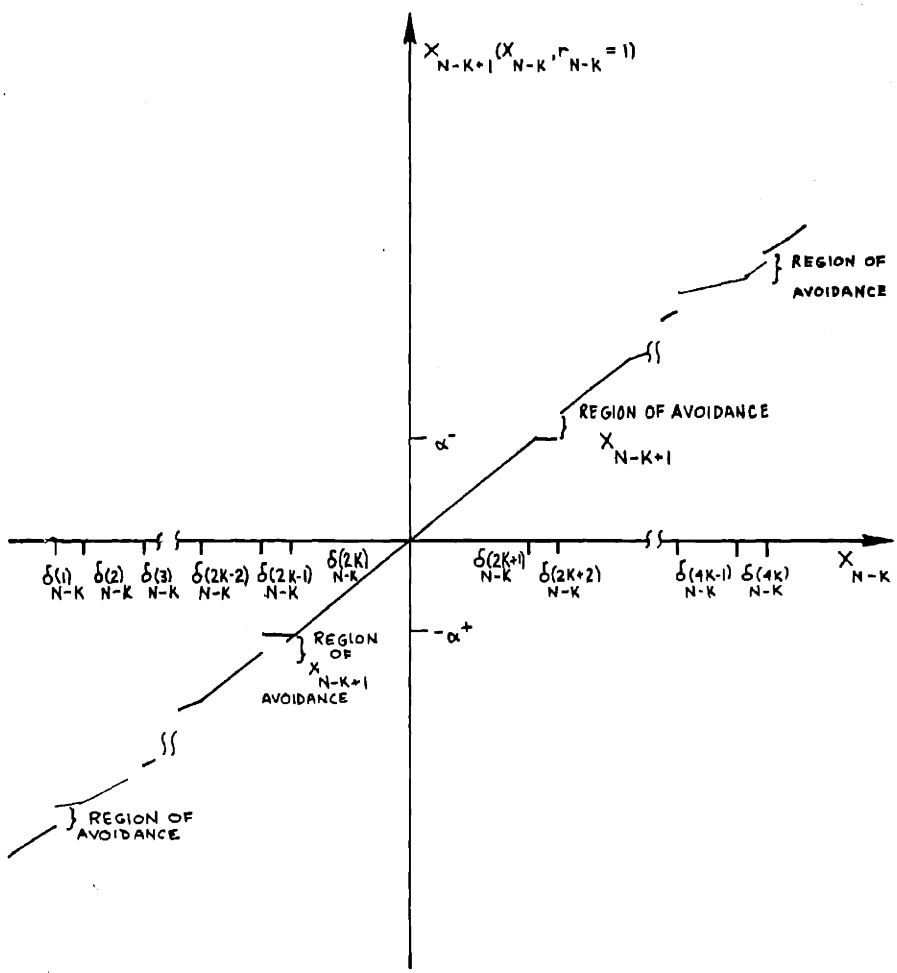

Figure 7.21: Optimal x_{N-k+1} given x_{N-k} and $r_{N-k}=1$ for the problems of Proposition 7.7.

in cost because the controller never drives x into the good p(1,2:x) region. The even-numbered pieces correspond to hedging-to-a-point at successively further times in the future (as we move away from the middle-piece in figure 7.19), with successively higher costs being incurred.

In figure 7.20 the optimal control law $u_{N-k}(x_{N-k}, r_{N-k}=1)$ is shown for these problems. Note that this control law is discontinuous at $\{\delta_{N-k}(1) \mid i=1,3,\ldots,(2k-1)\}$, where $V_{N-k}(x_{N-k}, r_{N-k}=1)$ is not differentiable. In figure 7.21 the optimal mapping from x_{N-k} to x_{N-k+1} (given $r_{N-k}=1$) is graphed. There is a region of avoidance associated with each control law discontinuity. Thus at all times (N-k) we have the type of behavior illustrated at time (N-1) in figures 6.10 - 6.12.

Let us now consider the JLQ optimal controller of Proposition 7.7 as the time horizon (N-k) grows large. From (7.40) we see that the number of pieces of the optimal controller grows without bound as (N-k) goes to infinity. Thus the exact infinite time horizon optimal controller is not obtainable precisely via any finite algorithm.

However, (as we hinted prior to stating Prop. 7.7), as (N-k) grows large, many of the additional controller pieces correspond to hedging very far into the future. As might be expected, the savings obtained p(1,2:x) domain that x is in becomes small as the time when this change is effected becomes distant. As a result, the structure of the optimal effected becomes distant. As a result, the structure of the optimal controller does converge to a steady-state controller which we can approximate with arbitrarily small error by choosing suitably large (N-k).

From (7.57) it is straightforward to show that for any k, the

k time-sequences of odd-indexed cost parameters:

$$\{K_{N-k}(2i-1:1)\}_{k=1}^{N} \qquad (i=1,\ldots,k)$$

are each given by the same recursive difference equation:

- compute $\{K_{N-k}(2i-1:1)\}_{k=1}^{N}$ via (7.55) - (7.56)

  from terminal condition

$$K_{N-i}(2i-1:1) = K_{N-i}^{Le}(1) \qquad (7.81)$$

Only the terminal times and conditions are different in the computation of each of these odd-indexed sequences. At a fixed time (N-k), these k cost parameters

$$\{K_{N-k}(2i-1:1), \quad i=1,\ldots k\}$$

correspond to all of the pieces of $V_{N-k}(x_{N-k}, r_{N-k}=1)$ to the left of the middlepiece where the optimal controller does not hedge-to-a-point with controls $u_{N-k},\ldots,u_{N-1}$. Here i=1 corresponds to the left end-piece $K_{N-k}(1:1)$; i = k corresponds to $x_{N-k+1} < -\alpha$ but all $x_{N-k+2},\ldots x_N$ greater than $-\alpha$; for an arbitrary i = 2,...,k, we have $x_{N-k+1},\ldots,x_{N-i+1}$ all less than $-\alpha$ and $x_{N-i+2},\ldots,x_N$ all greater than $-\alpha$.

We know[1] that $K_{N-k}^{Le}(1)$ increases monotonically to $K_{\infty}^{Le}(1)$ as $(N-k) \to \infty$ and $K_{N-k}(1:2) \to K_{\infty}(1:2)$ is monotonely increasing as well. Thus

$$\lim_{(N-k)\to\infty} K_{N-k}(2i-1:1) = K_{\infty}^{Le}(1) \qquad (7.82)$$

and this convergence is monotone increasing. That is, if one looks at

---

[1] From facts 7.1 - 7.3

a particular odd-indexed cost parameter $K_{N-k}(2i-1:1)$ (for $1 \leq i \leq k$; counting from the left) and lets $(N-k) \to \infty$, then this cost parameter looks increasingly like the limiting left-endpiece cost parameter $K_{\infty}^{Le}(1)$. That is, changing the transition probability piece in the far future looks like never changing at all. This is not suprising when one considers that the range of x values where

$$V_{N-k}(2i-1:1) = x_{N-k}^2 \, K_{N-k}(2i-1:1)$$

is optimal (i.e. the interval $(\delta_{N-k}(2i-2), \delta_{N-k}(2i-1))$) moves further and further leftwards as (N-k) increases.

Similarly, from (7.59) - (7.56) we see that the k time sequences of even-indexed cost parameters:

$$\{K_{N-k}(2i:1)\}_{k=1}^{N} \qquad (i=1,2,\ldots,k)$$

are each given by the same recursive difference equation:

- Compute $\{K_{N-k}(2i:1)\}_{k=i}^{N}$ via

  (7.55) - (7.56) from terminal condition

$$K_{N-i}(2i:1) = \frac{a^2(1)R(1)}{b^2(1)} \quad . \tag{7.83}$$

Only the terminal time is different for each i. At a fixed time (N-k), these k cost parameters $\{K_{N-k}(2i:1) \quad i = 1,\ldots,k\}$ correspond to all of the pieces of $V_{N-k}(x_{N-k}, r_{N-k}=1)$ to the left of $x_{N-k}=0$ from which the optimal controller will hedge-to-a-point at some (single) future time (i.e. with one of the controls $u_{N-k},\ldots,u_{N-1}$). Here i = 1 corresponds to using u_{N-1} to drive x_N to $-\alpha^+$; i=2 corresponds to using

u_{N-2} to drive x_{N-1} to $-\alpha^+$; i=k corresponds to <u>immediate</u> hedging-to-a-point (using u_{N-k} to obtain $x_{N-k+1} = -\alpha^+$).

Thus from facts 7.1 - 7.3

$$\lim_{(N-k)\to\infty} K_{N-k}(2i:1) = K_{\infty}^{Le}(1)$$

as well; however this convergence is monotone <u>decreasing</u>.

It is immediate from (7.65) and (7.66) that

$$\lim_{(N-k)\to\infty} H_{N-k}(2i:1) = 0$$

$$\lim_{(N-k)\to\infty} G_{N-k}(2i:1) = 0$$

for i=1,2,.., . So for <u>all</u> i=1,2,..,

$$\lim_{(N-k)\to\infty} V_{N-k}(i:1) = V_{\infty}^{Le}(1) \quad . \tag{7.84}$$

That is, as (N-k) increases for this problem, the number of pieces in $V_{N-k}(x_{N-k}, r_{N-k})$ increases without bound and, for any fixed i, the function $V_{N-k}(i:1)$ approaches the endpiece function $V_{\infty}^{Le}(1)$ in shape. The odd-indexed pieces $V_{N-k}(i:1)$ (i=1,3,5,...) approach this limit[1] from below (this follows from (7.77)); the even-indexed pieces $V_{N-k}(i:1)$ (i=2,4,6,...) approach it from above.

From parts 2,5 and 6 of Proposition 7.7 and from (7.78) it follows that the width of the switching regions $S_{N-k}^{1,L}$, $S_{N-k}^{1,R}$ (that is, the range of x values where active hedging at some future time is

---

[1] at each x

optimal) increases as (N-k) increases. However (7.84) implies that as (N-k) increases, active hedging in the far future[1] yields decreasing savings in the optimal cost relative to the endpiece cost function[2] $V^{Le}_{N-k}(1)$.

Condition (7.84) does not easily yield any further information about the structure of the infinite time horizon solution, however. In order to obtain further understanding of the infinite time horizon problem it is useful to alter the indexing of the controller pieces. Let us count from the middlepiece outwards instead of from left to right. This indexing will use the notation " < >" . Let

$V_{N-k} < i >$ $\quad$ $H_{N-k} < i >$

$u_{N-k} < i >$ $\quad$ $G_{N-k} < i >$

$K_{N-k} < i >$ $\quad$ $L_{N-k} < i >$

$F_{N-k} < i >$

for $i = -2k, -2k+1, \ldots, -1, 0, 1, 2, \ldots, 2k$.

denote the i^{th} piece to the left of zero if $i < 0$ (and to the right of zero if $i > 0$). Here $i=0$ denotes the middlepiece. Similarly let

$\delta_{N-k} < i >$ $\quad$ $i=-2k,-2k+1,-1,1,2,\ldots,2k$

denote the i^{th} joining point of $V_{N-k}(x_{N-k}, r_{N-k}=1)$ to the left or right of zero.

---

[1] that is, for pieces far from zero.

[2] which is also an upperbound for $V_{N-k}(x_{N-k}, r_{N-k}=1)$ for this problem by Fact 7.3.

Thus the middlepiece at time (N-k) is

$$V_{N-k}\,\langle 0{:}1\rangle \;=\; V^{LM}_{N-k}\,(1) \;=\; V_{N-k}(2k{:}1)$$

and the endpieces are

$$V_{N-k}\,\langle -2k\rangle \;=\; V^{Le}_{N-k}\,(1) \;=\; V_{N-k}(1{:}1)$$

$$V_{N-k}\,\langle 2k\,\rangle \;=\; V^{Re}_{N-k}(1) \;=\; V_{N-k}(4k{+}1{:}1)$$

These two methods of counting the pieces of $V_{N-k}(x_{N-k}, r_{N-k}{=}1)$ are illustrated in Figure 7.22

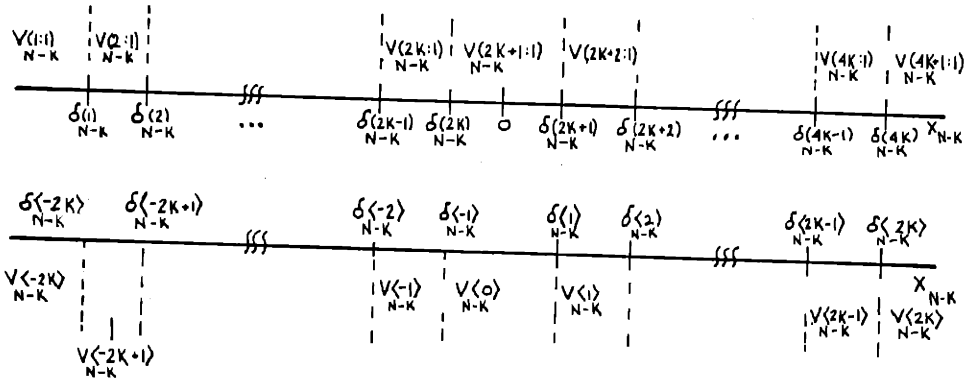

Figure 7.22: Counting $V_{N-k}(x_{N-k}, r_{N-k}=1)$ pieces from the left (as in the top line of the figure) and from the center outwards (as in the bottom line of the figure).

We already know[1] the steady-state behavior of the middlepiece and endpieces. Using the < > notation we can summarize and amplify the discussion above by the following:

Proposition 7.8: For the problem of Proposition 7.7, as $(N-k)\to\infty$ we have:

1. The number of pieces $m_{N-k}(1) = 4k+1$ of the controller becomes countably infinite.

2. In form r=2 the expected cost-to-go converges monotonely as (N-k) increases to $K_\infty(1:2)$ given by (6.98), and $L_{N-k}(1:2)$ converges to

$$L_\infty(1:2) = \frac{b(2)}{a(2)R(2)} K_\infty(1:2)$$

3. The middlepiece functions (of x) for k=1,2,...,N)

$$V_{N-k}\langle 0\rangle = V_{N-k}(2k+1:1)$$

$$u_{N-k}\langle 0\rangle = u_{N-k}(2k+1:1)$$

converge monotonely as $(N-k)\to\infty$ to the steady-state functions

$$V_\infty\langle 0\rangle = V_\infty^{LM}(1) = x^2\, K_\infty\langle 0\rangle$$

$$u_\infty\langle 0\rangle = u_\infty^{LM}(1) = -L_\infty\langle 0\rangle\, x$$

where

$$K_\infty\langle 0\rangle \equiv K_\infty^{LM}(1) = \lim_{(N-k)\to\infty} K_{N-k}\langle 0\rangle \text{ is the}$$

unique positive solution of (6.107):

---

[1] From Propositions 6.2 and 6.4, and (6.106)- (6.107)

$$K_\infty^{<0>} = \frac{\left[-\left\{ \begin{array}{l} R(1)\,[1-a^2(1)\,(1-\omega_1)] \\ + b^2(1)\,[Q(1) + \omega_1 (K_\infty(1:2)+Q(2)-Q(1)) \end{array} \right\} + \sqrt{\left\{ \begin{array}{l} R(1)\,[1-a^2(1)\,(1-\omega_1)] \\ + b^2(1)\,[Q(1) + \omega_1 (K_\infty(1:2) + Q(2) - Q(1))] \end{array} \right\}^2 + 4a^2(1)\, R(1)\, b^2(1)\,(1-\omega_1) \left[\begin{array}{l} Q(1) \\ + \\ \omega_1 \left(\begin{array}{l} K_\infty(1:2) \\ + Q(2) - Q(1) \end{array} \right) \end{array} \right]} \right]}{2\, b^2(1)\,(1-\omega_1)} \qquad (7.85)$$

and

$L_\infty^{<0>} \equiv L^{LM}(1) = \lim_{(N-k)\to\infty} L_{N-k}^{<0>}$ is given by

$$L_\infty^{<0>} = \frac{b(1)}{a(1)\, R(1)}\, K_\infty^{<0>} \quad .$$

4. The endpiece functions (of x) for k=1,2,...,N

$$V_{N-k}^{<-2k>} = V_{N-k}^{Le}(1) = V_{N-k}(1:1)$$

$$V_{N-k}^{<2k>} = V_{N-k}^{Re}(1) = V_{N-k}(4k+1:1)$$

$$u_{N-k}^{<-2k>} = u_{N-k}^{Le}(1) = u_{N-k}(1:1)$$

$$u_{N-k}^{<2k>} = u_{N-1}^{Re}(1) = u_{N-k}(4k+1:1)$$

converge monotonely as $(N-k)\to\infty$ to the steady-state

functions

$$V_{\infty}^{Le}(1) \equiv V_{\infty}^{Re}(1) = x^2 K_{\infty}^{Le}(1)$$

$$u_{\infty}^{Le}(1) \equiv u_{\infty}^{Re}(1) = -L_{\infty}^{Le}(1)x$$

where

$$K_{\infty}^{Le}(1) = \lim_{(N-k)\to\infty} K_{N-k}<-(N-k)> = \lim_{(N-k)\to\infty} K_{N-k}(1)$$

is the unique solution of (6.106):

$$K_{\infty}^{Le}(1) = \frac{\left[-\left\{ \begin{matrix} R(1)[1-a^2(1)(1-\omega_2)] \\ + b^2(1) \left[\dfrac{Q(1)}{\omega_2(K_{\infty}(1:2) + Q(2) - Q(1))} \right] \end{matrix} \right\} + \sqrt{\left\{ \begin{matrix} R(1)[1-a^2(1)(1-\omega_2)] \\ + b^2(1) \\ [Q(1) + \omega_2(K_{\infty}(1:2) + Q(2) - Q(1))] \end{matrix} \right\}^2 + 4a^2(1)R(1)b^2(1)(1-\omega_2) \left[\dfrac{Q(1)}{\omega_2(K_{\infty}(1:2) + Q(2) - Q(1))} \right]} \right]}{2b^2(1)(1-\omega_2)}$$

and

$$L_{\infty}^{Le} = \lim_{(N-k)\to\infty} L_{N-k}<-(N-k)> = \lim_{(N-k)\to\infty} K_{N-k}(1) \qquad (7.86)$$

is given by

$$L_{\infty}^{Le} = \frac{b(1)}{a(1)\ R(1)} K_{\infty}^{Le} \quad .$$

5. The functions

$$V_{N-k}^{<\pm 2i>} = x_{N-k}^2 K_{N-k}^{<\pm 2i>}$$

$$u_{N-k}^{<\pm 2i>} = -L_{N-k}^{<\pm 2i>} x_{N-k}$$

(for $i=1,2,\ldots,k$ and $k=1,2,\ldots,N$)

converge monotonely to $(N-k)\to\infty$ to the functions (of x)

$$V_\infty^{<\pm 2i>} = x^2 K_\infty^{<\pm 2i>}$$

$$u_\infty^{<\pm 2i>} = -L_\infty^{<\pm 2i>} x$$

for $i=1,2,3,\ldots$ where

$$K_\infty^{<\pm 2i>} = \frac{a^2(1)R(1)[(1-\omega_2)(K_\infty^{<-2(i-1)>}+Q(1)) + \omega_2(Q(2)+K_\infty(1:2))]}{R(1)+b^2(1)](1-\omega_2)(K_\infty^{<-2(i-1)>} + Q(1)) + \omega_2(Q(2)+K_\infty(1:2))]} \qquad (7.87)$$

and

$$L_\infty^{<-2i>} = \frac{b(1)}{a(1)R(1)} K_\infty^{<-2i>} = -L_\infty^{<2i>} \quad .$$

These pieces of the limiting controller correspond to <u>never</u> hedging-to-a-point. For $V_\infty^{<\pm 2i>}$, the x process stays outside of the advantageous p(1,2:x) piece $(-\alpha,\alpha)$ until i time steps in the future, after which it stays inside $(-\alpha,\alpha)$ forever.

6. The functions (for $k=1,2,\ldots,N$)

$$V_{N-k}^{<\pm 1>} = x_{N-k}^2 K_{N-k}^{<\pm 1>} + H_{N-k}^{<\pm 1>} x_{N-k} + G_{N-k}^{<\pm 1>}$$

converge monotonely as $(N-k)\to\infty$ to the functions (of x)

$$V_\infty\langle -1\rangle = x^2 K_\infty\langle \pm 1\rangle + H_\infty\langle \pm 1\rangle\, x + G_\infty\langle \pm 1\rangle$$

where

$$K_\infty\langle \pm 1\rangle \equiv K_{N-k}\langle \pm 1\rangle = \frac{a^2(1)R(1)}{b^2(1)} \tag{7.88}$$

$$H_\infty\langle -1\rangle \equiv H_{N-k}\langle -1\rangle = 2a(1)R(1)\alpha/b^2(1) \equiv -H_\infty\langle +1\rangle \tag{7.89}$$

$$G_\infty\langle \pm 1\rangle = \lim_{(N-k)\to\infty} G_{N-k}\langle \pm 1\rangle = \frac{\alpha^2}{b^2(1)}\left[R(1)+b^2(1)\left(\begin{array}{l}(1-\omega_1)(K_\infty\langle 0\rangle+Q(1))\\ +\omega_1(K_\infty(1{:}2)+Q(2))\end{array}\right)\right] \tag{7.90}$$

and the functions

$$u_\infty\langle \pm 1\rangle = -L_\infty\langle \pm 1\rangle\, x + F_\infty\langle \pm 1\rangle$$

at all k, where

$$L_\infty\langle -1\rangle \equiv L_{N-k}(2k{:}1) = a(1)/b(1) = -L_\infty\langle 1\rangle \tag{7.91}$$

$$F_\infty\langle \pm 1\rangle \quad F_{N-k}(2k{:}1) = -\alpha/b(1) \tag{7.92}$$

These pieces of the limiting controller correspond to hedging to-a-point <u>immediately</u> (using the very next control input).

7. For $k=2,\ldots,N$ and for each fixed $i\in\{1,\ldots,k-1\}$

$$V_{N-k}\langle \pm(2i+1)\rangle = x^2_{N-k}\langle (2i+1)\rangle + H_{N-k}\langle \pm(2i+1)\rangle\, x_{N-k} + G_{N-k}\langle \pm(2i+1)\rangle$$

and

$$u_{N-k}\langle \pm(2i+1)\rangle = -L_{N-k}\langle \pm(2i+1)\rangle\, x_{N-k} + F_{N-k}\langle \pm(2i+1)\rangle$$

converge monotonely as $(N-k)\to\infty$ to the functions (of x)

$$V_\infty\langle\pm(2i+1)\rangle = x^2\, K_\infty\langle\pm(2i+1)\rangle + H_\infty\langle\pm(2i+1)\rangle\, x + G_\infty\langle\pm(2i+1)\rangle$$

$$u_\infty\langle\pm(2i+1)\rangle = -L_\infty\langle\pm(2i+1)\rangle + F_\infty\langle\pm(2i+1)\rangle$$

where

$$K_\infty\langle\pm(2i+1)\rangle = \frac{a^2(1)R(1)\left[(1-\omega_2)\begin{pmatrix}K_\infty\langle\pm(2i-1)+1\rangle\\ +Q(1)\end{pmatrix} + \omega_2\begin{pmatrix}Q(2)\\ K_\infty(1:2)\end{pmatrix}\right]}{R(1) + b^2(1)\left[(1-\omega_2)\begin{pmatrix}K_\infty\langle\pm(2i-1)+1\rangle\\ +Q(1)\end{pmatrix} + \omega_2\begin{pmatrix}Q(2)\\ +\\ K_\infty(1:2)\end{pmatrix}\right]} \tag{7.93}$$

$$L_\infty\langle-(2i+1)\rangle = \frac{b(1)}{a(1)R(1)}\, K_\infty\langle-2i-1\rangle = -L_\infty\langle 2i+1\rangle \tag{7.94}$$

$$-H_\infty\langle 2i+1\rangle = H_\infty\langle-(2i+1)\rangle = \frac{a(1)R(1)(1-\omega_2)\, H_\infty\langle-2(i-1)-1\rangle}{R(1)+b^2(1)(1-\omega_2)\left[\begin{pmatrix}K_\infty\langle-2(i-1)-1\rangle\\ +Q(1)\end{pmatrix} + \omega_2\begin{pmatrix}Q(2)\\ +\\ K_\infty(1:2)\end{pmatrix}\right]} \tag{7.95}$$

$$F_\infty\langle\pm(2i+1)\rangle = \frac{-b(1)}{2a(1)R(1)}\, H_\infty\langle-(2i+1)\rangle = -F_\infty\langle 2i+1\rangle \tag{7.96}$$

$$G_\infty\langle\pm)2i+1)\rangle = (1-\omega_2)\, G_\infty\langle\pm(2i-1)+1)\rangle$$

$$\frac{-b^2(1)(1-\omega_2)^2(H_\infty\langle\pm(2(i-1)\rangle)^2}{4\left[R(1) + b^2(1)\left[(K_\infty\langle\pm(2(i-1)+1)\rangle)(1-\omega_2)+\omega_2\begin{pmatrix}Q(1)\\ +\\ K_\infty(1:2)\end{pmatrix}\right]\right]} \tag{7.97}$$

These pieces of the limiting controller correspond to hedging-to-a-point using the i^{th} control after the one that is immediately applied. That is, they correspond to hedging-to-a-point i time steps in the future.

8. As $(N-k)\to\infty$ the joining point

$$\delta_{N-k}\langle -1\rangle = \delta_{N-k}(2k) \quad \text{converges monotonely to}$$

$$\delta_{\infty}\langle -1\rangle = \lim_{N-k)\to\infty} \delta_{N-k}\langle -1\rangle = \frac{-\alpha}{a(1)}\left(1 + \frac{b^2(1)}{R(1)}\begin{bmatrix}(1-\omega_1)\begin{pmatrix}K_{\infty}\langle 0\rangle \\ + Q(1)\end{pmatrix} \\ +\omega_1(K_{\infty}(1{:}2)+Q(2))\end{bmatrix}\right) \tag{7.98}$$

and $\delta_{N-k}\langle +1\rangle \to \delta_{\infty}\langle +1\rangle = -\delta_{\infty}\langle -1\rangle$.

9. For $k=2,3,\ldots,N$ and each fixed $i\in\{1,\ldots,k-1\}$, the joining points

$\delta_{N-k}\langle -(2i+1)\rangle$ converge monotonely as $(N-k)\to\infty$ to

$$\delta_{\infty}\langle -(2i+1)\rangle = \frac{\delta_{\infty}\langle -(2(i-1)+1)\rangle}{a(1)}\left[1 + \frac{b^2(1)}{R(1)}\left[\begin{bmatrix}(1-\omega_2)\begin{pmatrix}K_{\infty}\langle -(2(i-1)+1)\rangle \\ + Q(1)\end{pmatrix} \\ +\omega_2(K_{\infty}(1{:}2) + Q(2))\end{bmatrix}\right]\right] \tag{7.99}$$

and $\delta_{N-k}\langle +(2i+1)\rangle \to \delta_{\infty}\langle 2i+1)\rangle = -\delta_{\infty}\langle -\langle 2i+1\rangle\rangle$.

10. For $k=1,2,\ldots,N$ and each fixed $i \in \{1,\ldots,k\}$,

$$\delta_{N-k}^{<-2i>} \quad \text{converges to}$$

$$\delta_{\infty}^{<-2i>} = \frac{-H_{\infty}^{<-2i+1>} - \sqrt{H_{\infty}^{<2i+1>)^2} - 4[K_{\infty}^{<-2i+1>} - K_{\infty}^{<-2i>}]\, G_{\infty}^{<-2i+1>}}}{2[K_{\infty}^{<-2i+1>} - K_{\infty}^{<-2i>}]} \tag{7.100}$$

and $\delta_{N-k}^{<+2i>} \to \delta_{\infty}^{<2i>} = -\delta_{\infty}^{<-2i>}$.

11. For the limiting problem solution parameters, as $(N-k)\to\infty$ the following relationships hold:

$$\text{(i)} \quad K_{\infty}^{<0>} < K_{\infty}^{<2>} < K_{\infty}^{<4>} < \ldots \leq K_{\infty}^{Le}(1) \tag{7.101}$$

$$\text{(ii)} \quad K_{\infty}^{<-1>} > K_{\infty}^{<-3>} > {}_{\infty}^{<-5>} > \ldots \geq K_{\infty}^{Le}(1) \tag{7.102}$$

$$\text{(iii)} \quad \delta_{\infty}^{<-2i-1>} < \delta_{\infty}^{<-2i>} < \delta_{\infty}^{<-2i+1>} \tag{7.103}$$

hence

$$\delta_{\infty}^{<2i+1>} - \delta_{\infty}^{<2i-1>} > 0$$

$$\delta_{\infty}^{<-2i+1>} - \delta_{\infty}^{<-2i-1>} > 0 \tag{7.104}$$

□

The proof of this proposition follows directly from Proposition 7.7. and our previous discussion. Proposition 7.8 says that as the time horizon becomes infinite, the number of pieces in the optimal controller also becomes infinite but that each piece (counting from the center out) converges to a constant steady state function that is optimal over a constant steady-state interval of x values. From (7.104) we see that the width of the switching regions will grow without bound as (N-k) increases.

From Prop. 7.8 it is clear that we cannot implement precisely a steady-state JLQ controller for the infinite time horizon problem using a finite algorithm, because there are infinitely many controller pieces. However the convergence of cost pieces to $V_{\infty}^{Le}(1)$ in (7.84) suggests a natural approximation of the steady-state controller. The idea is to use, at each time (N-k), the true optimal controller for a certain number of pieces around zero, and approximate the rest of $V_{N-k}(x_{N-k}, r_{N-k}=1)$ by the endpiece functions. As we will discuss in section 7.7, this allows us to approximate $V_{N-k}(x_{N-k}, r_{N-k}=1)$ arbitrarily well, and to relate the "complexity" of the controller (in terms of the number of pieces to be solved for and

implemented) to the approximation error. This approximate controller is essentially a finite look-ahead scheme; the option of active hedging is considered only for a finite number of future times. In section 7.7 a finite look-ahead approximation of the optimal JLQ controller is developed for the general class of problems of chapter 5.

In this section we have examined the structure of the optimal JLQ controller for a class of problems having commensurate reliability and performance goals. This class of problems has a solution structure that is particularly amenable to detailed analysis. Its solution illustrates the way the optimal controller uses active hedging to achieve fault tolerance in this commensurate goals case. In the next section we will consider the solution of an illustrative class of problems with conflicting performance and reliability goals.

7.6 Active Hedging When Reliability and Performance Goals are Conflicting

In this section we consider an example class of systems that illustrate how the optimal JLQ controller uses active hedging to achieve fault-tolerance when the system performance and reliability goals are conflicting.

We will examine here the "case 2" single form-transition problem of section 7.4, as (N-k) increases. Under certain additional parametric conditions (that are derived here) the optimal JLQ controller at all times $k = N, N-1, \ldots, k_o$ can be specified by recursive difference equations.

We will develop for this conflicting goals example results analogous to those of the previous section for a commensurate goals example. We are considering the scalar, single form-transition problem (7.2) - (7.5) where Facts 7.1, 7.2 and 7.3(2) hold. That is, we have

$$\omega_1 > \omega_2 \tag{7.105}$$

and figs. 7.9(b,c)[1] and 7.13(b) apply. We will also assume that (7.14) holds:

$$a(1) < \left(1 + \frac{b^2(1)}{R(1)} \hat{K}_N(2)\right)\left(1 - \sqrt{1 - \frac{R(1) + b^2(1)\,\hat{K}_N(1)}{R(1) + b^2(1)\,\hat{K}_N(2)}}\right), \tag{7.14}$$

Thus $\pm\alpha$ are the grid points of the x_{N-1} composite partition that are closest to zero. Note that when (7.10) holds (i.e., there are local minima in $V_{N-1}(x_{N-1}, r_{N-1}=1)$), then (7.14) holds for all[2] $a(1) < 1$.

---

[1] depending on whether (7.10) holds or not,

[2] see comments following (7.10).

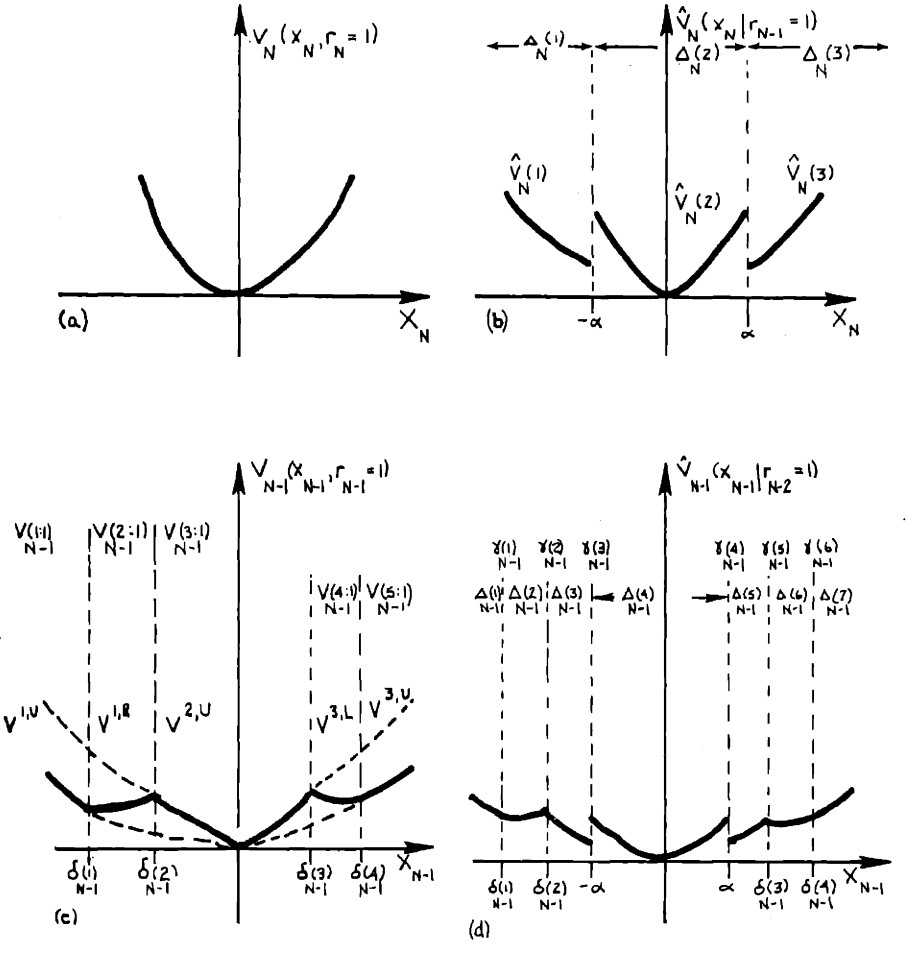

Figure 7.23: Curves for Case 2 Single Form-Transition Problem where Facts 7.1, 7.2 and 7.3 (2) hold: (a) $V_N(x_N, r_N=1)$, (b) $\hat{V}_N(x_N | r_{N-1}=1)$, (c) $V_{N-1}(x_{N-1}, r_{N-1}=1)$ and (d) $\hat{V}_{N-1}(x_{N-1} | r_{N-2}=1)$ when (7.14) holds.

In figure 7.23 we collect[1] for convenience the curves of $V_N(x_N, r_N=1)$, $\hat{V}_N(x_N|r_{N-1}=1)$, $V_{N-1}(x_{N-1}, r_{N-1}=1)$ and $\hat{V}_{N-1}(x_{N-1}|r_{N-2}=1)$ for this problem.

For this problem we have[2] that the endpieces of $V_k(x_k, r_k=1)$ coincide with the lower bound function $V_K^{LB}(1)$ and the middlepiece coincides with the upper bound (the opposite of section 7.5). The performance and reliability goals of the optimal controller conflict because driving x near zero (to the perfomance goal) necessitates driving x inside the region $(-\alpha, \alpha)$ where the probability of failure is high. Thus near zero, $V_k(x_k, r_k=1)$ reaches its upper bound cost. Far from zero, $V_k(x_k, r_k=1)$ approaches its lower bound because the risk of failure[3] (which, by Fact 7.1, is costly) is kept small.

Let us consider now the candidate cost-to-go functions that are eligible for $V_{N-2}(x_{N-2}, r_{N-2}=1)$. In Figure 7.24 we show the candidate functions (of x_{N-2}) $V_{N-2}^{i,U}$ (for i=1,2,...,7) for this problem?[4] These functions of x_{N-2} coincide with solutions of

$$\min_{u_{N-2}} \left\{ V_{N-2}(x_{N-2}, r_{N-2}=1) \right\}$$

s.t.

$$x_{N-1} \in \Delta_{N-1}(i) = (\gamma_{N-1}(i-1), \gamma_{N-1}(i))$$

for those x_{N-2} values where the resulting x_{N-1} is in the interior of $\Delta_{N-1}(i)$.

---

[1] As derived in Chapter 6 and sections 7.1 - 7.4

[2] By Facts 7.1 - 7.3

[3] That is, entering form r=2

[4] Fig. 7.24 corresponds with fig. 7.15 in the previous section.

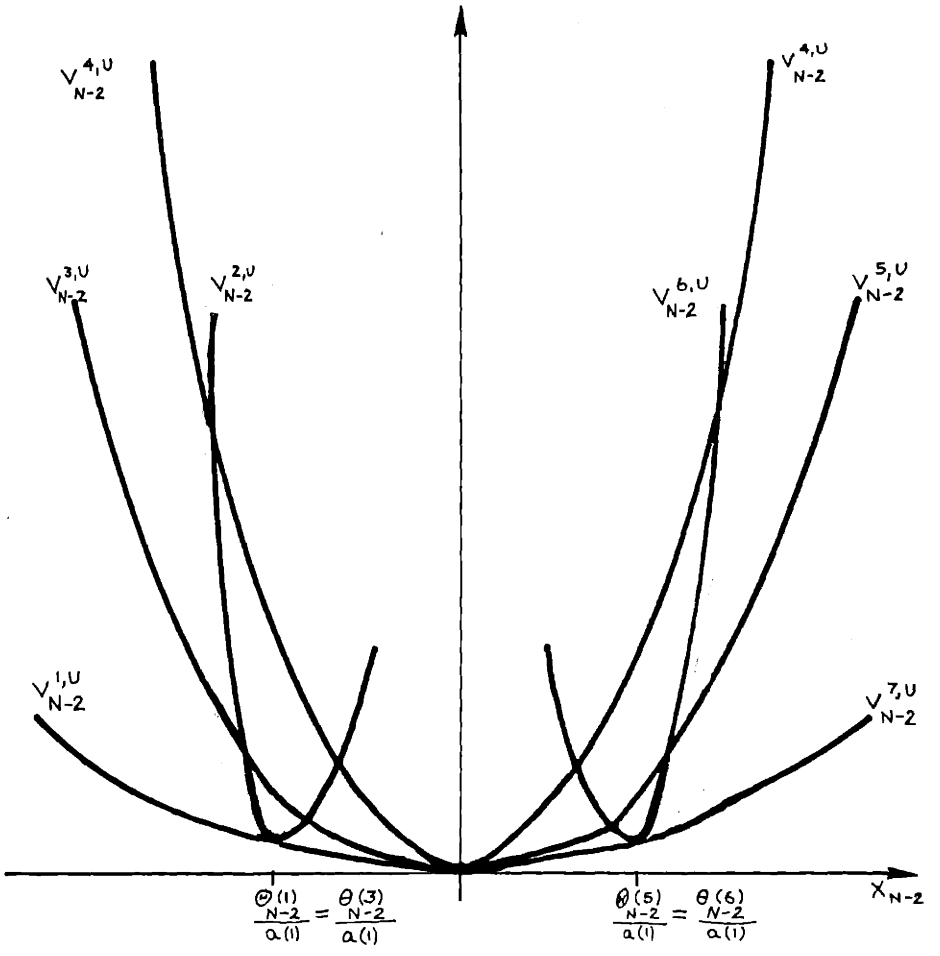

Figure 7.24: The candidate cost-to-go functions $V_{N-2}^{i,U}$ $(i=1,\ldots,7)$.

The following relationships that are pictured in Figure 7.24 are verified in Appendix C.15:

$$V_{N-2}^{1,U} \equiv V_{N-2}^{7,U} < V_{N-2}^{3,U} \equiv V_{N-2}^{5,U} < V_{N-2}^{4,U} \quad \text{at all } x_{N-2} \tag{7.106}$$

$$V_{N-2}^{2,U} > V_{N-2}^{1,U} \quad \text{for all } x_{N-2} \text{ except equality at } x_{N-2} = \theta_{N-2}^{(2)} \Big/ a(1) \tag{7.107}$$

$$V_{N-2}^{6,U} > V_{N-2}^{7,U} \quad \text{for all } x_{N-2} \text{ except equality at } x_{N-2} = \theta_{N-2}^{(7)} \Big/ a(1) \bullet \tag{7.108}$$

In addition to the seven candidate cost functions that are shown in Figure 7.24, there are two other condidate functions that are eligible for $V_{N-2}(x_{N-2}, r_{N-2}=1)$, according to Proposition 5.2.

The functions are

$V_{N-2}^{3,R}(x_{N-2}, r_{N-2}=1)$ driving x_{N-1} to $-\alpha^-$ (right boundary of $\Delta_{N-1}(3)$)

$V_{N-2}^{5,L}(x_{N-2}, r_{N-2}=1)$ driving x_{N-1} to $\alpha+$ (left boundary of $\Delta_{N-1}(5)$) •

These costs result from driving x_{N-1} to the <u>lower cost</u> side of a $\hat{V}_{N-1}(x_{N-1} | r_{N-2}=1)$ discontinuity. The parameters for $V_{N-2}^{3,R}$ and $V_{N-2}^{5,L}$ are listed in Appendix C.15.

We note that, by definition:

$$V_{N-2}^{3,R} > V_{N-2}^{3,U} \quad \text{except equality at } x_{N-2} = \Theta_{N-2}(3) \Big/ a(1) \tag{7.109}$$

$$V_{N-2}^{5,L} > V_{N-2}^{5,U} \quad \text{except equality at } x_{N-2} = \theta_{N-2}^{(5)} \Big/ a(1) \bullet \tag{7.110}$$

If we superimpose the curves of $V_{N-2}^{3,R}$ and $V_{N-2}^{5,L}$ on Figure 7.24 and compare the regions of x_{N-2} validity of each curve, we can obtain (as in Section 7.2) the optimal expected cost-to-go, $V_{N-2}(x_{N-2},r_{N-2}=1)$, at each value of x_{N-2}. However $V_{N-2}^{3,R}$ and $V_{N-2}^{5,L}$ can be in three different graphical positions relative to the $V_{N-2}^{i,u}$ (i=1,...,7) of Figure 7.24, depending upon the values of problem parameters. We will examine each of these three possibilities in turn.

We first refer to Figure 7.24. The functions $V_{N-2}^{1,U}$ and $V_{N-2}^{7,U}$ are (by Fact 7.3) lower bounds on $V_{N-2}(x_{N-2},r_{N-2}=1)$. Therefore they will be optimal over their entire domains of validity. That is,

$$V_{N-2}(x_{N-2},r_{N-2}=1) = V_{N-2}^{1,U} \quad \text{for } x_{N-2} < \Theta_{N-2}(1)/a(1) \tag{7.111}$$

$$V_{N-2}(x_{N-2},r_{N-2}=1) = V_{N-2}^{7,U} \quad \text{for } x_{N-2} > \Theta_{N-2}(7)/a(1) \ . \tag{7.112}$$

To the <u>right</u> of $x_{N-2} = \Theta_{N-2}(1)/a(1)$, the candidate cost $V_{N-2}^{2,U}$ will be optimal until, at some $x_{N-2} > \Theta_{N-2}(1)/a(1)$, $V_{N-2}^{2,U}$ intersects another valid eligible candidate cost. To the <u>left</u> of $\Theta_{N-2}(7)/a(1)$, $V_{N-2}^{6,U}$ will be optimal until, at some $x_{N-2} < \Theta_{N-2}(7)/a(1)$, $V_{N-2}^{6,U}$ intersects another valid eligible candidate cost. We know from Proposition 5.3 that the optimal controller mapping

$$x_{N-2} \longrightarrow \bar{x}_{N-1}(x_{N-2},r_{N-2}=1)$$

must be monotone. We also know (from Proposition 5.1) that $V_{N-2}(x_{N-2},r_{N-2}=1)$ is continuous in x_{N-2}. Thus we are left with the following question:

How does $V_{N-2}(x_{N-2}, r_{N-2}=1)$ get from the $V_{N-2}^{2,U}$ curve to $V_{N-2}^{4,U}$ and then from the $V_{N-2}^{4,U}$ curve to $V_{N-2}^{6,U}$ while satisfying the monotonicity and continuity requirements mentioned above? The three ways to superimpose $V_{N-2}^{3,R}$ and $V_{N-2}^{5,L}$ on Figure 7.24 each correspond to a different answer to this question. They are illustrated in Figure 7.25 - 7.27. We will examine each possibility in turn.

The first possibility (shown in Figure 7.25) results in $V_{N-2}(x_{N-2}, r_{N-2}=1)$ having (the maximum allowable number) $m_{N-2}(1) = 9$ pieces. Each piece corresponds to a different active hedging strategy using u_{N-2} and u_{N-1}. This case is analogous to Figure 7.16 for the commensurate goals problem of the previous section. The switching regions ($x_{N-2} \in S_{N-2}^{1,L}$ and $x_{N-2} \in S_{N-2}^{1,R}$) are divided into three parts:

- for $x_{N-2} \in (\delta_{N-2}(3), \delta_{N-2}(4))$ and $(\delta_{N-2}(5), \delta_{N-2}(6))$ the optimal controller uses u_{N-2} to <u>immediately</u> hedge-to-a-point (to $x_{N-1} = -\alpha^-$ or $x_{N-1} = \alpha^+$). This keeps the probability of failure at time N-1 (i.e., the probability that $r_{N-1} = 2$) <u>low</u>. Then u_{N-1} is used to drive x_N into the high risk piece $(-\alpha, \alpha)$ of $p(1,2:k)$. This increased risk at time N is compensated for by making x_N near zero, so that the performance ost

  $$x_N^2 \, [Q(r_N) + K_T(r_N)]$$

  is small for both $r_N = 1$ and $r_N = 2$.

- for $x_{N-2} \in (\delta_{N-2}(2), \delta_{N-2}(3))$ and $(\delta_{N-2}(6), \delta_{N-2}(7))$ the optimal controller keeps $|x_{N-1}| > \alpha$ <u>without</u> hedging-to-a-point with u_{N-2}. Then u_{N-1} is used to make $|x_N| < \alpha$ <u>without</u> hedging-to-a-point.

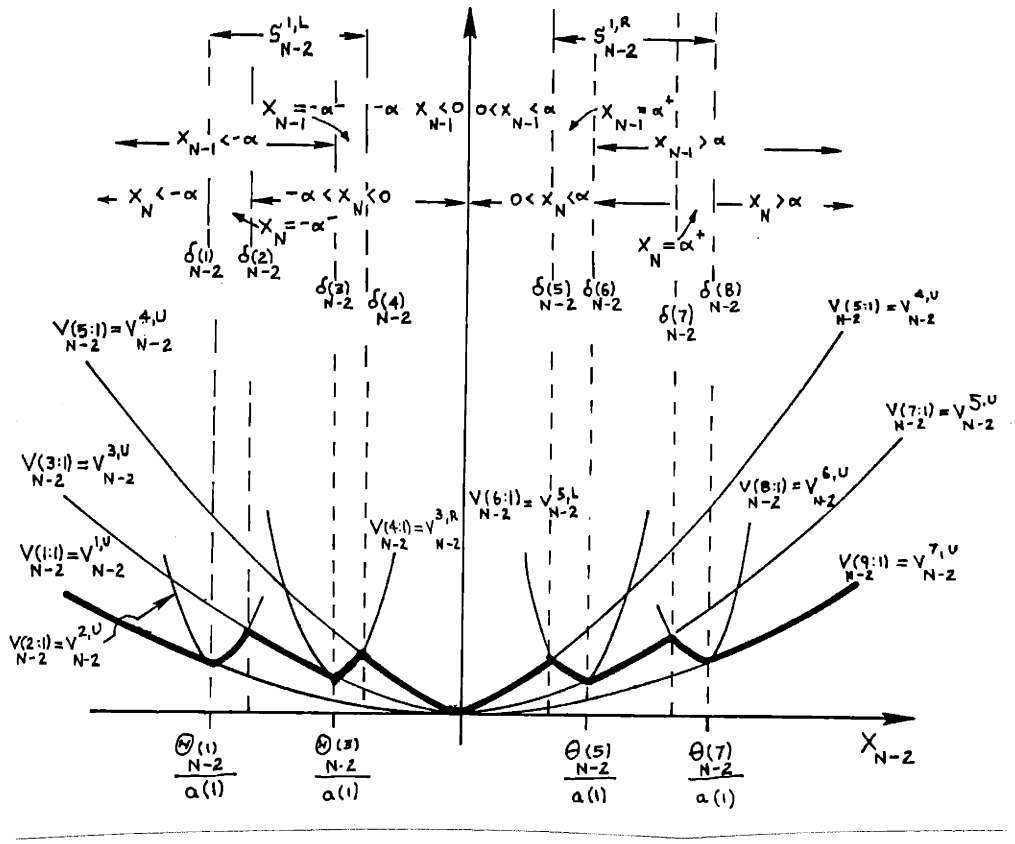

Figure 7.25: $V_{N-2}(x_{N-2}, r_{N-2}=1)$ in the first situation. The optimal is indicated by the heavier line. The resulting optimal values of x_N and x_{N-1} for each of the 9 pieces of $V_{N-2}(x_{N-2}, r_{N-2}=1)$ are also labelled.

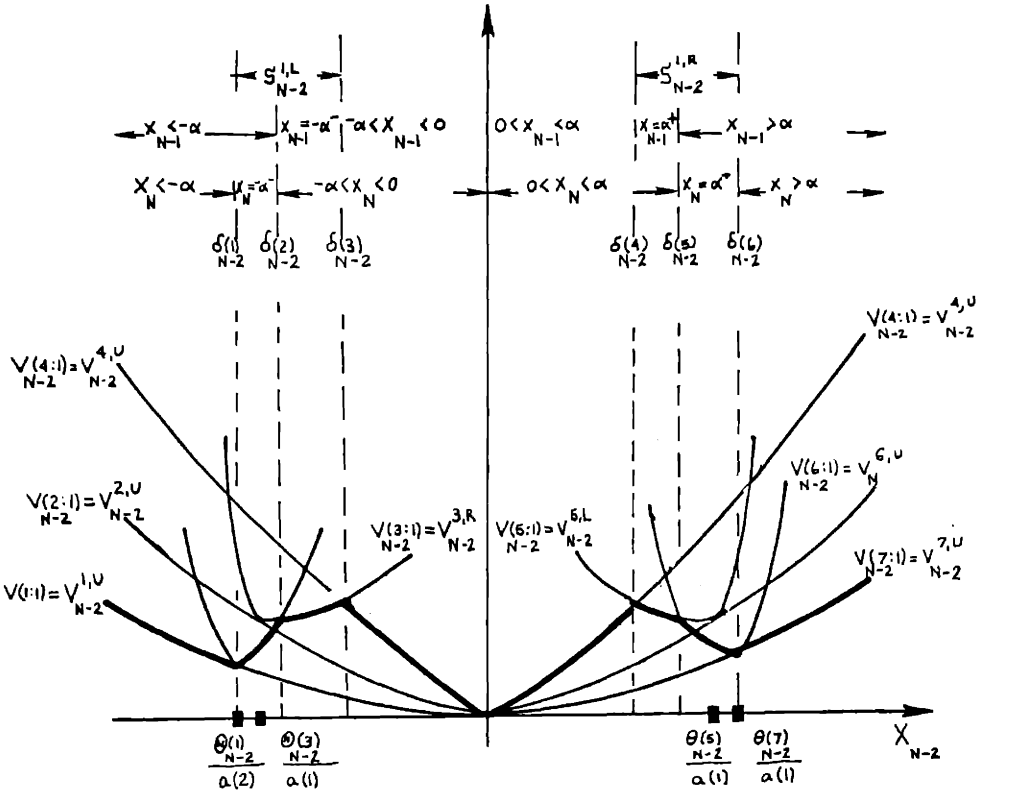

Figure 7.26: $V_{N-2}(x_{N-2}, r_{N-2}=1)$ in the second situation. The optimal is indicated by the heavier line. The resulting optimal values of x_N and x_{N-1} for each of the 7 pieces of $V_{N-2}(x_{N-2}, r_{N-2}=1)$ are also labelled.

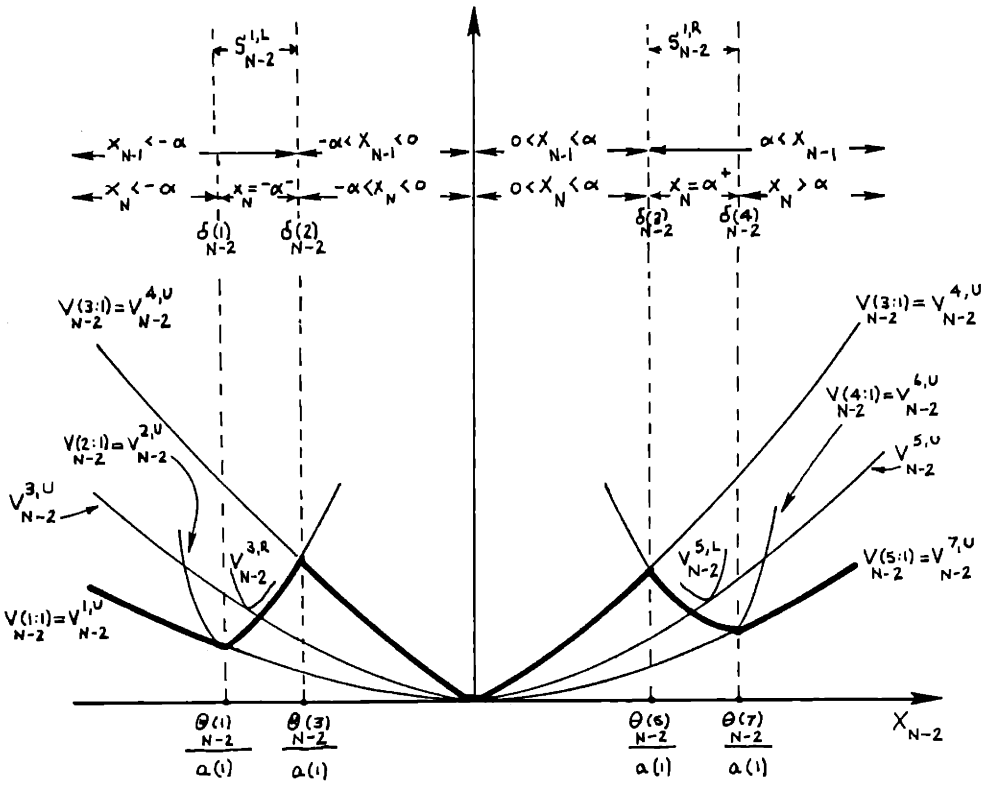

Figure 7.27: $V_{N-2}(x_{N-2}, r_{N-2}=1)$ in the third situation. The optimal cost is indicated by the heavier line. The resulting optimal values of x_N and x_{N-1} for each of the 5 pieces of $V_{N-2}(x_{N-2}, r_{N-2}=1)$ are also labelled.

	Situation 1 (Fig. 7.25)	Situation 2 (Fig.7.26)	Situation 3 (Fig.7.27)
Number of pieces of $V_{N-2}(x_{N-2}, r_{N-2}=1)$ and $u_{N-2}(x_{N-2}, r_{N-2}-1) = m_{N-2}(1)$	9 (maximum possible)	7	5
Endpiece functions	$V_{N-2}(1:1)$ $V_{N-2}(9:1)$	$V_{N-2}(1:1)$ $V_{N-2}(7:1)$	$V_{N-2}(1:1)$ $V_{N-2}(5:1)$
Middlepiece function	$V_{N-2}(5:1)$	$V_{N-2}(4:1)$	$V_{N-2}(3:1)$
Other pieces that do not involve hedging-to-$-\alpha^-$ or α^+	$V_{N-2}(3:1)$ $V_{N-2}(7:1)$	-	-
Pieces involving hedging-to-a-point with u_{N-2}	$V_{N-2}(4:1)$ $V_{N-2}(6:1)$	$V_{N-2}(3:1)$ $V_{N-2}(5:1)$	-
Pieces involving hedging-to-a-point with u_{N-1} (but not with u_{N-2})	$V_{N-2}(2:1)$ $V_{N-2}(8:1)$	$V_{N-2}(2:1)$ $V_{N-2}(6:1)$	$V_{N-2}(2:1)$ $V_{N-2}(4:1)$

TABLE 7.4: Comparison of Three Possible Situations for $V_{N-2}(x_{N-2}, r_{N-2}=1)$

- for $x_{N-2} \in (\delta_{N-2}(1), \delta_{N-2}(2))$ and $(\delta_{N-2}(7), \delta_{N-2}(8))$ the optimal controller keeps $|x_{N-1}| > \alpha$ without hedging-to-a-point with u_{N-2}. Then u_{N-1} is used to hedge-to-a-point (to $x_N = -\alpha^-$ or $x_N = \alpha^+$). That is, for these x_{N-2} values the optimal controller does not let x_N enter the high risk piece $(-\alpha,\alpha)$ of $p(1,2:x)$. It is better at time N to stay on the low failure probability sides of the $p(1,2:k)$ discontinuities.

The second possibility (shown in Figure 7.26) results in $V_{N-2}(x_{N-2}, r_{N-2}=1)$ having $m_{N-2}(1) = 7$ pieces. Unlike the first situation of Figure 7.25, there are <u>no</u> x_{N-2} values from which the optimal controller causes x_{N-1} and x_N to be in different $p(1,2:x)$ pieces <u>without</u> using hedging-to-a-point. Here the switching regions ($S_{N-2}^{1,L}$ and $S_{N-2}^{1,R}$) of x_{N-2} values are each divided into two parts:

- for $x_{N-2} \in (\delta_{N-2}(2), \delta_{N-2}(3))$ and $(\delta_{N-2}(4), \delta_{N-2}(5))$ the optimal controller uses u_{N-2} to keep x_{N-1} on the low probability side of the $p(i,2:x)$ discontinuity. That is, u_{N-2} is used to hedge-to-a-point $x_{N-1} = -\alpha^-$ or $x_{N-1} = \alpha^+$. Then u_{N-1} keeps x_N inside $(-\alpha,\alpha)$, making x_N^2 small,

- for $x_{N-2} \in (\delta_{N-2}(1), \delta_{N-2}(2))$ and $(\delta_{N-2}(5), \delta_{N-2}(6))$ the optimal controller keeps $|x_{N-1}| > \alpha$ without hedging-to-a-point with u_{N-2}. Then u_{N-1} is used to keep x_N outside the high-risk piece of $p(i,2:x)$ by hedging-to-points $x_N = -\alpha^-$ or $x_N = \alpha^+$.

In the third possible situation, as shown in Figure 7.27, the

optimal controller has

$$m_{N-2}(1) = 5 = m_{N-1}(1)$$

pieces. In this situation either x_N and x_{N-1} are in the same $p(1,2:x)$ piece (that is, x_{N-2} is in the domain of an endpiece or middlepiece of $V_{N-2}(x_{N-2}, r_{N-2}=1)$ or else the optimal controller hedges-to-a-point at time N, using u_{N-1} to obtain $x_N = -\alpha^-$ or $x_N = \alpha^+$). In this situation there is no immediate hedging-to-a-point (using u_{N-2}). This is in contrast to the third situation of the commensurate goal problem (Figure 7.28) where the only hedging-to-a-point is immediate.

In table 7.4 various aspects of these three situations for $V_{N-2}(x_{N-2}, r_{N-2}=1)$ are summarized. We want to relate these various active hedging strategies to the values of the problem parameters. From Figures 7.25 - 7.27 we can obtain the following graphical conditions relating to the three possible shapes of $V_{N-2}(x_{N-2}, r_{N-2}=1)$ in this problem.

Fact 7.9: For the problem (7.2) - (7.5) with fact 7.1, 7.2, 7.3(2) and (7,14) holding, we have the following:

(1) Situation (1), as in Figure 7.25, occurs if and only if the rightmost intersection of the two quadratic functions $V_{N-2}^{2,U}$ and $V_{N-2}^{3,U}$ is to the left of $x_{N-2} = \Theta_{N-2}(3) \big/ a(1)$.

(2) Situation (3), as in Figure 7.27 occurs if and only if the rightmost intersection of $V_{N-2}^{2,U}(x_{N-2})$ and $V_{N-2}^{4,U}(x_{N-2})$ occurs to the right of (or exactly at) the rightmost intersection of $V_{N-2}^{3,R}(x_{N-2})$ and $V_{N-2}^{4,U}(x_{N-2})$.

(3) Situation (2), as in Figure 7.26, occurs when (1) and (2) above are both not met. A necessary condition is that $V_{N-2}^{3,R}(x_{N-2})$ and $V_{N-2}^{2,U}(x_{N-2})$ intersect.

Proof: Immediate from Figures 7.25 - 7.27. □

In appendix C.15 the values of the rightmost intersections of $(V_{N-2}^{2,U}$ and $V_{N-2}^{3,U})$, $(V_{N-2}^{2,U}$ and $V_{N-2}^{4,U})$, $(V_{N-2}^{3,R}$ and $V_{N-2}^{4,U})$ and $(V_{N-2}^{3,R}$ and $V_{N-2}^{2,U})$ and the value of $\Theta_{N-2}(3)/a(1)$ are listed. From Fact 7.9 and these values we obtain:

Fact 7.10: For the problems of Fact 7.9,

(1) situation (1), as in Figure 7.25, occurs if and only if

$$a(1) < \left(1 + \frac{b^2(1)}{R(1)} \hat{K}_N(2)\right)\left(1 - \sqrt{1 - \chi_3}\right) \tag{7.113}$$

where χ_3 is given by (C.15.13).

(2) situation (3), as in Figure 7.27, occurs if and only if

$$a(1) > \frac{\left(1 + \frac{b^2(1)}{R(1)} \hat{K}_N(2)\right)(1 - \omega_2)\chi_6 \left(1 - \sqrt{1 - \chi_5}\right)}{\left(1 - \sqrt{1 - \frac{R + b^2 \hat{K}_{N-1}(3)}{R + b^2 \hat{K}_{N-1}(4)}}\right)} \tag{7.14}$$

where χ_5 is given by (C.15.27) and χ_6 by (C.15.28).

(3) Situation (2), as in Figure 7.26 occurs if and only if (7.113) and (7.114) are both not true. A necessary condition is that $\chi_4 \leq 1$ where χ_4 is given by (C.15.20).

Proof: These conditions are derived in Appendix C.15. □

Conditions (7.113) - (7.114) are implicit relationships that can be tested for any given set of problem parameters. We can use Facts 7.1, 7.2 and 7.3(1) to obtain sufficient conditions that are more easily analyzed, similar to those obtained in Fact 7.6 for the three cases of the commensurate goal problem. In particular we can use (7.113), (C.15.13) and condition (7.14) to obtain the following sufficient condition:

Fact 7.11 For the problem of Fact 7.9, situation (1) occurs if

$$a(1) < \left(1 + \frac{b^2(1)}{R(1)} \hat{K}_N(2)\right)\left[1 - \sqrt{1 - \frac{\left([R(1) + b^2(1)\,\hat{K}_N(1)]\cdot [R(1)+b^2(1)[(1-\omega_2)Q(1)+\omega_2(K_{N-1}(1:2)+Q(2)]]\right)}{\left([R(1)+b^2(1)\hat{K}_N(2)]\cdot [R(1)+b^2(1)[(1-\omega_2)Q(1)+\omega_2 Q(2)+K_{N-1}(1:2)]]\right)}}\right] \tag{7.115}$$

Another weaker sufficient condition for situation (1) is that

$$a(1) < (1 + \frac{b^2(1)}{R(1)} \hat{K}_N(2))\left(1 - \sqrt{1 - \frac{R(1) + b^2(1)\,\hat{K}_N(1)}{R(1) + b^2\,\hat{K}^{LM}_\infty(1)}}\right) \tag{7.116}$$

where $\hat{K}^{LM}_\infty(1)$ is given by

$$\hat{K}^{LM}_\infty(1) = (1 - \omega_1)(Q(1) + K^{LM}_\infty(1)) + \omega_1(Q(2) + K_\infty(1:2)) \tag{7.117}$$

for $K_\infty(1:2) = \lim_{(N-k)\to\infty} K_k(1:2)$ as given in (6.98)

and $K^{LM}_\infty(1) = \lim_{(N-k)\to\infty} K^{Le}_k(1)$ as given in (6.107) .

Proof: See Appendix C.15. □

As in the commensurate goals case (Facts 7.5, 7.6), for the conflicting goals case under study here the structure of $V_{N-2}(x_{N-2}, r_{N-2}=1)$ can be related to the value of a(1) (that is, to the stability of the open loop dynamics in form r=1). For sufficiently small a(1), where (7.113) is satisfied, we have the optimal controller of Figure 7.25. For larger a(1) (satisfying neither (7.113) nor (7.114)) the optimal controller must hedge-to-a-point with u_{N-2} or u_{N-1}, for all x_{N-2} that are not in the endpieces or middlepiece domains. This is the case shown in Figure 7.26. For sufficiently unstable a(1) (satisfying (7.114)), the optimal controller does not hedge-to-a-point until the last possible time. This is the situation shown in Figure 7.27. For $x_{N-2} \in (\delta_{N-2}(1), \delta_{N-2}(2))$ and $x_{N-2} \in (\delta_{N-2}(3), \delta_{N-2}(4))$ the optimal controller hedges to either $x_N = \alpha^+$ or $x_N = \alpha^-$ with control u_{N-1}.

Comparing the large a(1) case for the conflicting goals problem of this section and the commensurate goals problem of section 7.5. (that is, comparing Figures 7.18 and 7.27), we observe a basic difference in the nature of active hedging in these two cases. In both problems, for large a(1) the optimal controller either

- always puts x inside $(-\alpha,\alpha)$ (the middlepiece)

or

- always puts x outside $(-\alpha,\alpha)$ (the endpieces)

or it

- hedges to the advantageous side of a p(1,2:x) discontinuity at one (and only one) time.

For the commensurate goal problem, this hedging-to-a-point is immediate, using u_{N-2} to drive x_{N-1} to α^- or $-\alpha^+$. For the conflicting goals problem, the optimal controller doesn't hedge-to-a-point until the last possible time, using u_{N-1} to drive x_N to α^+ or $-\alpha^-$.

It is easy to see that hedging-to-a-point must be done quickly in the commensurate goals case, since if a(1) is large it tends to drive the system away from the desirable part of the x axis (with respect to both the performance and reliability goals). Spending extra control energy to drive x inside $(-\alpha,\alpha)$ leads to savings in the performance cost at all future times, and this strategy also reduces the likelihood of the undesirable form transition (from form 1 to form 2).

In the conflicting goals case, if a(1) is large it causes the system to move away from the performance goal (i.e., the origin), but it also tends to drive the system into the advantageous p(1,2:x) piece (or keeps it there). Hedging-to-a-point decreases the probability of a bad transition but it results in a much larger operating cost at all future times (since a(i) is large). Thus it is not desirable to hedge-to-a-point until there "isn't much future left" - that is, at the terminal time.

In the remainder of this section we will examine the optimal JLQ controller for problems satisfying the sufficient condition (7.116) of Fact 7.11. For these problems we find that at all times (N-k), the optimal JLQ controller follows the pattern of figure 7.25. This allows us to obtain a recursive description of $V_{N-k}(x_{N-k},r_{N-k}=1)$ and $u_{N-k}(x_{N-k},r_{N-k}=1)$ at each time (N-k) for this class of conflicting goals problems.

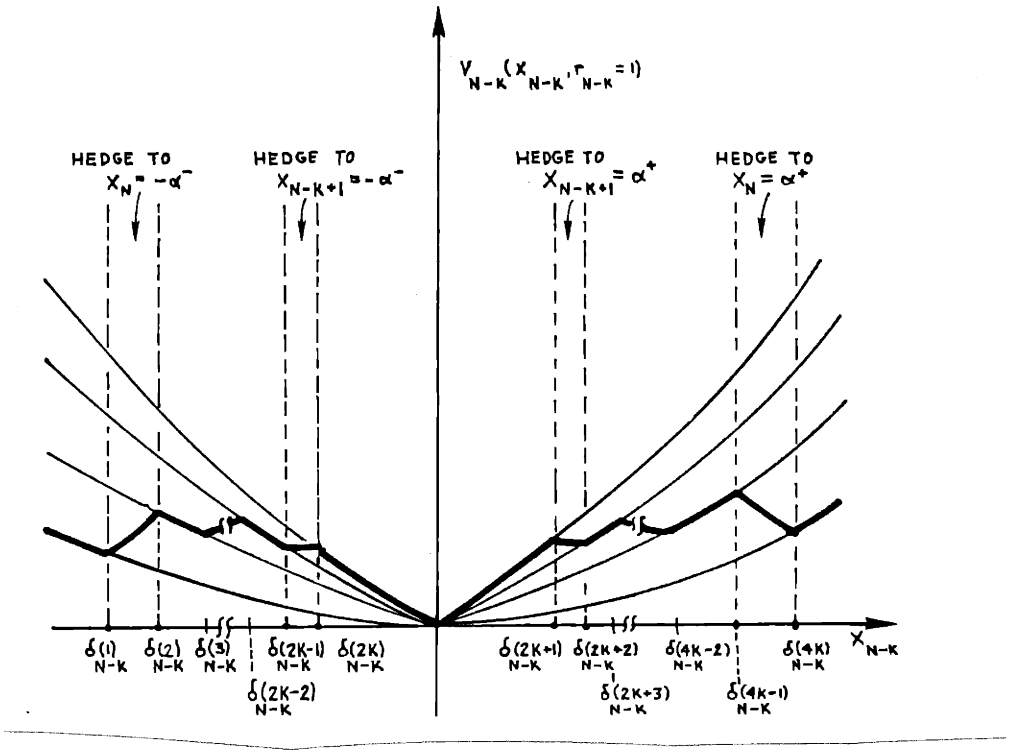

Figure 7.28: Optimal Expected Cost-to-go $V_{N-k}(x_{N-k}, r_{N-k}=1)$ for for the problems of Proposition 7.12.

A typical $V_{N-k}(x_{N-k}, r_{N-k}=1)$ curve is shown in figure 7.28. It has $m_{N-k}(1) = 4k+1$ pieces, and is symmetric about $x_{N-k} = 0$.

For x_{N-k} in the middlepiece (i.e., for $\delta_{N-k}(2k) < x_{N-k} < \delta_{N-k}(2k+1)$) the optimal controller will result in $|x_{N-k+\ell}| < \alpha$ for $\ell = 1,2,\ldots k$. That is, the x process will be kept in the high-failure-risk (but low cost) piece of p(i,2:x) at all future times.

The first piece to the left of the middlepiece (i.e., $\delta_{N-k}(2k-1) < x_{N-k} < \delta_{N-k}(2k)$) corresponds to using u_{N-k} to achieve $x_{N-k+1} = -\alpha^-$. That is, we use the control u_{N-k} to keep x_{N-k+1} out of the high-risk piece; we hedge to the low risk side of $-\alpha$. Then at the next time (for $k \geq 2$), the control u_{N-k+1} will drive x_{N-k+2} into the high-risk - low-cost middlepiece. The x process will then be kept inside $(-\alpha,0]$ through time N.

The second pieces to the left and right of the middlepice correspond to having $|x_{N-k+1}| > \alpha$ but $|x_{N-k+\ell}| < \alpha$ for $\ell = 2,3,\ldots k$ without hedging-to-a-point.

The third pieces of $V_{N-k}(x_{N-k}, r_{N-k}=1)$ to the left and right of the middlepiece correspond to hedging-to-a-point (to $-\alpha^-$ or α^+) one time step in the future; that is, u_{N-k+1} is used to obtain $|x_{N-k+2}| = -\alpha^-$. Then the x process is kept inside $(-\alpha,\alpha)$ from time (N-k) + 3 through N.

In general the $2m^{th}$ pieces of $V_{N-k}(x_{N-k}, r_{N-k}=1)$ to the left and right of the middlepiece correspond to never hedging-to-a-point. The x process will be in a low failure probability piece of p(1,2:x) for $x_{N-k+1}, \ldots, x_{N-k+m}$ and then it will be inside the high failure probability region $(-\alpha,\alpha)$ from time (N-k) + m + 1 through time N. Note that the

$2k^{th}$ pieces of $V_{N-k}(x_{N-k}, r_{N-k}=1)$ to the left and right of $x_{N-k}=0$ are the endpieces of the optimal cost. For $x_{N-k} < \delta_{N-k}(1)$ and $x_{N-k} > \delta_{N-k}(4k)$, the optimal controller does not drive the x process inside the high risk piece $(-\alpha,\alpha)$ of $p(1,2:k)$ at any future time.

The $(2m+1)^{st}$ pieces of $V_{N-k}(x_{N-k}, r_{N-k}=1)$ to the left and right of $x_{N-k} = 0$ correspond to using u_{N-k+m} to hedge to $x_{N-k+m+1} = -\alpha^-$ or $x_{N-k+m+1} = \alpha^+$. Then $|x_{N-k+\ell}| < \alpha$ for $\ell = m+2,\ldots,k$.

As in the commensurate goals problem of Section 7.5, this class of conflicting goal problems illustrates that using control to alter failure probabilities at future times is directly reflected in the expected cost-to-go. These two example classes motivate a finite-time-horizon approximation to the infinite time horizon problem (for the general problem of Chapter 5) that is developed in the next section.

The following Proposition states the general result for the problem of this section. We again use the shorthand notation of (7.39).

Proposition 7.12

For the problem of (7.2) - (7.5) with facts 7.1, 7.2, 7.3(2) and equation (7.116) of fact 7.11 holding, the optimal JLQ controller can be completely described as follows:

1) The number of pieces of $V_{N-k}(x_{N-k}, r_{N-k}=1)$ and $u_{N-k}(x_{N-k}, r_{N-k}=1)$ at time $(N-k)$ is

$$m_{N-k(1)} = 4k + 1. \tag{7.118}$$

2) This number of pieces is the maximum possible. That is, all eligible candidate cost-to-go functions (by Proposition 5.2) are optimal over

some portion of their regions of validity. These eligible candidate costs are

$V_{N-k}^{t,U}$ $\quad t = 1,\ldots,4k-1$ (driving x_{N-k+1} into $\Delta_{N-k+1}(t)$)

$V_{N-k}^{2k-1,R}$ (hedging to $x_{N-k+1} = -\alpha^{-}$)

$V_{N-k}^{2k+1,L}$ (hedging to $x_{N-k+1} = \alpha^{+}$)

3) $V_{N-k}(x_{N-k}, r_{N-k}=1)$ and $u_{N-k}(x_{N-k}, r_{N-k}=1)$ are symmetric about $x_{N-k}=0$. That is,

$$V_{N-k}(i:1)\Big|_{x_{N-k}=-x} = V_{N-k}(4k+2-i:1)\Big|_{x_{N-k}=x} \tag{7.119}$$

$$u_{N-k}(i:1)\Big|_{x_{N-k}=-x} = u(4k+2-i:1)\Big|_{x_{N-k}=x} \tag{7.120}$$

$$\delta_{N-k}(1) = -\delta_{N-k}(4k+1-i) \tag{7.121}$$

for $i = 1,2,\ldots,(2k+1)$.

4) The closest grid points to zero in the composite x_{N-k+1} partition are $\pm\,\alpha$. That is,

$$\begin{aligned}
&\gamma_{N-k+1}(i) = \delta_{N-k+1}(i) \qquad i = 1,\ldots,2k-2\\
&\gamma_{N-k+1}(2k-1) = -\alpha\\
&\gamma_{N-k+1}(2k) = \alpha\\
&\gamma_{N-k+1}(j) = \delta_{N-k+1}(j-2) \qquad j = 2k+1,\ldots,4k-2
\end{aligned} \tag{7.122}$$

5) The <u>odd-numbered</u> pieces of $V_{N-k}(x_{N-k},r_{N-k}=1)$ and $u_{N-k}(x_{N-k},r_{N-k}=1)$ are given by

$$V_{N-k}(i:1) = x_{N-k}^2\, K_{N-k}(i:1) \tag{7.123}$$

$$u_{N-k}(i:1) = -L_{N-k}(i:1)\, x_{N-k} \tag{7.124}$$

optimal for

$$\delta_{N-k}(i-1) \leq x_{N-k} \leq \delta_{N-k}(i)$$

$$i = 1,3,5,\ldots,(4k+1) \quad \bullet$$

These costs are optimal for x_{N-k} values where the best strategy is <u>not</u> to use <u>any</u> of the values $u_{N-k},\ldots,u_{N-1}$ to hedge-to-a-point. They include the left endpiece

$$V_{N-k}^{Le}(1) = V_{N-k}(1:1),$$

the middlepiece

$$V_{N-k}^{LM}(1) \equiv V_{N-k}^{RM}(1) = V_{N-k}(2k+1:1) \quad \bullet$$

and the right-endpiece

$$V_{N-k}^{Re}(1) = V_{N-k}(4k+1:1) \quad \bullet$$

6) The <u>even-numbered</u> pieces of $V_{N-k}(x_{N-k},r_{N-k}=1)$ and $u_{N-k}(x_{N-k},r_{N-k}=1)$ are given by

$$V_{N-k}(i:1) = x_{N-k}^2\, K_{N-k}(i:1) + x_{N-k}\, H_{N-k}(i:1) + G_{N-k}(i:1) \tag{7.125}$$

$$u_{N-k}(i:1) = -L_{N-k}(i:1)\, x_{N-k} + F_{N-k}(i:1) \tag{7.126}$$

optimal for $\delta_{N=k}(i;1) \leq x_{N-k} \leq \delta_{N-k}(i)$ $\quad i = 2,4,6,\ldots,4k$ $\bullet$

These costs correspond to actively hedging-to-a-point at one (and only one) future time. Specifically, at each time (N-k) < N, and for each i = 1,2,...,k:

$V_{N-k}(2i:1)$ is the cost associated with using control u_{N-i} to hedge to-a-point. That is, it is the expected cost-to-go which results if

- $u_{N-k+\ell-i}$ keeps $x_{N-k+\ell} < -\alpha$

  for each $1 \leq \ell \leq k-i$ (when $k \geq 2$)

and then

- u_{N-i} hedges to $x_{N-i+1} = -\alpha^-$

and then

$u_{N-k+\ell-1}$ keeps $-\alpha < x_{N-k+\ell} < 0$

for each $k-i+2 \leq \ell \leq k$ (when $k \geq 2$).

So $V_{N-k}(2k:1)$ corresponds to hedging-to-a-point immediately (using u_{N-k}) and $V_{N-k}(2:1)$ corresponds to hedging-to-a-point at the last time (using u_{N-1}).

Similarly for $V_{N-k}(j:1)$, where $j = 2k+2, \ldots, 4k$, the optimal controller uses

$$u_N - \left\lceil \frac{4k+2-j}{2} \right\rceil$$

to hedge to

$$x_N - \left\lceil \frac{4k-j}{2} \right\rceil = \alpha^+$$

•

7) The cost-parameters in (7.123) - (7.126) are given recursively by the following set of coupled difference equations:

- In form r=2, for k = N-1, N-2,..., the parameters $K_k(1:2)$, $L_k(1:2)$ are specified by (7.49) - (7.51) (as in the analogous commensurate goal problem of Proposition 7.7),

- For k = 1,...,N the middlepiece parameters $K_{N-k}(2k+1:1)$, $L_{N-k}(2k+1:1)$ are given by (7.52) - (7.54),
  Here $K_{N-k}(2k+1:1) = K^{UB}_{N-k}(1)$, the upperbound parameter,[1]

- For k = 1,2,...,N and i = 1,2,...,2k-1,
  $K_{N-k}(i:1)$ and $L_{N-k}(i:1)$ are given by (7.55) - (7.58)

- for k = 1,2,...,N the immediate-hedging-to-a-point parameters $K_{N-k}(2k:1)$, $H_{N-k}(2k:1)$, $L_{N-k}(2k:1)$ and $F_{N-k}(2k:1)$ are given by (7.59), (7.60), (7.62) and (7.63), respectively. Unlike Proposition 7.7, $G_{N-k}(2k:1)$ is given by

$$G_{N-k}(2k:1) = \frac{\alpha^2}{b^2(1)} \left[R(1) + b^2(1)\, \hat{K}_{N-k+1}(2k-1)\right], \tag{7.127}$$

- for k = 2,3,...,N and i = 2,4,...,2k-2
  the parameter $H_{N-k}(i:1)$, $G_{N-k}(i:1)$ and $F_{N-k}(i:1)$ are given by (7.64) - (7.67).

8) By symmetry we have (for each k = 1,2,...,N), for i = ,2,...,2k the relationships (7.72) - (7.76).

---

[1] Unlike the commensurate goals problem of Proposition 7.7, where $K_{N-k}(2k+1:1) = K^{LB}_{N-k}(1)$ (the lower-bound parameter).

9) The joining points $\{\delta_{N-k}(i) : i = 1,\ldots,4k\}$ are given by

- for $k = 1,2,\ldots,N$

$$\delta_{N-k}(2k) = \frac{-\alpha}{a(1)}\left(1 + \frac{b^2(1)}{R(1)}\hat{K}_{N-k+1}(2k)\right)\cdot$$

$$\cdot\left(1 - \sqrt{1 - \frac{R(1) + b^2(1)\,\hat{K}_{N-k+1}(2k-1)}{R(1) + b^2(1)\,\hat{K}_{N-k+1}(2k)}}\right) \tag{7.128}$$

- for $k = 1,2,\ldots,N$ and $i = 1,2,\ldots,k$

$$\delta_{N-k}(2i-1) = \frac{-\alpha}{a(1)}\left(1 + \frac{b^2(1)}{R(1)}\hat{K}_{N-i+1}(2i-1)\right)\prod_{\ell=1}^{k-i}\left[\frac{1+\frac{b^2(1)}{R(1)}\hat{K}_{N-k+\ell}(2i-1))}{a(1)}\right] \tag{7.129}$$

- for $k = 2,3,\ldots,N$ and $i = 1,2,\ldots,k-1$

$$\delta_{N-k}(2i) = \frac{-H_{N-k}(2i:1) + \sqrt{H^2_{N-k}(2i:1) - 4\begin{bmatrix}K_{N-k}(2i:1)\\ -K_{N-k}(2i+1:1)\end{bmatrix}G_{N-k}(2i:1)}}{2[K_{N-k}(2i:1) - K_{N-k}(2i+1:1)]}$$

$$= \frac{-\alpha}{a(1)}\left(1 + \frac{b^2(1)}{R(1)}\hat{K}_{N-i+1}(2i)\right)\left[\prod_{\ell=1}^{k-1}\frac{\left(1+\frac{b^2(1)}{R(1)}\hat{K}_{N-k+\ell}(2i+1)\right)}{a(1)}\right]\cdot$$

$$\cdot\left(1 - \sqrt{1 - \chi_k(1)}\right) \tag{7.130}$$

where $\chi_k(i)$ is given by (C.16,8).

Here we define

$$\prod_{t=1}^{9} = 1 \qquad \text{if } 9 < 1 \quad \bullet$$

10) At each time k = 1,2,... we have the following relationships:

$$\underbrace{K_{N-k}(1:1) < ,\ldots < K_{N-k}(2k-1:1) < K_{N-k}(2k+1:1) < K_{N-k}(2k:1)}_{\text{odd-indexed parameters}} \tag{7.131}$$

$$\underbrace{K_{N-k}(2k-1:1) < K_{N-k}(2:1) < \ldots < K_{N-k}(2k:1)}_{\text{even-indexed parameters}} \tag{7.132}$$

$$\delta_{N-k}(2i-1:1) < \delta_{N-k}(2i:1) < \delta_{N-k}(2i+1:1) \qquad i = 1,\ldots,k \tag{7.133}$$

$$\underbrace{\hat{K}_{N-k}(1) < \ldots < \hat{K}_{N-k}(2k-1) < \hat{K}_{N-k}(2k+1) < \hat{K}_{N-k}(2K)}_{\text{odd-indexed parameters}} \tag{7.134}$$

$$\underbrace{\hat{K}_{N-k}(2k-1) < \hat{K}_{N-k}(2) < \ldots < \hat{K}_{N-k}(2K)}_{\text{even-indexed parameters}} \tag{7.135}$$

and

$$\hat{K}_{N-k}(2k+1) < \hat{K}_{N-k}(2k+2) \quad \bullet \tag{7.136}$$

Here

$$K_{N-k}(2k+1:1) = K^{LM}_{N-k}(1) = K^{UB}_{N-k}(1) \qquad \text{and}$$

$$K_{N-k}(1:1) = K^{Le}_{N-k}(1) = K^{LB}_{N-k}(1)$$

11) For $i = 1,i,\ldots,k$

$$V_{N-k}(2i:1) > V_{N-k}(2i-1:1) \quad \text{except}$$

$$\text{equality at} \quad X_{N-k} = \delta_{N-k}(2i-1)$$

and

$\delta_{N-k}(2i)$ is the rightmost intersection of

$V_{N-k}(2i:1)$ and $V_{N-k}(2i+1:1)$. □

Proof: The proof of this proposition involves an induction on (N-k), starting with k=2. The proof is developed in appendix C.16.

For this problem the optimal control law and expected cost-to-go at each time $k = k_o,\ldots,N$ (for any finite time horizon problem) can be computed recursively from a growing number of difference equations running backwards in time. As with the commensurate goals problem of Proposition 7.7, for this conflicting goals problem we need not follow all the flowchart comparisons and tests of Section 7.2. This problem thus lends itself to detailed analysis and interpretation.

In particular we can see what each piece of the controller is trying to accomplish. Refer again to figure 7.28, where a typical $V_{N-k}(x_{N-k},r_{N-k}=1)$

is shown. The middlepiece is the upperbound cost function $V^{UB}_{N-k}(1)$, associated with always having x in the $p(1,2:x)$ region where the probability of failure is high. The endpieces coincide with the lowerbound cost function $V^{LB}_{N-k}(1)$, since the controller never drives x into the high $p(1,2:x)$ region if $x_{N-k} < \delta_{N-k}(1)$ or $x_{N-k} > \delta_{N-k}(4k)$. The even-numbered pieces correspond to hedging-to-a-point at successively further times in the future (as we move away from the middlepiece in figure 7.28), with successively higher costs being incurred.

In figure 2.29 the optimal control law $u_{N-k}(x_{N-k}, r_{N-k}=1)$ is shown for these problems. Note that this control law is discontinuous at the joining points $\{\delta_{N-k}(i) \mid i = 2,4,\ldots,2k\}$, where $V_{N-k}(x_{N-k}, r_{N-k}=1)$ is not differentiable. In figure 7.30 the optimal mapping from x_{N-k} to x_{N-k+1} (given $r_{N-k} = 1$) is graphed. There is a region of avoided x_{N-k+1} values associated with each control law discontinuity. Thus at all times (N-k) we have the type of behavior illustrated at time (N-1) in Fact 6.10.

Let us now consider the JLQ optimal controller of Proposition 7.12 as the time horizon (N-k) grows large. From (7.118) we see that the number of pieces of the optimal controller grows without bound as (N-k) goes to infinity. Thus the exact infinite time horizon optimal controller is not obtainable precisely via any finite algorithm. However, we can obtain a description of the Proposition 7.12 controller as (N-k) grows large which is similar to that given in Proposition 7.8 of the previous section.[1] As (N-k) grows large, many of the controller pieces correspond to moving the state from one $p(1,2:x)$ piece to another at a time far in

[1] describing the Proposition 7.7 controller as $(N-k) \to \infty$.

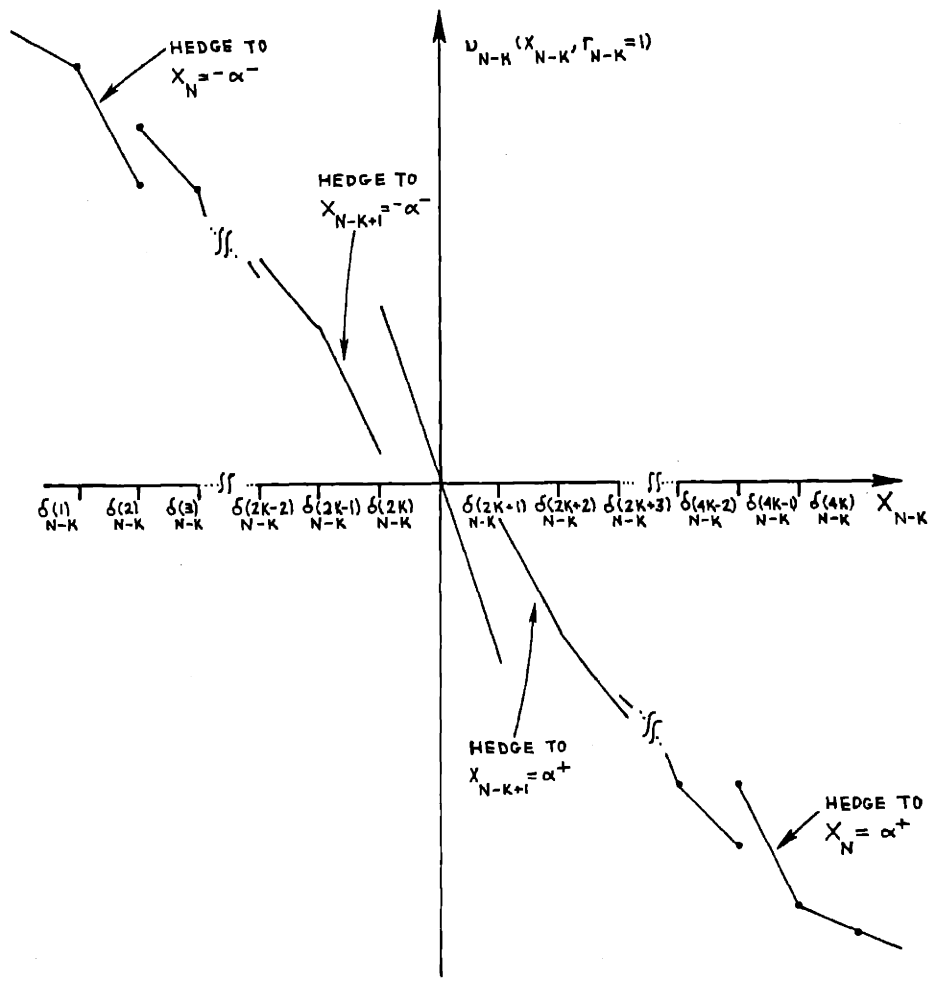

Figure 7.29: Optimal Control Law $u_{N-k}(x_{N-k}, r_{N-k}=1)$ for the Problems of Proposition 7.12.

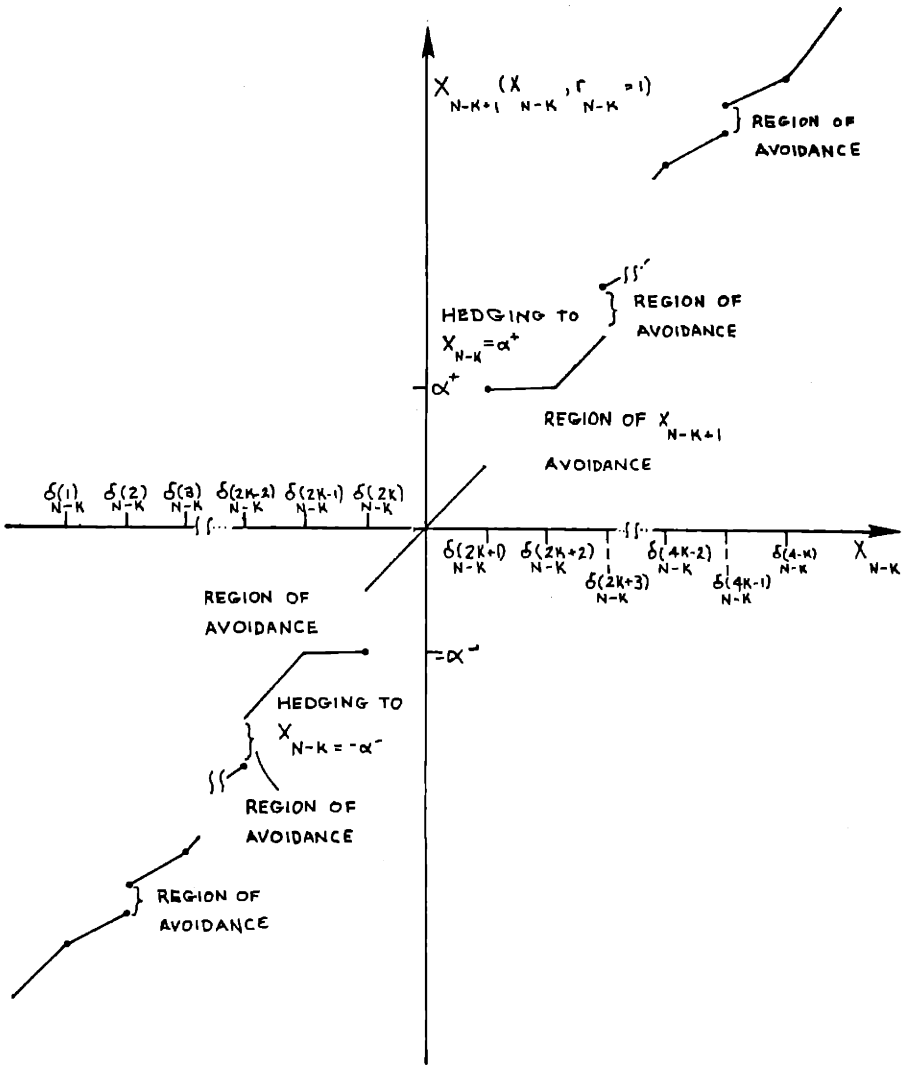

Figure 7.30: Optimal x_{N-k+1} given x_{N-k} and $r_{N-k} = 1$ for the problems of Proposition 7.12.

the future. The difference between any of these pieces and the endpiece cost function becomes small as the time when this change is effected becomes distant. Consequently the structure of the optimal controller converges to a steady-state controller which we can approximate with arbitrarily small error by choosing suitably large (N-k).

The discussion which precedes Proposition 7.8 in Section 7.5 is applicable here with the exceptions that

- hedging-to-a-point is to $-\alpha^-$ and α^+ (instead of to $-\alpha^+$ and α^-),
- the endpiece cost functions are lower bounds on $V_{N-k}(x_{N-k}, r_{N-k}=1)$ and odd-indexed pieces $V_{N-k}(i:1)$ $(i=1,3,5,\ldots)$ approach $V^{Le}_{N-k}(1)$ from above[1], at each x. The even-indexed pieces $V_{N-k}(i:1)$ $(i=2,4,6,\ldots)$ approach it from below.

As in section 7.5, it is easier to discuss the structure of the limiting optimal controller (as $(N-k)\to\infty$) if we count pieces from the middlepiece outwards. Using this indexing method (as described prior to Proposition 7.8 and as shown in figure 7.22), we can summarize the structure of the limiting controller for the problem of 7.12 as follows:

Proposition 7.13: For the problem of Proposition 7.12, as $(N-k)\to\infty$, items (1) - (7) of Proposition 7.8 hold except that (7.90) is replaced by

---

[1] instead of from below, as in section 7.5.

$$G_{\infty}\underline{<+1>} = \lim_{(N-k)\to\infty} G_{N-k}\underline{<+1>}$$

$$= \frac{\alpha^2}{b^2(1)}\left[R(1) + b^2(1)\left[\begin{matrix}(1-\omega_2)(K_{\infty}<0> + Q(1)\\ +\omega_2(K_{\infty}(1:2) + Q(2))\end{matrix}\right]\right] \quad . \qquad (7.137)$$

In addition we have the following:

1. As $(N-k)\to\infty$ the joining point

$\delta_{N-k}<-1> = \delta_{N-k}(2k)$ converges monotonely to

$$\delta_{\infty}<-1> = \lim_{(N-k)\to\infty} \delta_{N-k}<-1>$$

$$= \frac{-\alpha}{a(1)}\left(1 + \frac{b^2(1)}{R(1)}\hat{K}_{\infty}^{LM}(1)\right)\left(1 - \sqrt{1 - \frac{\left[R(1)+b^2(1)\left[\begin{matrix}(1-\omega_2)(K_{\infty}^{LM}(1)+Q(1)) +\\ \omega_2(K_{\infty}(1:1)+Q(2))\end{matrix}\right]\right]}{\left[R(1)+b^2(1)\left[\begin{matrix}(1-\omega_1)(K_{\infty}^{LM}(1)+Q(1)) +\\ +\omega_1(K_{\infty}(1:2)+Q(2))\end{matrix}\right]\right]}}\right) \qquad (7.138)$$

and $\delta_{N-1}<+1> \to \delta_{\infty}<+1> = -\delta_{\infty}<-1>$.

2. For $k=1,2,\ldots,N$, for each fixed $i \in \{1,2,\ldots,k\}$, the joining points $\delta_{N-k}<-2i>$ converge monotonely as $(N-k)\to\infty$ to

$$\delta_{\infty}<-2i> = \frac{\delta_{\infty}<-2(i:1)>}{a(1)}\left[1 + \frac{b^2(1)}{R(1)}\left[\begin{matrix}(1-\omega_2)(K_{\infty}<-2(i+1)> + Q(1))\\ +\omega_2(K_{\infty}(1:2) + Q(2))\end{matrix}\right]\right] \qquad (7.139)$$

and $\delta_{N-k}<2i> \to \delta_{\infty}<2i> = -\delta_{\infty}<-2i>$.

3. For $k = 2,3,\ldots,N$ for each fixed $i \in \{1,2,\ldots,k\}$ the joining points $\delta_{N-k}\langle -(2i+1)\rangle$ converge as $(N-k)\to\infty$ to

$$\delta_\infty\langle -(2i+1)\rangle = \frac{\left[-H_\infty\langle -(2i+2)\rangle - \sqrt{H_\infty\langle 2i-2\rangle)^2 - 4[K_\infty\langle -2i-2\rangle - K_\infty\langle -2i-1\rangle]G_\infty\langle -2i-2\rangle}\right]}{2[K_\infty\langle -2i-2\rangle - K_\infty\langle -2i-1\rangle]} \tag{7.140}$$

and

$$\delta_{N-k}\langle 2i+1\rangle \to \delta_\infty\langle 2i+1\rangle = -\delta_\infty\langle -(2i+1)\rangle \ .$$

4. For the limiting problem solution parameters, as $(N-k)\to\infty$ the following relationships hold:

$$\text{(i)} \quad K_\infty^{Le}(1) \equiv K_\infty^{Re}(1) < \ldots < K_\infty\langle \pm 4\rangle \leq K_\infty\langle \pm 2\rangle < K_\infty\langle 0\rangle < K_\infty\langle \pm 1\rangle \tag{7.141}$$

$$\text{(ii)} \quad K_\infty\langle \pm 2\rangle < \ldots < K_\infty\langle \pm 3\rangle < K_\infty\langle \pm 1\rangle \tag{7.142}$$

$$\text{(iii)} \quad \delta_\infty\langle -2(i+1)\rangle < \delta_\infty\langle -2i\rangle < \delta_\infty\langle -2(i-1)\rangle \tag{7.143}$$

hence

$$\delta_\infty\langle 2i+1\rangle - \delta_\infty\langle 2i-1\rangle > 0 \tag{7.144}$$

$$\delta_\infty\langle -(2i+1)\rangle - \delta_\infty\langle -(2i-1)\rangle > 0$$

Proposition 7.13 says that as the time horizon becomes infinite, the number of pieces in the optimal controller also becomes infinite but each piece (counting from the center outwards) converges to a constant steady-state function that is optimal over a constant steady-state interval of x values. From figure 7.30 we see that there will be certain steady-state

intervals of x values that the system will avoid. From (7.144) we see that the width of the switching regions will grow without bounds as (N-k) increases. We cannot implement precisely the steady-state JLQ controllers of Proposition 7.13 and 7.8 using a finite algorithm, because there are infinitely many controller pieces. However, we can approximate the steady-state controller by using, at each time (N-k), the true optimal controller for a certain number of pieces around zero and approximating the rest of $V_{N-k}(x_{N-k}, r_{N-k}=1)$ by the endpiece functions. This method of approximation is discussed in the next section.

In this section we have examined the structure of the optimal JLQ controller for a class of problems having conflicting reliability and performance goals. This problem class has a solution structure that is particularly amenable to detailed analysis. Its solution illustrates the way that the optimal controller uses active hedging to achieve fault tolerance in this conflicting goals case. The major difference between this case and the commensurate goals problems of section 7.5 is the following:

- When the pefromance and reliability goals are commensurate, the JLQ controller uses hedging-to-a-point to drive the x process into the advantageous probability region sooner than the probability region x-independent JLQ controller (of chapter 3) would.
- In the case where these goals are conflicting, the JLQ controller uses hedging-to-a-point to keep the x process out of the disadvantageous piece for a longer time than the x-independent JLQ controller (of chapter 3) would.

7.7 Finite Look-Ahead Approximations of the Optimal JLQ Controller

The solution algorithm flowchart of section 7.2 lets us obtain the optimal JLQ controller for the general problem of chapter 5.[1] This algorithm is more efficient that the brute force approach used in chapter 5, in that Propositions 5.2 and 5.3 are used to greatly reduce the number of calculations and comparisons that are needed to obtain the optimal controller. However, the algorithm of section 7.2 is burdensome to compute and difficult to implement when the time horizon of the control problem is large. This is because the number of pieces of the optimal control law (in each form) grows linearly with the time horizon. In this section we develop an approximation of the true optimal JLQ controller that requires less computation and is easier to implement. This approximation is applicable for any problem in the class that was formulated in section 5.2.

Our approximation of the optimal JLQ controller for the general class of problems of chapter 5 is motivated by the structures of the optimal controllers in the special problems that were studied in sections 7.3 - 7.6. We will first develop suboptimal approximations of the optimal JLQ controller for these problems. Then we will develop a similar approximation that applies to the general case.

Recall that for the optimal controllers described by Propositions 7.7 and 7.12, the optimal control laws and expected cost-to-go can be computed off-line, backwards in time via sets of (growing numbers of)

---

[1] as formulated in section 5.2

recursive difference equations. In Propositions 7.8 and 7.13, the limiting structures of the optimal controllers for these problems as the time horizon becomes infinite are specified by (countably) infinite sets of difference equations. That is, even for these relatively simple problems, the optimal controller for the infinite time horizon situation cannot be obtained using a finite algorithm. However, pieces of the optimal controller (for the controllers of Propositions 7.7, 7.8, 7.12 and 7.13) that are succesively further from the middlepiece are seen to converge to the controller endpieces (as functions of x). This suggests a natural approximate controller for these problems: at each time N-k ($k > p$, for some fixed specified p), we apply the true optimal controller when the x process is in the domain of the $(4p + 1)$ pieces closest to (and including) $x_{N-k} = 0$, and we approximate the optimal controller for other x_{N-k} values by the endpiece control laws.

Proposition 7.14 (4p+1 piece suboptimal controller):

1. For JLQ problems satisfying the assumptions of Proposition 7.7 or 7.12, the optimal JLQ controller can be approximated as follows:

   For $p \geq 1$ fixed,

   - at times N-p,...,N-1 use the true optimal control laws (if in form 1):

     $$u_{N-p}(x_{N-p}, r_{N-p}=1), \ldots, u_{N-1}(x_{N-1}, r_{N-1}=1)$$

     (as computed using the algorithm of section 7.2), with expected cost-to-go

     $$V_{N-p}(x_{N-p}, r_{N-p}=1), \ldots, V_{N-1}(x_{N-1}, r_{N-1}=1), V_N(x_N, r_N=1)$$

, at times (N-k), for $k > p$, if $r_{N-k}=1$,

(i) use the middlepiece control law

$$u_{N-k}(2k+1:1) = u^{IM}_{N-k}(1) \text{ if}$$

$$\delta_{N-k}(2k) < x_{N-k} < \delta_{N-k}(2k+1)$$

(ii) use

$$u_{N-k}(2k:1) \quad \text{if} \quad \delta_{N-k}(2k-1) < x_{N-k} < \delta_{N-k}(2k)$$

$$u_{N-k}(2k+2:1) \quad \text{if} \quad \delta_{N-k}(2k+1) < x_{N-k} < \delta_{N-k}(2k+2)$$

(iii) if $p \geq 2$ then for $\ell = 1,\ldots,p-1$ use

$$u_{N-k}(2(k-\ell):1) \quad \text{if} \quad \delta_{N-k}(2(k-\ell)-1) < x_{N-k} < \delta_{N-k}(2(k-\ell))$$

$$u_{N-k}(2(k-\ell)+1:1) \quad \text{if} \quad \delta_{N-k}(2(k-\ell)) < x_{N-k} < \delta_{N-k}(2(k-\ell)+1)$$

$$u_{N-k}(2(k+\ell)+1:1) \quad \text{if} \quad \delta_{N-k}(2(k+\ell)) < x_{N-k} < \delta_{N-k}(2(k+\ell)+1)$$

$$u_{N-k}(2(k+\ell)+2:1) \quad \text{if} \quad \delta_{N-k}(2(k+\ell)+1) < x_{N-k} < \delta_{N-k}(2(k+\ell+1))$$

(iv) use the endpiece controllers

$$u^{Le}_{N-k}(1) = u_{N-k}(1:1) \quad \text{if} \quad x_{N-k} < \delta_{N-k}(2(k-p))$$

$$u^{Re}_{N-k}(1) = u_{N-k}(4k+1:1) \quad \text{if} \quad x_{N-k} > \delta_{N-k}(2(k+p)+1),$$

2. The resulting suboptimal controller has (4p+1) pieces at all times $(N-k) \leq (N-p)$. Let us denote the expected cost-to-go from

$(x_{N-k}, r_{N-k}=1)$ that corresponds to this approximate controller by $\tilde{V}_{N-k}(x_{N-k}, r_{N-k}=1)$. It is related to the true optimal JLQ expected cost to go $V_{N-k}(x_{N-k}, r_{N-k}=1)$ by

(i) For problems satisfying the assumptions of Proposition 7.7 commensurate goals):

$$x_{N-k}^2 \, K_{N-k}(2(k-p+1)+1:1) \leq V_{N-k}(x_{N-k}, r_{N-k}=1) \leq \tilde{V}_{N-k}(x_{N-k}, r_{N-k}=1)$$

$$\leq x_{N-k}^2 \, K_{N-k}(1:1) \qquad (7.145)$$

for x_{N-k} outside $(\delta_{N-k}(2(k-p)), \delta_{N-k}(2(k+p)+1))$.

(ii) For problems satisfying the assumptions of Proposition 7.12 (conflicting goals):

$$x_{N-k}^2 \, K_{N-k}(1:1) \leq V_{N-k}(x_{N-k}, r_{N-k}=1) \leq \tilde{V}_{N-k}(x_{N-k}, r_{N-k}=1) \leq$$

$$\leq x_{N-k}^2 \, K_{N-k}(2(k-p+1)+1:1) \qquad (7.146)$$

for x_{N-k} outside $(\delta_{N-k}(2(k-p)), \delta_{N-k}(2(k+p)+1))$.

3. Consequently the suboptimality of the approximate controller at any x_{N-k} is bounded by

$$\left(\tilde{V}_{N-k}(x_{N-k}, r_{N-k}=1) - V_{N-k}(x_{N-k}, r_{N-k}=1) \right) \leq x_{N-k}^2 \left| K_{N-k}(1:1) - K_{N-k}(2(k-p+1)+1:1) \right| \qquad (7.147)$$

□

Proof:

This Proposition follows almost immediately from Facts 7.1 - 7.3, and Propositions 7.7, 7.12. Details are given in Appendix C.17.

The special structure of the JLQ controllers of Propositions 7.12 and 7.7 lets us describe the suboptimality of this time-varying approximate controller. In Figure 7.31 we illustrate the bounds of (7.145) and (7.146). Notice that as the controller pieces (of the optimal controller) have domains further from the middlepiece, they look more and more like the endpieces. This observation motivates our substitution of the endpiece control law for those optimal control law pieces that are far from zero (i.e., outside $(\delta_{N-k}(2k-p),\ \delta_{N-k}(2(k+p)+1))$.

In Figures 7.32 and 7.33 we show the control laws and $x_{N-5} \mapsto x_{N-4}$ mapping for the optimal JLQ controller and a p = 3 approximation, for an example problem of the type that is addressed by Proposition 7.7. The solid lines indicate the optimal controller quantities. The thick, checkered line denotes the p=3 approximation. Note that the p=3 approximation coincides with the optimal solution in figures 7.32 and 7.33 except for

$$x_N \in (\delta_{N-4}(1), \delta_{N-4}(3)) \quad \text{and} \quad x_N \in (\delta_{N-4}(14),\ \delta_{N-4}(16)) \quad ,$$

By making p larger and larger, we can increase the width of the interval about the origin where the true optimal controller is used (for finite time horizon problems, if we make p = N-1 then the approximate controller is in fact optimal).

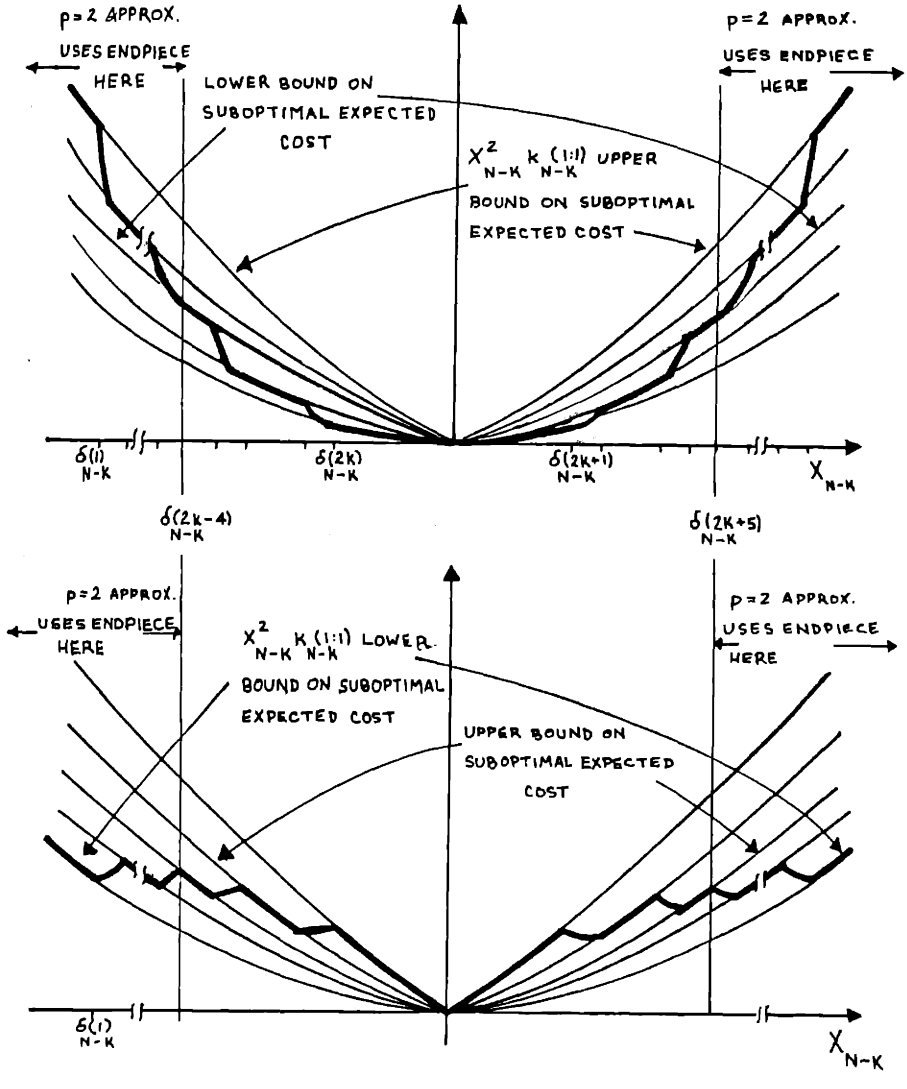

Figure 7.31: Optimal Expected (Thick Line) and p=2 Suboptimal Approximation for Problems of (a) Proposition 7.7, (b) Proposition 7.12

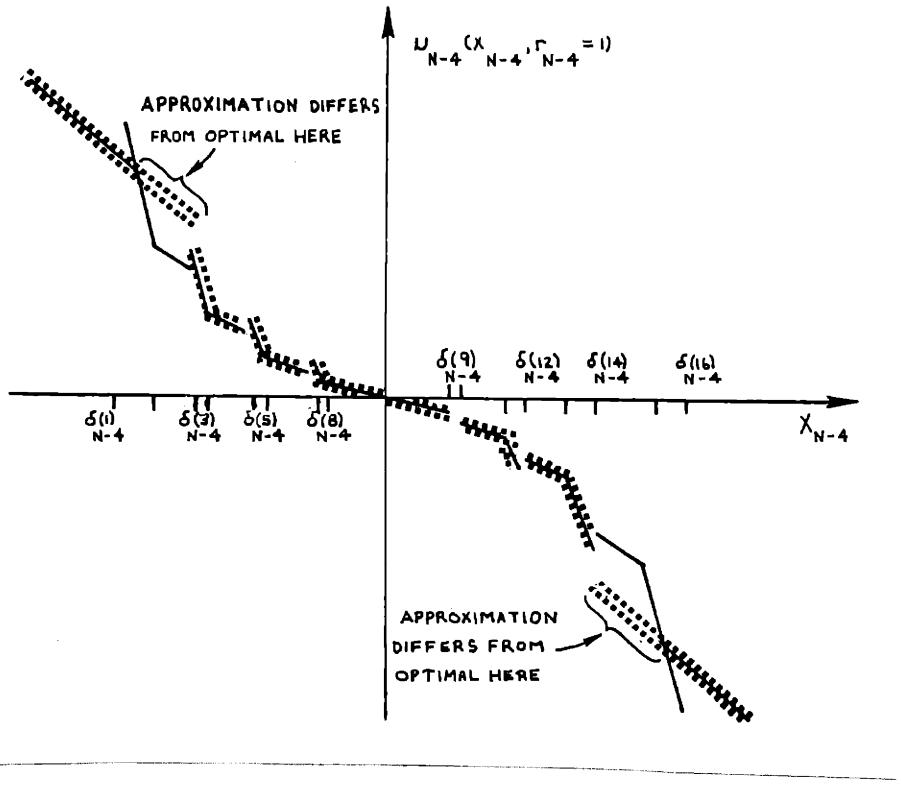

Figure 7.32: Optimal JLQ control law and p =3 approximation at time (N-4) for a problem addressed by Proposition 7.7. The thick checkered line denotes the approximation and the solid line indicates the optimal controller.

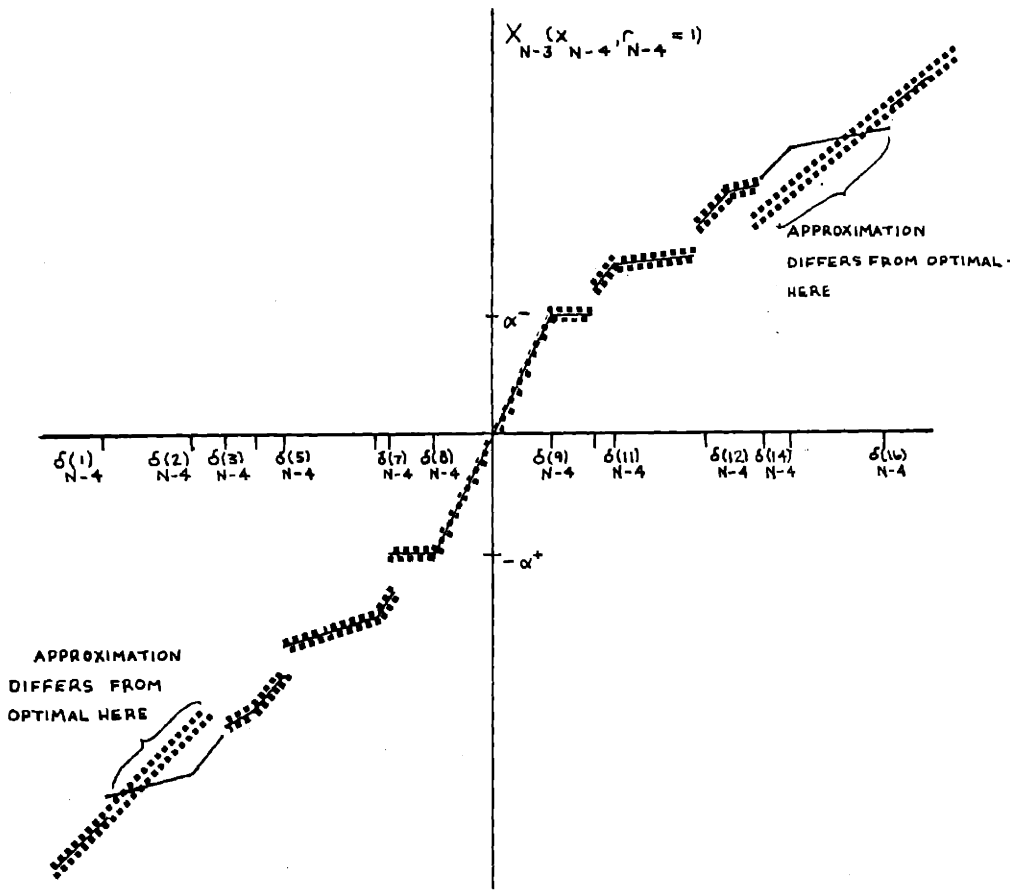

Figure 7.33: Optimal controller and p = 3 approximate controller $x_{N-4} \longmapsto x_{N-3}$ mappings for a problem addressed by Proposition 7.7. The thick checkered line denotes the p = 3 approximation and the solid line indicates the optimal controller.

In sections 7.5 and 7.6 we saw that for fixed k, we have the convergence

$$K_{N-k}(2(k-p+1) + 1:1) \rightarrow K_{N-k}(1;1) = K^{Le}_{N-k}(1) \qquad (7.148)$$

as p grows large. Therefore as p is made larger we also reduce the suboptimality of the approximate controller of Proposition 7.14 at each x_{N-k} outside $(\delta_{N-k}(2(k-p)$, $\delta_{N-k}(2(k+p)+1))$. However, the number of controller pieces that must be calculated and implemented increases linearly with p. Thus we have a tradeoff between controller suboptimality and complexity.

The approximation algorithm that is described above results in time-varying control laws. All 4p+1 pieces of the approximate controller must be computed anew at each time (N-k). We can further simplify the computational burden of controller determination if we use the 4p+1 closest pieces (to zero) of the <u>steady-state</u> controllers, as given by Proposition 7.8 and 7.13, instead of the finite time horizon ones.

<u>Proposition 7.15</u>

1. For JLQ problems satisfying the assumptions of Propositions 7.7., 7.8 or 7.12, 7.13, the optimal JLQ controller can be approximated by a <u>constant</u> suboptimal controller as follows:

(1) In the form r=2 use the steady-state controller, and for $p \geq 1$ fixed, at all times (N-k):

(i) use the steady-state middle-piece control law

$$u_\infty^{<0>} \quad \text{if} \quad \delta_\infty^{<-1>} < x_{N-k} < \delta^{<1>}$$

(ii) use

$$u_\infty^{<1>} \quad \text{if} \quad \delta_\infty^{<1>} < x_{N-k} < \delta_\infty^{<2>}$$

$$u_\infty^{<-1>} \quad \text{if} \quad \delta_\infty^{<-2>} < x_{N-k} < \delta_\infty^{<-1>}$$

(iii) if $p \geq 2$ amd $k \geq 2$, then for $\ell = 1,\ldots,\min(p-1,k-1)$ use

$$u_\infty^{<-2\ell>} \quad \text{if} \quad \delta_\infty^{<-(2\ell+1)>} < x_{N-k} < \delta_\infty^{<-2\ell>}$$

$$u_\infty^{<-(2\ell+1)>} \quad \text{if} \quad \delta_\infty^{<-(2\ell+2)>} < x_{N-k} < \delta_\infty^{<-(2\ell+1)>}$$

$$u_\infty^{<2\ell>} \quad \text{if} \quad \delta_\infty^{<2\ell>} < x_{N-k} < \delta_\infty^{<2\ell+1>}$$

$$u_\infty^{<2\ell+1>} \quad \text{if} \quad \delta_\infty^{<2\ell+1>} < x_{N-k} < \delta_\infty^{<2\ell+2>}$$

(iv) use the steady-state endpiece controllers

$$u_\infty^{Le}(1) \quad \text{if} \quad \delta_\infty^{<-2p>} > x_{N-k}$$

$$u_\infty^{Re}(1) \quad \text{if} \quad \delta_\infty^{<2\ell>} < x_{N-k}$$

(Note: we are using the < > notation, indicating indexing from the middle outwards, that was introduced in section 7.5 and was used in Propositions 7.8 and 7.13).

2. At times $(N-k) > (N-p)$ the resulting controller has $(4k+1)$ pieces. When $(N-k) \leq (N-p)$, the controller has $(4p+1)$ pieces. As the time horizon becomes infinite (as $N-k) \to \infty$), the suboptimality of the approximate controller at each x value is bounded by

$$x^2 \left| K_\infty^{Le}(1) - K_\infty\langle 2(p-1)\rangle \right| \qquad (7.149)$$

and as $p \to \infty$ this error at each x converges to zero, since

$$\lim_{p\to\infty} K_\infty\langle 2(p-1)\rangle = K_\infty^{Le}(1) \ .$$

Proof: Immediate from Propositions 7.8, 713 and 7.14. □

The approximate steady-state controller does not coincide, in general, with the true optimal JLQ controller at any x value. However, for large time horizons the steady-state control law pieces (including the joining points $\{\delta_\infty(i)\}$) do become close to the true optimal. In addition, bounds like those of Proposition 7.14 hold as $(N-k) \to \infty$.

In example 7.2 we compare the controllers and expected performance of the optimal JLQ controller and both the time-varying and steady-state approximate controllers.

Example 7.2 (= 7.1, 6.1, 5.1):

Consider the following system having M=2 forms:

$$x_{k+1} = x_k + u_k \qquad \text{if } r_n=1$$

$$x_{k+1} = 2x_k + u_k \qquad \text{if } r_k=2$$

$$p(1,2:x) = \begin{cases} 1/4 & |x|<1 \\ 3/4 & |x|>1 \end{cases}$$

$p(1,1:x) = 1-p(1,2:x)$ $\quad p(2,2)=1$ $\quad p(2,1)=0$.

We seek to minimize

$$\min_{u_o,\ldots,u_{N-1}} E\left\{ \sum_{k=0}^{N-1} (u_k^2 + x_{k+1}^2) + x_N^2 K_T(r_N) \right\}$$

where $K_T(1) = 0$, $K_T(2) = 3$. The form structure and form transition probability p(1,2:x) for this example were shown in figure 5.4.

This problem was examined earlier in sections 5.3, 5.5, 6.3 and 7.2. It is a "Case 1" problem at time (N-1), in the sense of section 6.5. That is, it satisfies (6.108):

$$(\omega_2-\omega_1)[K_T(2) + Q(2)) - (K_T(1) + Q(1)] = \frac{1}{2}[4-1] = 3/2 > 0.$$

The optimal controller in form 1 at time (N-1) is specified by fact 6.9.

This example problem satisfies the assumptions of facts 7.1, 7.2 and 7.3(1): (7.22) becomes $0 \leq K_T(2) = 3 < 3.236068$. For this example problem, (7.35) is satisfied:

$$a(1) = 1 < \frac{1}{2}(1 + \frac{b^2(1)}{R(1)} \hat{K}_N(2)) = \frac{1}{2}(1 + 7/4) = 11/8.$$

Thus by fact 7.6, we have "situation (1)" of figure 7.16 at time (N-2). Consequently the optimal controller in form 1 at each time is specified by Proposition 7.7 and the limiting controller as $(N-k) \to \infty$ is given by Proposition 7.8.

In table 7.5 the optimal JLQ controller parameters are given for three time steps when the system is in form r=2.

(N-k)	$K_{N-k}(1:2)$	$L_{N-k}(1:2)$	$a(2) - b(2) L_{N-k}(1:2)$
N	3	-	-
N-1	3.2	1.6	.4
N-2	3.231	1.615	.3846
N-3	3.235	1.618	.3824
∞	3.236	1.618	.3820

Table 7.5: Optimal JLQ Controller Parameters in Form r=2 for Example 7.2

The optimal JLQ controller parameters in form r=1 for three time steps and for the 13 pieces of the steady-state controller closest to zero are given in Table 7.6 Only the left sides ($x_{N-k} < 0$) of the controllers are specified since the right-side parameters are obtained by the symmetry relations of Propositions 7.7, 7.8. Also since $L_{N-k}(i:1) = K_{N-k}(i:1)$, the L_{N-k}'s are not listed separately.

Comparing the columns for (N-k) = (N-3) and (N-k) = ∞ in Table 7.6, we see that the values of each parameter $\{K_{N-k}<-i>, H_{N-k}<-i>, i=1,\ldots,5\}$ are very close. This suggests that the approximation in Proposition 7.15 is a good one.

Let us compare the performance of the optimal JLQ controller and the approximate controllers of Propositions 7.14 and 7.15, for a problem where N=3. This is, of course, a limited calculation that has only academic importance. But it does provide some insight into the behavior of the various controllers. From Table 7.6 we see that the optimal JLQ controller[1] is:

(1) Optimal JLQ Controller:

$$u_o(x_o, r_o=1) = \begin{cases} -(.78348)x_o & x_o < -138.13 \\ -(.78352)x_o - .00291 & -138.13 < x_o < -54.686 \\ -(.78347)x_o & -54.686 < x_o < -32.285 \\ -(.78600)x_o - .05350 & -32.285 < x_o < -15.315 \\ -(.78245)x_o & -15.315 < x_o < -7.0110 \\ -x_o - 1.000 & -7.0110 < x_o < -3.2329 \\ -(.6996)x_o & -3.2329 < x_o < 3.2329 \end{cases}$$

[1] We have listed the control laws for $x < 0$, since the $x > 0$ laws are directly obtained by symmetry.

$(N-k)$ =	N	N-1	N-2	N-3	∞
$K^{LM}_{N-k}(1) = K_{N-k}(2k+1:1)=K_{N-k}\langle 0\rangle$	0	.6364	.6949	.6996	.7007
$K_{N-k}(2k:1) = K_{N-1}\langle -1\rangle$	-	1.000	1.000	1.000	1.000000
$K_{N-k}(2k-1:1) = K_{N-k}\langle -2\rangle$	-	.7647	.7807	.78245	.7827063
$K_{N-k}(2k-2:1) = K_{N-k}\langle -3\rangle$	-	-	.7849	.78600	.786190
$K_{N-k}(2k-3:1) = K_{N-k}\langle -4\rangle$	-	-	.7822	.78347	.7836775
$K_{N-k}(2k-4:1) = K_{N-k}\langle -5\rangle$	-	-	-	.78352	.7837182
$K^{Le}_{N-k}(1) = K_{N-k}(1:1)$	0	.7647	.7822	.78348	.7836889
$H_{N-k}(2k:1) = H_{N-k}\langle -1\rangle$	-	2.0000	2.0000	2.00000	2.000000
$H_{N-k}(2k-2:1) = H_{N-k}\langle -3\rangle$	-	-	.1075	.10700	.1069049
$H_{N-k}(2k-4:1) = H_{N-k}\langle -5\rangle$	-	-	-	.00582	.0057804
$G_{N-k}(2k:1) = G_{N-k}\langle -1\rangle$	-	2.75	3.2773	3.32884	3.3340644
$G_{N-k}(2k-2:1) = G_{N-k}\langle -3\rangle$	-	-	.6741	.80594	.8201529
$G_{N-k}(2k-4:1) = G_{N-k}\langle -5\rangle$	-	-	-	.16848	.2049996
$F_{N-k}(2k:1) = F_{N-k}\langle -1\rangle$	-	-1.0000	-1.0000	-1.0000	-1.00000
$F_{N-k}(2k-2:1) = F_{N-k}\langle -3\rangle$	-	-	-.05375	-.05350	-.053452
$F_{N-k}(2k-4:1) = F_{N-k}\langle -5\rangle$	-	-	-	-.00291	-.002890
$\delta_{N-k}(2k) = \delta_{N-k}\langle -1\rangle$	-	-2.75	-3.2773	-3.23288	-3.3345113
$\delta_{N-k}(2k-1) = \delta_{N-k}\langle -2\rangle$	-	-6.7749	-6.9765	-7.00102	-7.0177289
$\delta_{N-k}(2k-2) = \delta_{N-k}\langle -3\rangle$	-	-	-12.5375	-15.31494	-15.595679
$\delta_{N-k}(2k-3) = \delta_{N-k}\langle -4\rangle$	-	-	-31.1791	-32.28468	-32.507589
$\delta_{N-k}(2k-4) = \delta_{N-k}\langle -5\rangle$	-	-	-	-54.68637	-72.108158
$\delta_{N-k}(1)$	-	-6.7749	-31.1991	-138.1297	-∞
$m_{N-k}(1)$	1	5	9	13	∞

Table 7.6: Optimal JLQ Controller Parameters in Form r=1, for Example 7.2

$$u_1(x_1,r_1=1)=\begin{cases}-(.7822)x_1 & x_1 < -31.179\\ -(.7849)x_1 - .05375 & -31.179 < x_1 < -12.538\\ -(.7807)x_1 & -12.538 < x_1 < -6.9765\\ -x_1 - 1.000 & -6.9765 < x_1 < -3.2773\\ -(.6949)x_1 & -3.2773 < x_1 < 3.2773\end{cases}$$

$$u_2(x_2,r_2=1)=\begin{cases}-(.7647)x_2 & x_2 < -6.7749\\ -x_2 - 1.00 & -6.7749 < x_2 < -2.75\\ -(.6364)x_2 & -2.75 < x_2 < 2.75\end{cases}$$

The control laws for the suboptimal controllers of Propositions 7.14 and 7.15 for various p values are as follows:

(2) Proposition 7.14 : Controller with p=2

$$u_o(x_o,r_o=1)=\begin{cases}-(.78348)x_o & x_o < -32.285\\ -(.78600)x_o - .05350 & -32.285 < x_o < -15.315\\ -(.78245)x_o & -15.315 < x_o < -7.0110\\ -x_o - 1.000 & -7.0110 < x_o < -3.23329\\ -(.6996)x_o & -3.23329 < x_o < 3.23329\end{cases}$$

$u_1(x_1,r_1=1)$ and $u_2(x_2,r_2=1)$ as in (1) above.

(3) Proposition 7.14 Controller with p=1

$$u_o(x_o,r_o=1)=\begin{cases}-(.78348)x_o & x_o < -7.0110\\ -x_o - 1.000 & -7.0110 < x_o < -3.23329\\ -(.6996)x_o & -3.23329 < x_0 < 3.23329\end{cases}$$

$$u_1(x_1, r_1=1) = \begin{cases} -(.7822)x_1 & x_1 < -6.9765 \\ -x_1 - 1.0000 & -6.9765 < x_1 < -3.2773 \\ -(.6949)x_1 & -3.2773 < x_1 < 3.2773 \end{cases}$$

$u_2(x_2, r_2=1)$ as in (1), (2) above.

(4) Proposition 7.15 Controller with p=2

$$u_i(x_i, r_i=1) = \begin{cases} -(.78369)x_i & x_i < -32.5076 \\ -(.78619)x_i - .05345 & -32.5076 < x_i < -15.5957 \\ -(.782706)x_i & -15.5957 < x_i < -7.0177 \\ -x_i - 1.0000 & -7.0177 < x_i < -3.3345 \\ -(.700659)x_i & -3.3345 < x_i < 3.3345 \end{cases}$$

for i = 0,1.

$$u_2(x_2, r_2=1) = \begin{cases} -(.78369)x_2 & x_2 < -7.0177 \\ -x_2 - 1.0000 & -7.0177 < x_2 < -3.3345 \\ -(.700659)x_2 & -3.3345 < x_2 < 3.3345 \end{cases}$$

and

$$u_i(x_i, r_i=2) = (-1.618)x_i \qquad \text{for } i=1,2.$$

In table 7.7 the expected costs-to-go from $(x_o, r_o=1)$, for several different x_o values, are listed for these four controllers.

Note that the p=2 controller (1) obtains the same performance as the optimal (when rounded for four digits). The p=1 controller does almost as well. Thus for this example, the (4p+1) - piece controllers of Proposition 7.14 perform well despite their simplicity (relative to

the optimal controller). Note also that using the steady-state control laws in (4) does not seriously degrade performance (compare with (2), which has the same number of pieces).

x_o =	-200	-100	-20	.10	-5	-1
controller (1) (optimal)	31340	7835	313.1	78.25	18.33	.6996
controller (2) p=2	31340	7835	313.1	78.25	18.33	.6996
controller (3) p=1	31340	7835	313.2	78.28	18.33	.7087
controller (4) p=2 steady-state	31340	7835	313.1	78.25	18.33	.7024

Table 7.7: Expected Costs-to-go from $(x_o, r_o=1)$ for Different Controllers in Example 7.2 (entries rounded to four places).

It is important to note that it is the special structure of the JLQ problems which are addressed by Propositions 7.7, 7.8, 7.12 and 7.13 that enables us to implement the approximate controllers denoted above. We are able to obtain the controller pieces that are required by the approximate controllers of Propositions 7.14, 7.15 without using the algorithm of section 7.2 for these special problems.

For the general class of problems of Chapter 5, the optimal JLQ controller will not have the nice structure of the problems of sections 7.5 and 7.6. We will not be able to compute only the (4p+1) closest pieces to zero of the optimal controller. However, the approximations that we used above can be interpreted in a way that suggests an alternate

suboptimal approximate controller that is applicable to the general problem class. This alternate controller does not coincide with the controllers in Propositions 7.14, 7.15. It does not assume the special problem structure possessed by the problems of Sections 7.3 - 7.6.

In figures 7.19 and 7.28 we saw that the cost-to-go pieces that correspond to changing the transition probability pieces that x is in at far future times tend to look alike. That is, using the control to change transition probability pieces at times further and further in the future has less and less effect. In particular, the expected costs of such strategies became close to the endpiece costs (ie., of never changing the transition probability pieces that x is in).

One interpretation of the time-varying controller of Proposition 7.14 is that it is a finite look-ahead approximation of the controllers in Propositions 7.7 and 7.12. It assumes that the transition probability pieces that the x process is located in will either change in the next p time steps, or not at all. The approximate controller ignores eventualities that might occur[1] beyond a fixed planning time. Ignoring the far future, optimality is lost but the computational burden of determining and the complexity of implementing the resulting controller is greatly reduced.

In the remainder of this section we present and demonstrate a general p-step (finite) look ahead approximation to the optimal JLQ controller, that is obtained directly from p iterations of the algorithm in section 7.2 and from the endpiece computations of Proposition 6.1. This p-step look ahead controller is the optimal controller for a different

[1] with respect to the p(1,2:x) piece that x will be in.

problem than the true one.

The true optimal JLQ controller minimizes

$$V_{N-k}(x_{N-k},r_{N-k}) = \min_{u_{N-k},\ldots,u_{N-1}} E\left\{\sum_{\ell=0}^{N-1}\left[\begin{array}{l} x^2_{N-k+\ell+1}\, Q(r_{N-k+\ell+1}) \\ + \\ x_{N-k+\ell+1}\, S(r_{N-k+\ell+1}) \\ + \\ P(r_{N-k+\ell+1}) \\ + \\ u^2_{N-k+\ell}\, R(r_{N-k+\ell}) \end{array}\right] + V_N(x_N,r_N)\right\},$$

for $k \geq 1$ where

$$V_N(x,r) = x^2\, K_T(r) + x\, H_T(r) + G_T(r).$$

The p-step look ahead controller that will be derived in Proposition 7.16 is the optimal solution of the control problem:

$$\tilde{V}_{N-k}(x_{N-k},r_{N-k}) = \min_{u_{N-k},\ldots,u_{N-k+p-1}} E\left\{\sum_{\ell=0}^{p-1}\left[\begin{array}{l} x^2_{N-k+\ell+1}\, Q(r_{N-k+\ell+1}) \\ + \\ x_{N-k+\ell+1}\, S(r_{N-k+\ell+1}) \\ + \\ P(r_{N-k+\ell+1}) \\ + \\ u^2_{N-k+\ell}\, R(r_{N-k+\ell}) \end{array}\right] + V_N(x_{N-k+p},r_{N-k+p})\right\},$$

for $k \geq 1$. That is, we only consider costs p times in the future and

we charge the terminal cost at time N-k+p. At times (N-p),(N-p-1),...,(N-1) the controllers are the same for both problems. At all other times we use the u_{N-p} control law instead of the true problem optimal control u_{N-k}.

The performance of this p-step look ahead controller and of the true JLQ controller can be bounded by the solutions of two other, different control problems.

Proposition 7.16 (p step Look-Ahead Controllers):

1. For any JLQ problem as formulated in (5.1) - (5.6) of section 5.2, the optimal JLQ controller can be approximated as follows:

for $p \geq 1$ fixed,

- at times (N-p),...,(N-1) use the true optimal control laws

$$u_{N-p}(x_{N-p}, r_{N-p}=j), \ldots, u_{N-1}(x_{N-1}, r_{N-1}=j)$$

for each form $j \in \underline{M}$; these laws are computed using the algorithm of section 7.2.

- at all times (N-k) for $k > p$, use the control law

$$u_{N-p}(x_{N-k}, t_{N-k}=j)$$

for each $j \in \underline{M}$.

2. For $k \geq p$, this control law applied at time (N-k) has a fixed number, $m_{N-p}(j)$ of pieces (for each $j \in \underline{M}$). These control laws need only be calculated once. Let us denote the expected cost-to-go from (x_{N-k}, r_{N-k}) that corresponds to this approximate controller by $\tilde{V}_{N-k}(x_{N-k}, r_{N-k})$. It is related to the true optimal JLQ expected cost-to-go, $V_{N-k}(x_{N-k}, r_{N-k})$,

$$V^{L,P}(x_{N-k},r_{N-k}=j) \leq V_{N-k}(x_{N-k},r_{N-k}=j) \leq \tilde{V}_{N-k}(x_{N-k},r_{N-k}=j) \leq V^{U,P}_{N-k}(x_{N-k},r_{N-k}=j)$$

(7.150)

for each $j \in \underline{M}$

where $V^{L,P}(x_{N-k},r_{N-k}=j)$ is the solution of the problem

$$V^{L,P}(x_{N-k},r_{N-k}=j) = \min_{u_{N-k},\ldots,u_{N-k+p+1}} E \left\{ \sum_{\ell=0}^{p-1} \left[x^2_{N-k+\ell+1} Q(r_{N-k+\ell+1}) + x_{N-k+\ell+1} s(r_{N-k+\ell+1}) + P(r_{N-k+\ell+1}) + u^2_{N-k+\ell} R(r_{N-k+\ell}) \right] \right\} \tag{7.151}$$

and $V^{U,P}_{N-k}(x_{N-k},r_{N-k}=j)$ is the solution of the problem

$$V^{U,P}_{N-k}(x_{N-k},r_{N-k}=j) = \min_{u_{N-k},\ldots,u_{N-k+p-2}} E \left\{ \sum_{\ell=0}^{p-2} \left[x^2_{N-k+\ell+1} Q(r_{N-k+\ell+1}) + x_{N-k+\ell+1} S(r_{N-k+\ell+1}) + P(r_{N-k+\ell+1}) + u^2_{N-k+\ell} R(r_{N-k+\ell}) \right] + V^U_T(x_{N-k+p-1},r_{N-k+p-1}) \right\} \tag{7.152}$$

where

$$V_T^U(x_{N-k+p-1}, r_{N-k+p-1}) = \frac{a^2(r_{N-k+p-1})\, R(r_{N-k+p-1})\, x^2_{N-k+p-1}}{b^2(r_{N-k+p-1})}$$

$$+$$

$$\sum_{\ell=p}^{N} E\{P(r_\ell) \,|\, x_\ell = 0\}$$

$$+$$

$$E\{G_T(r_N) \,|\, x_N = 0\} \quad , \tag{7.153}$$

3. Consequently the suboptimality incurred by using the approximate controller instead of the optimal one is bounded as follows:

$$\begin{bmatrix} \tilde{V}_{N-k}(x_{N-k}, r_{N-k}) \\ -V_{N-k}(x_{N-k}, r_{N-k}) \end{bmatrix} \leq \begin{bmatrix} V^{U,p}_{N-k}(x_{N-k}, r_{N-k}) \\ -V^{L,p}(x_{N-k}, r_{N-k}) \end{bmatrix} , \tag{7.154}$$

□

Proof: See Appendix C.18.

Note that $V^{L,p}(x_{N-k}, r_{N-k})$ in (7.151) is the optimal expected cost for a problem where no costs are incurred after time (N-p). The cost $V^{L,p}(x_{N-k}, r_{N-k})$ can be computed using p-steps of the algorithm of section 7.2, if we set the terminal costs to zero:

$$K_T(i) = H_T(j) = G_T(j) = 0, \qquad \forall\, j \in \underline{M} .$$

This cost will nost exceed the optimal expected cost-to-go from (x_{N-k}, r_{N-k}) for the true problem (since in the true problem $V_{N-p}(x_{N-p}, r_{N-p}) \geq 0$).

The upperbound cost function $V^{U,p}_{N-k}(x_{N-k}, r_{N-k})$ in (7.152) corresponds to the true problem with the added constraint that x be driven to zero in p steps, and that x be kept at zero thereafter. This problems's solution will exceed the optimal expected cost-to-go of the true problem because of the extra constraint. The first term in (7.153) is the $u^2_{N-k+p-1}\, R(r_{N-k+p-1})$ cost that results from driving x_{N-k+p} to zero. The second and third terms are costs incurred by keeping x at zero. Note that they are zero for the problems discussed in chapter 6.

We conclude this section with an example that demonstrates the use of the section 7.2 algorithm for a more general problem than those of chapt. 6 and that illustrates the application of the preceding proposition.

Example 7.3 :

Consider a system whose form structure is as shown in figure 7.34. This system might represent the following situation:

$r_k = 1$	normal operation
$r_k = 2$	degraded operation (repairable failure)
$r_k = 3$	nonrepairable failure
p(1,2:x)	one-step probability of repairable failure occurrence (x-dependent)
p(2,1)	one-step probability of repair
p(1,3:x)	one-step probability of nonrepairable system failure occurrence.

The form transition probabilities from r_k=1 are piecewise constant in x (but p(2,1), p(2,2) and p(3,3) are x-independent).

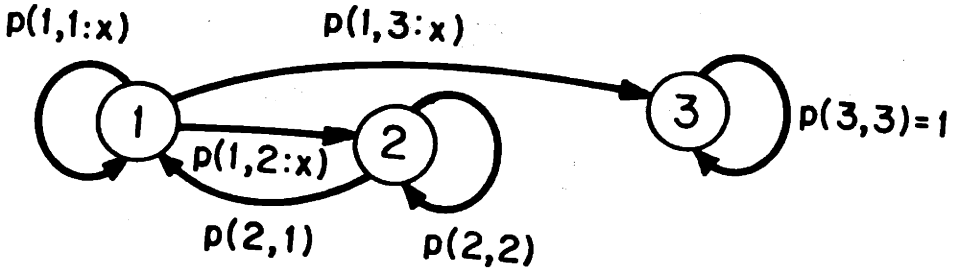

Figure 7.34: Form Structure for Example 7.3. Form r=1 = Normal Operation, r=2=Degraded Operation, r=3=System Failure (Same as Example 5.2.)

$$\Big(p(1,1{:}x)\ p(1,2{:}x)\ p(1,3{:}x)\Big) = \begin{cases} (.89 \quad .1 \quad .01) & \text{if } |x| < 1 \\ (.7 \quad .2 \quad .1) & \text{if } 1<|x| < 2 \\ (0 \quad .2 \quad .8) & \text{if } |x| > 2 \end{cases}$$

$$p(2,1)=p(2,2)= .5$$

Thus the numbers of pieces in each of the form transition probabilities are

$$\bar{\nu}_{11} = \bar{\nu}_{12} = 5$$

$$\bar{\nu}_{12} = 3$$

$$\bar{\nu}_{21} = \bar{\nu}_{22} = \bar{\nu}_{23} = \bar{\nu}_{31} = \bar{\nu}_{32} = \bar{\nu}_{33} = 1 .$$

The x-dependent transition probabilities are shown in figure 7.35.

The dynamic equations of this system are:

$x_{k+1} = x_k + u_k$ in form r=1 (normal operation)

$x_{k+1} = x_k + \frac{u_k}{2}$ in form r=2 (degraded operation)

$x_{k+1} = x_k$ in form r=3 (system failure),

That is, $b(1) = 1 \quad b(2) = 1/2 \quad b(3) = 0$

$a(1) = a(2) = a(3) = 1$

The cost-parameters are

$Q(1) = Q(2) = 1$

$Q(3) = 0$

$R(1) = 2$

$R(2) = R(3) = 1$

$K_T(1) = K_T(2) = K_T(3) = 0$

$G_T(3) = 1000$ (penalty for system failure)

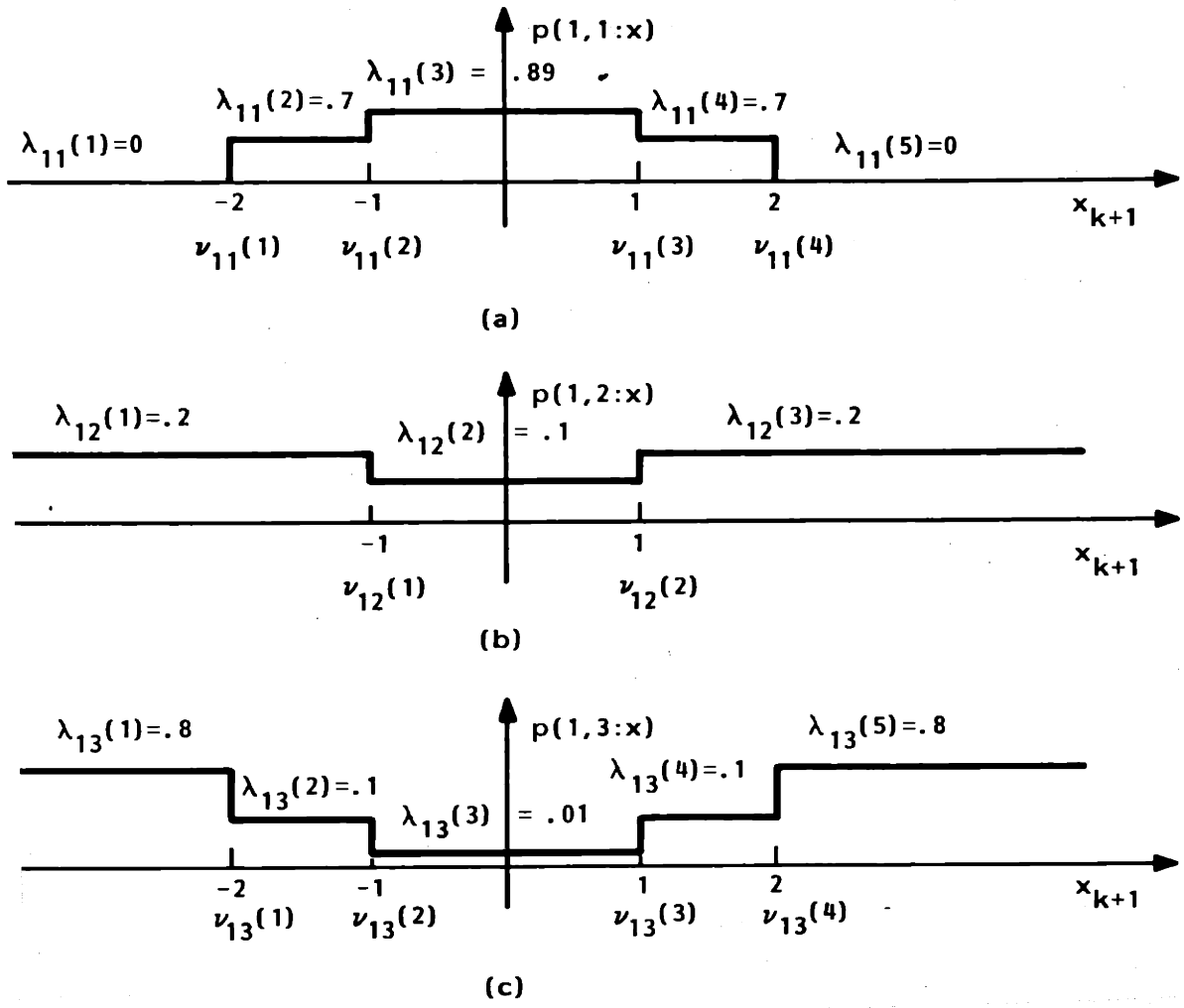

Figure 7.35: Piecewise-Constant Form Transition Probabilities from Form r =1 in Example 7.3; (a) p(1,1=x) with ν_{11}=5 Pieces, (b) p(1,2=x) with ν_{12}=3 Pieces, (c) p(1,3=x) with ν_{13}=5 Pieces

Note that we are willing to spend more control energy when the system is in a degraded mode than when it is operating normally.

Clearly we have at all (N-k)

$$V_{N-k}(x_{N-k}, r_{N-k}=3) = 1000.$$

$$u_{N-k}(x_{N-k}, r_{N-k}=3) = 0.$$

If the nonrepairable failure occurs (that is, if we enter form 3), then we are charged $G_T(3) = 1000$ regardless of what we do. The optimal strategy is to shut the system off (set u=0).

Using the algorithm of section 7.2 we can compute the optimal controllers in forms r=1 and 2, backwards in time. We find that at time k = (N-1), the numbers of pieces of the optimal JLQ controllers in each form are

$$m_{N-1}(1) = 5 \qquad m_{N-1}(2) = 1 \qquad m_{N-1}(3) = 1 \quad .$$

In form $r_{N-1} = 2$,

$$V_{N-1}(x_{N-1}, r_{N-1}=2) = .8\, x_{N-1}^2$$

$$u_{N-1}(x_{N-1}, r_{N-1}=2) = -.4\, x_{N-1}$$

$$x_N(x_{N-1}, r_{N-1}=2) = .8\, x_{N-1}$$

The controller in form $r_{N-1}=1$ is summarized by table 7.8 below.

for	$V_{N-1}(x_{N-1}, r_{N-1}=1)$	$u_{N-1}(x_{N-1}, r_{N-1}=1)$	$x_N(x_{N-1}, r_{N-1}=1)$
$x_{N-1} < -21.934$	$(.18182)x_{N-1}^2 + 800$	$-(.09091)x_{N-1}$	$(.90909)x_{N-1}$
$21.934 < x_{N-1} < -1.495$	$2x_{N-1}^2+4x_{N-1}+12.99$	$-x_{N-1} - 1^*$	-1^+
$-1.495 < x_{N-1} < 1.495$	$(.66221)x_{N-1}^2 +10$	$-(.3311)x_{N-1}$	$(.6689)x_{N-1}$
$1.495 < x_{N-1} < 21.934$	$2x_{N-1}^2 - 4x_{N-1}+12.99$	$-x_{N-1} + 1^-$	1^-
$21.934 < x_{N-1}$	$(.18182)x_{N-1}^2 + 800$	$-(.09091)x_{N-1}$	$(.90909)x_{N-1}$

Table 7.8: Optimal Controller at time k = N-1 in form $r_{N-1}=1$, for example 7.3.

In form $r_{N-1}=1$ the optimal controller actively hedges-to-a-point for certain x_{N-1} values. Specifically, from $(x_{N-1}, r_{N-1}=1)$ the optimal controller

- drives $|x_N| > 2$ for $|x_{N-1}| > 21.934$
- hedges-to-a-point, obtaining

  $x_N = 1^+$ for $-21.934 < x_{N-1} < -1.495$

  $x_N = 1^-$ for $1.495 < x_{N-1} < 21.934$

- drives $|x_N| < 1$ for $|x_{N-1}| < 1.495$.

The optimal controller from $(x_{N-1}, r_{N-1}=1)$ avoids the values in the intervals (-19.93999, -1) and (1,19.9399).

Note that the controller completely avoids the intervals (-2,-1) and (1,2) where the one-step probabilities of normal operation and nonrepairable failure take intermediate values[1]. Either the controller resigns

[1] See figure 7.35

itself to failure of some kind (for $|x_{N-1}| > 21.934$) or it forces the system into the region of x_{N-1} values where the probabilities of both nonrepairable and repairable failures are lowest.

If the repairable actuator failure has already occurred (that is, $r_{N-1}=2$), then the system is equally likely to be in forms 1 or 2 at the next time regardless of the control that is applied. Thus the single-piece structure of $u_{N-1}(x_{N-1},r_{N-1}=2)$ results. Another way of viewing this is as follows: when $r_{N-1}=2$, the conditional cost $\hat{V}_N(x_N|r_{N-1}=2)$ has no discontinuities and therefore there is no hedging-to-a-point from $(x_{N-1},r_{N-2}=1)$. Since $\hat{V}_N(x_N|r_{N-1}=2)$ has only one piece, the same control law is used for all x_{N-1} when $r_{N-1}=2$. Thus there is no region of avoided x_N values from $(x_{N-1},r_{N-1}=2)$.

Using the algorithm of section 7.2 again, we find that at time k = (N-2), the numbers of pieces of the optimal controller are

$$m_{N-2}(1) = 5 \qquad m_{N-2}(2) = 5 \qquad m_{N-2}(3) = 1.$$

In form $r_{N-2}=1$ we have the controller that is summarized in table 7.9.

for $V_{N-2}(x_{N-2},r_{N-2}=1$	$u_{N-2}(x_{N-2},r_{N-2}=1)$	$x_{N-1}(x_{N-2},r_{N-2}=1)$
$x_{N-2} < -22.630$	$(.30508)x_{N-2}^2+800$	$-(.15254)x_{N-2}$	$(.84746)x_{N-2}$
$-22.630 < x_{N-2} < -1.8297$	$2x_{N-2}^2+4x_{N-2}+22.559$	$-x_{N-2}$ $-1+$	-1^+
$-1.8297 < x_{N-2} < 1.8297$	$(.90691)x_{N-2}^2+18.9$	$-(.45346)x_{N-2}$	$(.54654)x_{N-2}$
$1.8297 < x_{N-2} < 22.630$	$2x_{N-2}^2 - 4x_{N-2}+22.559$	$-x_{N-2} + 1^-$	1^-
$22.630 < x_{N-2}$	$(.30508)x_{N-2}^2 + 800$	$-(.15254)x_{N-2}$	$(.84746)x_{N-2}$

Table 7.9: Optimal Controller at time k = N-2 in form $r_{N-2}=1$, for example 7.3

In form $r_{N-2}=1$ the optimal controller does the following:

- keeps $|x_{N-1}| > 19.1803$ if $|x_{N-2}| < -22.630$
- hedges-to-a-point, obtaining

$$x_{N-1} = -1^{+} \quad \text{for} \quad -22.630 < x_{N-2} < -1.8297$$

$$x_{N-1} = 1^{-} \quad 1.8297 < x_{N-2} < 22.630$$

- keeps $|x_{N-1}| < 1$ and

$$|x_N| < 1 \quad \text{if} \quad |x_{N-2}| < 1.8297 \quad .$$

The optimal controller from $(x_{N-2}, r_{N-2}=1)$ avoids (-19.1803,-1) and (1,19.1803). Thus as at time k = N-1, the optimal controller from $r_{N-2}=1$ completely avoids the intermediate-level failure risk regions (-2,-1) and (1,2).

In table 7.10 the optimal controller from $r_{N-2}=2$ is summarized. Here the optimal controller does not hedge-to-a-point with u_{N-2} since $\hat{V}_{N-1}(x_{N-1} | r_{N-2}=2)$ has no discontinuities. However, there are intervals of avoided x_{N-1} values:

(-23.607123, - 20.41)

(20.41, 23.607123) .

for	$V_{N-2}(x_{N-2}, r_{N-2}=2)$	$u_{N-2}(x_{N-2}, r_{N-2}=2)$	$x_{N-1}(x_{N-2}, r_{N-2}=2)$
$x_{N-2} < -32.406$	$(1.0861)x_{N-2}^2+400$	$-(.54305)x_{N-2}$	$(.72848)x_{N-2}$
$-32.406 < x_{N-2} < 3.4428$	$(1.5)x_{N-2}^2+(1.25)x_{N-2}+5.845$	$-(.75)x_{N-2}-.3125$	$(.625)x_{N-2}-.15625$
$-3.4428 < x_{N-2} < 3.4428$	$(1.2082)x_{N-2}^2 + 5$	$-(.60411)x_{N-2}$	$(.697945)x_{N-2}$
$3.4428 < x_{N-2} < 32.406$	$(1.5)x_{N-2}^2-1.25x_{N-2}+5.845$	$-(.75)x_{N-2}+.3125$	$(.625)x_{N-2}+.15625$
$32.406 < x_{N-2}$	$(1.0861)x_{N-2}^2 + 400$	$-(.54305)x_{N-2}$	$(.72848)x_{N-2}$

Table 7.10: Optimal controller at time k = N-2 in form $r_{N-3} = 1$, for example 7.3

for	$V_{N-3}(x_{N-3}, r_{N-3}=1)$	$u_{N-3}(x_{N-3}, r_{N-3}=1)$	$x_{N-2}(x_{N-3}, r_{N-3}=1)$
$x_{N-3} < -39.800$	$(.34521)x_{N-3}^2+880$		$(.8274)x_{N-3}$
$-39.800 < x_{N-3} < -23.156$	$(.4)x_{N-3}^2+(.2)x_{N-3}+801.16$	$-.2\,x_{N-3}-.05$	$.8x_{N-3}-.05$
$-23.156 < x_{N-3} < -1.9590$	$2x_{N-3}^2 + 4x_{N-3} + 31.2390$	$-x_{N-3}-1^+$	-1^+
$-1.9590 < x_{N-3} < 1.9590$	$(.97906)x_{N-3}^2+27.321$	$-(.48953)x_{N-3}$	$(.51047)x_{N-3}$
$1.9590 < x_{N-3} < 23.156$	$x_{N-3}^2 - 4x_{N-3} +31.2390$	$-x_{N-3} + 1^-$	1^-
$23.156 < x_{N-3} < 39.800$	$(.4)x_{N-3}^2-.2x_{N-3}+801.16$	$-.2x_{N-3}+.05$	$.8x_{N-3}+.05$
$39.800 < x_{N-3}$	$(.34521)x_{N-3}^2 + 880$	$-(.17260)x_{N-3}$	$(.8274)x_{N-3}$

Table 7.11: Optimal Controller at time k = (N-3) in form $r_{N-3} = 1$, for example 7.3

Using the algorithm of section 7.2 once again, we find that at time k = (N-3):

$$m_{N-3}(1) = 7 \qquad m_{N-3}(2) = 9 \qquad m_{N-3}(3) = 1.$$

In form r_{N-3} =1, the optimal controller is given in table 7.11. In form r_{N-3}=1 the optimal controller hedges-to-a-point for $|23.156| < x_{N-3} < |1.950|$. The optimal controller avoids the intervals of x_{N-2} values:

(-32.93052, -31.89)	(31.89, 32,93052)
(-18.5748, -1)	(1, 18.5748)

Once again, the optimal controller in form 1 avoids the regions of x values that correspond to an intermediate level of failure risk.

The optimal controller from r_{N-3}=2 is given in table 7.12. As before, the optimal controller form $(x_{N-3}, r_{N-3}=2)$ does not hedge-to-a-point. The regions of x_{N-2} values that are avoided by the optimal JLQ controller from $(x_{N-3}, r_{N-3}=2)$ are

(-32.962, -31.8608)	(31.8608, 32.962)
(-24.1187, -21.2383)	(21.2383, 24.1187)

We will compare the performance of the optimal controller above to that of a p = 1 step look-ahead suboptimal controller. As specified by Proposition 7.16, the p=1 step look-ahead controller uses the optimal controller of time k=(N-1) at <u>all</u> times. In table 7.13 we compare the expected cost-to-go achieved by the optimal controller and the p=1 suboptimal for a N=3 time step problem.

for	$V_{N-3}(x_{N-3}, r_{N-3}=2)$	$u_{N-3}(x_{N-3}, r_{N-3}=2)$	$x_{N-2}(x_{N-3}, r_{N-3}=2)$
$x_{N-3} < -46.935$	$(1.1908)x_{N-3}^2+600$	$-(.5954)x_{N-3}$	$(.7023)x_{N-3}$
$-46.935 < x_{N-3} < -35.511$	$(1.2893)x_{N-3}^2+(.42355)x_{N-3}+402.91$	$-(.64465)x_{N-3}-.10589$	$(.6777)x_{N-3}-.0529$
$-35.511 < x_{N-3} < -5.4816$	$(1.6296)x_{N-3}^2+(1.5556)x_{N-3}+13.938$	$-(.81482)x_{N-3}-.3889$	$(.5926)x_{N-3}-.1945$
$-5.4816 < x_{N-3} < -2.7709$	$(1.5773)x_{N-3}^2+(1.2114)x_{N-3}+13.626$	$-(.78863)x_{N-3}-.3028$	$(.6057)x_{N-3}-.1514$
$-2.7709 < x_{N-3} < 2.7709$	$(1.3587)x_{N-3}^2+11.95$	$-(.67933)x_{N-3}$	$(.6603)x_{N-3}$
$2.7709 < x_{N-3} < 5.4816$	$(1.5773)x_{N-3}^2-(1.2114)x_{N-3}+13.626$	$-(.78863)x_{N-3}+.3028$	$(.6057)x_{N-3}+.1514$
$5.4816 < x_{N-3} < 35.511$	$(1.6296)x_{N-3}^2-(1.5556)x_{N-3}+13.938$	$-(.81482)x_{N-3}+.3889$	$(.5926)x_{N-3}+.1945$
$35.511 < x_{N-3} < 46.935$	$(1.2893)x_{N-3}^2-(.42355)x_{N-3}+402.91$	$-(.64465)x_{N-3}+.10589$	$(.6777)x_{N-3}+.0529$
$< x_{N-3} < 46.935$	$(1.1908)x_{N-3}^2 + 600$	$-(.5954)x_{N-3}$	$(.7023)x_{N-3}$

Table 7.12: Optimal Controller at time k = (N-3) in form $r_{N-3}=2$, for example 7.3.

x_o =	±1	±5	±20	±40
Optimal expected cost from $r_o = 1$	28.3001	61.239	751.239	1432.34
p=1 suboptimal expected cost from $r_o = 1$	28.4229	61.2765	751.2765	1465.57
optimal expected cost from $r_o = 2$	13.3087	47.0015	634.666	2448.85
p=1 suboptimal expected cost from $r_o = 2$	13.4635	52.8952	740.795	2611.25
suboptimality of p=1 controller from $r_o = 1$	.1228 (0.43%)	.0375 (0.06%)	.0375 (0.005%)	33.33 (2.33%)
suboptimality of p = 1 controller from $r_o = 2$	.1548 (1.157%)	5.8937 (12.54%)	106.129 (16.72%)	162.4 (6.63%)

Table 7.13: Optimal Expected Costs Obtained by the Optimal and p=1 Look-ahead controllers.

The suboptimal controller performs well at each x_o value when the system begins in $r_o = 1$. This is because in form 1 the p=1 suboptimal controller can hedge-to-a-point. In form 2 the p=1 controller has a single control law; thus the suboptimal controller cannot hedge-to-a-point until the system is repaired (that is, until it leaves form r=2). Despite this fact the p=1 controller performs well for $r_o=2$.

In this section we have presented and illustrated via examples certain suboptimal approximations to the optimal JLQ controller. We first developed an approximate controller for the single-form transition control problems that were described in Propositions 7.7,7.8,7.12 and 7.13. Then a p-step look-ahead controller was described in Proposition 7.16. This p-step suboptimal controller is applicable for the general class of JLQ problems of chapter 5.

7.8 Summary of Part III

In part III (chapters 5, 6 and 7) we have considered scalar JLQ control problems that involve state-dependent structural changes. This class of nonlinear stochastic control problems yields controller designs which endow systems with fault-tolerance, in that the controller takes into account known system limitations and failure likelihoods so as to achieve the best tradeoff between system reliability and performance goals. The optimal controller attempts to minimize the cost incurred by the usual LQ regulator action, and by driving the system state to regions where the likelihoods of undesirable form shifts are reduced. We have formulated and solved a class of scalar-in-x, noiseless JLQ problems with x-dynamics that would be linear, if not for random x-dependent jumping parameters. These problems possess form transition probabilities that depend upon x in a piecewise-constant way. For this class of problems we have developed a procedure that calculates the optimal expected costs-to-go and control laws "off-line", in advance of system operation. The procedure determines the optimal controller inductively, backwards in time (for finite time-horizon problems).

The basic idea of the solution procedure is simple, and the solution structure is conceptually straightforward. However, the notation that is required to describe the solution becomes quite complex. Essentially, the nonlinearity of the system dynamics (due to the x-dependence of the form transition probabilities) is converted into computational complexity in the determination of the controller. At each time the optimal controller is obtained by calculating and comparing growing number of quadratic functions. These quadratic functions are computed via Riccati-

like difference equations. It is the piecewise-constant structure of the form transition probabilities that allows us to do this. In chapter 5 the general problem under consideration was formulated and one stage of a simple problem was solved from first principles. Guided by intuition gained from this example, a general one-stage solution procedure was developed in section 5.4. We established that the optimal control laws are piecewise-linear in x (with x^1, x^0 terms) and the optimal expected costs-to-go are piecewise-quadratic in x (with x^2, x^1, x^0 terms). The different controller pieces arise from using the control to actively hedge. Intuitively, at each stage the optimal controller must take into account what the expected cost of driving x into different regions will be, where different values of the form transition probabilities apply. As the control problem is solved backwards in time (using dynamic programming), the controller must take into account what the effects of active hedging will be at the intervening times. The number of pieces of the controller grows additively. This additive increase depends upon the number of different forms into which the system can change (from its current one) and the number of pieces in the relevant piecewise-constant-in-x transition probabilities. Thus there is a tradeoff between the accuracy of the modeling of failure probability state-dependence (via piecewise-constant approximations) versus the computational burden of control law determination and the complexity of the controller. In chapter 5 we also identified several basic qualitative properties of the optimal JLO controller. These included hedging-to-a-point, regions of avoidances and the endpieces and middle-pieces of the expected costs-to-go and control laws.

In chapter 6 we investigated these properties in detail. In particular we examined the behavior of the optimal control laws and expected

costs-to-go when x is far from zero ("endpieces")[1] and when x is near zero ("middlepieces")[2]. Over these regions of x values, $V_k(x_k, r_k=j)$ can be computed from sets of recursive difference equations.

The equations specifying these endpieces are middlepieces of the optimal controller are the same as those that solve certain corresponding x-independent JLQ problems (as in chapter 3). Upper and lower bounds on the expected optimal cost-to-go when x is between these endpiece and middlepiece domains were also obtained[2]. In chapter 7 we used the combinatoric properties established in chapter 5 and the results of chapter 6 to construct an algorithm for the efficient computation of the optimal controller. This algorithm was presented in flowchart form and described in detail. The basic idea is to compute the optimal cost function $V_k(x_k, r_k=j)$ at time stage k (and in each form j) one piece at a time, starting on the left (with the left end-piece). Using Propositions 5.2 and 5.3, the number of calculations and computations that this solution algorithm must make is greatly reduced from those of the "brute force" solution technique in chapter 5. This solution algorithm (developed in section 7.2) is applicable to all problems satisfying the requirements of Proposition 5.1. The class of JLQ problems addressed by Proposition 5.1 is extremely rich. The resulting optimal controllers can exhibit a wide variety of qualitative behaviors. Analytical characterizations of these JLQ controllers that are sufficiently general to encompass the entire problem class tend to be uninformative, since so many diverse behaviors must be simultaneously considered. We chose, therefore, to focus our attention on problems that lend

---

[1] For all problems of chapter 5.

[2] For problems with purely quadratic costs (no x_k^1 and x_k^o terms).

insight into the kinds of qualitative JLQ controller behaviors that are appropriate in fault-tolerant control applications. Our vehicle for doing this was the single form-transition problem that was developed in sections 6.5 and 6.6 and specialized to two archetypical problems in sections 7.3-7.6. In one of these classes the two goals of high performance and high reliability are commensurate. In the other class they are at cross purpose. We examined the parametric dependence of the hedging regions, regions of avoidance, stability properties, and local minima in the expected costs-to-go for these controllers. Under certain assumptions for algorithm of section 7.2 reduces to the solution of (increasingly many) sets of difference equations as N-k increases. This makes these problems amenable to further detailed analysis, and it lets us illustrate some of the controller properties and qualitative issues that arise from the use of control to achieve both reliability and performance goals.

For the general problem of Part III, as the time horizon of the problem becomes infinite the number of pieces in the optimal controller becomes infinite. That is, the optimal infinite time-horizon problem cannot be obtained by any finite algorithm. For the two problem classes of sections 7.5 and 7.6 we could analyze the infinite time horizon behavior of the controller and obtain the optimal steady-state controllers as $(N-k)\rightarrow\infty$, since the optimal controller at each time can be obtained from the solution of increasingly many difference equations without making the comparisons and tests in the solution algorithm (of section 7.2) that are needed in general.

The steady-state solutions that are obtained for these two problem classes exhibit a structure that suggests a "natural" approximation to the steady-state optimal controller (both for these problems and the general

class of problems in Chapter 5). These approximations correspond to "finite look-ahead" controllers which ignore eventualities that might occur beyond some fixed planning time. By ignoring the far future, optimality is lost in these controllers but the computational burden of determining them and the complexity (and cost) of their implementation is reduced. This finite look-ahead controller was developed in section 7.7.

In conclusion, in this part of the thesis we have formulated and solved a class of nonlinear discrete-time stochastic control problems. The optimal controller is obtained recursively, backwards in time, by an algorithm which was presented in flowchart form. Less complex but suboptimal approximations of this optimal controller were also presented. For special classes of these problems, the optimal controller algorithm collapses to a set of recursive difference equations. These special problems are examined in detail. In the next part of this thesis we will extend the results of Part III to address more general problems than those of chapter 5.

PART IV

EXTENSIONS TO THE SCALAR X-DEPENDENT NOISELESS JLQ PROBLEM

8. THE JUMP LINEAR PIECEWISE-QUADRATIC CONTROL PROBLEM

8.1 Introduction

In this part of the thesis we extend the range of control problems for which the methods of Parts II and III are applicable. In this chapter we modify the scalar JLQ problem of chapters 5-7 to include a more general class of x-operating and terminal costs. Specifically, we consider x operating costs $Q(x_k,r_k)$ and terminal costs $Q_T(x_N,r_N)$ that are piecewise -quadratic in x (with x^2, x^1 and x^0 terms); these nonnegative costs may have constant pieces, linear pieces and quadratic pieces that are concave-up $\left(\frac{\partial^2 Q}{\partial x^2} > 0\right)$ or concave-down $\left(\frac{\partial^2 Q}{\partial x^2} < 0\right)$.

We call this the jump linear piecewise quadratic (JLPQ) control problem. Our study of this class of problems is motivated by two factors:

- The solution of the JLPQ control problem is a necessary step in the extension of the JLQ solution to systems having additive input noise and more general x-dependent form transition probabilities; we will use the results of this chapter in Chapter 9.
- The JLPQ formulation broadens the range of problems that can be addressed by the methodology of Part III.

In particular, the JLPQ formulation includes x-operating costs that are

- constant in x

  eg: $Q(x,j) = 100$

- piecewise-constant in x with discontinuities

  eg: $$Q(x,j) = \begin{cases} 100 & |x| > 10 \\ 0 & |x| \leq 10 \end{cases}$$

- piecewise-quadratic in x with concave-down pieces

  eg: $$Q(x,j) = \begin{cases} x^2 & |x| > .5 \\ -x^2-x & -.5<x<0 \\ -x^2+x & 0<x<.5 \end{cases}$$

Example problems with these kinds of x costs will be examined in this chapter.

The basic structure of the optimal controllers for the JLPQ problem is similar to those for the JLQ problems. The optimal expected costs-to-go are piecewise-quadratic and the control laws are piecewise-linear in x_k, in each form. The derivation of the JLPQ solution uses the same idea that was used in Chapter 5:

> We break up the JLPQ problem into constrained subproblems that are easier to solve, and then we compare these subproblem solutions to determine the optimal controller.

At each time step k, the control problem involving the search for $V_k(x_k, r_k=j)$ is transformed into the comparison of many constrained -in-x_{k+1} JLQ control problems with x-independent form transitions and quadratic x-costs. One such constrained problem arises over each interval of x_{k+1} values having

- constant form transition probabilities

  $$p(j,i;x_{k+1}) \qquad (\forall i \in C_j)$$

- a quadratic expected cost-to-go (with x^2_{k+1}, x^1_{k+1} and x^o_{k+1} terms),

  $$V_{k+1}(x_{k+1}, r_{k+1}=i) \qquad \text{for all } i \in C_j$$

- a quadratic x-cost (with x^2_{k+1}, x^1_{k+1} and x^o_{k+1} terms), $Q(x_{k+1}, r_{k+1}=i)$ for all $i \in C_j$.

The number of costs-to-go that must be compared at each stage, and the number of pieces, $m_k(j)$, in the optimal expected cost-to-go $V_{k+1}(x_{k+1}, r_{k+1}=j)$ may grow at a <u>faster than linear</u> rate with the number of form transition probability pieces and x-cost pieces (unlike the JLQ problem of Chapter 5). The "piecewise" structure of the optimal expected costs-to-go and control laws for the JLPQ problems of this chapter is caused by both

- the piecewise-constant nature of the form transition probabilities (as in Chapters 5-7).

and

- the piecewise-quadratic nature of the x-costs.

We develop in this chapter a recursive procedure for the determination of the optimal expected costs-to-go and control laws when the system is in each form. This procedure can be done off-line, in advance of system operation. It is carried out by pursuing a sequence of computations and comparisons that are described in a flowchart. This solution procedure is a generalization of the algorithm of section 7.2. Certain modifications are necessitated by the qualitative controller properties which result from the piecewise nature of the x-costs $Q(x_{k+1},r_{k+1})$ and $Q_T(x_N,r_N)$.

Although the basic idea of this chapter is simple, the deviation and presentation of the general result involves unavoidably complicated notation and "bookkeeping" problems. For this reason this chapter has been organized as follows:

1. In Section 8.2 the general JLPQ problem is formulated.
2. In Section 8.3 we solve for the last-stage controller for four JLPQ control problem examples, and we we compare these results.

3. Guided by the intuition gained from these examples, a general one-step solution procedure is developed in Section 8.4. We state and prove Proposition 8.1 which is a generalization (to JLPQ problems) of Proposition 5.1.

4. In Section 8.5 we establish a number of qualitative properties of the JLPQ controller (essentially generalization of the results of Chapters 5 and 6). These results are then used to develop the solution algorithm, which is presented in the flowcharts of figures 8.5-8.12.

5. In Section 8.6 we illustrate the use of this algorithm by solving for the k=(N-2) controller for the problem of example 8.2.

From the study of the optimal JLPQ controllers developed here we can gain additional insight into the structures of controllers that use active hedging, and into the qualitative effects of their control actions. The algorithm of Section 8.5 provides the basis for the approximate solution of the scalar JLPC (jump-linear-piecewise-convex) control problems of the next chapter. These problems have x-costs, form transition probabilities and additive input noise densities that are piecewise-convex or concave in x. They can be solved approximately using the algorithm of section 8.5 and certain approximations motivated by the qualitative results of this chapter.

8.2 JLPQ Problem Formulation

In this section we formulate the jump linear piecewise quadratic (JLPQ) control problem that is addressed in this chapter. As in Part III, we restrict our attention to the time-invariant case so as to simplify notation somewhat. All of the results of this chapter can be directly extended to the time-varying case.

Consider the discrete-time jump linear system

$$x_{k+1} = a(r_k)x_k + b(r_k)u_k \tag{8.1}$$

$$P_r\{r_{k+1}=j \,|\, r_k=i,\ x_{k+1}=x\} = p(i,j;x) \tag{8.2}$$

$$x(k_0) = x_0 \qquad r(k_0) = r_0 \ .$$

Each transition probability $p(i,j;x)$ of the form process is assumed to be piecewise-constant in x, having a finite number of pieces $\bar{\nu}_{ij}$. That is, the real line is partitioned into $\bar{\nu}_{ij}$ disjoint intervals with the transition probabilities taking constant values over each interval:

$$p(i,j;x) = \lambda_{ij}(s) \tag{8.3}$$

if

$$\nu_{ij}(s-1) < x < \nu_{ij}(s) \tag{8.4}$$

where

$$s = 1,2,\ldots,\bar{\nu}_{ij}$$

$$-\infty \triangleq \nu_{ij}(0) < \nu_{ij}(1) < \ldots < \nu_{ij}(\bar{\nu}_{ij}-1) < \nu_{ij}(\bar{\nu}_{ij}) \triangleq \infty.$$

The grid points $\nu_{ij}(s)$ may be different for each pair $(i,j) \in \underline{M}x\underline{M}$. For all $s=1,2,\ldots,\bar{\nu}_{ij}$,

$$\lambda_{ij}(s) \geq 0 \qquad \text{for each} \quad i,j \in \underline{M}$$

$$\sum_{j=1}^{M} \lambda_{ij}(s)=1 \qquad \text{for each} \quad i \in \underline{M} .$$

We assume (as in Part III) that the state (x_k,r_k) is perfectly observed at each k. The problem is to find the optimal control laws.

$$u_k = \phi_k(x_0,\ldots,x_k;\ r_0,\ldots,r_k)$$

that minimize the cost criterion

$$J_{k_0}(x_0,r_0) = E\left\{\sum_{k=k_0}^{N-1}\left[u_k^2 R(r_k) + Q(x_{k+1},r_{k+1})\right] + Q_T(x_N,r_N)\right\} \tag{8.5}$$

where the expectation is over $\{r_{k_0},\ldots,r_N\}$.

As in the JLQ problems of Chapters 5-7 we assume that the penalty on the control magnitude is quadratic. It is assumed that

$$R(j) > 0 \quad \text{for each} \quad j \in \underline{M} \tag{8.6}$$

The x-operating costs $Q(x,j)$ and terminal costs $Q_T(x,j)$ make the above problem formulation more general than in Part III. We assume here that for each $j \in \underline{M}$, $Q(x,j)$ and $Q_T(x,j)$ are piecewise-quadratic functions having $\bar{\mu}^j$ and $\bar{\eta}^j$ pieces, respectively:

$$Q(x,j) = Q^j(t)x^2 + S^j(t)x + P^j(t)$$
$$\text{if } \mu^j(t-1) < x < \mu^j(t) \tag{8.7}$$
$$t=1,\ldots,\bar{\mu}^j$$

$$Q_T(x,j) = K_T^j(t)x_N^2 + H_T^j(t)x_N + G_T^j(t)$$
$$\text{if } \eta^j(t-1) < x_N < \eta^j(t) \tag{8.8}$$
$$t=1,\ldots,\bar{\eta}^j .$$

We also assume that

$$Q(x,j) \geq 0$$
$$Q_T(x,j) \geq 0 \qquad \text{for all } x . \tag{8.9}$$

Note that (8.9) requires that the endpiece x-costs have

$$K_T^j(1),\ K_T^j(\bar{\eta}^j),\ Q^j(1),\ Q^j(\bar{\mu}^j-1) \geq 0 \tag{8.9}$$

for all $j \in \underline{M}$.

The term $Q_T(x_N,r_N)$ in (8.5) is a terminal cost changed in addition to the time-invariant x-operating cost $Q(x_N,r_N)$. Since $\{(x_k,r_k): k=k_o,\ldots,N)\}$ is a Markov process we need only consider feedback laws of the type

$$u_k = \phi_k(x_k,r_k) \ .$$

Defining the expected cost-to-go $V_k(x_k,r_k)$ as before and applying dynamic programming from finite terminal k=N, we have the relationship

$$V_k(x_k,r_k) = \min_{u_k} \left\{ u_k^2 R(r_k) + E \left\{ \begin{matrix} Q(x_{k+1},r_{k+1}) \\ + V_{k+1}(x_{k+1},r_{k+1}) \end{matrix} \middle| \begin{matrix} x_k' \\ r_k' \\ u_k \end{matrix} \right\} \right. \qquad (8.10)$$

$$\text{for } k=N-1,N-2,\ldots,k_0$$

where

$$V_N(x_N,r_N=j) = Q_T(x_N,r_N=j)$$

with

$$m_N(j) = \bar{\eta}^j$$

and

$$\delta_N^j(t) = \eta^j(t) \qquad t=1,\ldots,\bar{\eta}^j-1 \ ,$$

from which we can (in principle) solve for the optimal controls

$u_{N-1},\ldots,u_{k_0}$.

In the next section we will solve the last stage control problem (k=N-1) for several example problems that satisfy (8.1)-(8.10).

8.3 Several JLPQ Examples

In this section we examine several example problems that satisfy (8.1)-(8.10). We solve for the last-stage optimal controller (i.e., at time k=N-1) for these examples from first principles. These controllers are then analyzed and compared. They will provide insight regarding the solution of the general JLPQ problem later in this chapter. All of the examples of this section are variations of the following control problem: consider a system with M=2 forms where

$$\begin{aligned} &\text{(normal operation)} && x_{k+1} = x_k + u_k && \text{if } r_k=1 \\ &\text{(failure)} && x_{k+1} = x_k && \text{if } r_k=2 \end{aligned} \tag{8.11}$$

$$p(1,2:x) = \begin{cases} 1/4 & |x|< 1 \\ 3/4 & |x|> 1 \end{cases} \tag{8.12}$$

$$p(1,1:x) = \quad 1-p(1,2:x) \qquad p(2,2)=1 \qquad p(2,1)=0.$$

We seek to minimize

$$\min_{u_0,\ldots,u_{N-1}} E\left\{ \sum_{k=0}^{N-1} [u_k^2+Q(x_{k+1},r_{k+1})] + Q_T(r_N,r_N)] \right\} \tag{8.13}$$

where

$$\begin{aligned} &Q(x_{k+1},r_{k+1}=2) = 0 \\ &Q_T(x_N,r_N=2) = 1000 \\ &Q_T(x_N,r_N=1) = 0 \end{aligned} \tag{8.14}$$

and $Q(x_{k+1},r_{k+1}=1)$ is piecewise-quadratic in x_{k+1} and satisfies $Q(x_{k+1},r_{k+1}=1) \geq 0$ at each x_k. In this problem, if the system fails (jumps into form r=2), it stays there. There is no repair possible.

In form r=2 the value of x does not change; a terminal penalty of $Q_\tau(x_N,r_N=2)=1000$ is incurred. Clearly in form r=2,

$$\begin{aligned} V_k(x_k,r_k=2) &= 1000 \\ U_k(x_k,r_k=2) &= 0 \end{aligned} \tag{8.15}$$

at all times. That is, if the system fails then the optimal strategy is to turn it off (by setting u=0).

In this section we will consider four different piecewise-quadratic x-costs, $Q(x_{k+1},r_{k+1}=1)$. Recall that the conditional expected cost-to-go, $\hat{V}_N(x_N|r_{N-1}=1)$ is defined by:

$$\hat{V}_N(x_N|r_{N-1}=1) = E\left\{ Q(x_N,r_N) + V_N(x_N,r_N) \,\middle|\, \begin{matrix} x_N \\ r_{N-1}=1 \end{matrix} \right\}, \tag{8.16}$$

which for (8.11)-(8.15) is given by

$$\begin{aligned} \hat{V}_N(x_N|r_{N-1}=1) = {} & p(1,1:x_N)\,[Q(x_N,r_N)] \\ & + \\ & p(1,2:x_N)\,1000 \end{aligned} \tag{8.17}$$

$\hat{V}_N(x_N|r_{N-1}=1)$ is a piecewise-quadratic function of x_N having ψ_N pieces:

$$\hat{V}_N(x_N|r_{N-1}=l) = \hat{V}_N(t) = \begin{cases} x_N^2\hat{K}_N(t) + x_N\hat{H}_N(t) + \hat{G}_N(t) \\ \text{for } x_N \in \Delta_N(t) = (\gamma_N(t-1),\gamma_N(t)) \end{cases} \bullet$$

$$t=1,\ldots,\psi_N \qquad (8.18)$$

Our task is to find the u_{N-1} value, as a function of x_{N-1}, which minimizes

$$V_{N-1}(x_{N-1},r_{N-1}=l) = \min_{u_{N-1}} \left\{ u_{N-1}^2 + \hat{V}_N(x_N|r_{N-1}=l) \right\}$$

$$= \min_{t=1,..,s} \; \min_{\substack{u_{N-1} \text{ s.t.} \\ x_N \in \Delta_N(t)}} \left\{ u_{N-1}^2 + x_N^2\hat{K}_N(t) + x_N\hat{H}_N(t) + \hat{G}_N(t) \right\}$$

$$= \min_{t=1,..,s} V_{N-1}(x_{N-1},r_{N-1}=l|t) \quad \bullet \qquad (8.19)$$

In (8.19) we are following the basic idea of Part III:

> We convert the control problem (8.11)-(8.15) into the <u>comparison</u> (for each x_{N-1}) of the solutions of a set of constrained-in-x_N JLQ subproblems. Each subproblem corresponds to driving x_N into one of the domains $\Delta_N(t)$ of the $\hat{V}_N(x_N|r_{N-1}=l)$ pieces (as in (8.18)).

We begin with a single one-piece concave upwards quadratic x-cost. This problem is solvable by the algorithm of Section 7.2. We present it here for comparison with-the other examples of this section.

Example 8.1:

$$\text{Let } Q(x,r) = x^2 \qquad (8.20)$$

Applying the algorithm of Section 7.2 to the last stage (k=N-1) of (8.11)-(8.19), we find that

$$\hat{V}_N(x_N|r_{N-1}=1) = \begin{cases} (.25)x_n^2 + 750 & \text{if } x_N < -1 \\ (.75)x_N^2 + 350 & \text{if } -1 < x_N < 1 \\ (.25)x_N^2 + 750 & \text{if } 1 < x_N \end{cases}$$

That is, $\psi_N=3$ and

$$\Delta_N(1) = (-\infty,-1)$$

$$\Delta_N(2) = (-1,1)$$

$$\Delta_N(3) = (1,\infty)$$

in (8.18). This conditional cost function is discontinuous at $x_N = \pm 1$.

The optimal controller from $(x_{N-1},r_{N-1}=1)$ is specified by Table 8.1 and shown[1] in Figure 8.1.

[1] In Figure 8.1 and all of the graphs of this chapter, the scales are distorted so that the behavior of the functions at joining points is highlighted.

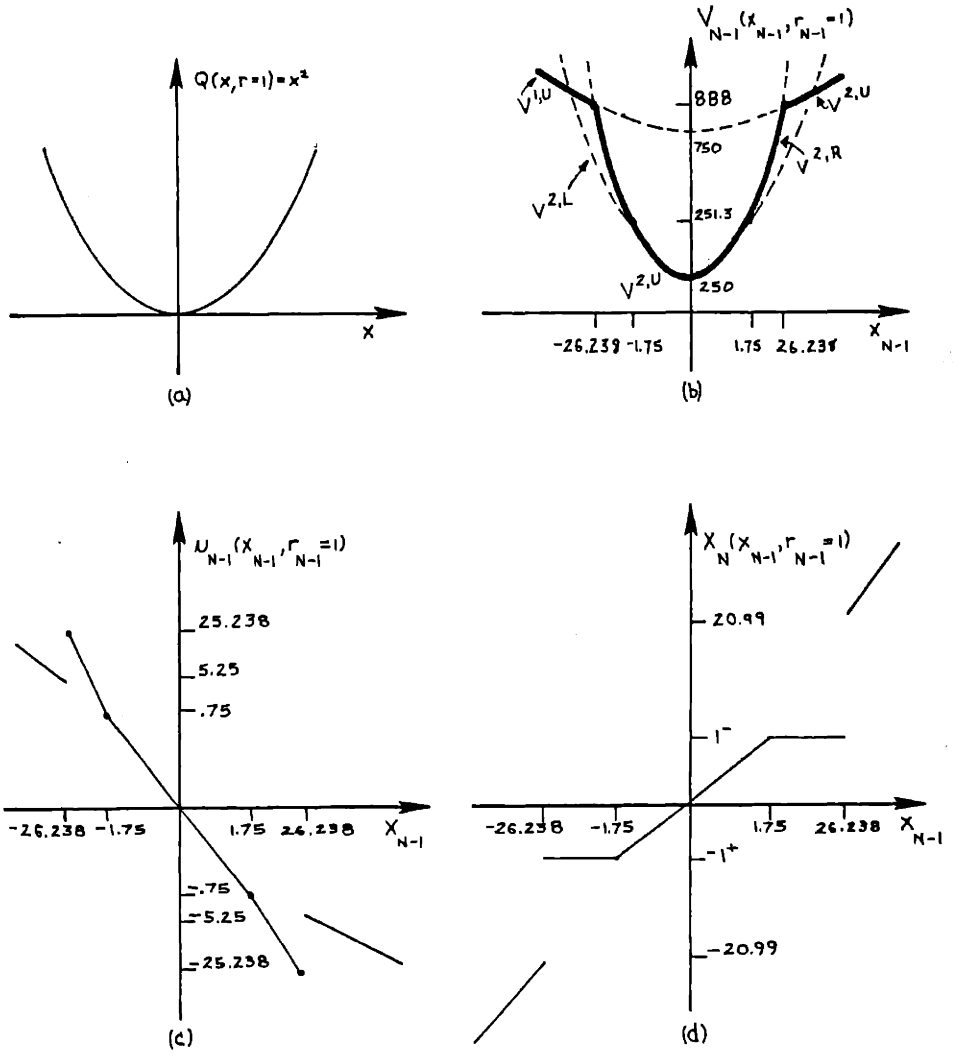

Figure 8.1: Q(x,r=1) and k=(N-1) Solution for Example 8.1. Not Drawn to Scale so as to Emphasize Behavior at Joining Points

if	$V_{N-1}(x_{N-1}, r_{N-1}=1)$	$u_{N-1}(x_{N-1}, r_{N-1}=1)$	$x_N(x_{N-1}, r_{N-1}=1)$
$x_{N-1} < -26.238$	$(.2)x_{N-1}^2 + 750$	$-.2x_{N-1}$	$.8x_{N-1}$
$-26.238 < x_{N-1} < -1.75$	$x_{N-1}^2 + 2x_{N-1} + 251.73$	$-x_{N-1} - 1^+$	-1^+
$-1.75 < x_{N-1} < 1.75$	$(.4285)x_{N-1}^2 + 250$	$-.4285\ x_{N-1}$	$.57143x_{N-1}$
$1.75 < x_{N-1} < +26.38$	$x_{N-1}^2 - 2x_{N-1} + 251.73$	$-x_{N-1} + 1^-$	1^-
$26.38 < x_{N-1}$	$.2x_{N-1}^2 + 750$	$-.2x_{N-1}$	$.8x_{N-1}$

TABLE 8.1: Optimal controller from $(x_{N-1}, r_{N-1}=1)$ in Example 8.1.

Let us recall the following general properties of this class of JLQ problems that were established in Chapter 5 and are illustrated by this example:

1. $V_{N-1}(x_{N-1}, r_{N-1}=1)$ is piecewise-quadratic in x_{N-1} and $u_{N-1}(x_{N-1}, r_{N-1}=1)$ and the optimal mappings $x_N(x_{N-1}, r_{N-1}=1)$ are piecewise-linear. (Proposition 5.1)

2. $V_{N-1}(x_{N-1}, r_{N-1}=1)$ is continuous in x_{N-1}. Between joining points its slope is continuous. At joining points the slopes is either continuous (as at $x_{N-1} = \delta_{N-1}(2) = -1.75$)

or else the slope of $V_{N-1}(x_{N-1}, r_{N-1}=1)$ decreases discontinuously (as at $x_{N-1} = \delta_{N-1}(1) = -26.238$ and $x_{N-1} = \delta_{N-1}(4) = 26.238$). (Proposition 5.1)

3. The optimal control law $u_{N-1}(x_{N-1}, r_{N-1}=1)$ is a continuous nonincreasing function of x_{N-1} except at joining points where $V_{N-1}(x_{N-1}, r_{N-1}=1)$ has a discontinuous-slope; at such points ($x_{N-1} = \pm 26.238$ in Example 8.1), the control law increases discontinously. (Proposition 5.3).

4. The optimal controller can hedge-to-a-point only to the low cost side of a $\hat{V}_N(x_N | r_{N-1}=1)$ discontinuity. These arise from form transition probability discontinuities. In example 8.1 these are

$$x_N = -1^+ , 1^- .$$

(Proposition 5.2).

5. The mapping

$$x_{N-1} \longmapsto x_N(x_{N-1}, r_{N-1}=1)$$

is monotonely nondecreasing. It consists of five line segments:

- a segment with positive slope in each region of x_{N-1} values where an "unconstrained" cost (driving x_N into the interior of one of the $\hat{V}_N(x_N | r_{N-1}=1)$ piece domains) is optimal.

- a <u>constant</u> line segment for each x_{N-1} region from which there is hedging-to-a-point

$$\left.\begin{array}{ll} & -26.238 < x_{N-1} < -1.75 \qquad x_N = -1^+ \\ \text{and} & \\ & +1.75 < x_{N-1} < 26.238 \qquad x_N = 1^- \end{array}\right)$$

in example 8.1.

(Proposition 5.3)

6. There are regions of x_N avoidance associated with (and only with) each joining point where the slope of $V_{N-1}(x_{N-1}, r_{N-1}=1)$ decreases discontinuously. These are

(-20.9904,-1) and (1,20.9904) in example 8.1.

(Proposition 5.3). □

We will now present examples of the problem (8.11)-(8.18) where not all of the above facts will hold, due to the structure of the x-cost $Q(x_N, r_N)$.

<u>Example 8.2</u>: (Hedging to discontinuities of the x-cost $Q(x,r)$)

Let the x-cost be piecewise-constant in x:

$$Q(x_{k+1}, r_{k+1}=1) = \begin{cases} 100 & |x_{k+1}| > .5 \\ 0 & |x_{k+1}| < .5 \end{cases} \qquad (8.21)$$

•

This cost is shown in Figure 8.2(a). The control problem (8.11)-(8.15), (8.21) corresponds to a situation where we want the x process to be inside a certain interval (i.e., inside (-.5,.5)), and we penalize <u>equally</u> any x value outside of the desired interval.

The conditional expected cost-to-go in (8.18) for this problem is

$$\hat{V}_N(x_N|r_{N-1}=1) = \begin{cases} 775 & \text{if} \quad x_N < -1 \\ 325 & \text{if} \quad -1 < x_N < -.5 \\ 250 & \text{if} \quad -.5 < x_N < .5 \\ 325 & \text{if} \quad .5 < x_N < 1 \\ 775 & \text{if} \quad 1 < x_N \end{cases} \tag{8.22}$$

Solving the first of the constrained subproblems in (8.19) we obtain the following:

for $x_N \in \Delta_N(1) = (-\infty,-1)$,

$$V_{N-1}(x_{N-1},r_{N-1}=1|1) = \left\{ \min_{\substack{u_{N-1} \\ \text{s.t } x_N < -1}} u_{N-1}^2 + 775) \right\} . \tag{8.23}$$

Differentiating V_{N-1} with respect to u_{N-1} and setting to zero, we find that (8.23) is minimized by $u_{N-1}=0$ with resulting cost $V_{N-1}=775$ <u>if</u> $x_N = x_{N-1} < -1$. If, however, we have $x_{N-1} > 1$ then the constraint in (8.23) is active. Since

$$\frac{\partial^2 V_{N-1}(x_{N-1},r_{N-1}=1|1)}{\partial x_N^2} > 0 \quad \text{for any fixed } x_{N-1} ,$$

we minimize (8.23) for $x_{N-1}<-1$ by driving x_N to -1^-, using control

$$u_{N-1} = -x_{N-1}^{-1}$$

and attaining cost

$$V_{N-1} = x_{N-1}^2 + 2x_{N-1} + 776.$$

We can solve each of the constrained subproblems of (8.23) in a similar way, obtaining the following:

$$V_{N-1}(x_{N-1}, r_{N-1}=1 \mid 1) = \begin{cases} v^{1,U} = 775 & \text{if } x_{N-1}<-1 \\ v^{1,R} = x_{N-1}^2+2x_{N-1}+776 & \text{if } x_{N-1}>-1 \end{cases}$$

with

$$u_{N-1}(x_{N-1}, r_{N-1}=1 \mid 1) = \begin{cases} u^{1,U} = 0 & \text{if } x_{N-1}<-1 \\ u^{1,U} = -x_{N-1}^{-1} & \text{if } x_{N-1}>-1 \end{cases}$$

$$V_{N-1}(x_{N-1}, r_{N-1}=1 \mid 2) = \begin{cases} v^{2,L} = x_{N-1}^2+2x_{N-1}+326 & \text{if } x_{N-1}<-1 \\ v^{2,U} = 325 & \text{if } -1<x_{N-1}<-.5 \\ v^{2,R} = x_{N-1}^2+x_{N-1}+325.25 & \text{if } -.5<x_{N-1} \end{cases}$$

$$u_{N-1}(x_{N-1}, r_{N-1}=1 \mid 2) = \begin{cases} u^{2,L} = -x_{N-1}^{-1} & \text{if } x_{N-1}<-1 \\ u^{2,U} = 0 & \text{if } -1<x_{N-1}<-.5 \\ u^{2,R} = -x_{N-1}^{-.5} & \text{if } -.5<x_{N-1} \end{cases}$$

and

$$V_{N-1}(x_{N-1}, r_{N-1}=1 \mid 3) = \begin{cases} v^{3,L} = x_{N-1}^2 + x_{N-1} + 250.25 & \text{if } x_{N-1} < -.5 \\ v^{3,U} = 250 & \text{if } -.5 < x_{N-1} < .5 \\ v^{3,R} = x_{N-1}^2 - x_{N-1} + 250.25 & \text{if } .5 < x_{N-1} \end{cases}$$

$$u_{N-1}(x_{N-1}, r_{N-1}=1 \mid 3) = \begin{cases} u^{3,L} = -x_{N-1} - .5^{+} & \text{if } x_{N-1} < .5 \\ u^{3,U} = 0 & \text{if } -.5 < x_{N-1} < .5 \\ u^{3,L} = -x_{N-1} + .5^{-} & \text{if } .5 < x_{N-1} \end{cases}$$

By the symmetry of the problem, for each x_{N-1}

$$V_{N-1}(x_{N-1}, r_{N-1}=1 \mid 4) = V_{N-1}(-x_{N-1}, r_{N-1}=1 \mid 2)$$

$$V_{N-1}(x_{N-1}, r_{N-1}=1 \mid 5) = V_{N-1}(-x_{N-1}, r_{N-1}=1 \mid 1)$$

$$u_{N-1}(x_{N-1}, r_{N-1}=1 \mid 4) = -u_{N-1}(-x_{N-1}, r_{N-1}=1 \mid 2)$$

$$u_{N-1}(x_{N-1}, r_{N-1}=1 \mid 5) = -u_{N-1}(-x_{N-1}, r_{N-1}=1 \mid 1)$$

Performing the comparison in (8.19) at each x_{N-1} we obtain the solution for the last time stage of this example, as listed in Table 8.2 and shown in Figure 8.2.

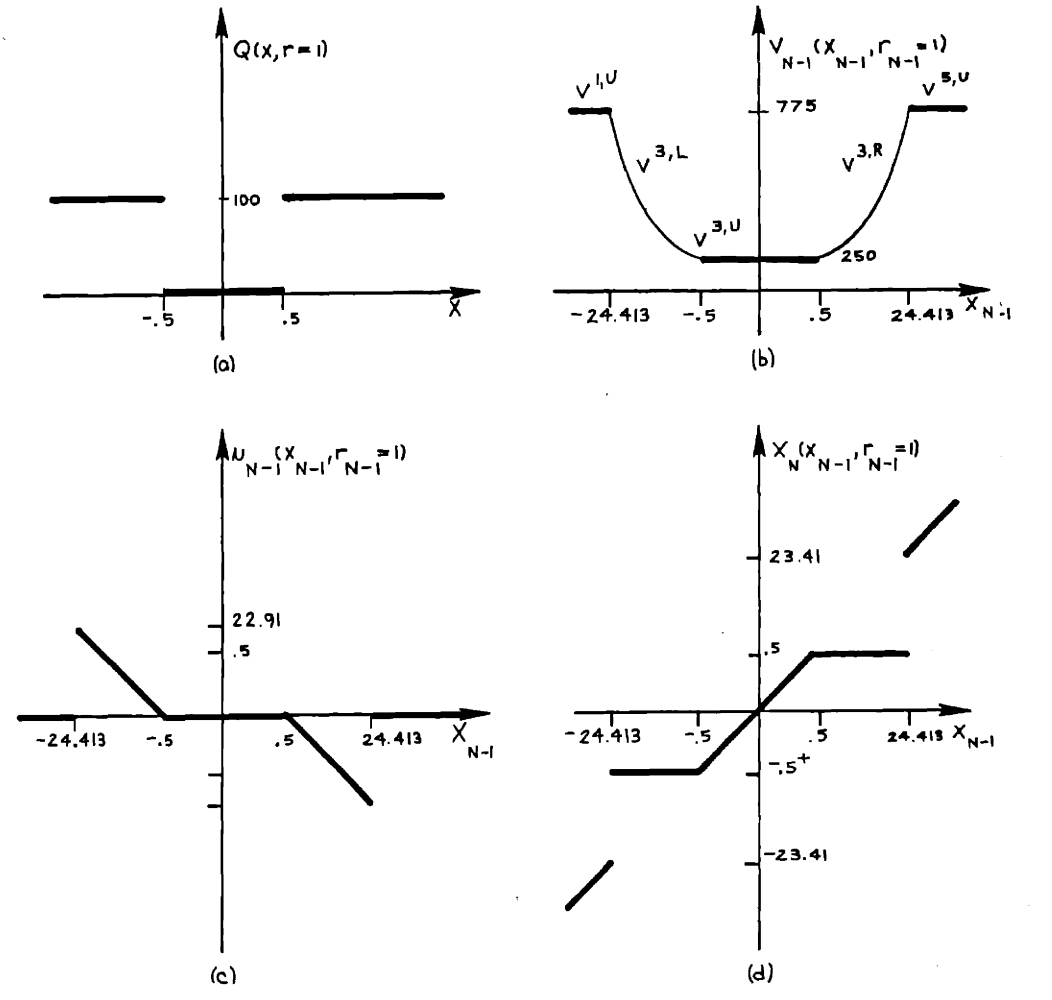

Figure 8.2: Q(x,r=1) and k=(N-1) Solution for Example 8.2

(Not Drawn to Scale)

if	$V_{N-1}(x_{N-1}, r_{N-1}=1)$	$u_{N-1}(x_{N-1}, r_{N-1}=1)$	$x_N(x_{N-1}, r_{N-1}=1)$
$x_{N-1} < -23.413$	775	0	x_{N-1}
$-23.413 < x_{N-1} < -.5$	$x_{N-1}^2 + x_{N-1} + 250.25$	$-x_{N-1} - .5^+$	$-.5^+$
$-.5 < x_{N-1} < .5$	250	0	x_{N-1}
$.5 < x_{N-1} < 23.413$	$x_{N-1}^2 - x_{N-1} + 250.25$	$-x_{N-1} + .5^-$	$.5^-$
$23.413 < x_{N-1}$	775	0	x_{N-1}

TABLE 8.2: Optimal controller from $(x_{N-1}, r_{N-1}=1)$ in Example 8.2.

For small $|x_{N-1}|$ ($|x_{N-1}| < .5$) the optimal controller spends no control to move the x process, since it is already in the domain where $Q(x, r=1)=0$. For large $|x_{N-1}|$ ($|x_{N-1}| > 23.413$) the optimal control is also zero. For $23.413 > |x_{N-1}| > .5$ however, the optimal strategy is to exert control so as to drive x_N inside the lowest $\hat{V}_N(x_N | r_{N-1}=1)$ interval in (8.22).

Note that it is never optimal in this example to drive x_N into the intervals ((-1,-.5) and (.5,1)) where the $Q(x, r=1)$ cost is high but the failure probability $p(1,2:x)$ is low.

Comparing examples 8.1 and 8.2 we note that:

- The optimal controller hedges to the points $x_N = -.5, .5^-$ in example 8.2.

These values of x_N are discontinuities of $\hat{V}_N(x_N|r_{N-1}=1)$ in (8.22). However the optimal hedging is not to form transition probability discontinuity locations but, rather, to discontinuities of the x-cost $Q(x,r=1)$.

- The mapping $x_{N-1} \longmapsto x_{N-1}(x_{N-1},r_{N-1}=1)$ is once again monotonely nondecreasing. The regions of x_N avoidance for example 8.2 are

$$(-23.413,-.5),(5,\ 23.413).$$

As in Example 8.1, each region of avoidance is associated with a joining point of $V_{N-1}(x_{N-1},r_{N-1}=1)$ where the slope decreases discontinuously. In Section 8.6 the optimal controller at time k=(N-2) will be obtained for this example using the solution algorithm that is developed in Section 8.5. □

The next example x-cost that we will examine involves quadratic pieces that are concave-up as well as concave down. This leads to a controller that has somewhat different qualitative properties than those that we have examined previously. In particular, the following example shows that for the JLPQ controllers of this chapter,

- active hedging-to-a-point can occur to points other than conditional cost, $\hat{V}_k(x_k|r_{k-1}=j)$, discontinuities.

Example 8.3: (x-operating cost having concave-down quadratic pieces)

Let $Q(x_{k+1}, r_{k+1}=1)$ be as follows:

$$Q(x_{k+1}, r_{k+1}=1) = \begin{cases} x_{k+1}^2 & x_{k+1} < -.5 \\ -x_{k+1}^2 - x_{k+1} & -.5 \; x_{k+1} < 0 \\ -x_{k+1}^2 + x_{k+1} & 0 < x_{k+1} < .5 \\ x_{k+1}^2 & .5 < x_{k+1} \end{cases} \quad \bullet \tag{8.24}$$

This cost is shown in Figure 8.3(a). Note that the inner two pieces are concave-down.

The conditional expected cost-to-go for the problem (8.11)-(8.15), (8.24) from form $r_{N-1}=1$ is

$$\hat{V}_N(x_N | r_{N-1}=1) = \begin{cases} (.25)x_N^2 + 750 & x_N < -1 \\ (.75)x_N^2 + 250 & -1 < x_N < -.5 \\ (.75)[-x_N^2 - x_N] + 250 & -.5 < x_N < .0 \\ (.75)[-x_N^2 + x_N] + 250 & 0 < x_N < .5 \\ (.75)x_N^2 + 250 & .5 < x_N < 1 \\ (.25)x_N^2 + 750 & 1 < x_N \end{cases} \quad \bullet \tag{8.25}$$

We note in passing that that $\hat{V}_N(x_N | r_{N-1}=1)$ is <u>continuous</u> at $x_N = \pm .5$ and $x_N = 0$. It is discontinuous at $x_N = \pm 1$.

Note that $\hat{V}_N(x_N|r_{N-1}=1)$ is not differentiate at any of its joining points in (8.25) (i.e., at ± 1, $\pm .5$, 0).

Solving the constrained subproblems in (8.19) we obtain the following:

$$V_{N-1}(x_{N-1},r_{N-1}=1|1) = \begin{cases} V^{1,U} = .2\,x_{N-1}^2 + 750 & x_{N-1}<-1.25 \\ V^{1,L} = x_{N-1}^2 + 2x_{N-1} + 751.25 & -1.25<x_{N-1} \end{cases}$$

$$u_{N-1}(x_{N-1},r_{N-1}=1|1) = \begin{cases} u^{1,U} = -.2\,x_{N-1} & x_{N-1}<-1.25 \\ u^{1,L} = -1^- - x_{N-1} & -1.25<x_{N-1} \end{cases}$$

and

$$V_{N-1}(x_{N-1},r_{N-1}=1|2) = \begin{cases} V^{2,L}=x_{N-1}^2+2x_{N-1}+251.7286 & x_{N-1}<-1.75 \\ V^{2,U}=.4285x_{N-1}^2+250 & -1.75<x_{N-1}<-.875 \\ V^{2,R}=x_{N-1}^2+x_{N-1}+250.4372 & -.875<x_{N-1} \end{cases}$$

$$u_{N-1}(x_{N-1},r_{N-1}=1|2) = \begin{cases} u^{2,L}= -x_{N-1}-1^+ & x_{N-1}<-1.75 \\ u^{2,U}= -.4285x_{N-1} & -1.75<x_{N-1}<-.875 \\ u^{2,R}= -x_{N-1}-.5^- & -.875<x_{N-1} \end{cases}$$

By the symmetry of the problem, for each x_{N-1}

$$V_{N-1}(x_{N-1}, r_{N-1}=1|5) = V_{N-1}(-x_{N-1}, r_{N-1}=1|2)$$

$$V_{N-1}(x_{N-1}, r_{N-1}=1|6) = V_{N-1}(-x_{N-1}, r_{N-1}=1|1)$$

$$u_{N-1}(x_{N-1}, r_{N-1}=1|5) = -u_{N-1}(-x_{N-1}, r_{N-1}=1|2)$$

$$u_{N-1}(x_{N-1}, r_{N-1}=1|6) = -u_{N-1}(-x_{N-1}, r_{N-1}=1|1) \quad \bullet$$

For $x_N \in \Delta_N(3)$ and $x_N \in \Delta_N(4)$, however, the associated subproblems are different than any we have examined here previously. Specifically, $\hat{V}_N(x_N|r_{N-1}=1)$ is concave-down over $\Delta_N(3)$ and $\Delta_N(4)$. Consider the constrained subproblem $V_{N-1}(x_{N-1}, r_{N-1}=1|3)$:

$$V_{N-1}(x_{N-1}, r_{N-1}=1|3) = \min_{\substack{u_{N-1} \text{ s.t.} \\ -.5<x_N<0}} \left\{ u_{N-1}^2 - .75x_N^2 - .75x_N + 250 \right\} \quad \bullet \tag{8.26}$$

Differentiating with respect to u_{N-1} and setting to zero we find that (8.26) is minimized by

$$u_{N-1} = 3x_{N-1} + 1.50$$

$$\left(\text{since } \frac{\partial^2 V_{N-1}(x_{N-1}, r_{N-1}=1|3)}{(\partial u_{N-1})^2} = .5 > 0 \right). \quad \text{The resulting cost is}$$

$$V_{N-1} = -3x_{N-1}^2 - 3x_{N-1} + 249.4375 \quad .$$

This solution is only valid, however, if the constraint in (8.26) is inactive. That is, if the resulting x_N satisfies

$$.5 < x_N = 4x_{N-1} + 1.5 < 0,$$

which is the case when $-.5<x_{N-1}<-.375$. Otherwise, we must drive to the best x_N value in $(-.5,0)$. Note that for each <u>fixed</u> x_{N-1} value, we can write (8.26) as a minimization over x_N values in $(-.5,0)$:

$$V_{N-1}(x_{N-1},r_{N-1}=1\,|\,3) = \min_{-.5<x_N<0} \{(x_N-x_{N-1})^2 - .75x_N^2 - .75x_N + 250$$

$$= \min_{-.5<x_N<0} \{(.25)x_N^2 + (-2x_{N-1}-.75)x_N + (x_{N-1}^2+250)\} .$$

Since

$$\frac{\partial^2}{(\partial x_N)^2} V_{N-1}(x_{N-1},r_{N-1}=1\,|\,3) = .25 > 0 ,$$

the optimal strategy is to

- make $x_N = -.5^+$ if $x_{N-1} < -.5$
- make $x_N = 0^-$ if $-.375 < x_{N-1}$.

Consequently we obtain

$$V_{N-1}(x_{N-1},r_{N-1}=1\,|\,3) = \begin{cases} V^{3,L} = x_{N-1}^2 + x_{N-1} + 250.4375 & x_{N-1} < -.5 \\ V^{3,U} = -3x_{N-1}^2 - 3x_{N-1} + 249.4375 & -.5 < x_{N-1} < -.375 \\ V^{3,R} = x_{N-1}^2 + 250 & -.375 < x_{N-1} \end{cases}$$

$$u_{N-1}(x_{N-1}, r_{N-1}=1 \mid 3) = \begin{cases} u^{3,L} = -x_{N-1} - .5^{+} & x_{N-1} < -.5 \\ u^{3,U} = 3x_{N-1} + 1.50 & -.5 < x_{N-1} < -.375 \\ u^{3,R} = -x_{N-1} & -.375 < x_{N-1} \end{cases}$$

and, by the symmetry of the problem,

$$V_{N-1}(x_{N-1}, r_{N-1}=1 \mid 3) = V_{N-1}(-x_{N-1}, r_{N-1}=1 \mid 4)$$

$$u_{N-1}(x_{N-1}, r_{N-1}=1 \mid 3) = -u_{N-1}(-x_{N-1}, r_{N-1}=1 \mid 4) \ .$$

Performing the comparison in (8.19) for the six constrained subproblem solutions (at each x_{N-1}) we obtain the last time-stage solution of this example, as listed in Table 8.3 and shown in Figure 8.3.

In Figure 8.3(b) we see that, as in earlier examples, the optimal cost $V_{N-1}(x_{N-1}, r_{N-1}=1)$ is piecewise-quadratic in x_{N-1}. This example differs from those considered earlier in that some of these pieces have $\partial^2 V_{N-1}/(\partial x_{N-1})^2 < 0$.

The only nondifferentiable points of $V_{N-1}(x_{N-1}, r_{N-1})$ are at $x_{N-1} = \pm 26.238$. At the other joining points of $V_{N-1}(x_{N-1}, r_{N-1}=1)$,

$$\frac{\partial V_{N-1}(x_{N-1}, r_{N-1}=1)}{\partial x_{N-1}} = \begin{cases} \pm 1.5 \text{ at } x_{N-1} = \pm 1.75 \\ \pm .75 \text{ at } x_{N-1} = \pm .875 \\ 0 \quad \text{at } x_{N-1} = \pm .5 \\ \pm .75 \text{ at } x_{N-1} = \pm .375 \end{cases}$$

At $x_{N-1} = \pm .5$, $V_{N-1}(x_{N-1}, r_{N-1}=1)$ has inflection points.

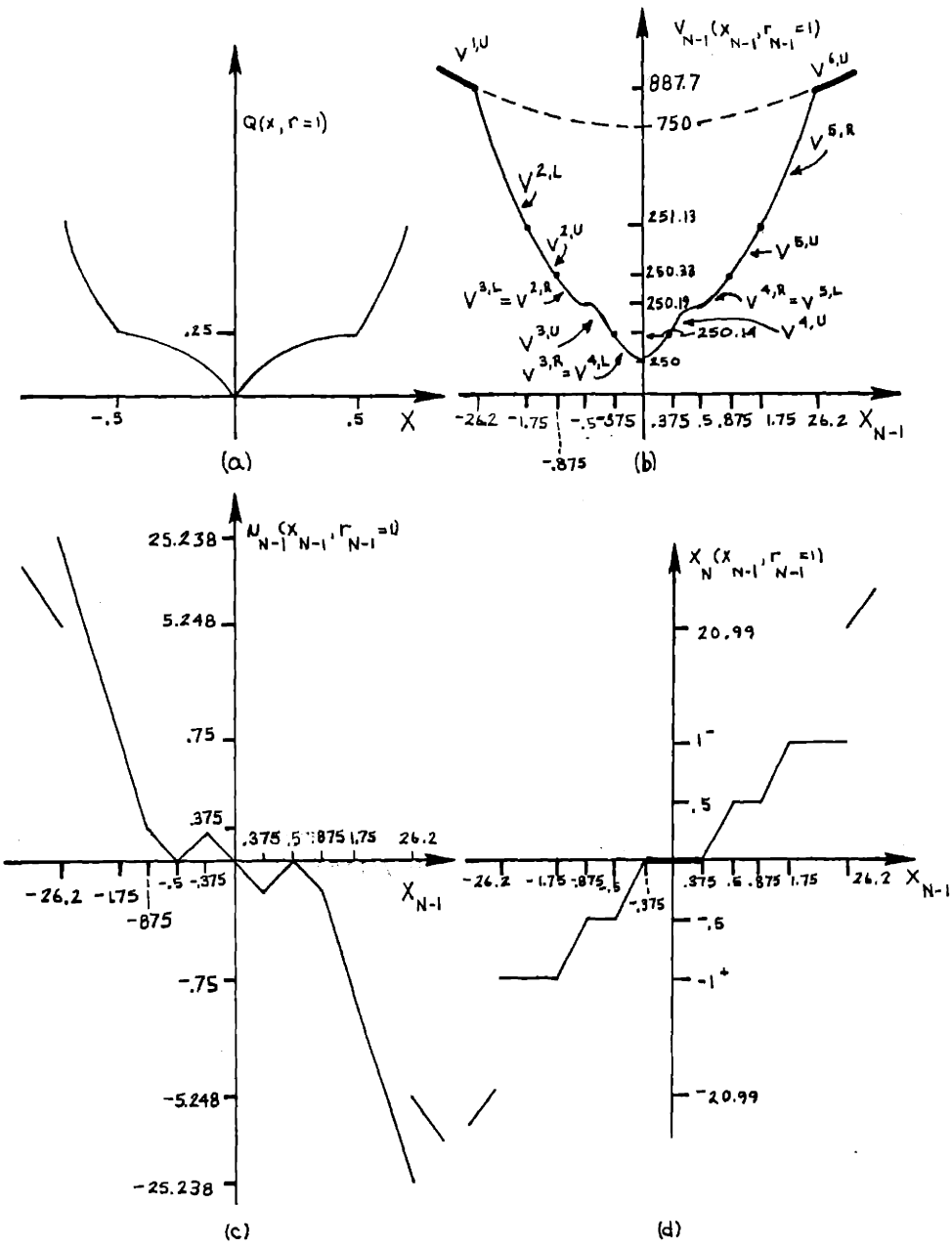

Figure 8.3: Q(x,r=1) and k=(N-1) Solution for Example 8.3

if	$V_{N-1}(x_{N-1}, r_{N-1}=1)$	$u_{N-1}(x_{N-1}, r_{N-1}=1)$	$x_N(x_{N-1}, r_{N-1}=1)$
$x_{N-1} < -26.238$	$.2x_{N-1}^2 + 750$	$-.2x_{N-1}$	$.8x_{N-1}$
$-26.238 < x_{N-1} < -1.75$	$x_{N-1}^2 + 2x_{N-1} + 251.73$	$-x_{N-1} - 1^+$	-1^+
$-1.75 < x_{N-1} < -.875$	$.4285x_{N-1}^2 + 250$	$-.4285x_{N-1}$	$.5715x_{N-1}$
$-.875 < x_{N-1} < -.5$	$x_{N-1}^2 + x_{N-1} + 250.44$	$-x_{N-1} - .5$	$-.5$
$-.5 < x_{N-1} < -.375$	$-3x_{N-1}^2 - 3x_{N-1} + 249.44$	$3x_{N-1} + 1.5$	$4x_{N-1} + 1.5$
$-.375 < x_{N-1} < .375$	$x_{N-1}^2 + 250$	$-x_{N-1}$	0
$.375 < x_{N-1} < .5$	$-3x_{N-1}^2 + 3x_{N-1} + 249.44$	$3x_{N-1} - 1.5$	$4x_{N-1} - 1.5$
$.5 < x_{N-1} < .875$	$x_{N-1}^2 - x_{N-1} + 250.44$	$-x_{N-1} + .5$	$.5$
$.875 < x_{N-1} < 1.75$	$.4285x_{N-1}^2 + 250$	$-.4285x_{N-1}$	$.5715x_{N-1}$
$1.75 < x_{N-1} < 26.238$	$x_{N-1}^2 - 2x_{N-1} + 251.73$	$-x_{N-1} + 1^-$	1^-
$26.238 < x_{N-1}$	$.2x_{N-1}^2 + 750$	$-.2x_{N-1}$	$.8x_{N-1}$

TABLE 8.3: Optimal controller from $(x_{N-1}, r_{N-1}=1)$ in Example 8.3.

As in earlier examples, the optimal control law is a piecewise-linear function of x_{N-1}. The control law in example 8.3 does not decrease between all joining points (unlike examples 8.1, 8.2 and any problem in Chapters 5-7 with $b(j), a(j) > 0$). The slope of $u_{N-1}(x_{N-1}, r_{N-1}=1)$ is positive in the intervals $(-.5,-.375)$ and $(.375,.5)$ but negative everywhere else it exists (see Figure 8.3(c)).

The optimal controller in example 8.3 hedges to the points $x_N=-1^+$, $x_N=-.5$, $x_N=.5$, $x_N=1^-$ and $x_N=0$. Two of these values $(x_N=-1^+,1^-)$ are hedging to the low cost side of a $\hat{V}_N(x_N|r_{N-1}=1)$ discontinuity, as in previously studied examples.

However, $\hat{V}_N(x_N|r_{N-1}=1)$ is not discontinuous at $x_N=\pm.5$ and $x_N=0$, yet we hedge to these values. From (8.25) note that $x_N=\pm.5$, 0 are the boundaries of $\hat{V}_N(x_N|r_{N-1}=1)$ pieces that are concave. Necessary conditions for hedging-to-a-point will be stated in Section 8.5 (corollary 8.3).

As in example 8.1 and 8.2, we see from Figure 8.3(d) that the mapping

$$x_{N-1} \longmapsto x_N(x_{N-1}, r_{N-1}=1)$$

is monotonely nondecreasing. Note that the regions of avoidance

$$(-20.99,-1) \text{ and } (1,20.99)$$

are associated once again with x_{N-1} values when the slope of $V_{N-1}(x_{N-1}, r_{N-1}=1)$ decreases discontinuously (i.e., at $x_N=\pm 26.230$).

There are no regions of x_N avoidance associated with hedging to $x_N = \pm .5$ or $x_N = 0$. □

The next example illustrates additional issues that the modified solution algorithm must cope with in solving the JLPQ problems of this chapter.

Example 8.4: (Subproblem with no unconstrained minimum)

Let the x-cost be piecewise-quadratic in x with concave-up endpieces:

$$Q(x_{k+1}, r_{k+1}=1) = \begin{cases} x_{k+1}^2 & x_{k+1} < -.5 \\ -2x_{k+1}^2 - 1.5x_{k+1} & -.5 < x_{k+1} \leq 0 \\ -2x_{k+1}^2 + 1.5x_{k+1} & 0 < x_{k+1} < .5 \\ x_{k+1}^2 & .5 < x_{k+1} \end{cases} \quad (8.27)$$

This cost is shown in Figure 8.4(a). The conditional expected cost-to-go for the problem (8.11)-(8.15), (8.27) from form $r_{N-1}=1$ is

$$\hat{V}_N(x_N | r_{N-1}=1) = \begin{cases} (.25)x_N^2 + 750 & x_N < -1 \\ (.75)x_N^2 + 250 & -1 < x_N < -.5 \\ (.75)[-2x_N^2 - 1.5x_N] + 250 & -.5 < x_N < 0 \\ (.75)[-2x_N^2 + 1.5x_N] + 250 & 0 < x_N < .5 \\ (.75)x_N^2 + 250 & .5 < x_N < 1 \\ (.25)x_N^2 + 750 & 1 < x_N \end{cases} \quad (8.28)$$

For $|x_N| > .5$, $\hat{V}_N(x_N|r_{N-1}=1)$ in (8.28) is the same as that of example 8.3 in (8.25). As in the last example, $\hat{V}_N(x_N|r_{N-1}=1)$ is continuous at $x_N = \pm .5$ and at $x_N=0$. It is discontinuous at $x_N = \pm 1$. As in Example 8.2, $\hat{V}_N(x_N|r_{N-1}=1)$ is not differentiable at $x_N = \pm 1, \pm .5, 0$.

Solving the constrained subproblems in (8.19) we obtain the same $V_{N-1}(x_{N-1}, r_{N-1}=1|t)$ for t=1,2,5,6 as in Example 8.2:

$$V_{N-1}(x_{N-1}, r_{N-1}=1|1) = \begin{cases} V^{1,U} = .2x_{N-1}^2 + 750 & x_{N-1} < -1.25 \\ V^{1,L} = x_{N-1}^2 + 2x_{N-1} + 751.25 & x_N > -1.25 \end{cases}$$

$$V_{N-1}(x_{N-1}, r_{N-1}=1|2) = \begin{cases} V^{2,L} = x_{N-1}^2 + 2x_{N-1} + 251.7286 & x_{N-1} < -1.75 \\ V^{2,U} = .4285x_{N-1}^2 + 250 & -1.75 < x_{N-1} < -.875 \\ V^{2,R} = x_{N-1}^2 + x_{N-1} + 250.4375 & -.875 < x_{N-1} \end{cases}$$

and

$$V_{N-1}(x_{N-1}, r_{N-1}=1|1) = V_{N-1}(-x_{N-1}, r_{N-1}=1|6)$$

$$V_{N-1}(x_{N-1}, r_{N-1}=1|2) = V_{N-1}(-x_{N-1}, r_{N-1}=1|5) \ .$$

Consider now the constrained subproblem $V_{N-1}(x_{N-1}, r_{N-1}=1|3)$:

$$V_{N-1}(x_{N-1}, r_{N-1}=1|3) = \min_{\substack{u_{N-1} \text{ s.t} \\ -.5 < x_N < 0}} \left\{ \begin{array}{l} u_{N-1}^2 + .75(-2x_N^2 - 1.5x_N) \\ \quad + 250 \end{array} \right\} \qquad (8.29)$$

Differentiating twice with respect to u_{N-1} we obtain

$$\frac{\partial V_{N-1}(x_{N-1}, r_{N-1}=1|3)}{\partial u_{N-1}} = 2u_{N-1} + (.75)(-2)(x_{N-1}+u_{N-1}) + (.75)(-1.5) \tag{8.30}$$

$$\frac{\partial^2 V_{N-1}(x_{N-1}, r_{N-1}=1|3)}{(\partial u_{N-1})^2} = 2-4(.75) = -1 < 0 . \tag{8.31}$$

Thus for u_{N-1} such that $\frac{\partial V_{N-1}(x_{N-1}, r_{N-1}=1|3)}{\partial u_{N-1}} = 0$ we obtain a maximum instead of a minimum . For a fixed x_{N-1} value, we can rewrite (8.29) as

$$V_{N-1}(x_{N-1}, r_{N-1}=1|3) = \min_{-.5\leq x_N \leq 0} \left\{ \begin{matrix} (x_N - x_{N-1})^2 + 250 \\ + (.75)(-2x_N^2 - 1.5x_N) \end{matrix} \right\} \tag{8.32}$$

$$= \min_{-.5<x_N<0} \left\{ \begin{matrix} -.5x_N^2 - (2x_{N-1}+1.125)x_N \\ +[x_{N-1}^2+250] \end{matrix} \right\} .$$

Since

$$\frac{\partial^2}{(\partial x_N)^2} V_{N-1}(x_{N-1}, r_{N-1}=1) = -1 < 0 \tag{8.33}$$

the optimal choice of x_N inside $\Delta_N(3)=(-.5,0)$ is on a boundary (either $x_N=-.5^+$ or $x_N=o^-$) for every x_{N-1}.

If we make $x_N = .5^+$ we will use control

$$u_{N-1}^{3,L} = -x_{N-1} - .5^+ \tag{8.34}$$

and incur cost

$$V^{3,L} = x_{N-1}^2 + x_{N-1} + 250.4375 \quad .$$

If we make $x_N = 0^-$ we will use control

$$u_{N-1}^{3,R} = -x_{N-1}$$

and incur cost

$$V^{3,R} = x_{N-1}^2 + 250. \tag{8.35}$$

From (8.34)-(8.35) we see that

$$V^{3,L}(x_{N-1}, r_{N-1}=1) < V^{3,R}(x_{N-1}, r_{N-1}=1)$$

if

$$x_{N-1} < -.4375 \quad .$$

Consequently we obtain

$$V_{N-1}(x_{N-1}, r_{N-1}=1 \mid 3) = \begin{cases} V^{3,L} = x_{N-1}^2 + x_{N-1} + 250.4375 & \text{if } x_{N-1} \leq -.4375 \\ V^{3,R} = x_{N-1}^2 + 250 & \text{if } x_{N-1} \leq -.4375 \end{cases}$$

$$u_{N-1}(x_{N-1}, r_{N-1}=1 \mid 3) = \begin{cases} -x_{N-1} - .5^+ & \text{if } x_{N-1} \leq -.4375 \\ -x_{N-1} & \text{if } x_{N-1} > -.4375 \end{cases}$$

We don't list $V^{3,U}$ and $u^{3,U}$ (the inactive constraint cost and control) since they do not solve (8.29) for any x_{N-1}. By the symmetry of the problem,

$$V_{N-1}(x_{N-1}, r_{N-1}=1 \mid 3) = V_{N-1}(-x_{N-1}, r_{N-1}=1 \mid 4)$$

$$u_{N-1}(x_{N-1}, r_{N-1}=1 \mid 3) = -u_{N-1}(-x_{N-1}, r_{N-1}=1 \mid 4) \quad .$$

Note that

$$V^{3,L}(x_{N-1}, r_{N-1}=1) = V^{2,R}(x_{N-1}, r_{N-1}=1)$$

$$V^{3,R}(x_{N-1}, r_{N-1}=1) = V^{4,L}(x_{N-1}, r_{N-1}=1)$$

$$V^{4,R}(x_{N-1}, r_{N-1}=1) = V^{5,L}(x_{N-1}, r_{N-1}=1) \quad .$$

This is because (as we noted before) $\hat{V}_N(x_N \mid r_{N-1}=1)$ is continuous at $x_N = \pm .5, 0$. Performing the comparison of subproblem solutions in (8.19) for the six problems here, we obtain the last time-stage solution for this example. This solution is listed in Table 8.4 and shown in Figure 8.4.

Comparing the results of Examples 8.3 and 8.4 we see that

1. Examples 8.3 and 8.4 have the same solution at k=(N-1) except for $.375 < |x_{N-1}| < .5$.
2. In Example 8.3 the cost $V_{N-1}(x_{N-1}, r_{N-1}=1) = V^{3,U}$ in $.375 < |x_{N-1}| < .5$ is concave down (Figure 8.3(b)).

In Example 8.4 this cost piece of $V_{N-1}(x_{N-1}, r_{N-1}=1)$ is missing. The adjacent cost pieces $V^{2,R}$ and $V^{3,L}$ are

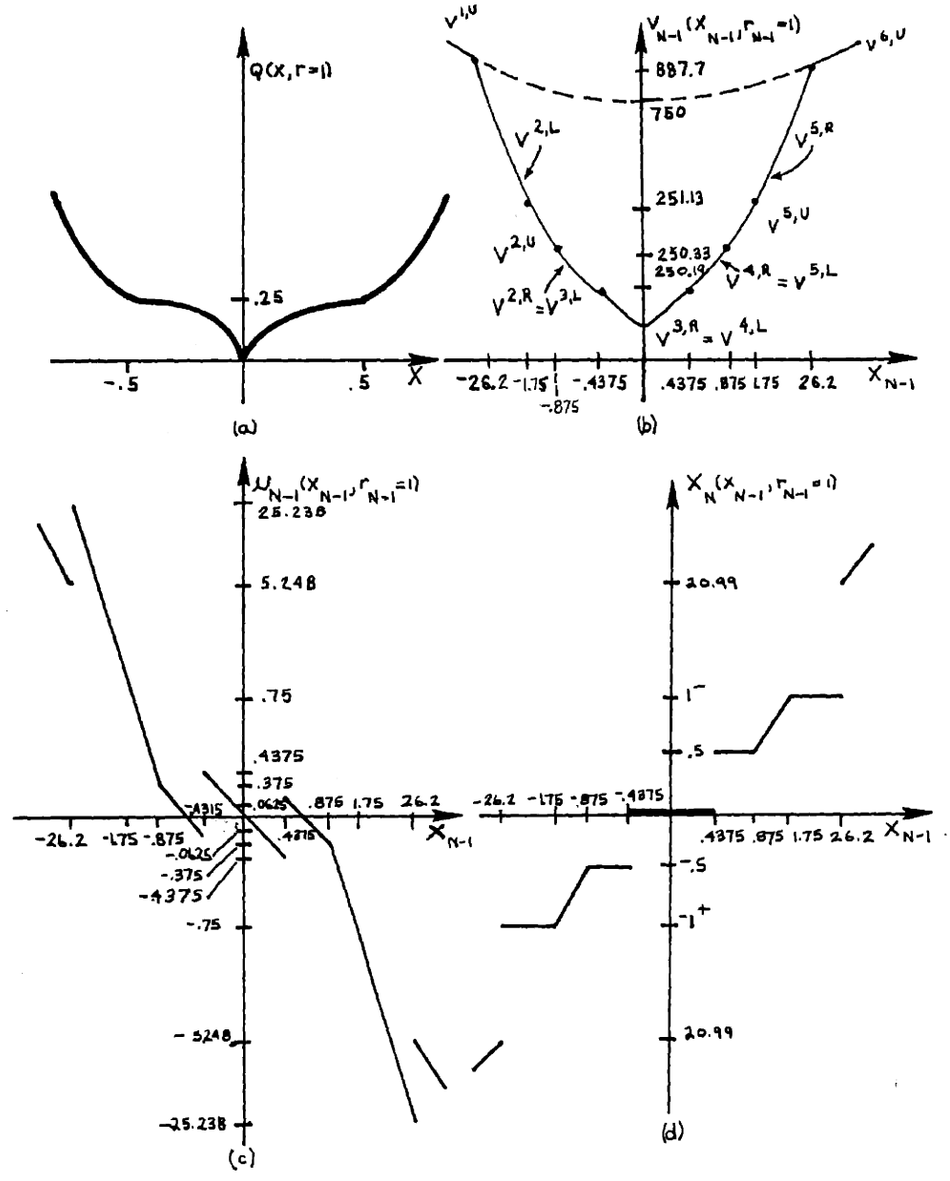

Figure 8.4: Q(x,r=1) and k=(N-1) Solution for Example 8.4.

if	$V_{N-1}(x_{N-1}, r_{N-1}=1)$	$u_{N-1}(x_{N-1}, r_{N-1}=1)$	$x_N(x_{N-1}, r_{N-1}=1)$
$x_{N-1} < -26.238$	$.2x_{N-1}^2 + 750$	$-.2x_{N-1}$	$.8x_{N-1}$
$-26.238 < x_{N-1} < -1.75$	$x_{N-1}^2 + 2x_{N-1} + 251.73$	$-x_{N-1} - 1^+$	-1^+
$-1.75 < x_{N-1} < -.875$	$.4285x_{N-1}^2 + 250$	$-.4285x_{N-1}$	$.5715x_{N-1}$
$-.875 < x_{N-1} < -.4375$	$x_{N-1}^2 + x_{N-1} + 250.44$	$-x_{N-1} - .5$	$-.5$
$-.4375 < x_{N-1} < .4375$	$x_{N-1}^2 + 250$	$-x_{N-1}$	0
$.4375 < x_{N-1} < .875$	$x_{N-1}^2 - x_{N-1} + 250.44$	$-x_{N-1} + .5$	$.5$
$.875 < x_{N-1} < 1.75$	$.4285x_{N-1}^2 + 250$	$-.4285x_{N-1}$	$.5715x_{N-1}$
$1.75 < x_{N-1} < 26.238$	$x_{N-1}^2 - 2x_{N-1} + 251.73$	$-x_{N-1} + 1^-$	1^-
$26.238 < x_{N-1}$	$.2x_{N-1}^2 + 750$	$-.2x_{N-1}$	$.8x_{N-1}$

TABLE 8.4: Optimal control from $(x_{N-1}, r_{N-1}=1)$ in Example 8.4.

optimal over (-.375,-.5). Cost $V^{3,U}$ is missing in Figure 8.4(b) because it is never valid.

Here

$$\frac{\partial^2 V_{N-1}(x_{N-1}, r_{N-1}=1|3)}{(\partial u_{N-1})^2} < 0,$$

hence the constraint in (8.29) is always active.

3. In Example 8.4 we have two additional regions of x_N avoidance;

   $(-.5,0)$ and $(0,.5)$.

   Although it is optimal to drive x_N to exactly zero for $|x_{N-1}| < .4375$, it is never optimal to place x_N near zero.

□

In the above examples of JLPQ problems, the last-stage controllers exhibit certain qualitative behaviors that are not manifested by the JLQ problems of Part III. These aspects of the JLPQ controller must be accounted for in the development of a solution algorithm. We list them here for convenience:

1. Hedging need not only be to form transition probability discontinuities in JLPQ problems. It can be to conditional cost $\hat{V}_k(x_k|r_{k-1})$ discontinuities that arise from x-cost discontinuities in $Q(x_k,r_k)$ or $Q_T(x_N,r_N)$. (Example 8.2)
2. Hedging-to-a-point can occur to points that are not discontinuities of the conditional cost $\hat{V}_k(x_k|r_{k-1})$. However, these points are the boundaries of $\hat{V}_k(x_k|r_{k-1})$ pieces that are concave down. (Examples 8.3,8.4).

3. The optimal control law $u_k(x_k, r_k=j)$ may be discontinuous at x_k values where the optimal cost $V_k(x_k, r_k=j)$ is differentiable. (Examples 8.3,8.4).

4. Hedging-to-a-point $x_k=x$ can occur without an accompanying region of x_k avoidance (example 8.3).

5. Regions of x_k avoidance are associated with (and only with) x_{k-1} values where u_{k-1} is discontinuous (i.e., where $V_{k-1}(x_{k-1}, r_{k-1}=1)$ is not differentiable). Thus there is no region of avoidance associated with hedging to a continuous point of $\hat{V}_k(x_k | r_{k-1}=1)$. (Example 8.3,8.4).

6. In some instances, the constrained subproblem $V_k(x_k, r_k=j | t)$, corresponding to driving x_{k+1} into $\Delta_{k+1}(t)$ where $\hat{V}_{k+1}(x_{k+1} | r_k=j)$ is concave down in $\Delta_{k+1}(t)$, may result in a subproblem controller that never drives x_{k+1} into the interior of $\Delta_{k+1}(t)$, for any x_k value. (Example 8.4, but not example 8.3).

In the next section we will solve the general JLPQ control problem (of Section 8.2) for one time-stage. This result will then be used in Section 8.5 to construct a solution algorithm for these problems. The examples of this chapter will provide insight regarding how the solution algorithm of Chapter 7 must be altered for JLPQ problems.

8.4 One Stage Solution of the JLPQ Problem

In this section we use intuition gained from the example problems of the last section to solve the optimal control problem of Section 8.2 for one time stage. As we indicated earlier, the notation and "book-keeping" becomes quite complex, but the basic idea is the same as illustrated in the previous section. Inductive application of the one stage solution (backwards in time from finite terminal time N) then establishes that the solution of problem (8.1)-(8.10) yields optimal expected costs-to-go that are piecewise-quadratic in x and optimal control law that are piecewise-linear, for all forms $j \in \underline{M}$:

$$V_k(x_k, r_k=j) = x_k^2 K_k(t:j) + x_k H_k(t:j) + G_k(t:j) \tag{8.36}$$

$$u_k(x_k, r_k=j) = -L_k(t:j)x_k + F_k(t:j) \tag{8.37}$$

when

$$\delta_k^j(t-1) < x_k < \delta_k^j(t),$$

where

$$\delta_k^j(1) < \delta_k^j(2) < \ldots < \delta_k^j(m_k(j)-1)$$

are the points where the pieces of $V_k(x_k, j)$ are joined together (the boundaries of the x_k intervals) and

$$\delta_k^j(0) \triangleq -\infty, \quad \delta_k^j(m_k(j)) \triangleq \infty.$$

The proof of the one-stage optimal controller result is constructive. It suggests an algorithm for the recursive determination of the optimal expected costs-to-go and control laws for this problem. An efficient algorithm for this determination of the optimal controller (8.36)-(8.37) is presented in flowchart form in Section 8.5. The one-stage solution result is as follows:

Proposition 8.1: (One Stage Solution)

Consider the problem (8.1)-(8.10). If at time k+1, for each $r_{k+1} = j \in \underline{M}$ we have

(i) $V_{k+1}(x_{k+1}, r_{k+1}=j)$ is piecewise-quadratic with $m_{k+1}(j)$ pieces joined continuously at

$$\{\delta^j_{k+1}(1) < \delta^j_{k+1}(2) < \ldots < \delta^j_{k+1}(m_{k+1}(j)-1)\}$$

(ii) $$\begin{pmatrix} K_{k+1}(t:1) & H_{k+1}(t:1)/2 \\ H_{k+1}(t:1)/2 & G_{k+1}(t:1) \end{pmatrix} \geq 0$$ for $t=1$ and $t=m_{k+1}(j)$

(iii) $\dfrac{\partial V_{k+1}(x_{k+1}, r_{k+1}=j)}{\partial x_{k+1}}$ is either continuous, or

decreases discontinuously at the joining points

$$\{\delta^j_{k+1}(1), \ldots, \delta^j_{k+1}(m_{k+1}(j)-1)\},$$

then for each $r_k = j \varepsilon \underline{M}$

(1) $V_k(x_k, r_k=j)$ is piecewise-quadratic and $u_k(x_k, r_k=j)$ is piecewise-linear (as in (8.36)-(8.37)), each having $m_k(j)$ pieces joined continuously at

$$\{\delta_k^j(1) < \delta_k^j(2) < \ldots < \delta_k^j(m_k(j)-1)\}$$

(2) $$\begin{pmatrix} K_k(t:j) & H_k(t:j)/2 \\ H_k(t:j)/2 & G_k(t:j) \end{pmatrix} \geq 0 \qquad \text{at } t=1 \text{ and } t=m_k(j)$$

(3) $\dfrac{\partial V_k(x_k, r_k=j)}{\partial x_k}$ is either continuous or decreases discontinuously at the joining points $\{\delta_k^j(1), \ldots, \delta_k^j(m_k(j)-1)\}$.

□

At time k=N, conditions (i)-(ii) are clearly satisfied. If we consider the sum of the x-terminal cost $Q_T(x_N, r_N)$ and x-operating cost $Q(x_N, r_N)$ to be the last-stage x-operating cost (that is, we think of $V_N(x_N, r_N)=0$) then (iii) is also satisfied at time k=N. Thus this proposition can be applied inductively, backwards in time from k=N. Equations for the iterative computation of the quantities $m_k(j)$, $K_k(t:j)$, $H_k(t:j)$, $G_k(t:j)$ and $\{\delta_k^j(\ell): \ell=1,\ldots,m_k(j)-1\}$ for each $i,j \in \underline{M}$ are listed in Appendix D.1. These equations are developed in the proof of Proposition 8.1, which constitutes the remainder of this section (with some details in Appendix D.2).

Proof of Proposition 8.1:

For each form $r_k = j \in \underline{M}$, the minimization in (8.10) subject to (8.1)-(8.9) is converted into the comparison of a finite set of constrained-in-x_{k+1} JLQ problems, each with x-independent forms.

This is done conceptually via the following steps:

Step 1: Obtain a composite partition of x_{k+1} values from the partitions associated with the x-costs $Q(x_{k+1}, r_{k+1}=i)$, with the form transition probabilities $p(j,i:x)$ and the expected costs-to-go

$$V_{k+1}(x_{k+1}, r_{k+1}=i) \text{ for each } i \in c_j .$$

The composite partition grid points are the boundaries of the pieces of the piecewise-quadratic function (in x_{k+1}):

$$\hat{V}_{k+1}(x_{k+1} | r_k=j) = E\left\{ \begin{array}{l} V_{k+1}(x_{k+1}, r_{k+1}) \\ \quad + Q(x_{k+1}, r_{k+1}) \end{array} \middle| \begin{array}{l} r_k=j \\ x_{k+1} \end{array} \right\} . \qquad (8.38)$$

This step is similar to step 1 of Section 5.4, except that here we must include $Q(x_{k+1}, r_{k+1})$ discontinuities.

Step 2: Formulating a set of constrained (in x_{k+1}) JLQ problems having x-independent form transition probabilities and one-piece quadratic costs; one problem for each region of values in the partition of Step 1. This step is like step 2 in Section 5.4.

Step 3: Solving the constrained subproblems that are formulated in Step 2. These problems solutions represent the optimal

expected costs-to-go from $(x_k, r_k=j)$ if x_{k+1} is constrained to be in one of the specific regions of values defined in Step 1.

Step 4: Comparing the constrained costs. The optimal expected cost -to-go $V_k(x_k, r_k=j)$ from any x_k value is the minimum of the constrained expected costs-to-go that are obtained in Step 3. This minimization involves the comparison of piecewise-quadratic functions in x_k. The implementation of this step in the algorithm developed in Section 8.5 is more complicated than for the JLQ problems of Part III.

We will describe each of these conceptual steps in sequence so as to demonstrate the validity of Proposition 8.1. The actual solution algorithm mixes these steps and uses other facts (that will be developed) to solve the control problem efficiently (i.e., with fewer calculations).

Proof Step 1: For each form $j \in M$ we construct a composite partition of the real line (of x_{k+1} values) by superimposing the grids associated with $p(j,i:x)$, $Q(x,i)$ and $V_{k+1}(x_{k+1}, r_{k+1}=i)$, for all $i \in c_j$.

The general procedure for obtaining the composite partitions is as follows:

For each $r_k=j \in \underline{M}$ the real line can be divided into a finite number of intervals of x_{k+1} values by superimposing the grids

$$\{\mu^i(t):\ t=1,\ldots,\bar{\mu}^i-1\}$$

$$\{\delta^i_{k+1}(t):\ t=1,2,\ldots,m_{k+1}(i)-1\}$$

$$\{\nu_{ji}(t):\ t=1,\ldots,\bar{\nu}_{ji}-1\}$$

$$\text{for each } i \in c_j\ ,$$

obtaining the composite partition

$$-\infty \triangleq \gamma^j_{k+1}(0) < \gamma^j_{k+1}(1) < \gamma^j_{k+1}(2) < \ldots < \gamma^j_{k+1}(\psi^j_{k+1}-1) < \gamma^j_{k+1}(\psi^j_{k+1}) \triangleq \infty$$

of unique grid points. We define

$$\psi^j_{k+1} \triangleq \text{the (finite) number of such nonempty } x_{k+1} \text{ intervals}$$

where the t^{th} such interval is

$$\Delta^j_{k+1}(t) \triangleq \{x_{k+1}:\ \gamma^j_{k+1}(t-1) < x_{k+1} < \gamma^j_{k+1}(t)\}$$

$$t=1,\ldots,\psi^j_{k+1}-1$$

These intervals of x_{k+1} values are the domains of the individual quadratic-in-x_{k+1} pieces of the function

$$\hat{V}_{k+1}(x_{k+1}|r_k=j) = \hat{V}^j_{k+1}(t) \triangleq x^2_{k+1}\hat{K}^j_{k+1}(t) + x_{k+1}\hat{H}^j_{k+1}(t) + \hat{G}^j_{k+1}(t) \tag{8.39}$$

$$\text{for } x_{k+1} \in \Delta^j_{k+1}(t)$$

$$t=1,\ldots,\psi^j_{k+1}-1$$

where $\hat{K}^j_{k+1}(t)$, $\hat{H}^j_{k+1}(t)$ and $\hat{G}^j_{k+1}(t)$ are specified by (D.1.1)-(D.1.3).

Here

$$\psi^j_{k+1}=1+\left|\bigcup_{i\in C_j}\left[\{\nu_{ji}(\ell):\ \ell=1,\ldots,\bar{\nu}_{ji}-1\}\ \ \{\delta^i_{k+1}(\ell):\ \ell=1,\ldots,m_{k+1}(i)-1\}\right.\right.$$
$$\left.\left.\{\mu^i(\ell):\ \ell=1,\ldots,\bar{\mu}^i-1\}\right]\right| \tag{8.40}$$

where $|\cdot|$ denotes cardinality. An upper bound on ψ^j_{k+1} is given by

$$\psi^j_{k+1}\leq 1+\sum_{i\in C_j}[\bar{\nu}_{ji}+\bar{\mu}^i+m_{k+1}(i)-3] \tag{8.41}$$

where equality in (8.41) holds if

$$\nu_{ji}(\ell)\neq\nu_{jn}(\rho) \qquad \text{for all } i,\ n\in C_j$$
$$\nu_{ji}(\ell)\neq\mu^i(q) \qquad \delta^i_{k+1}(t)\neq\mu^i(q)$$
$$\nu_{ji}(\ell)\neq\delta^i_{k+1}(t)$$

where $\ell=1,\ldots,\bar{\nu}_{ji}-1$, $\rho=1,\ldots,\bar{\nu}_{jn}-1$; $q=1,\ldots,\bar{\mu}^i-1$; $t=1,\ldots,m_{k+1}(i)-1$.

Proof Step 2: Formulating the Constrained Subproblems

In Step 1 we obtained for each $r_k=j\in\underline{M}$ a composite partition of x_{k+1} values into ψ^j_{k+1} intervals. We can formulate (for each $r_k=j\in\underline{M}$) a set of ψ^j_{k+1} constrained JLQ problems having x_{k+1}-independent form transition probabilities and quadratic (not piecewise-quadratic) expected costs and x-costs; one corresponding to each

region of x_{k+1} values. To see this, note that over each such region $\Delta^j_{k+1}(t)$, $Q(x_{k+1}, r_{k+1}=i)$ and $V_{k+1}(x_{k+1}, r_{k+1}=i)$ are quadratic and $p(j,i;x_{k+1})$ is constant in x_{k+1}, for all $i \in c_j$. These constrained problems are:

$$V_k[x_k, r_k=j \,|\, x_{k+1} \in \Delta^j_{k+1}(t)] \triangleq V_k[x_k, j|t] =$$

$$= \min_{\substack{u_k \text{ s.t.} \\ x_{k+1} \in \Delta^j_{k+1}(t)}} E\left\{ \begin{array}{l} u_k^2 R(j) + x_{k+1}^2 Q^j(t) \\ + S^j(t) x_{k+1} + P^j(t) \\ + V_{k+1}(x_{k+1}, r_{k+1}) \end{array} \right\} \tag{8.42}$$

$$= \min_{\substack{u_k \text{ s.t.} \\ x_{k+1} \in \Delta^j_{k+1}(t)}} \left\{ \begin{array}{c} u_k^2 R(j) \\ + \\ \sum_{i=1}^{M} p(j,i,x_{k+1}) \end{array} \left[\begin{array}{l} x_{k+1}^2 Q^i(t) + x_{k+1} S^i(t) \\ + P^i(t) \\ + V_{k+1}(x_{k+1}, i) \end{array} \right] \right\}$$

$$= \min_{\substack{u_k \text{ s.t.} \\ x_{k+1} \in \Delta^j_{k+1}(t)}} \left\{ u_k^2 R(j) + \hat{V}_{k+1}(x_{k+1} \,|\, r_k=j) \right\} , \tag{8.43}$$

subject to (8.1)-(8.3) for each $t=1,2,\ldots,\psi^j_{k+1}$.

Proof Step 3: Solving the constrained subproblems

The third step in this constructive proof of Proposition 8.1 is to solve the contrained JLQ problems of (8.42). For each $r_k=j \in \underline{M}$ the solutions of these ψ^j_{k+1} constrained optimization problems involve optimal expected costs-to-go that are piecewise-quadratic in x_k with two or three parts:

$$V_k[x_k, r_k=j \,|\, x_{k+1} \in \Delta^j_{k+1}(t)] = \begin{cases} V^{t,L}_k(x_k, j) & \text{if } a(j)x_k \leq \theta^j_k(t) \\ V^{t,U}_k(x_k, j) & \text{if } \theta^j_k(t) \leq a(j)x_k \leq \Theta^j_k(t) \\ V^{t,R}_k(x_k, j) & \text{if } \Theta^j_k(t) \leq a(j)x_k \end{cases} \tag{8.44}$$

with corresponding optimal control laws

$$u_k[x_k, r_k=j \,|\, x_{k+1} \in \Delta^j_{k+1}(t)] = \begin{cases} u^{t,L}_k(x_k, j) & \text{if } a(j)x_k < \theta^j_k(t) \\ u^{t,U}_k(x_k, j) & \text{if } \theta^j_k(t) < a(j)x_k < \Theta^j_k(t) \\ u^{t,R}_k(x_k, j) & \text{if } \Theta^j_k(t) < a(j)x_k \,. \end{cases} \tag{8.45}$$

As in Chapter 5, the superscripts L, R and U correspond, respectively, to driving x_{k+1} to the left endpoint, the right endpoint, or the interior[1] of the region

$$\Delta^j_{k+1}(t) = (\gamma^j_{k+1}(t-1), \gamma^j_{k+1}(t)) \,.$$

[1] Where constraint (8.42) is inactive.

For t=1 there are no left parts $V_k^{t,L}$ and $u_k^{t,L}$ in (8.44)-(8.45). For $t = \psi_{k+1}^j$ there are no right parts $V_k^{t,R}$ and $u_k^{t,R}$. If

$$\frac{\partial^2 V_k^{t,U}}{(\partial x_{k+1})^2} = 2\left[\frac{R(j)}{b^2(j)} + \hat{K}_{k+1}^j(t)\right] < 0$$

for some t, then the inactive-constraint control $u_k^{t,U}$ is never valid; that is, for this t

$$\theta_k^j(t) = \Theta_k^j(t)$$

in (8.44)-(8.45), and therefore $V_k(x_k, r_k=j|t)$ has only two pieces. This kind of subproblem solution in (8.42) is the result of a sufficiently concave-down piece of the x-cost $Q(x,r=j)$. We saw an example of this in t=3 of Example 8.4. The derivation of expressions for these control law and expected cost pieces involves straightforward (but tedious) algebraic manipulations that are described in Appendix D.2. Formulae for the quantities in (8.44)-(8.45) are listed for reference in Appendix D.1.

The $V_k^{t,L}(x_k,j)$, $V_k^{t,U}(x_k,j)$ and $V_k^{t,R}(x_k,j)$ in (8.44)-(8.45) are similar to those of Chapter 5. In particular, when $\partial^2 V_k^{t,U}/(\partial x_{k+1})^2 \geq 0$ we have the following:

- at $x_k = \theta_k^j(t)/a(j)$ the values and slopes of $V_k^{t,L}(x_k,j)$ and $V_k^{t,U}(x_k,j)$ are the same. At $x_k = \Theta_k^j(t)/a(j)$, the values and slopes of

$V_k^{t,R}(x_k,j)$ and $V_k^{t,U}(x_k,j)$ are the same. At all other x_k values, the constrained costs are greater than the unconstrained costs. That is, for $t=2,\ldots,\psi_{k+1}^j$ (with $\partial^2 V_k^{t,U}/(\partial x_{k+1})^2 \geq 0$):

$$V_k^{t,L}(x_k,j) > V_k^{t,U}(x_k,j) \qquad x_k \neq \theta_k^j(t)/a(j)$$

$$V_k^{t,L}(x_k,j)\Big|_{x_k = \frac{\theta_k^j(t)}{a(j)}} = V_k^{t,U}(x_k,j)\Big|_{x_k = \frac{\theta_k^j(t)}{a(j)}} \tag{8.46a}$$

$$\frac{\partial V_k^{t,L}(x_k,j)}{\partial x_k}\Bigg|_{x_k = \frac{\theta_k^j(t)}{a(j)}} = \frac{\partial V_k^{t,U}(x_k,t)}{\partial x_k}\Bigg|_{x_k = \frac{\theta_k^j(t)}{a(j)}}$$

and for $t=1,\ldots,\psi_{k+1}^j-1$

$$V_k^{t,R}(x_k,j) > V_k^{t,U}(x_k,j) \qquad x_k \neq \frac{\Theta_k^j(t)}{a(t)}$$

$$V_k^{t,R}(x_k,j)\Big|_{x_k = \frac{\Theta_k^j(t)}{a(t)}} = V_k^{t,U}(x_k,j)\Big|_{x_k = \frac{\Theta_k^j(t)}{a(j)}} \tag{8.47a}$$

$$\frac{\partial V_k^{t,R}(x_k,j)}{x_k}\Bigg|_{x_k = \frac{\Theta_k^j(t)}{a(j)}} = \frac{\partial V_k^{t,U}(x_k,j)}{\partial x_k}\Bigg|_{x_k = \frac{\Theta_k^j(t)}{a(j)}} \quad \bullet$$

When $\partial^2 V_k^{t,U}/(\partial x_{k+1})^2 \leq 0$ we have, for $t=2,\ldots,\psi_{k+1}^j - 1$:

$$V_k^{t,L}(x_k,j)\Big|_{x_k=\frac{\theta_k^j(t)}{a(j)}=\frac{\Theta_k^j(t)}{a(j)}} = V_k^{t,R}(x_k,j)\Big|_{x_k=\frac{\theta_k^j(t)}{a(j)}=\frac{\Theta_k^j(t)}{a(j)}}$$

$$\frac{\partial V_k^{t,L}(x_k,j)}{\partial x_k}\Big|_{x=\frac{\theta_k^j(t)}{a(j)}=\frac{\Theta_k^j(t)}{a(j)}} > \frac{\partial V_k^{t,R}(x_k,j)}{\partial x_k}\Big|_{x=\frac{\theta_k^j(t)}{a(j)}=\frac{\Theta_k^j(t)}{a(j)}} \tag{8.46b}$$

For all $t=2,\ldots,\psi_{k+1}^j-1$ (regardless of the value of $\frac{\partial 2V_k^{t,U}}{(\partial x_{k+1})^2}$), (8.47b)

since $V_k^{t,R}(x_k,j)$ and $V_k^{t,L}(x_k,j)$ have the same curvature it follows that:

$$\begin{aligned} V_k^{t,R}(x_k,j) &< V_k^{t,L}(x_k,j) \quad \text{for} \quad a(j)x_k > \Theta_k^j(t) \\ V_k^{t,L}(x_k,j) &< V_k^{t,R}(x_k,j) \quad \text{for} \quad a(j)x_k < \Theta_k^j(t) \quad . \end{aligned} \tag{8.48}$$

Proof Step 4: Comparing the Constrained Costs

The fourth step in this proof of Proposition 8.1 is to compare the solutions of the ψ_{k+1}^j constrained JLQ problems specified by (8.42). For each $r_k = j \in \underline{M}$, $V_k(x_k, r_k=j)$ at each x_k value is the smallest of the constrained costs in (8.43). That is,

$$V_k(x_k,r_k=j) = \min_{t=1,\ldots,\psi_{k+1}^j} \{V_k(x_k,r_k=j \,|\, x_{k+1} \in \Delta_{k+1}^j(t))\} \quad . \tag{8.49}$$

This minimization involves the comparison of piecewise-quadratic functions in x_k.

In principle we can use (8.49) to find $V_k(x_k,r_k=j)$ and $u_k(x_k,r_k=j)$ (that is, the quantities $K_k(t:j)$, $H_k(t:j)$, $G_k(t:j)$, $L_k(t:j)$, $F_k(t:j)$, $\{\delta_k^j(t): t=1,\ldots,m_k(j)-1\}$ and $m_k(j)$ as in (8.36)-(8.37)). This minimization was done graphically for the examples of Section 8.3. In general, we must accomplish the minimization of (8.49) by finding the intersections of the quadratic functions

$$\left\{ \begin{array}{l} V_k^{1,U}(x_k,j),\ V_k^{1,R}(x_k,j),\ V_k^{2,L}(x_k,j),\ V_k^{2,U}(x_k,j),\ V_k^{2,R}(x_k,j),\ldots, \\ V_k^{\psi_{k+1}^j-1,L}(x_k,j), V_k^{\psi_{k+1}^j-1,U}(x_k,j), V_k^{\psi_{k+1}^j-1,R}(x_k,j), V_k^{\psi_{k+1}^j-1,L}(x_k,j) V_k^{\psi_{k+1}^j-1,U}(x_k,j) \end{array} \right\} \tag{8.50}$$

and choosing $V_k[x_k,r_k=j]$ at each value of x_k to be the one having the lowest value there (for those costs that are valid at x_k). Thus $V_k[x_k,r_k=j]$ is piecewise-quadratic in x_k and $u_k(x_k,r_k=j)$ is piecewise-linear, as claimed in (1) of Proposition 8.1. The verification of (2) in the proposition is straightforward, given our requirement that $Q^j(1)\geq 0$ and $Q^j(\bar{\mu}^j)\geq 0$ in (8.9).

The fact that

$$\frac{\partial V_k(x_k,r_k=j)}{\partial x_k} \quad \text{is either continuous or decreases discontinuously}$$

at the joining points $\{\delta_k^j(1),\ldots,\delta_k^j(m_k(j)-1)\}$ follows directly from the comparison in (8.49); a particular joining point $\delta_k^j(\ell)$ can arise in two ways:

(1) two (or more) of the constrained costs-to-go in (8.49) may cross at $\delta_k^j(\ell)$. Since $V_k(x_k,r_k=j)$ is the smallest candidate cost at each x_k value, the slope of $V_k(x_k,r_k=j)$ must decrease discontinuously at such a $\delta_k^j(\ell)$.

(2) $\delta_k^j(\ell)$ may be an x_k value where the optimal candidate cost in (8.49) changes from one of its parts ($V_k^{t,L}$, $V_k^{t,U}$, $V_k^{t,R}$) to another.

When $\dfrac{\partial V_k^{t,U}}{(\partial x_{k+1})^2} > 0$ we can have

- $\delta_k^j(\ell) = \theta_k^j(t)/a(j)$; where the left endpoint constraint becomes inactive (i.e., $V_k(x_k, j|t)$ changes from $V_k^{t,L}(x_k,j)$ to $V_k^{t,U}(x_k,j)$)

or

- $\delta_k^j(\ell) = \Theta_k^j(t)/a(j)$; where the right endpoint constraint becomes inactive (i.e., $V_k(x_k, j|t)$ changes from $V_k^{t,U}(x_k,j)$ to $V_k^{t,R}(x_k,j)$.

In either of these cases the slope of $V(x_k, r_k=j)$ is continuous at $S_k^j(\ell)$.

When $\dfrac{\partial 2V_k^{t,U}}{(\partial x_{k+1})^2} \leq 0$ we can have

- $\delta_k^j(\ell) = \Theta_k^j(t)/a(j) = \theta_k^j(t)/a(j)$, where the left endpoint constraint becomes inactive and the right endpoint constraint becomes active (i.e., $V_k(x_k, j|t)$ changes from $V_k^{t,L}(x_k,j)$ to $V^{t,R}(x_k,j)$). This occurs at the crossing point of $V_k^{t,L}(r_k,j)$ and $V_k^{t,R}(x_k,j)$. Consequently the slope of $V_k(x_k, r_k=j)$ decreases discontinuously here.

□

This concludes the proof of the one-stage solution given by Proposition 8.1. Certain qualitative properties of the optimal controller that are developed later in this chapter will be used to simplify the procedure that is described above.

8.5 An algorithm for computation of the optimal controller

In this section we examine several combinatoric and qualitative issues related to the (off-line) determination of the optimal control laws and costs of Proposition 8.1. Aspects of the problem that are addressed here include:

- the nature of active hedging; examining what values of an optimal controller will hedge to and why, and what values of will be avoided and why (Corollary 8.3),
- determining how many of the candidate costs (and control laws) must actually be computed and compared (Proposition 8.2),
- characterizing the number of pieces, $m_k(j)$ of the optimal expected costs $V_k(x_k, r_k=j)$ and control law $u_k(x_k, r_k=j)$.

The topics studied here are useful in the specification of an efficient way to carry out the algorithm steps that is indicated in the proof of Proposition 8.1.

These facts will be established as we pursue the following:

(1) First we show that many of the candidate costs in (8.50) cannot be optimal (for any x_k value) and hence they need not be computed (Proposition 8.2).

(2) Next we show that each candidate cost in (8.50) can be optimal over, at most, a single interval of x_k values. This bounds the number of pieces $m_k(j)$ of $V_k(x_k, r_k=j)$. (Proposition 8.4 and Corollary 8.5).

(3) We then describe the endpieces (Proposition 8.6) of the optimal JLQ controller for these problems.

(4) Finally, we use these results to devise an algorithm for the computation of the optimal controller in Proposition 8.1 that is efficient in the sense that many of the candidate costs in (8.49) need not be computed and compared.

The solution algorithm is presented in flowchart form and is described in detail. It is basically similar to the solution algorithm of section 7.2 (for the problems of chapter 5).

The following proposition eliminates many of the candidate costs in (8.50) from eligibility for the optimal cost.

Proposition 8.2: In performing the minimization in (8.49), the following candidate costs of (8.50) need not the examined:

(i) if

$$\hat{K}^j_{k+1}(t) > \frac{-R(j)}{b^2(j)} \tag{8.51}$$

and

$$\hat{K}^j_{k+1}(t+1) > \frac{-R(j)}{b^2(j)} \tag{8.52}$$

and $\hat{V}_{k+1}(x_{k+1}|r_k=j)$ is continuous at $\gamma^j_{k+1}(t)$ with

$$\begin{pmatrix} 2\,\hat{K}^j_{k+1}(t+1)\gamma^j_{k+1}(t) \\ + \\ \hat{H}^j_{k+1}(t+1) \end{pmatrix} \leq \begin{pmatrix} 2\,\hat{K}^j_{k+1}(t)\ \gamma^j_{k+1}(t) \\ + \\ \hat{H}^j_{k+1}(t) \end{pmatrix} \tag{8.53}$$

then we need not examine

$$V^{t,R}_k(x_k,j) \equiv V^{t+1,L}_k(x_k,j) \quad .$$

(ii) if

$$\hat{K}^j_{k+1}(t) \leq \frac{-R(j)}{b^2(j)} \tag{8.54}$$

then we need not examine

$$V^{t\ ,U}_k \quad .$$

(iii) if $\hat{V}_{k+1}(x_{k+1}|r_k=j)$ is discontinuous at $\gamma^j_{k+1}(t)$ with

$$\begin{pmatrix} [\gamma^j_{k+1}(t)]^2[\hat{K}^j_{k+1}(t)-\hat{K}^j_{k+1}(t+1)] \\ + \\ \gamma^j_{k+1}(t)\,[\hat{H}^j_{k+1}(t)-\hat{H}^j_{k+1}(t+1)] \\ + \\ [\hat{G}^j_{k+1}(t)-\hat{G}^j_{k+1}(t+1)] \end{pmatrix} < 0 \tag{8.55}$$

then we need not examine $V^{t+1,L}_k(x_k,j)$.

(iv) if $\hat{V}_{k+1}(x_{k+1}|r_k=j)$ is discontinuous at $\gamma_{k+1}^{j}(t)$ with the inequality in (8.55) reversed, then we need not examine

$$V_k^{t,R}(x_k,j) \ .$$

The proof of this proposition is in Appendix D.3. □

This proposition is a generalization of Proposition 5.2. For the problems of Chapter 5, (8.51)-(8.53) are always true and (8.54) never occurs. For the more general problems of section 8.2 we must account (in Proposition 8.2) for additional possibilities. Consequently we must examine a different (and usually more numerous) set of candidate costs than for those of Chapter 5 in the minimuzation of (8.49).

For example, if either (8.51) or (8.52) does not hold, then we must examine $V_k^{t,R}(x_k,j) = V_k^{t+1,L}(x_k,i)$ even though $V_{k+1}(x_{k+1}|r_k = j)$ is continuous at $\gamma_{k+1}^{j}(t)$. In examples 8.3 and 8.4 the optimal controller hedged to continuous points of $\hat{V}_N(x_N|r_{N-1} = 1)$ for x_{N-1} intervals over which these additional eligible candidates were optimal. Hedging to continuous points of the conditional expected cost-to-go was <u>not</u> possible for the JLQ problems of Part III.

An illustration of Proposition 8.2 (ii) appeared in example 8.4. The candidate cost $V_{N-1}^{3,U}(x_{N-1} = 1)$ was shown to never be valid, because

$$\frac{\partial^2 V_{N-1}^{3,U}}{(\partial U_{N-1})^2} < 0.$$

This second derivative is negative if and only if $\hat{K}_N^1(3) \leq \frac{-R(1)}{b^2(1)}$, as in (8.54). Thus Proposition 8.2 (ii) specifies that for example 8.3 we need not examine $V_{N-1}^{3,U}$ but we do have to examine $V_{N-1}^{3,L}$ and $V_{N-1}^{3,R}$.

Our requirements on $K_T^k(i)$, $K_T^j(\eta^{-j})$ $Q^j(1)$ and $Q^j(\eta^{-j})$ in (8.9) guarantee that (8.54) does not hold for t=1, ψ_{k+1}^j. That is, we must always examine $V_k^{1,U}$ and $V_k^{\psi_{k+1}^j,U}$.

Therefore the endpiece candidate costs $V_k^{1,U}(x_k,j)$ and $V_k^{\psi_K^j}(x_k,j)$ are eligible candidates for consideration.

The following corollary specifies necessary conditions for a point x_{k+1} to be hedged to.

Corollary 8.3:

If the optimal controller in Proposition 8.1 hedges from $(x_k,r_k=j)$ to the point $x_{k+1}=x$ then one (or more) of the following is true:

(1) x is a discontinuous point of the conditional cost $\hat{V}_{k+1}(x_{k+1}|r_k=j)$,

or

(2) x is a boundary ($\gamma_{k+1}^j(t)$ or $\gamma_{k+1}^j(t-1)$) of an interval $\Delta_{k+1}^j(t)$ over which the conditional cost $\hat{V}_{k+1}(x_{k+1}|r_k=j)$ has

$$\hat{K}_{k+1}^j(t) \leq -R(j)/b^2(j),$$

or

(3) $x = \gamma_{k+1}^j(t)$ is a boundary of intervals $\Delta_k^j(t)$ and $\Delta_k^j(t+1)$ where $\hat{V}_{k+1}(x_{k+1}|r_k=j)$ is continuous and

$$2\gamma_{k+1}^j(t)[\hat{K}_{k+1}^j(t+1)-\hat{K}_{k+1}^j(t)] \geq \hat{H}_{k+1}^j(t)-\hat{H}_{k+1}^j(t+1) \qquad (8.56)$$

Proof: Hedging-to-a-point can occur only to finite boundary points of the x_{k+1} intervals $\{\Delta_{k+1}^j(t): t=1,\ldots,\psi_{k+1}^j\}$; that is, to

an element of the set $\{\gamma_{k+1}^{j}(t): t=1,\ldots,\psi_{k+1}^{j}-1\}$. When the optimal controller drives x_{k+1} to such a point from x_k, then either $V_k^{t,R}$ or $V_k^{t+1,L}$ is the optimal cost from that x_k. Proposition 8.2 excludes many of these constrained candidate costs from eligibility. Corollary 8.3 lists the possible ways that a constrained cost $V_k^{t,R}$ or $V_k^{t+1,L}$ associated with $\gamma_{k+1}^{j}(t)$ can be eligible. Corollary 8.3(1) occurs when either Proposition 8.2(iii) or 8.2(iv) holds. Here we hedge to the low-cost side of a $\hat{V}_{k+1}(x_{k+1}|r_k=j)$ discontinuity. Corollary 8.3(2) occurs when Proposition 8.2(ii) holds, When (8.54) is true, $V_k^{t,U}$ is not eligible but both $V_k^{t,L}$ and $V_k^{t,R}$ are eligible (unless excluded by Proposition 8.2(iii) or (iv)). Corollary 8.3(3) holds when (8.53) of Proposition 8.2(i) is not satisfied. □

Note that if one or more of the conditions of Corollary 8.3 is satisfied for some $x = \gamma_{k+1}^{j}(t)$, we are not guaranteed that the optimal controller hedges to that x; the associated constrained costs $V_k^{t,R}$ and $V_k^{t+1,L}$ need not be optimal in (8.49).

From Proposition 8.2 we know that the mapping

$$x_k \longmapsto x_{k+1}(x_k, r_k=j)$$

need not be one-to-one, in that hedging to points may occur. Proposition 5.3, which lists a number of general qualitative properties of the optimal controller, applies for the JLPQ problems of this chapter. We repeat this proposition here. The proof of this result for the JLPQ case is somewhat different in detail from the JLQ case.

Proposition 8.4:

The optimal controller of Proposition 8.1 has the following properties:

(1) At each time k and in each form $j \in M$, between joining points $\{\delta_k^j(t): t=1,\ldots,m_k(j)-1\}$ of $V_k(x_k, r_k=j)$:

$$u_k(x_k, r_k=j) = \frac{-b(j)}{2a(j)R(j)} \frac{\partial V_k(x_k, r_k=j)}{\partial x_k} \tag{8.57}$$

$$x_{k+1}(x_k, r_k=j) = a(j)x_k - \frac{b^2(j)}{2a(j)R(j)} \frac{\partial V_k(x_k, r_k=j)}{\partial x_k} \tag{8.58}$$

(here $a(j)R(j)\neq 0$, $b(j)\neq 0$).

(2) At those joining points δ where the slope of $V_k(x_k, r_k=j)$ does not change $\left(\text{ie, } \frac{\partial V_k(x_k, r_k=j)}{\partial x_k}\Big|_{x_k=\delta} \text{ exists} \right)$,

$u_k(x_k, r_k=j)$ and $x_{k+1}(x_k, r_k=j)$ are continuous functions of x_k.

(3) At those joining points $\delta_k^j(t)$ where the slope of $V_k(x_k, r_k=j)$ decreases discontinuously

$$\left(\text{i.e., } \frac{\partial V_k(x_k, r_k=j)}{\partial x_k}\Big|_{x_k=\delta^+} < \frac{\partial V_k(x_k, r_k=j)}{\partial x_k}\Big|_{x_k=\delta^-} \right),$$

(i) $u_k(x_k, r_k=i)$ <u>increase</u> discontinuously at δ when

$\frac{b(j)}{a(j)} > 0$ (and <u>decreases</u> discontinuously at δ when $\frac{b(j)}{a(j)} < 0$)

(ii) the mapping $x_k \longmapsto x_{k+1}(x_k, r_k=j)$ <u>increases</u> discontinuously at δ when $a(j) > 0$) (and decreases discontinuously at δ when $a(j) < 0$).

(4) The mapping

$$x_k \longmapsto x_{k+1}(x_k, r_k=j)$$

has the following properties:

(i) the mapping is <u>monotonely nondecreasing</u> if $a(j) > 0$ (and monotonely nonincreasing if $a(j) < 0$) for each $j \in \underline{M}$

(ii) it consists of $m_k(j)$ line segments:

- one line segment with positive slope if $a(j) > 0$ (negative slope if $a(j) < 0$) for each x_k region where an "unconstrained cost" $V_k^{t,U}(x_k, r_k=1)$ is optimal:

$$V_k(x_k, r_k=j) = V_k^{t,U}(x_k, r_k=j)$$

$$x_{k+1} = \left[\frac{a(j)R(j)}{R(j)+b^2(j)\hat{K}_{k+1}^j(t)}\right] x_k - \frac{b^2(j)\hat{H}_{k+1}^j(t)}{2[R(j)+b^2(j)\hat{K}_{k+1}^j(t)]} \tag{8.59}$$

. a <u>constant</u> line segment for each x_k region where there is active hedging-to-a-point:

$$x_{k+1} = \gamma^j_{k+1}(t) \quad t\in\{1,\ldots,\psi^j_{k+1}\}.$$

(iii) there are regions of x_{k+1} avoidance associated with (and only with) each $x_k=\delta$ value where the slope of $V_k(x_k,r_k=j)$ decreases discontinuously.

(5) Each candidate linear control law associated with the costs listed in (8.50) can be optimal over, at most, a single interval of x_k values.

□

<u>Proof</u>: Items ((1)-(3) and are proven exactly as for Proposition 5.3 in Appendix C-4. For item (4): From 3(ii) we have that the mapping

$$x_k \longmapsto x_{k+1}(x_k,r_k=j)$$

increases discontinuously at joining points where $V_k(x_k,r_k=j)$ is not differentiable, and from (2) the mapping is continuous at other joining points.

Now between joining points, if the optimal cost corresponds to hedging-to-a-point then clearly the mapping is constant. If the optimal cost does not correspond to hedging-to-a-point, then in such a region

$$V_k(x_k,r_k=j) = V_k^{t,U}(x_k,j) = x_k^2K_k^j(t) + x_kH_k^j(t) + G_k^j(t)$$

for some $t\in\{1,\ldots,\psi^j_{k+1}\}$. Thus from (8.58)

$$x_{k+1}(x_k,r_k=j) = a(j)x_k - \frac{b^2(j)}{2a(j)R(j)} \frac{\partial V_k(x_k,r_k=1)}{\partial x_k}$$

hence

$$\frac{\partial x_{k+1}}{\partial x_k} = a(j) \frac{b^2(j)}{2a(j)R(j)} \frac{\partial^2 V_k(x_k,r_k=j)}{(\partial x_k)^2}$$

$$= a(j) - \frac{b^2(j)}{2a(j)R(j)} 2K^j_k(t) \quad .$$

If $R(j) + b^2K^j_{k+1}(t)=0$ then $\hat{K}^j_k(t)=0$, so $\frac{\partial x_{k+1}}{\partial x_k} = a(j)>0$.

If $R(j) + b^2K^j_{k+1}(t)\neq 0$ then

$$\frac{\partial x_{k+1}}{\partial x_k} = a(j) - \frac{b^2(j)}{2a(j)R(j)} \frac{2a^2(j)R(j)\hat{K}^j_{k+1}(t)}{R(j)+b^2(j)\hat{K}^j_{k+1}(t)}$$

$$= \frac{a(j)R(j)}{R(j)+b^2(j)\hat{K}^j_{k+1}(t)} \quad . \tag{8.60}$$

If $\hat{K}^j_{k+1}(t) > -R(j)/b^2(j)$ then $\frac{\partial x_{k+1}}{\partial x_k} > 0$ in (8.60) if $a(j)> 0$ $\left(\text{and } \frac{\partial x_{k+1}}{\partial x_k} < 0\right)$. But for $V^{t,U}_k(x_k,r_k=j)$

to be optimal over some interval of x_k values, we must have

$$\hat{K}^j_{k+1}(t) > - R(j)/b^2(j)$$

by Proposition 8.2. Thus we have 4(i), (ii). The remainder of the Proof of Proposition 8.4 follows the proof of Proposition 5.3 in Appendix C.4, exactly.

□

Proposition 8.2 restricts the number of candidate costs that must be considered in (8.49) and fact (5) of Proposition 8.4 says that each candidate can be optimal over at most one x_k interval. Thus we immediately have from (8.50):

Corollary 8.5:

The number of pieces of the optimal expected costs-to-go $V_k(x_k, r_k=j)$ and their associated control laws are bounded above by

$$m_k(j) \leq 3\psi^j_{k+1} - 2 \quad . \tag{8.61}$$

A weaker bound which follows from (8.41) is

$$m_k(j) \leq 3 \sum_{i \in c_j} [\bar{\nu}_{ji} + \bar{\mu}^i + m_{k+1}(i)] - 8 \quad . \tag{8.62}$$

□

The bound on the growth of the number of pieces, $m_k(j)$, (as (k-N) increases) in Corollary 8.5 is much larger than for the JLQ problems (in Corollary 5.4). Corollary 8.5 suggests that

the number of pieces in each optimal expected cost $V_k(x_k,r_k=j)$ may grow geometrically rather than linearly (because of the factor $3m_{k+1}(i)$ in (8.62)).

We examine next the behavior of the optimal JLPQ controller when x is far from zero. As in the JLQ controller, over their endpieces $V_k(x_k,r_k=j)$ and $u_k(x_k,r_k=j)$ can be computed from sets of recursive difference equations. These equations correspond to the solutions of x-independent form probability, single-piece x cost JLQ problems (as in Chapter 3).

For finite time horizon problems, if x_k is negative enough or positive enough the optimal strategy will be to keep x in the same extreme piece of the form transition probabilities p(j,i:x) and x-costs $Q(x;\ell)$, $Q_T(x,j)$, for all if c_j from each $j\in\underline{M}$, for all future times.

Proposition 8.6: Endpieces

Consider the JLQ problem of Proposition 8.1.

(1) For $x_k \leq \delta_k^j(1)$, the optimal control laws and expected costs-to-go are

$$V_k(x_k,r_k=j) = V_k^{1,U}(x_k,j)$$
$$\triangleq V_k^{Le}(x_k,j) = x_k^2 K_k^{Le}(j) + x_k H_k^{Le}(j) + G_k^{Le}(j) \quad (8.63)$$

$$u_k(x_k, r_k=j) = u_k^{1,U}(x_k, j)$$

$$\triangleq u_k^{Le}(x_k, j) = -L_k^{Le}(j)x_k + F_k^{Le}(j) \quad \bullet \tag{8.64}$$

(2) For $x_k \geq \delta_k^j(m_k(j)-1)$, the optimal expected costs-to-go and control laws are

$$V_k(x_k, r_k=j) = V_k^{\psi_{k+1}^j, U}(x_k, j)$$

$$\triangleq V_k^{Re}(x_k, j) = x_k^2 K_k^{Re}(j) + x_k H_k^{Re}(j) + G_k^{Re}(j) \tag{8.65}$$

$$u_k(x_k, r_k=j) = u_k^{\psi_{k+1}^j, U}(x_k, j)$$

$$\triangleq u_k^{Re}(x_k, j) = -L_k^{Re}(j)x_k + F_k^{Re}(j) \quad \bullet \tag{8.66}$$

(3) The parameters in (8.63)-(8.66) are computed recursively, backwards in time from N by

$$K_k^{Le}(j) = \frac{a^2(j)R(j)\hat{K}_{k+1}^{Le}(j)}{R(j)+b^2(j)\hat{K}_{k+1}^{Le}(j)} \tag{8.67}$$

$$H_k^{Le}(j) = \frac{a(j)R(j)\hat{H}_{k+1}^{Le}(j)}{R(j)+b^2(j)\hat{K}_{k+1}^{Le}(j)} \tag{8.68}$$

$$G_k^{Le}(j) = \hat{G}_{k+1}^{Le}(j) - \frac{b^2(j)[\hat{H}_{k+1}^{Le}(j)]^2}{4[R(j)+b^2(j)\hat{K}_{k+1}^{Le}(j)]} \tag{8.69}$$

where

$$\hat{K}^{Le}_{k+1}(j) = \sum_{i \in c_j} \lambda_{ji}(1)\,[K^{Le}_{k+1}(i) + Q^{j}(1)] \tag{8.70}$$

$$\hat{H}^{Le}_{k+1}(j) = \sum_{i \in c_j} \lambda_{ji}(1)\,[H^{Le}_{k+1}(i) + S^{i}(1)] \tag{8.71}$$

$$\hat{G}^{Le}_{k+1}(j) = \sum_{i \in c_j} \lambda_{ji}(1)\,[G^{Le}_{k+1}(i) + P^{i}(1)] \tag{8.72}$$

and

$$K^{Re}_{k}(j) = \frac{a^2(j)R(j)\hat{K}^{Re}_{k+1}(j)}{R(j)+b^2(j)\hat{K}^{Re}_{k+1}(j)} \tag{8.73}$$

$$H^{Re}_{k}(j) = \frac{a(j)R(j)\hat{H}^{Re}_{k+1}(j)}{R(j)+b^2(j)\hat{K}^{Re}_{k+1}(j)} \tag{8.74}$$

$$G^{Re}_{k}(j) = \hat{G}^{Re}_{k+1}(j) - \frac{b^2(j)[\hat{H}^{Re}_{k+1}(j)]^2}{4[R(j)+b^2(j)\hat{K}^{Re}_{k+1}(j)]} \tag{8.75}$$

where

$$\hat{K}^{Re}_{k+1}(j) = \sum_{i \in c_j} \lambda_{ji}(\bar{\nu}_{ji})\,[K^{Re}_{k+1}(j) + Q^{i}(\bar{\mu}^{i})] \tag{8.76}$$

$$\hat{H}^{Re}_{k+1}(j) = \sum_{i \in c_j} \lambda_{ji}(\bar{\nu}_{ji})\,[H^{Re}_{k+1}(i) + S^{i}(\bar{\mu}^{i})] \tag{8.77}$$

$$\hat{G}^{Re}_{k+1}(j) = \sum_{i \in c_j} \lambda_{ji}(\bar{\nu}_{ji}) [G^{Re}_{k+1}(i) + P^i(\bar{\mu}^i)] \tag{8.78}$$

with terminal conditions

$$K^{Le}_k(j) = K^j_T(1) \tag{8.79}$$

$$K^{Re}_N(j) = K^j_T(\bar{\eta}^j) \tag{8.80}$$

$$H^{Le}_N(j) = H^j_T(1) \tag{8.81}$$

$$H^{Re}_N(j) = H_T(\bar{\eta}^j) \tag{8.82}$$

$$G^{Le}_N(j) = G^j_T(1) \tag{8.83}$$

$$G^{Re}_N(j) = G^j_T(\bar{\eta}^j) \tag{8.84}$$

The control law gains are

$$L^{Le}_K(j) = \frac{a(j)b(j)\hat{K}^{Le}_{k+1}(j)}{R(j)+b^2(j)\hat{K}^{Le}_{k+1}(j)} \tag{8.85}$$

$$F^{Le}_k(j) = \frac{-b(j)\hat{H}^{Le}_{k+1}(j)}{2[R(j)+b^2(j)\hat{K}^{Le}_{k+1}(j)]} \tag{8.86}$$

$$L^{Re}_k(j) = \frac{a(j)b(j)\hat{K}^{Re}_{k+1}(j)}{R(j)+b^2(j)\hat{K}^{Re}_{k+1}(j)} \tag{8.87}$$

$$F^{Re}_k(j) = \frac{-b(j)\hat{H}^{Re}_{k+1}(j)}{2[R(j)+b^2(j)\hat{K}^{Re}_{k+1}(j)]} \tag{8.88}$$

Proof: This proposition is essentially the same as Proposition 6.1, except for the parameters of the extreme x-cost pieces in (8.70)-(8.72), (8.76)-(8.78) and terminal conditions (8.79)-(8.84).

In these extreme pieces since we have assumed (in (8.9)) that

$$Q^j(1) \geq 0 \qquad Q^j(\bar{\mu}^j) \geq 0$$

$$K_T^j(1) \geq 0 \qquad K_T(\bar{\eta}^j) \geq 0$$

for all $j \in \underline{M}$, we will have

$$\hat{K}_{k+1}^j(1) > \frac{-R(j)}{b^2(j)} \qquad \text{and}$$

$$\hat{K}_{k+1}^j(\psi_{k+1}^j) \geq 0 \qquad .$$

Thus by Proposition 8.2, $V_k^{1,U}(x_k,j)$ and $V_k^{\psi_{k+1}^j,U}(x_k,j)$ will be valid subproblem solutions in (8.49) for some range of x_k values. Therefore we can apply the arguments of Appendix C.5 directly to establish Proposition 8.6. □

The conditions for the existence of steady-state endpiece cost parameters and control law parameters are the same as in Proposition 6.2, and will not be repeated here.

We have identified some basic qualitative properties of the JLPQ problem that can be used to reduce the combinatories involved in the "brute-force" solution of the one-stage problem that was

presented in the proof of Proposition 8.1. We now present a solution algorithm that exploits these properties, enabling us to solve the general JLPQ problem (8.1)-(8.10) efficiently.

This algorithm is based upon the application of the one-stage solution of Proposition 8.1 recursively, backwards in time, for each, $j \in \underline{M}$ that the system can take. The basic idea of the JLPQ solution algorithms is the same as in the JLQ solution algorithm of Section 7.2. For each form $j \in \underline{M}$ at time k, we can compute $V_k(x_k, r_k=j)$ and $u_k(x_k, r_k=j)$ one piece at a time, sweeping from left to right along the axis of $a(j)x_k$ values.

An overview of the solution algorithm is shown in Figure 8.5. The algorithm is initialized with the terminal time (k=N) cost parameter (block 2). Then for successively decreasing times through $k=k_o$ (block 13), the one-stage solution of Proposition 8.1 is obtained for each form $j \in \underline{M}$ (block 10). Figure 8.5 differs substantially from the analogous flowchart (figure 7.1) of Section 7.2 only in the initialization block (block 1).

In the following discussions we refer to the algorithm flowchart shown in Figures 8.5-8.11. All of the steps indicated in this flowchart constitute one iteration of block 10 in Figure 8.5. That is, they determine the one-stage JLPQ solution that is specified by Proposition 8.1 for some time stage k and form j. For the reader's convenience, a table of block number locations and entry points is given in Table 8.5.

Figure Number	Block Numbers	Entry Points	Exit Points
8.5	1-15	Start (blk. 1)	Stop (blk. 14)
8.6	16-26	from block 10	① (blk. 22)
8.7	27-51	① (blk. 27)	② (blk. 46,48) ③ (blk. 31)
8.8	52-63	② (blk. 52)	③ (blk. 63)
8.9	64-68	③ (blk. 64)	④ (blk. 68) ⑦ (blk. 68)
8.10	69-76	④ (blk. 69) ⑥ (blk. 76)	⑤ (blk. 70)
8.11	77-86	⑤ (blk. 77) ⑦ (blk. 80)	⑥ (blk. 84) ④ (blk. 86)
		return to block 10 from blk. 82)	

TABLE 8.5: Block Number Locations and entry points for JLPQ solution algorithm flowchart.

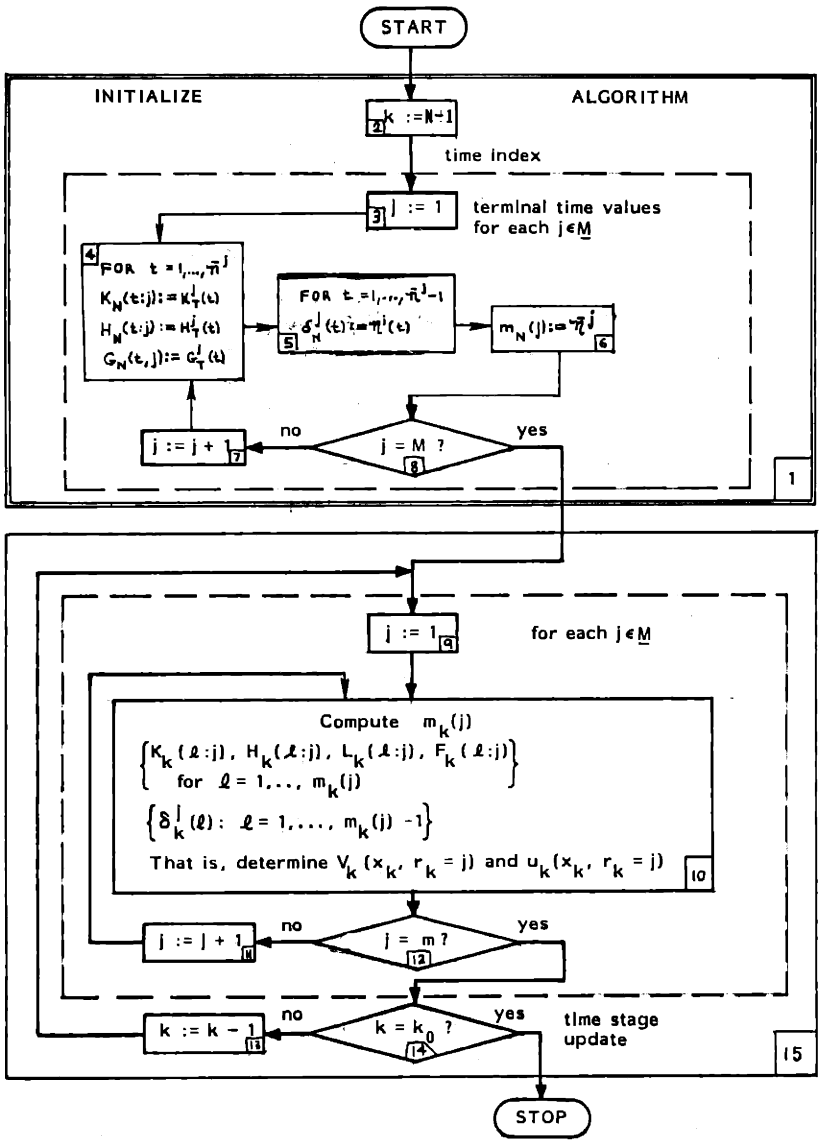

Figure 8.5 Algorithm Overview

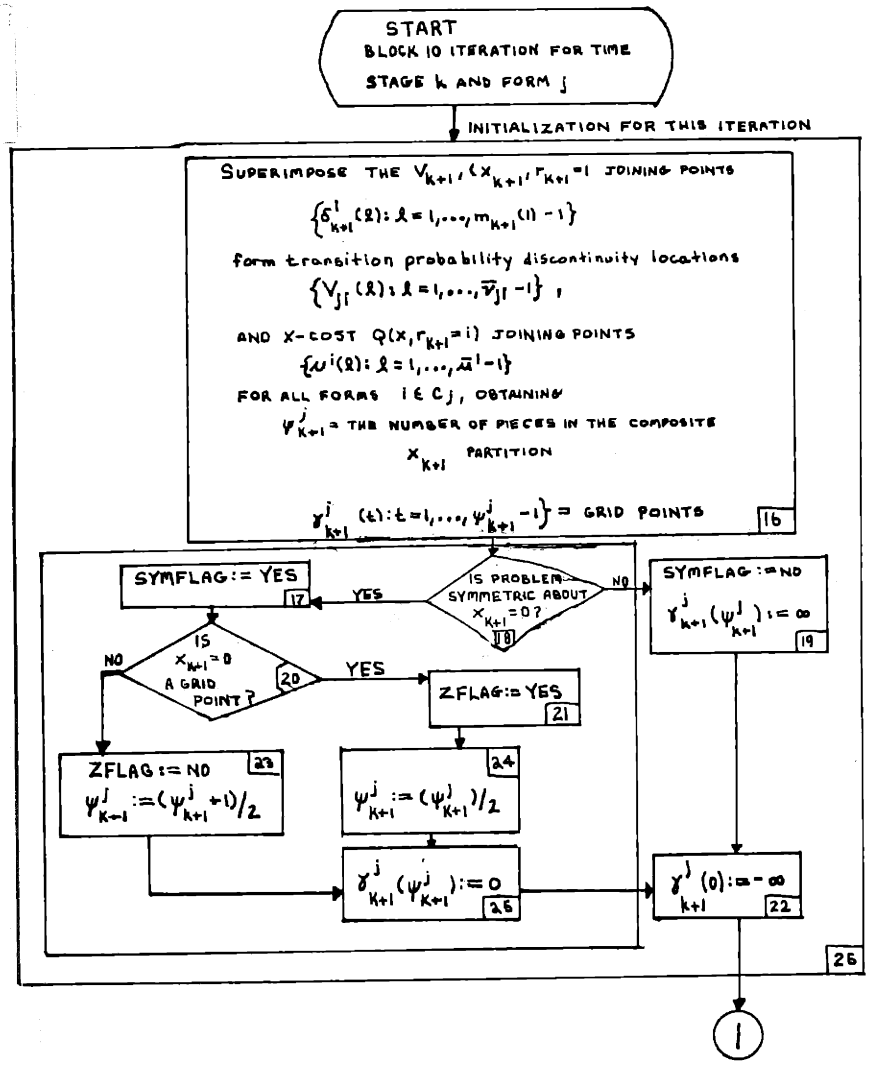

Figure 8.6: One Stage Solution Flowchart - Part II

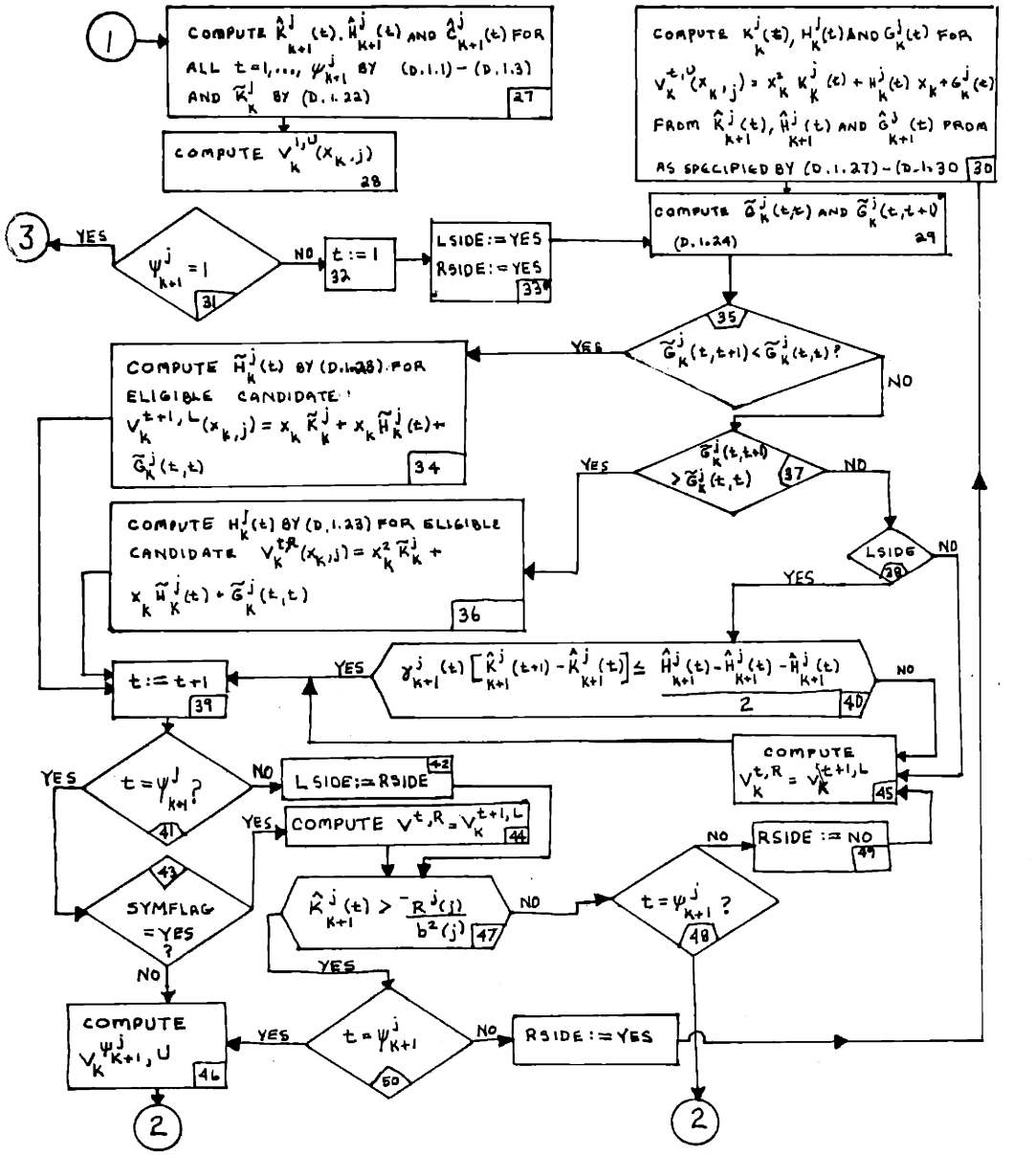

Figure 8.7: Flowchart, Part III: Using Proposition 8.2

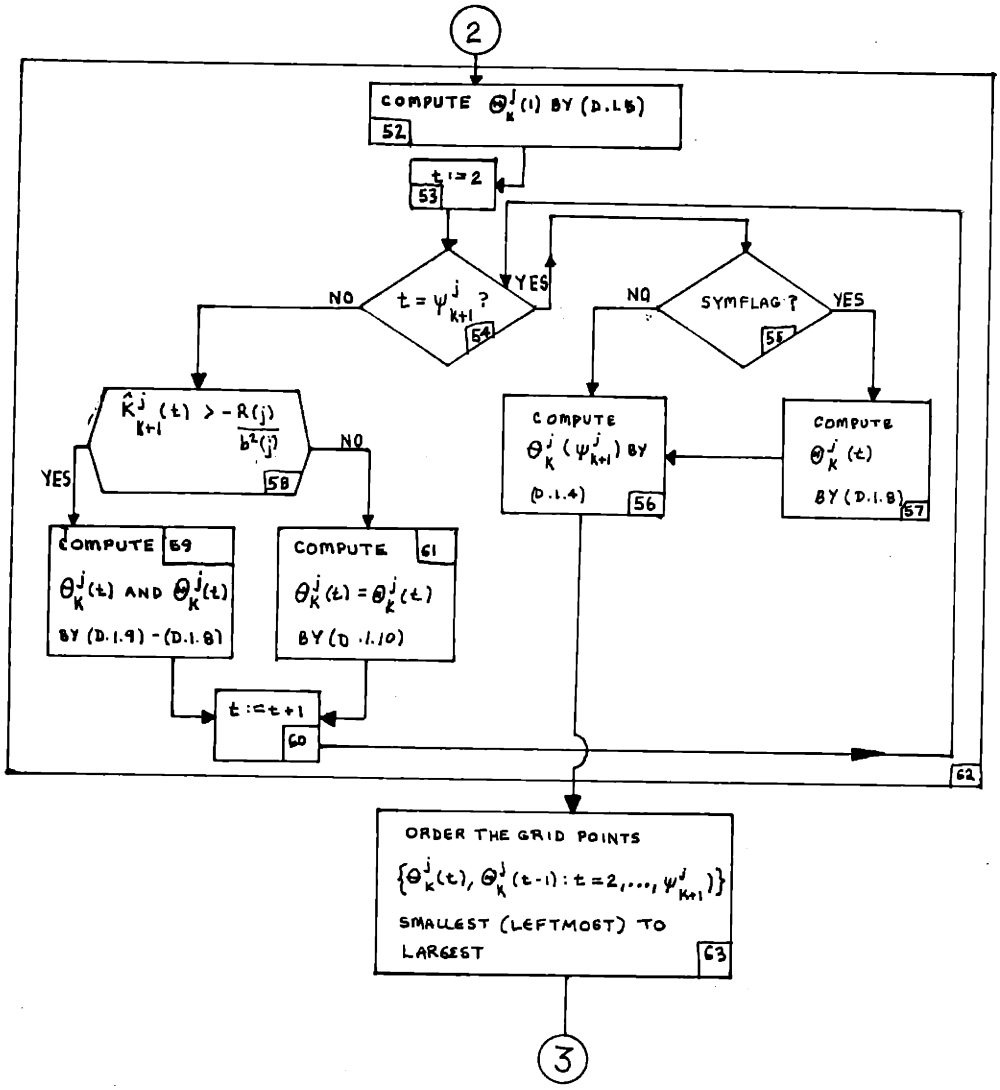

Figure 8.8: Flowchart, Part IV: Obtaining the θ -- Θ Grid

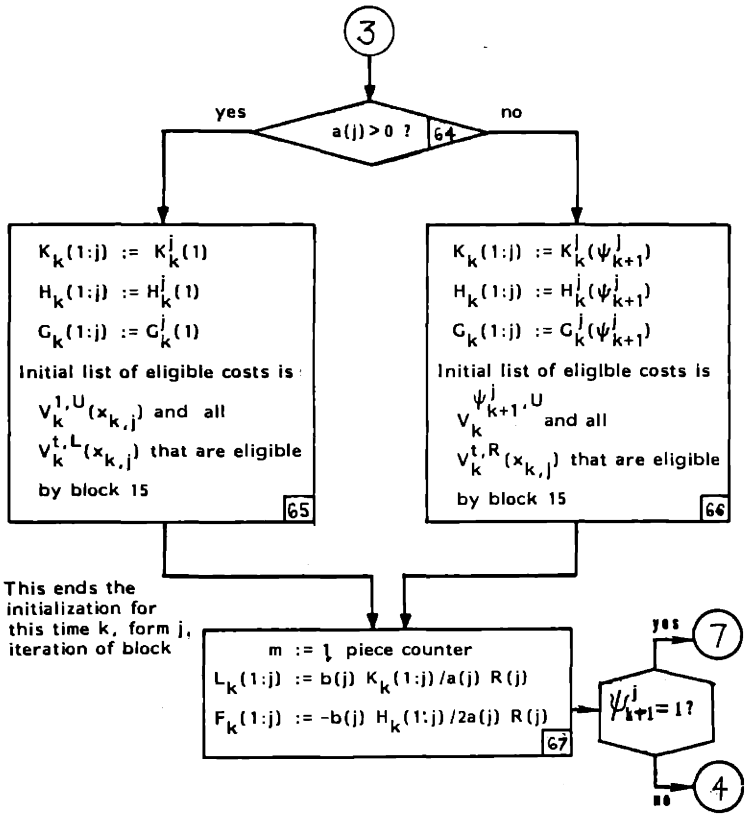

Figure 8.9: Flowchart, Part V: End of Initialization

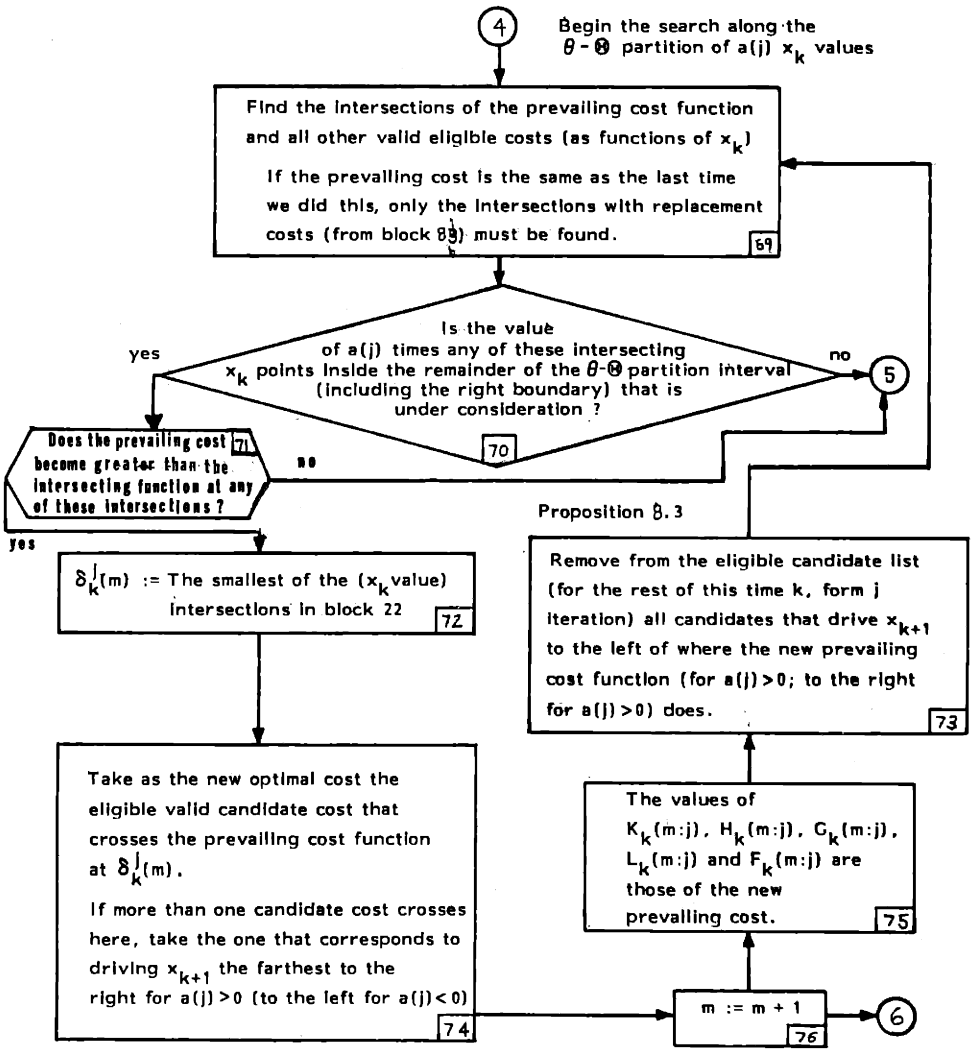

Figure 8.10: Flowchart, Part IV: Comparison within a θ--Θ Interval

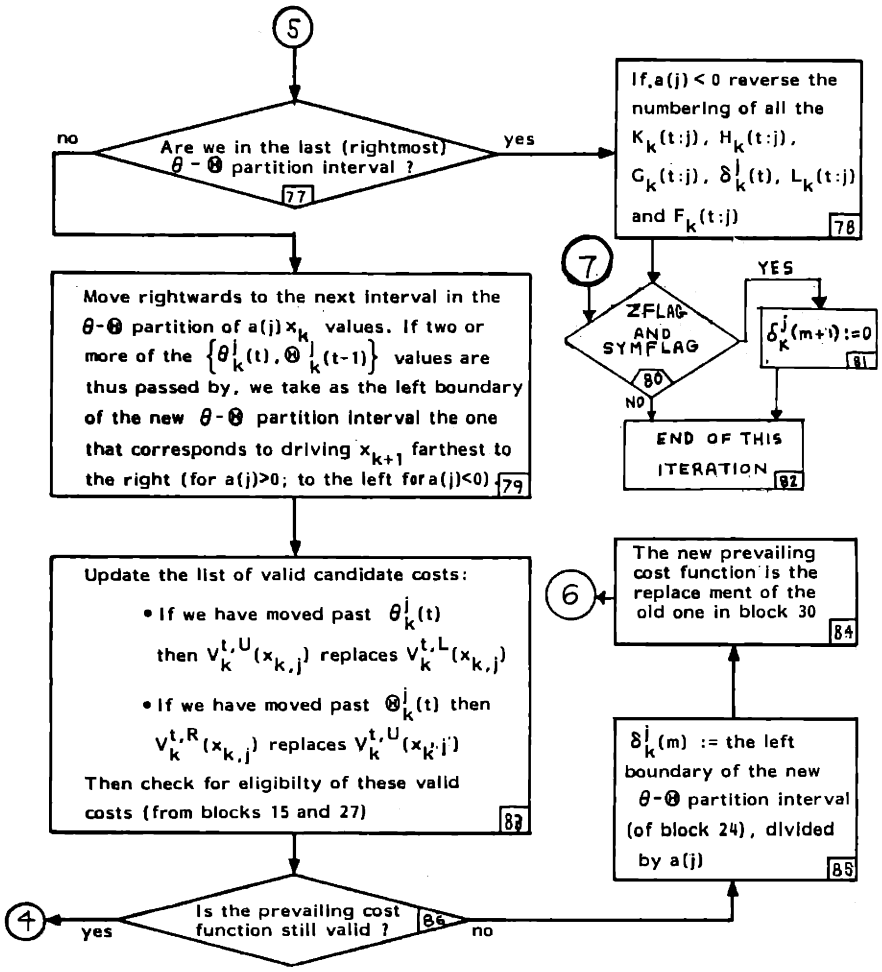

Figure 8.11: Flowchart, Part VII: Moving Rightwards

A macroscopic overview of the algorithm specified by this flowchart is as follows:

1. The algorithms is first initialized (in block 1) at time N with the terminal x-cost $Q_T(x,j)$ for each $j \in \underline{M}$.

2. The determination of the optimal controller at time k for a fixed j value constitutes one iteration in block 10.

3. The computations of block 9 begin in block 26 with the determination of the composite x_{k+1} partition (block 16). This partition is obtained from the joining points of $V_{k+1}(x_{k+1}, r_{k+1}=i)$ for all $i \in c_j$ that were computed in the previous time stage, and from known parameters of the problem.

4. For symmetric problems about zero we only compute this grid for $x_{k+1} \leq 0$. This is accomplished by blocks 17,23,24 and 25. If $x_{k+1}=0$ is agrid point we must be sure to include it in later calculations (blocks 20,21).

5. The next task is to determine which candidate cost-to-go functions are eligible for optimality with respect to Proposition 8.2, and to compute the parameters for these eligible functions. This is done in Figure 8.7. We begin by computing the conditional cost parameters for $\hat{V}_{k+1}(x_{k+1} | r_k=j)$ for all $t=1,\ldots,\psi_{k+1}^j$ in block 27. We also calculate $\hat{K}_k^j$ here.

6. By Proposition 6.1, the endpiece cost $V_k^{1,U}(x_k,j)$ is always an eligible candidate. It is computed in block 28. If $\psi_{k+1}^j=1$ then we are done (block 31). If not, then the x_{k+1} partition piece counter is set to t=1 in block 32, and the variable Lside is set to "yes" in block 33. The variable Lside answers the question:

"is $\hat{K}_{k+1}^j(t) > -R(j)/b^2(j)$?"

That is, is (8.51) satisfied on the left side of $\gamma_{k+1}^j(t)$?

7. In blocks 29,35,37 we determine if $\hat{V}_{k+1}(x_{k+1}|r_k=j)$ has a discontinuity at $x_{k+1} = \gamma_{k+1}^j(t)$. If there is a discontinuity, then either $V_k^{t,R}$ or $V_k^{t+1,L}$ is computed (as specified by (iii)-(iv) of Proposition 8.2) in block 34 or 36.

8. If $\gamma_{k+1}^j(t)$ is not a discontinuous point of $\hat{V}_{k+1}(x_{k+1}|r_k=j)$ then we enter block 38. If Lside=no then either t=1 or

$$\hat{K}_{k+1}^j(t-1) \leq \frac{-R(j)}{b^2(j)} \quad \bullet$$

That is, (8.51) of Proposition 8.2(i) is not satisfied so we must compute $V_k^{t,R}(x_k,j)$ and $V_k^{t+1,L}(x_k,j)$, in block 45.

9. If Lside=yes in block 38 then we check condition (8.53) of Proposition 8.2(i) in block 40, and compute $V_k^{t,R}(x_k,j)$ and $V_k^{t+1,L}(x_k,j)$ if required (in block 45).

10. The x_{k+1} partition piece counter, t, is incremented in block 39. If $t=\psi_{k+1}^j$ (block 41) and the problem is not symmetric (block 43) then we compute $V_k^{\psi_{k+1}^j,U}$ (in block 46) which, by Proposition 8.6, is an eligible cost candidate.

11. If $t=\psi_{k+1}^j$ (block 41) and the problem <u>is</u> symmetric (block 43)then $V^{\psi_{k+1}^j,U}$ is <u>not</u> an endpiece (because of block 24). Therefore we compute $V_k^{t,R} = V_k^{t+1,L}$ (in block 44) and test to see if $V^{\psi_{k+1}^j,U}$ should also be calculated (in block 47), according to (8.54) of Proposition 8.2(ii). If it should, we pass from block 47 to 50 to 46. If not, we exit via block 48.

12. If $t < \psi_{k+1}^j$ in block 41 then we assign the Rside value to Lside (in block 42) and then test (8.54) of Proposition 8.2(ii) (in block 47) to see if $V_k^{t,U}$ should be calculated. If it should, we set Rside to yes (in block 51) and perform the calculations in block 30. If not, we set Rside to no (in block 49) and compute $V_k^{t,R} = V_k^{t+1,L}$ (in block 45).

13. Upon leaving figure 8.7, we have calculated all of the cost parameters for eligible candidate cost functions. Figure 8.7 is substantially different from figure 7.3 of the algorithms of section 7.2, due to the major differences between Propositions 5.2 and 8.7.

14. We next prepare for the rightward sweep along the $a(j)x_k$ axis by obtaining in Figure 8.8 the partition of the real line (of $a(j)x_k$ values) that is caused by the points $\{\theta_k^j(t), \Theta_k^j(t-1): t=2,..,\psi_{k+1}^j\}$. If the problem is symmetric we compute $\Theta_k^j(\psi_{k+1}^j)$ as well, in block 57. In block 63 we obtain the grid ordering required for the righthand sweep. Initialization of the righthand sweep is completed in Figure 8.9, where the endpiece result of Proposition 8.6 is applied. Figures 8.8 and 8.9 are more complicated than figure 7.9 in the section 7.2 algorithms, due to the different θ and Θ computations that arise when $\hat{K}_{k+1}^j(t) < -R(j)/b^2(j)$.

15. Finally, the algorithm performs the minimization in (8.49) over each interval of $a(j)x_k$ values in the θ-Θ partition, starting on the left. This task, shown in Figures 8.10-8.11, is <u>identical</u> to the steps in Figures 7.5-7.6 in the section 7.2 algorithm, except for blocks 80 and 81. If $x_{k+1}=0$ was a grid point of the x_{k+1} partition (that is, if zflag=yes) and the problem is symmetric, then we have $\delta_k^j(m+1)=0$.

This completes the derivation of a solution algorithm that computes, off line, the optimal control laws and expected cost-to-go parameters for the general class of finite time-horizon JLPQ problems formulated in Section 8.2.

In the next section we conclude this chapter with the application of this algorithm to an example problem.

8.6 Using the JLPQ Solution Algorithm

In this section we will use the algorithm of Figures 8.5-8.11 to solve the jump linear piecewise-quadratic control problem of Example 8.2 for another time stage.

Example 8.5: (Example 8.2 at k=N-2):

Recall that the x-cost $Q(x_k, r_{k=1})$ for this problem has three constant pieces (specified by (8.21) and shown in Figure 8.2(a)). The optimal controller parameters at time k=N-1 are listed in Table 8.2 and are shown in Figure 8.4.

We apply the solution algorithm of Figures 8.5-8.11 at time k=N-2, for j=1:

1. Obtaining the composite x_{N-1} partition in block 26 we have

$\psi^1_{N-1} = 1$ (symflag=yes)

$\gamma^1_{N-1}(0) = -\infty$

$\gamma^1_{N-1}(1) = -23.413$

$\gamma^1_{N-1}(2) = 1$

$\gamma^1_{N-1}(3) = -.5$

$\gamma^1_{N-1}(4) = 0$ (zflag=no)

2. Computing in block 27:

$\tilde{K}^1_{N-1}=1$

$\hat{K}^1_{N-1}(1)=0$	$\hat{H}^1_{N-1}(1)=0$	$\hat{G}^1_{N-1}(1)=968.75$
$\hat{K}^1_{N-1}(2)=.25$	$\hat{H}^1_{N-1}(2)=.25$	$\hat{G}^1_{N-1}(2)=837.5625$
$\hat{K}^1_{N-1}(3)=.75$	$\hat{H}^1_{N-1}(3)=.75$	$\hat{G}^1_{N-1}(3) = 512.6875$
$\hat{K}^1_{N-1}(4)=0$	$\hat{H}^1_{N-1}(4)=0$	$\hat{G}^1_{N-1}(4)=437.5$

3. In block 28: $V^{1,U}_{N-2} = 968.75$

4. In blocks 29 → 35 → 37:

$$\tilde{G}^1_{N-2}(1,1) = 151.92 = \tilde{G}^1_{N-2}(1,2)$$

5. In block 40:

$$\gamma^1_{N-1}(1)\ [\hat{K}^1_{N-1}(2)-\hat{K}^1_{N-1}(1)] = -5.853 < -.125 = \frac{\hat{H}^1_{N-1}(1)-\hat{H}^1_{N-1}(2)}{2}$$

6. In blocks 39→41→42→47:

$$\hat{K}^{1}_{N-1}(2) = .25 > \frac{-R(1)}{b^{2}(1)} = -1$$

7. In blocks 50→51→30:

$$V^{2,U}_{N-2} = (.2)x^{2}_{N-2} + (.2)x_{N-2} + 837.55$$

8. In blocks 29→35→34:

$$\tilde{G}^{1}_{N-2}(2,2) = 838.5625$$

$$\tilde{G}^{1}_{N-2}(2,3) = 438.6875$$

$$V^{3,L}_{N-1}(x_{N-2},j) = x^{2}_{N-1} + 2x_{N-2} + 438.6875$$

9. In blocks 39→41→42→47→50→51→30:

Lside=yes

$$\hat{K}^{1}_{N-1}(3) = .75 > \frac{-R(1)}{b^{2}(1)} = -1$$

Rside=yes

$$V^{3,U}_{N-2} = (.4286)x^{2}_{N-2} + (.4286)x_{N-2} + 437.607$$

10. In blocks 29→35→37→36:

$$\tilde{G}^{1}_{N-2}(3.3) = 437.75$$

$$\tilde{G}^{1}_{N-2}(3.4) = 512.9375$$

$$V^{3,R}_{N-2}(x_{N-2},j) = x^{2}_{N-2} + x_{N-2} + 437.75$$

11. In block 39, $t=4=\psi^1_{N-1}$ and symflag=yes in block 43, so we compute

$$V^{4,R}_{N-2} = x^2_{N-2} + 437.5$$

in block 44 and, since

$$\hat{K}^1_{N-1}(4) = 0 > \frac{-R(1)}{b^2(1)} = -1 ,$$

we compute

$$V^{4,U}_{N-1} = 968.75$$

in block 46.

12. We have now computed the eligible candidate costs-to-go (according to Proposition 8.2):

$$V^{1,U}_{N-2},\ V^{2,U}_{N-2},\ V^{3,L}_{N-2},\ V^{3,U}_{N-2},\ V^{3,R}_{N-2},\ V^{4,U}_{N-2},\ V^{4,R}_{N-2}$$

13. We compute the grid of θ-Θ values in Figure 8.8:

$\Theta^1_{N-2}(1) = -.23.413$ (block 52)

$\theta^1_{N-2}(2) = -29.141$

$\Theta^1_{N-2}(2) = -1.125$

$\theta^1_{N-2}(3) = -1.375$ (block 59)

$\Theta^1_{N-2}(3) = -.5$

$\Theta^1_{N-2}(4) = .0$ (block 57)

$\theta^1_{N-2}(4) = -.5$ (block 56)

14. Ordering these grid points as specified in block 63:

$$\theta^1_{N-2}(2) < \Theta^1_{N-2}(1) < \theta^1_{N-2}(3) < \Theta^1_{N-2}(2) < \theta^1_{N-2}(4) = \Theta^1_{N-2}(3) < \Theta^1_{N-2}(4).$$

15. In blocks 65→67→68:

$$K_{N-2}(1{:}1) = 0 \qquad = L_{N-2}(1{:}1)$$

$$H_{N-2}(1{:}1) = 0 \qquad = F_{N-2}(1{:}1)$$

$$G_{N-2}(1{:}1) = \sum_{m=1} 968.75$$

16. We begin the search along the θ-Θ partition of $a(j)x_k$ values in the interval

$$(-\infty, -29.141) = (-\infty, \theta^1_{N-2}(2)).$$

The initial list of eligible costs is

$$V^{1,U}_{N-2} \text{ (prevailing cost) and } V^{3,L}_{N-2}.$$

17. In block 69 we find that the leftmost intersection of $V^{1,U}_{N-2}$ and $V^{3,L}_{N-2}$ is at

$$x_{N-2} = -24.04$$

18. In blocks 70→71→77→79:

we move into the next partition piece

$$(\theta^1_{N-2}(2), \Theta^1_{N-2}(1)) = (-29.141, -23.413).$$

Here the prevailing cost $V^{1,U}_{N-2}$ and $V^{3,L}_{N-2}$ are the eligible and valid candidate costs.

19. Since the prevailing cost $V_{N-2}^{1,U}$ is still valid we go to block 69 (Figure 8.10). The intersection of $V_{N-2}^{1,U}$ $V_{N-2}^{3,L}$ is at $x_{N-2} = -24.04$, so we go to block 72:

$$\delta_{N-2}^{1}(1) = -24.04$$

$V_{N-2}^{3,L}$ now prevailing

20. Setting m=2 (block 76) we have (by block 75):

$$K_{N-2}(2:1) = 1 = L_{N-2}(2:1)$$

$$H_{N-2}(2:1) = 2$$

$$G_{N-2}(2:1) = 438.6875$$

$$F_{N-2}(2:1) = -1$$

21. In block 73 we remove $V_{N-2}^{1,U}$ and $V_{N-2}^{2,U}$ from the eligibility list. The only currently eligible valid cost is the prevailing cost $V_{N-2}^{3,L}$, so no new intersection need to be found in block 69.

22. In block 79 we move rightward into

$$(\Theta_{N-2}^{1}(1),\ \theta_{N-2}^{1}(3)) = (-23.413,\ -1.375)$$

The list of valid eligible costs still contains only $V^{3,L}$.

23. In blocks 86→83→70→77→79→83:

we move righthand into

$$(\theta_{N-2}^{1}(3), \Theta_{N-2}^{1}(2)) = (-1.375,\ -1.125)\ .$$

$V^{3,L}_{N-2}$ ceases to be valid and is replaced by $V^{3,U}_{N-2}$ (which is now the only eligible valid cost).

24. In 86↪85→84→76→75:

$$\delta^{1}_{N-2}(2) = -1.375$$

and

$V^{3,U}_{N-2}$ is the new prevailing cost (block 49).

m=3

$$K_{N-2}(3:1) = .4286 \qquad = L_{N-2}(3:1)$$

$$H_{N-2}(3:1) = .4286$$

$$G_{N-2}(3:1) = 437.607$$

$$F_{N-2}(3:1) = -.2143$$

25. We remove $V^{3,L}_{N-2}$ from the eligibility list (block 73) and since only $V^{3,U}_{N-2}$ is valid and eligible, there are no new intersections to compute in block 69.

26. In blocks 70→77→79→83→86→69:

$$(\Theta^{1}_{N-2}(2),\ \theta^{1}_{N-2}(4) = \Theta^{1}_{N-2}(3)) = (-1.125,\ -.5)$$

The eligible valid costs still include only the prevailing cost $V^{3,U}_{N-2}$ so no new intersections are computed in block 69.

27. In blocks 70→77→79→83→86→85→84

we move into the interval

$$(\theta^1_{N-2}(4) = \Theta^1_{N-2}(3),\ \Theta^1_{N-2}(4)) = (-.5,\ 0).$$

We have moved past both $\theta^1_{N-2}(4)$ and $\Theta^1_{N-2}(3)$, so the list of valid eligible candidates becomes $V^{4,U}_{N-2}$ only. Thus the prevailing cost $V^{3,U}_{N-2}$ is no longer valid. We set $\delta^1_{N-2}(3) = -.5$ and the new prevailing cost is $V^{4,U}_{N-2}$.

28. In blocks 76→77:

m=4

$K_{N-2}(4:1) = 0 = L_{N-2}(4:1)$

$H_{N-2}(4:1) = 0 = F_{N-2}(4:1)$

$G_{N-2}(4:1) = 437.5$

29. In blocks 73→69→70→77→78:

Only $V^{4,U}_{N-2}$ is eligible, so there are no intersections to compute. We are in the last partition interval and a(1)> 0.

30. The problem is symmetric but zflag=no, so this k=N-2 iteration for j=1 is completed.

Collecting the results of the above steps, we have the optimal controller from (x_{N-2},r_{N-2}=1) in example 8.2=8.5, as listed in Table 8.6 below, and shown in Figure 8.12.

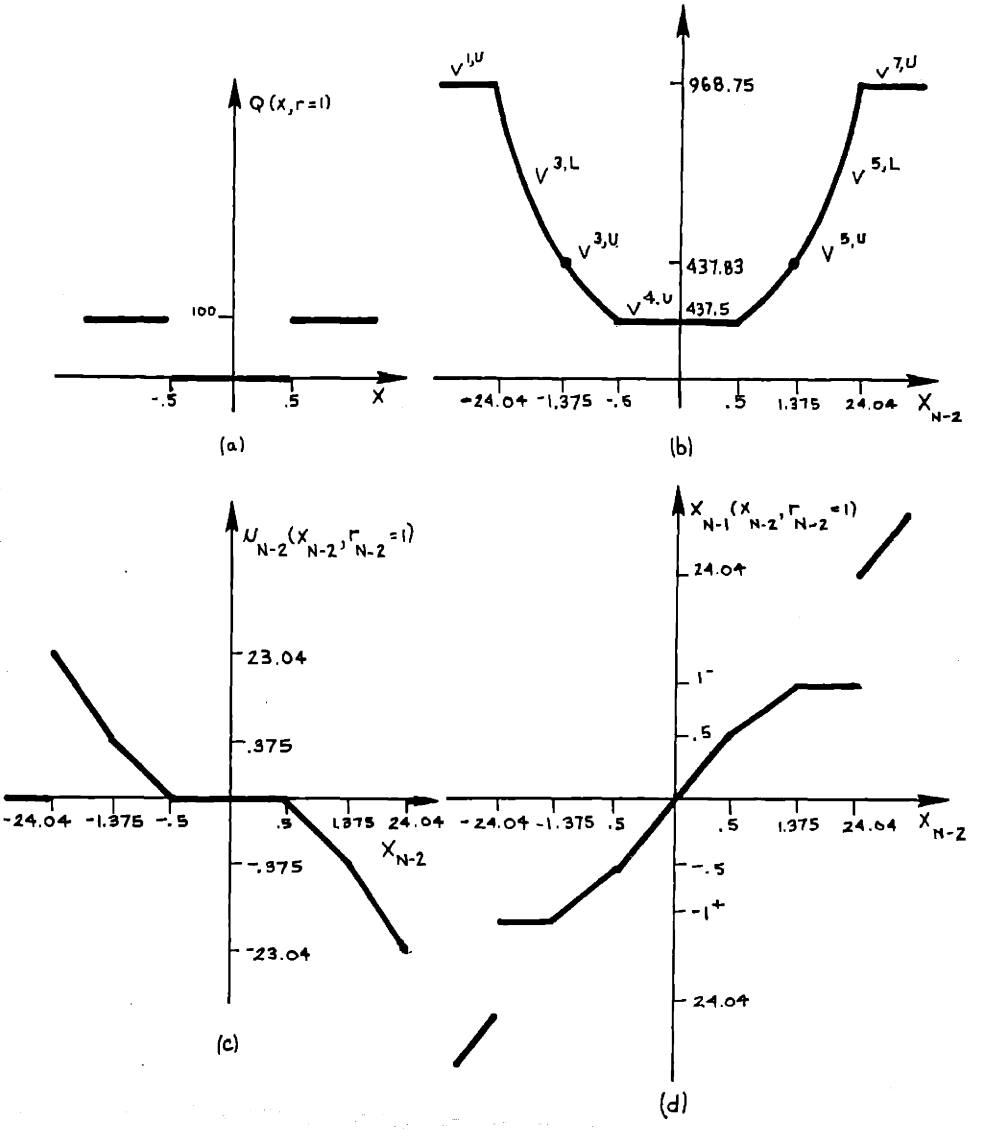

Figure 8.12: Q(x,r=1) and k=(N-2) Solution for Example 8.2=8.5

(Not Drawn to Scale)

if	$V_{N-2}(x_{N-2}, r_{N-2}=1)$	$u_{N-2}(x_{N-2}, r_{N-2}=1)$	$x_{N-1}(x_{N-2}, r_{N-2}=1)$
$x_{N-2} < -24.04$	968.78	0	x_{N-2}
$-24.04 < x_{N-2} < -1.375$	$x_{N-2}^2 + 2x_{N-2} + 438.6875$	$-x_{N-2} - 1^+$	-1^+
$-1.375 < x_{N-2} < -.5$	$(.4286)x_{N-2}^2 + (.4286)x_{N-2} + 437.607$	$-(.4286)x_{N-2} - .2143$	$(.5714)x_{N-2} - .2143$
$-.5 < x_{N-2} < .5$	437.5	0	x_{N-2}
$.5 < x_{N-2} < 1.375$	$(.4286)x_{N-2}^2 - .4286x_{N-2} + 437.607$	$-(.4286)x_{N-2} + .2143$	$(.5714)x_{N-2} + .2143$
$1.375 < x_{N-2} < 24.04$	$x_{N-2}^2 + 2x_{N-2} + 438.6875$	$-x_{N-2} + 1^-$	1^-
$24.04 < x_{N-2}$	968.75	0	x_{N-2}

Table 8.6: Optimal Controller from $(x_{N-2}, r_{N-2}=1)$ in Example 8.5.

Comparing these results at k=N-2 with the k=(N-1) results of Table 8.2 and Figure 8.2 we see that:

1. For small $|x_k|$ ($|x_k| < .5$) the optimal controller spends no control energy to move the x-process, since it is already in the $Q(x,r=1)=0$ piece. This is true at k=N-1 and k=N-2 (and at all other times for this example).

2. For large $|x_k|$ ($|x_{N-1}| > 23.413$ and $|x_{N-2}| > 24.04$) the optimal control is also zero.

3. In example 8.5, for $1.375 < |x_{N-2}| < 24.04$ the optimal controller hedges to $x_{N-1} = -1^+$ or 1^-. These are the low-cost sides of $\hat{V}_{N-1}(x_{N-1}|r_{N-2}=1)$ discontinuities. At time k=(N-1) we did not hedge to these discontinuities for any x_{N-1}.

   Note that we not only hedge to $x_{N-1}=-1^+$ or $x_{N-1}=1^-$ but, by Figure 8.2(d), we will also hedge at the following time step to $x_N = -.5^+$ or $.5^-$. That is, at time N-2 the controller actively hedges to place the x process in the advantageous p(1,2:x) piece. Then at time N-1 the controller actively hedges to place the x process in the advantageous Q(x,r=1) piece as well.

4. In example 8.5, for

$$.5 < |x_{N-2}| < 1.375 ,$$

we choose control $u_{N-2}^{3,U}(x_{N-2},1)$ which results in $.5 < |x_{N-1}| < 1$. Then at time k=(N-1), the optimal controller hedges to the joining points $x_N = \pm .5$ of Q(x,r=1). Here the optimal controller doesn't have to hedge to-a-point with u_{N-2} to place x_{N-1} in the advantageous probability piece ($|x_{N-1}| < 1$), but it does hedge-to-a-point to get x_N into the preferred Q(x,r=1) piece ($|x_N| < .5$).

8.7 Summary

In this chapter we have extended the kinds of x-operating costs that can be incorporated in the formulation and solution of control problems for jump linear systems. We have developed a solution algorithm that determines the optimal controller for perfectly observed, noiseless, scalar jump linear systems where the form transition probabilities are piecewise-constant in x and the x-operating and terminal costs are piecewise-quadratic. These costs may contain discontinuities and they may be concave over any but their extreme pieces.

The qualitative results and solution algorithm for the JLPQ problem that has been developed here provides a basis for the

approximate solution of scalar jump linear control problems with quadratic control operating costs and

- x-operating costs $Q(x_{k+1}, r_{k+1})$
- x-terminal costs $Q\ (x_N, r_N)$
- form transition probabilities
- input noise densities

that are piecewise convex and concave. This is the topic of the next chapter.

9. CONTROL OF JUMP LINEAR SYSTEMS WITH ADDITIVE INPUT NOISE

9.1 Introduction

In this chapter we extend the solution methodology of chapters 5-8 to address a larger class of scalar jump linear control problems, possessing additive input noise and a more general class of x-dependent form transition probabilities, x-operating costs and x-terminal costs. Specifically we consider scalar jump linear control problems with quadratic control penalties and

- input noise densities that are twice continuously differentiable except at a finite number of points,
- x-operating costs $Q(x, r)$, x-terminal costs $Q_T(x,r)$ and form transition probabilities $p(i,j;x)$ that are twice continuously differentiable in x, except at a finite number of points; they consist of a finite number of convex or concave (in x) pieces.

We call this the jump linear piecewise convex (JLPC) control problem.

Our study of this class of problems is motivated by a desire to make the solution approach of chapters 5-7 applicable to more realistic control problems. The discussion in this chapter builds directly upon the JLPQ problem formulation and solution of chapter 8. In turn, the results of this chapter provide a basis for the study of jump linear control problems possessing n-dimensional state process and control-dependent form transition probabilities, in chapter 10.

The major extension of this chapter is the inclusion of additive input noise in the x-process dynamics. As we indicated in earlier

chapters, we can approximate general x-dependent form transition probabilities in piecewise-constant way, and general x-operating and terminal costs by piecewise-quadratic functions. We cannot , however, reasonably approximate the behavior of jump linear controllers subject to additive noise by noiseless JLQ or JLPQ controllers. As we shall see in this chapter, additive input noise profoundly changes the nature of the optimal controller. It is not possible, in general, to use the control input to drive the x process into a specified interval of values (or to a boundary of such an interval) with certainty, because of the noise. Consequently, we cannot solve a noisy JLQ or JLPQ problem by comparing the solutions of constrained-in-x subproblems.

For JLPQ problems like those in chapter 8, the presence of additive input noise leads to the loss (in general) of the piecewise-quadratic structure of the optimal controllers, due to the "blurring" effects of the noise. If the noise density has a piecewise structure (that is, if it is twice differentiable except at a finite number of points (the piece boundaries)), then the optimal controller's expected cost will also have a piecewise (but not quadratic) structure. We have included more general piecewise structures for the x-operating costs, x-terminal costs, from transition probabilities and noise densities in the JLPC problem formulation because the piecewise-quadratic structure of the solution optimal cost is lost in any event.

In this chapter we will show how JLPC control problems with additive input noise can be reformulated at each time stage k as different, equivalent JLPC control problems that do not possess input noise. These

reformulated problems involve an artificial variable z, which replaces x.

These reformulated JLPC problems can be solved using the approach of chapters 5 and 8:

> We break up the reformulated JLPC problem into constrained subproblems, and then we compare these subproblems solutions to determine the optimal controller. These constraints are in the artificial variable z_k (instead of x_k).

At each step in time, the control problem involving the search for $V_k(x_k, r_k=j)$ results in a set of noiseless, constrained-in-z_{k+1} subproblems with z-independent form transition probabilities and single-piece z-costs. Each subproblem can be solved analytically, and the resulting subproblem optimal costs are compared at each x_k value to obtain $V_k(x_k, r_k=j)$. However, since the subproblem solutions are not in general quadratic in z_k (or x_k), we don't have the nice inductive solution structure of the problems of chapters 5 and 8. At each time, the analytical steps required to minimize the constrained subproblems may be quite different.

We propose, therefore, a suboptimal approximation of the one-step JLPC control problem (at each time stage k) that results in controllers that are piecewise-linear in x_k. This approximation method constrains the controller to drive the system to one of an arbitrary grid of points (z_{k+1} values). This is essentially is a brute force approach which is subject to significant error as the number of time stages of approximation increases. Better approximation methods that utilize knowledge of the problem structure

can probably be obtained, at least for certain classes of JLPC problems. We have not investigated approximate solutions in detail here.

This chapter is organized as follows:

1. In section 9.2 we formulate the general JLPC control problem with additive input noise.

2. In section 9.3 we describe how the basic solution approach of chapters 5 and 8 must be modified when there is additive input noise in the x dynamics. We use two example problems to illustrate this process.

3. In section 9.4 we solve for the last stage controller of a JLPC example problem (example 9.3). The example problem is the same as example 8.5, except for the additive input noise. We compare the resulting controllers for each problem to illustrate the effects of the additive noise. An approximate solution method is also developed for example 9.3.

4. In section 9.5 we derive a general one-step solution procedure for the JLPC problems that are formulated in section 9.2. This procedure is patterned after the examples of sections 9.3 and 9.4.

5. In section 9.6 we establish a number of qualitative properties of the optimal one-step JLPC solution. In particular, we describe active hedging in JLPC controllers.

6. In section 9.7 these results are then used to construct an algorithm for the efficient determination of the optimal controller. This algorthm is presented in flowchart form.

7. In section 9.8 we demonstrate the application of the optimal controller derivation algorithm to an example problem. This example serves to illustrate the need for numerical methods (as opposed to analytical methods) in certain steps of the algorithm.

8. In section 9.9 we consider the approximation method that was discussed above. The resulting controller is applied to two time stages of the example of section 9.8, and the performance of the approximate and optimal controllers are compared.

9.2 JLPC Problem Formulation

In this section we formulate the jump linear piecewise convex (JLPC) control problem with additive input noise that is addressed in this chapter. As in earlier problems we restrict our attention to the time-invariant case so as to simplify notation. The results of this chapter can be directly extended to the time-varying case.

Consider the discrete-time jump linear system with additive input noise and scalar x:

$$x_{k+1} = a(r_k)x_k + b(r_k)u_k + \Xi(r_k)v_k \tag{9.1}$$

$$\Pr\{r_{k+1}=j \,|\, r_k=i,\ x_{k+1}=x\} = p(i,j:x) \tag{9.2}$$

$$x(k_o) = x_o \qquad r(k_o) = r_o$$

Each transition probability $p(i,j;x)$ of the form process is assumed to be piecewise-convex or concave in x, having a finite number of pieces, $\bar{\nu}_{ij}$. That is, the real line is partitioned into $\bar{\nu}_{ij}$ disjoint intervals by the points

$$-\infty \triangleq \nu_{ij}(0) < \nu_{ij}(1) <,\ldots, \nu_{ij}(\bar{\nu}_{ij}-1) < \nu_{ij}(\bar{\nu}_{ij}) \triangleq \infty \tag{9.3}$$

and

$$p(i,j:x) = \lambda_{ij}(x;s) \quad \text{if } \nu_{ij}(s-1) < x < \nu_{ij}(s)\ , \tag{9.4}$$

for $s = 1,\ldots,\bar{\nu}_{ij}$. Each function $\lambda_{ij}(x;s)$ is twice continuously

differentiable in x over the interval $(\nu_{ij}(s-1),\nu_{ij}(s))$ and either

$$\frac{\partial^2 \lambda_{ij}(x;s)}{\partial x^2} > 0 \qquad \text{for all } x\in(\nu_{ij}(s-1),\nu_{ij}(s))$$

or

$$\frac{\partial^2 \nu_{ij}(x,s)}{\partial x^2} \leq 0 \qquad \text{for all } x\in(\nu_{ij}(s-1),\nu_{ij}(s)) \quad \bullet$$

We require that

$$p(i,j=x) \geq 0 \qquad \forall i,j \text{ and } x$$

and

$$\sum_{j=1}^{M} p(i,j:x) = 1 \qquad \text{for each } i\in\underline{M}. \text{ at each } x\in\mathbb{R} \ . \tag{9.5}$$

The input noise process $\{v_k\}$ is assumed to be a white noise sequence with a probability density that is piecewise-convex or concave in v_k, having a finite number of pieces, $\bar{\sigma}$. That is, the real line is partitioned into $\bar{\sigma}$ disjoint intervals by the points

$$-\infty \triangleq \sigma(0) < \sigma(1) < \ldots < \sigma(\bar{\sigma}-1) < \sigma(\bar{\sigma}) \triangleq \infty \tag{9.6}$$

and at each time k

$$p(v_k) = \omega(v_k;s) \qquad \text{if } \sigma(s-1) < v_k < \sigma(s) \ , \tag{9.7}$$

for $s=1,\ldots,\bar{\sigma}$. Each function $\omega(v;s)$ is twice continuously differentiable in v over the interval $(\sigma(s-1),\sigma(s))$ and either

$$\frac{\partial^2 \omega(v:s)}{\partial x^2} \geq 0 \qquad \text{for all } v\in(\sigma(s-1),\sigma(s))$$

or

$$\frac{\partial^2 \omega(v:s)}{\partial x^2} \leq 0 \qquad \text{for all } v\in(\sigma(s-1),\sigma(s)) \ .$$

Since $p(v_k)$ is a probability density we require that

$$p(v) \geq 0 \qquad \text{(at each v)}$$

and $$\int_{-\infty}^{\infty} p(v)dv = 1$$

Consequently

$$\lim_{v\to\pm\infty} p(v) = 0$$

$$\lim_{v\to\pm\infty} \frac{dp(v)}{dv} = 0$$

$$\lim_{v\to\pm\infty} \frac{d^2p(v)}{dv^2} = 0 \quad .$$

By assumption, the input noise is white:

$$Pr(v_k | v_n) = Pr(v_k) \qquad \text{for } k \neq n \tag{9.8}$$

We assume (as in Part III and Chapter 8) that the state (x_k, r_k) is perfectly observed at each k. The problem is to find the optimal control laws

$$u_k = \phi_k(x_o,\ldots,x_k;\ r_o,\ldots,r_k)$$

that minimize the cost criterion

$$J_{k_o}(x_o,r_o) = E\left\{ \sum_{k=k_o}^{N-1} [u_k^2 R(r_k) + Q(x_{k+1},r_{k+1})] + Q_T(x_N,r_N) \right\}, \tag{9.10}$$

where the expectation is over $\{r_{k_o},\ldots,r_N\}$ and the input noise sequence

$\{v_{k_o},\ldots,v_N\}$.

As in the JLQ problems of Part III and JLPQ problems of Chapter 8, we assume that the penalty on the control signal is quadratic, where

$$R(j) > 0 \quad \text{for each } j \in \underline{M} \tag{9.11}$$

The x-operating costs $Q(x,j)$ and terminal costs $Q_T(x,j)$ are assumed to be piecewise-convex or concave in x, having a finite number of pieces, $\bar{\mu}^j$. That is, the real line is partitioned into $\bar{\mu}^j$ disjoint intervals by the points

$$-\infty \triangleq \mu^j(0) < \mu^j(1) < \ldots < \mu^j(\bar{\mu}^j-1) < \mu^j(\bar{\mu}^j) \triangleq \infty \tag{9.12}$$

and

$$Q(x,j) = Q^j(x;s) \quad \text{if } \mu^j(s-1) < x < \mu^j(s) , \tag{9.13}$$

for $s = 1,\ldots,\bar{\mu}^j$.

The real line is also partitioned into $\bar{\eta}^j$ disjoint intervals by the points

$$-\infty \triangleq \eta^j(0) \leq \eta^j(1) \leq \ldots \quad \eta^j(\bar{\eta}^j-1) \leq \eta^j(\bar{\eta}^j) \triangleq \infty \tag{9.14}$$

and

$$Q_T(x,j) = Q_T^j(x;s) \quad \text{if } \eta^j(s-1) < x < \eta^j(s) , \tag{9.15}$$

for $s = 1,\ldots,\bar{\eta}^j$.

We require that at each x value,

$$Q(x,j) \geq 0$$

$$Q_T(x,j) \geq 0 \quad . \tag{9.16}$$

The term $Q_T(x_N,r_N)$ in (9.10) is a terminal cost charged in addition to the

time-invariant x-operating cost $Q(x_N, r_N)$. Since $\{(x_k, r_k) : k = k_o, \ldots, N\}$ is a Markov process we need only consider feedback laws of the type

$$u_k = \phi_k(x_k, r_k) \quad .$$

The JLPC control problem formulation (9.1) - (9.16) includes as special cases the problems of chapters 3, 5-7 and 8. In the next section we begin our analysis of this problem with an examination of the effects of the additive noise, and how the solution approach of chapters 5 and 8 must be modified to handle this noise.

9.3 Reformulating JLPC Problems with Additive White Input Noise as Noiseless Problems.

In this section we will describe how the basic solution approach of chapters 5 and 8 must be modified when there is additive white input noise in the x dynamics. As we indicated in section 9.1, this modified solution approach involves the reformulation of the noisy problem, at each time stage k, as a different (but equivalent) control problem in an artificial variable z_k (which replaces x_k). This reformulated problem does not have additive noise (it is absorbed in z_k). We will derive and describe this reformulation process via two example problems.

Defining the expected cost-to-go $V_k(x_k, r_k)$ as in previous chapters, and applying dynamic programming from finite terminal time $k = N$, we have the relationship:

$$V_k(x_k,r_k) = \min_{u_k} \left\{ u_k^2 R(r_k) + E\left\{ \begin{array}{c} Q(x_{k+1},r_{k+1}) \\ + \\ V_{k+1}(x_{k+1},r_{k+1}) \end{array} \middle| \begin{array}{c} x_k, \\ r_k, \\ u_k \end{array} \right\} \right\} \qquad (9.17)$$

$$\text{for } k = N-1, N-2, \ldots, k_o$$

where

$$V_N(x_N,r_N=j) = Q_T(x_N,r_N=j)$$

with

$$m_N(j) = \bar{\eta}^j \qquad (9.18)$$

and

$$\delta_N^j(t) = \eta^j(t) \qquad t = 1,\ldots,\eta^j - 1 \quad .$$

From (9.17) - (9.18) we can, in principle, solve for the optimal controls $u_{N-1},\ldots,u_{k_o}$.

As in part III and chapter 8 , let us define the conditional expected cost-to-go by:

$$\hat{V}_{k+1}(x_{k+1}|r_k=j) \triangleq E\left\{ \begin{array}{l} V_{k+1}(x_{k+1},r_{k+1}) \\ + Q(x_{k+1},r_{k+1}) \end{array} \middle| \begin{array}{l} r_k = j \\ x_k \end{array} \right\} \quad . \qquad (9.19)$$

This is a function of x_{k+1}. We can rewrite the minimization in (9.17) as

$$V_k(x_k,r_k=j) \min_{u_k} \left\{ u_k^2 R(r_k) + E\left\{ \hat{V}_{k+1}(x_{k+1}|r_k=j) \right\} \right\} \quad . \qquad (9.20)$$

The expectation in (9.20) is over values of the input noise v_k.

The conditional expected cost-to-go in (9.19) will have a piecewise

structure

$$\hat{V}_{k+1}(x_{k+1}|r_k=j) = \hat{V}^j_{k+1}(x_{k+1};t) \qquad \text{for } x_{k+1} \in \Delta^j_{k+1}(t)$$

$$t = 1,\ldots,\psi^j_{k+1} - 1 \qquad (9.21)$$

where the x_{k+1} intervals are

$$\Delta^j_{k+1}(t) = (\gamma^j_{k+1}(t-1),\ \gamma^j_{k+1}(t)) \qquad (9.22)$$

Here

$$-\infty \triangleq \gamma^j_{k+1}(0) < \gamma^j_{k+1}(1) < ,\ldots, < \gamma^j_{k+1}(\psi^j_{k+1}-1) < \gamma^j_{k+1}(\psi^j_{k+1}) \triangleq \infty \qquad (9.23)$$

are the unique grid points obtained by superimposing the quantities

$$\{\mu^i(t) : t = 1,\ldots,\overline{\mu}^i - 1\} \qquad \text{(x-operating costs grid)}$$

$$\{\nu_{ji}(t) : t=1,\ldots,\overline{\nu}_{ji} - 1\} \qquad \text{(form-transition probability grid)}$$

$$\{\delta^i_{k+1}(t) : t = 1,\ldots,m_{k+1}(i)-1\} \qquad \begin{pmatrix}(V_{k+1}(x_{k+1},r_{k+1}=i)\\ \text{joining points})\end{pmatrix}$$

$$\text{for each } i \in \mathcal{C}_j . \qquad (9.24)$$

The solution approach of chapters 5 and 8 might suggest that the way to solve (9.20) is to convert it into the comparison of a finite set of constrained-in-x_{k+1} subproblems:

$$V_k(x_k,r_k=j) = \min_{t=1,\ldots,\psi^j_{k+1}} \{V_k(x_k,t_k=j) \mid x_{k+1} \in \Delta^j_{k+1}(t)\}$$

where the ψ^j_{k+1} subproblems are

$$V_k(x_k, r_k=j) \,|\, x_{k+1} \in \Delta^j_{k+1}(t)) = \min_{\substack{u_k \\ \text{s.t.}}} \{u_k^2 R(j) + \hat{V}_{k+1}(x_{k+1} \; r_k=j)\}$$

$$x_{k+1} \in \Delta^j_{k+1}(t)$$

This will not work because of the additive white input noise. We cannot choose x_{k+1} with certainty. Thus the subproblems above are not well posed.

Let us now consider an example problem that is identical to example 5.1 (and 6.1, 7.1) except for the presence of additive input noise. From its solution we will develop a general method for the reformulation of (9.1) - (9.16) as a comparison of constrained subproblems that are constrained in a deterministic[1] quantity.

Example 9.1 (Uniformly Distributed Input Noise)

Consider the following system having uniformly distributed (in magnitude) bounded white driving noise and $m = 2$ forms:

$$x_{k+1} = x_k = u_k + v_k \qquad \text{if } r_k = 1$$

$$x_{k+1} = 2x_k + u_k \qquad \text{if } r_k = 2$$

$$p(1,2:x) = \begin{cases} 1/4 & \text{if } |x| < 1 \\ 3/4 & \text{if } |x| > 1 \end{cases}$$

$$p(1,1:x) = 1 - p(1,2:x) \qquad p(2,2) = 1 \qquad p(2,1) = 0$$

[1] deterministic, given x_k, r_k and u_k

where the input noise sequence $\{v_k\}$ is a white noise sequence with uniformly distributed magnitude:

$$\text{noise density} \qquad p(v) = \begin{cases} 0 & |v| > 2 \\ 1/4 & |v| < 2 \end{cases}$$

hence

$$E\{v_k\} = 0$$

$$E\{v_k^2\} = \frac{1}{4}\int_{-2}^{2} v^2 dv = 4/3 \qquad \text{(all k)}$$

and

$$E\{v_k\, v_s\} = 0 \qquad \text{if } k \neq s$$

We seek to minimize

$$\min_{u_o,\ldots,u_{N-1}} E\left\{\sum_{k=0}^{N-1} [u_k^2 + x_{k+1}^2] + x_N^2\, K_T(r_N)\right\}$$

where $K_T(1) = 0, \quad K_T(2) = 3.$

Once the system attains form r = 2, it stays there and the usual LQ solution applies:

$$V_k(x_k, r_k{=}2) = x_k^2\, K_k(1{:}2)$$

$$u_k(x_k, r_k{=}2 = -L_k(1{:}2)x_k$$

where

$$K_N(1{:}2) = K_T(2) = 3$$

$$K_k(1{:}2) = \frac{a^2(2)\, R(2)[K_{k+1}(1{:}2) + Q(2)]}{R(2) + b^2(2)[K_{k+1}(1{:}2) + Q(2)]} = \frac{4[K_{k+1}(1{:}2) + 1]}{2 + K_{k+1}(1{:}2)}$$

$$L_k(1{:}2) = \frac{a(2)\, b(2)[K_{k+1}(1{:}2) + Q(2)]}{R(2) + b^2(2)[K_{k+1}(1{:}2) + Q(2)]} = \frac{2[K_{k+1}(1{:}2) + 1]}{2 + K_{k+1}(1{:}2)}$$

Now let us examine what happens in form $r_{N-1} = 1$. We are given that $V_N(x_N, r_N=1) = x^2 K_T = 0$. Applying dynamic programming,

$$V_{N-1}(x_{N-1}, r_{N-1}=1) = \min_{u_{N-1}} \left\{ u_{N-1}^2 + E\left\{ x_N^2 + V_N(x_N, r_N) \,\middle|\, \begin{matrix} x_{N-1} \\ r_{N-1}=1 \\ u_{N-1} \end{matrix} \right\} \right\}$$

$$= \min_{u_{N-1}} \left\{ u_{N-1}^2 + E\left\{ x_N^2 + p(1,1:x_N)\ V_N(x_N, r_N=1) + p(1,2:x_N)\ V_N(x_N, r_N=2) \,\middle|\, \begin{matrix} x_{N-1} \\ r_{N-1}=1 \\ u_{N-1} \end{matrix} \right\} \right\} \tag{9.25}$$

$$= \min_{u_{N-1}} \left\{ u_{N-1}^2 + E\left\{ x_N^2 [p(1,1:x_N) + 4p(1,2:x_N)] \,\middle|\, \begin{matrix} x_{N-1} \\ r_{N-1}=1 \\ u_{N-1} \end{matrix} \right\} \right\}$$

The expectation is over values of the noise v_{N-1}. We can influence the probabilities $p(1,1:x_N)$ and $p(1,2:x_N)$ by our choice of u_{N-1}, but we cannot precisely specify them because the value of x_N depends upon the noise v_{N-1} as well as x_{N-1} and u_{N-1}.

Substituting the noise density in (9.25),

$$V_{N-1}(x_{N-1}, r_{N-1}=1) =$$

$$= \min_{u_{N-1}} \left\{ u_{N-1}^2 + \int_{-\infty}^{\infty} p(v) \; (x_{N-1} + u_{N-1} + v)^2 \begin{bmatrix} p(1,1:x_{N-1}+u_{N-1}+v \\ +d \\ 4p(1,2:x_{N-1}+u_{N-1}+v) \end{bmatrix} dv \right\}$$

$$= \min_{u_{N-1}} \left\{ u_{N-1}^2 + \frac{1}{4} \int_{-2}^{2} (x_{N-1} + u_{N-1} + v)^2 \begin{bmatrix} p(1,1:x_{N-1}+u_{N-1}+v) \\ + \\ 4p(1,2:x_{N-1}+u_{N-1}+v) \end{bmatrix} dv \right\} .$$

(9.26)

If u_{N-1} is chosen so that $|x_{N-1} + u_{N-1}| > 3$ then $|x_N| = |x_{N-1}+u_{N-1}+v_{N-1}| > 1$ for all possible values of v_{N-1}, and therefore $p(1,2:x_N) = 3/4$ and $p(1,1:x_N) = 1/4$. That is, for $|x_{N-1} + u_{N-1}| > 3$ in this example, the value of the input noise v_{N-1} will not affect the form transition probabilities; we will have

$$\frac{1}{4}\int_{-2}^{2} (x_{N-1}+u_{N-1}+v)^2 \begin{bmatrix} p(1,1:x_{N-1}+u_{N-1}+v) \\ + \\ 4p(1,2:x_{N-1}+u_{N-1}+v) \end{bmatrix} dv = \frac{13}{16}\int_{-2}^{2} (x_{N-1}+u_{N-1}+v)^2 \, dv$$

$$= \frac{13}{4}(x_{N-1} + u_{N-1})^2 + \frac{13}{3} . \qquad (9.27)$$

If we chose u_{N-1} so that $|x_{N-1} + u_{N-1}| < 3$ then the form transition probabilities will depend upon the value of the input noise. In this case,

$$\frac{1}{4}\int_{-2}^{2} (x_{N-1}+u_{N-1}+v)^2 \begin{bmatrix} p(1,1:x_{N-1}+u_{N+1}+v) \\ + \\ 4p(1,2:x_{N-1}+u_{N-1}+v) \end{bmatrix} dv =$$

$$= \frac{13}{16}\int_{-2}^{-1-(x_{N-1}+u_{N-1})} (x_{N-1}+u_{N-1}+v)^2 dv + \frac{7}{16}\int_{-1-(x_{N-1}+u_{N-1})}^{1-(x_{N-1}+u_{N-1})} (x_{N-1}+u_{N-1}+v)^2 dv +$$

$$+ \frac{13}{16}\int_{1-(x_{N-1}+u_{N-1})}^{2} (x_{N-1}+u_{N-1}+v)^2 \, dv$$

$$= \frac{19}{4}(x_{N-1} + u_{N-1})^2 + 49/12. \qquad (9.28)$$

Thus we have different minimization problems, depending upon the value of $(x_{N-1} + u_{N-1})$.

Surprisingly, in each case the expected cost term

$$E\{x_N^2 + V_N(x_N,r_N) \mid x_{N-1}, r_{N-1}=1, u_{N-1}\} \tag{9.29}$$

is only quadratic in $(x_{N-1} + u_{N-1})$. This <u>will not</u> be the case, in general, for problems of type (9.1) - (9.16) having piecewise-constant form transition probabilities, piecewise constant noise densities, and piecewise-quadratic x costs. As we will see in the next example, the cost in (9.29) is generally cubic in $(x_{N-1} + u_{N-1})$ for such problems. The expression in (9.28) does not contain cubic terms because of the symmetric nature of the limits of integration and the fact that p(1,2:x), p(1,1:x) and p(v) all have only three constant pieces. We have chosen to study this somewhat unrepresentative example problem here because it highlights the solution approach for handling JLPC problems possessing additive input noise, without introducing extraneous complications.

The following strategy for computing $V_{N-1}(x_{N-1},r_{N-1}=1)$ and the associated optimal control law is suggested by (9.26) - (9.28):

> For each of regions of $(x_{N-1} + u_{N-1})$ values, solve the <u>constrained</u> optimization problem that assumes $(x_{N-1} + u_{N-1})$ is in the specified region. Once we have the solutions to these problems, we compare them and obtain the optimal solution by choosing the smallest of these for each value of x_{N-1}.

As we have indicated, in this example there are three $(x_{N-1}+u_{N-1})$ regions:

(1) $x_{N-1} + u_{N-1} \leq -3^-$ where $p(1,2:x_N) = 3/4$,

(2) $-3^+ \leq x_{N-1} + u_{N-1} \leq 3^-$ where $p(1,2:x_N) = 1/4$ if

$-1-(x_{N-1}+u_{N-1}) < v_{N-1} < 1 - (x_{N-1}+u_{N-1})$

and $p(1,2:x_N) = 3/4$ otherwise ,

(3) $x_{N-1} + u_{N-1} \geq 3^+$ where $p(1,2:x_N) = 3/4$

The three corresponding constrained control problems are:

$$V_{N-1}(x_{N-1}, r_{N-1}=1 \,|\, 1) = \min_{u_{N-1} \text{ s.t. } x_{N-1}+u_{N-1} \leq -3^-} \left\{ u_{N-1}^2 + \frac{13}{4}(x_{N-1} + u_{N-1})^2 + \frac{13}{3} \right\} \tag{9.30}$$

$$V_{N-1}(x_{N-1}, r_{N-1}=1 \,|\, 2) = \min_{u_{N-1} \text{ s.t. } -3^+ \leq x_{N-1}+u_{N-1} \leq 3^-} \left\{ u_{N-1}^2 + \frac{19}{4}(x_{N-1} + u_{N-1})^2 + \frac{49}{12} \right\} \tag{9.31}$$

$$V_{N-1}(x_{N-1}, r_{N-1}=1 \,|\, 3 = \min_{u_{N-1} \text{ s.t. } x_{N-1}+u_{N-1} \geq 3^+} \left\{ u_{N-1}^2 + \frac{13}{4}(x_{N-1} + u_{N-1})^2 + \frac{13}{3} \right\} \bullet \tag{9.32}$$

The costs in the first and third problems are the same, because of the symmetry of $p(1,2:x_N)$ and $p(v)$ about zero.

Consider the second $(x_{N-1} + u_{N-1})$ region:

$$-3^+ \leq x_{N-1} + u_{N-1} \leq 3^- \quad \bullet$$

Differentiating $V_{N-1}(x_{N-1}, r_{N-1}=1|2)$ in (9.27) with respect to u_{N-1}:

$$\frac{\partial V_{N-1}(x_{N-1}, 1|2)}{\partial u_{N-1}} = \left(\frac{19}{2}\right) x_{N-1} + \left(\frac{23}{2}\right) u_{N-1} \tag{9.33}$$

$$\frac{\partial^2 V_{N-1}(x_{N-1}, 1|2)}{\partial u_{N-1}^2} = \frac{23}{2} > 0 \tag{9.34}$$

hence setting (9.29) to zero yields the minimizing

$$u_{N-1}(x_{N-1}, r_{N-1}=1|2) = \left(\frac{-19}{23}\right) x_{N-1} = (-.82609)\, x_{N-1} \tag{9.35}$$

with the resulting cost

$$V_{N-1}(x_{N-1}, r_{N-1}=1|2) = \left(\frac{19}{23}\right) x_{N-1}^2 + \frac{49}{12} = (.82609) x_{N-1}^2 + 4.0833 . \tag{9.36}$$

But u_{N-1} in (9.35) solves (9.31) only if the resulting $(x_{N-1} + u_{N-1})$ value satisfies the constraint

$$|x_{N-1} + u_{N-1}| \leq 3^- \tag{9.37}$$

This holds if and only if

$$-17.25 < x_{N-1} < 17.25 \quad .$$

From (9.34) we see that for $x_{N-1} > 17.25$, the best choice of u_{N-1} that satisfies (9.37) is

$$u_{N-1} = 3^- - x_{N-1} \quad .$$

The resulting cost is

$$V_{N-1} = (3^- - x_{N-1})^2 + \frac{19}{4}(-3)^2 + \frac{49}{12}$$

$$= x_{N-1}^2 - 6x_{N-1} + \frac{335}{6} \quad .$$

Similarly for $x_{N-1} < -17.25$, the best choice of u_{N-1} that satisfies (9.37) is

$$u_{N-1} = -3^{+} - x_{N-1}$$

with resulting cost

$$V_{N-1} = x_{N-1}^2 + 6x_{N-1} + 335/6 \quad .$$

Thus the optimal cost-to-go in (9.31) has a three-piece quadratic structure in x_{N-1}.

The other two constrained control problems (9.30), (9.32) have two-piece quadratic structures. The optimal expected costs-to-go for all three constrained subproblems are:

$$V_{N-1}(x_{N-1},1|1) = \begin{cases} (.7647)\ x_{N-1}^2 + 4.333 & \text{if } x_{N-1} \leq -12.75 \\ x_{N-1}^2 + 6x_{N-1} + 42.58 & \text{if } x_{N-1} \geq -12.75 \end{cases} \tag{9.38}$$

$$V_{N-1}(x_{N-1}\ 1|2) = \begin{cases} x_{N-1}^2 + (6x_{N-1} + 55.83 & \text{if } x_{N-1} \leq -17.25 \\ (.82069)x_{N-1}^2 + 4.083 & \text{if } -17.25 \leq x_{N-1} \leq 17.25 \\ x_{N-1}^2 - 6x_{N-1} + 55.83 & \text{if } 17.25 \geq x_{N-1} \end{cases} \tag{9.39}$$

$$V_{N-1}(x_{N-1},1|3) = \begin{cases} x_{N-1}^2 - 6x_{N-1} + 42.58 & \text{if } x_{N-1} \leq 12.75 \\ .7647\ x_{N-1}^2 + 4.333 & \text{if } x_{N-1} \geq 12.75 \end{cases} \tag{9.40}$$

and the corresponding control laws are

$$u_{N-1}(x_{N-1},1\,|1) = \begin{cases} -.7647\ x_{N-1} & \text{if } x_{N-1} \leq -12.75 \\ -x_{N-1} - 3^{-} & \text{if } x_{N-1} \geq -12.75 \end{cases} \tag{9.41}$$

$$u_{N-1}(x_{N-1},1\,|2) = \begin{cases} -x_{N-1} = 3^{+} & \text{if } x_{N-1} \leq -17.25 \\ -.82069\ x_{N-1} & \text{if } -17.25 \leq x_{N-1} \leq 17.25 \\ -x_{N-1} + 3^{-} & \text{if } 17.25 \leq x_{N-1} \end{cases} \tag{9.42}$$

$$u_{N-1}(x_{N-1},1\,|3) = \begin{cases} -x_{N-1} + 3^{+} & \text{if } x_{N-1} \leq 12.75 \\ -.7647\ x_{N-1} & \text{if } x_{N-1} \geq 12.75 \end{cases} \tag{9.43}$$

Having solved the constrained problems (9.30) - (9.32) we are now ready to compare them:

$$V_{N-1}(x_{N-1},r_{N-1}=1) = \min_{t=1,2,3} V_{N-1}(x_{N-1},r_{N-1}=1\,|t) \tag{9.44}$$

This is done graphically in figure 9.1. Choosing the lowest of the three constrained costs at each x_{N-1} value, we see that the optimal expected cost-to-go of control law, and optimal $(u_{N-1} + x_{N-1})$ values are as listed in table 9.1.

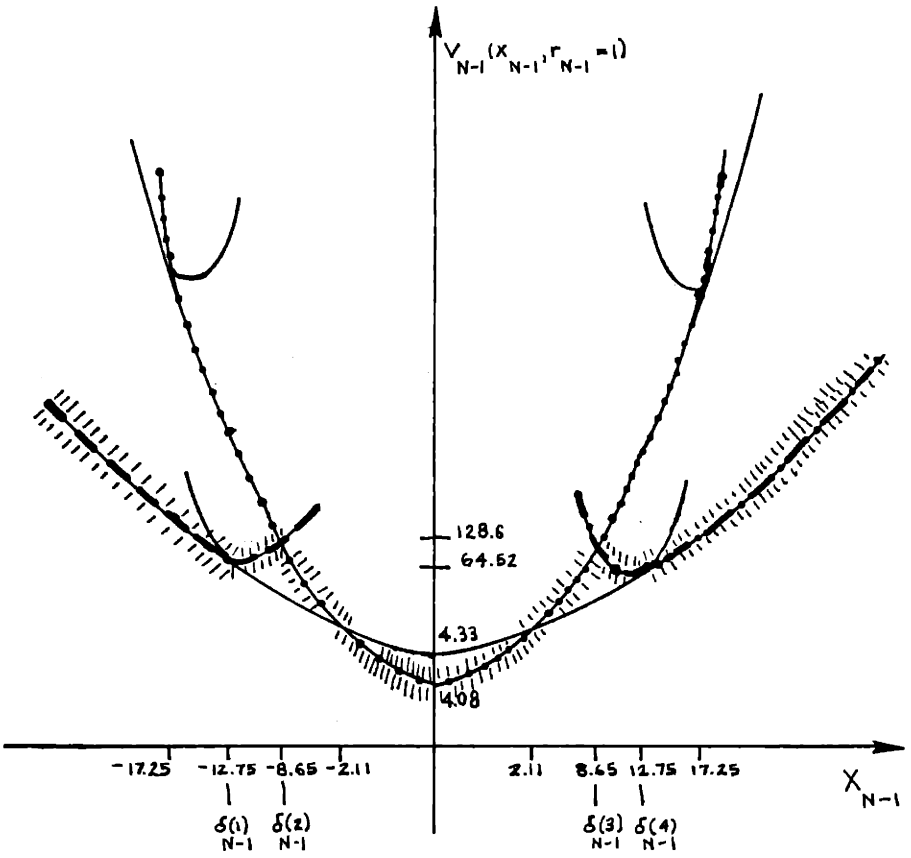

Figure 9.1: $V_{N-1}(x_{N-1}, r_{N-1}=1)$ in example 9.1 and subproblem costs; $V_{N-1}(x_{N-1}, 1 \mid 1)$ is indicated by the dashed line, $V_{N-1}(x_{N-1}, 1 \mid 2)$ by the dotted line and $V_{N-1}(x_{N-1}, 1 \mid 3)$ by the dot-dash line. The optimal cost $V_{N-1}(x_{N-1}, r_{N-1}=1)$ is indicated by the solid overline.

if	$V_{N-1}(x_{N-1}, r_{N-1}=1)$	$u_{N-1}(x_{N-1}, r_{N-1}=1)$	$x_{N-1} + u_{N-1}$
$x_{N-1} < -12.75$	$(.7647)x_{N-1}^2 + 4.333$	$-.7647\ x_{N-1}$	$.2353\ x_{N-1}$
$-12.75 < x_{N-1} < -8.655$	$x_{N-1}^2 + 6x_{N-1} + 42.58$	$-x_{N-1} - 3^-$	-3^-
$-8.655 < x_{N-1} < 8.655$	$(.8207)x_{N-1}^2 + 4.083$	$-.8207\ x_{N-1}$	$.1793\ x_{N-1}$
$8.655 < x_{N-1} < 12.75$	$x_{N-1}^2 - 6x_{N-1} + 42.58$	$-x_{N-1} + 3^+$	3^+
$12.75 < x_{N-1}$	$(.7647)\ x_{N-1}^2 + 4.333$	$-.7647\ x_{N-1}$	$.2353\ x_{N-1}$

Table 9.1 Optimal Expected Cost-to-go, Control Law, and $x_{N-1} + u_{N-1}$ from $(x_{N-1}, r_{N-1}=1)$ in Example 9.1.

In figure 9.2 we can compare the last-stage solution of this problem and the noiseless version of this example (example 5.1 in Section 5.3). We make the following observations:

1. In both example 9.1 and example 5.1 the optimal expected cost $V_{N-1}(x_{N-1}, r_{N-1}=1)$ is piecewise-quadratic in x_{N-1} and the optimal control law is piecewise-linear. When we go back another stage in time, the optimal cost $V_{N-2}(x_{N-2}, r_{N-2}=1)$ can be obtained using a similar approach. The piecewise-quadratic structure will be lost, however, in example 9.1.

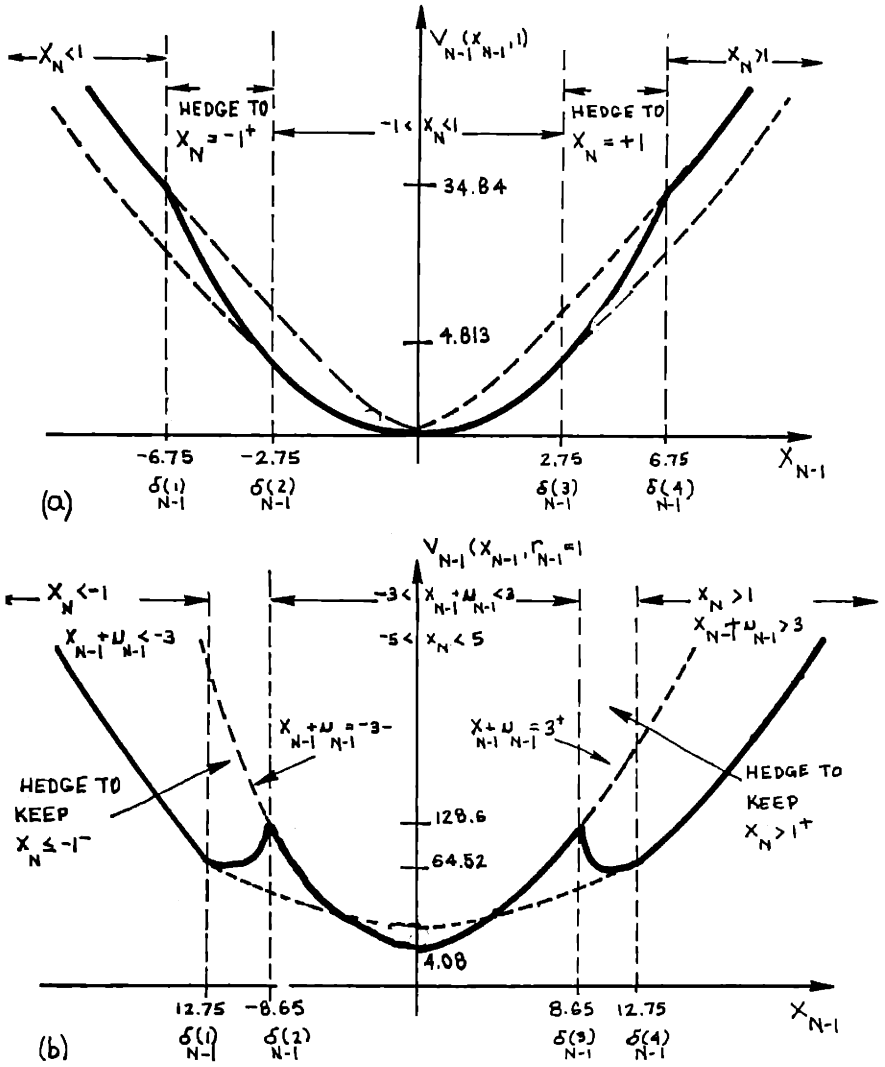

Figure 9.2: $V_{N-1}(x_{N-1}, r_{N-1}=1)$ in (a) example 6.1 and (b) example 9.1 (not to scale).

2. The endpiece control laws in both examples are the same:

$$u_{N-1}(x_{N-1}, r_{N-1}=1) = (-.7647)\ x_{N-1}\ .$$

In both examples this control law corresponds to making

$$|x_N| > 1$$

with certainty. In example 5.1, where there is no input noise, this is done by making

$$|x_{N-1} + u_{N-1}| > 1 \quad .$$

In example 9.1 we must make

$$|x_{N-1} + u_{N-1}| > 3$$

to guarantee that $|x_N| > 1$ (since no matter what value in $(-2,2)$ the noise v_{N-1} takes, we will have $|x_N| > 1$).

3. In example 5.1 we use control

$$u_{N-1} = -x_{N-1} = 1^+$$

to hedge to point $x_N = -1^+$ when

$$8.65 = \delta_{N-1}(1) \leq x_{N-1} \leq \delta_{N-1}(2) = 12.75.$$

In example 9.1 we cannot place x_N with certainty. However we can place $(x_{N-1} + u_{N-1})$. In example 9.1 when $8.65 \leq x_{N-1} \leq 12.75$ we use the control

$$u_{N-1} = -x_{N-1} - 3$$

to obtain

$$(x_{N-1} + u_{N-1}) = -3^{-} \quad \bullet$$

This corresponds to using control u_{N-1} to guarantee $x_N \leq -1^{-}$ with certainty.

4. Note that in example 5.1 we hedge-to-a-point to get x_N <u>inside</u> $(-1,1)$. In example 9.1, however, we hedge to keep x_N <u>outside</u> $(-1,1)$ even though the probability of failure is larger there. The reason is that for

$$8.65 < |x_{N-1}| < 12.75 \quad ,$$

it is better to keep x_N in the disadvantageous $p(1,2:x)$ pieces $|x_N| > 1$ with certainty (by making $x_{N-1} + u_{N-1} > 3$) than it is to risk having either $|x_N| > 1$ or $|x_N| < 1$ (by making $|x_{N-1} + u_{N-1}| < 3$). That is, it is not worth spending extra control energy to try to get x_N inside the advantageous $p(1,2:x_N)$ piece because we can not do it with certainty.

5. As in the JLQ problems of chapter 5, the optimal controller has regions of avoidance. However for example 9.1 they are regions of $(x_{N-1} + u_{N-1})$ avoidance (instead of x_N avoidance). From Table 9.1 we see that the optimal controller chooses u_{N-1} so that $(x_{N-1} + u_{N-1})$ does not take values in the intervals

$$(-3^{+}, -1.55) \quad \text{and} \quad (1.55, 3^{-}) \quad .$$

□

Example 9.2 Let us now modify example 9.1 so that the expected cost term

$$E\{x_N^2 + V_N(x_N,r_N) \,|\, x_{N-1},r_{N-1}=1,\ u_{N-1}\} \tag{9.45}$$

is piecewise-cubic in $(x_{N-1} + u_{N-1})$. Consider the control problem of example 9.1, but with

$$p(1,2:x) = \begin{cases} 1/4 & \text{if } x < 1 \\ 3/4 & \text{if } x > 1 \end{cases} \tag{9.46}$$

In form r = 2 the solution is the same as in example 9.1, and (9.25) - (9.26) apply in form r = 1.

If u_{N-1} is chosen so that $(x_{N-1} + u_{N-1}) > 3$ then $x_N > 1$, and therefore $p(1,2:x_N) = 3/4$. The expected cost (9.45) in this case is given by (9.27).

If u_{N-1} is chosen so that $(x_{N-1} + u_{N-1}) < -1$ then $x_N < 1$ with certainty, and therefore $p(1,2:x_N) = 3/4$. When this is the case,

$$\frac{1}{4}\int_{-2}^{2} (x_{N-1} + u_{N-1} + v)^2 \begin{bmatrix} p(1,1:x_{N-1} + u_{N-1} + v) \\ + \\ 4p(1,1:x_{N-1} + u_{N-1} + v) \end{bmatrix} dv =$$

$$\frac{7}{16}\int_{-2}^{2} (x_{N-1}+u_{N-1}+v)^2 dv = \frac{7}{4}(x_{N-1} + u_{N-1})^2 + 7/3. \tag{9.47}$$

If we choose u_{N-1} so that $-1 < (x_{N-1} + u_{N-1}) < 3$ then the form transition probabilities will depend upon the value of the input noise. In this case,

$$\frac{1}{4}\int_{-2}^{2} (x_{N-1} + u_{N-1} + v)^2 \begin{bmatrix} p(1,1:x_{N-1} + u_{N-1} + v) \\ + \\ 4p(1,1:x_{N-1} + u_{N-1} + v) \end{bmatrix} dv$$

$$= \frac{13}{16}\int_{-2}^{1-(x_{N-1}+u_{N-1})} x_{N-1} + u_{N-1} + v)^2 \, dv + \frac{7}{16}\int_{1-(x_{N-1}+u_{N-1})}^{2} (x_{N-1} + u_{N-1} + v)^2 \, dv$$

$$= (\frac{-1}{8})(x_{N-1} + u_{N-1})^3 + (\frac{5}{2})(x_{N-1} + u_{N-1})^2 - (\frac{3}{2})(x_{N-1} + u_{N-1}) + \frac{83}{24} \quad .$$

(9.48)

Thus the expected cost in (9.45) is piecewise-cubic in $(x_{N-1} + u_{N-1})$.

$V_{N-1}(x_{N-1}, r_{N-1}=1)$ is obtainable by comparing the solutions of the constrained-in-$(x_{N-1} + u_{N-1})$ subproblems.

$$V_{N-1}(x_{N-1}, r_{N-1}=1 \mid 1) = \min_{\substack{u_{N-1} \text{ s.t.} \\ (x_{N-1}+u_{N-1})<-1}} \left\{ u_{N-1}^2 + \frac{7}{4}(x_{N-1} + u_{N-1})^2 + 7/3 \right\}$$

(9.49)

$$V_{N-1}(x_{N-1}, r_{N-1}=1 \mid 2) = \min_{\substack{u_{N-1} \text{ s.t.} \\ -1<(x_{N-1}+u_{N-1})<3}} \left\{ \begin{matrix} u_{N-1}^2 - \frac{1}{8}(x_{N-1} + u_{N-1})^3 + \frac{5}{2}(x_{N-1}+u_{N-1})^2 \\ - \frac{3}{2}(x_{N-1} + u_{N-1}) + 83/24 \end{matrix} \right\}$$

$$V_{N-1}(x_{N-1}, r_{N-1}=1 \mid 3) = \min_{\substack{u_{N-1} \text{ s.t.} \\ 3<(x_{N-1} + u_{N-1})}} \left\{ u_{N-1}^2 + \frac{3}{4}(x_{N-1} + u_{N-1})^2 + \frac{13}{3} \right\}$$

(9.51)

We will defer solution of these subproblems and the determination of $V_{N-1}(x_{N-1}, r_{N-1}=1)$ until section 9.8 .

Let us return to the general control problem of this chapter. We can follow the idea used in the above examples and reformulate (9.20) as a comparison of a set of constrained subproblem solutions. Let z_{k+1} be the value that x_{k+1} would have given r and assuming that the noise is zero:

$$z_{k+1} = a(r_k)x_k + b(r_k)u_k \quad . \tag{9.52}$$

That is

$$z_{k+1} = x_{k+1} - \Xi(r_k)v_k \quad . \tag{9.53}$$

We define the z-conditional expected cost-to-go as follows:

$$\hat{\hat{V}}_{k+1}(z_{k+1}|r_k=j) \triangleq E\left\{ \begin{array}{l|ll} V_{k+1}(x_{k+1}, r_{k+1}) & r_k = j & \\ + & & \\ Q(x_{k+1}, r_{k+1}) & z_{k+1} = a(j)x_k + b(j)u_k & \end{array} \right\}$$

$$= E\left\{ \begin{array}{l|ll} V_{1+1}(a(j)x_k + b(j)u_k + \Xi(j)v_k, r_{k+1}) & r_k = j, & \\ + & & \\ Q(a(j)x_k + b(j)u_k + \Xi(j)v_k, r_{k+1}) & u_k, x_k & \end{array} \right\}$$

$$= E\left\{ \hat{V}_{k+1}(x_{k+1}|r_k=j) \,\middle|\, \begin{array}{l} r_k=j \\ x_k, u_k \end{array} \right\} \quad . \tag{9.54}$$

The minimization in (9.17), (9.20) then becomes

$$V_k(x_k, r_k) = \min_{u_k} \left\{ u_k^2 R(r_k) + \hat{\hat{V}}_{k+1}(z_{k+1}|r_k=j) \right\} \quad . \tag{9.55}$$

As we shall see in later sections of this chapter, the behavior of this z-conditional expected cost function is intimately related to qualitative properties of the optimal controller and combinatoric properties of the solution.

We can solve for $V_k(x_k,r_k)$ in (9.55) by comparing (at each x_k value) a finite set of constrained-in-z_{k+1} subproblems:

$$V_k(x_k,r_k=j) = \min_{t=1,\ldots,\hat{\psi}^j_{k+1}} \{ V_k(x_k,r_k=j \,|\, z_{k+1} \in \hat{\Delta}^j_{k+1}(t)) \} , \tag{9.56}$$

where the $\hat{\psi}^j_{k+1}$ subproblems are

$$V_k(x_k,r_k=j \,|\, z_{k+1} \in \hat{\Delta}^j_{k+1}(t)) = \min_{\substack{u_k \text{ s.t} \\ z_{k+1} \in \hat{\Delta}^j_{k+1}}} \left\{ u_k^2 R(j) + \hat{\hat{V}}_{k+1}(z_{k+1} \,|\, r_k=j) \right\} \tag{9.57}$$

$$\triangleq V_k(x_k,r_k=j \,|\, t)$$

and the $\hat{\Delta}^j_{k+1}(t)$ are intervals of z_{k+1} values.

In principle, we can solve for the optimal controllers for (9.1) - (9.16) at each time stage k and in each form $j \in \underline{M}$ if we can solve (9.55) - (9.57) subject to (9.52) - (9.54).

We have now incorporated additive input noise in the problem solution approach of chapters 5 and 8, by reformulating the noisy JLPC problem (9.1) - (9.16) as a comparison of subproblems constrained in the deterministic quantity z_{k+1} (given u_k,x_k,r_k). Note that if there is no input noise then $z_{k+1} = x_{k+1}$ and $\hat{\hat{V}}_{k+1}(z_{k+1} \, r_k=j) = \hat{V}_{k+1}(x_{k+1} \,|\, r_k=j)$.

Two issues must be resolved before we can use this reformulation to solve (9.1) - (9.16):

(1) How do we obtain the partition of z_{k+1} values (that is, the intervals $\hat{\Delta}^j_{k+1}(t)$; $t = 1,\ldots,\hat{\psi}^j_{k+1}$) in (9.56) - (9.57)?

(2) How do we solve the subproblems in (9.57) when $\hat{\hat{V}}_{k+1}(z_{k+1}|r_k)$ is not piecewise-quadratic in z_{k+1}?

We address these questions in the remainder of this chapter.

9.4 Solution of a One-Stage Example Problem:

In the previous section we described how a JLPC problem specified by (9.1) - (9.16) can be transformed into the comparison of a finite number of constrained-in-z_{k+1} subproblems. In this section we will carry out this reformulation for one stage of an example problem, and we will solve for the optimal controller.

As we obtain the solution of this example problem we will make a number of observations regarding JLPC problems possessing additive noise. Using insight gained from the solution of this example problem, we will develop a general one-step solution procedure in section 9.5, and two approximate (suboptimal) controllers in section 9.9.

Example 9.3: This example is the same as example 8.4, except for the inclusion of additive input noise. It involves x-costs that are piece-quadratic in x, form transition probabilities that are piecewise -

constant in x, and a piecewise-constant input noise density.

We consider a system with M = 2 forms where

(normal operation) $x_{k+1} = x_k + u_k + v_k$ if $r_k = 1$

(failure) $x_{k+1} = x_k$ if $r_k = 2$

$$p(1,2:x) = \begin{cases} 1/4 & \text{if } |x| < 1 \\ 3/4 & \text{if } |x| > 1 \end{cases}$$

$$p(1,1:x) = 1 - p(1,2:x) \qquad p(2,2) = 1 \quad p(2,1) = 0$$

(noise density)
$$p(v) = \begin{cases} 3/8 & \text{if } |v| < 1 \\ 1/8 & \text{if } 1 < |v| < 2 \\ 0 & \text{if } |v| > 2 \end{cases}$$

hence

$$E\{v_k\} = 0 \quad , \quad E\{v_k^2\} = 5/6 \qquad \forall\ k$$

and

$$E\{v_k\ v_s\} = 0 \qquad \text{for} \quad k \neq s.$$

In the notation of section 9.2 we have noise-density piece boundaries

$\sigma(1) = -2$ $\sigma(3) = 1$ ($\bar{\sigma}$ = 5 pieces)

$\sigma(2) = -1$ $\sigma(4) = 2$

We seek to minimize

$$\min_{u_o,\ldots,u_{N-1}} E\left\{\sum_{k=0}^{N-1}\left[u_k^2 + Q(x_{k+1},r_{k+1})\right] + Q_T(x_N,r_N)\right\}$$

where

$$Q(x_{k+1},r_{k+1}=2) = 0$$

$$Q_T(x_N,r_N=2) = 1000.$$

$$Q_T(x_N,r_N=1) = 0$$

and

$$Q(x_{k+1},r_{k+1}=1) = \begin{cases} x_{k+1}^2 & x_{k+1} < -.5 \\ -2x_{k+1}^2 - 1.5x_{k+1} & -.5 < x_{k+1} < 0 \\ -2x_{k+1}^2 + 1.5x_{k+1} & 0 < x_{k+1} < .5 \\ x_{k+1}^2 & .5 < x_{k+1} \end{cases}$$

•

As in example 8.4, in form r = 2 (i.e., in the failure mode) the optimal expected cost-to-go and control law is

$$V_k(x_k,r_k=2) = 1000$$

$$u_k(x_k,r_k=2) = 0$$

at all times k. In form r=1 we have

$$V_N(x_N,r_N=1) = 0$$ •

As in example 8.4, the conditional expected cost $\hat{V}_N(x_N|r_{N-1}=1)$ for this problem is

$$\hat{V}_N(x_N|r_{N=1}=1) = \begin{cases} \hat{V}_N(x_N;1) = (.25)x_N^2 + 750 & x_N < -1 \\ \hat{V}_N(x_N;2) = (.75)x_N^2 + 250 & -1 < x_N < -.5 \\ \hat{V}_N(x_N;3) = (-1.5)x_N^2 - (.375)x_N + 250 & -.5 < x_N < 0 \\ \hat{V}_N(x_N;4) = (-1.5)x_N^2 + (.375)x_N + 250 & 0 < x_N < .5 \\ \hat{V}_N(x_N;5) = (.75)x_N^2 + 250 & .5 < x_N < 1 \\ \hat{V}_N(x_N;6) = (.25)x_N^2 + 750 & 1 < x_N \end{cases} \tag{9.58}$$

where we have a partition of x_N values with $\psi_N = 6$ pieces, specified by

$$\begin{array}{lll} \gamma_N(1) = -1 = -\gamma_N(5) & \Delta_N(1) = (-\infty,-1) & \Delta_N(4) = (0,.5) \\ \gamma_N(2) = -.5 = -\gamma_N(4) & \Delta_N(2) = (-1,-.5) & \Delta_N(5) = (.5,1) \\ \gamma_N(3) = 0 & \Delta_N(3) = (.5,0) & \Delta_N(6) = (1,\infty) \end{array} . \tag{9.59}$$

$\hat{V}_N(x_N|r_{N=1}=1)$ is discontinuous at $x_N = \pm 1$ (the form transition probability discontinuities).

The grid points in (9.59) are joining points of the x-operating cost $Q(x,r=1)$ and discontinuities of the form transition probability $p(1,2:x)$.

Now let us compute the z-conditional expected cost-to-go $\hat{\hat{V}}_N(z_N|r_{N-1}=1)$. From (9.54) we have

$$\hat{\hat{V}}_N(z_N|r_{N-1}=1) = \int_{-\infty}^{\infty} p(v)\ \hat{V}_N(z_N+v|r_{N-1}=1)dv \quad . \tag{9.60}$$

In this example the input noise density p(v) is piecewise-constant with $\bar{\sigma} = 5$ pieces and p(v) = 0 over the leftmost and rightmost pieces. Here $\hat{V}_N(x_N|r_{N-1}=1)$ has $\psi_N = 6$ pieces. Thus we can rewrite (9.50) as a sum of

$$(\bar{\sigma} - 2)\psi_N = 18$$

integrals:

$$\hat{\hat{V}}_N(z_N|r_{N-1}=1) = \sum_{S=2}^{\bar{\sigma}=1} \left\{ \begin{array}{l} \displaystyle\int_{\sigma(s-1)}^{\max[\sigma(s-1),\min[\gamma_N(1)-z_N,\sigma(s)]]} \omega(v:s)\ \hat{V}_N(z_N+v;1)dv \\ + \displaystyle\sum_{t=2}^{\psi_N-1} \int_{\min[\sigma(s),\max[\gamma_N(t-1)-z_N,\sigma(s-1)]]}^{\max[\sigma(s-1),\min(\gamma_N(t)-z_N,\sigma(s))]} \{\omega(v;s)\ \hat{V}_N(z_N+v;t)dv\} \\ + \displaystyle\int_{\min[\sigma(s),\ \max\{\gamma_N(\psi_N-1)-z_N,\sigma(s-1)\}]}^{\sigma(s)} \omega(v;s)\ \hat{V}_N(z_N+v;\psi_N)dv \end{array} \right. \tag{9.61}$$

(where $\hat{V}_N(z_N+v:t)$ denotes the t^{th} piece of $\hat{V}_N(z_N+v_N|r_{N-1}=1)$, as in (9.21), and p(s:v) denotes the s^{th} piece of noise density $p(v_k)$ as in (9.6), and the $\gamma_N(t)$ are as in (9.59)).

The numerical values of the limits of integration in (9.61) depend upon the value of z_N. This gives $\hat{\hat{V}}_N(z_N|r_{N-1}=1)$ a piecewise structure in z_N:

We have a boundary between pieces of $\hat{\hat{V}}_N(z_N|r_{N-1}=1)$ at each z_N value where one (or more) of the limits of integration (9.61) changes.

It is straightforward to verify that for each $s = 2,3,\ldots,\bar{\sigma}-1 = 4$ and $t = 1,2,\ldots,\psi_N-1=5$ we have

$$\max\{\sigma(s-1), \min(\gamma_N(t) - z_N, \sigma(s))\} = \min\{\sigma(s), \max(\gamma_N(t) - z_N, \sigma(s-1))\} =$$

$$= \begin{cases} \sigma(s) & \text{if } z_N \leq \gamma_N(t) - \sigma(s) \\ \gamma_N(t) - z_N & \text{if } \gamma_N(t) - \sigma(s) \leq z_N \leq \gamma_N(t) - \sigma(s-1) \\ \sigma(s-1) & \text{if } \gamma_N(t) - \sigma(s-1) \leq z_N \end{cases} \quad . \tag{9.62}$$

The boundaries of the $\hat{\hat{V}}_N(z_N|r_{N-1}=1)$ pieces' domains are the set of values

$$\{\gamma_N(t) - \sigma(s) : \quad s=2,\ldots,\sigma-1; \quad t=1,\ldots,\psi_N-1\}$$

which, for this example, are

$$\{-3, -2.5, -2, -1.5, -1, -.5, 0, .5, 1, 1.5, 2, 2.5, 3\} \quad .$$

Ordering these 13 quantities from smallest to largest, and denoting them by $\hat{\gamma}_N(t)$ $(t=1,\ldots,13)$ we obtain a partition of the real line of z_N values into $\hat{\psi}_N = 14$ intervals,

$$\hat{\Delta}_N(t) = (\hat{\gamma}_N(t-1), \hat{\gamma}_N(t)) \qquad t = 1,\ldots,13$$

(where $\hat{\gamma}_N(0) \triangleq -\infty$, $\hat{\gamma}_N(14) \triangleq +\infty$) as follows:

$$
\begin{aligned}
\hat{\Delta}_N(1) &= (\hat{\gamma}_N(0), \hat{\gamma}_N(1)) = (-\infty, -3) \\
\hat{\Delta}_N(2) &= (\hat{\gamma}_N(1), \hat{\gamma}_N(2)) = (-3, -2.5) \\
\hat{\Delta}_N(3) &= (\hat{\gamma}_N(2), \hat{\gamma}_N(3)) = (-2.5, -2) \\
\hat{\Delta}_N(4) &= (\hat{\gamma}_N(3), \hat{\gamma}_N(4)) = (-2, -1.5) \\
\hat{\Delta}_N(5) &= (\hat{\gamma}_N(4), \hat{\gamma}_N(5)) = (-1.5, -1) \\
\hat{\Delta}_N(6) &= (\hat{\gamma}_N(5), \hat{\gamma}_N(6)) = (-1, -.5) \\
\hat{\Delta}_N(7) &= (\hat{\gamma}_N(6), \hat{\gamma}_N(7)) = (-.5, 0) \\
\hat{\Delta}_N(8) &= (\hat{\gamma}_N(7), \hat{\gamma}_N(8)) = (0, .5) \\
\hat{\Delta}_N(9) &= (\hat{\gamma}_N(8), \hat{\gamma}_N(9)) = (.5, 1) \\
\hat{\Delta}_N(10) &= (\hat{\gamma}_N(9), \hat{\gamma}_N(10)) = (1, 1.5) \\
\hat{\Delta}_N(11) &= (\hat{\gamma}_N(10), \hat{\gamma}_N(11)) = (1.5, 2) \\
\hat{\Delta}_N(12) &= (\hat{\gamma}_N(11), \hat{\gamma}_N(12)) = (2, 2.5) \\
\hat{\Delta}_N(13) &= (\hat{\gamma}_N(12), \hat{\gamma}_N(13)) = (2.5, 3) \\
\hat{\Delta}_N(14) &= (\hat{\gamma}_N(13), \hat{\gamma}_N(14)) = (3, \infty)
\end{aligned}
\qquad (9.63)
$$

Applying the integration limit values specified by (9.62) to the computation of (9.61), we can obtain each $\hat{\hat{V}}_N(z_N | r_{N-1}=1)$ piece.

These calculations can be simplified if we first calculate $\hat{\hat{V}}_N(z_N:1)$ (i.e. for $z_N \in \hat{\Delta}_N(1)$) and we then successively calculate (for each $t = 2, \ldots, \hat{\psi}_N - 1$) the piece $\hat{\hat{V}}_N(z_N;t)$ from $\hat{\hat{V}}_N(z_N;t-1)$, by adding or subtracting (as appropriate) those integrals in (9.61) whose limits change when we move from $\hat{\Delta}_N(t-1)$ to $\hat{\Delta}_N(t)$.

For $z_N \in \hat{\Delta}_N(1) = (-\infty, 3)$ we obtain

$$\begin{aligned}\hat{\hat{V}}_N(z_N;1) &= \int_{-2}^{-1} \frac{1}{8} \hat{V}_N(z_N + v:1)\, dv + \int_{-1}^{1} \frac{3}{8} \hat{V}_N(z_N + v;1)dv \\ &\quad + \int_{1}^{2} \frac{1}{8} \hat{V}_N(z_N + v;1)dv \\ &= (.25)z_N^2 + 750.208 \,.\end{aligned} \tag{9.64}$$

For $z_N \in \hat{\Delta}_N(1)$, each of the other fifteen integrals in (9.61) has the same upper and lower limit of integration; hence they are zero. As is evident in (9.64), $x_N = z_N + v$ is in $\Delta_N(1)$ for any noise magnitude in $(-2,2)$. Consequently $\hat{\hat{V}}_N(z_N;1)$ is quadratic in z_N.

For $z_N \in \hat{\Delta}_N(2) = (-3, -2.5)$ we have

$$\begin{aligned}\hat{\hat{V}}_N(z_N;2) &= \hat{\hat{V}}_N(z_N;1) + \int_{-1-z_N}^{2} \frac{1}{8}(\hat{V}_N(z_N + v;2) - \hat{V}_N(z_N + v;1))dv \\ &= (.020833)z_N^3 + (.375)z_N^2 - (62.25)z_N + 562.896.\end{aligned}$$

Following this procedure for the remaining z_N intervals, we obtain the z-conditional cost for this example:

$$\hat{\hat{V}}_N(z_N|r_{N-1}=1) = \begin{cases} +(.25)z_N^2 + 750.208 & \text{if } z_N \in \hat{\Delta}_N(1) \\ +(.020833)z_N^3 + (.375)z_N^2 - (62.25)z_N + 562.896 & \text{if } z_N \in \hat{\Delta}_N(2) \\ -(.072917)z_N^3 - (.210938)z_N^2 - (63.4688)z_N + 562.046 & \text{if } z_N \in \hat{\Delta}_N(3) \\ -(.031250)z_N^3 - (.039063)z_N^2 - (188.156)z_N + 312.317 & \text{if } z_N \in \hat{\Delta}_N(4) \\ -(.125)z_N^3 - (.108645)z_N^2 - (187.781)z_N + 312.721 & \text{if } z_N \in \hat{\Delta}_N(5) \\ -(.145833)z_N^3 - (.140625)z_N^2 - (125.343)z_N + 375.169 & \text{if } z_N \in \hat{\Delta}_N(6) \\ (.041667)z_N^3 + (.375)z_N^2 - (124.875)z_N + 375.298 & \text{if } z_N \in \hat{\Delta}_N(7) \\ -(.041667)z_N^3 + (.375)z_N^2 + (124.875)z_N + 375.298 & \text{if } z_N \in \hat{\Delta}_N(8) \\ +(.145833)z_N^3 - (.140625)z_N^2 + (125.343)z_N + 375.169 & \text{if } z_N \in \hat{\Delta}_N(9) \\ +(.125)z_N^3 - (.108645)z_N^2 + (187.781)z_N + 312.721 & \text{if } z_N \in \hat{\Delta}_N(10) \\ +(.03250)z_N^3 - (.039063)z_N^2 + (188.156)z_N + 312.317 & \text{if } z_N \in \hat{\Delta}_N(11) \\ +(.072917)z_N^3 - (.210938)z_N^2 + (63.4688)z_N + 562.046 & \text{if } z_N \in \hat{\Delta}_N(12) \\ -(.020833)z_N^3 + (.375)z_N^2 + (62.25)z_N + 562.896 & \text{if } z_N \in \hat{\Delta}_N(13) \\ +(.25)z_N^2 + 750.208 & \text{if } z_N \in \hat{\Delta}_N(14) \end{cases} \tag{9.65}$$

This z-conditional cost $\hat{\hat{V}}_N(z_N|r_{N-1}=1)$ is continuous in z_N. The additive noise smooths out the discontinuities in $\hat{V}_N(x_N|r_{N-1}=1)$ at $x_N = \pm 1$.

For this example problem the $\hat{\psi}_N = 14$ constrained subproblems are

$$V_{N-1}(x_{N-1},r_{N-1}=1\,|t) = \min_{\substack{u_{N-1} \text{ s.t.} \\ z_N \in \hat{\Delta}_N(t)}} \left\{ u_{N-1}^2 + \hat{\hat{V}}_N(z_n;t) \right\} \tag{9.66}$$

for $t = 1,2,\ldots, \hat{\psi}_N = 14$. Substituting

$$u_{N-1} = \frac{z_N - a(1)\, x_{N-1}}{b(1)} = z_N - x_{N-1} \tag{9.67}$$

in (9.66) we obtain

$$V_{N-1}(x_{N-1},r_{N-1}=1\,|t) = \min_{z_N \in \hat{\Delta}_N(t)} \left\{ \begin{array}{l} z_N^2 - 2z_N\, x_{N-1} + x_{N-1}^2 \\ + \hat{\hat{V}}_N(z_N;t) \end{array} \right\} . \tag{9.68}$$

Each of the subproblems in (9.66) can be solved analytically. The extreme-piece subproblems (i.e., t=1 and t=14) have optimal expected costs that are piecewise-quadratic in x_{N-1} with two pieces:

$$V_{N-1}(x_{N-1},r_{N-1}=1\,|1) = \begin{cases} V_{N-1}^{1,U} = .2x_{N-1}^2 + 750.2 & \text{if } x_{N-1} < -3.75 \\ V_{N-1}^{1,R} = x_{N-1}^2 + 6x_{N-1} + 761.5 & \text{if } x_{N-1} > \theta_{N-1}(1) \end{cases}$$

$$u_{N-1}(x_{N-1}, r_{N-1}=1 \mid 1) = \begin{cases} u_{N-1}^{1,U} = -.2x_{N-1} & \text{if } x_{N-1} < \Theta_{N-1}(1) \\ u_{N-1}^{1,R} = -x_{N-1} - 3^{-} & \text{if } x_{N-1} > \Theta_{N-1}(1) \end{cases}$$

$$V_{N-1}(x_{N-1}, r_{N-1}=1 \mid 14 = \begin{cases} V_{N-1}^{14,L} = x_{N-1}^2 - 6x_{N-1} + 761.5 & \text{if } x_{N-1} < 3.75 \\ V_{N-1}^{14,U} = .2x_{N-1}^2 + 750.2 & \text{if } x_{N-1} > \theta_{N-1}(14) \end{cases}$$

$$u_{N-1}(x_{N-1}, r_{N-1}=1 \mid 14 = \begin{cases} u_{N-1}^{14,L} = -x_{N-1} + 3^{+} & \text{if } x_{N-1} < \theta_{N-1}(14) \\ u_{N-1}^{14,U} = -.2x_{N-1} & \text{if } x_{N-1} > \theta_{N-1}(14) \end{cases}$$

$V_{N-1}^{1,U}$ and $V_{N-1}^{14,U}$ are quadratic in x_{N-1} because $\hat{\hat{V}}_N(z_{N:1})$ and $\hat{\hat{V}}_N(z_N{:}14)$ quadratic in z_N.

The other subproblems in (9.66) for this example have a three-piece solution structure:

$$V_{N-1}(x_{N-1}, r_{N-1}=1 \mid t) = \begin{cases} V_{N-1}^{t,L}(x_{N-1}, 1) & \text{if } x_{N-1} \leq \theta_{N-1}(t) \\ V_{N-1}^{t,U}(x_{N-1}, 1) & \text{if } \theta_{N-1}(t) \leq x_{N-1} \leq \Theta_{N-1}(t) \\ V_{N-1}^{t,R}(x_{N-1}, 1) & \text{if } \Theta_{N-1}(t) \leq x_{N-1} \end{cases} \tag{9.69}$$

with

$$\theta_{N-1}(t) < \Theta_{N-1}(t)$$

We can find the actively constrained cost pieces $V_{N-1}^{t,L}(x_{N-1},1)$ and $V_{N-1}^{t,R}(x_{N-1},1)$ in (9.69) quite easily:

- For $t = 2,\ldots, \hat{\psi}_N = 14$ find $V_{N-1}^{t,L}(x_{N-1},1)$ by evaluating (9.68) with $z_N = \hat{\gamma}_N(t-1)$.

- For $t = 1,\ldots, \hat{\psi}_{N-1}=13$ find $V_{N-1}^{t,R}(x_{N-1},1)$ by evaluating (9.68) with $z_N = \hat{\gamma}_N(t)$.

Following these steps for this example we obtain:

$$
\begin{aligned}
V_{N-1}^{1,R} &= V_{N-1}^{2,L} = x_{N-1}^2 + 6x_{N-1} + 761.5 \\
V_{N-1}^{2,R} &= V_{N-1}^{3,L} = x_{N-1}^2 + 5x_{N-1} + 726.8 \\
V_{N-1}^{3,R} &= V_{N-1}^{4,L} = x_{N-1}^2 + 4x_{N-1} + 692.7 \\
V_{N-1}^{4,R} &= V_{N-1}^{5,L} = x_{N-1}^2 + 3x_{N-1} + 596.8 \\
V_{N-1}^{5,R} &= V_{N-1}^{6,L} = x_{N-1}^2 + 2x_{N-1} + 501.5 \\
V_{N-1}^{6,R} &= V_{N-1}^{7,L} = x_{N-1}^2 + x_{N-1} + 438.0 \\
V_{N-1}^{7,R} &= V_{N-1}^{8,L} = x_{N-1}^2 + 375.3 \\
V_{N-1}^{8,R} &= V_{N-1}^{9,L} = x_{N-1}^2 - x_{N-1} + 438.0 \\
V_{N-1}^{9,R} &= V_{N-1}^{10,L} = x_{N-1}^2 - 2x_{N-1} + 501.5 \\
V_{N-1}^{10,R} &= V_{N-1}^{11,L} = x_{N-1}^2 - 3x_{N-1} + 596.8 \\
V_{N-1}^{11,R} &= V_{N-1}^{12,L} = x_{N-1}^2 - 4x_{N-1} + 692.7 \\
V_{N-1}^{12,R} &= V_{N-1}^{13,L} = x_{N-1}^2 - 5x_{N-1} + 726.8 \\
V_{N-1}^{13,R} &= V_{N-1}^{14,L} = x_{N-1}^2 - 6x_{N-1} + 761.5
\end{aligned}
\qquad (9.70)
$$

$$
\begin{aligned}
u_{N-1}^{1,R} &= u_{N-1}^{2,L} = -x_{N-1} - 3 \\
u_{N-1}^{2,R} &= u_{N-1}^{3,L} = -x_{N-1} - 2.5 \\
u_{N-1}^{3,R} &= u_{N-1}^{4,L} = -x_{N-1} - 2 \\
u_{N-1}^{4,R} &= u_{N-1}^{5,L} = -x_{N-1} - 1.5 \\
u_{N-1}^{5,R} &= u_{N-1}^{6,L} = -x_{N-1} - 1 \\
u_{N-1}^{6,R} &= u_{N-1}^{7,L} = -x_{N-1} - .5 \\
u_{N-1}^{7,R} &= u_{N-1}^{8,L} = -x_{N-1} \\
u_{N-1}^{8,R} &= u_{N-1}^{9,L} = -x_{N-1} + .5 \\
u_{N-1}^{9,R} &= u_{N-1}^{10,L} = -x_{N-1} + 1 \\
u_{N-1}^{10,R} &= u_{N-1}^{11,L} = -x_{N-1} + 1.5 \\
u_{N-1}^{11,R} &= u_{N-1}^{12,L} = -x_{N-1} + 2 \\
u_{N-1}^{12,R} &= u_{N-1}^{13,L} = -x_{N-1} + 2.5 \\
u_{N-1}^{13,R} &= u_{N-1}^{14,L} = -x_{N-1} + 3
\end{aligned}
\qquad (9.71)
$$

•

From (9.69) we see that the actively-constrained cost-pieces ($V_{N-1}^{t,L}$ and $V_{N-1}^{t,R}$) of $V_{N-1}(x_{N-1}, r_{N-1}=1 \mid t)$ will <u>always</u> be quadratic in x_{N-1} (with x_{N-1}^2, x_{N-1}^1, x_{N-1}^0 terms) regardless of the form of $\hat{V}_N(z_N;t)$.

The unconstrained costs $V_{N-1}^{t,U}$ are <u>not</u> quadratic in x_{N-1}, in general. The difficulty in solving for nonquadratic $V_{N-1}^{t,U}$ may necessitate the use of an approximation to $V_{N-1}(x_{N-1}, r_{N-1}=1 \mid t)$. One such approximation is as follows:

For $t=2,3,\ldots,\hat{\psi}_N-1$ - 13, each subproblem's optimal cost $V_{N-1}(x_{N-1},r_{N-1}=1|t)$ is bounded above at every x_{N-1} value as follows:

$$V_{N-1}(x_{N-1},r_{N-1}=1|t) \leq \tilde{V}_{N-1}(t) \triangleq \begin{cases} V_{N-1}^{t,L}(x_{N-1},1) & \text{if } x_{N-1} \leq \Omega_{N-1}(t) \\ V_{N-1}^{t,R}(x_{N-1},1) & \text{if } x_{N-1} \geq \Omega_{N-1}(t) \end{cases} \tag{9.72}$$

where we define

$$\Omega_{N-1}(t) \triangleq x_{N-1} \text{ value where } V_{N-1}^{t,L}(x_{N-1},1) \text{ and } V_{N-1}^{t,R}(x_{N-1},1) \text{ intersect} \quad . \tag{9.73}$$

Note that

$$\theta_{N-1}(t) < \Omega_{N-1}(t) < \Theta_{N-1}(t) \quad .$$

Using these upper bounds on the subproblem optimal costs, a suboptimal approximation of the optimal expected cost-to-go,

$$V_{N-1}(x_{N-1},r_{N-1}=1) = \min_{t=1,..,\hat{\psi}_N} \{V_{N-1}(x_{N-1},r_{N-1}=1|t)\} \ , \tag{9.74}$$

can be obtained by performing the following comparison at each x_{N-1} value:

$$\tilde{V}_{N-1}(x_{N-1},r_{N-1}=1) = \min \left\{ \begin{array}{l} V_{N-1}(x_{N-1},r_{N-1}=1|1),\ V_{N-1}(x_{N-1},r_{N-1}=1|14) \\ \{\tilde{V}_{N-1}(t) \ ; \ t=2,\ldots,\hat{\psi}_{N-1}=13\} \end{array} \right\} . \tag{9.75}$$

This approximate controller involves the comparison of cost functions that are all piecewise-quadratic in x_{N-1}. This comparison can therefore be carried out using the JLPQ algorithm of chapter 8. The resulting suboptimal controller has an expected cost-to-go that is piecewise-quadratic in x_{k+1}, and a control law that is piecewise-linear.

The suboptimal controller (9.73), (9.75) can be interpreted as follows: for each x_{N-1} value we either

- use the left-endpiece of the optimal controller,

$$u_{N-1}^{Le}(x_{N-1},1) = u_{N-1}^{1,U}(x_{N-1},1)$$

or

- hedge to one of the $\hat{\psi}_{N-1} = 13$ joining points of the z-conditional cost $\hat{\hat{V}}_N(z_N|r_{N-1}=1)$; that is, we hedge one of the $\hat{\gamma}_N(t)$

or

- use the right-endpiece of the optimal controller

$$u_{N-1}^{Re}(x_{N-1},1) = u_{N-1}^{14,U}(x_{N-1},1) .$$

For this example the intersections $\Omega_{N-1}(t)$ of (9.73) are as follows:

t	$V_{N-1}^{t,L}$ and $V_{N-1}^{t,R}$ intersect at $\Omega_{N-1}(t)$ =	Value of $V_{N-1}^{t,L}$ and $V_{N-1}^{t,R}$ at $\Omega_{N-1}(t)$
2	-34.7	1757.
3	-34.1	1719.
4	-95.9	9505.
5	-95.3	9393.
6	-63.5	4407.
7	-62.7	4307.
8	62.7	4307.
9	63.5	4407.
10	95.3	9393.
11	95.9	9506.
12	34.1	1719.
13	34.7	1757.

Table 9.2 Intersections of Constrained Costs in Example 9.3

Performing the comparison in (9.75) we find that the approximate controller is given by

$$\tilde{V}_{N-1}(x_{N-1},r_{N-1}=1) = \begin{cases} V^{1,U} = .2x_{N-1}^2 + 750.2 & \text{if } x_{N-1} < -21.648 \\ V^{7,R} = V^{8,L} = x_{N-1}^2 + 375.3 & \text{if } -21.648 < x_{N-1} < 21.648 \\ V^{14,U} = .2x_{N-1}^2 + 750.2 & \text{if } 21.648 < x_{N-1} \end{cases}$$

$$\tilde{u}_{N-1}(x_{N-1},r_{N-1}=1) = \begin{cases} u^{1,U} = -.2x_{N-1} & \text{if } x_{N-1} < 21.648 \\ u^{7,R} = u^{8,L} = -x_{N-1} & \text{if } -21.648 < x_{N-1} < 21.648 \\ u^{14,U} = -.2x_{N-1} & \text{if } 21.648 < x_{N-1} \end{cases} . \tag{9.76}$$

This suboptimal controller has three obvious advantageous properties:

(1) it is obtained without computing the inactive-constraint costs $V^{t,U}$ for $t \neq 1$, $\hat{\psi}_N$.

(2) All of the comparisons in (9.75) are between quadratic functions, so they can be easily obtained using the quadratic formula.

(3) The resulting controller is piecewise-linear in x_k, which facilitates implementation.

To investigate the accuracy of this approximate controller for this example, let us return to the optimal solution derivation. The inactive-

constraint cost pieces $V^{t,U}$ in (9.69), when they are valid, are not quadratic in x_{N-1} (in general), so they are more difficult to determine than the active constraint costs. We will demonstrate how they can be obtained by considering the subproblem

$$V_{N-1}(x_{N-1},r_{N-1}=1|7) = \min_{\substack{u_{N-1} \text{ s.t.} \\ -.5<z_N<0}} \left\{ u_{N-1}^2 + \hat{\hat{V}}_N(z_N;7) \right\} \tag{9.77}$$

in detail. From (9.65) we can rewrite (9.77) as

$$V_{N-1}(x_{N-1},t_{N-1}=1|7) = \min_{z_N \in (-.5,0)} \left\{ \begin{array}{l} (.0416667)\ z_N^3 + (1.375)z_N^2 \\ -(124.875 + 2x_{N-1})z_N \\ + 375.298 + x_{N-1}^2 \end{array} \right\} , \tag{9.78}$$

Differentiating with respect to z_N we have

$$\frac{\partial V_{N-1}(x_{N-1},r_{N-1}=1|7)}{\partial z_N} = (.125)z_N^2 + (2.75)z_N - (124.875 + 2x_{N-1}) \tag{9.79}$$

$$\frac{\partial^2 V_{N-1}(x_{N-1},r_{N-1}=1|7)}{(\partial z_N)^2} = .25z_{N-1} + 2.75 \quad , \tag{9.80}$$

From (9.80) we see that

$$\frac{\partial^2 V_{N-1}(x_{N-1},r_{N-1}=1|7)}{(\partial z_N)^2} > 0 \quad \text{for } z_N \in \hat{\Delta}_N(7) = (-.5,0) \quad , \tag{9.81}$$

Setting (9.79) to zero and solving for z_N, we obtain the stationary points of $V_{N-1}(x_{N-1}, r_{N-1}=1|7)$:

$$z_N = -11 \pm \sqrt{1120 + 16x_{N-1}} \qquad (9.82)$$

$$\text{if and only if } x_{N-1} \geq -70 \ .$$

If $x_{N-1} < -70$, there are no stationary points. From (9.79) we see that if $x_{N-1} < -70$ then

$$\frac{\partial V_{N-1}(x_{N-1}, r_{N-1}=1|7)}{\partial z_N} > 0 \qquad , \quad \forall\, z_N$$

hence the minimizing z_N in (9.78) is on the left boundary of $\hat{\Delta}_N(7)$ (i.e., at $z_N = \hat{\gamma}_N(6) = -.5^+$) when $x_{N-1} < -70$.

From (9.81) we have that the optimal z_N value in (9.78) is given by

$$z_N = -11 + \sqrt{1120 + 16x_{N-1}}$$

if this z_N is, in fact, in $\hat{\Delta}_N(7) = (-.5, 0)$ (and $x_{N-1} \geq -70$). That is, if

$$-63.09375 \leq x_{N-1} \leq 62.4375 \ .$$

When $x_{N-1} < -63.04375$, the minimizing z_N in $\hat{\Delta}_N(7)$ is on the left boundary:

$$z_N^{7,L} = -.5 \ .$$

This is obtained with control $u_{N-1}^{7,L}(x_{N-1},1)$. If $x_{N-1} > -62.4375$ then the minimizing z_N in $\hat{\Delta}_N(7)$ is the right boundary

$$z_N^{7,R} = 0.$$

This is obtained using control $u_{N-1}^{7,R}(x_{N-1},1)$ when

$$-63.09375 \leq x_{N-1} \leq -62.4375$$

then the minimizing z_N in (9.61) is

$$z_N^{7,U} = -11 + \sqrt{1120 + 16x_{N-1}} \quad ;$$

this is obtained using the control

$$u_{N-1}^{7,U} = -11 - x_{N-1} + \sqrt{1120 + 16x_{N-1}} \quad .$$

The resulting expected cost-to-go is

$$V_{N-1}^{7,U} = \left[\begin{array}{l} x_{N-1}^2 + 22x_{N-1} + 1859.83 \\ - [93.333 - 1.33333\, x_{N-1}] \sqrt{1120 + 16x_{N-1}} \end{array} \right] .$$

Following this optimization procedure for each subproblem in (9.68) we obtain the subproblem solution joining points $\theta_{N-1}(t)$, $\Theta_{N-1}(t)$, the costs $V_{N-1}^{t,U}(x_{N-1},1)$ and the controls $u_{N-1}^{t,U}(x_{N-1},1)$ as in (9.69). These are

$$V_{N-1}^{1,U} = .2x_{N-1}^2 + 750.2$$

$$V_{N-1}^{2,U} = x_{N-1}^2 + 44.00x_{N-1} + 2376. + [-61.67 - 1.333x_{N-1}]\sqrt{1480 + 32x_{N-1}}$$

$$V_{N-1}^{3,U} = x_{N-1}^2 - 4.509x_{N-1} + 422.4 + [56.29 + 1.833x_{N-1}]\sqrt{-69.14 - 2.286x_{N-1}}$$

$$V_{N-1}^{4,U} = x_{N-1}^2 - 20.67x_{N-1} - 1564. + [118.8 + 1.333x_{N-1}]\sqrt{-1900. - 21.33x_{N-1}}$$

$$V_{N-1}^{5,U} = x_{N-1}^2 - 4.754x_{N-1} - 130.3 + [123.8 + 1.333x_{N-1}]\sqrt{-495.1 - 5.333x_{N-1}}$$

$$V_{N-1}^{6,U} = x_{N-1}^2 - 3.929x_{N-1} + 134.4 + [41.22 + 1.333x_{N-1}]\sqrt{-565.3 - 4.571x_{N-1}}$$

$$V_{N-1}^{7,U} = x_{N-1}^2 + 22x_{N-1} + 1860. + [-93.33 - 1.333x_{N-1}]\sqrt{1120 + 16x_{N-1}}$$

$$V_{N-1}^{8,U} = x_{N-1}^2 - 22x_{N-1} + 1860. + [-93.33 + 1.333x_{N-1}]\sqrt{1120 - 16x_{N-1}}$$

$$V_{N-1}^{9,U} = x_{N-1}^2 + 3.929x_{N-1} + 134.4 + [41.22 - 1.333x_{N-1}]\sqrt{-565.3 + 4.571x_{N-1}}$$

$$V_{N-1}^{10,U} = x_{N-1}^2 + 4.754x_{N-1} - 130.3 + [123.8 - 1.333x_{N-1}]\sqrt{-495.1 + 5.333x_{N-1}}$$

$$V_{N-1}^{11,U} = x_{N-1}^2 + 20.67x_{N-1} - 1564. + [118.8 - 1.333x_{N-1}]\sqrt{-1900 + 21.33x_{N-1}}$$

$$V_{N-1}^{12,U} = x_{N-1}^2 + 4.509x_{N-1} + 422.4 + [56.29 - 1.833x_{N-1}]\sqrt{-69.14 + 2.286x_{N-1}}$$

$$V_{N-1}^{13,U} = x_{N-1}^2 - 44.00x_{N-1} + 2376. + [-61.67 + 1.333x_{N-1}]\sqrt{1480 - 32x_{N-1}}$$

$$V_{N-1}^{14,U} = .2x_{N-1}^2 + 750.2 \qquad (9.83)$$

$$
\begin{aligned}
u_{N-1}^{1,U} &= -.8x_{N-1} \\
u_{N-1}^{2,U} &= -x_{N-1} - 22 + \sqrt{1480 + 32x_{N-1}} \\
u_{N-1}^{3,U} &= -x_{N-1} + 1.804 - \sqrt{-69.14 - 2.286x_{N-1}} \\
u_{N-1}^{4,U} &= -x_{N-1} + 10.34 - \sqrt{-1900. - 21.33x_{N-1}} \\
u_{N-1}^{5,U} &= -x_{N-1} + 2.377 - \sqrt{-495.1 - 5.333x_{N-1}} \\
u_{N-1}^{6,U} &= -x_{N-1} + 1.964 - \sqrt{-565.3 - 4.571x_{N-1}} \\
u_{N-1}^{7,U} &= -x_{N-1} - 11 + \sqrt{1120 + 16x_{N-1}} \\
u_{N-1}^{8,U} &= -x_{N-1} + 11 - \sqrt{1120 - 16x_{N-1}} \\
u_{N-1}^{9,U} &= -x_{N-1} - 1.964 + \sqrt{-565.3 + 4.571x_{N-1}} \\
u_{N-1}^{10,U} &= -x_{N-1} - 2.377 + \sqrt{-495.1 + 5.333x_{N-1}} \\
u_{N-1}^{11,U} &= -x_{N-1} - 10.34 + \sqrt{-1900. + 21.33x_{N-1}} \\
u_{N-1}^{12,U} &= -x_{N-1} - 1.804 + \sqrt{-69.14 + 2.286x_{N-1}} \\
u_{N-1}^{13,U} &= -x_{N-1} + 22 - \sqrt{1480 - 32x_{N-1}} \\
u_{N-1}^{14,U} &= -.8x_{N-1}
\end{aligned}
\tag{9.84}
$$

with $\theta_{N-1}(t)$, $\Theta_{N-1}(t)$ as listed in table 9.3 below

t	$\theta_{N-1}(t)$	$\Theta_{N-1}(t)$
1	---	- 3.75
2	-34.9688	- 34.3672
3	-38.3531	- 36.4484
4	-96.2037	- 95.6370
5	-95.6494	- 94.9694
6	-125.577	-124.983
7	-63.0938	- 62.4375
8	62.4375	63.0938
9	124.983	125.577
10	94.9694	95.6494
11	95.6321	96.1968
12	36.4484	38.3531
13	34.3672	34.9688
14	3.75	---

Table 9.3: Joining Points of Constrained Subproblem Solutions $V_{N-1}(x_{N-1}, r_{N-1}=1 \mid t)$ of Example 9.3

Performing the minimization[1] in (9.74) we obtain the optimal expected cost-to-go

$$V_{N-1}(x_{N-1},r_{N-1}=1) = \begin{cases} V^{1,U} = .2x_{N-1}^2 + 750.2 & \text{if } x_{N-1} \leq -21.6 \\ V^{7,R} = V^{8,L} = x_{N-1}^2 + 375.3 & \text{if } -21.6 \leq x_{N-1} \leq 21.6 \\ V^{14,U} = .2x_{N-1}^2 + 750.2 & \text{if } 21.6 \leq x_{N-1} \end{cases} \tag{9.85}$$

$$u_{N-1}(x_{N-1},t_{N-1}=1) = \begin{cases} u^{1,U} = -.2x_{N-1} & \text{if } x_{N-1} < -21.6 \\ u^{7,U}=u^{8,L} = -x_{N-1} & \text{if } -21.6 < x_{N-1} < 21.6 \\ u^{14,U} = -.2x_{N-1} & \text{if } 21.6 < x_{N-1} \end{cases} \tag{9.86}$$

$$z_N(x_{N-1},r_{N-1}=1) = \begin{cases} z^{1,U} = .8x_{N-1} & \text{if } x_{N-1} < -21.6 \\ z^{7,R} = z^{8,L} = 0 & \text{if } -21.6 < x_{N-1} < 21.6 \\ z^{14,U} = .8x_{N-1} & \text{if } 21.6 < x_{N-1} \end{cases} \tag{9.87}$$

This optimal controller (9.85) - (9.97) is identical to the approximate controller (9.75) for this example problem. That is, at no point other than the endpieces are any unconstrained costs $V_{N-1}^{t,U}$ optimal. □

Comparing the solution to example 9.3 with that of example 8.4 (same problem but without noise) we note that the optimal controller in the noisy case is simpler than in the noiseless case. In example 8.4

[1] graphically, or by finding the intersection of all of the subproblem solutions.

(figure 8.4), $V_{N-1}(x_{N-1}, r_{N-1}=1)$ had $m_{N-1}^{(1)} = 9$ pieces. In example 9.3, $V_{N-1}(x_{N-1}, r_{N-1}=1)$ has only $m_{N-1}^{(1)} = 3$ pieces. The presence of additive input noise in example 9.3 makes many of the optimal strategies of example 8.4 (in particular hedging to $x_N = -1^+, -5, .5, 1^-$) impossible.

We note that the optimal control laws in (9.86) are the same as the endpiece and middlepiece control laws of example 8.4 (see table 8.4). The resulting optimal expected cost is, of course, higher for example 9.3 because of the added uncertainty caused by the input noise.

In this section we have obtained the solution of an example problem having nonquadratic $\hat{\hat{V}}_N(z_N|r_{N-1})$ pieces. In the process we also developed an approximate controller (which, for this example, yields the true optimal). In the next section we will derive a general one-step solution to JLPC problems described by (9.1) - (9.16), patterned after the solution of example 9.3. The investigation of approximate solutions will be continued in section 9.9.

9.5 One Stage Solution of the Noisy JLPC Problem

In this section we develop a formal procedure for the solution of the noisy JLPC problem that was formulated in section 9.2. We begin by presenting a proposition which describes the one-stage solution. The proof of this result is constructive; it is essentially a formalization of the solution technique applied to examples 9.1 and 9.3. The one-stage solution can be applied inductively (backwards in time from finite terminal time N) to solve (9.1) - (9.16) at each time stage.

The one-stage solution result is as follows:

Proposition 9.1:

Consider a noisy JLPC problem as in (9.1) - (9.16). If at time $k = \ell + 1$ the following three statements are true for each $r_{\ell+1} = j \in \underline{M}$, then they are also true at time $k = \ell$ for each $r_\ell = j \in \underline{M}$.

(i) $V_k(x_k, r_k=j)$ consists of $m_k(j)$ pieces joined continuously at

$$\{\delta_k^j(1) < \delta_k^j(2) < \ldots < \delta_k^j(m_k(j)-1)\} :$$

$$V_k(x_k, r_k=j) = V_k^j(x_k;t) \quad \text{for } \delta_k^j(t-1) < x_k < \delta_k^j(t)$$

$$t = 1, \ldots, m_k(j) \tag{9.88}$$

(here $\delta_k^j(0) \triangleq -\infty$, $\delta_k^j(m(j)) \triangleq \infty$).

(ii) Over its domain $(\delta_k^j(t-1), \delta_k^j(t))$, each piece $V_k^j(x_k;t)$ is twice continuously differentiable in x_k, with either

$$-\frac{\partial^2 V_k^j(x_k;t)}{(\partial x_k)^2} > 0$$

or

$$\frac{\partial^2 V_k^j(x_k;t)}{(\partial x_k)^2} < 0 \tag{9.89}$$

or

$$\frac{\partial^2 V_k^j(x_k;t)}{(\partial x_k)^2} = 0$$

throughout $\delta_k^j(t-1) < x_k < \delta_k^j(t)$.

That is, over each piece $V_k(x_k, r_k=j)$ is either everywhere convex or everywhere concave.

(iii) At each joining point $\delta_k^j(t)$ $(t=1,\ldots,m_k(j)-1)$ either

$$\frac{\partial V_k(x_k, r_k=j)}{\partial x_k} \quad \text{is continuous}$$

or it decreases discontinuously. □

This proposition is a generalization of the JLPQ and JLQ one step solutions (Propositions 5.1 and 8.1). If we think of the x-operating cost at time k = N as the sum of $Q(x_N; r_N)$ and $Q_T(x_N; r_N)$ (and thus think of $V_N(x_N, r_N) = 0$), then conditions (i) - (iv) are met at k = N. This proposition can then be applied inductively to solve (9.1) - (9.16) at each time stage.

Proof of Proposition 9.1:

This proposition is proven in a constructive manner, similar to the proofs of Proposition 5.1 (JLQ one step solution) and Proposition 8.1 (JLPQ one step solution). We will sketch the proof here; details appear in appendix D,4.

For each form $r_k = j \in \underline{M}$ the minimization in (9.17) is converted into the comparison of a finite set of constrained in z_{k+1} sub-problems, where 2_{k+1} is as defined in (9.50) - (9.53). These are then solved and compared at each x_k to obtain $V_k(x_k, r_k=j)$. This is done via the following steps:

STEP 1: Obtain a composite partition of x_{k+1} values from the partitions associated with the x-costs, $Q(x_{k+1}, r_{k+1}=i)$, the form transition probabilities $p(j,i:x_{k+1})$ and the expected costs-to-go $V_{k+1}(x_{k+1}, r_{k+1}=i)$ for each $i \in C_j$.

This x_{k+1} partition

$$\{\Delta^j_{k+1}(t) = (\gamma^j_{k+1}(t-1),\ \gamma^j_{k+1}(t) \quad : \quad t=1,\ldots,\psi^j_{k+1}\}$$

is obtained as described in section 9.3 (in (9.22) - (9.24)). This step is the same as for the noiseless JLPQ problems of chapter 8.

STEP 2: Obtaining $\hat{V}_{k+1}(x_{k+1}|r_k=j)$.

For each x_{k+1} interval, Δ^j_{k+1}, compute the conditional expected cost-to-go $\hat{V}_{k+1}(x_{k+1}|r_k=j)$ by

$$\hat{V}^j_{k+1}(x_{k+1};t) = \sum_{i \in C_j} p(j,i:x_{k+1}) \left[\begin{array}{l} V_{k+1}(x_{k+1}, r_{k+1}=i) \\ \quad + \\ Q(x_{k+1}, r_{k+1}=i) \end{array} \right], \tag{9.90}$$

obtaining

$$\hat{V}_{k+1}(x_{k+1}|r_k=j) = \hat{V}^j_{k+1}(x_{k+1};t) \qquad \begin{array}{l} \text{for } x_{k+1} \in \Delta^j_{k+1}(t) \\ t=1,\ldots,\psi^j_{k+1} - 1 \end{array} . \tag{9.91}$$

Since $p(j,i:x_{k+1})$, $V_{k+1}(x_{k+1}, r_{k+1}=i)$ and $Q(x_{k+1}, r_{k+1}=i)$ are each twice continuously differentiable in x_{k+1} except at a finite number of points (for each $i \in C_j$),

$\hat{V}_{k+1}(x_{k+1}|r_k=j)$ is also twice continuously differentiable except at finitely many points. Each piece $\hat{V}^j_{k+1}(x_{k+1};t)$ is twice continuously differentiable in x_{k+1} over $\Delta^j_{k+1}(t)$.

STEP 3: Obtaining $\hat{\hat{V}}_{k+1}(z_{k+1}|r_k=j)$ and a partition of z_{k+1} values:

We now have

$$V_k(x_k,r_k=j) = \min_{u_k} \{u_k^2 R(j) + E\{V_{k+1}(x_{k+1}|r_k=j)\}\}, \tag{9.92}$$

We seek to reformulate (9.92) as

$$V_k(x_k,r_k=j) = \min_{t=1,..,\hat{\psi}^j_{k+1}} \{V_k(x_k,r_k=j|t)\} \tag{9.93}$$

where

$$V_k(x_k,r_k=j|t) \triangleq V_k(x_k,r_k=j|z_{k+1} \in \hat{\Delta}^j_{k+1}(t))$$

$$= \min_{\substack{u_k \text{ s.t.} \\ z_{k+1} \in \hat{\Delta}^j_{k+1}(t)}} \{u_k^2 R(j) + \hat{\hat{V}}_{k+1}(z_{k+1}|r_k=j)\} \tag{9.94}$$

and

$$z_{k+1} = a(r_k)x_k + b(r_k)u_k = x_{k+1} - \Xi(r_k)V_k \quad . \tag{9.95}$$

Here

$$\hat{\hat{V}}_{k+1}(z_{k+1}|r_k=j) \triangleq E\left\{\hat{V}_{k+1}(x_{k+1}|r_k=j) \;\middle|\; \begin{matrix} r_k = j, \\ x_k,\ u_k \end{matrix}\right\} \quad . \tag{9.96}$$

We claim that the z-conditional cost $\hat{\hat{V}}_{k+1}(z_{k+1}|r_k=j)$ has a piecewise structure in z_{k+1}.

Specifically,

$$\hat{\hat{V}}_{k+1}(z_{k+1}|r_k=j) = \hat{\hat{V}}^j_{k+1}(z_{k+1};t) \qquad \text{for } z_{k+1} \in \hat{\Delta}^j_{k+1}(t)$$
$$(t = 1, \ldots, \hat{\psi}^j_{k+1}) \qquad (9.97)$$

where the z_{k+1} intervals in (9.94), (9.97) are

$$\hat{\Delta}^j_{k+1}(t) = (\hat{\gamma}^j_{k+1}(t-1),\ \hat{\gamma}^j_{k+1}(t)) \ ,$$

forming a partition of the real line with

$$-\infty \triangleq \hat{\gamma}^j_{k+1}(0) < \hat{\gamma}^j_{k+1}(1) < \ldots < \hat{\gamma}^j_{k+1}(\hat{\psi}^j_{k+1}-1) < \hat{\gamma}^j_{k+1}(\hat{\psi}^j_{k+1}) \triangleq \infty \ . \qquad (9.98)$$

We can express the z-conditional cost in (9.96) as

$$\hat{\hat{V}}_{k+1}(z_{k+1}|r_k=j) = \int_{-\infty}^{\infty} p(v)\ \hat{V}_{k+1}(z_{k+1} + \Xi(j)v|r_k=j)dv \ . \qquad (9.99)$$

Recall from section 9.2 that the noise density p(v) has a piecewise structure with $\bar{\sigma}$ pieces. We can rewrite (9.99) to reflect this:

$$\hat{\hat{V}}_{k+1}(z_{k+1}|r_k=j) = \sum_{s=1}^{\bar{\sigma}} \int_{\sigma(s-1)}^{\sigma(s)} \omega(v_k;s)\ \hat{V}_{k+1}(z_{k+1} + \Xi(j)v|r_k=j)dv. \qquad (9.100)$$

Incorporating the piecewise-structure of $\hat{V}_{k+1}(x_{k+1}|r_k=j)$ in (9.100) we have

$$\hat{\hat{V}}_{k+1}(z_{k+1}|r_k=j) = \sum_{s=1}^{\bar{\sigma}} \left\{ \begin{array}{l} \int_{\sigma(s-1)}^{\max[\sigma(s-1),\min[\gamma^j_{k+1}(1)-z_{k+1},\sigma(s)]]} \omega(v;s)\hat{V}^j_{k+1}(z_{k+1}+v;1)\,dv \\ + \sum_{t=2}^{\psi^j_{k+1}-1} \int_{\min[\sigma(s),\max[\gamma^j_{k+1}(t-1)-z_{k+1},\sigma(s-1)]]}^{\max[\sigma(s-1),\min[\gamma^j_{k+1}(t)-z_{k+1},\sigma(s)]]} \omega(v;s)\,\hat{V}^j_{k+1}(z_{k+1}+v;t)\,dv \\ + \int_{\min[\sigma(s),\max[\gamma^j_{k+1}(\psi^j_{k+1}-1)-z_{k+1},\sigma(s-1)]]}^{\sigma(s)} \omega(v;s)\,\hat{V}^j_{k+1}(z_{k+1}+v;\psi^j_{k+1})\,dv \end{array} \right\}. \quad (9.101)$$

From (9.101) we see that for each value of z_{k+1}, the z-conditional cost is a sum of

$$\bar{\sigma}\ \psi^j_{k+1}$$

integrals. The numerical values of the limits of integration in (9.101) depends upon the value of z_{k+1}. This gives $\hat{\hat{V}}_{k+1}(z_{k+1}|r_k=j)$ a piecewise structure in z_{k+1} :

> We have a z_{k+1} partition boundary, $\hat{\gamma}^j_{k+1}(t)$, at each z_{k+1} value where one (or more) of the limits of integration in (9.101) changes.

Since $\omega(v;s)$ is twice continuously differentiable in v for each s over $(\sigma(s-1), \sigma(s))$ and each $\hat{V}^j_{k+1}(x_{k+1};1)$ is twice continuously differentiable (in $x_{k+1} = z_{k+1} + v$) over

$(\gamma^j_{k+1}(t-1),\ \gamma^j_{k+1}(t))$, it follows from (9.101) that each z-conditional cost piece $\hat{\hat{V}}^j_{k+1}(z_{k+1};t)$ is twice continuously differentiable (with respect to z_{k+1}) over its domain.

In order to satisfy (iii) of Proposition 9.1 (i.e., (9.89) and for reasons we will discuss later, it is desirable to have additional grid points in the z_{k+1} partition: We also have a z_{k+1} partition boundary $\hat{\gamma}^j_{k+1}(t)$, at each z_{k+1} value where the quantity

$$\frac{\partial^2 V^j_{k+1}(z_{k+1}|r_k=j)}{(\partial z_{k+1})^2} + \frac{2R(j)}{b^2(j)} \qquad (9.102)$$

changes sign, becomes zero or ceases to be zero and we have a z_{k+1} partition boundary at each z_{k+1} value where the quantity

$$\frac{\partial^2 V^j_{k+1}(z_{k+1}\ r_k=j)}{\partial(\ z_{k+1})^2}$$

changes sign. Consequently over each z_{k+1} interval $\hat{\Delta}^j_{k+1}(t) = (\hat{\gamma}^j_{k+1}(t-1),\ \hat{\gamma}^j_{k+1}(t))$ the z-conditional cost piece $\hat{\hat{V}}^j_{k+1}(z_{k+1};t)$ is twice continuously differentiable in z_{k+1}, and it is everywhere convex or concave over $\hat{\Delta}^j_{k+1}(t)$.

STEP 4: Solving the constrained-in-z_{k+1} subproblems:

Having formulated the $\hat{\psi}^j_{k+1}$ constrained-in-z_k subproblems we must now solve them. Sustituting the definition of z_{k+1} of (9.95) into (9.94), these constrained subproblems become

$$V_k(x_k, r_k=j \mid t) = \min_{z_{k+1} \in \hat{\Delta}^j_{k+1}(t)} \left\{ \begin{array}{l} \dfrac{z^2_{k+1}\, R(j)}{b^2(j)} - \dfrac{2a(j)\, z_{k+1}\, x_k\, R(j)}{b^2(j)} \\ + \dfrac{a^2(j)\, x^2_{k+1}\, R(j)}{b^2(j)} + \hat{\hat{V}}^j_{k+1}(z_{k+1};t) \end{array} \right\}$$

(for $t=1,\ldots,\hat{\psi}^j_{k+1}$) . (9.103)

We can solve each subproblem analytically, using the basic approach that was followed in example 9.3.

The endpiece problems (i.e., $t=1$ and $t=\hat{\psi}^j_{k+1}$) will have two-piece optimal expected costs:

$$V_k(x_k, r_k=j \mid 1) = \begin{cases} V^{1,U}_k(x_k, j) & \text{if } a(j)\, x_k \leq \Theta^j_k(1) \\ V^{1,R}_k(x_k, j) & \text{if } a(j)\, x_k \geq \Theta^j_k(1) \end{cases} \quad (9.104)$$

$$V_k(x_{k+1}, r_k=j \mid \hat{\psi}^j_{k+1}) = \begin{cases} V^{\hat{\psi}^j_{k+1},L}_k(x_k, j) & \text{if } a(j)\, x_k \leq \theta^j_k(\hat{\psi}^j_{k+1}) \\ V^{\hat{\psi}^j_{k+1},U}_k(x_k, j) & \text{if } \theta^j_k(\hat{\psi}^j_{k+1}) \leq a(j)\, x_k \end{cases} , \quad (9.105)$$

The other subproblems in (9.103) will have either a three-piece solution structure:

$$V_k(x_k, r_k=j \mid t) = \begin{cases} V^{t,L}_k(x_k, j) & \text{if } a(j)\, x_k \leq \theta^j_k(t) \\ V^{t,U}_k(x_k, j) & \text{if } \theta^j_k(t) \leq a(j) x_k \leq \Theta^j_k(t) \\ V^{t,R}_k(x_k, j) & \text{if } \Theta^j_k(t) \leq a(j)\, x_k . \end{cases} \quad (9.106)$$

with

$$\theta^j_k(t) < \Theta^j_k(t)$$

or they will have a two-piece solution structure

$$V_k(x_k, r_k=j \mid t) = \begin{cases} V_k^{t,L}(x_k,j) & \text{if } a(j)\ x_k \leq \theta_k^j(t) = \Theta_k^j(t) \\ V_k^{t,R}(x_k,j) & \text{if } a(j)\ x_k \geq \theta_k^j(t) = \Theta_k^j(t) \end{cases} . \tag{9.107}$$

As in chapters 5 and 8, the superscripts L,R and U correspond, respectively, to driving x_{k+1} to the left endpoint, the right-endpoint, or the interior of the region

$$\hat{\Delta}_{k+1}^j(t) = (\hat{\gamma}_{k+1}^j(t-1), \hat{\gamma}_{k+1}^j(t)) .$$

As we indicated in the solution of example 9.3, the actively-constrained costs $V_k^{t,L}(x_k,j)$ and $V_k^{t,R}(x_k,j)$ are quadratic in x_k. Direct substitution in (9.103) yields the formulas

$$V_k^{t,L}(x_k,j) = \left(\frac{a^2(j)\ R(j)}{b^2(j)}\right) x_k^2 - \left(\frac{2a(j)\ R(j)\ \hat{\gamma}_{k+1}^j(t-1)}{b^2(j)}\right) x_k + \left[\frac{\hat{\gamma}_{k+1}^2(t-1)}{b^2(j)}\ R(j) + \hat{\hat{V}}_{k+1}^j(z_{k+1};t)\Big|_{z_{k+1}=\gamma_{k+1}^j(t-1)}\right] \tag{9.108}$$

$$\text{for } t = 2,\ldots,\hat{\psi}_{k+1}^j$$

and

$$V_k^{t,R}(x_k,j) = \left(\frac{a^2(j)R(j)}{b^2(j)}\right) x_k^2 - \left(\frac{2a(j)\ R(j)\ \hat{\gamma}_{k+1}^j(t)}{b^2(j)}\right) x_k + \left[\frac{\hat{\gamma}_{k+1}^2(t)\ R(j)}{b^2(j)} + \hat{\hat{V}}_{k+1}^j(z_{k+1};t)\Big|_{z_{k+1}=\hat{\gamma}_{k+1}^j(t)}\right] \tag{9.109}$$

$$t=1,\ldots,\hat{\psi}_{k+1}^j - 1 .$$

The cost functions $V_k^{t,U}(x_k i))$ in (9.106) are not piecewise-quadratic in x_k, in general, as we saw in example 9.3. Recall that we are considering (9.103) as an optimization over z_{k+1}. The inactive-constraint solution $z_{k+1}^{t,U}$ to (9.103) (if one exists) is a z_{k+1} value <u>in the interior</u> of $\hat{\Delta}_{k+1}^{j}(t)$ that satisfies

$$0 = \frac{\partial V_k(x_k, r_k=j|t)}{\partial z_{k+1}} = \frac{2\,R(j)}{b^2(j)}\,z_{k+1} - \frac{2\,a(j)\,R(j)\,x_k}{b^2(j)} + \frac{\partial \hat{\hat{V}}_{k+1}^{j}(z_{k+1};t)}{\partial z_{k+1}} \tag{9.110}$$

with

$$0 < \frac{\partial^2 V_k(x_k, r_k=j|\,t)}{(\partial z_{k+1})^2}\Bigg|_{z_{k+1}=z_{K+1}^{t,U}} = \frac{2\,R(j)}{b^2(j)} + \frac{\partial^2 \hat{\hat{V}}_{k+1}^{j}(z_{k+1}:t)}{(\partial z_{k+1})^2}\,, \tag{9.111}$$

By making each $\hat{\hat{V}}_{k+1}^{j}(z_{k+1};t)$ piece either concave or convex over its domain (by adding "extra" points to the z_{k+1} partition), where necessary, we have insured that there is, at most, one value of $z_{k+1}^{t,U}$ in the interval $\hat{\Delta}_{k+1}^{j}(t)$. It also insures that the cost function $V_k^{t,U}(x_k,j)$ is everywhere convex or everywhere concave over $(\theta_k^j(t),\ \Theta_k^j(t))$ in (9.106); this is needed to obtain (iii) of Proposition 9.1 (i.e., (9.89)).

A procedure for solving each of the $\hat{\psi}_{k+1}^{j}$ subproblems in (9.103) is described in Appendix D4.

The $V_k^{t,L}(x_k,j)$, $V_k^{t,U}(x_k,j)$ and $V_k^{t,R}(x_k,j)$ in (9.104) - (9.107) possess similar properties at $\theta_k^j(t)$ and $\Theta_k^j(t)$ to the analogous quantities in chapters 5 and 8. In particular, we have the following:

- when (9.105) or (9.106) applies, at $x_k = \theta_k^j(t)/a(j)$ the slopes and values of $V_k^{t,L}(x_k,j)$ and $V_k^{t,U}(x_k,j)$ are the same,

- when (9.104) or (9.106) applies, at $x_k = \Theta_k^j(t)/a(j)$ the slopes and values of $V_k^{t,R}(x_k,j)$ and $V_k^{t,U}(x_k,j)$ are the same,

- when (9.107) applies (i.e., there is no $V_k^{t,U}$) then at $x_k = \theta_k^j(t)/a(j) = \Theta_k^j(t)/a(j)$, the value of $V_k^{t,R}(x_k,j)$ and $V_k^{t,L}(x_k,j)$ are the same but

$$\left.\frac{\partial V_k^{t,L}(x_k,j)}{\partial x_k}\right|_{x_k = \frac{\theta_k^j(t)}{a(j)} = \frac{\Theta_k^j(t)}{a(j)}} > \left.\frac{\partial V_k^{t,R}(x_k,j)}{\partial x_k}\right|_{x_k = \frac{\theta_k^j(t)}{a(j)} = \frac{\Theta_k^j(t)}{a(j)}} . \tag{9.112}$$

STEP 5: Comparing the Constrained Costs:

The fifth step in this proof of Proposition 9.1 is to compare the solutions of the $\hat{\psi}_{k+1}^j$ constrained problems specified by (9.103), as indicated in (9.93). This minimization involves the comparison of piecewise functions in x_k (with structures as given in (9.104) - (9.107)). Since these function pieces are not all quadratic in x_k, this comparson is much more difficult (in general) than for the JLQ and JLPQ problems. We choose $V_k(x_k,r_k=j)$ at each x_k value to be the candidate function in (9.93) having the least value. Thus $V_k(x_k,r_k=j)$ has the piecewise

structure described by (i) of the Proposition. As we mentioned earlier, we partitioned the axis of z_k values so that (ii) of the Proposition is satisfied by each $V_k^{t,U}(x_k,j)$ (and for each $V_k^{t,L}(x_k,j)$, $V_k^{t,R}(x_k,j)$ we see from (9.108) - (9.109) that (ii) is satisfied).

The fact that $\frac{\partial V_k(x_k,r_k=j)}{\partial x_k}$ is either continuous or decreases discontinuously follows directly from the comparison in (9.93). A joining point $\delta_k^j(\ell)$ can arise either from a <u>crossing</u> of candidates (here the slope decreases discontinuously), or from a change between parts of a subproblem solution $V_k(x_k,r_k=j|t)$ (i.e., from $v_k^{t,L}$ to $V_k^{t,U}$ in (9.105), (9.106), or from $V_k^{t,L}$ to $V_k^{t,R}$ in (9.107), or from $V_k^{t,U}$ to $V_k^{t,R}$ in (9.104), (9.105); in these cases the slope of $V_k(x_k,r_k=j)$ is continuous or it decreases discontinuously at $\delta_k^j(\ell)$.

□

This concludes the proof of the one-stage solution given by Proposition 9.1.

9.6 Qualitative Properties of the Optimal JLPC Controller

In this section we examine several qualitative issues related to the (off-line) determination of the optimal control laws and costs of Proposition 9.1. The results of this examination are used in the next section to devise an algorithm for the efficient computation of the optimal controller.

We begin with a description of the subproblem solution in (9.94) - (9.97). Some of the properties that are listed in the following proposition were mentioned in the preceding section.

Proposition 9.2: Consider the constrained subproblem of finding u_k satisfying

$$V_k(x_k, r_k=j \mid t) = \min_{\substack{u_k \text{ s.t} \\ z_{k+1} \in \hat{\Delta}^j_{k+1}(t)}} \{u_k^2 R(j) + \hat{\hat{V}}^j_{k+1}(z_{k+1};t)\} \tag{9.113}$$

s.t.

$$z_{k+1} = a(j)\, x_k + b(j)\, u_k \tag{9.114}$$

$$\hat{\Delta}^j_{k+1}(t) = (\hat{\gamma}^j_{k+1}(t-1)\ ,\ \hat{\gamma}^j_{k+1}(t))$$

$$R(j) > 0 \qquad a(j) \neq 0 \qquad b(j) \neq 0 \qquad \bullet$$

The subproblem solutions possess the following properties:

1. For $t = 2,\ldots, \hat{\psi}^j_{k+1}$:

if $a(j)\, x_k < \theta^j_k(t)$ then the minimizing u_k in (9.113) is given by the control law

$$u_k = u_k^{t,L}\,(x_k, r_k=j) = \frac{\hat{\gamma}_{k+1}(t-1) - a(j)x_k}{b(j)} \tag{9.115}$$

with the resulting z_{k+1} value

$$z_{k+1} = z_{k+1}^{t,L}\,(x_k, r_k=j) = [\hat{\gamma}^j_{k+1}(t-1)]^+ \tag{9.116}$$

and

$$V_k = V_k^{t,L}(x_k, r_k=j) = \left(\frac{\hat{\gamma}_{k+1}(t-1) - a(j)x_k}{b(j)}\right)^2 R(j) + \hat{\hat{V}}^j_{k+1}\left([\hat{\gamma}^j_{k+1}(t-1)]^+; t\right), \tag{9.117}$$

which is quadratic in x_k.

2. For $t = 1,\ldots, \hat{\psi}^j_{k+1} - 1$:

if $a(j)x_k > \theta^j_k(t)$ then the minimizing u_k in (9.113) is given by the control law

$$u_k = u_k^{t,R}(x_k, j) = \frac{\hat{\gamma}^j_{k+1}(t) - a(j)x_k}{b(j)} \tag{9.118}$$

with the resulting z_{k+1} value

$$z_{k+1} = z_{k+1}^{t,R}(x_k, r_k=j) = [\hat{\gamma}^j_{k+1}(t)]^- \tag{9.119}$$

and

$$V_k = V_k^{t,R}(x_k, j) = \left(\frac{\hat{\gamma}_{k+1}(t) - a(j)x_k}{b(j)}\right)^2 R(j) + \hat{\hat{V}}^j_{k+1}\left([\hat{\gamma}^j_{k+1}(t)]^-; t\right), \tag{9.120}$$

which is quadratic in x_k.

3. For $t = 2,\ldots,\hat{\psi}^j_{k+1} - 1$,

if

$$\frac{\partial^2 \hat{V}^j_{k+1}(z_{k+1};t)}{(\partial z_{k+1})^2} + \frac{2R(j)}{b^2(j)} \leq 0 \tag{9.121}$$

for all $z_{k+1} \in \hat{\Delta}^j_{k+1}(t)$ then

$$\text{(i)}\quad \theta^j_k(t) = \Theta^j_k(t) = \frac{1}{2}\left[\hat{\gamma}^j_{k+1}(t-1) + \hat{\gamma}^j_{k+1}(t) + \frac{b^2(j)}{R(j)}\left[\hat{V}^j_{k+1}([\hat{\gamma}^j_{k+1}(t-1)]^+;t) - \hat{V}^j_{k+1}([\hat{\gamma}^j_{k+1}(t)]^-;t)\right]\right] \tag{9.122}$$

$$\text{(ii) At}\quad x_k = \frac{\theta^j_k(t)}{a(j)} = \frac{\Theta^j_k(t)}{a(j)}\ ,$$

$$V^{t,R}_k(x_k,j)\Big|_{x_k = \frac{\theta^j_k(t)}{a(j)}} = V^{t,L}_k(x_k,j)\Big|_{x_k = \frac{\theta^j_k(t)}{a(j)}} \tag{9.123}$$

and

$$\frac{\partial V^{t,R}_k(x_k,j)}{\partial x_k}\Big|_{x_k = \frac{\theta^j_k(t)}{a(j)}} = \frac{2a(j)R(j)}{b^2(j)}\left[\theta^j_k(t) - \hat{\gamma}^j_{k+1}(t-1)\right] <$$

$$< \frac{2a(j)R(j)}{b^2(j)}\left[\theta^j_k(t) - \hat{\gamma}^j_{k+1}(t)\right] = \frac{\partial V^{t,L}_k(x_k,j)}{\partial x_k}\Big|_{x_k = \frac{\theta^j_k(t)}{a(j)}} \tag{9.124}$$

4. For $t = 1,\ldots, \hat{\psi}^j_{k+1}$, if

$$\frac{\partial^2 \hat{V}^j_{k+1}(z_{k+1};t)}{(\partial z_{k+1})^2} + \frac{2R(j)}{b^2(j)} > 0 \qquad (9.125)$$

for all $z_{k+1} \in \hat{\Delta}^j_{k+1}(t)$ then

(i) for $\theta^j_k(t) < a(j)x_k < \Theta^j_k(t)$ the minimizing u_k in (9.113) is given by the control law

$$u_k = u^{t,U}_k(x_k,j) = \frac{-b(j)}{2R(j)} \left.\frac{\partial \hat{V}^j_{k+1}(z\ ;t)}{\partial z}\right|_{z\ =\ z^{t,U}_{k+1}(x_k,j)} \qquad (9.126)$$

with

$$z_{k+1} = z^{t,U}_{k+1}(x_k,j) = a(j)x_k \frac{-b^2(j)}{2R(j)} \left.\frac{\partial \hat{V}^j_{k+1}(z\ ;t)}{\partial z}\right|_{z=\ z^{t,U}_{k+1}(x_k,j)}$$

(9.127)

and

$$V_k = V_k^{t,U}(z_k,j) = \frac{b^2(j)}{4R(j)} \left[\left. \frac{\partial \hat{\hat{V}}_{k+1}^{j}(z:t)}{\partial z} \right|_{z = z_{k+1}^{t,U}(x_k,j)} \right]^2 +$$

$$+ \left. \hat{\hat{V}}_{k+1}^{j}(z:t) \right|_{z = z_{k+1}^{t,U}(x_k,j)} \qquad (9.128)$$

(ii) Here

$$\theta_k^j(t) = \hat{\gamma}_{k+1}^j(t-1) + \frac{b^2(j)}{2R(j)} \left. \frac{\partial \hat{\hat{V}}_{k+1}^j(z;t)}{\partial z} \right|_{z = [\hat{\gamma}_{k+1}^j(t-1)]^+} \tag{9.129}$$

$$\Theta_k^j(t) = \hat{\gamma}_{k+1}^j(t) + \frac{b^2(j)}{2R(j)} \left. \frac{\partial \hat{\hat{V}}_{k+1}^j(z;t)}{\partial z} \right|_{z = [\hat{\gamma}_{k+1}^j(t)]^-} , \tag{9.130}$$

and

$$\theta_k^j(t) < \Theta_k^j(t) \tag{9.131}$$

For $t = 1$ and $t = \hat{\psi}_{k+1}^j$, (9.125) is always true (and $\theta_k^j(1) \triangleq -\infty$, $\Theta_k^j(\hat{\psi}_k^j) \triangleq +\infty$).

(iii) For $t = 1, \ldots, \hat{\psi}_{k+1}^j - 1$:

$$\left. V_k^{t,R}(x_k,j) \right|_{x_k = \frac{\Theta_k^j(t)}{a(j)}} = \left. V_k^{t,U}(x_k,j) \right|_{x_k = \frac{\Theta_k^j(t)}{a(j)}} \tag{9.132}$$

$$\left. \frac{\partial V_k^{t,R}(x_k,j)}{\partial x_k} \right|_{x_k = \frac{\Theta_k^j(t)}{a(j)}} = \left. \frac{\partial V_k^{t,U}(x_k,j)}{\partial x_k} \right|_{x_k = \frac{\Theta_k^j(t)}{a(j)}} \tag{9.133}$$

(iv) For $t = 2,\ldots, \hat{\psi}^j_{k=1}$:

$$V_k^{t,U}(x_k,j)\Big|_{x_k = \frac{\theta_k^j(t)}{a(j)}} = V_k^{t,L}(x_k,j)\Big|_{x_k = \frac{\theta_k^j(t)}{a(j)}} \tag{9.134}$$

$$\frac{\partial V_k^{t,U}(x_k,j)}{\partial x_k}\Big|_{x_k = \frac{\theta_k^j(t)}{a(j)}} = \frac{\partial V_k^{t,L}(x_k,j)}{\partial x_k}\Big|_{x_k = \frac{\theta_k^j(t)}{a(j)}} \tag{9.135}$$

(v) • If

$$\frac{\partial^2 \hat{V}^j_{k+1}(z_{k+1};t)}{(\partial z_{k+1})^2} > 0 \quad \text{for all } z_{k+1} \in \hat{\Delta}^j_{k+1}(t) \tag{9.136}$$

then

$$\frac{\partial^2 V_k^{t,U}(x_k,j)}{(\partial x_k)^2} > 0 \quad \text{for all } \theta_k^j(t) < a(j)x_k < \Theta_k^j(t) \,. \tag{9.137}$$

• If

$$\frac{\partial^2 \hat{V}^j_{k+1}(z_{k+1};t)}{(\partial z_{k+1})^2} = 0 \text{ for all } z_{k+1} \in \hat{\Delta}^j_{k+1}(t) \tag{9.138}$$

then

$$\frac{\partial^2 V_k^{t,U}(x_k,j)}{(\partial x_k)^2} = 0 \quad \text{for all } \theta_k^j(t) < a(j)x_k < \Theta_k^j(t) \,. \tag{9.139}$$

- If

$$\frac{\partial^2 \hat{V}^j_{k+1}(z_{k+1};t)}{(\partial z_{k+1})^2} < 0 \quad \text{for all } z_{k+1} \in \hat{\Delta}^j_{k+1}(t) \tag{9.140}$$

then

$$\frac{\partial^2 V^{t,U}_k(x_k,j)}{(\partial x_k)^2} < 0 \quad \text{for all } \theta^j_k(t) < a(j)x_k < \Theta^j_k(t) . \tag{9.141}$$

- For the extreme cases t = 1 and t = $\hat{\psi}^j_{k+1}$, either (9.136) - (9.137) or (9.138) - (9.139) applies. □

This proposition is proved in appendix D.5. It says that each subsystem optimal cost $V_k(x_k,r_k=j|t)$ in (9.113) has a two or three part structure. Note that we have constructed the partition of z_{k+1} (i.e., the grid points $\{\hat{\gamma}^j_{k+1}(t)\}$) so that for each t, only one of the conditions (9.121), (9.136), (9.138) or (9.140) applies over the entire interval $\hat{\Delta}^j_{k+1}(t)$.

The unconstrained cost $V^{1,U}_k(x_k,r_k=j)$, which corresponds to driving z_{k+1} into the leftmost z_{k+1} interval, $\hat{\Delta}^j_{k+1}(1)$, has the two-part structure shown in figure 9.3(a). The actively constrained piece $V^{1,R}_k(x_k,j)$ is quadratic in x_k; the unconstrained piece $V^{1,U}_k(x_k,j)$ is, in general, not quadratic in x_k. The unconstrained cost $V^{\hat{\psi}^j_{k+1},U}_k(x_k,j)$, which corresponds to driving z_{k+1} into the

rightmost x_{k+1} interval, $\hat{\Delta}^j_{k+1}(\hat{\psi}^j_{k+1})$, also has a two-piece structure, as shown in figure 9.3(b). The unconstrained extreme pieces $V_k^{1,U}(x_k,r_k=j)$ and $V_k^{\hat{\psi}^j_{k+1},U}(x_k,j)$ each have nonnegative second derivatives over the regions of x_k values where they are valid.

For $t = 2, \hat{\psi}^j_{k+1}-1$, if (9.121) holds then $V_k(x_k,r_k=j|t)$ in (9.113) has a piecewise-quadratic (in x_k) structure with two pieces, as shown in figure 9.4(a). From (9.124) we see that at their joining point, the slope of this subproblem optimal cost decreases discontinuously.

For $t = 2,\ldots,\hat{\psi}^j_{k+1}-1$ with (9.125) holding, $V_k(x_k,r_k=j|t)$ has a three piece structure, as shown in figure 9.4(b). The actively constrained pieces $V_k^{t,L}(x_k,j)$ and $V_k^{t,R}(x_k,j)$ are each quadratic in x_k. The unconstrained piece $V_k^{t,U}(x_k,j)$ need not be quadratic. However from (9.137), (9.139), (9.141) we see that $V_k^{t,U}(x_k,j)$ is either convex or concave over its entire domain of validity (i.e. for all x_k values where $V_k(x_k,r_k=j|t) = V_k^{t,U}(x_k,j)$). At the joining points the slope of $V_k(x_k,r_k=j|t)$ is continuous.

From (9.126) - (9.127) we see that it may be quite difficult to determine the unconstrained control law $u_k^{t,U}(x_k,j)$. When $\hat{V}^j_{k+1}(z;t)$ is quadratic in z there is clearly no difficulty. But for other $\hat{V}^j_{k+1}(z;t)$ structures, (9.126) - (9.127) must be simultaneously solved to obtain $u_k^{t,U}(x_k,j)$ and $z_k^{t,U}(x_k,j)$. It is this difficulty that motivates the development of a

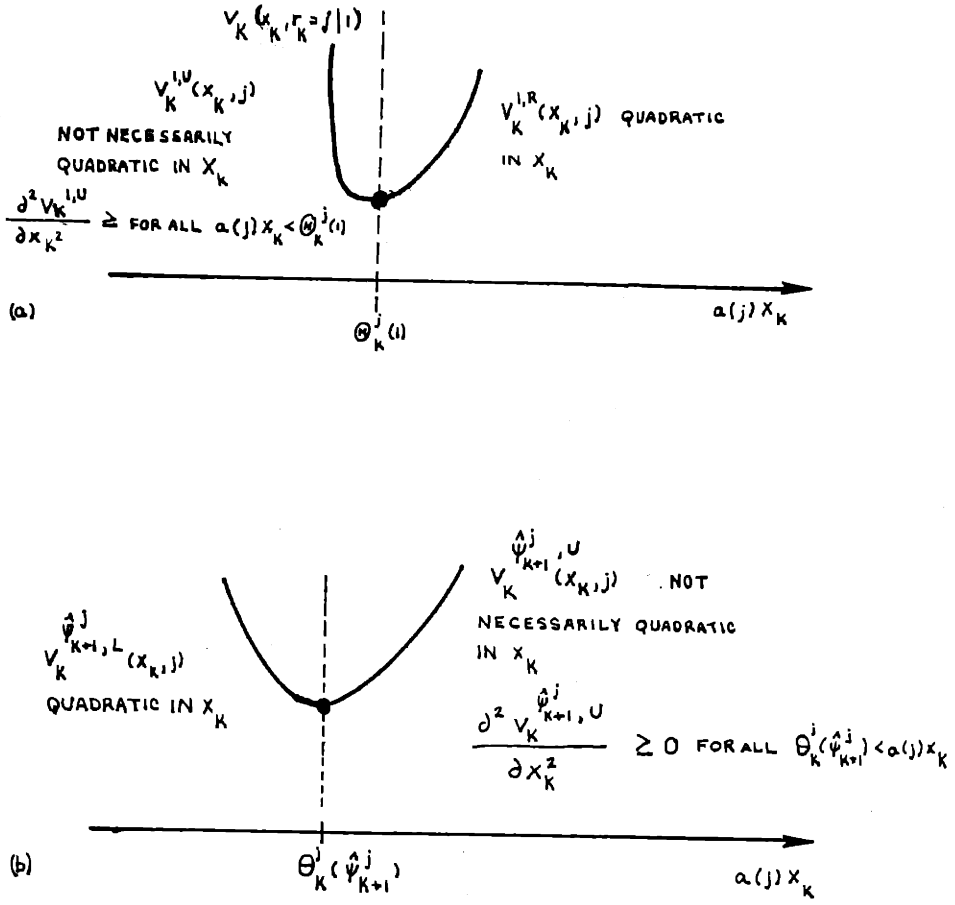

Figure 9.3: Constrained subproblem solutions for extreme pieces of the z_{k+1} partition; (a) $V_k(x_k, r_k = j \mid 1)$; (b) $V_k(x_k, r_k = j \mid \psi_{k+1}^j)$.

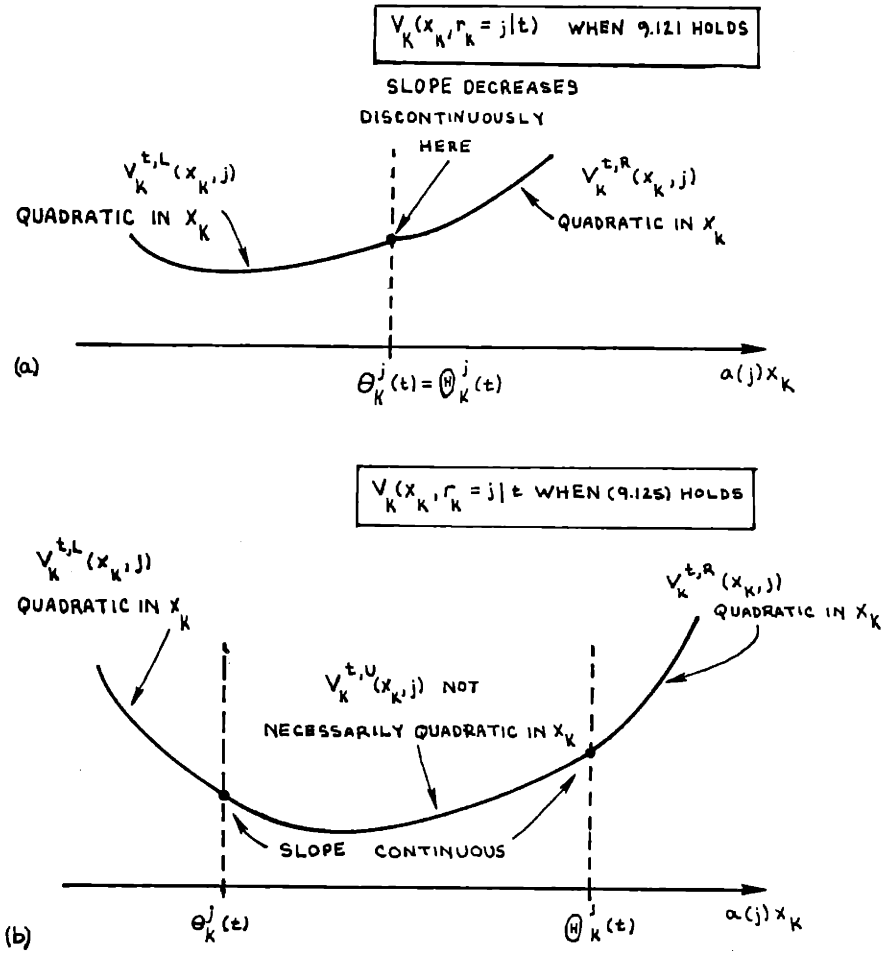

Figure 9.4: Constrained subproblems and optimal costs for $t = 2,\ldots,\psi_{k+1}^j - 1$ (a) when (9.121) holds and (b) when (9.125) holds.

suboptimal controller described later in this chapter.

We will next show that many of the candidate cost pieces in (9.104) - (9.107) cannot be optimal from any x_k; consequently they need not be calculated.

The following proposition eliminates many of the candidate costs in (9.92) from eligibility for the optimal cost.

Proposition 9.3: In performing the minimization in (9.92), the following candidate costs need not be examined:

(i) if

$$\frac{\partial^2 \hat{\hat{V}}^j_{k+1}(z_{k+1};t)}{(\partial x_{k+1})^2} + \frac{2R(j)}{b^2(j)} > 0$$

for all $z_{k+1} \in \hat{\Delta}^j_{k+1}(t)$

and

$$\frac{\partial^2 \hat{\hat{V}}^j_{k+1}(z_{k+1};t+1)}{(\partial z_{k+1})^2} + \frac{2R(j)}{b^2(j)} > 0$$

for all $z_{k+1} \in \hat{\Delta}^j_{k+1}(t+1)$

and $\hat{\hat{V}}_{k+1}(z_{k+1}|r_k=j)$ is continuous at $\hat{\gamma}^j_{k+1}(t)$ with

$$\left.\frac{\partial \hat{\hat{V}}^j_{k+1}(z_{k+1};t+1)}{\partial z_{k+1}}\right|_{z_{k+1}=\hat{\gamma}^j_{k+1}(t)} \leq \left.\frac{\partial \hat{\hat{V}}^j_{k+1}(z_{k+1};t)}{\partial z_{k+1}}\right|_{z_{k+1}=\hat{\gamma}^j_{k+1}(t)}$$

then we need not examine

$$V_k^{t,R}(x_k,j) \equiv V_k^{t+1,L}(x_k,j) \quad .$$

(ii) if for all $z_{k+1} \in \hat{\Delta}_{k+1}^j(t)$ we have

$$\frac{\partial^2 V_{k+1}^j(z_{k+1};t)}{(\partial z_{k+1})^2} + \frac{2R(j)}{b^2(j)} \leq 0$$

then $V_k^{t,U}(x_k,j)$ does not exist but we must examine $V_k^{t,R}(x_k,j)$ and $V_k^{t,L}(x_k,j)$.

(iii) if $\hat{\hat{V}}_{k+1}(z_{k+1}|r_k=j)$ is discontinuous at $z_{k+1} = \hat{\gamma}_{k+1}^j(t)$ with

$$\left.\hat{\hat{V}}_{k+1}(z_{k+1}|r_k=j)\right|_{z_{k+1}=[\hat{\gamma}_{k+1}^j(t)]^-} < \left.\hat{\hat{V}}_{k+1}(z_{k+1}|r_k=j)\right|_{z_{k+1}=[\hat{\gamma}_{k+1}^j(t)]^+}$$

then we need not examine $V_k^{t+1,L}(x_k,j)$.

(iv) if $\hat{\hat{V}}_{k+1}(z_{k+1}|r_k=j)$ is discontinuous at $z_{k+1} = \hat{\gamma}_{k+1}^j(t)$ with (9.141) reversed, then we need not examine $V_k^{t,R}(x_k,j)$.

This proposition is a generalization of Propositions 5.2 and 8.2. It is proved in appendix D.6. □

As we have seen in the examples of this chapter, the optimal controller hedges to certain values of the artificial variable z_{k+1}. The following corollary specifies necessary conditions for a point $z_{k+1} = z$ to which the system hedges.

Corollary 9.4:

If the optimal controller in Proposition 9.1 hedges from $(x_k, r_k=j)$ to the point $z_{k+1} = z$ then one (or more) of the following is true:

(1) z is a discontinuous point of the conditional cost $\hat{\hat{V}}_{k+1}(z_{k+1}|r_k=j)$,

or

(2) z is a boundary ($\hat{\gamma}^j_{k+1}(t)$ or $\hat{\gamma}^j_{k+1}(t-1)$ of an interval $\hat{\Delta}^j_{k+1}(t)$ over which the conditional cost $\hat{\hat{V}}_{k+1}(z_{k+1}|r_k=j)$ has

$$\frac{\partial^2 \hat{\hat{V}}^j_{k+1}(z_{k+1};t)}{(\partial z_{k+1})^2} + \frac{2R(j)}{b^2(j)} \leq 0 \tag{9.142}$$

or

(3) $z = \hat{\gamma}^j_{k+1}(t)$ is a boundary of intervals $\hat{\Delta}^j_k(t)$ and $\hat{\Delta}^j_{k+1}(t+1)$ where $\hat{\hat{V}}_{k+1}(z_{k+1}|r_k=j)$ is continuous and

$$\frac{\partial \hat{\hat{V}}^j_{k+1}(z;t+1)}{\partial x_{k+1}} - \frac{\partial \hat{\hat{V}}^j_{k+1}(z;t)}{\partial z_{k+1}} > 0 \tag{9.143}$$

Proof: Hedging-to-a-point can occur only to finite boundary points of the z_{k+1} intervals $\{\hat{\Delta}^j_{k+1}(t) : t=1,\ldots,\hat{\psi}^j_{k+1}\}$; that is, to an element of the set $\{\hat{\gamma}^j_{k+1}(t) : t=1,\ldots,\hat{\psi}^j_{k+1}-1\}$. When the optimal controller drives z_{k+1} to such a point from some x_k, then either $V_k^{t,R}$ or $V_k^{t+1,L}$ is the optimal cost from that x_k. Proposition 9.3 excludes many of these constrained candidate costs from elibility. Corollary 9.4 lists the possible ways that a constrained cost $V_k^{t,R}$ or $V_k^{t+1,L}$ associated with $\hat{\gamma}^j_{k+1}(t)$ can be eligible. Corollary 9.4(1) occurs when either Proposition 9.3(iii) or 9.3(iv) holds. Here we hedge to the low-cost side of a $\hat{V}_{k+1}(z_{k+1}|r_k=j)$ discontinuity. Corollary 9.4(2) occurs when Proposition 9.3(ii) holds. When (9.142) is true, $V_k^{t,U}$ is not eligible but both $V_k^{t,L}$ abd $V_k^{t,R}$ are eligible (unless excluded by Proposition 9.3(ii) or iv). Corollary 9.4(3) holds when the slope condition of Proposition 9.3(i) is not satisfied. □

Note that if one or more of the if one or more of the conditions of Corollary 9.4 is satisfied for some $z = \hat{\gamma}^j_{k+1}(t)$, we are not guaranteed that the optimal controller hedges to that z; the associated constrained costs $V_k^{t,R}$ and $V_k^{t+1,L}$ need not be optimal in (9.92).

For finite time horizon problems, if x_k is negative enough or positive enough, the optimal strategy will be to keep x in the same extreme piece of the form transition probabilities p(j,i:x)

and x-costs $Q(x,j)$, $Q_T(x,j)$, for all $i \in \mathbf{C}_j$; from each $j \in \underline{M}$, for all future times. The following proposition is a generalization of the JLQ endpiece result (Proposition 6.1) and the JLPQ endpiece result (Proposition 8.6).

Proposition 9.5: (JLPC endpieces)

(1) for $x_k < \delta_k^j(1)$ the optimal control laws and expected costs-to-go are

$$V_k(x_k, r_k=j) = V_k^{1,U}(x_k,j) \triangleq V_k^{Le}(x_k,j)$$

$$u_k(x_k, r_k=j) = u_k^{1,U}(x_k,j) \triangleq u_k^{Le}(x_k,j)$$

(2) for $x_k > \delta_k^j(m_k(j)-1)$ the optimal control laws and expected costs-to-go are

$$V_k(x_k, r_k=j) = V_k^{\hat{\psi}_{k+1}^j,U}(x_k,j) \triangleq V_k^{Re}(x_k,j)$$

$$u_k(x_k, r_k=j) = u_k^{\hat{\psi}_{k+1}^j,U}(x_k,j) \triangleq u_k^{Re}(x_k,j) .$$

Consequently

(3) $$\frac{\partial^2 V_k^{Le}(x_k,j)}{(\partial x_k)^2} \geq 0 \qquad \text{for all } x_k < \delta_k^j(1)$$

$$\frac{\partial^2 V_k^{Re}(x_k,j)}{(\partial x_k)^2} \geq 0 \qquad \text{for all } x_k > \delta_k^j(m_k(j) - 1),$$

□

Proof: (1) and (2) above are immediate generalizations of Propositions 6.1 and 8.6. Item (3) follows directly from Proposition 9.2(v). □

The following proposition lists a number of general qualitative properties of the optimal controller for the noisy JLPC problems of this chapter. This proposition is a generalization of Propositions 5.3 and 8.4.

Proposition 9.6: The optimal controller of Proposition 9.1 has the following properties:

(1) At each time k and in each form $j \in M$, between joining points $\{\delta_k^j(t) : t=1,\ldots,m_k(j)-1\}$ of $V_k(x_k, r_k=j)$:

$$u_k(x_k, r_k=j) = \frac{-b(j)}{2a(j)R(j)} \frac{\partial V_k(x_k, r_k=j)}{\partial x_k} \tag{9.144}$$

$$z_{k+1}(x_k, r_k=j) = a(j)x_k - \frac{b^2(j)}{2a(j)R(j)} \frac{\partial V_k(x_k, r_k=j)}{\partial x_k} \tag{9.145}$$

(here $a(j)R(j) \neq 0$, $b(j) \neq 0$).

(2) At those joining points δ where the slope of $V_k(x_k, r_k=j)$ does not change $\left(\text{ie., } \left.\frac{\partial V_k(x_k, r_k=j)}{\partial x_k}\right|_{x_k=\delta} \text{exists}\right)$,

$u_k(x_k, r_k=j)$ and $z_{k+1}(x_k, r_k=j)$ are continuous functions of x_k.

(3) At those joining points $\delta_k^j(t)$ where the slope of $V_k(x_k, r_k=j)$ decreases discontinuously

$$\left(\text{ie, } \left.\frac{\partial V_k(x_k, r_k=j)}{\partial x_k}\right|_{x_k=\delta^+} \qquad \left.\frac{\partial V_k(x_k, r_k=j)}{\partial x_k}\right|_{x_k=\delta^-} \right),$$

(i) $u_k(x_k, r_k=i)$ increases discontinuously at δ when $\frac{b(j)}{a(j)} > 0$ (and decreases discontinuously at δ when $\frac{b(j)}{a(j)} < 0$)

(ii) the mapping $x_k \longmapsto z_{k+1}(x_k, r_k=j)$ increases discontinuously at δ when $a(j) > 0$) (and decreases discontinuously at δ when $a(j) < 0$).

(4) The mapping

$$x_k \longmapsto z_{k+1}(x_k, r_k=j)$$

has the following properties:

(i) the mapping is monotonely nondecreasing if $a(j) > 0$ (and monotonely nonincreasing if $a(j) < 0$) for each $j \in \underline{M}$

(ii) it consists of $m_k(j)$ line segments:

one line segment with positive slope if $a(j) > 0$ (negative slope if $a(j) < 0$) for each x_k region where an "unconstrained cost" $V_k^{t,U}(x_k, r_k=1)$ is optimal

$$V_k(x_k, r_k=j) = V_k^{t,U}(x_k, r_k=j)$$

a <u>constant</u> line segment for each x_k region where there is active hedging-to-a-point:

$$z_{k+1} = \hat{\gamma}_{k+1}^{j}(t) \qquad t \in \{1, \ldots, \hat{\psi}_{k+1}^{j}\} \quad .$$

(iii) there are regions of z_{k+1} avoidance associated with (and only with) each $x_k = \delta$ value where the slope of $V_k(x_k, r_k=j)$ decreases discontinuously.

(5) Each candidate linear control law (associated with the costs listed in (9.92)) can be optimal over, at most, a single interval of x_k values. □

The proof of this proposition is presented in appendix D.7.

We have identified some basic qualitative properties of the JLPC problem that can be used to reduce the combinatories involved in the "brute-force" solution of the one-stage problem that was presented in the proof of Proposition 9.1. In the next section we will develop a solution algorithm that exploits these properties, enabling us to solve the general JLPC problem (9.1) - (9.16) efficiently.

9.7 An Algorithm for Obtaining the Optimal JLPC Controller

In this section we develop an algorithm for obtaining the optimal controller for general JLPC control problems (9.1) - (9.16). This algorithm is based upon the application of the one-stage solution of Proposition 9.1 recursively, backwards in time, for each $j \in \underline{M}$ that the system can take. The basic idea of the noisy JLPC problem solution algorithm here is the same as in the JLQ solution algorithm of section 7.2 and the JLPQ algorithm of section 8.5.

For each form $j \in \underline{M}$ at time k, we can compute $V_k(x_k, r_k=j)$ and $u_k(x_k, r_k=j)$ one piece at a time, sweeping from left to right along the axis of $a(j)x_k$ values.

The solution algorithm is presented in flowchart form and is described in detail. In principle it can be applied at successive time stages to solve any JLPC control problem of the type in section 9.2. However, since the optimal costs are not piecewise quadratic in x_k, the analytical steps specified by this algorithm may often be quite difficult to carry out.

An overview of the solution algorithm is shown in figure 9.5. The algorithm is initialized with the terminal time (k=N) cost parameter (block 2). Then for successively decreasing time through $k = k_o$ (block 13), the one-step solution of Proposition 9.1 is obtained for each form $j \in M$ (block 9).

In the following discussion we refer to the algorithm flowchart shown in figures 9.6 - 9.14. All of the steps indicated in this

flowchart constitute one iteration of block 9 in figure 9.5. That is, they determine the one-stage JLPQ solution that is specified by Proposition 9.1 for some time stage k and form j. For the reader's convenience, a table of block number locations and entry points is given in table 9.4.

A macroscopic overview of the algorithm specified by this flowchart is as follows:

1. The algorithm is first initialized (in block 1) at time N with the terminal x-cost $Q_T(x,j)$ for each $j \in \underline{M}$,

2. The determination of the optimal controller at time k for a fixed j value constitutes one iteration in block 10. Figure 9.5 differs from figure 8.5 only in blocks 4 and 10.

3. The computations of block 10 begin in block 26 with the determination of the composite x_{k+1} partition (block 14). This partition is obtained exactly as for the JLPQ problems of chapter 8 (figures 8.6 and 9.6 are the same).

4. In figure 9.7 we obtain the tentative z_{k+1} partition and its associated $\hat{V}^j_{k+1}(z_{k+1} | r_k=j,\ z_{k+1} \in \tilde{\Delta}(\ell))$, for $\ell = 1,\ldots,\tilde{\psi}$ as described in appendix D.4.

Figure Number	Block Numbers	Entry Points	Exit Points
9.5	1-13	start (block 1)	Stop (block 12)
9.6	14-26	from block 10	① (block 22)
9.7	27-42	① (block 27)	② (block 33)
9.8	43-61	② (block 43)	③ (block 61)
9.9	62-84	③ (block 63)	④ (block 64)
			⑤ (blocks 77,80)
9.10	85-96	⑤ (block 85)	④ (block 96)
9.11	97-101	④ (block 97)	⑥ (block 101)
			⑦ (block 101)
9.12	102-108	⑦ (block 102)	⑨ (blocks 103,104)
		⑧ (block 108)	
9.13	109-118	⑥ (block 111)	⑧ (block 118)
		⑨ (block 109)	⑦ (block 116)

Table 9.4: Block Number Locations, Entry Points and Exit Points for Optimal JLPC Solution Algorithm Flowchart.

5. We next add extra z_{k+1} grid points, as needed, so each $\hat{\hat{V}}_{k+1}(z_{k+1} \mid r_k=j)$ piece satisfies one of the following for all $z_{k+1} \in \hat{\Delta}^j_{k+1}(t)$:

$$\frac{\partial^2 \hat{\hat{V}}^j_{k+1}(z_{k+1};t)}{\partial z^2_{k+1}} \leq \frac{-2R(j)}{b^2(j)}$$

or

$$\frac{-2R(j)}{b^2(j)} < \frac{\partial^2 \hat{\hat{V}}^j_{k+1}(z_{k+1};t)}{\partial z^2_{k+1}} \leq 0$$

or

$$\frac{\partial^2 \hat{\hat{V}}^j_{k+1}(z_{k+1};t)}{\partial z^2_{k+1}} > 0$$

This is done in figure 9.8 via the specifications described in appendix D.4.

6. The next task is to determine which candidate cost-to-go functions are eligible for optimality with respect to Proposition 9.3 and to compute the parameters for these eligible functions. This is done in figure 9.9. The steps here are directly analogous to those of figure 8.7 (applying Proposition 8.2 in the JLPQ problem).

7. We next prepare for the rightward sweep along the $a(j)x_k$ axis by obtaining in figure 9.10 the partition of the real line (of $a(j)x_k$ values) that is caused by the points $\{\theta_k^j(t), \Theta_k^j(t-1) : t=2,\ldots,\hat{\psi}_{k+1}^j\}$. Figure 9.10 is the same as figure 8.8 (for the JLPQ problem) except for block 88.

8. Initialization of the rightward sweep is completed in figure 9.11, where the endpiece result of Proposition 9.5 is applied. Figure 9.11 is essentially the same as figure 8.9.

9. Finally the algorithm performs the minimization in (9.93) over each interval of $a(j)x_k$ values in the θ - Θ partition, starting on the left. This task, shown in figures 9.12 - 9.13, is identical to the steps is figures 8.10 - 8.11 (In the JLPQ problem) and in figures 7.5 - 7.6 (for the JLQ problem) - except for blocks 111,112.

As we mentioned previously, it may be quite difficult to carry out some of the algorithm steps for general JLPC problems. In particular it may be difficult to do the following:

(1) Perform the integrations in blocks 30,40,41

(2) Solve for $\frac{\partial^2 V}{\partial z^2} = 0$ in figure 9.8

Determine $V_K^{t,U}(x_k,j)$ in blocks 84,63 and 77

Determine $\theta_k^j(t)$ and $\Theta_k^j(t)$ in blocks 90,91,92

Find the intersections specified in blocks 102 and 103.

These difficulties arise because of the non-quadratic structure of $V_k(x_k,r_k=j)$. They will be illustrated in the next section when we apply this optimal JLPC algorithm to two time stages of an example problem.

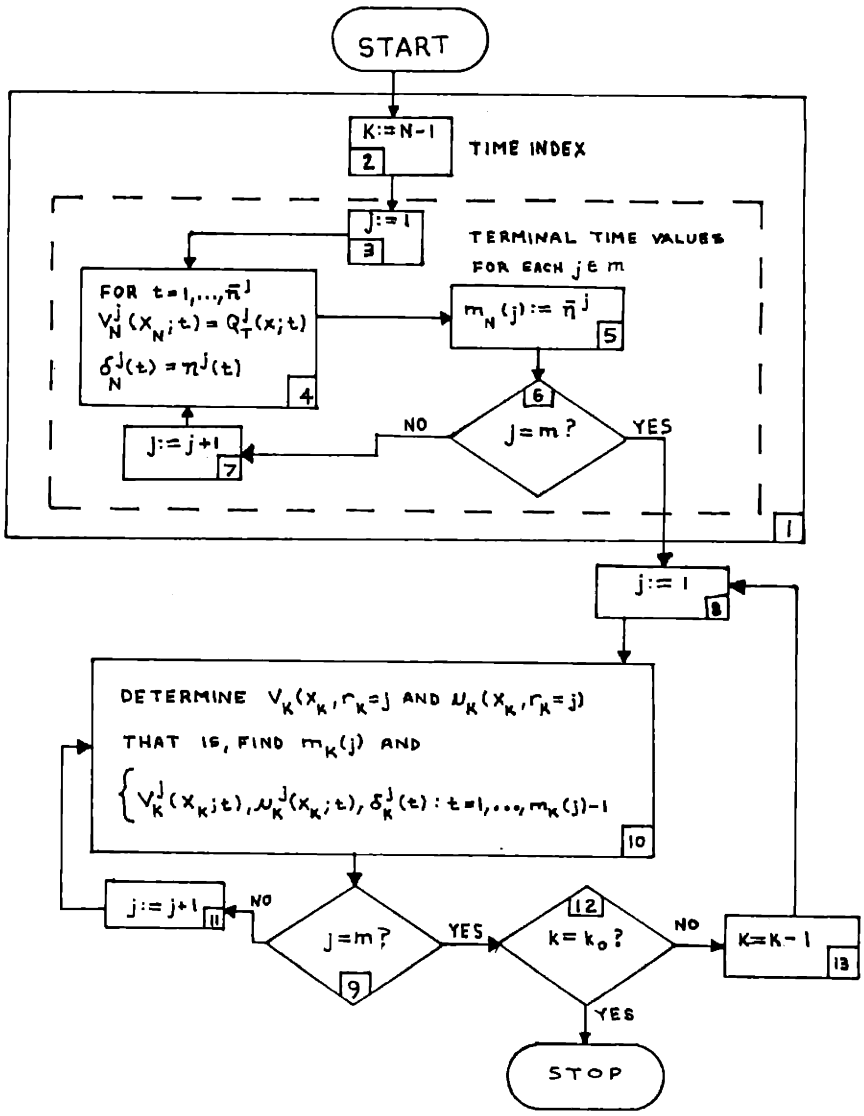

Figure 9.5: Algorithm Overview

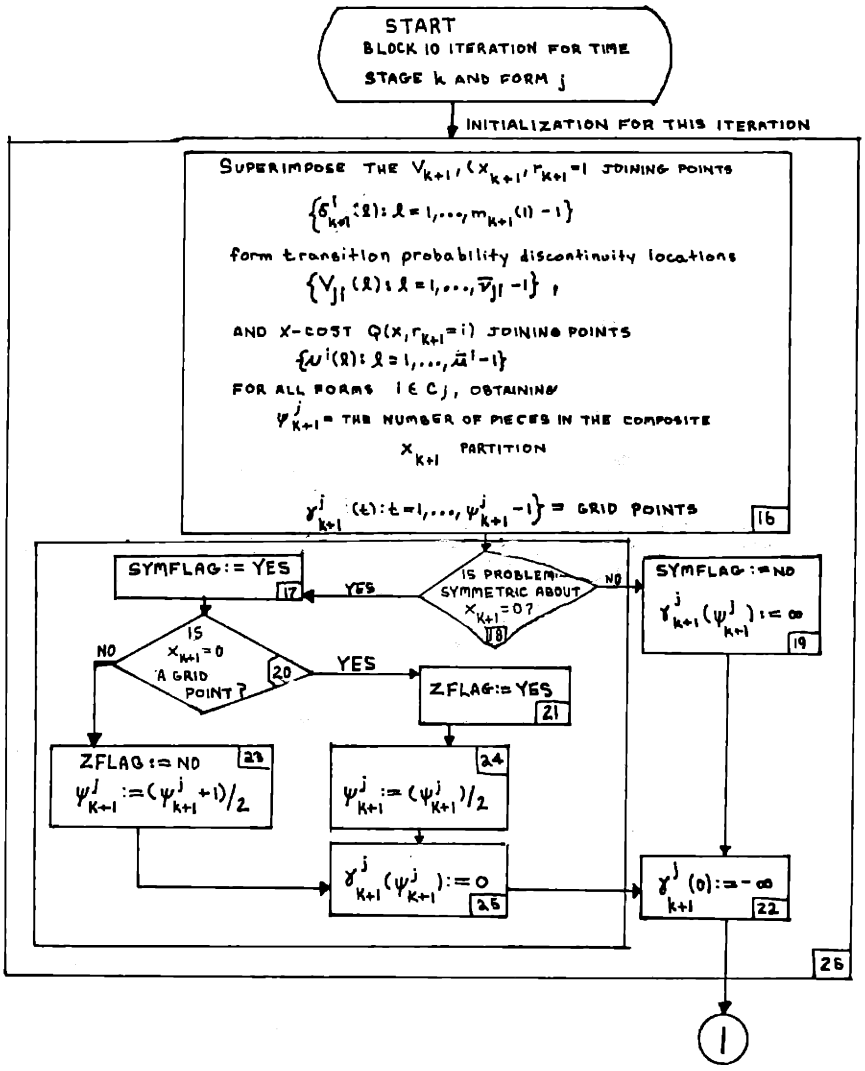

Figure 9.6: One Stage Solution Flowchart -- Part II

(same as figure 8.6)

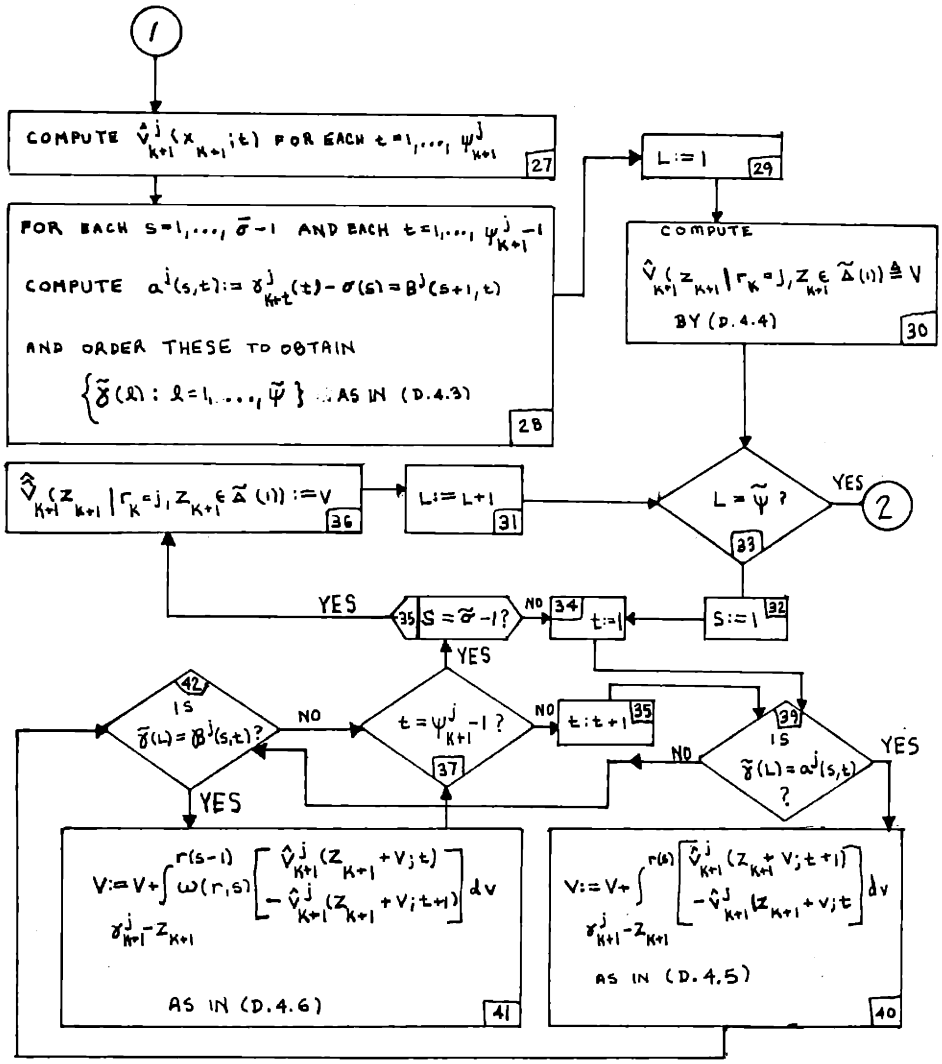

Figure 9.7: Algorithm Solution Flowchart- Part III; Obtaining the tentative z_{k+1} partition as in Appendix D.4.

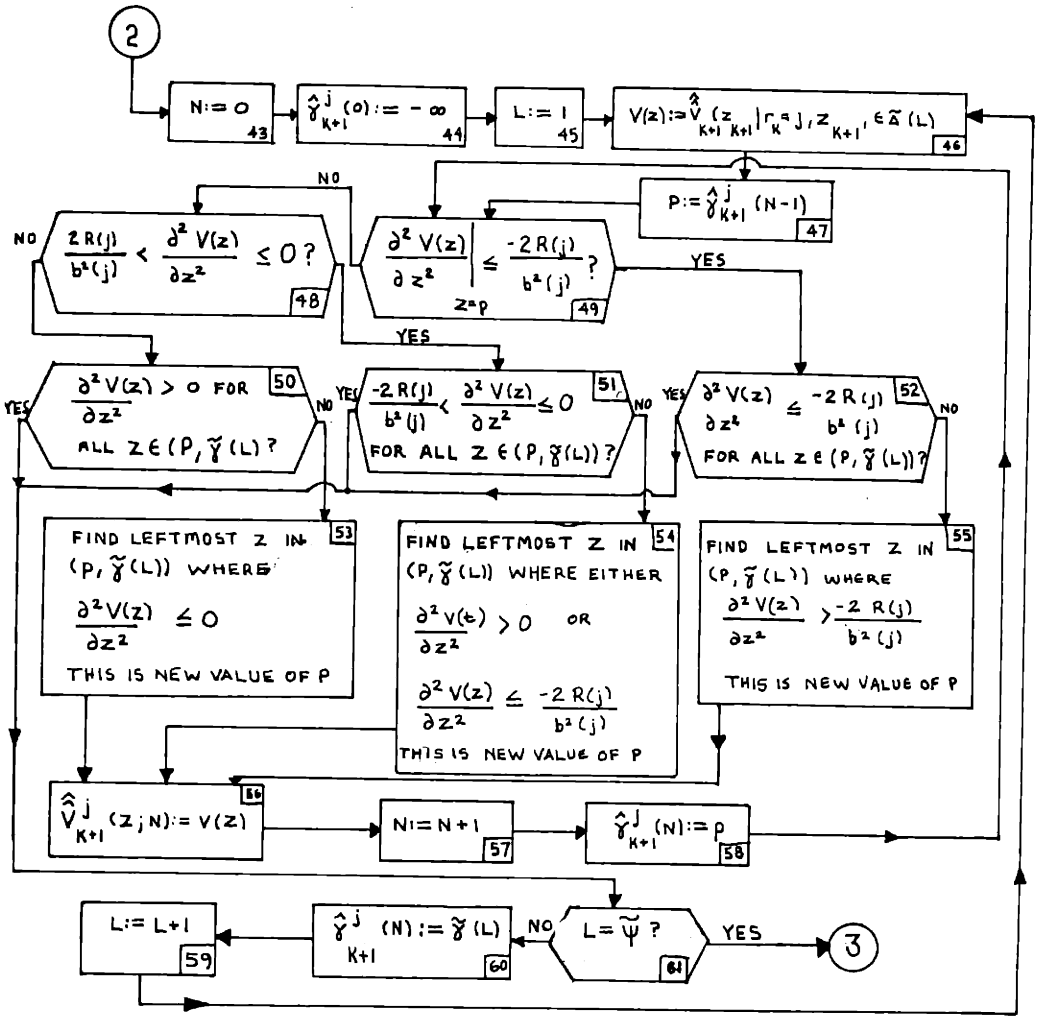

Figure 9.8: Algorithm Flowchart-Part IV: Obtaining the complete z_{k+1} partition, as in Appendix D.4.

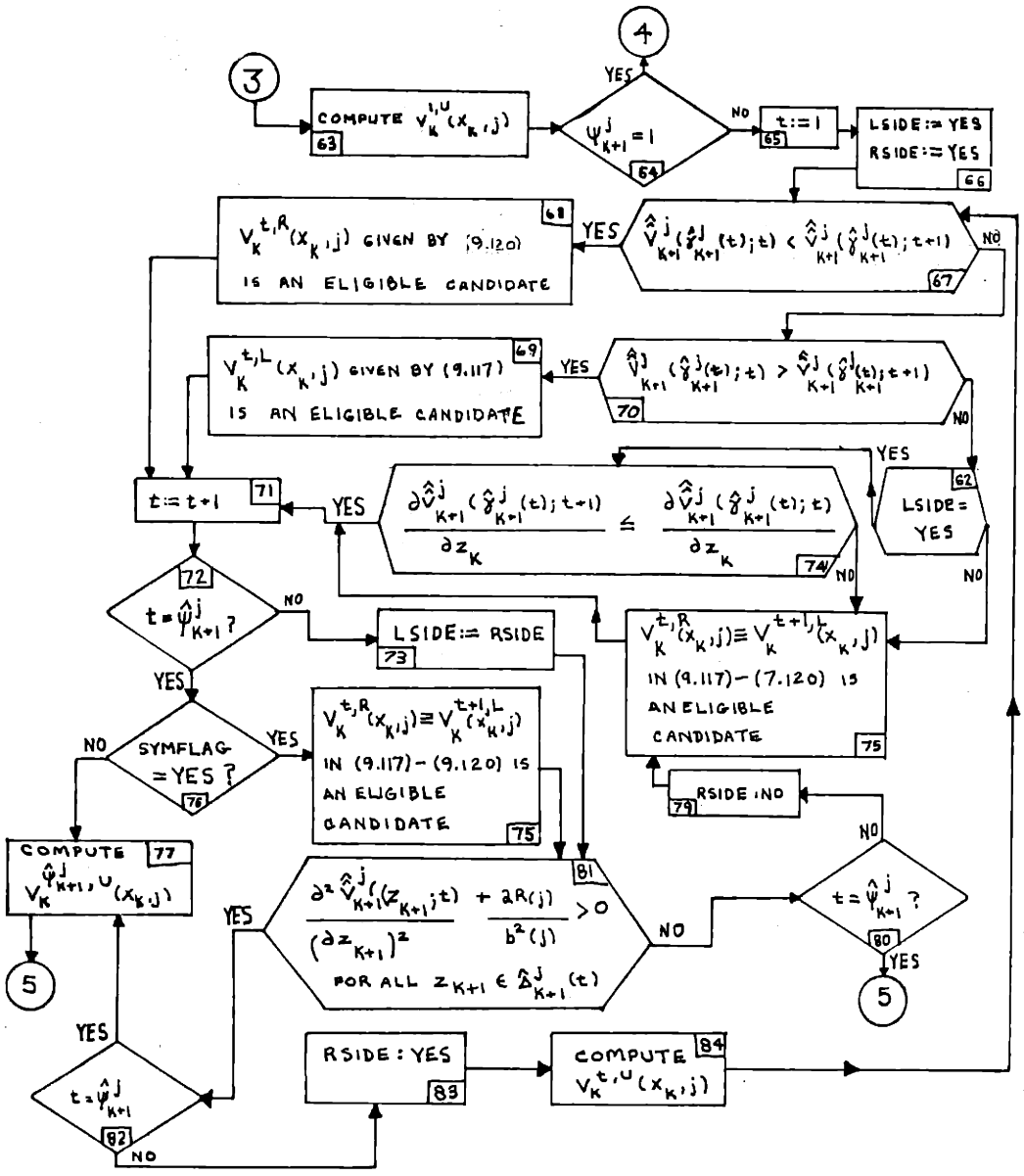

Figure 9.9: Algorithm Flowchart-Part V: Using Proposition 9.3.

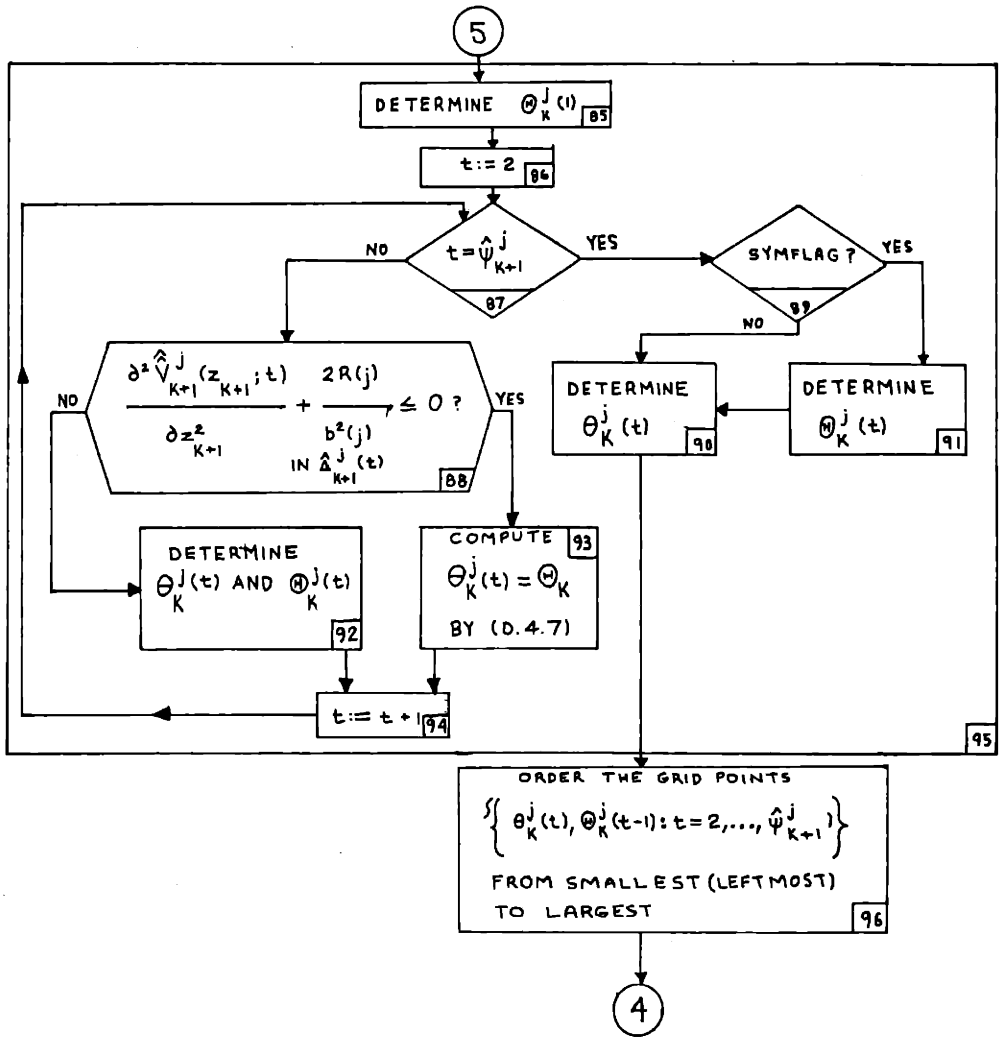

Figure 9.10: Algorithm Flowchart-Part VI: Obtaining the θ-Θ Grid

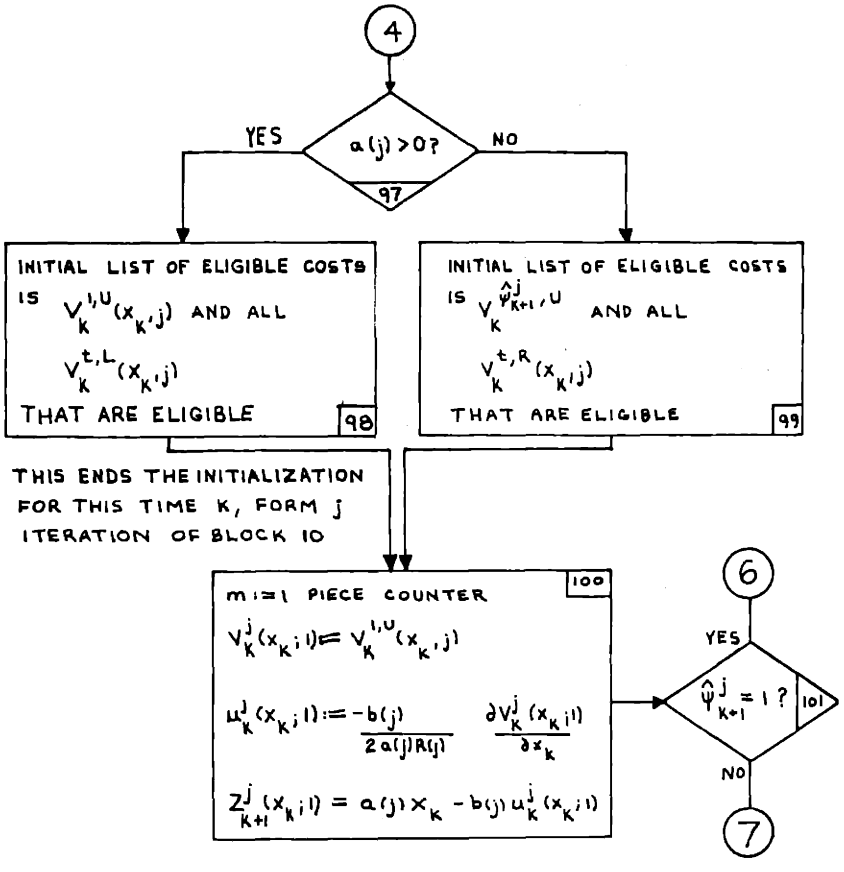

Figure 9.11: Algorithm Flowchart-Part VII: End of Initialization

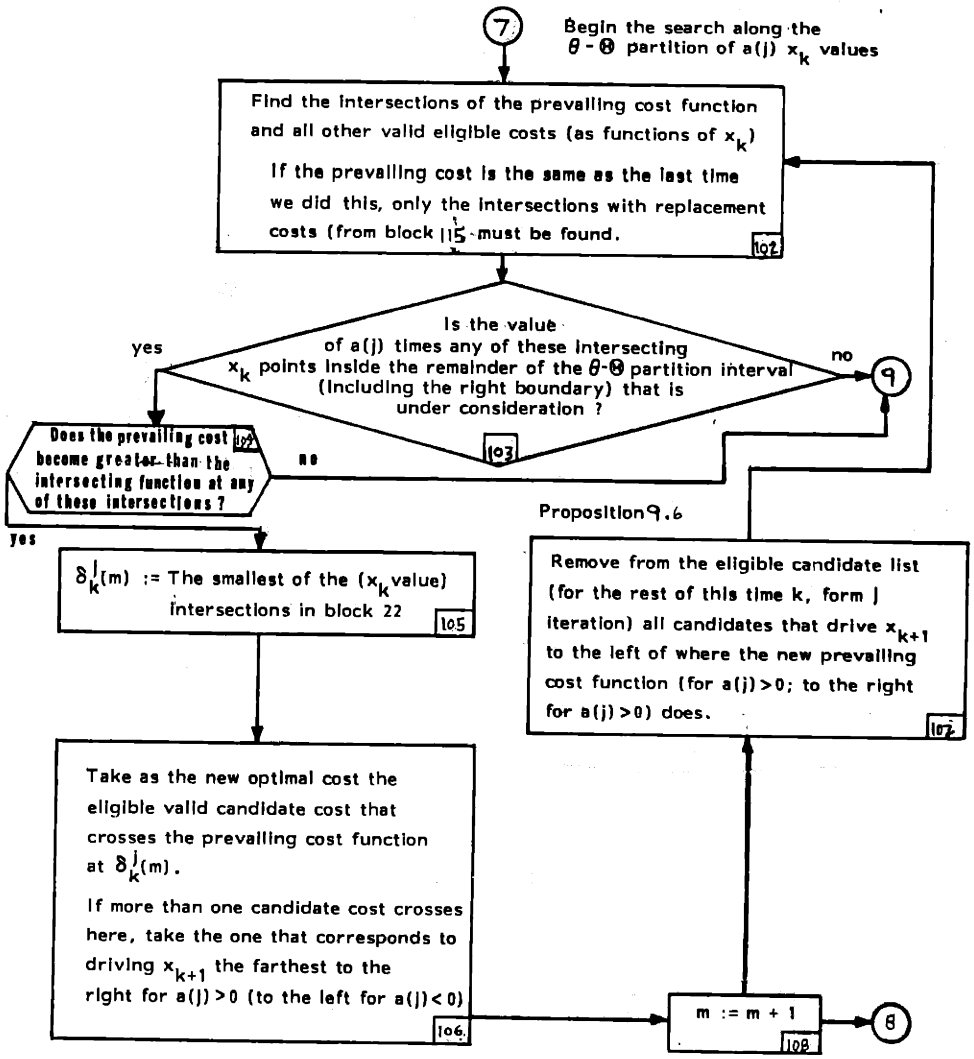

Figure 9.12: Algorithm - Part VIII: Comparisons Within a θ-Θ interval.

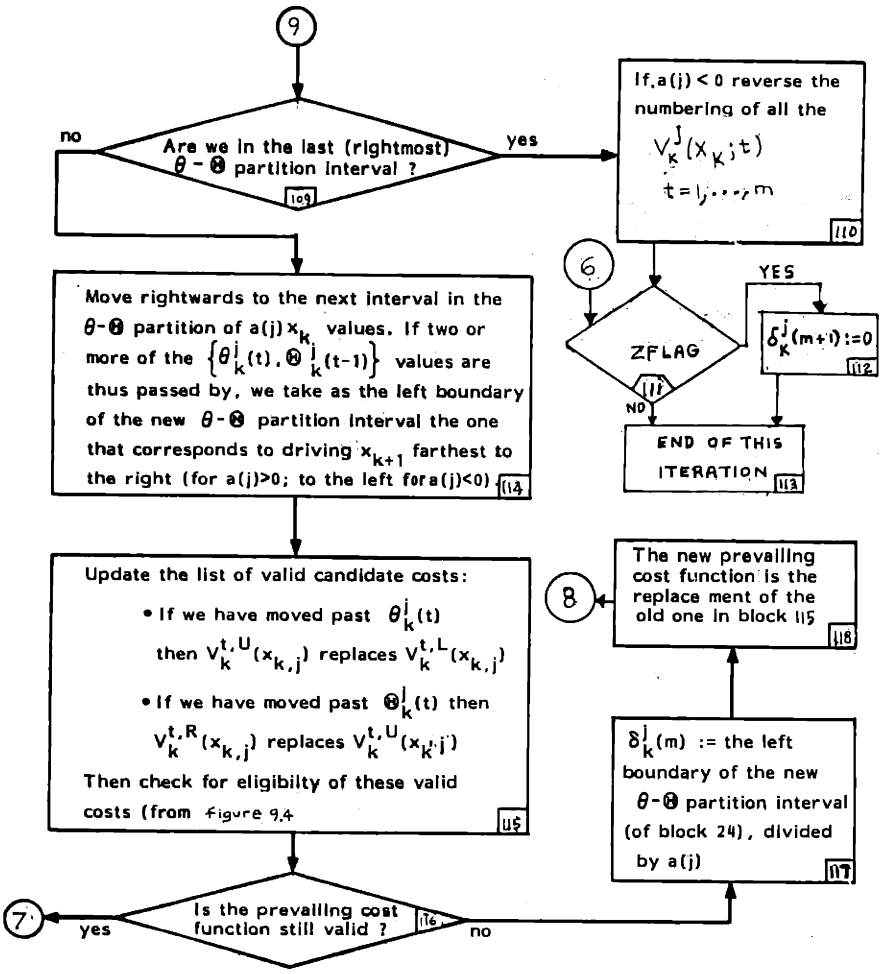

Figure 9.13: Algorithm Flowchart-Part IX: Moving Rightwards.

9.8 Numerical Solution of the Optimal Controller

In the previous section we developed an algorithm flowchart that describes the steps required to obtain the optimal controller for JLPC problems specified by (9.1) - (9.16). However, since the optimal JLPC controller is not piecewise quadratic in x_k, in general, we don't have the nice inductive solution structure of chapters 5 and 8. At each time stage the steps specified by the optimal controller algorithm may be difficult or impossible to carry out analytically. Numerical methods are generally required. These difficulties motivate the development of suboptimal approximations to the optimal JLPC controller that are easier to obtain and implement.

In this section we will illustrate the optimal JLPC algorithm of figures 9.5 - 9.13 by applying it to the last two time stages of the noisy JLPC control problem. That was begun in example 9.2 (section 9.3). This example yields an optimal controller that has optimal control laws that are <u>not</u> piecewise-linear in x_k. We will use this example to demonstrate some of the qualitative properties of optimal JLPC controllers that were established in section 9.6.

The determination of the optimal controller at time $k = N-2$ requires the solution of equations that are difficult or impossible to obtain analytically. Numerical methods for obtaining the optimal controller will be described and illustrated for this example.

The difficulties encountered in solving this example at time $k = N-2$ motivate the development of a suboptimal approximation to

the one-stage JLPC controller solution that is analytically tractable in section 9.9.

We begin by considering the application of the optimal solution algorithm to example 9.2 at time k = N-1:

Example 9.4: Example 9.2, continued at k = N-1

In section 9.3 we derived the tentative z_N partition and the $\hat{\hat{V}}_N(z_N|r_{N-1}=1,\ z_N \in \tilde{\Delta}(t))$ pieces in (9.47) - (9.48) by following the steps described in figures 9.5 - 9.7:

$$\hat{\hat{V}}_N(z_N|r_{N-1}=1) = \begin{cases} \frac{7}{4} z_N^2 + 7/3 & \text{if } z_N < -1 \\ \frac{-1}{8} z_N^3 + \frac{5}{2} z_N^2 - \frac{3}{2} z_N + \frac{83}{24} & \text{if } -1 < z_N < 3 \\ \frac{13}{4} z_N^2 + \frac{13}{3} & \text{if } 3 < z_N \end{cases} \qquad (9.146)$$

Following the steps of figure 9.8, we find that inside $\tilde{\Delta}_N^1(2) = (-1,3)$ we have

$$\frac{\partial 2\ \hat{\hat{V}}_N(z_N|r_{N-1}=1,\ z_N \in \tilde{\Delta}(2))}{\partial z_N^2} = -\frac{6}{8} z_N + 5 > 0.$$

Consequently no additional grid points are needed; we have

$$\hat{\gamma}_N^1(1) = -1$$

$$\hat{\gamma}_N^1(2) = 3$$

and

$$\hat{\psi}_N(1) = 3 \quad \bullet$$

In block 63 we obtain (from (9.126) - (9.128)):

$$u_{N-1}^{1,U} = -7/11\ x_{N-1}$$

$$z_{N-1}^{1,U} = 4/11\ x_{N-1}$$

$$V_{N-1}^{1,U}(x_{N-1},1) = \frac{7}{11} x_{N-1}^2 + \frac{7}{3} \quad .$$

In block 67, at $z = \hat{\gamma}_N^1(1) = -1$ we have

$$\hat{\hat{V}}_N^1(z;1) = 4.0833 < 7.5833 = \hat{\hat{V}}_N^1(z;2)$$

so

$$V_{N-1}^{1,R}(x_{N-1},1) = x_{N-1}^2 + 2\ x_{N-1} + 5.0833$$

is an eligible candidate cost. As we have shown above, $V_N^{2,U}$ has a positive second derivative, hence the answer to the question in block 81 is "yes". Therefore we compute $V_{N-1}^{2,U}(x_{N-1},1)$ in block 84:

$$u_{N-1}^{2,U} = -x_{N-1} + 9.3333 - \sqrt{83.1111 - 5.3333\ x_{N-1}}$$

$$z_{N-1}^{2,U} = 9.333 - \sqrt{83.1111 - 5.3333\ x_{N-1}}$$

$$V_{N-1}^{2,U}(x_{N-1},1) = x_{N-1}^2 - 18.6667\ x_{N-1} + 192.718$$

$$+ [-20.7778 + 1.3333 x_{N-1}]\sqrt{83.1111 - 5.3333 x_{N-1}} \quad .$$

Returning to block 67, at $z = \hat{\gamma}_N^1(2) = 3$ we have

$$\hat{\hat{V}}_N^1(z;2) = 18.0833 < 33.5833 = \hat{\hat{V}}_N^1(z;3)$$

hence from (9.120),

$$V^{2,R}_{N-1}(x_{N-1},1) = x^2_{N-1} - 6x_{N-1} + 27.0833$$

is an eligible candidate cost. Proceeding through blocks 68 → 71 → 72 → 76 → 77 we compute (from (9.126) - (9.128)):

$$V^{3,U}_{N-1}(x_{N-1},1) = \frac{13}{17} x^2_{N-1} + 13/3$$

$$u^{3,U}_{N-1}(x_{N-1},1) = -\frac{13}{17} x_{N-1}$$

$$z^{3,U}_{N-1}(x_{N-1},1) = \frac{4}{17} x_{N-1} \quad .$$

The eligible[1] candidate costs-to-go for $V_{N-1}(x_{N-1},r_{N-1}=1)$ are thus $V^{1,U}_{N-1}$, $V^{1,R}_{N-1}$, $V^{2,U}_{N-1}$, $V^{2,R}_{N-1}$ and $V^{3,U}_{N-1}$. Following the steps indicated in figure 9.10 we obtain the θ-Θ grid:

$$\Theta^1_{N-1}(1) = -2.75 \qquad \Theta^1_{N-1}(2) = 8.0625$$

$$\theta^1_{N-1}(2) = -2.4375 \qquad \theta^1_{N-1}(3) = 12.75 \quad .$$

These values are computed using (9.129) - (9.130). The ordering specified by block 96 is

$$\Theta^1_{N-1}(1) < \theta^1_{N-1}(2) < \Theta^1_{N-1}(2) < \theta^1_{N-1}(3).$$

Figures 9.11 - 9.13 are then followed to obtain $V_{N-1}(x_{N-1},r_{N-1}=1)$.

---

[1] according to Proposition 9.3

Since these steps are almost identical to those in figures 8.9 - 8.11, we will not describe them in detail here. There is one step that is difficult to carry out in this example. That is the determination of the intersections of $V_{N-1}^{2,U}(x_{N-1},1)$ with $V_{N-1}^{1,R}(x_{N-1},1)$ in block 102. We obtain the value $x_{N-1} = -.813$ numerically.

The optimal expected cost-to-go has 5 pieces:

$$V_{N-1}(x_{N-1},r_{N-1}=1)=\begin{cases} V_{N-1}^{1,U} = .636364\, x_{N-1}^2 + 2.3333 & \text{if } x_{N-1} \leq -.275 \\ V_{N-1}^{1,R} = x_{N-1}^2+2x_{N-1}+5.08333 & \text{if } -2.75 \leq x_{N-1} \leq -.813 \\ V_{N-1}^{2,U} = x_{N-1}^2 - 18.6667\, x_{N-1} = 192.718 & \\ \quad + [1.3333x_{N-1} - 20.7778]\sqrt{83.1111 - 5.333\, x_{N-1}} & \\ \qquad\qquad \text{if } -.813 \leq x_{N-1} \leq 8.0625 & \\ V_{N-1}^{2,R} = x_{N-1}^2 - 6x_{N-1} + 27.083 & \text{if } 8.0625 \leq x_{N-1} \leq 20.866 \\ V_{N-1}^{3,U} = .76471\, x_{N-1}^2 + 4.3333 & \text{if } x_{N-1} \geq 20.866 \end{cases} \tag{9.147}$$

This optimal cost has a piecethat is not quadratic in x_{N-1}. The corresponding optimal control law and $x_{N-1} \mapsto z_N$ mappings are as follows:

$$u_{N-1}(x_{N-1}, r_{N-1}=1) = \begin{cases} u_{N-1}^{1,U} = -.636364\, x_{N-1} & \text{if } x_{N-1} < -2.75 \\ u_{N-1}^{1,R} = -x_{N-1} - 1^{-} & \text{if } -2.75 < x_{N-1} < -.813 \\ u_{N-1}^{2,U} = -x_{N-1} + 9.3333 - \sqrt{83.1111 - 5.3333\, x_{N-1}} & \text{if } -.813 < x_{N-1} < 8.0625 \\ u_{N-1}^{2,R} = -x_{N-1} + 3^{-} & \text{if } 8.0625 < x_{N-1} < 20.866 \\ u_{N-1}^{3,U} = -.76471\, x_{N-1} & \text{if } x_{N-1} > 20.866 \end{cases}$$

(9.148)

$$z_N(x_{N-1}, r_{N-1}=1) = \begin{cases} z_N^{1,U} = .363636\, x_{N-1} & \text{if } x_{N-1} < -2.75 \\ z_N^{1,R} = -1^{-} & \text{if } -2.75 < x_{N-1} < -.813 \\ z_N^{2,U} = 9.3333 - \sqrt{83.1111 - 5.3333\, x_{N-1}} & \text{if } -.813 < x_{N-1} < 8.0625 \\ z_N^{2,R} = 3^{-} & \text{if } 8.0625 < x_{N-1} < 20.866 \\ z_N^{3,U} = .23529\, x_{N-1} & \text{if } x_{N-1} > 20.866 \end{cases}$$

(9.149)

These optimal quantities are shown in figures 9.14 - 9.16. Note that the slope of $V_{N-1}(x_{N-1}, r_{N-1}=1)$ is discontinuous at $x_N = -.813,\ 20.866$. Associated with these discontinuities are the regions of z_N avoidance:

$(-1, -.0179827)$ and $(3, 4.90951)$,

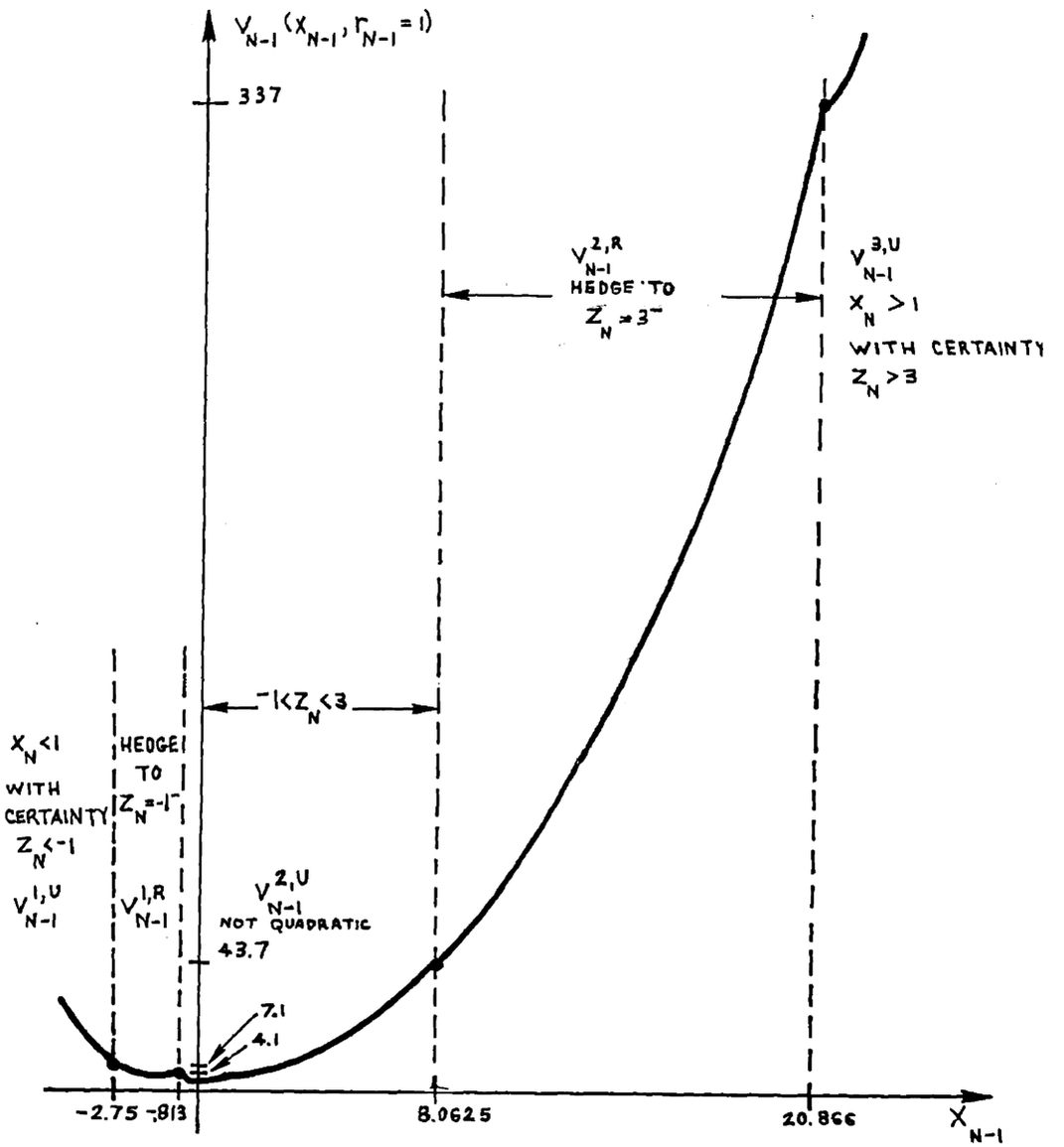

Figure 9.14: $V_{N-1}(x_{N-1}, r_{N-1}=1)$ in Example 9.2 (to scale)

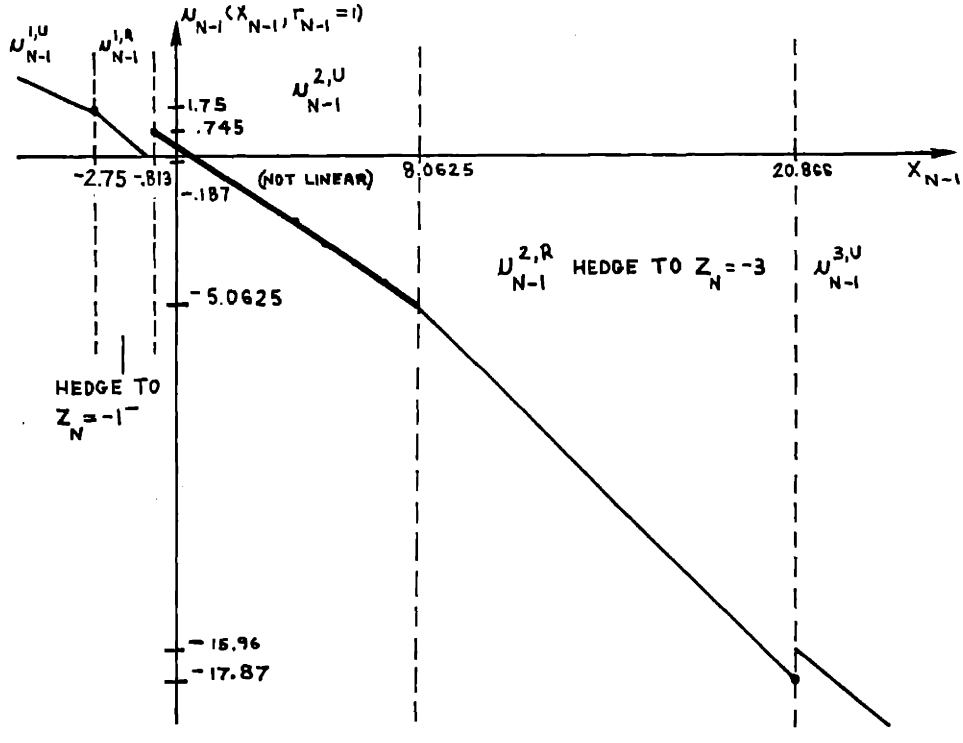

Figure 9.15: $u_{N-1}(x_{N-1}, r_{N-1}=1)$ in Example 9.2 (to scale)

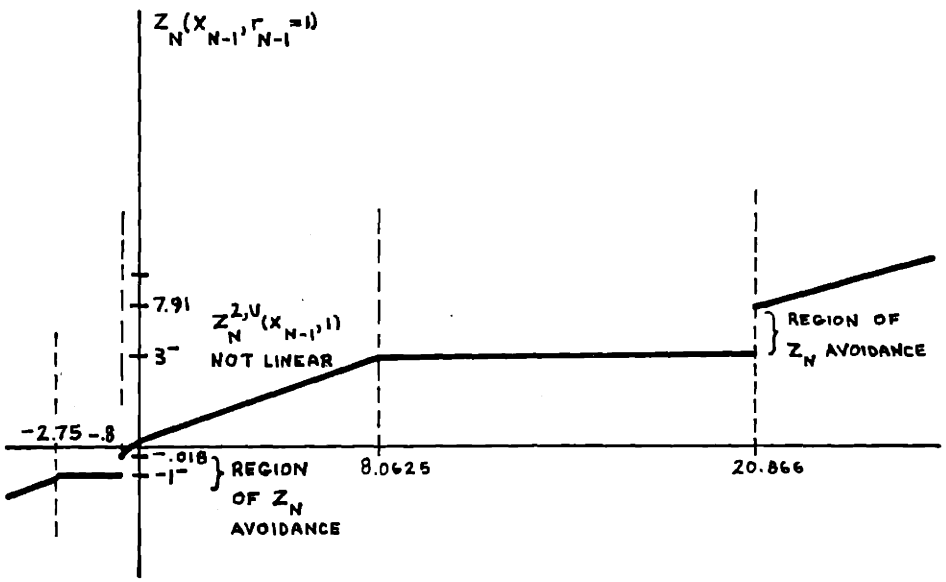

Figure 9.16: $z_N(x_{N-1}, r_{N-1}=1)$ in example 9.2 (to scale).

as specified by Proposition 9.6. Note that the mapping $z_N(x_{N-1}, r_{N-1}=1)$ shown in figure 9.16 is monotonely nondecreasing, as claimed in Proposition 9.6. □

Example 9.5: Example 9.2 at k = N-2

Obtaining $V_{N-1}(x_{N-1}, r_{N-1}=1)$ for example 9.2 via the algorithm of section 9.7 presents no significant difficulties. At time k = N-2, however, things are much different. Many of the algorithm steps must be done numerically. In particular, it is difficult or impossible to analytically obtain some of the unconstrained candidate costs $V_{N-2}^{t,U}$ (and their associated control laws), and it is difficult to analytically find the intersections of these $V_{N-2}^{t,U}$ with other candidate costs. In this example we demonstrate how the algorithm steps can be followed without analytically determining the $V_{N-2}^{t,U}$ functions.

To obtain $V_{N-2}(x_{N-2}, r_{N-2}=1)$ we first follow the steps in figure 9.6, to obtain the x_{N-1}- conditional cost $\hat{V}_{N-1}(x_{N-1} | r_{N-2}=1)$ as follows:

$$\hat{V}_{N-1}(x_{N-1}|r_{N-2}=1)=\begin{cases}(1.2773)x_{N-1}^2+1.75 & \text{if } x_{N-1}<-2.75\\ (1.55)x_{N-1}^2+1.5x_{N-1}=3.8125 & \text{if } -2.75<x_{N-1}<-.813\\ \left[(1.55)x_{N-1}^2-14x_{N-1}+144.54\right. & \\ \left.+[x_{N-1}-15.5833]\sqrt{83.1111-5.333x_{N-1}}\right] & \text{if } -.813<x_{N-1}<1\\ \left[(2.65)x_{N-1}^2-4.6667x_{N-1}+48.1795\right. & \\ \left.+[.3333x_{N-1}-5.1944]\sqrt{83.1111-5.333\,x_{N-1}}\right] & \text{if } 1<x_{N-1}<8.065\\ 2.65x_{N-1}^2-1.5x_{N-1}+6.7708 & \text{if } 8.065<x_{N-1}<20.866\\ 2.59x_{N-1}^2+1.0833 & \text{if } 20.866<x_{N-1}\end{cases}. \tag{9.150}$$

Here

$$\psi_{N-1}^1 = 6 \quad \text{and}$$

$$\gamma_{N-1}^1(1) = -2.75 \qquad \gamma_{N-1}^1(4) = 8.065$$

$$\gamma_{N-1}^1(2) = -.813 \qquad \gamma_{N-1}^1(5) = 20.866$$

$$\gamma_{N-1}^1(3) = 1$$

The computation of $\hat{V}_k(x_k|r_{k-1}=1)$ via (9.90) (in block 27) can be done analytically for any JLPC problem at each time stage, since it involves only multiplication and addition known functions of x_k.

Next we determine $\hat{\hat{V}}_{N-1}(z_{N-1}|r_{N-2}=1)$ for this example. Following the steps in figure 9.7 with

$$\sigma(1) = -2 \qquad \sigma(2) = 2 \qquad (\bar{\sigma} = 3)$$

we obtain the tentative z_{N-1} grid points (in block 28):

$$\begin{aligned}
A(1,1) &= B(2,1) = -.75 = \tilde{\gamma}(4)\\
A(2,1) &= B(3,1) = -4.75 = \tilde{\gamma}(1)\\
A(1,2) &= B(2,2) = 1.187 = \tilde{\gamma}(5)\\
A(2,2) &= B(3,2) = -2.813 = \tilde{\gamma}(2)\\
A(1,3) &= B(2,3) = 3 = \tilde{\gamma}(6)\\
A(2,3) &= B(3,3) = -1 = \tilde{\gamma}(3)\\
A(1,4) &= B(2,4) = 10.065 = \tilde{\gamma}(8)\\
A(2,4) &= B(3,4) = 6.065 = \tilde{\gamma}(7)\\
A(1,5) &= B(2,5) = 22.866 = \tilde{\gamma}(10)\\
A(2,5) &= B(3,5) = 18.866 = \tilde{\gamma}(9)
\end{aligned}$$

with $\tilde{\psi} = 11$.

The z_{N-1} conditional cost $\hat{\hat{V}}_{N-1}(z_{N-1}|r_{N-2}=1)$ is then determined via blocks 29-33 of figure 9.7. Its $\tilde{\psi} = 11$ pieces are as follows:

1. if $z_{N-1} < -4.75$,

$$\hat{\hat{V}}_{N-1}(z_{N-1}|r_{N-2}=1) = (1.2773)z_{N-1}^2 + 3.45307$$

2. if $-4.75 < z_{N-1} < -2.813$,

$$\hat{\hat{V}}_{N-1}(z_{N-1}|r_{N-2}=1) = (.022724)z_{N-1}^3 + (1.60115)z_{N-1}^2 + (1.53833)z_{N-1} + 5.88873$$

3. if $-2.813 < z_{N-1} < -1$,

$$\hat{\hat{V}}_{N-1}(z_{N-1}|r_{N-2}=1) = (.022725)z_{N-1}^3 - (.33635)z_{N-1}^2 + (28.9702)z_{N-1} + (153.019) + [-(.01875)z_{N-1} + .254693]\sqrt{\left(\begin{matrix}72.444\\-5.333z_{N-1}\end{matrix}\right)^3}$$

4. if $-1 < z_{N-1} < -.75$,

$$\hat{\hat{V}}_{N-1}(z_{N-1}|r_{N-2}=1) = (.114391)z_{N-1}^3 + (1.38032)z_{N-1}^2 + (10.6467)z_{N-1} - (42.9246) + [-(.00625)z_{N-1} + .084898]\sqrt{\left(\begin{matrix}72.444\\-5.333z_{N-1}\end{matrix}\right)^3}$$

5. if $-.75 < z_{N-1} < 1.187$,

$$\hat{\hat{V}}_{N-1}(z_{N-1}|r_{N-2}=1) = (.091666)z_{N-1}^3 + (1.32917)z_{N-1}^2 + (10.6084)z_{N-1} - (47.9342) + [-(.00625)z_{N-1} + .084898]\sqrt{\left(\begin{matrix}72.444\\-5.333z_{N-1}\end{matrix}\right)^3}$$

6. if $1.187 < z_{N-1} < 3$,

$$\hat{\hat{V}}_{N-1}(z_{N-1}|r_{N-1}=1) = (.091666)z_{N-1}^3 + (3.26667)z_{N-1}^2 - (32.3235)z_{N-1}$$

$$+ (251.697)$$

$$+ [-(.00625)z_{N-1} + .084898]\sqrt{\left(\begin{matrix}72.444\\-5.333z_{N-1}\end{matrix}\right)^3}$$

$$+ [(.01875)z_{N-1} - .329693]\sqrt{(93.7778 - 5.333z_{N-1})^3}$$

7. if $3 < z_{N-1} < 6.065$,

$$\hat{\hat{V}}_{N-1}(z_{N-1}|r_{N-2}=1) = (2.65)z_{N-1}^2 - (4.66667)z_{N-1} + 51.7128$$

$$+ [-(.00625)z_{N-1} + .084898]\sqrt{(72.4444 - 5.33333z_{N-1})^3}$$

$$+ [+(.00625)z_{N-1} - .109898]\sqrt{(93.7778 - 5.33333z_{N-1})^3}$$

8. if $6.065 < z_{N-1} < 10.065$,

$$\hat{\hat{V}}_{N-1}(z_{N-1}|r_{N-2}=1) = (3.04583)z_{N-1}^2 - (13.4355)z_{N-1} + 102.159$$

$$+ [(.00625)z_{N-1} - .109898]\sqrt{(93.7778 - 5.33333z_{N-1})^3}$$

9. if $10.065 < z_{N-1} < 18.866$,

$$\hat{\hat{V}}_{N-1}(z_{N-1}|r_{N-1}=1) = (2.65)z_{N-1}^2 - (1.5)z_{N-1} + (10.3041)$$

10. if $18.866 < z_{N-1} < 22.866$,

$$\hat{\hat{V}}_{N-1}(z_{N-1}|r_{N-2}=1) = -(.005)z_{N-1}^3 + (2.8075)z_{N-1}^2 - (2.23188)z_{N-1} + 1.6278$$

11. if $22.866 < z_{N-1}$,

$$\hat{\hat{V}}_{N-1}(z_{N-1}|r_{N-2}=1) = (2.59)z_{N-1}^2 + 4.53663 \quad .$$

Obtaining the z_{N-1} partition for this example, and obtaining the z_{k+1} partition for arbitrary JLPC problems at time k (as in block 28) does not present any special difficulties. For some problems, however, it may be difficult to determine the z-cost $\hat{\hat{V}}_{k+1}(z_{k+1}|r_k=j)$ as a function of z_{k+1}. In example 9.2, finding $\hat{\hat{V}}_{N-1}(z_{N-1}|r_{N-2}=1)$ via figure 9.7 is straightforward since the integrals in blocks 40 and 41 can be done analytically. For arbitrary $\hat{\hat{V}}_{k+1}(z_{K+1}|r_k=j)$, if these integrations cannot be done analytically then numerical methods of integration must be used.

Comparing $\hat{\hat{V}}_{N-1}(z_{N-1}|r_{N-2}=1)$ with $\hat{\hat{V}}_N(z_N|r_{N-1}=1)$ in (9.146), we see that the z-conditional cost is much more complicated at stage N-2. Following the steps of figure 9.8, we find[1] that no additional z_{N-1} grid points are needed. Thus the complete z_{N-1} partition is

---

[1] this can be done by numerical methods (substitution of values and testing) or analytically in this example. For some examples only numerical methods are feasible.

$$\gamma^1_{N-1}(1) = -4.75 \qquad \hat{\gamma}^1_{N-1}(7) = 6.065$$

$$\gamma^1_{N-1}(2) = -2.813 \qquad \hat{\gamma}^1_{N-1}(8) = 10.065$$

$$\gamma^1_{N-1}(3) = -1 \qquad \hat{\gamma}^1_{N-1}(9) = 18.866$$

$$\gamma^1_{N-1}(4) = -.75 \qquad \hat{\gamma}^1_{N-1}(10) = 22.866$$

$$\gamma^1_{N-1}(5) = 1.187$$

$$\gamma^1_{N-1}(6) = 3$$

with $\hat{\psi}^1_{N-1}(1) = 11$. The second derivative of $\hat{\hat{V}}_{N-1}(z_{N-1}|r_{N-2}=1)$ is everywhere positive in this example. That is

$$\frac{\partial^2 \hat{\hat{V}}^1_{N-1}(z_{N-1};t)}{\partial z^2_{N-1}} > 0 \qquad \text{for } z_{N-1} \in \hat{\Delta}^1_{N-1}(t) = (\hat{\gamma}^1_{N-1}(t-1), \hat{\gamma}^1_{N-1}(t)),$$

Next we follow figure 9.9 to determine which candidate costs are eligible in terms of Proposition 9.3. The tests in figure 9.9 can be done without actually computing any of the candidate costs. Only the values of

$$\hat{\hat{V}}^j_{k+1}(z_{k+1};t) \qquad \text{and} \qquad \frac{\partial \hat{\hat{V}}^j_{k+1}(z_{k+1};t)}{\partial z_{k+1}}$$

at the grid points $\{\hat{\gamma}^j_{k+1}(t) : t = 1,\ldots, \hat{\psi}^j_{k+1}\}$ are needed in blocks 67,70 and 74.

For this example, the values of $\hat{\hat{V}}_{N-1}(z_{N-1}|r_{N-1}=1)$ and its derivative at the z_{N-1} grid points are listed in table 9.5. Note that $\hat{\hat{V}}_{N-1}(z_{N-1}|r_{N-1}=1)$ is continuous in z_{N-1}.

Using these values in figure 9.9, the list of eligible candidate costs for $V_{N-2}(x_{N-2},r_{N-2}=1)$ is found to be

$$V_{N-2}^{t,U}(x_{N-2},r_{N-2}=1) \qquad \text{for } t = 1,\ldots,11$$

and

$$V_{N-2}^{6,R}(x_{N-2},r_{N-2}=1) = V_{N-2}^{7,L}(x_{N-2},r_{N-2}=1) \quad .$$

The next task is to obtain the θ - Θ grid, as in figure 9.10. For this example

$$\frac{\partial^2 \hat{\hat{V}}_{N-1}^{l}(z_{N-1};t)}{\partial z_{N-1}^2} + \frac{2\,R(j)}{b^2(j)} > 0$$

for each t = 1,...,11, We compute $\{\theta_k^j(t),\ \Theta_k^j(t-1) \quad t = 1,\ldots,11\}$ directly in block 92 from (9.129) - (9.130), using the values in table 9.5.

z_{N-1}	$\hat{\hat{V}}_{N-1}(z_{N-1}\ r_{N-2}=1)$	$\frac{\partial \hat{\hat{V}}_{N-1}(z_{N-1}\ r_{N-2}=1)}{\partial z_{N-1}}$	
-4.75^-	32.272	-12.134	
-4.75^+	32.272	-12.134	
-2.813^-	13.725	-6.930	
-2.813^+	13.725	-6.930	
-1^-	5.216	-2.4425	discontinuity
-1^+	5.216	-2.4886	
$-.75^-$	4.695	-1.6741	
$-.75^+$	4.695	-1.6741	
1.187^-	8.33	5.7516	
1.187^+	8.33	5.7516	
3^-	27.09	15.2791	discontinuity
3^+	27.09	15.3251	
6.065^-	98.16	31.034	
6.065^+	98.16	31.034	
10.065^-	263.66	51.845	
10.065^+	263.66	51.845	
18.866^-	905.62	98.4898	discontinuity
18.866^+	905.62	98.3524	
22.866^-	1358.73	118.4459	
22.866^+	1358.73	118.4459	

Table 9.5: Values of z_{N-1} - conditional Cost and its Derivative to the Left and Right of each grid point $\{\hat{\gamma}_{N-1}(t) \quad :t = 1,\ldots, \hat{\psi}^1_{N-1} = 11\}$.

$$\theta^1_{N-2}(1) = -10.817 = \theta^1_{N-2}(2)$$

$$\theta^1_{N-2}(2) = -6.278 = \theta^1_{N-2}(3)$$

$$\theta^1_{N-2}(3) = -2.221$$

$$\theta^1_{N-2}(4) = -2.244$$

$$\theta^1_{N-2}(4) = -1.587 = \theta^1_{N-2}(5)$$

$$\theta^1_{N-2}(5) = 4.0628 = \theta^1_{N-2}(6)$$

$$\theta^1_{N-2}(6) = 10.6395$$

$$\theta^1_{N-2}(7) = 10.6625$$

$$\theta^1_{N-2}(7) = 21.582 = \theta^1_{N-2}(8)$$

$$\theta^1_{N-2}(8) = 35.987 = \theta^1_{N-2}(9)$$

$$\theta^1_{N-2}(9) = 68.111$$

$$\theta^1_{N-2}(10) = 68.042$$

$$\theta^1_{N-2}(10) = 82.089 = \theta^1_{N-2}(11)$$

Now we follow the steps outlined in figures 9.11 - 9.13 to determine $V_{N-2}(x_{N-2}, r_{N-2}=1)$ for each x_{N-2} value. We can find all of the boundaries of unconstrained cost domains of validity and most of the intersections between candidate costs without explicitly analytically determining all of the $V^{t,U}_{N-2}(x_{N-2},1)$ functions. To do this we need to find the <u>constrained</u> cost functions $V^{t,L}_{N-2}$ and $V^{t+1,R}_{N-2}$ for t = 1,...,10.

From (9.117), (9.120) of Proposition 9.2 and table 9.5 we have

$$
\begin{aligned}
V_{N-2}^{1,R} &= V_{N-2}^{2,L} = x_{N-2}^2 + 9.5x_{N-2} + 54.8346 \\
V_{N-2}^{2,R} &= V_{N-2}^{3,L} = x_{N-2}^2 + 5.626z_{N-2} + 21.638 \\
V_{N-2}^{3,R} &= V_{N-2}^{4,L} = x_{N-2}^2 + 2x_{N-2} + 6.21595 \\
V_{N-2}^{4,R} &= V_{N-2}^{5,L} = x_{N-2}^2 + 1.5x_{N-2} + 6.2573 \\
V_{N-2}^{5,R} &= V_{N-2}^{6.L} = x_{N-2}^2 - 2.374x_{N-2} + 9.7420 \\
V_{N-2}^{6,R} &= V_{N-2}^{7,L} = x_{N-2}^2 - 6x_{N-2} + 36.09 \\
V_{N-2}^{7,R} &= V_{N-2}^{8,L} = x_{N-2}^2 - 12.13x_{N-2} + 134.88 \\
V_{N-2}^{8,R} &= V_{N-2}^{9,L} = x_{N-2}^2 - 20.13x_{N-2} + 364.9 \\
V_{N-2}^{9,R} &= V_{N-2}^{10,L} = x_{N-2}^2 - 37.732x_{N-2} + 1254.01 \\
V_{N-2}^{10,R} &= V_{N-2}^{11,L} = x_{N-2}^2 - 45.732x_{N-2} + 1881.58 \quad .
\end{aligned}
\tag{9.151}
$$

Using these easily obtained constrained cost functions we can avoid having to analytically determine the unconstrained cost functions, as we will demonstrate below in detail.[1]

Now we consider in turn each x_{N-2} interval in the $\theta - \Theta$ partition specified by (9.150).

For x_{N-2} sufficiently negative, we know that

$$V_{N-2}(x_{N-2}, r_{N-2}=1) = V_{N-2}^{1,U}(x_{N-2}, 1) \quad .$$

Since $\hat{V}_{N-2}^{1}(z_{N-1};1)$ is quadratic in z_{N-1}, $V_{N-2}^{1,U}(x_{N-2},1)$ is quadratic in x_{N-2}.

[1] these details are expounded in the next five pages.

In the interval $(-\infty, -10.817 = \theta^1_{N-1}(1))$, the only two valid eligible candidate cost functions are $V^{1,U}_{N-2}$ and $V^{6,U}_{N-2} \equiv V^{7,L}_{N-2}$. From (9.151) and Proposition 9.2 we have

$$V^{6,R}_{N-2} = V^{7,L}_{N-2} = 217.995 \quad \text{at } x_{N-2} = 10.817$$

$$V^{1,U}_{N-2} = V^{1,R}_{N-2} = 69.081 \quad \text{at } x_{N-2} = -10.817 \ .$$

Consequently (from Proposition 9.6(5)),

$$V_{N-2}(x_{N-2}, r_{N-2}=1) = V^{1,U}_{N-2}(x_{N-2}, 1) \quad \text{for } x_{N-2} < -10.817 \ .$$

In $-10.817 < x_{N-2} < -6.278$, $V^{1,U}_{N-2}$ ceases to be valid. The valid eligible costs are $V^{2,U}_{N-2}$ and $V^{6,R}_{N-2} = V^{7,L}_{N-2}$. Using (9.151) and (9.132), (9.134) of Proposition 9.2:

- at $x_{N-2} = \theta^1_{N-2}(2) = -10.817$,

$$V^{2,U}_{N-2} = V^{2,L}_{N-2} = 69.081$$

- at $x_{N-2} = \theta^1_{N-2}(2) = 6.278$,

$$V^{2,U}_{N-2} = V^{2,R}_{N-2} = 25.731256$$

and

$$V^{6,R}_{N-2} = V^{7,L}_{N-2} = 113.17128 \ .$$

Consequently $V_{N-2}(x_{N-2}, r_{N-2}=1) = V^{2,U}_{N-2}(x_{N-2}, 1)$ over $(-10.817, -6.278)$.

In the interval $-6.278 < x_{N-2} < -2.244$, $V^{2,U}_{N-2}$ ceases to be valid.

The valid eligible costs are $V_{N-2}^{3,U}$ and $V_{N-2}^{6,R} = V_{N-2}^{7,L}$. At

$x_{N-2} = \theta_{N-2}^{1}(3) = -6.278,$

$$V_{N-2}^{3,U} = V_{N-2}^{3,L} = 25.732 ,$$

so $V_{N-2}^{3,U}$ is optimal there. But what is the numerical value of $V_{N-2}^{3,U}$ at $x_{N-2} = -2.244 = \theta_{N-2}^{1}(4)$? From Proposition 9.2 we know that

$$u_{N-2}^{3,U}(x_{N-2},1) = -\frac{1}{2} \left. \frac{\partial \hat{\hat{V}}_{N-1}^{1}(z_{N-1};3)}{\partial z_{N-1}} \right|_{z_{N-1} = z_{N-1}^{3,U} = x_{N-2} + u_{N-2}^{3,U}} \tag{9.152}$$

from

$$x_{N-2} = z_{N-1}^{3,U} - u_{N-2}^{3,U} \tag{9.153}$$

with resulting cost

$$V_{N-2}^{3,U}(x_{N-2},1) = (u_{N-2}^{3,U})^2 + \left. \hat{\hat{V}}_{N-1}^{1}(z_{N-1};3) \right|_{z_{N-1} = z_{N-1}^{3,U}} , \tag{9.154}$$

where

$$z_{N-1}^{3,U} \in (\hat{\gamma}_{N-1}^{1}(2), \hat{\gamma}_{N-1}^{1}(3)) = (-1,-2.813) .$$

Using (9.152) - (9.154) we need to find $V_{N-2}^{3,U}(x_{N-2},1)$ for x_{N-2} near -2.244 and compare it with the value of $V_{N-2}^{6,R} \equiv V_{N-2}^{7,L}$ at that x_{N-2},

in order to determine if $V_{N-2}^{6,R} \equiv V_{N-2}^{7,L}$ is optimal for any x_{N-2} in (-6.278, -2.244). We find that to obtain $z_{N-1}^{3,U} = -1$, the control is

$$u_{N-2}^{3,U} = +1.2213 \quad ,$$

applied to

$$x_{N-2} = -2.22$$

with resulting cost

$$V_{N-1}^{3,U} = 6.7074.$$

Since

$$V_{N-2}^{6,R} = V_{N-2}^{7,L} = 54.34 \quad \text{at}$$

$x_{N-2} = -2.22$, it is clear that $V_{N-2}^{3,U}$ is optimal over the entire interval (-6.278, -2.244).

Next we consider the interval $\theta_{N-2}^{1}(4) = -2.244 < x_{N-2} < -2.221 = \theta_{N-2}^{1}(3)$. Here $V_{N-2}^{3,U}$ is the prevailing optimal at $x_{N-2} = -2.244$ and the costs $V_{N-2}^{4,U}$ and $V_{N-2}^{6,R} = V_{N-2}^{7,L}$ are valid, eligible candidates for optimality. At $x_{N-2} = -2.221 = \theta_{N-2}^{1}(3)$,

$$V_{N-2}^{3,U} = V_{N-2}^{3,R} = V_{N-2}^{4,L} = 6.7067$$

and since $V_{N-2}^{4,U} < V_{N-2}^{4,L}$ for all $x_{N-2} \neq \theta_{N-2}^{1}(4)$, we know that $V_{N-2}^{3,U}$ will cross $V_{N-2}^{4,U}$ somewhere inside (-2.244, -2.221). We will call this point of intersection $\delta_{N-1}^{1}(3)$. We will defer its determination until later in this discussion.

$$V_{N-2}^{6,R} = V_{N-2}^{7,L} = 54.36 \qquad \text{at } x_{N-2} = -2.221 \ ,$$

we have that

$$V_{N-2}(x_{N-2},1) = \begin{cases} V_{N-2}^{3,U} & \text{for } -2.244 < x_{N-2} < \delta_{N-2}^{1}(3) \\ V_{N-2}^{4,U} & \text{for } \delta_{N-2}^{1}(3) < x_{N-2} < -2.221 \end{cases}$$

where $-2.244 < \delta_{N-2}^{1}(3) < -2.221$.

In the interval (-2.221, -1.587) the only eligible valid candidate costs are $V_{N-2}^{4,U}$ and $V_{N-2}^{6,R} = V_{N-2}^{7,L}$. Since at $x_{N-2} = 1.587$ we have

$$V_{N-2}^{6,R} = V_{N-2}^{7,L} = 48.1306$$

$$V_{N-2}^{4,U} = V_{N-2}^{4,L} = 6.3954 \ ,$$

we see that $V_{N-2}^{4,U}$ is optimal over the entire interval (-2.221, -1.587).

In (-1.587, 4.0628) the eligible valid candidates are $V_{N-2}^{5,U}$ and $V_{N-2}^{6,R} = V_{N-2}^{7,L}$. Now

- at $x_{N-2} = -1.587 = \theta_{N-2}^{1}(5) = \Theta_{N-2}^{1}(4)$,

$$V_{N-2}^{5,U} = V_{N-2}^{5,L} = 6.395$$

- at $x_{N-2} = 4.0628 = \Theta_{N-2}^{1}(5) = \theta_{N-2}^{1}(6)$,

$$V_{N-2}^{5,U} = V_{N-2}^{5,R} = 16.6033$$

$$V_{N-2}^{6,R} = V_{N-2}^{7,L} = 28.2195 \ .$$

Therefore $V_{N-2}^{5,U}$ is optimal over (-1.587, 4.0628).

Over the next interval (4.0628, 10.639), the eligible valid candidates are $V_{N-2}^{6,U}$ and $V_{N-2}^{6,R} = V_{N-2}^{7,L}$. Since $V_{N-2}^{6,U} < V_{N-2}^{6,R}$ except at $\theta_{N-2}^{1}(6)$,

$$V_{N-2}(x_{N-2}, r_{N-2}=1) = V_{N-2}^{6,U} \quad \text{for} \quad 4.0628 < x_{N-2} < 10.639.$$

Over (10.639, 10.662) the only eligible valid candidate is $V_{N-2}^{6,R} = V_{N-2}^{7,L}$, so it is optimal. Over (10.662, 21.582) the only eligible valid candidate is $V_{N-2}^{7,U}$, so it is optimal. Similarly, $V_{N-2}^{8,U}$ is optimal over (21.582, 35.987) and $V_{N-2}^{9,U}$ is optimal over (35.987, 68.042).

Now in the interval ($68.042 = \theta_{N-2}^{1}(10)$, $\theta_{N-2}^{1}(9) = 68.111$) the cost functions $V_{N-2}^{9,U}$ and $V_{N-2}^{10,U}$ are both valid eligible candidates. At $x_{N-2} = 68.042$, $V_{N-2}^{9,U}$ is optimal. At $x_{N-2} = 68.111$ $\theta_{N-2}^{1}(9)$,

$$V_{N-2}^{9,U} = V_{N-2}^{9,R} = V_{N-2}^{10,L} > V_{N-2}^{10,U},$$

so $V_{N-2}^{10,U}$ is optimal here. In (68.042,68.111) we have the intersection of $V_{N-2}^{9,U}$ and $V_{N-2}^{10,U}$ which we will denote by $\delta_{N-2}^{1}(10)$.

$$V_{N-2}(x_{N-2}, r_{N-2}=1) = \begin{cases} V_{N-2}^{9,U} & \text{for } 68.042 < x_{N-2} < \delta_{N-2}^{1}(10) \\ V_{N-2}^{10,U} & \text{for } \delta_{N-2}^{1}(10) < x_{N-2} < 68.111 . \end{cases}$$

In (68.111, 82.089), $V_{N-2}^{10,U}$ is the only valid eligible candidate so it is optimal. Similarly, $V_{N-2}^{11,U}$ is optimal for $x_N > 82.089$.

We have now determined the basic structure of the optimal controller, using the procedure of figures 9.11 - 9.13. This has been done without explicitly computing the costs $V_{N-2}^{t,U}(x_{N-2}, r_{N-2}=1)$ Instead, we used the quadratic, constrained costs in (9.151), as specified by Proposition 9.2

Summarizing the preceding discussion, we have found that

$$V_{N-2}(x_{N-2}, r_{N-2}=1) = \begin{cases} V_{N-2}^{1,U} \text{ for } & x_{N-2} \leq -10.817 = \delta_{N-2}^{1}(1) \\ V_{N-2}^{2,U} \text{ for } & -10.817 \leq x_{N-2} \leq -6.278 = \delta_{N-2}^{1}(2) \\ V_{N-2}^{3,U} \text{ for } & -6.278 \leq x_{N-2} \leq \delta_{N-2}^{1}(3) \\ V_{N-2}^{4,U} \text{ for } & \delta_{N-2}^{1}(3) \leq x_{N-2} \leq -1.587 = \delta_{N-2}^{1}(4) \\ V_{N-2}^{5,U} \text{ for } & -1.587 \leq x_{N-2} \leq 4.0628 = \delta_{N-2}^{1}(5) \\ V_{N-2}^{6,U} \text{ for } & 4.0628 \leq x_{N-2} \leq 10.639 = \delta_{N-2}^{1}(6) \\ V_{N-2}^{6,R} = V_{N-2}^{7,L} \text{ for } & 10.639 \leq x_{N-2} \leq 10.662 = \delta_{N-2}^{1}(7) \\ V_{N-2}^{7,U} \text{ for } & 10.662 \leq x_{N-2} \leq 21.582 = \delta_{N-2}^{1}(8) \\ V_{N-2}^{8,U} \text{ for } & 21.582 \leq x_{N-2} \leq 35.987 = \delta_{N-2}^{1}(9) \\ V_{N-2}^{9,U} \text{ for } & 35.987 \leq x_{N-2} \leq \delta_{N-2}^{1}(10) \\ V_{N-2}^{10,U} \text{ for } & \delta_{N-2}^{1}(10) \leq x_{N-2} \leq 82.089 = \delta_{N-2}^{1}(11) \\ V_{N-2}^{11,U} \text{ for } & 82.089 \leq x_{N-2} \end{cases} \quad (9.155)$$

where we have yet to determine the two joining points which lie in the intervals

$$-2.244 < \delta^1_{N-2}(3) < -2.221$$

$$68.042 < \delta^1_{N-2}(10) < 68.111 \quad .$$

Some of the unconstrained costs in (9.155) and their corresponding control laws can be easily obtained analytically. In particular the optimal controller endpieces are

$$V^{1,U}_{N-2}(x_{N-2},1) = (.56088)\, x^2_{N-2} + 3.45307$$

$$u^{1,U}_{N-2}(x_{N-2},1) = -(.56088)\, x_{N-2}$$

$$V^{11,U}_{N-2}(x_{N-2},1) = (.72145)\, x^2_{N-2} + 4.5366$$

$$u^{11,U}_{N-2}(x_{N-2},1) = -(.72144)\, x_{N-2}$$

However, the other unconstrained cost pieces $V^{t,U}_{N-2}(t=2,\ldots,10)$ are harder to obtain. In particular, in order to analytically solve for $u^{7,U}_{N-2}$ and $V^{7,U}_{N-2}$ (as functions of x_{N-2}), we must solve a sixth degree polynomial in u which must in general be done numerically.

However, we can numerically obtain the value of the optimal control and expected cost-to-go for <u>any</u> x_{N-2}. Therefore we can determine the optimal controller for as fine a mesh of x_{N-2} values as desired.

The procedure for doing this is as follows:

1. For intervals of x_k values where a constrained cost ($V_k^{t,L}(x_k,j)$ or $V_k^{t,R}(x_k,j)$) is optimal we obtain $u_k(x_k,j)$ and $V_k(x_k,j)$ directly from (1) - (2) of Proposition 9.2.

2. For intervals where an unconstrained cost $V_k^{t,U}(x_k,j)$ is optimal we obtain $u_k(x_k,j)$ and $V_k(x_k,j) = V_k^{t,U}$ as follows:

(i) for arbitrarily chosen z_{k+1} values in the constraint region $(\hat{\gamma}_{k+1}^{j}(t-1), \hat{\gamma}_{k+1}^{j}(t))$ find u_k from (9.126):

$$u_k = \frac{-b(j)}{2R(j)} \left. \frac{\partial \hat{\hat{V}}_{k+1}^{j}(z;t)}{\partial z} \right|_{z=z_{k+1}}$$

Since we have $\hat{\hat{V}}_{k+1}^{j}(z_{k+1};t)$, we can differentiate (numerically or analytically) to obtain the above quantity,

(ii) We then find the x_k value that corresponds to obtaining $z_{k+1}^{t,U}(x_k,j) = z$ with this u_k:

$$x_k = z - u_k$$

(iii) We can then obtain the corresponding value of $V_k^{t,U}(x_k,j)$ from (9.128):

$$V_k^{t,U}(x_k,j) = u_k^2 + \hat{\hat{V}}_{k+1}^{j}(z;t)$$

for this z and u_k value.

We repeat this procedure for as many x_k values as needed.

We can use this procedure with each candidate cost in block 102 (of figure 9.12) to determine the intersections of candidate costs. Applying this procedure to example 9.2 we obtain the optimal control, expected cost-to-go and resulting z_{N-1} value for a number of x_{N-2} values, as shown in tables 9.6 - 9.7. The joining points resulting from crossing candidate cost are found to be approximately

$$\delta^1_{N-1}(3) \approx -2.233$$

$$\delta^1_{N-2}(10) \approx 68.10 \ .$$

From tables 9.6, 9.7 we see that the optimal control law $u_{N-2}(x_{N-2}, r_{N-2}=1)$ is <u>discontinuous</u> at

$$x_{N-2} = \delta^1_{N-2}(3) \approx -2.233$$

$$x_{N-2} = \delta^1_{N-2}(1) \approx 68.10 \ .$$

Associated with each control law discontinuity is a region of z_{N-1} avoidance:

$$(-1.005, \ -.996) \quad \text{and} \quad (18.863, \ 18.882) \ .$$

We also note that $V_{N-2}(x_{N-2}, r_{N-2}=1)$ has its minimum value near $x_{N-2} = -.2204$. Evaluating $V_{N-2}(x_{N-2}, r_{N-2}=1)$ for x_{N-2} near -.2204, we find that the minimizing x_{N-2} is

$$x_{N-2} \approx -.26$$

with

$$u_{N-2} = -.003 \qquad \text{and } V_{N-2} = 4.28517.$$

□

x_{N-2}	u_{N-2}	z_{N-2}	$V_{N-2}(x_{N-2}, r_{N-2}=1)$
-20	11.2167	-8.7833	227.806
-12	6.7300	-5.2694	84.213
$-10.817 = \delta^1_{N-2}(1)$	6.0665	-4.75	69.075
-10	5.7938	-3.933	60.032
- 8	4.4650	-3.535	36.004
- 7	3.8861	-3.1139	31.040
$-6.278 = \delta^1_{N-2}(2)$	3.4651	-2.813	25.732
- 5.581	3.0809	-2.5	21.168
- 3.344	1.8443	-1.5	10.151
- 2.243	1.2337	-1.010	6.763
$-2.233^- \approx \delta^1_{N-2}(3)^-$	1.2275	-1.005	6.73
$-2.233^+ \approx \delta^1_{N-2}(3)^+$	1.2379	-.996	6.73
- 2.114	1.1644	-.95	6.482
- 1.984	1.0838	-.90	6.158
$-1.587 = \delta^1_{N-2}(4)$	.8371	-.75	5.395
-.9117	.4117	-.5	4.551
-.2204	-.0296	-.25	4.287
-.0802	-.1198	-.2	4.308
.2021	-.3021	-.1	4.427
.4869	-.4869	0	4.651
1.2102	-.9602	.25	5.697
1.9493	-1.449	.5	7.478

Table 9.6: Optimal Controller at Time k=N-2 for Example 9.2 (Part I)

x_{N-2}	u_{N-2}	z_{N-2}	$V_{N-2}(x_{N-2}, r_{N-2}=1)$
3.4756	- 2.476	1	13.463
4.0628 = $\delta^1_{N-2}(5)$	- 2.876	1.187	16.605
4.2743	- 3.024	1.25	17.849
6.8866	- 4.887	2	38.491
10.639 = $\delta^1_{N-2}(6)$	- 7.639	3	85.44
10.662 = $^1_{N-2}(7)$	- 7.662	3	85.79
14.229	-10.229	4	149.62
17.792	-12.792	5	231.64
21.351	-15.351	6	331.79
21.582 = $\delta^1_{N-2}(8)$	-15.517	6.065	338.93
24.916	-17.916	7	450.29
28.504	-20.50	8	588.12
35.987 = $\delta^1_{N-2}(9)$	-25.92	10.065	935.52
40	-28.84	11.164	1155.4
50	-36.10	13.904	1804.7
68.042	-49.19	18.847	3343.5
68.10^- $\delta^1_{N-1}(10)^-$	-49.24	18.863	3349.2
68.10^+	-49.22	18.882	3349.2
68.111	-49.23	18.885	3350.3
70	-50.58	19.422	3538.8
75	-54.15	20.849	4062.5
82.089 = $\delta^1_{N-2}(11)$	-59.20	22.886	4866.1
90	-64.93	25.07	5848.3
100	-72.14	27.86	7219.0

Table9.7 : Optimal Controller at time k=N-2 for Example 9.2 (Part II)

It is important to note that we can obtain the optimal controller for any JLPC problem of this chapter in the manner demonstrated for example 9.2. However, a large number of numerical calculations may be necessary in order to accurately approximate the optimal controller, and the resulting controller may not be easy to implement. In the next section we will consider a suboptimal approximation of the JLPC controller.

9.9 Suboptimal Approximations of the Optimal Controller

The algorithm for determining the optimal controller of section 9.7 and illustrated in section 9.8 allows us to obtain (or to numerically approximate arbitrarily well) the optimal controller for any noisy JLPC problem. However, this controller may have certain undesirable properties. Specifically,

- it may be too difficult (i.e., require too many calculations) to perform all of the analytical and/or numerical tasks required to derive the optimal controller

  the resulting controller may be too complicated for cost-effective implementation.

Consider the example described in the previous section at time stage k=N-2. If we need to obtain the optimal control law for a fine mesh of x_{N-2} values then the number of calculations may be prohibitive. Implementation of the optimal controller for x_{N-2} intervals where the optimal control law is not analytically available will require a "table look-up" operation (and interpolation for x_{N-2} values between table entries) in order to determine the control input to be applied for any encountered x_{N-2}. These implementation tasks may be too expensive or too time consuming to be economically feasible.

These difficulties motivate the development of a suboptimal approximation of the optimal controller that is easier to determine and implement. In this section we will consider a suboptimal approximation of the optimal controller that drives the system to one of a set of arbitrarily chosen z_{k+1} values. The basic idea is as follows:

- at each time stage k we designate a set of z_{k+1} values that the controller may hedge to from $(x_k, r_k=j)$. The cost of hedging from any

x_k to a specified z_{k+1} is quadratic in x_k. These quadratic costs are compared for each x_k, and the control law corresponding to the lowest one is chosen.

This approximation method yields a controller that has control laws that are piecewise-linear in x_k, and piecewise-quadratic expected costs-to-go. This is essentially a brute force approximation of the optimal controller. In principle, if we choose enough target z_{k+1} values at each time k, we can obtain arbitrarily good approximations. An open question is how to intelligently choose these target values. One reasonable set of target choices are the discontinuous points of the z-conditional cost $\hat{V}_{k+1}(z_{k+1}|r_k=j)$, since we know that the optimal controller may hedge to such points. In the example below we have chosen these points and a grid of values in between. The performance of the suboptimal controller is unsatisfactory after two time stages. At least for special classes of JLPC problems, it should be possible to use knowledge of the structure of the problem to obtain a better approximation of the optimal controller. We have not addressed the topic of approximation of the optimal JLPC controller in detail here.

This approximation of the optimal JLPC controller consists of the tasks specified in the flowcharts of figures 9.5-9.7 and 9.17, which can be summarized as follows:

1. The overall algorithm framework is described by figure 9.5, as in the optimal algorithm,
2. The x_{k+1}-conditional cost and x_{k+1} grid are obtained in figure 9.6 and block 27 of figure 9.7 as in the optimal algorithm except that the approximate $V_{k+1}(x_{k+1},r_{k+1}=i)$ (obtained in the preceeding iteration) is used instead of the true optimal cost.

3. The z_{k+1}-conditional cost $\hat{V}_{k+1}(z_{k+1}|r_k=j)$ is computed via figure 9.7, exactly as in the optimal algorithm (except that the $V_{k+1}(x_{k+1}\ r_k=j)$ from step 2 is used instead of the true one.

4. We then follow the steps of figure 9.17 (replacing figures 9.8-9.13) of the optimal controller derivation algorithm.

In table 9.8 we list the block numbers of the flowchart for this approximation scheme. The circled numbers in the table refer to points where the flowchart control path enters and leaves the different figures.

Figure Number	Block Numbers	Entry Points	Exit Points
9.5	1-13	start (block 1)	stop (block 12)
9.6	14-26	from block 10	(1) (block 22)
9.7	27-42	(1) (block 27)	(2) (block 33)
9.17	43-59	(2) (block 43)	block 59

Table 9.8: Block number locations, entry points and exit points for sub-optimal approximate controller derivation.

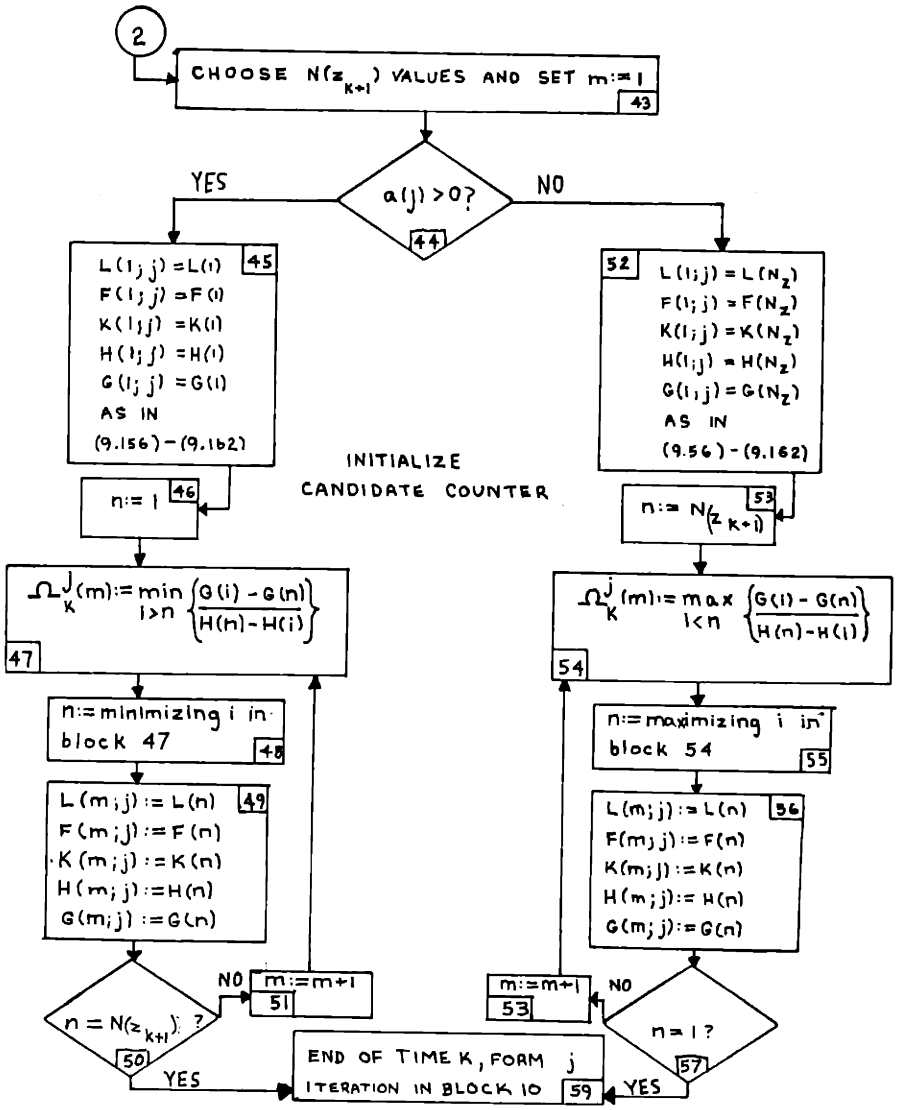

Figure 9.17: Calculating and Comparing Candidate Costs in the Suboptimal Approximation of the JLPC Optimal Controller.

Let us now consider the suboptimal approximation method in detail. At each time stage k and in each form $j \in \underline{M}$ we begin by calculating the z_{k+1} cost $V_{k+1}(z_{k+1} \; r_k=j)$ via the steps specified in figure 9.7. This $\hat{\hat{V}}_{k+1}(z_{k+1} \mid r_x=j)$ is based upon the <u>approximate</u>[1] expected cost-to-go $\tilde{V}_{k+1}(x_{k+1}, r_k=j)$ (computed in the preceeding iteration).

In the process of determining $\hat{\hat{V}}_{k+1}(z_{k+1} \mid r_k=j)$ in figure 9.7 we also obtain the partition grid-points $\{\gamma(1), \ldots, \gamma(L)\}$. Note that for this suboptimal controller we do not need to differentiate $\hat{\hat{V}}_{k+1}(z_{k+1} \mid r_k=j)$, nor do we have to add the extra z_{k+1} partition grid points that are used in the optimal controller derivation (in figure 9.8).

As we indicated above, the basic approximation idea is to calculate and compare the costs associated with hedging to each member of a set of specified z_{k+1} values. Included in this list z_{k+1} grid points (obtained in figure 9.7) where $\hat{\hat{V}}_{k+1}(z_{k+1} \mid r_k=j)$ is discontinuous. Let $N(z_{k+1})$ denote the number of these target z_{k+1} values; that is, we designate a list[2] of values $\{z_{k+1} = z(i): i = 1, \ldots, N(z_{k+1})\}$ that the system is <u>required</u> (by our suboptimal approximation) to hedge to. This list of target points includes the discontinuous points of the z-conditional cost (where we know that the true optimal controller may hedge to) and we have chosen additional target points in between. (hopefully enough for a good approximation). For each of these target points z(i), the control law

$$u(i) = -L(i)\; x_k + F(i) \tag{9.156}$$

---

[1] The symbol $\sim$ is used to denote approximations in this section.

[2] ordered from left to right; i.e., z

drives the system to $z_{k+1} = z(i)$ from any $(x_k, r_k=j)$ with the resulting quadratic cost

$$V(i) = K(i)x_k^2 + H(i)x_k + G(i) \tag{9.157}$$

where the coefficients in (9.157) are

$$L(i) = a(j)/b(j) \tag{9.158}$$

$$F(i) = z(i)/b(j) \tag{9.159}$$

$$K(i) = a^2(j)\ R(j)/b^2(j) \tag{9.160}$$

$$H(i) = -2a(j)R(j)z(i)/b^2(i) \tag{9.161}$$

$$G(i) = z^2(i)R(j)/b^2(j) + V_{k+1}(z(i)\ r_k=j) \quad . \tag{9.162}$$

Note that the index i in (9.156)-(9.162) refers to the target point z(i). The parameters F(i), H(i) and G(i) here depend upon z(i). Note that G(i) (and hence V(i)) is not quadratic in z; however V(i) is quadratic in x_k. This is the motivation for this approximation scheme; we are obtaining a quadratic controller structure by evaluating $V_{k+1}(z(i)\ r_k=j)$ only at specific points.

For each x_k value we choose $\tilde{u}_k(x_k, r_k=j)$ to be the control law in (9.156) that yields the least expected cost in (9.157). To do this we must find the intersections of the costs $V(i): i=1,\ldots,N(z_{k+1})$ in (9.157). That is, we obtain the approximate controller expected cost $V_k(x_k, r_k=j)$ via the minimization

$$V_k(x_k, r_k=j) = \min_{i\ =\ 1,\ldots,N(z_{k+1})} \left\{ V(i) \right\} \tag{9.163}$$

at each x_k value. Consequently the approximate controller cost $\tilde{V}_k(x_k, r_k=j)$ is piecewise-quadratic in x_k. Consider now the minimization

in (9.163). From (9.157), V(i) intersects V(j) at

$$x_k = \frac{G(j) - G(i)}{H(i)-H(j)} \quad . \qquad (9.164)$$

Therefore we can solve (9.163) for all x_k by determining the intersections of the V(i) using (9.164). Following the basic idea of the controller algorithms of chapters 7-9, we need not solve for all of these intersections. For x_k sufficiently negative, the lowest cost in $\{ V(i) : i = 1,\ldots,N(z_{k+1}) \}$ will be V(1) (that is, the leftmost target value is hedged to), when $a(j)>0$ (or the rightmost when $a(j)<0$).

We then sweep rightward along the axis of $a(j)x_k$ values. At some value one of the other V(j) costs in (9.157) will intersect V(1) and will then become the prevailing optimal cost until it in turn is intersected by another cost. Since the mapping

$$x_k \longmapsto z_{k+1}$$

is monotone nondecreasing for $a(j) > o$ we need only consider the intersections of the prevailing cost V(n) with $V(n+1),\ldots,V(N(z_{k+1}))$.

This suboptimal controller will consist of $\tilde{m}_K(j)$ pieces (at time k from form j), where $\tilde{m}_K(j)$ increases at most linearly with the number of target z_{k+1} values, $N(z_{k+1})$.

The computational and implementation advantages of this suboptimal controller, relative to the optimal JLPC controller derivation algorithm, are as follows: for the approximate controller

1. We need not compute the functions

$$\frac{\partial \hat{\hat{V}}_{k+1}(z_{k+1}|r_k=j)}{\partial z_{k+1}} \quad , \quad \frac{\partial^2 \hat{\hat{V}}_{k+1}(z_{k+1}|r_k=j)}{(\partial z_{k+1})^2} \quad .$$

2. We need not determine (analytically or numerically) any of the $V_k^{t,U}$ costs, nor do we have to determine a θ-$\dot{\theta}$ grid as in figure 9.10.

3. The candidate cost functions are all quadratic in x_k, so it is easy to determine their intersections.

4. The suboptimal control law is piecewise-linear, unlike the optimal controller; thus the suboptimal controller will often be easier to implement.

5. The suboptimal controller has the same type of structure (i.e., piecewise-linear control laws) at each time stage, unlike the (in general) changing structure of the optimal controller. This also facilitates implementation of the suboptimal controller.

6. The suboptimal controller specifies a control input for every x_k. The numerical implementation of the optimal JLPC controller (as in the previous section) requires interpolation between stored values.

To illustrate this suboptimal controller we apply it to two time stages (example 9.2) and compare the resulting controller with the optimal controllers obtained in section 9.8.

Example 9.5: (Applying Suboptimal Approximation to Example 9.2)

In the previous section we found that at time k=N-1 the optimal JLPC controller for example 9.2 has five pieces. One of these pieces involves a control law that is nonlinear in x_{n-1}. Let us now consider the suboptimal approximation of this controller that is specified by figures 9.5-9.7, 9.17. In section 9.3 we obtained (9.146):

$$V_N(z_N | r_{N-1}=1) = \begin{cases} \frac{7}{4} z_N^2 + \frac{7}{3} & \text{if } z_N < -1 \\ \frac{-1}{8} z_N^3 + \frac{5}{2} z_N^2 - \frac{3}{2} z_N + \frac{83}{24} & \text{if } -1 < z_N < 3 \\ \frac{13}{4} z_N^2 + \frac{13}{3} & \text{if } 3 < z_N \end{cases}$$

This z_n-conditional cost was obtained via the steps of figures 9.5 - 9.7. In order to apply the approximation technique of figure 9.17 we must choose a set of $N(z_N)$ target values of z_N to which the suboptimal controller is constrained to hedge. In table 9.9 we list a set of $N(z_N) = 34$ such values. Note that we have included the values of z_N where $V_N(z_N\ r_{N-1}=1)$ is discontinuous (ie, -1^-, -1^+, 3^- and 3^+). The remaining points have been chosen arbitrarily.

Following the instructions of figure 9.17 we obtain the following approximation of the optimal JLPC controller for example 9.2 at time k=N-1:

$$\tilde{V}_{N-1}(x_{N-1}, r_{N-1}=1) = x_{N-1} + H_{N-1}(t:1) x_{N-1} + G_{N-1}(t:1) \qquad (9.165)$$

$$\tilde{u}_{N-1}(x_{N-1}, r_{N-1}=1) = -x_{N-1} + F_{N-1}(t:1) \qquad (9.166)$$

$$\tilde{z}_{N-1}(x_{N-1}, r_{N-1}=1) = F_{N-1}(t:1) \qquad (9.167)$$

$$\text{for } \Omega_{N-1}(t-1) \quad x_{N-1} \quad \Omega_{N-1}(t)$$

$$t = 1, \ldots, \tilde{m}_{N-1}(1)$$

where the parameters in (9.165)-(9.167) are as defined in (9.157)-(9.162) and the $\{\Omega_{N-1}(t)\}$ are determined in blocks 47 or 54 of figure 9.17. In table 9.10 we list the parameters for this example when the z_N grid of table 9.9 is used. Here $\tilde{m}_{N-1}(1) = 25$. That is, the approximate controller has 25 pieces at time k = N-1.

i	z(i)	i	z(i)
1	-6	18	.75
2	-3	19	1
3	-2.75	20	1.25
4	-2.5	21	1.5
5	-2.25	22	1.75
6	-2	23	2
7	-1.75	24	2.25
8	-1.5	25	2.5
9	-1.25	26	2.75
10	$-1^- = \gamma_N'(1)^-$	27	$3^- = \gamma_N'(2)^-$
11	$-1^+ = \gamma_N'(1)^+$	28	$3^+ = \gamma_N'(2)^+$
12	-7.5	29	3.25
13	- .5	30	3.5
14	- .25	31	3.75
15	0	32	4
16	.25	33	5
17	.5	34	10

Table 9.9: The $N(z_N) = 34$ target z_N values at time $k = N-1$ in example 9.5.

$V_{N-2}(x_{N-2}, r_{N-2}=1)$ piece, t	H(t;1)	G(t;1)	target $z_N=F(t;1)$	$\Omega_{N-1}(t)$	choice of i
1	30	782.43	-15	- 43.23	1
2	20	350.17	-10	- 30.34	2
3	15	198.98	- 7.5	- 21.62	3
4	10	90.380	- 5	- 16.86	4
5	9.5	81.949	- 4.75	- 13.39	5
6	6	35.075	- 3	- 8.626	6
7	4	17.824	- 2	- 5.140	7
8	2	7.5437	- 1	- 2.627	8
9	1.5	6.2298	- .75	- 1.949	9
10	1.28	5.8009	- .64	- .5153	10
11	0	5.1414	0	1.069	11
12	- .34	5.5033	.17	2.968	12
13	- 1.9	10.133	.95	5.052	13
14	- 2374	12.528	1.187	6.691	14
15	- 3.42	19.526	1.71	9.408	15
16	- 4.88	33.262	2.44	11.24	16
17	- 5.07	35.398	2.535	12.51	17
18	- 6	47.032	3	13.61	18
19	- 6.3	51.116	3.15	15.42	19
20	- 7.68	72.396	3.84	17.75	20
21	-10.28	118.55	5.14	27.02	22
22	-12.13	168.54	60.65	28.12	23
23	-14	221.12	7	32.02	24
24	-16	285.16	8	36.03	25

Table 9.10: Suboptimal Controller of Example 9.5 at k = N-1.

Comparing the hedging behavior of the optimal JLPC controller (see figure 9.16) and the suboptimal controller of table 9.10, we see that

- The optimal controller hedges to $z_N=-1^-$ for $-2.75 < x_{N-1} < .8125$; the suboptimal controller hedges to $z_N=-1^-$ for $-2.226 < x_{N-1} < -.8125$
- The optimal controller hedges to $z_N=3^-$ for $8.0625 < x_{N-1} < 20.866$; the suboptimal controller hedges to $z_N=3^-$ for $7.762 < x_{N-1} < 20.875$.

At time stage k=N-1 the optimal controller (see (9.148)) has $m_{N-1}(1)=6$ pieces, one of which is not linear in x_{N-1}. The approximate controller has $\tilde{m}_{N-1}(1)=25$ pieces, but all are linear in x_{N-1}. Of course, we can reduce the number of pieces in the suboptimal controller by reducing the number of grid points.

In table 9.11 we list the optimal and approximate controls, expected costs and resulting z_N values for various x_{N-1} values. Note that the percentage of excess cost incurred using the suboptimal controller is small for all of these values. As $|x_{N-1}|$ becomes large, the error will become large since the suboptimal controller drives z_N to either -6 or +10 (the extreme values of the target grid). However for x_{N-1} within the interval of interest, the suboptimal controller is quite accurate at this first time stage.

Let us now apply the suboptimal controller to time stage k = N-2. Using the approximate expected cost-to-go we obtain an approximate $\tilde{\tilde{V}}_{N-1}(z_{N-1}|r_{N-2}=1)$ which has the structure

$$\tilde{\tilde{V}}_{N-1}(z_{N-1}|r_{N-1}=1) = W_3(t)z_{N-1}^3 + W_2(t)z_{N-1}^2 + W_1(t)z_{N-1} + W_o(t) \qquad (9.168).$$

$$\tilde{\tilde{\gamma}}_{N-1}(t-1) < z_{N-1} < \tilde{\tilde{\gamma}}_{N-1}(t)$$

	OPTIMAL CONTROLLER			SUBOPTIMAL CONTROLLER			% increase in cost of suboptimal
x_{N-1}	u_{N-1}	z_{N-1}	V_{N-1}	$\tilde{u}_{N-1}$	$\tilde{z}_{N-1}$	$\tilde{V}_{N-1}$	
-15	9.545	-5.4545	145.52	9	-6	146.33	.557
-10	6.364	-3.6364	65.970	7	-3	67.08	2.774
- 5	3.182	-1.8182	18.242	3.25	-1.75	18.33	1.68
- 3	1.909	-1.0909	8.0606	2	-1^-	8.08	.241
-2.75^-	1.75	-1^-	7.1458	1.75	-1^-	7.1458	0
-2.75^+	1.75	-1^-	7.1458	1.75	-1^-	7.1458	0
- 2	1	-1^-	5.0833	1	-1^-	5.0833	0
- 1.5	.5	-1^-	4.3333	.5	-1^-	4.3333	0
- 1	0	-1^-	4.0833	0	-1^-	4.0833	0
$-.8125^-$	- .187	-1^-	4.1183	- .187	-1^-	4.1183	0
$-.8125^+$	.795	- .0178	4.1176	.8125	0	4.1182	.015
- .5	.572	.0717	3.6906	.5	0	3.708	.471
0	.2168	.2168	3.2966	.25	.25	3.300	.103
.5	- .1357	.3643	3.2562	- .25	.25	3.300	1.345
1	- .4858	.5142	3.5672	- .5	.5	3.568	.022
1.5	- .8333	.6667	4.2270	- .75	.75	4.249	.520
2	- 1.178	.8219	5.2330	- 1.25	.75	5.249	.306
5	- 3.180	1.820	18.368	- 3.25	1.75	18.38	.065
8.0625^-	- 5.0625	3^-	43.712	- 5.0625	3^-	43.712	0
8.0625^+	- 5.0625	3^-	43.712	- 5.0625	3^-	43.712	0
10	- 7	3^-	67.083	- 7	3^-	67.083	0
15	-12	3^-	162.08	-12	3^-	162.08	0
20.866^-	-17.866	3^-	337.28	-17.866	3^-	337.28	0
20.866^+	-15.956	4.9096	337.28	-15.866	5	337.33	.015
25	-19.118	5.8823	482.28	-20	5	485.6	.688

Table 9.11: Performance of the optimal and suboptimal controller at various x_{N-1} values.

This approximate cost is computed via the steps of figure 9.7. It has $\tilde{\tilde{\psi}}_{N-1} = 51$ pieces which are listed in table 9.12. Note that each piece of this approximate z_{N-1} cost is either quadratic or cubic in z_{N-1}. This is similar to $\hat{\hat{V}}_N(z_N | r_{N-1}=1)$, which has quadratic and cubic pieces in z_N. In section 9.8 we found that the true z_{N-1} cost $\hat{V}_{N-1}(z_{N-1} | r_{N-2}=1)$ has many fewer pieces than this approximate version has, and several of the true cost pieces have complicated terms such as

$$[(-.00625)z_N + .08489]\sqrt{(72.44-5.33z_{N-1})}^3$$

in them. Thus we see that for this example the approximate z_{N-1} cost has more pieces, but a simpler structure. At successive time stages the true z_k-cost $\hat{\hat{V}}_k(z_k | r_{k-1}=j)$ will have even more complicated pieces; the approximate cost $\tilde{\tilde{V}}_k(z_k | r_{k-1}=j)$ will always have pieces that are at most cubic in z_k. Note that in this example $\tilde{\tilde{\tilde{V}}}_{N-1}(z_{N-1} | r_{N-2}=1)$ is continuous in z_{N-1}. Therefore we have no specific values to include in the target set of z_{N-1} values.

The next step in the determination of the suboptimal controller is the selection of a set of $N(z_{N-1})$ values. In table 9.13 a set of $N(z_{N-1}) = 34$ such values have been arbitrarily chosen. Following the steps of figure 9.17 we obtain the following approximation of the optimal controller for example 9.2 at time k = N-2.

$$\tilde{V}_{N-2}(x_{N-2}, r_{N-2}=1) = x_{N-2}^2 + H_{N-2}(t:1)x_{N-2} + G_{N-2}(t:1) \qquad (9.169)$$

$$\tilde{u}_{N-2}(x_{N-2}, r_{N-2}=1) = -x_{N-2} + F_{N-2}(t:1) \qquad (9.170)$$

$$\tilde{z}_{N-1}(x_{N-2}, r_{N-2}=1) = F_{N-2}(t:1) \qquad (9.171)$$

$$\text{for } \Omega_{N-2}(t-1) < x_{N-2} < \Omega_{N-2}(t)$$

$$t = 1, \ldots, \tilde{m}_{N-2}(1)$$

where the parameters in (9.169)-(9.171) are as defined in (9.157)-(9.162) and the $_{N-1}(t)$ are defined in blocks 47, 54 of figure 9.17. In table 9.15 we list the parameters for this example when the z_{N-2} grid of table 9.13 is used. Here $m_{N-2}(1) = 33$. That is, the suboptimal approximate controller has 33 pieces at time k = N-2. The suboptimal controller described in table 9.14 has almost three times as many pieces as the optimal controller. However all of the suboptimal controller pieces are linear control laws in x_{N-2}. Many of the optimal control law pieces are difficult or impossible to obtain analytically.

In section 9.8 we obtained numerically the optimal control law, expected cost and attained z_{N-1} value for each item in a set of x_{N-2} values (see table 9.6). In table 9.15 we compare the suboptimal controller's behavior at these x_{N-2} values. Note that with the 34 target values that we have arbitrarily chosen (in table 9.13), the resulting suboptimal has large errors for all x_{N-2} values (20%-30%). Thus the error at the second time stage is an order of magnitude greater than at k = N-1. In order to reduce this error we can increase the density of the z_{k+1} grid , but this increases the complexity of the approximate controller.

The approximate controller described in this section is a brute force approach to obtaining an approximation of the optimal JLPC controller that has an easily implementable structure. As we have seen, this approximation is prone to large errors after only two time steps. We have not considered more successful approximation methods in detail here.

t	$W_3(t)$	$W_2(t)$	$W_1(t)$	$W_o(t)$	$\tilde{\tilde{\gamma}}_{N-1}(t)$
1	---	2.55	3	28.7325	-14.375
2	---	2.3625	-2.3906	-10.0126	-10.375
3	---	2.55	1.5	10.17	- 9.906
4	---	2.5344	1.1906	8.6386	- 9.219
5	---	2.5188	.9025	7.3103	- 8.531
6	---	2.5031	.6363	6.2074	- 7.844
7	---	2.4875	.3906	5.2421	- 7.156
8	---	2.4719	.1694	4.4589	- 6.462
9	---	2.4563	- .0331	3.8032	- 5.906
10	---	2.4719	.1513	4.3471	- 5.7813
11	---	2.4563	- .0294	3.8248	- 5.219
12	---	2.4719	.1338	4.2505	- 5.0937
13	---	2.4563	- .0254	3.8451	- 4.531
14	---	2.4719	.1158	4.1643	- 3.844
15	---	2.4875	.2364	4.3971	- 3.156
16	---	2.5031	.3346	4.5512	- 2.8125
17	---	2.4875	.1705	4.2133	- 2.462
18	---	2.5031	.2479	4.3093	- 2.316
19	---	2.4875	.1756	4.2255	- 1.7813
20	---	2.5031	.2313	4.2751	- 1.465
21	---	2.4875	.1855	4.2416	- 1.0937
22	---	2.5031	.2197	4.2603	- 1
23	.0917	2.9906	1.5157	5.1605	- .64
24	.0917	2.9438	1.4559	5.1414	.17
25	.0917	2.8969	1.4711	5.1401	.95
26	.0917	2.85	1.5607	5.0973	1.1875

Table 9.12, Part I: Parameters for approximate z_{N-1} cost $\tilde{\tilde{V}}_{N-1}(z_{N-1} | r_{N-2}=1)$ in example 9.5.

t	$W_3(t)$	$W_2(t)$	$W_1(t)$	$W_0(t)$	$\hat{Y}_{N-1}(t)$
27	.0917	2.8656	1.5997	5.0289	1.684
28	.0917	2.8813	1.5471	5.0732	1.71
29	.0917	2.8344	1.7071	4.9368	2.44
30	.0917	2.7875	1.9356	4.6581	2.535
31	.0917	2.8031	1.8564	4.7610	3
32	---	3.4156	.0604	7.1115	3.15
33	---	3.3688	.3566	6.6433	3.36
34	---	3.3844	.1664	7.1060	3.84
35	---	3.3375	.5264	6.4148	4.17
36	---	3.3531	.2612	7.2489	4.50
37	---	3.3063	.6831	6.2997	4.95
38	---	3.3219	.3435	7.5980	5.14
39	---	3.275	.8254	6.3596	5.71
40	---	3.2906	.4154	8.1909	5.76
41	---	3.2438	.9554	6.6357	6.44
42	---	3.2594	.4769	9.0696	7.15
43	---	3.275	- .0694	12.1765	7.84
44	---	3.2906	- .6794	15.9985	8.50
45	---	3.3063	-1.3513	20.5806	9.14
46	---	3.3219	-2.0831	25.9646	9.76
47	---	3.3375	-2.8731	32.1866	18.866
48	---	3.2906	12.5994	-243.034	22.866
49	---	3.3063	-3.1231	108.308	29.88
50	---	3.2594	56.4456	-1629.76	33.88
51	---	3.275	-3.3731	378.968	---

Table 9.12, continued .

i	z(i)	i	z(i)
1	-15	18	3
2	-10	19	3.15
3	- 7.5	20	3.84
4	- 5	21	4.50
5	- 4.75	22	5.14
6	- 3	23	6.065
7	- 2	24	7
8	- 1	25	8
9	- .75	26	9
10	- .64	27	10.065
11	0	28	13
12	.17	29	15
13	.95	30	18.866
14	1.187	31	22.866
15	1.71	32	25
16	2.44	33	30
17	2.535	34	35

Table 9.13: The $N(z_{N-1}) = 34$ target z_{N-1} values at time $k = N-2$ in example 9.5.

$V_{N-2}(x_{N-2}, r_{N-2}=1)$ piece, t	H(t;1)	G(t;1)	target $z_N=F(t;1)$	$\Omega_{N-1}(t)$	choice of i
1	30	782.43	-15	- 43.23	1
2	20	350.17	-10	- 30.34	2
3	15	198.98	- 7.5	- 21.62	3
4	10	90.380	- 5	- 16.86	4
5	9.5	81.949	- 4.75	- 13.39	5
6	6	35.075	- 3	- 8.626	6
7	4	17.824	- 2	- 5.140	7
8	2	7.5437	- 1	- 2.627	8
9	1.5	6.2298	- .75	- 1.949	9
10	1.28	5.8009	- .64	- .5153	10
11	0	5.1414	0	1.069	11
12	- .34	5.5033	.17	2.968	12
13	- 1.9	10.133	.95	5.052	13
14	- 2374	12.528	1.187	6.691	14
15	- 3.42	19.526	1.71	9.408	15
16	- 4.88	33.262	2.44	11.24	16
17	- 5.07	35.398	2.535	12.51	17
18	- 6	47.032	3	13.61	18
19	- 6.3	51.116	3.15	15.42	19
20	- 7.68	72.396	3.84	17.75	20
21	-10.28	118.55	5.14	27.02	22
22	-12.13	168.54	60.65	28.12	23
23	-14	221.12	7	32.02	24
24	-16	285.16	8	36.03	25
25	-18	357.23	9	40.12	26
26	-20.13	442.68	10.065	48.59	27
27	-26	727.87	13	59.29	28
28	-30	965.03	15	74.58	29
29	-37.732	1541.7	18.866	93.34	30
30	-45.732	2288.4	22.866	101.5	31
31	-50	2721.7	25	117.5	32
32	-60	3897.1	30	160.1	33
33	-70	5497.8	35	---	34

Table 9.14: Suboptimal controller of example 9.5 at time k = N-2.

	OPTIMAL CONTROLLER			SUBOPTIMAL CONTROLLER			
x_{N-2}	u_{N-2}	z_{N-2}	V_{N-2}	u_{N-2}	z_{N-2}	V_{N-2}	% increase in cost of suboptimal controller
3.4756	- 2.476	1	13.463	- 2.526	.95	15.61	15.94
4.0628	- 2.876	1.187	16.605	- 3.113	.95	18.92	13.94
4.2743	- 3.024	1.25	17.849	- 3.324	.95	20.28	13.61
6.8866	- 4.887	2	38.491	- 5.177	1.71	43.40	12.75
10.639	- 7.639	3	85.44	- 8.199	2.44	94.53	10.64
10.662	- 7.662	3	85.79	- 8.222	2.44	94.91	10.63
14.229	-10.229	4	149.62	-11.079	3.15	163.9	9.57
17.792	-12.792	5	231.64	-12.652	5.14	252.2	8.88
21.351	-15.351	6	331.79	-16.211	5.14	354.9	6.97
21.582	-15.517	6.065	338.93	-16.44	5.14	362.5	6.95
24.916	-17.916	7	450.29	-19.78	5.14	483.2	7.31
28.504	-20.50	8	588.12	21.50	7	634.5	7.89
35.987	-25.92	10.065	935.52	-27.99	8	1004.4	7.37
40	-28.84	11.164	1154.4	-32	8	1245.2	7.77
50	-36.10	13.904	1804.7	-37	13	1927.9	6.82
68.042	-49.19	18.847	3343.5	-53.04	15	3553.4	6.28
68.10^{-}	-49.24	18.863	3349.2	-53.1	15	3559.6	6.28
68.10^{+}	-49.22	18.882	3349.2	-53.1	15	3559.6	6.28
68.111	-49.23	18.885	3350.3	-53.1	15	3560.1	6.28
70	-50.58	19.422	3538.8	-55	15	3765.0	6.39
75	-54.15	20.849	4062.5	-56.13	18.87	4336.8	6.75
82.089	-59.20	22.886	4866.1	-63.22	18.87	5182.9	6.51
90	-64.93	25.07	5848.3	-71.13	18.87	6245.8	6.80
100	-72.14	27.86	7219.0	-81.13	18.87	7768.5	7.61

Table 9.15 , Part I: Performance of the optimal and suboptimal controller at various x_{N-1} values.

	OPTIMAL CONTROLLER			SUBOPTIMAL CONTROLLER			% increase in
x_{N-2}	u_{N-2}	z_{N-2}	V_{N-2}	u_{N-2}	z_{N-2}	V_{N-2}	cost of suboptimal controller
-20	11.2167	-8.7833	227.806	12.5	- 7.5	298.98	31.24
-12	6.7300	-5.2694	84.213	.9	- 3	107.075	27.15
-10.817	6.0665	-4.75	69.075	7.817	- 3	87.180	26.21
-10	5.7938	-3.933	60.032	7	- 3	75.075	25.06
- 8	4.4650	-3.535	36.004	6	- 2	49.824	38.38
- 7	3.8861	-3.1139	31.040	5	- 2	38.824	25.08
- 6.278	3.4651	-2.813	25.732	4.278	- 2	32.125	24.85
- 5.581	3.0809	-2.5	21.168	3.581	- 2	26.648	25.89
- 3.344	1.8443	-1.5	10.151	2.344	- 1	12.038	18.59
- 2.243	1.2337	-1.010	6.763	1.493	- .75	7.896	16.76
- 2.233	1.2275	-1.005	6.73	1.483	- .75	7.867	16.89
- 2.233^{+}	1.2379	- .996	6.73	1.483	- .75	7.867	16.89
- 2.114	1.1644	- .95	6.482	1.364	- .75	7.528	16.13
- 1.984	1.0838	- .90	6.158	1.234	- .75	7.190	16.76
- 1.587	.8371	- .75	5.395	.947	- .64	6.288	16.55
- .9117	.4117	- .5	4.551	.2717	- .64	5.465	20.09
- .2204	- .0296	- .25	4.287	.2204	0	5.110	21.06
- .0802	- .1198	- .2	4.308	.0802	0	5.148	19.49
.2021	- .3021	- .1	4.427	- .2021	0	5.182	17.06
.4869	- .4869	0	4.651	- .4869	0	5.378	15.64
1.2102	- .9602	.25	5.697	- 1.04	.17	6.556	15.09
1.9493	-1.449	.5	7.478	- 1.779	.17	8.640	15.54

Table 9.16, continued.

9.10 Summary

In this chapter we have extended the solution methodology of chapters 5-8 to encompass jump linear control problems that involve additive input noise in the x-dynamics. The presence of additive input noise profoundly changes the nature of the optimal controller in that it is not possible to use the control input to drive the x process into a specified interval of values with certainty.

In extending the methodology of chapter 8 to include input noise we lose the piecewise-quadratic nature of the optimal controller. We have therefore relaxed the restrictions on the k-operating costs, x-terminal costs and from transition probabilities (requiring only a finite number of convex or concave pieces) because the piecewise-quadratic structure of the optimal controller cost is lost in any event.

In sections 9.2 - 9.7 we formulated the general JLPC control problem, obtained a general one-step solution procedure, investigated the qualitative properties of the optimal one-step solution, and presented an algorithm (flowchart) for the computation of the optimal controller for finite time-horizon problems. This algorithm was applied to two time stages of an example in section 9.8. In section 9.9 we developed a suboptimal JLPC approximation that results in controllers which have piecewise-linear control laws (in x_k), at all times $k=N-1,\ldots,k_o$. This suboptimal controller was applied to the example of section 9.8 and the optimal

and suboptimal controllers were compared.

In the next chapter we will consider the application of the methodology of this thesis to jump linear control problems possessing n-dimensional states with x-dependent and u-dependent form transitions and having form controls. These problems can be addressed using approximations similar to the approximation technique of section 9.9.

10. JUMP LINEAR CONTROL PROBLEMS WITH NONSCALAR x AND CONTROL-DEPENDENT FORM TRANSITIONS

10.1 Introduction

In part III and chapters 8-9 of this thesis we have developed and applied a basic approach for the solution of optimal jump linear feedback control problems. This methodology is based upon the following tactic:

- at each time stage k and from each form $r_k=j$, the control problem is broken up into a set of constrained subproblems that are relatively easy to solve.
- then the solutions of these constrained subproblems are compared at each x_k value to determine the optimal controller.

In this chapter we will briefly consider how this general solution approach can be applied to several other classes of jump linear control problems. Specifically, we will examine

- JLPC problems involving nonscalar x process (Section 10.2)
- JLPC problems involving u-dependent form transitions (Section 10.3)

and

- JLPQ (and JLPC) problems where the form process can be directly or indirectly controlled by a separate form control (Section 10.4).

Combining these extensions, we obtain the general control problem formulation that was introduced and motivated in detail in chapter 1. Our motivation for addressing these issues here is to demonstrate that the basic idea of this thesis can potentially be applied to

more realistic fault-tolerant optimal control problems. As we will see, each of these problems represents a generalization of the results of chapters 5-9 that involves an increase in complexity in both the optimal controller derivation and the implementation of the resulting control laws. However the basic solution approach of Part III remains valid for these problems and it yields methods for their solution.

10.2 Nonscalar x Processes

When the x-process in a JLQ,JLPQ or JLPC problem is n-dimensional, the basic solution idea of dividing the problem into constrained subproblems is still a valid one. However there are fundamental differences in the resulting subproblems.

The basic difference involves the nature of the subproblem constraints. Recall that in the problems of chapters 5-9 the optimal JLPC control problem is converted into the comparison of a set of subproblems constrained in x_{k+1} (or in z_{k+1} for noisy JLPC problems), which is determined by the control u_k when x_k and $r_k=j$ are known. The $\hat{\psi}^j_{k+1}$ different subproblems involve constraining z_{k+1} to be in a certain interval

$$\hat{\Delta}^j_{k+1}(t)=(\hat{\gamma}^j_{k+1}(t-1),\ \hat{\gamma}^j_{k+1}(t))$$

of values on the real number line. Thus the optimal solution of each subproblem either places z_{k+1} in the interior of the constraint interval $\hat{\Delta}_{k+1}(t)$ or on one of the (at most two) boundary points. When the x process is nonscalar, the constraint set $\hat{\Delta}^j_{k+1}(t)$ $\{t=1,..,\hat{\psi}^j_{k+1}\}$ for each subproblem is not an interval on the real line but, rather, a surface in n-space. If, for some $(x_k,r_k=j)$, the constraint in a particular subproblem is <u>active</u>, we must determine the best location

for z_{K+1} on the constraint surface. Thus we have uncountably many points to consider (instead of two).

A second complicating factor in the consideration of n-dimensional x-processes in JLQ, JLPQ or JLPC problems relates to the comparison of subproblem solutions (so as to determine the optimal control law for each x_k. In the scalar x case this involved finding the intersections of convex functions of x. Using the monotonicity property of the mapping

$$(x_k,\ r_k = j) \longmapsto z_{k+1}$$

in the scalar case (as in Proposition 9.6), only one such intersection needed to be found for some (but not all) pairs of valid, eligible candidate costs. For nonscalar x_k we must find the curves described by the intersection of valid, eligible candidate cost surfaces. This comparison was greatly simplified for scalar problems by the ordering of the real line. For n-dimensional problems the lack of as simple an ordering in n-space complicates matters. For some classes of problems there may be special orderings that facilitate detailed analysis. In particular ideas such as the endpiece and middlepiece (in scalar problems) appear to have natural extensions in nonscalar problems. Some of the difficulties involved with the analysis of these problems are illustrated in the following example:

These difficulties are illustrated in the following example;

Example 10.1: Consider the following control problem:

$$\min_{u_0,\ldots,u_{N-1}} E\left\{ \sum_{k=1}^{N} (u_k'R(r_k)u_k + x_{k+1}' Q(r_{k+1})x_{k+1}) + x_N'Q_N(r_N)x_N \right\} \tag{10.1}$$

where $R(j) > 0$, $Q(j) \geq 0$, $Q_N(j) \geq 0$ for $j = 1,2$ and

$$x_{k+1} = A(r_k)x_k + B(r_k)u_k \tag{10.2}$$

$$\text{Prob}\{r_{k+1} = j \mid r_k = i,\ x_{k+1} = x\} = p(i;j:x) \qquad r_k \in \{1,2\} \tag{10.3}$$

with form transition probabilities

$$p(2.1)=0$$

$$p(2,2)=1$$

$$p(1,2:x) = \begin{cases} \lambda_1 & \text{if } x'Sx < \alpha^2 \\ \lambda_2 & \text{if } x'Sx > \alpha^2 \end{cases}, \tag{10.4}$$

where $S=S' > 0$ is an $n*n$ matrix. In figure 10.1 we show the two form transition probability pieces in (10.4). Here $p(1,2:x)=\lambda_1$ if x is inside an n-dimensional ellipsoid centered at zero. For convenience we will assume that the x process has dimension n=2.

The conditional expected cost-to-go $\hat{V}_N(x_N \mid r_{N-1}=1) = \hat{\hat{V}}_N(z_N \mid r_{N-1}=1)$ is (here $z_N = x_N$ since there is no noise):

$$\hat{V}_N(x_N \mid r_{N-1} = 1) = \begin{cases} x_N'\hat{K}_N(1)x_N & \text{if } x_N'Sx_N < \alpha^2 \\ x_N'\hat{K}_N(2)x_N & \text{if } x_N'Sx_N > \alpha^2 \end{cases} \tag{10.5}$$

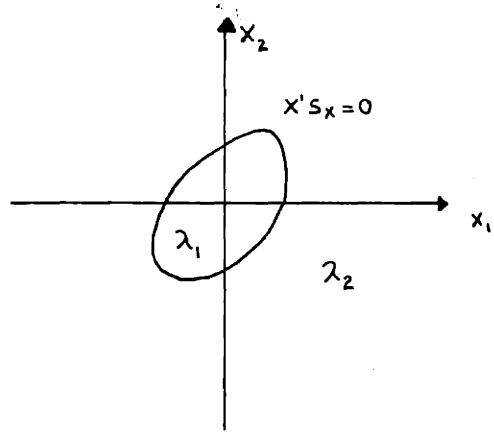

Figure 10.1: Form transition probability p(1,2:x) in example 10.1.

where

$$\hat{K}_N(i) = (1-\lambda_i)(Q(1) + Q_N(1)) + \lambda_i(Q(2) + Q_N(2)) \qquad (10.6)$$

for i = 1,2.

If we assume that

$$\hat{K}_N(1) < \hat{K}_N(2) \qquad (10.7)$$

(as in the commensurate goals problem of chapter 7) then $\hat{V}_N((x_N|r_{N-1}=1)$ has the general shape that is shown in figure 10.2. Note that this function is discontinuous for any x_N such that $x_N'Sx_N = \alpha^2$.

We can rewrite (10.1) - (10.6) at time k=N-1 as the comparison of two constrained subproblems:

$$V_{N-1}(x_{N-1}, r_{N-1}=) = \min_{t=1,2} V_{N-1}(x_{N-1}, r_{N-1}= 1;\ t) \qquad (10.8)$$

where

$$V_{N-1}(x_{N-1}, r_{N-1}; t) = \min_{u_{N-1}} \left\{ \begin{array}{l} u_{N-1}' R(1)\, u_{N-1} \\ + \\ x_N \hat{K}_N(t) x_N \end{array} \right\} \qquad (10.9)$$

s.t.

$x_N \epsilon \Delta_N(t)$

where the constraint regions are

$$\Delta_N(1) = \{x_N : x_N'Sx_N < \alpha^2\}$$
$$\Delta_N(2) = \{x_N : x_N'Sx_N > \alpha^2\} \qquad (10.10)$$

If the two conditional cost matrices $\hat{K}_N(1)$ and $\hat{K}_N(2)$ are scalar multiples of each other, then the ellipses described by

$$x_N' \hat{K}_N(2) x_N = \gamma_2 \quad , \quad x_N' \hat{K}_N(1) x_N = \gamma_1$$

in figure 10.2 will be oriented along the same axes in the x-plane. In

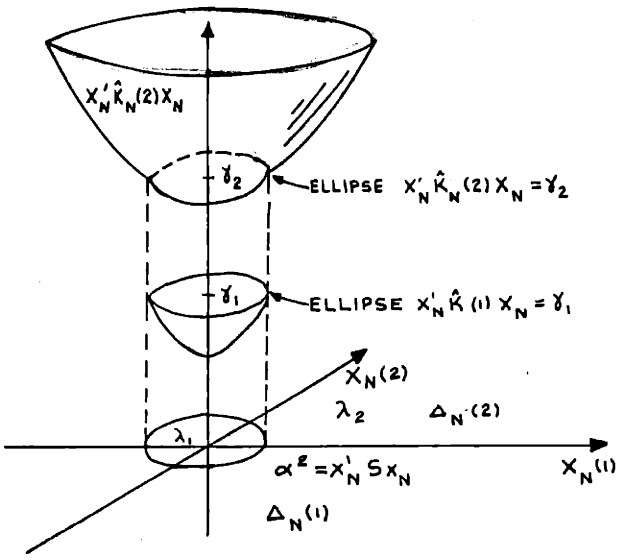

Figure 10.2: Conditional expected cost $\hat{V}_N(x_N|r_{N-1}=1)$ in example 10.1 when $\hat{K}_N(1) < \hat{K}_N(2)$. The upper "bottomless cone" is $x_N'\hat{K}_N(2)x_N$. The lower cone is $x_N'\hat{K}_N(1)x_N$, which applies when $x_N'Sx_N < \alpha^2$.

this case the optimal controller will have the three-part structure that is shown in figure 10.3. For x_{N-1} in the ellipsoidal region $\delta_{N-1}(1)$, the optimal controller places x_N in $\Delta_N(1)$. For x_{N-1} in the ellipsoidal ring $\delta_{N-1}(2)$, the optimal controller places x_N somewhere on the ellipse

$$x_N' \hat{K}_N(2) x_N = \alpha^2$$

in figure 10.2. Here the controller is hedging to this smooth curve. For x_{N-1} in $\delta_{N-k}(3)$, the optimal controller places x_N in $\Delta_N(2)$. If the conditional cost matrices $\hat{K}_N(1)$ and $\hat{K}_N(2)$ are not scalar multiples of each other, then the domains of the optimal controller at k = N-1 may take any ot the shapes in figure 10.4.

At the next time stage, the conditional cost $\hat{V}_{N-1}(x_{N-1} | r_{N-1}=2)$ will have a domain similar to those in figure 10.4 even if figure 10.2 applies (unless the ellipse $x'Sx$ is aligned with the x-plane boundary ellipses in figure 10.3). Thus for all but the most trivial cases, the shapes of the optimal controller domain (in the x plane) will vary greatly (and be difficult to describe, in general) as (N-k) increases.

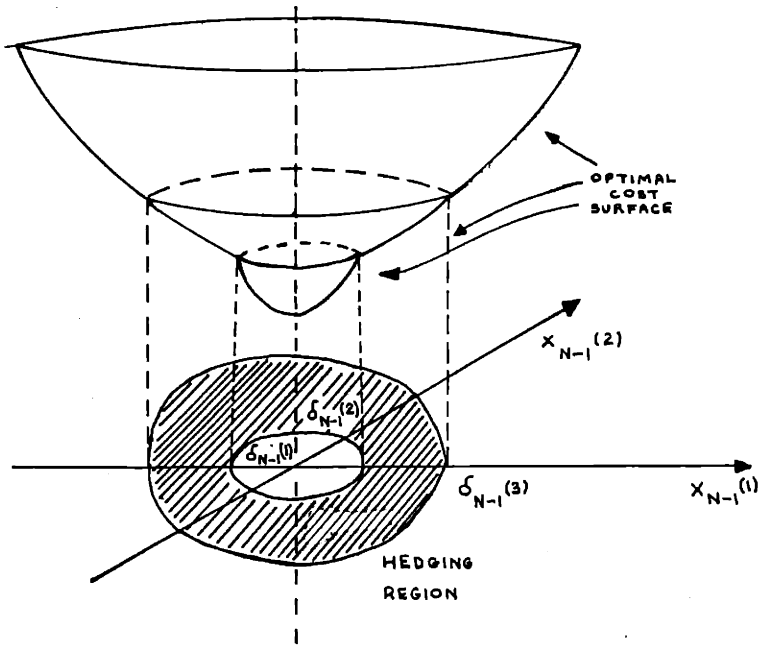

Figure 10.3: $V_{N-1}(x_{N-1}, r_{N-1}=1)$ in example 10.1 if the conditional cost boundary ellipses in figure 10.2 are aligned.

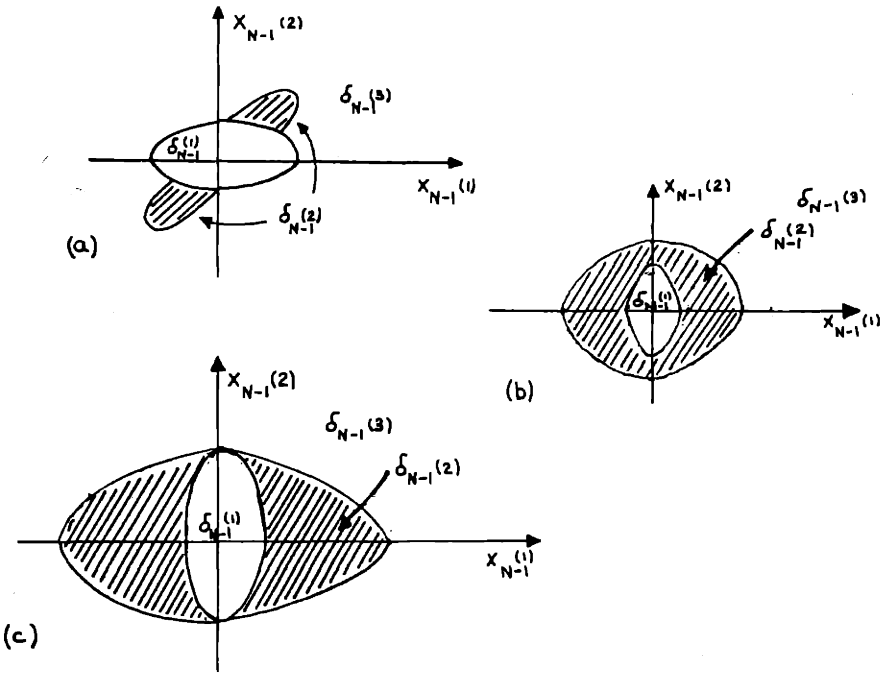

Figure 10.4: Three other $V_{N-1}(x_{N-1}, r_{N-1}=1)$ domain shapes in example 10.1 if the conditional cost boundary ellipses are not aligned. In each case, the region $\delta_{N-1}^{(2)}$ corresponds to hedging to the curve $x_N' S x_N = \alpha^2$.

Example 10.1 suggests that it is extremely difficult, in general, to obtain the solutions of n-dimensional versions of the problems of chapters 7-9. However for certain subclasses of these problems with special structures we can obtain greater insight into the nature of the optimal controller. One such class consists of JLQ (or JLPQ) problems with scalar x and u and form transition probabilities that are piecewise-constant in u and x.[1] As we will discuss in the next section, such problems are solvable with a relatively minor modification of the solution algorithm of chapters 7 and 8. The analysis of other special classes of n-dimensional problems for which the x-dependent problem is solvable is a topic for future investigation.

We can also think of obtaining approximations of the optimal controller for n-dimensional problems. One way to do this would be to use the approach of section 9.9. Basically, this would involve carrying out the following tasks at each time stage k (and in each form j):

1. Compute (by numerically integrating over x) the x_k-conditional cost surface $\hat{V}_{k+1}(x_{k+1}|r_k=j)$. This is done by generalizing the steps of figures 9.6-9.7 to account for the n-dimensional x.

2. Compute (numerically) the z_{k+1}-conditional cost surfact $\hat{\hat{V}}_{k+1}(z_{k+1}|r_k=j)$ at (only) a set of target z_{k+1} values. As in section 9.9, these target values are chosen arbitrarily. Finding an intelligent way to choose them is an open question.

3. For each x_k value of interest, compute the cost incurred

---

[1] These systems can be thought of as two-dimensional x problems by augmenting x with the control.

if the controller drives z_{k+1} to one of the chosen target values.

4. Select as the optimal control law at each x_k of interest the control in step 3 that results in the lowest expected cost-to-go.

This approximation scheme can be used (in principle) to obtain an approximation of the optimal controller for any specific problem of interest . It does not offer us much insight into the qualitative properties of the optimal controller, however. The investigation and analysis of the general nonscalar x problem (or special classes of it) remains a topic for future investigation.

10.3 Form Transitions that are u-Dependent

From a practical standpoint, control-dependent form transitions are an important part of the overall fault-tolerant control problem. A large class of component failures are related to dynamic control input choices. Indeed, actuator -dependent failures are a major source of difficulty in many transportation, military, electric power and communication systems.

We have deferred examining this class of problems because unless there is no x-cost in the problem formulation, after one time step the optimal expected cost-to-go (and conditional expected costs) will have a piecewise structure in x (as well as in u) if the transition probabilities are piecewise in u. When both x and u are scalar, however, this does not present a serious difficulty. Conceptually, such problems are basically the same as in the scalar-x, x-dependent only case.

Consider form transition probabilities

$$\Pr\{r_{k+1}=j \mid r_k=i, x_{k+1}=x, u_k=u\} = p(i,j;x,u) \tag{10.11}$$

that are piecesiwe-constant in x and u. At each time step the optimal expected cost-to-go $V_k(x_k, r_k=j)$ is given by

$$V_k(x_k, r_k=j) = \min_{u_k} \left\{ u_k^2 R(j) + \hat{V}_{k+1}(x_{k+1} \mid r_k=j, u_k=u) \right\} \tag{10.12}$$

where the conditional expected cost-to-go is parameterized by <u>both</u> x_{k+1} and u_k. The minimizations in (10.12) is solved by breaking up the problem into a collection of subproblems, each correspondint to keeping x_{k+1} in a certain interval <u>and</u> simultaneously keeping u_k in a certain interval. The solutions of these subproblems are piecewise-quadratic in x_k, with <u>unconstrained pieces</u> (resulting from u_k in the interior of the u-constraint interval in question and the resulting x_{k+1} also in the interior of its constraint interval) and the subproblems also have <u>actively constrained pieces</u> (where either u_k or x_{k+1} (or both) is at a constraint boundary point). The effect of the constrains in u_k is to complicate the book-keeping regarding the intervals of x_k values where each subproblem solution cost function piece is valid. Nevertheless, we obtain the optimal cost $V_k(x_k, r_k=j)$ and control $u_k(x_k, r_k=j)$ by comparing a collection of piecewise-quadratic in x_k cost functions, as in chapters 5-9. We consider the following simple example that illustrates the effect of having u-dependent form transitions:

Example 10.2:
Let

$$x_{k+1} = x_k + u_k \qquad \text{if } r_k = 1$$

$$x_{k+1} = 2x_k + u_k \qquad \text{if } r_k = 2$$

$$p(1,2:u) = \begin{cases} 1/4 & |u| < 1 \\ 3/4 & |u| > 1 \end{cases}$$

$$p(1,1:u) = 1 - p(1,2:u) \qquad p(2,2)=1 \quad p(2,1)=0$$

where we minimize

$$\min_{u_o, \ldots, u_{N-1}} E\left\{ \sum_{k=0}^{N-1} (u_k^2 + x_{k+1}^2) + x_N^2 K_T(r_N) \right\} \tag{10.13}$$

with terminal conditions

$$K_T(1) = 0 \qquad K_T(2) = 3 \quad .$$

This is similar to example 5.1 (which was modified in chapters 6,7,8 and 9), except that the form transition probability is piecewise-constant in u.

In form $r_k = 2$ we have

$$V_k(x_k, r_k=2) = x_k^2 K_k(2) \tag{10.14}$$

where

$$K_N(2) = 3$$

$$K_k(2) = \frac{4(K_{k+1}(2) + 1)}{2 + K_{k+1}(2)} \tag{10.15}$$

as in earlier versions of this example since, once the system enters form r = 2 it cannot leave.

We also have that

$$V_N(x_N, r_N = 1) = x_N^2 K_T(1) = 0 \quad . \tag{10.16}$$

Applying dynamic programming we have at time k = N-1:

$$V_{N-1} = \min_{u_{N-1}} \left\{ \begin{array}{l} u_{N-1}^2 + p(1,1:u_{N-1})[x_N^2 + V_N(x_N, r_N=1)] \\ + p(1,2:u_{N-1})[x_N^2 + V_N(x_N, r_N=2)] \end{array} \right\}$$

$$= \min_{u_{N-1}} \left\{ u_{N-1}^2 + p(1,1:u_{N-1}) x_N^2 + p(1,2:u_{N-1}) 4 x_N^2 \right\}. \tag{10.17}$$

Here the conditional expected cost-to-go is

$$\hat{V}_N(x_N | r_{N-1}=1, u_{N-1}) = \begin{cases} (13/4) x_N^2 & \text{if } |u_{N-1}| > 1 \\ (7/4)\ x_N^2 & \text{if } |u_{N-1}| < 1 \end{cases} \quad . \tag{10.18}$$

The two constrained subproblems that arise at the last time stage are

$$V_{N-1}(x_{N-1}, r_{N-1}=1 \mid |u_{N-1}|>1) = \min_{|u_{N-1}|>1} \left\{ u_{N-1}^2 + (13/4) x_N^2 \right\} \tag{10.19}$$

$$V_{N-1}(x_{N-1}, r_{N-1}=1 \mid |u_{N-1}|<1) = \min_{|u_{N-1}|<1} \left\{ u_{N-1}^2 + (7/4)\ x_N^2 \right\} \tag{10.20}$$

.

For $|u_{N-1}|>1$ we have

$$V_{N-1} = \min_{u_{N-1}} \left\{ u_{N-1}^2 + (13/4)(x_{N-1}^2 + 2x_{N-1}u_{N-1} + u_{N-1}^2) \right\}. \tag{10.21}$$

Differentiating with respect to u_{N-1} and setting to zero we find that the unconstrained solution to (10.21) is

$$u_{N-1}^{2,U} = -(13/17) x_{N-1} \tag{10.22}$$

with

$$V_{N-1}^{2,U} = (13/17)\, x_{N-1}^2 \quad . \tag{10.23}$$

This is valid if

$$|x_{N-1}| > (17/13) \tag{10.24}$$

(ie, in this case we have $|u_{N-1}| > 1$). If

$$|x_{N-1}| \leq (17/13) \tag{10.25}$$

we can drive the system to the constraint boundary

$$u_{N-1}^{2,+} = 1^- \tag{10.26}$$

obtaining

$$x_N^{2,+} = x_{N-1} + 1^- \tag{10.27}$$

with the cost

$$V_{N-1}^{2,+} = (13/4)x_{N-1}^2 + 13x_{N-1} + (15/2). \tag{10.28}$$

Alternatively we can drive the system to the constraint boundary

$$u_{N-1}^{2,-} = -1^+ \tag{10.29}$$

obtaining

$$x_N^{2,-} = x_{N-1} - 1^+ \tag{10.30}$$

with the cost

$$V_{N-1}^{2,-} = (13/4)x_{N-1}^2 - 13x_{N-1} + (15/2) \quad . \tag{10.31}$$

Similarly if $|u_{N-1}| < 1$ we have

$$u_{N-1}^{1,U} = -(7/11)x_{N-1} \tag{10.32}$$

with

$$V_{N-1}^{1,U} = (7/11)x_{N-1}^2 \tag{10.33}$$

which is valid for

$$|x_{N-1}| < (11/7) \quad . \tag{10.34}$$

If

$$x_{N-1} \geq (11/7) \tag{10.35}$$

we can drive to the boundary

$$u_{N-1}^{1,+} = 1^{+} \tag{10.36}$$

obtaining

$$x_{N}^{1,+} = x_{N-1} + 1^{+} \tag{10.37}$$

with the cost

$$V_{N-1}^{1,+} = (7/4)x_{N-1}^{2} + 7x_{N-1} + (9/2) \quad . \tag{10.38}$$

If

$$x_{N-1} \leq -(11/7) \tag{10.39}$$

we can drive to the boundary

$$u_{N-1}^{1,-} = -1^{-} \tag{10.40}$$

obtaining

$$x_{N}^{1,-} = x_{N-1} - 1^{-} \tag{10.41}$$

with

$$V_{N-1}^{1,-} = (7/4)x_{N-1}^{2} - 7x_{N-1} + (9/2). \tag{10.42}$$

Note that all six of the above candidate cost-to-go pieces are quadratic in x_{N-1}, and are defined over regions of validity in terms of x_{N-1} (and not u_{N-1}). Thus once these candidate costs and their regions of validity are established we can find the optimal controller by finding the intersections of quadratic functions, as in chapters 5-8. In figure 10.5 we show the regions of validity for each of the candidate cost functions in this example.

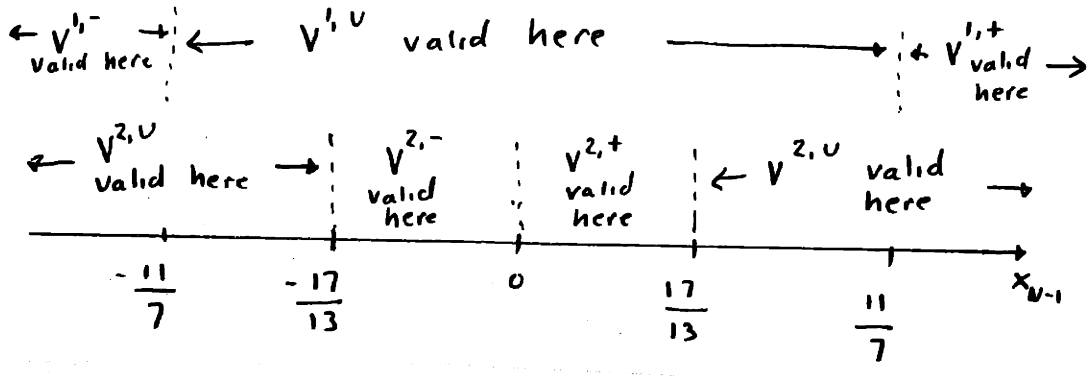

Figure 10.5: Candidate cost functions and regions of validity for example 10.2 at k = N-1.

Since $(13/17) > (7/11)$ we have

$$V_{N-1}^{2,U} > V_{N-1}^{1,U} \qquad \text{for all } x_{N-1} \neq 0.$$

Thus $V_{N-1}^{1,U}$ is optimal over the interval $(-11/7, 11/7)$. For x_{N-1} sufficiently large, $V_{N-1}^{2,U}$ will be optimal. We find that $V_{N-1}^{2,U}$ and $V_{N-1}^{1,-}$ intersect in $(-\infty, -11/7)$ at

$$x_{N-1} = -6.3897.$$

Consequently the optimal controller at time k = N-1 for this example is

$$V_{N-1}(x_{N-1}, r_{N-1}=1) = \begin{cases} V_{N-1}^{2,U} & \text{for } x_{N-1} > -6.3897 \\ V_{N-1}^{1,-} & \text{for } -6.3897 < x_{N-1} < -11/7 \\ V_{N-1}^{1,U} & \text{for } -1.571 = -11/7 < x_{N-1} < 11/7 \\ V_{N-1}^{1,+} & \text{for } 11/7 < x_{N-1} < 6.3897 \\ V_{N-1}^{2,U} & \text{for } x_{N-1} > 6.3897 \end{cases} \tag{10.43}$$

The optimal expected cost is thus piecewise-quadratic in x_{N-1}. At the next time stage we will have a conditional cost that is dependent on x_{N-1} and u_{N-2}, and the resulting optimal cost $V_{N-2}(x_{N-2}, r_{N-2}=1)$ will be piecewise-quadratic in x_{N-2}. Thus at time k= N-2 (and thereafter) the optimal controller must take into account both u constrants and x constraints.

In this section we have not investigated the qualitative properties of the control-dependent JLQ problem in detail. However it is reasonable to assume that results similar to those of chapters 5-6 and 8 are

accessible. One important area for future research is an examination of how controllers involving piecewise-constant u-dependent form transitions differ from x-dependent problems. One difference is immediately apparent from the above example: the optimal controller here hedges to values of u_{N-1} as well as to values of x_N. Thus for the scalar case, the optimal controller can hedge to either points or lines in the two-dimensional u-and-x space.

10.4 JLPC Problems with Form Controls

In this section we consider JLQ, JLPQ and JLPC problems where the form process can be controlled. The optimal controller chooses, at each time $_k$, between a finite number of control options. These options either entail changing form transition probabilities ("indirect from control" in the terminology of chapter 1) or deterministically switching between forms ("direct form control"). The form control decision is made using observations of
It is assumed that the form would be x-independent if no such controls were applied.

Through the use of $_{form}$ controls, we can endow the JLQ controller with the active hedging behavior that is one attribute of fault-tolerant control systems.

Let us consider the following problem formulation (as in (1.1)-(1.10)):

$$\bar{x}_{k+1} = A(r_k)x_k + B(r_k)u_k + \Xi(r_k)v_k \tag{10.43}$$

$$\text{Prob}\{r_{k+1} = j \mid r_k = i, q_k = q\} = p(i,j;q) \tag{10.44}$$

$$x_{k+1} = \bar{A}(r_k, r_{k+1})\bar{x}_{k+1} + Z(r_k, r_{k+1}) \tag{10.45}$$

$$q_k \varepsilon \underline{L} = \{1,2,\ldots,L\} \qquad L < \infty$$

where $\underline{L}$ is a set of form control options. We assume that (x_k, r_k) is perfectly observed at each time k, and we seek to minimize

$$\min_{\substack{u_{k_o},\ldots,u_{N-1} \\ q_{k_o},\ldots,q_{N-1}}} J_{k_o}(x_o, r_o) = E\left\{ \sum_{k=k_o}^{N-1} \left[u_k' R(r_k) u_k + x_{k+1}' Q(r_k, r_{k+1}; q_k) x_{k+1} + S(r_k, r_{k+1}; q_k) x_{k+1} + P(r_k, r_{k+1}; q_k) \right] + x_N' K_T(r_{N-1}, r_N; q_{N-1}) x_N + H_T(r_{N-1}, r_N; q_{N-1}) x_N + G_T(r_{N-1}, r_N; q_{N-1}) \right\} \tag{10.46}$$

where $R(j) > 0$, (10.47)

$$\begin{pmatrix} Q(i,j;q) & S'(i,j;q)/2 \\ S(i,j;q)/2 & P(i,j;q) \end{pmatrix} \geq 0 \tag{10.48}$$

and

$$\begin{pmatrix} K_T(i,j;q) & H_T'(i,j;q)/2 \\ H_T(i,j;q)/2 & G_T(i,j;q) \end{pmatrix} \geq 0 \tag{10.49}$$

for all $i,j \varepsilon \underline{M}$ and $q \varepsilon \underline{L}$. We will optimize over all feedback control laws of the types

$$u_k = f_k(x_{k_o},\ldots,x_k; r_{k_o},\ldots,r_k; u_{k_o},\ldots,u_{k-1}; q_{k_o},\ldots,q_{k-1}) \tag{10.50}$$

$$q_k = g_k(x_{k_o},\ldots,x_k; r_{k_o},\ldots,r_k; u_{k_o},\ldots,u_{k-1}; q_{k_o},\ldots,q_{k-1}) \; . \tag{10.51}$$

Thus this problem is a modification of the problems addressed in chapter 4. Note that we allow for different costs $Q(\cdot)$, $S(\cdot)$, $P(\cdot)$, $K_T(\cdot)$, $H_T(\cdot)$, and $G_T(\cdot)$, depending upon the form control. This lets us model costs of maintenance, switching to backup systems and the like. Also note that in (10.44), the form transition probability $p(i,j;q)$ takes a different value for each form control option q.

We could obtain the optimal controller for any pre-specified sequence of form controls $q_{k_o}, \cdots q_{N-1}$, using Proposition 4.2. These quadratic -in-x_k solutions (not piecewise-quadratic) would then have to be compared to determine the best sequence of options. This method of finding the optimal controls is clearly unsatisfactory since the number of form control options to be evaluated grows geometrically as (N-k) increases i.e., as $L^{(N-k-1)}$.

An alternative approach is to apply dynamic programming. At each time step we find the optimal cost by considering the intersections of the L optimal costs-to-go from $(x_k, r_k=j)$ that correspond to each choice of form control.

Applying dynamic programming, we have

$$V_N(x_N, r_{N-1}, r_N, q_{N-1}) = x_N' K_T(r_{N-1}, r_N; q_{N-1}) x_N + H_T(r_{N-1}, r_N; q_{N-1}) x_N + \\ + G_T(r_{N-1}, r_N; q_{N-1}) \tag{10.52}$$

$$V_{N-1}(x_{N-1}, r_{N-1}=j) = \min_{\substack{u_{N-1} \\ q_{N-1}}} \left\{ \begin{array}{l} u_{N-1}' R(j) u_{N-1} \\ \quad + \\ E\left\{ \begin{array}{l} x_N' Q(j, r_N, q_{N-1}) x_N + S(j, r_N, q_{N-1}) x_N + \\ + P(j, r_N, q_{N-1}) + V_N(x_N, r_{N-1}=j, r_N, q_{N-1}) \end{array} \right\} \end{array} \right\} \tag{10.53}$$

and for $k = N-2, N-3, \ldots, k_o$

$$V_k(x_k, r_k=j) = \min_{\substack{u_k \\ q_k}} \left\{ \begin{array}{l} u_k' R(j) u_k \\ \quad + \\ E \left\{ \begin{array}{l} x_{k+1}' \, Q(j, r_{k+1}, q_k) x_{k+1} \\ \quad + S(j, r_{k+1}, q_k) x_{k+1} + P(j, r_{k+1}, q_k) \\ \\ \quad + V_{k+1}(x_{k+1}, r_{k+1}) \end{array} \right\} \end{array} \right\}.$$

If x_k is scalar and there is no input noise, we can use the algorithm of chapters 5-7 to find the L piecewise-quadratic (in x_k) costs associated with the different form control options at time k. These cost functions are then evaluated and compared at each x_k (by finding their intersections), and the best choisce of q is chosen for each x_k value. That is, the control q_k depends explicitly on the observed value of x_k as well as r_k. The resulting optimal expected cost-to-go is thus also piecewise-quadratic in x_k. The use of dynamic programming lets us "prune" the tree of form control options; at each time we must compare at most L of them.

This approach to form control problems can als0 be used for scalar problems subject to additive input noise, using the JLPC algorithm of chapter 9.

10.5 Summary of Part IV

In part III of this thesis we developed a basic approach to the solution of jump linear feedback control problems that consists of the following tactic:

- at each time stage k and from each form $r_k=j$, the control problem is broken up into a set of constrained subproblems that are relatively easy to solve
- the solutions of these constrained subproblems are then compared to determine the optimal control law and expected cost-to-go.

In part IV of this thesis we have used this solution approach to determine the optimal feedback controllers for several more general classes of jump linear control problems. The results of chapters 8 - 10 allow the application of the methodology of chapters 5 - 7 to more realistic control problems.

In chapter 8 we considered a modification of the solution algorithm of chapter 7 that lets us solve problems involving:

- x operating costs and terminal costs that are piecewise-quadratic in x (rather than just quadratic)
- cost pieces that are concave-up as well as concave-down.

This jump linear piecewise quadratic (JLPQ) control problem is solved using an off-line, recursive algorithm. As in the JLQ problem of part III, the optimal JLPQ control laws are piecewise-linear in x and the optimal expected costs-to-go are piecewise-quadratic. Unlike the JLQ case, the number of optimal controller pieces may grow at a faster-than-linear rate as the number of stages

from the finite terminal time increases. The piecewise structure of the optimal controller is caused by both the piecewise-constant nature of the form transition probabilities (as in part III) and by the piecewise-quadratic nature of the x-operating and terminal costs.

In chapter 9 we extended the solution methodology of chapters 5 - 8 to address a larger class of scalar jump linear control problems, possessing additive input noise and a more general class of x-dependent form transition probabilities, x-operating costs and x-terminal costs. Specifically we considered scalar jump linear control problems with quadratic control penalties and

- input noise densities that are twice continuously differentiated except at a finite number of points,
- x-operating costs $Q(x,r)$, x-terminal costs $Q_T(x,r)$ and form transition probabilities $p(i,j=x)$ that consist of a finite number of convex or concave (in x) pieces.

We call this the jump linear piecewise convex (JLPC) control problem. The major extension in chapter 9 is the inclusion of additive input noise in the x-dynamics. Additive input noise profoundly changes the nature of the optimal controller. The piecewise-quadratic structure of the optimal cost and piecewise-linear structure of the optimal control laws is lost due to the "blurring" effects of the noise. In chapter 9 we show how JLPC control problems with additive input noise can be reformulated (at each time stage) as problems that do not possess input noise. This is done by breaking the noisy JLPC problem into a comparison of subproblems that are constrained in the value of the artificial variable z_{k+1}:

$$z_{k+1}=a(j)k_k+b(j)u_k$$

$$=x_{k+1}- \quad (j)V_k$$

which is determined by control u_k when x_k and $r_k=j$ are given. These reformulated problems can be solved using the approach of chapters 5 - 8.

The optimal JLPC controller can be obtained following the steps of an algorithm which is a generalization of those developed in chapters 7 and 8. However many of the algorithm steps are quite difficult or impossible to carry out analytically. Consequently, numerical methods must be used, as was illustrated in chapter 9. This requirement of numerical approximations, and the fact the optimal JLPC controller does not have the nice inductive piecewise-quadratic cost structure (at each time stage) motivated consideration of approximations of the optimal controller that are easier to determine and to implement than the optimal controller. We examined one approximation scheme that yields controllers that have piecewise-linear control laws at each time.

In chapter 10 we examined further extensions of the solution methodology of Part III. We first considered jump linear control problems where the x process is not scalar. This class of problems is far more complicated than in the scalar case. We can, however, obtain approximate controllers for these problems using the ideas of section 9.9. The next topic of chapter 10 was jump linear quadratic control problems with u-dependent form transitions. This problem is of practical importance since it captures the issue of

actuator-dependent failures and it allows us to examine conflicts between system performance and reliability requirements. We demonstrated (via an example) that these problems are accessible using the ideas of chapters 5-8 when both x and u are scalar.

In chapter 10 we also consider JLQ problems (and JLPQ problems) where the form process can be controlled on the basis of observed x_k and r_k values. This allows us to study controllers that use strategies such as preventive maintenance, switching to backup systems in anticipation of failures and the like. For such problems with scalar x and x-dependent form transition probabilities (a priori), after one time stage (solving backwards from a finite terminal time) the optimal control problem resembles the x-dependent JLPQ problem of chapter 8. The optimal expected costs-to-go are piecewise-quadratic in x and are indexed by the choice of form control q_k as well as the current form r_k, at each time k.

In conclusion, in part IV we have extended the results of chapters 5 - 7 to more general jump linear control problems that involve more complicated system and cost descriptions. These extensions are motivated by a desire to make the solution approach of part III applicable to more realistic control problems. We believe that the results of parts III and IV comprise an important step in the development of techniques for fault-tolerant control system design.

PART V

CONCLUSIONS

11. CONCLUSIONS AND SUGGESTIONS FOR FUTURE RESEARCH

Using dynamic programming, several classes of the discrete time jump linear control problem formulation of chapter 1 have been solved. In this chapter we will briefly summarize the results obtained and we will identify a number of directions for future research.

Let us begin by considering the basic assumptions of the control problems we have studied. This thesis focuses on systems where the form observations are not noisy. This has not been done because the noisy observation case is unimportant. The reason for this problem restriction is that, even when the form is perfectly observed, the solution of control problems of this kind for the x- and u-dependent form transition probability cases is very difficult, previously unsolved, important, and useful in terms of the insight which it provides us regarding the tradeoffs between reliability and system performance goals in fault-tolerant controller designs. An important task for future research is the study of these problems when the form process is not perfectly observed. Two cases which merit investigation are

- problems where only x_k is observed, in the presence of additive noise
- problems where a noisy version of r_k is observed

One recommended strategy for this analysis is to consider suitably modified versions of the two archetypical single form-transition problems (i.e., commensurate and conflicting performance and reliability goals) of chapter 7.

In this work we have restricted our attention to the fault-tolerant control of discrete time systems. As described in chapter 1, there are several practical reasons for doing this. In addition, the discrete-time formulations of these problems are much more easily analyzed than continuous-time ones. When dynamic programming is used to solve discrete-time trajectory control problems there is no partial differential equation that must be solved. Thus we need not grapple with the unsolved nonlinear partial differential equations that arise from continuous-time versions of the control problems of parts III and IV. The use of discrete-time problem formulations in this work has enabled us to gain considerable conceptual insight into the structure of fault-tolerant control systems. The continuous-time version of the Markovian form JLQ problem (of part II) was first formulated and solved by Krasovskii and Lidskii [34], and later by Wonham [76] and Sworder [63]. The study of continuous-time versions of the problems of parts III and IV is a challenging topic for future research. The solution of a class of nontrivial continuous time jump linear control problems with nonmarkovian, x-dependent form transitions would be a significant contribution.

In part II of this thesis we considered JLQ control problems for n-dimensional systems with Markovian form transitions. The noiseless case was addressed in chapter 3, and in chapter 4. This problem formulation was extended to include jump costs, affine resets of x and additive white input and x-observation noises (but with the form process still perfectly observed). The optimal

control laws that are obtained are linear in x, with a different law for each form. The expected costs-to-go are quadratic in x (for each form). All of the control gains and costs are obtained by solving off-line a set of precomputable Riccati-like difference equations (one for each form). Necessary and sufficient conditions are derived for the existence of a set of steady-state constant expected cost-to-go functions. It is shown that the corresponding set of time-invariant steady-state control laws stabilizes the controlled system, in that $E\{x_k' x_k\} \to 0$ as $(k-k_0) \to \infty$ and that the steady-state control laws minimize the limiting expected cost-to-go as $(N-k_0) \to \infty$, with finite optimal expected cost.

The presence of additive (usually Gaussian) white observation and input noise does not complicate these problems. Since the form is perfectly observed (with delay), a separation theorem like that of the standard LQG problem follows. In each form, a Kalman filter estimates x, and this estimate is then used by the control law for that form.

The results of chapters 3 and 4 suggest several directions for future research:

1. Proposition 3.1 specifies a set of coupled recursive Riccati-like difference equations whose solution specifies the optimal JLQ controller. An efficient technique for solving these coupled equations is needed.
2. Proposition 3.2 provides necessary and sufficient conditions for existence of the optimal steady-state JLQ controller. These conditions are not easily

tested for nonscalar-x problems, however since they require the simultaneous solution of coupled matrix equations containing infinite sums. In Corollaries 3.4 and 3.5 sufficient conditions that are based upon singular values are presented that are somewhat more testable for some problems. However the derivation of easily calculable conditions for the JLQ steady state problem (like the controllability and observability conditions of the LQ problem) remains an open question.

3. A more restrictive sufficient condition for the existence of steady-state optimal controllers for the continuous time version of the problem was developed by Wonham [76]. The attainment of necessary conditions for the continuous time problem remains an open question.

In part III (chapters 5,6 and 7) we have considered scalar JLQ control problems that involve state-dependent structural changes. This class of nonlinear stochastic control problems yields controller designs which endow systems with fault-tolerance, in that the controller takes into account known system limitations and failure likelihoods so as to achieve the best tradeoff between system reliability and performance goals. The optimal controller attempts to minimize the cost incurred by the usual LQ regulator action, and by driving the system state to regions where the likelihood of undesirable form shifts is reduced.

We have formulated and solved a class of scalar-in-x, noiseless JLQ problems with x-dynamics that would be linear, if

not for random x-dependent jumping parameters. These problems possess form transition probabilities that depend upon x in a piecewise-constant way. For this class of problems we have developed a procedure that calculates the optimal expected costs-to-go and control laws "off-line", in advance of system operation. The procedure determines the optimal controller inductively, backwards in time (for finite time-horizon problems). At each time the optimal controller is obtained by calculating and comparing a growing number of quadratic functions. These quadratic functions are computed via Riccati-like difference equations. We established that the optimal control laws are piecewise-linear in x (with x^1, x^0 terms) and the optimal expected costs-to-go are piecewise-quadratic in x (with x^2, x^1, x^0 terms). The different controller pieces arise from using the control to actively hedge. We also identified and examined several basic qualitative properties of the optimal JLQ controller. These included hedging-to-a-point, regions of avoidances and the endpieces and middlepieces of the expected costs-to-go and control laws. In chapter 7 we used the combinatoric properties established in chapter 5 and the results of chapter 6 to construct an algorithm for the efficient computation of the optimal controller. This algorithm was presented in flowchart form and described in detail. A very useful topic for future efforts is the development of mechanized schemes for implementing the flowchart steps for general JLQ problems. This will probably require the use of a high-level symbolic-manipulation computer language,

The class of JLQ control problems addressed by chapter 5 is extremely rich. The resulting optimal controllers can exhibit a wide variety of qualitative behaviors. Analytical characterizations of these JLQ controllers that are sufficiently general to encompass the entire problem class tend to be uninformative, since so many diverse behaviors must be simultaneously considered. We chose, therefore, to focus our attention on problems that lend insight into the kinds of qualitative JLQ controller behaviors that are appropriate in fault-tolerant control applications. We considered two archetypical problem classes in detail. In one of these classes the two goals of high performance and high reliability are commensurate. In the other class they are at cross purposes. We examined the parametric dependence of the hedging regions, regions of avoidance, stability properties, and local minima in the expected costs-to-go for these controllers. Under certain assumptions for these problems, the solution algorithm of chapter 7 reduced to the solution of (increasingly many) sets of difference equations (as N-k increases). This made these problems amenable to detailed analysis and it let us illustrate some of the controller properties and qualitative issues that arise from the use of control to achieve both reliability and performance goals. There are probably many other special classes of problems within the general problem class of chapter 5 for which similar detailed study can be effected. Of course, they need not correspond to fault-tolerant control applications. The search for other special problem classes and their study may be a fruitful line of research.

For the general problem of part III, as the time horizon

of the problem becomes infinite the number of pieces in the optimal controller becomes infinite. That is, the optimal infinite time-horizon problem cannot be obtained by any finite algorithm. For the two problem classes examined in chapter 7 we could analyze the infinite time behavior of the controller and obtain the optimal steady-state controllers as $(N-k)\to\infty$, since the optimal controller at each time can be obtained from the solution of increasingly many difference equations without making the comparisons and tests in the solution algorithm that are needed in general. The establishment of general conditions for the existence of steady-state optimal controllers for JLQ problems is an open question.

The steady-state solutions that were obtained for the two problem classes studied in detail here exhibit a structure that suggests a natural approximation to the steady-state optimal controller (both for these problems and the general class of problems in chapter 5). These approximations correspond to "finite look-ahead" controllers which ignore eventualities that might occur beyond some fixed planning time. By ignoring the far future, optimality is lost in these controllers but the computational burden of determining them and the complexity (and cost) of their implementation is reduced. This finite look-ahead controller was developed in section 7.7. The evaluation of this controller for general JLQ problems and the derivation of better suboptimal controllers are open questions for future research.

In part IV (chapters 8, 9 and 10) we considered a number of extensions to the basic solution approach of part III, as described in section 10.5. Among the myriad "next steps" arising

from these chapters we suggest that the following may be particularly fruitful:

1. For the noisy JLPC problem of chapter 9, consider in detail the approximation of problems involving input noise densities that are piecewise-constant and form transition probabilities that are piecewise-constant in x. At the first time stage the z-conditional cost will be piecewise-cubic. If we approximate $_{it}$ by a piecewise-quadratic function then the JLPQ algorithm of chapter 8 can be applied for one time step. This will result in a piecewise-quadratic (in x) expected cost. Therefore at the next time stage back we will again have a piecewise-cubic z-conditional cost. Thus there is a nice recursive structure to this approximation idea. The key question is how to efficiently approximate the cubic in z pieces by quadratics.

2. For the n-dimensional x problems of section 10.2, consider special cases that look similar to the scalar-x-and-u example of section 10.3. In particular, what kind of hedging behaviors will the optimal controller demonstrate?

In this thesis we have considered the control of dynamic systems subject to abrupt structural changes at random times. This work was motivated by the need for design techniques that yield fault-tolerant systems. We have concentrated on the tradeoffs and conflicts between system reliability and performance goals. Specifically, we considered the attainment of fault-tolerance through control strategies rather than by direct redundancy. This is, of course, only part of the overall fault-tolerant design problem. However the problem formulations here capture many important issues. We believe that the problems that are addressed and the results obtained in this thesis provide an important step in the development of a general theory of fault-tolerant control.

APPENDICES

APPENDIX TO PART I

Some Notational Conventions Used

We list here several notational conventions used in this thesis.

1. $\wedge$ above a cost or cost parameter indicates that it is conditioned on the value of the form process at the previous time step

2. $\wedge$ above a boundary interval ($\hat{\gamma}$) indicates that this is a conditional quantity parameterized by the z process of chapter 9.

3. $\wedge\wedge$ above a cost or cost parameter indicates that this is a quantity that is parameterized by the z process and is conditioned on the previous time step 's form process value.

4. $\sim$ above a quantity indicates that it is an approximate version of the true optimal controller's whatever.

5. Cost parameters followed by arguments (t:i) denote the t^{th} controller piece's parameters, if the system is in form i.

6. superscript t,U indicates the "unconstrained" solution (control law,cost, etc) to a constrained subproblem

   superscript t,L indicates the constrained left-boundary solution

   superscript t,R indicates the constrained quantity on the right boundary.

B. APPENDICES TO PART II

B.1 Proof of Proposition 3.1

The cost is quadratic for k=N. Given that $V_k(x_k,j) = x_k^2 K_k(j) x_k$ for each j at some time k, the optimal u_{k-1} given (x_{k-1},r_{k-1}) can be obtained by minimizing

$$u'_{k-1}R_{k-1}(r_{k-1})u_{k-1} + E\left\{\begin{array}{l} x'_k Q_k(r_k) x_k \\ + \\ V_k(x_k,r_k) \end{array} \middle| \, x_{k-1},r_{k-1}\right\} \qquad \text{(B.1.1)}$$

$$= u'_{k-1}R_{k-1}(r_{k-1})u_{k-1} + E\left\{ x'_k \left[\begin{array}{c} Q_k(r_k) \\ + \\ K_k(r_k) \end{array}\right] x_k \middle| \, x_{k-1},r_{k-1}\right\}$$

subject to the dynamic constraint (3.1).

Using the fact that r_k and x_k are conditionally independent (given x_{k-1},r_{k-1}), and that

$$E\left\{Q_k(r_k) + K_k(r_k) \middle| r_{k-1}\right\} = \sum_{j=1}^{M} P_k(r_{k-1},j) \left[\begin{array}{c} Q_k(j) \\ + \\ K_k(j) \end{array}\right],$$

(B.1.1) can be minimized by substituting for x_k (using (3.1)), differentiating with respect to u_{k-1} and setting the result to zero, resulting in (3.7). Condition (3.5) guarantees that the inverse matrix in (3.7) exists for each $j \in \underline{M}$. Substitution of (3.7) in (3.6) yields (3.8). It is easily verified that $K_{k-1}(j)$ is a symmetric positive

semi-definite matrix for each j, that the solution given above always exists if conditions (3.5) one met (and all parameters are finite) and, by contradiction, it can easily be shown that this optimal solution is unique. Recursive application of this argument yields the desired results.

□

B.2 Establishing Condition (4) of Proposition 3.2

First of all we observe that since in finite expected time the system will have entered a closed communicating class, the transient forms need not be considered here.

Now suppose that condition (4) is true: for at least one form i in each closed communicating subset of $\underline{M}$ the nullspaces

$$\eta(Q_i^{1/2}) \cap \eta(L_i) = \{0\}.$$

Then for any $x \neq 0$.

$$x'(Q_i + L_i' R_i L_i)x \neq 0$$

for these forms.

We must show that with condition (4) holding, the optimal steady-state controller guaranteed by conditions (1)-(3) of the Proposition must result in

$$\lim_{(k-k_0)\to\infty} E\{x_k' x_k\} = 0 .$$

From (3.17) we see that

$$x_{k+1} = (A_j - B_j L_j)x_k = D_j x_k \qquad \text{if} \quad r_k = j$$

where L_j and D_j are the steady-state values established by condition (1)-(3) of the Proposition. Thus if $r_{k+1}=i$,

$$\begin{aligned} x_{k+1}' K_i x_{k+1} - x_k' K_j x_k \\ &= x_k' [D_j' K_i D_j - K_j] x_k \\ &= -x_k' [Q_j + L_j' R_j L_j] x_k \end{aligned}$$

where the last equality follows from (3.12).

Hence

$$x_{k+1}' K_i x_{k+1} = x_0' K_{r_0} x_0 - \sum_{i=0}^{k} x_i' (Q_{r_i} + L_{r_i} R_{r_i} L_{r_i}) x_i \quad . \qquad \text{(B.2.1)}$$

Now the left side of (B.2.1) is bounded below by zero, and thus

$$x_k' (Q_j + L_j' R_j L_j) x_k \to 0 \qquad \text{(B.2.2)}$$

for all nontransient $j \in M$.

A contrapositive argument now shows the sufficiency of condition (4): Suppose that the steady-state optimal controller yields

$$\lim_{k-k_0 \to \infty} x_k = x > 0 \quad .$$

hence

$$\lim_{(k-k_0) \to \infty} ||x_k|| = ||x|| > 0$$

but that the expected cost is finite.

Since the system will return (with probability one) countably infinitely many times to each form in one of the closed communicating subsets of $\underline{M}$, an infinite cost must be incurred by (B.2.2).

□

B.3 Proof of Proposition 3.2 conditions (1)-(3) and Corollary 3.4

For Proposition 3.2: Let $k_0=0$ for simplicity. Note that

$$\text{Expected Cost} = E\sum_{k=0}^{\infty}\left\{[x'_{k+1}Q(r_{k+1})x_{k+1} + u'_kR(r_k)u_k]\right\}$$

$$= \begin{pmatrix}\text{expected cost}\\ \text{while}\\ r \in \underline{T}\end{pmatrix} + \begin{pmatrix}\text{expected cost while the}\\ \text{form is in a closed}\\ \text{communicating subset}\end{pmatrix}$$

$$= E\left\{\sum_{k=0}^{\tau-1}\left[x'_{k+1}Q(r_{k+1})x_{k+1} + u'_kR(r_k)u_k\right] + \sum_{k=\tau}^{\infty}\left[x'_{k+1}Q(r_{k+1})x_{k+1}+u'_kR(r_k)u_k\right]\right\}$$

(If $\tau=0$ (i.e.: $r_0 \notin \underline{T}$) then the first sum is zero).

Conditions (1) and (2) of Proposition 3.2 concern the second sum above; condition (3) relates to the first one. If i is an absorbing form, then

$$E\left\{\begin{matrix}\text{expected cost to go}\\ \text{from}\\ (x_k, r_k=i)\text{at } k\end{matrix}\right\} = x'_k\left[\sum_{t=0}^{\infty}(A_i-B_iF_i)'^t(Q_i+F'_iR_iF_i)(A_i-B_iF_i)^t\right]x_k$$

and thus (3.18) follows immediately.

From above it is clear that

$$x'(s_i)G_j x(s_i) = x'(s)\left[(1-p_{jj})\sum_{t=1}^{\infty} p_{jj}^{t-1}(A_j-B_jF_j)'^t\left[(Q_j+F_j'R_jF_j) + \sum_{\substack{k\in\underline{T}\\ k\neq j}} G_k \frac{p_{jk}}{1-p_{jj}}\right](A_j-B_jF_j)^t\right]x'(s)$$

for any $x'(s_i)$, thus for each $j \in \underline{T}$:

$$G_j = (1-p_{jj})\sum_{t=1}^{\infty} p_{jj}^{t-1}(A_j-B_jF_j)'^t\left[(Q_j+F_j'R_jF_j) + \sum_{\substack{k\in\underline{T}\\ k\neq j}} G_k \frac{p_{jk}}{1-p_{jj}}\right](A_j-B_jF_j)^t$$

as in (3.20). If and only if there exist $\{G_j : j\in\underline{T}\}$ that are <u>positive-definite</u> and finite valved (each element) satisfying these coupled equations, are the above equalities valid (the positive-definitness must be a property of the G_j's by (3.5)).

Similar arguments yields the $\{Z_i\}$ in (3.19). □

For Proposition 3.4, note that for absorbing forms i

$$x_k'\left[\sum_{\tau=0}^{\infty}(A_i-B_iF_i)'^t(Q_i+F_i'R_iF_i)(A_i-B_iF_i)^t\right]x_k \leq$$

$$\leq ||x_k||^2\,||Q_i+F_i'R_iF_i||\sum_{t=0}^{\infty}||(A_i-B_iF_i)^t||^2$$

Now suppose the system is in a transient form $i \in \underline{T}$.

Let s_i $(i=1,2,\ldots)$ be the times when the system form changes, with

$$r(s_i) = r_i$$

$$s_o = 0 \quad .$$

Then the $\{(s_{j+1}-s_j);\ j=0,1,\ldots,\}$ are independent random variables.

Given that we are in $(x(s_i),\ r_i=j)$ at s_i,

$$E\left\{x'(s_{i+1})x(s_{i+1}) \,\middle|\, \begin{matrix} x(s_i) \\ r_i=j \end{matrix}\right\} =$$

$$(1-p_{jj}) \sum_{t=1}^{\infty} p_{jj}^{t-1}\, x'(s_i)(A_i-B_iF_i)'^t (A_i-B_iF_i)^t x(s_i) \quad .$$

Let

$$x'(s_i)G_jx(s_i) = \left[\begin{matrix} \text{expected cost from } j \in \underline{T} \text{ until } \underline{T} \text{ is} \\ \text{exited, given} \\ \qquad x(s_i),\ s_i < \tau,\ r_i=j \end{matrix}\right] \quad .$$

Clearly.

$$x'(s_i)G_jx(s_i) = \left[\begin{matrix} \text{expected cost} \\ \text{while in} \\ j \end{matrix}\right] + \sum_{\substack{k\in\underline{T} \\ k\neq j}} \frac{p_{jk}}{1-p_{jj}}\, E\left\{\begin{matrix} x'(s_{i+1})G_kx(s_{i+1}) \\ \text{given} \quad x(s_i) \end{matrix}\right\}$$

$$= \left[\begin{matrix} x'(s_i)(1-p_{jj}) \sum_{t=1}^{\infty} p_{jj}^{t-1}(A_j-B_jF_j)'^t(Q_j+F_j'R_jF_j)(A_j-B_jF_j)^t x(s_i) \\ + \\ \sum_{\substack{k\in\underline{T} \\ k\neq j}} \frac{p_{jk}}{1-p_{jj}}\, E\left\{x'(s_{i+1})G_kx(s_{i+1}) \,\middle|\, x(s_i)\right\} \quad . \end{matrix}\right]$$

hence (3.28) implies (3.18). Similarly (3.29) implies (3.19) and (3.30) implies (3.20). For nonre-enterable transient forms, the sum of G_ℓ terms ($\ell \in \underline{T}$, $\ell \neq j$) in (3.20) is zero; thus (3.31) implies (3.20) trivially.

□

B.4 Proof of Proposition 4.1 (Sketch)

Let us first consider the minimum mean square (minimum variance) filtering problem for (4.1) - (4.2). This is just the Kalman-Buccy filter for discrete-time systems since we have perfect observations of the form process r_k (see, for example, [ ] pp. 528-531); (4.15) - (4.19) yield the optimal filter. Note that the extrapolation equations (4.15) - (4.16) use the value of r_{k-1} on the right side. The update and Kalman gain equations (4.17) - (4.19) use the r_k value (since y_k depends on r_k and x_k).

The Gaussianity of x_o and the noise sequences insure the separation result; (4.6) - (4.12) are the same as in the deterministic JLQ problem (see appendix C and chapter 5). The equation (4.23) for $G_k(j)$ includes a factor

$$\sum_{k=1}^{m} p(j,i)\ \mathrm{tr}\ \{\Xi^{1}(i)\begin{bmatrix} K_{k+1}(i) \\ + \\ Q(i) \end{bmatrix}\Xi(i)\}$$

that reflects the cost of the input noise uncertainty. It is the same as in the standard LQG problem, except for the form dependence. The last two terms in the cost $V_{k_o}(x_o,r_o)$ in (4.22) are due to the filter error (as in the LQG problem). □

C. APPENDICES TO PART III

C.1 One-Step Solution Equations (for Proposition 5.1)

For $t = 1,2,\ldots,\psi^j_{k+1}$ let

ℓ^{ji}_t be the index of $\lambda_{ji}(\ )$ valid in (5.3) when $x_{k+1} \in \Delta^j_{k+1}(t)$

ξ^{ji}_t be the index of the piece of $V_{k+1}(x_{k+1}, r_{k+1}=i)$ valid when $x_{k+1} \in \Delta^j_{k+1}(\ )$,

as in (5.27) - (5.28).

Define the conditional cost parameters

$$\hat{K}^j_{k+1}(t) = \sum_{i=1}^{M} \lambda_{ji}(\ell^{ji}_t)\,[K_{k+1}(\xi^{ji}_t;i) + Q(i)] \tag{C.1.1}$$

$$\hat{H}^j_{k+1}(t) = \sum_{i=1}^{M} \lambda_{ji}(\ell^{ji}_t)\,[H_{k+1}(\xi^{ji}_t;i) + S(i)] \tag{C.1.2}$$

$$\hat{G}^j_{k+1}(t) = \sum_{i=1}^{M} \lambda_{ji}(\ell^{ji}_t)\,[G_{k+1}(\xi^{ji}_t;i) + P(i)] \tag{C.1.3}$$

where

$$\theta^j_k(t) = \gamma^j_{k+1}(t-1)\left[1 + \frac{b^2(j)\,\hat{K}^j_{k+1}(t)}{R(j)}\right] + \frac{b^2(j)}{2R(j)}\,\hat{H}^j_{k+1}(t) \tag{C.1.4}$$

$t = 2,3,\ldots,\psi^j_{k+1}$

$$\Theta^j_k(t) = \gamma^j_{k+1}(t)\left[1 + \frac{b^2(j)\,\hat{K}^j_{k+1}(t)}{R(j)}\right] + \frac{b^2(j)}{2R(j)}\,\hat{H}^j_{k+1}(t) \tag{C.1.5}$$

$t = 1,2,\ldots,\psi^j_{k+1} - 1$

Note that

$$E\left\{ V_{k+1}\ (x_{k+1}, r_{k+1}) \;\middle|\; \begin{matrix} x_{k+1} \in \Delta_{k+1}^{j}(t) \\ r_k = j \end{matrix} \right\} = \left[\begin{matrix} x_{k+1}^2\ \hat{K}_{k+1}^{j}(t) \\ + \\ x_{k+1}\ \hat{H}_{k+1}^{j}(t) \\ + \\ \hat{G}_{k+1}^{j}(t) \end{matrix} \right] . \qquad \text{(C/1.6)}$$

Then the candidate costs-to-go in (5.29) and corresponding optimal control laws in (5.30), and the optimal $x_{k+1} \in \Delta_{k+1}^{j}(t)$ values achieved by these controls are:

$$V_k^{t,L}(x_k, j) = x_k^2\ \tilde{K}_k^j + x_k\ \tilde{H}_k^j\ (t-1) + \tilde{G}_k^j(t-1;t) \qquad \text{(C.1.7)}$$

$$U_k^{t,L}(x_k, j) = -\ \tilde{L}_k^j\ x_k + \tilde{F}_k^j\ (t-1) \qquad \text{(C.1.8)}$$

$$x_{k+1}^{t,L}\ (x_k, j) = \gamma_{k+1}^{t}\ (t-1) \qquad \text{(C.1.9)}$$

$$\text{for } t = 2,3,\ldots, \psi_{k+1}^{j} \quad \text{if}$$

$$a(j)\ x_k \leq \theta_k^j(t)$$

$$V_k^{t,U}(x_k, j) = x_k^2\ K_k^j(t) + x_k\ H_k^j(t) + G_k^j(t) \qquad \text{(C.1.10)}$$

$$u_k^{t,U}(x_k, j) = -L_k^j(t)\ x_k + F_k^j\ (t) \qquad \text{(C.1.11)}$$

$$x_{k+1}^{t,U}(x_k, j) + [a(j) - B(j)\ L_k^j(t)]x_k + b(j)\ F_k^j(t) \qquad \text{(C.1.12)}$$

$$\text{for } t = 1,2,\ldots\ \psi_{k+1}^{j} \quad \text{if}$$

$$\theta_k^j(t) \leq a(j)\ x_k \leq\ \theta_k^j(t)$$

$$V_k^{t,R}(x_k,j) = x_k^2 \tilde{K}_k^j + x_k \tilde{H}_k(t) + \tilde{G}_k^j(t,t) \qquad \text{(C.1.13)}$$

$$u_k^{t,R}(x_k,j) = -\tilde{L}_k^j x_k + \tilde{F}_k^j(t) \qquad \text{(C.1.14)}$$

$$x_{k+1}^{t,R}(x_k,j) = \bar{\gamma}_{k+1}(t) \qquad \text{(C.1.15)}$$

$$\text{for } t = 1,2,\ldots,\psi_{k+1}^j - 1 \qquad \text{if}$$

$$\Theta_k^j(t) \leq a(j)\, x_k \quad .$$

The quantities on the right-hand side of (C.1.10) - (C.1.12) are computed by

$$\left.\begin{aligned} K_N^j(t) &= K_T(j) \qquad \text{(all } j\text{)} \\ K_k^j(t) &= \frac{a^2(j)\, R(j)\, \hat{K}_{k+1}^j(t)}{R(j) + b^2(j)\, \hat{K}_{k+1}^j(t)} \end{aligned}\right\} \qquad \text{(C.1.16)}$$

$$\left.\begin{aligned} H_N^j(t) &= H_T(j) \qquad \text{(all } j\text{)} \\ H_k^j(t) &= \frac{a(j)\, R(j)\, \hat{H}_{k+1}^j(t)}{R(j) + b^2(j)\, \hat{K}_{k+1}^j(t)} \end{aligned}\right\} \qquad \text{(C.1.17)}$$

$$\left.\begin{aligned} G_N^j(t) &= G_T(j) \qquad \text{(all } j\text{)} \\ G_k^j(t) &= \hat{G}_{k+1}^j(t) - \frac{b^2(j)\, [\hat{H}_{k+1}^j(t)]^2}{4[R(j) + b^2(j)\, \hat{K}_{k+1}^j(t)]} \end{aligned}\right\} \qquad \text{(C.1.18)}$$

and

$$L_k^j(t) = \frac{a(j)\, b(j)\, \hat{K}_{k+1}^j(t)}{R(j) + b^2(j)\, \hat{K}_{k+1}^j(t)} \qquad \text{(C.1.19)}$$

$$F_k^j(t) = \frac{-b(j)\ \hat{H}_{k+1}^j(t)}{2[R(j) + b^2(j)\ \hat{K}_{k+1}^j(t)]} \quad \bullet \qquad \text{(C.1.20)}$$

The quantities on the righthand sides (C.1.7) - (C.1.9) and (C.1.13)-(C.1.15) are computed by

$$\tilde{K}_k^j = \frac{a^2(j)\ R(j)}{b^2(j)} \qquad \text{(C.1.21)}$$

$$\tilde{H}_k^j(t) = \frac{-2a(j)\ R(j)\ \gamma_{k+1}^j(t)}{b^2(j)} \qquad \text{(C.1.22)}$$

$$\text{for } t = 1, \ldots, \psi_{k+1}^j - 1$$

$$\tilde{G}_k^j(S,t) = \left\{ \begin{array}{l} \hat{G}_{k+1}^j(t) + \gamma_{k+1}^j(S)\ \hat{H}_{k+1}^j(t) \\ + \ [\gamma_{k+1}^j(s)]^2\ [\hat{K}_{k+1}^j(t) + \frac{R(j)}{b^2(j)}] \end{array} \right\} \qquad \text{(C.1.23)}$$

defined for

$$S = t \quad \text{for } t = 1, \ldots, \psi_{k+1}^j - 1$$

$$\text{and} \quad S = t-1 \quad \text{for } t = 2, \ldots, \psi_{k+1}^j$$

and

$$\tilde{L}_k^j = a(j)/b(j) \qquad \text{(C.1.24)}$$

$$\tilde{F}_k^j(t) = \gamma_{k+1}^j(t)/b(j) \qquad \text{(C.1.25)}$$

$$\text{for } t = 1, \ldots, \psi_{k+1}^j - 1 \ .$$

Regarding the notation used here,

$\sim$ denotes an actively-constrained quantity

$\wedge$ denotes a conditional quantity .

It is straightforward to verify that (5.6) and (ii) of Proposition 5.1 imply that

$$\begin{pmatrix} \tilde{K}_k^j & \tilde{H}_k^j(t)/2 \\ \tilde{H}_k^j(t)/2 & \tilde{G}_k^j(t,t) \end{pmatrix} \geq 0 \qquad t=1,\ldots,\psi_{k+1}^j - 1 \tag{C.1.26}$$

$$\begin{pmatrix} \tilde{K}_K^j & \tilde{H}_k^j(t-1)/2 \\ \tilde{H}_k^j(t-1)/2 & \tilde{G}_k^j(t-1,t) \end{pmatrix} \geq 0 \qquad t=2,\ldots,\psi_{k+1}^j \tag{C.1.27}$$

$$\begin{pmatrix} K_k^j(t) & H_k^j(t)/2 \\ H_k^j(t)/2 & G_k^j(t) \end{pmatrix} \geq 0 \qquad t=1,\ldots,\psi_{k+1}^j \tag{C.1.28}$$

for each $j \in \underline{M}$, and thus (2) of Proposition 5.1 holds.

The values of $m_k(j)$, $\{\delta_k^j(t):t=1,\ldots,m_k(j)-1\}$, and $K_k(t:j)$, $H_k(t:j)$, $G_k(t:j)$, $L_k(t:j)$ and $F_k(t:j)$ are assigned, for each $j \in \underline{M}$, by performing the minimization indicated in (5.37). The derivation of (C.1.7) - (C.1.25) is done in the next section.

C.2 Derivation of (C.1.7) - (C.1.25).

From (5.15), (C.1.1) - (C.1.3) we have that

$$V_k[x_k, r_k=j|t] = \min_{\substack{u_k \\ \text{s.t.} \\ x_{k+1} \in \Delta^j_{k+1}(t)}} \left\{ \begin{array}{c} u_k^2 \, R(j) \\ + \\ x_{k+1}^2 \, \hat{K}^j_{k+1}(t) + \hat{H}^j_{k+1}(t) \, x_{k+1} \\ + \\ \hat{G}^j_{k+1}(t) \end{array} \right\}. \qquad (C.2.1)$$

From (5.1) we have that

$$u_k = \frac{x_{k+1} - a(j)\, x_k}{b(j)} \qquad (b(j) \neq 0). \qquad (C.2.2)$$

Thus (C.2.1) becomes

$$V_k[x_k, r_k=j|t) = \min_{x_{k+1} \in \Delta^j_{k+1}(t)} \left[\begin{array}{c} x_{k+1}^2 [\hat{K}'_{k+1}(t) + \frac{R(j)}{b^2(j)}] \\ + \\ x_{k+1} [\hat{H}^j_{k+1}(t) - \frac{2a(j)\, R(j)\, x_k}{b^2(j)}] \\ [\hat{G}^j_{k+1}(t) + \frac{a^2(j)\, R(j)\, x_k^2}{b^2(j)}] \end{array} \right]. \qquad (C.2.3)$$

To minimize (C.2.3), differentiate with respect to x_{k+1} and set to zero. We find that the optimal x_{k+1} is

$$x_{k+1} = \frac{2a(j)\, R(j)\, x_k - b^2(j)\, \hat{H}^j_{k+1}(t)}{2[R(j) + b^2(j)\, \hat{K}^j_{k+1}(t)]} \qquad (C.2.4)$$

(if this x_{k+1} is, in fact, in $\Delta^j_{k+1}(t)$.

Also,

$$\frac{\partial^2 V_k[x_k, r_k=j|t]}{\partial x^2_{k+1}} = 2\left[\frac{R(j)}{b^2(j)} + \hat{K}^j_{k+1}(t)\right] > 0 \quad . \tag{C.2.5}$$

Now $x_{k+1} \in \Delta^j_{k+1}(t)$ if and only if

$$\frac{\left[\gamma^j_{k+1}(t-1)\left[R(j) + b^2(j)\,\hat{K}_{k+1}(t)\right] + \frac{b^2(j)}{2}\,\hat{H}^j_{k+1}(t)\right]}{R(j)} \leq a(j)\,x_k \leq \frac{\left[\gamma^j_{k+1}(t)\left[R(j) + b^2(j)\,\hat{K}^j_{k+1}(t)\right] + \frac{b^2(j)}{2}\,\hat{H}^j_{k+1}(t)\right]}{R(j)} \tag{C.2.6}$$

The left and right sides of (C.2.6) are defined to be $\theta^j_k(t)$ and $\Theta^j_k(t)$, respectively, as in (C.1.4) - (C.1.5).

With the definitions of (C.1.10) - (C.1.12) holding, the substitution of (C.2.4) into (C.2.3) yields (C.1.16) - (C.1.18) and the substitution of (C.2.4) into (C.2.2) yields (C.1.19) - (C.1.20).

Now if

$$a(j)x_k \leq \theta^j_k(t),$$

(C.2.5) implies that the best we can do is to drive x_{k+1} to $\gamma^{j+}_{k+1}(t-1)$, the left boundary of $\Delta^j_{k+1}(t)$. Thus from (C.2.2)

$$u_k^{*,L}(\alpha_{k+1},j) = -\frac{-a(j)\,x_k + \gamma_{k+1}^{j}(t-1)}{b(j)} \qquad (C.2.7)$$

which yields (C.1.8) with (C.1.21) - (C.1.22).

Substituting $x_{k+1} = \gamma_{k+1}^{j}(t-1)$ into (C.2.3) yields (C.1.8) with (C.1.21) - (C.1.23); here S = t-1 and t=2,..., ψ_{k+1}^{j}. Similarly

$$a(j)\,x_k \geq \Theta_k^{j}(t)$$

case yields (C.1.13) - (C.1.15); here S = t and t=1,..., ψ_{k+1}^{j} in (C.1.18).

If b(j) = 0 then the optimal control is

$$u_k(x_k, r_k=j) = 0$$

with

$$x_{k+1} = a(j)\,x_k$$

and cost

$$V_k(x_k, r_k=j) = a^2(j)\,\hat{K}_{k+1}^{j}(t)\,x_k^2 + a(j)\,\hat{H}_{k+1}^{j}(t)\,x_k + \hat{G}_{k+1}^{j}(t)$$

where the index t is determined by which region $\Delta_{k+1}^{j}(t)$ the x_{k+1} value is in (for each x_k value).

C.3 Proof of Proposition 5.2

To prove this proposition we must first establish the following relationships between $\theta_k^j(t)$, $\Theta_k^j(t)$ and the slopes of $\hat{V}_{k+1}(x_{k+1}|r_{k+1}=j)$ at the points $r_{k+1}^j(t)$: $t = 1,\ldots, \psi_{k+1}^j - 1\}$.

Lemma C.3.1: The following relationships hold:

1. $\theta_k^j(t) > \theta_k^j(\ell)$ if and only if

$$\left.\frac{\partial \hat{V}_{k+1}^j}{\partial x_{k+1}}\right|_{x_{k+1}=[\gamma_{k+1}^j(t-1)]^+} - \left.\frac{\partial \hat{V}_{k+1}^j}{\partial x_{k+1}}\right|_{x_{k+1}=[\gamma_{k+1}^j(\ell-1)]^+} > \frac{2R(j)}{b^2(j)}\,[\gamma_{k+1}^j(\ell-1) - \gamma_{k+1}^j(t-1)] \tag{C.3.1}$$

2. $\Theta_k^j(t) > \Theta_k^j(\ell)$ if and only if

$$\left.\frac{\partial \hat{V}_{k+1}^j}{\partial x_{k+1}}\right|_{x_{k+1}=[\gamma_{k+1}^j(t)]^-} - \left.\frac{\partial \hat{V}_{k+1}^j}{\partial x_{k+1}}\right|_{x_{k+1}=[\gamma_{k+1}^j(\ell)]^-} > \frac{2R(j)}{b^2(j)}\,[\gamma_{k+1}^j(\ell) - \gamma_{k+1}^j(t)] \tag{C.3.2}$$

3. $\Theta_k^j(t) > \theta_k^j(\ell)$ if and only if

$$\left.\frac{\partial \hat{V}_{k+1}^j}{\partial x_{k+1}}\right|_{x_{k+1}=[\gamma_{k+1}^j(t)]^-} - \left.\frac{\partial \hat{V}_{k+1}^j}{\partial x_{k+1}}\right|_{x_{k+1}=[\gamma_{k+1}^j(\ell-1)]^+} > \frac{2R(j)}{b^2(j)}\,[\gamma_{k+1}^j(\ell-1) - \gamma_{k+1}^j(t)] \tag{C.3.3}$$

Proof of Lemma C.3.1

Note from (C.1.6) that

$$\left.\frac{\partial \hat{V}^j_{k+1}(t)}{\partial x_{k+1}}\right|_{x_{k+1} = x} = 2X\ \hat{K}^j_{k+1}(t) + \hat{\bar{H}}^j_{k+1}(t)$$

and thus by (C.1.4),

$$\theta^j_k(t) = \gamma^j_{k+1}(t-1)\ \left[1 + \frac{b^2(j)}{R(j)}\ \hat{K}^j_{k+1}(t)\right] + \frac{b^2(j)\ \hat{\bar{H}}^j_{k+1}(t)}{2R(j)}$$

$$= \gamma^j_{k+1}(t-1) + \left(\frac{b^2(j)}{2R(j)}\ \left.\frac{\partial \hat{V}^j_{k+1}(t)}{\partial x_{k+1}}\right|_{x_{k+1} = [\gamma^k_{k+1}(t-1)]^+}\right).$$

Hence (1) of the lemma follows for any $t,\ell \in \{2,\ldots,\psi^j_{k+1}\}$. The other two relationships are proved in the same manner (using (C.1.5) for $\Theta^j_k(t)$). □

PROOF OF PROPOSITION 5.2, CONTINUED

Suppose that $\hat{V}_{k+1}(x_{k+1};r_k=j)$ is continuous at $\gamma^j_{k+1}(t)$. Then clearly

$$V^{t,R}_k\ x_k,j) \equiv V^{t+1,L}_k\ (x_k,j) \qquad \text{(C.3.4)}$$

since we are driving to the same x_{k+1} value in each, with the same cost. Hence from (C.1.23),

$$\tilde{G}^j_k(t,t) = \tilde{G}^j_k(t,t+1)\ .$$

Since (by Proposition 5.1) $\dfrac{\partial V_{k+1}(x_{k+1},\ r_k=j)}{\partial x_{k+1}}$ (C.3.5)

is nonincreasing at $\gamma^j_{k+1}(t)$, we have

$$\left.\frac{\partial}{\partial x_{k+1}} \hat{V}_{k+1}(x_{k+1}|r_k=j)\right|_{x_{k+1}=[\gamma^j_{k+1}(t)]^+} \leq$$

$$\left.\frac{\partial}{\partial x_{k+1}} \hat{V}_{k+1}(x_{k+1}|t_k=j)\right|_{x_{k+1}=[\gamma^j_{k+1}(t)]^-}$$

and hence, by lemma C.3.1, $\theta^j_k(t+1) \leq \theta^j_k(t)$. (C.3.7)

Now (C.3.4), (C.3.7) are sufficient to guarantee that neither $V^{t,R}_k(x_k,j)$ nor $V^{t+1,L}_k(x_k,j)$ can be optimal for any x_k since

$$V^{t,R}_k(x_k,j) \geq V^{t,U}_k(x_k,j)$$

$$V^{t+1,L}_k(x_k,j) \geq V^{t+1,U}_k(x_k,j) \quad .$$

This situation is illustrated in Figure C.3.1 (for a(j) 0).

Thus for each $\gamma^j_{k+1}(t)$ with $\hat{V}_{k+1}(x_{k+1}|r_k=j)$ continuous,

$$\min\{V^{t,U}_k(x_k,j),\ V^{t,R}_k(x_k,j),\ V^{t+1,L}_k(x_k,j),\ V^{t+1,U}_k(x_k,j)\}$$

$$= V^{t,U}_k(x_k,j) \text{ or } V^{t+1,U}_k(x_k,j)$$

for each x_k (C.3.8)

Suppose instead that

$$\hat{V}_{k+1}([\gamma^j_{k+1}(t)]^-|j) < \hat{V}_{k+1}([\gamma^j_{k+1}(t)]^+|j) \quad (C.3.9)$$

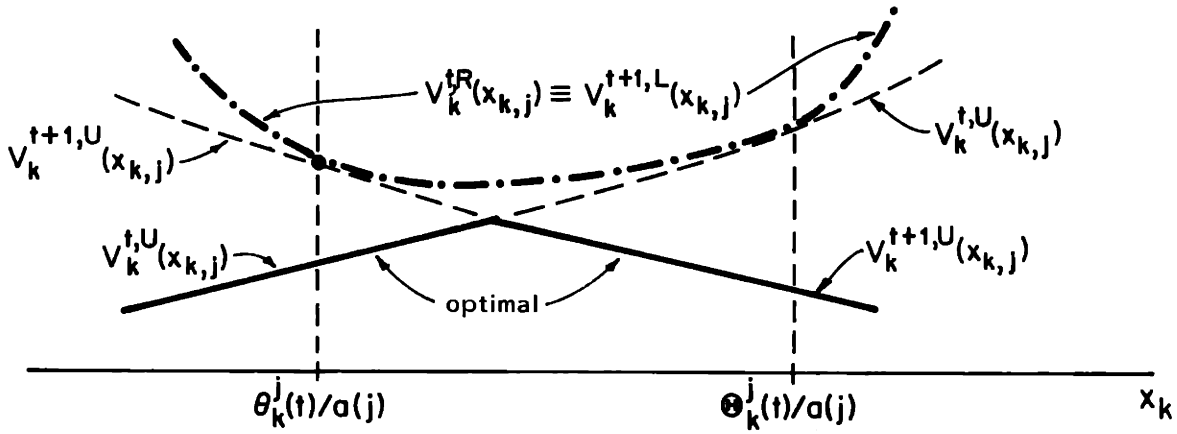

Figure C.3.1: Adjacent constrained and Unconstrained Costs when the conditional expected cost is continuous at their common boundary.

That is, $\hat{V}_{k+1}(x_{k+1}|j)$ has a discontinuous <u>increase</u> at $\gamma^j_{k+1}(t)$. This can happen only if $\gamma^j_{k+1}(t)$ is a form transition probability discontinuity $\bar{\nu}_{ji}(\ell)$ (for $i \in C_j, \ell \in \{1,\ldots,\bar{\nu}_{ji}-1\}$).

Then clearly

$$V_k^{t,R}(x_k,j) < V_k^{t+1,L}(x_k,j) \quad . \tag{C.3.10}$$

So in this case $V_k^{t+1,L}(x_k,j)$ <u>cannot</u> be optimal for any x_k. However, $V_k^{t,R}(x_k,j)$ may be. Similarly, if

$$\hat{V}_{k+1}([\gamma^j_{k+1}(t)]^-|j) > \hat{V}_{k+1}([\gamma^j_{k+1}(t)]^+|j)$$

(which implies that $\gamma^j_{k+1}(t)$ is a form transition probability discontinuity) then

$$V_k^{t+1,L}(x_k,j) < V_k^{t,R}(x_k,j) \tag{C.3.11}$$

hence $V_k^{t,R}(x_k,j)$ cannot be optimal. Thus we need consider only the candidate costs-to-go listed in the statement of Proposition 5.2. □

C.4 Proof of Proposition 5.3

1. Differentiation of $V^{t,U}_{(x_{k,j})}$, $V^{t,R}_{K(x_{k,j})}$ and $V^{t,L}_{K}(x_{k},j)$ and comparison with $u^{t,U}_{K}(x_{k},j)$, $u^{t,R}_{K}(x_{k},j)$ and $u^{t,L}_{k}(x_{k},j)$ (for appropriate values of t) yields (1) directly

2. At joining points δ where $\left.\frac{\partial V_k(x_k,r_k=j)}{\partial x_k}\right|_{x_k=\delta}$, exists, $u_k(x_k,r_k=j)$ and $x_{k+1}(x_k,r_k=j)$ are clearly continuous from (1),

3. At a joining point $x_k = \delta$ where the slope of $V_k(x_k,r_k=j)$ decreases.

$$u_k(\delta^+) - u_k(\delta^-) = \frac{-b(j)}{2a(j)R(j)}\left[\left.\frac{\partial V_k(x_{k,j})}{\partial x_k}\right|_{\delta^+} - \left.\frac{\partial V_k(x_{k,j})}{\partial x_k}\right|_{\delta^-}\right]$$

but

$$\left.\frac{\partial V_k(x_k,r_k=j)}{\partial x_k}\right|_{x_k=\delta^+} < \left.\frac{\partial V_k(x_k,r_k=j)}{\partial x_k}\right|_{x_k=\delta^-}$$

we have

$$\frac{b(j)}{a(j)} > 0 \Longrightarrow u_k(\delta^+) > u_k(\delta^-)$$

$$\frac{b(j)}{a(j)} < 0 \Longrightarrow u_k(\delta^+) < u_k(\delta^-)$$

hence 3(i), and from (5.48),

$$x_{k+1}(\delta^+,j) - x_{k+1}(\delta^-,j)$$

$$= a(j)[\delta^+ - \delta^-] - \frac{b^2(j)}{2a(j)R(j)}\left[\frac{\partial V_k(\delta^+,j)}{\partial x_k} - \frac{\partial V_k(\delta^-,j)}{\partial x_k}\right]$$

$$= \frac{-b^2(j)}{2a(j)R(j)}\left[\frac{\partial V_k(\delta^+,j)}{\partial x_k} - \frac{\partial V_k(\delta^-,j)}{\partial x_k}\right] > 0$$

hence 3(ii).

4. From 3(ii) we have that the mapping

$$x_k \longmapsto x_{k+1}(x_k, r_k=j)$$

increases discontinously at joining points where $V_k(x_k,r_k=j)$ is not differentiable, and from (2), the mapping is continuous at other joining points.

Now between joining points, if the optimal cost corresponds to hedging to a point then clearly the mapping is constant. If the optimal cost does not correspond to hedging to a point, then in such a region

$$V_k(x_k,r_k=j) = x_k^2 K_k^j(t) + x_k H_k^j(t) + G_k^j(t)$$

for some $t \in \{1,\ldots,\psi_{k+1}^j\}$ (from C1.10). Thus from (5.48)

$$x_{k+1}(x_k,r_k=j) = a(j)x_k - \frac{b^2(j)}{2a(j)R(j)} \frac{\partial V_k(x_k,r_k=1)}{\partial x_k}$$

hence

$$\frac{\partial x_{k+1}}{\partial x_k} = a(j) - \frac{b^2(j)}{2a(j)R(j)} \frac{\partial^2 V_k(x_k, r_k=j)}{(\partial x_k)^2}$$

$$= a(j) - \frac{b^2(j)}{2a(j)R(j)} \; 2\, K_k^j(t)$$

$$= a(j) - \frac{b^2(j)}{2a(j)R(j)} \frac{2a^2(j)R(j)\, \hat{K}_{k+1}(t)}{R(j) + b^2(j)\, \hat{K}_{k+1}^j(t)} \qquad \text{by (C.1.16)}$$

$$= \frac{a(j)R(j)}{R(j) + b^2(j)\, \hat{K}_{k+1}^j(t)} \geq 0$$

if $a(j) > 0$ $\left(\text{and } \frac{\partial x_{k+1}}{\partial x_k} < 0 \quad \text{if } a(j) < 0\right)$.

Thus we have 4(i), (ii) .

Clearly from (5.48) we cannot have regions of avoidance except when $\frac{\partial V_k(x_k, r_k=j)}{\partial x_k}$ is discontinuous, and from 4(i), 3(ii) we must have a region of x_{k+1} values that are not attainable using the optimal control associated with each discontinuous joining point.

5. Fact (5) follows directly from the monotonicity of the mapping

$$x_k \longmapsto x_{k+1} \; (x_k, r_k=j)$$

in 4(i), since each candidate cost corresponds to driving x_{k+1} into a different region of values; if a certain candidate cost is optimal over two disconnected intervals then the monotonicity of the mapping is violated.

C.5 Proof of Proposition 6.1

Condition (6.1) - (6.4) quarantees that $\hat{K}^j_{k+1}(t)$ and hence $K^j_k(t)$ are nonzero for all k = N, N-1,...,0 (see appendix C.2). As $|x_k|$ grows large, the candidate costs-to-go $V^{t,u}_k(x_k,j)$, $V^{t,L}_k(x_k,j)$, $V^{t,R}_k(x_k,j)$ are dominated by their x^2_k terms.

For constrained costs ($V^{t,U}_k(x_k,j)$ or $V^{t,}_k(x_k,j)$) this term is

$$x^2_k \ \tilde{K}^j_k \qquad \text{(all k)}$$

and for unconstrained costs $V^{t,u}_k(x_k,j)$ is

$$x^2_k \ K^j_k(t) \quad .$$

For any $t = 1,\ldots, \psi^j_{k+1}$,

$$K^j_k(t) \ < \tilde{K}^j_k \qquad \text{(C.5.1)}$$

To see this, note from (C.1.16), (C.1.21) that

$$\tilde{K}^j_k = \frac{a^2(j)\ R(j)}{b^2(j)}$$

$$K^j_k(i) = \frac{a^2(j)\ R(j)\ \hat{K}^j_{k+1}(i)}{R(j) + b^2(j)\ \hat{K}^j_{k+1}(i)} \quad .$$

Thus for x_k large enough, the optimal expected cost-to-go $V_k(x_k,r_k-j)$ must be one of the unconstrained ones. But for x_k small (large) enough, $V^{1,U}_k(x_k,j)$ $\left(V^{\psi^j_{k+1},U}_k(x_k,j)\right)$ is the only unconstrained cost that is eligible, and (6.6) - (6.24) follow directly from Appendix C.1. □

C.6 Proof of Proposition 6.3, part (iv).

We first verify (6.48). Each form j is assumed to be stabilizable. Thus by Proposition 6.2 the steady-state endpieces of the optimal expected costs-to-go in each form are finite (for finite x). The closed-loop optimal gain in the left endpiece of $V_k(x_k,j)$ thus approaches the following limiting value as $(N-k) \to \infty$:

$$a(j) - b(j)\, L_{\infty}^{Le}(j) \qquad \text{by} \quad (6.39)$$

$$= a(j) - \frac{b^2(j)}{a(j)\, R(j)}\, K_{\infty}^{Le}(j) \qquad \text{by} \quad (6.40)$$

$$= a(j)\left[1 - \frac{b^2(j)\, \hat{K}_{\infty}^{Le}(j)}{R(j) + b^2(j)\, \hat{K}_{\infty}^{Le}(j)}\right] \qquad \text{by} \quad (6.37)$$

$$= a(j)\left[\frac{1}{1 - \frac{b^2(j)}{R(j)}\, \hat{K}_{\infty}^{Le}(j)}\right] \quad .$$

Now for each j this limiting value of the closed loop optimal gain magnitude must be less than one (i.e. stable) since the steady-state endpiece of the cost function is finite. That is, we have (6.48):

$$0 < a(j) < 1 + \frac{b^2(j)}{R(j)}\, \hat{K}_{\infty}^{Le}(j) \quad .$$

In particular there exists a positive integer $z < \infty$ such that for each $j \in \underline{M}$ we have

$$\left[1 + \frac{a(j)}{1 + \frac{b^2(j)}{R(j)}\, \hat{K}_{k}^{Le}(j)}\right] < 1 \qquad (C.6.1)$$

for all $(N-k) > z$.

Now by (iv), there exists a form ℓ that is accessible from j which has an x-dependent form transition probability and can be repeatedly re-entered. Thus there is some finite number $\bar{\ell}$ such that

$$\Pr\{r_{k+\rho} = \ell \,|\, r_k = \ell\} > 0 \qquad \forall\ \rho \geq \bar{\ell}$$

and, by (C.6.1), the closed-loop optimal control driving $(x_k, r_k=\rho)$ to $(x_{k+\rho}, r_{k+\rho}=\ell)$ is greater than one for any form sequence from $r_k = \ell$ to $r_{k+\rho} = \ell$.

Thus

$$x_{k+\rho} = \delta^{\ell}_{k+\rho}(1) \Longrightarrow x_k > \delta^{\ell}_{k}(j)$$

hence

$$\delta^{\ell}_{k}(1) < \delta^{\ell}_{k+\rho}(1) \quad .$$

Similarly,

$$\delta^{\ell}_{k}(m_k(\ell)-1) > \delta^{\ell}_{k+\rho}(m_{k+\rho}(\ell)-1$$

Hence

$$|S^{\ell}_{k+\rho}| < |S^{\ell}_{k}|$$

Since ℓ can be repeatedly re-entered

$$|S^{\ell}_{k}| \to \infty \quad \text{as } (N-k) \to \infty$$

consequently since ℓ is accessible from j, $|S_k| \to \infty$ as well. □

C.7 Proof of Proposition 6.5

Parts (1) and (2) of Proposition 6.5 are obvious. Let us consider part(3), with β_j defined, as in the Proposition, to be the smallest positive form transition probability discontinuity location, for all p(j,i) where i$\in$ $\mathcal{C}_j$.By Proposition 6.4, for x_k in the right middlepiece of $V_k(x_k,r_k=j)$ -- that is, for

$$0 \leq x_k \leq \bar{\delta}_k j \tag{C.7.1}$$

we have the optimal control law (6.57) yielding the optimal x_{k+1} value

$$x_{k+1} = [a(j) - b(j)\, L_k^{RM}(j)]\, x_k$$

$$= a(j) \left[1 - \frac{b^2(j)\, \hat{K}_{k+1}^{RM}(j)}{R(j) + b^2(j)\, \hat{K}_{k+1}^{RM}(j)}\right] x_k$$

$$= \left[\frac{a(j)}{1 + \frac{b^2(j)}{R(j)}\, \hat{K}_{k+1}^{RM}(j)}\right] x_k \tag{C.7.2}$$

Now by definition, $x_k \in [0, \bar{\delta}_k^{\,j}]$ implies that $x_{k+1} \in [0, \bar{\delta}_{k+1}^{\,i}]$ for all i $\in$ $\mathcal{C}_j$ as well as $x_{k+1} \in [0, \nu_{ji}(t)]$ for all i $\in$ $\mathcal{C}_j$ and t = $1,\ldots,\bar{\nu}_{ji}-1$.

Thus, in particular we have

$$0 \leq x_{k+1} \leq \beta_j \quad ;$$

hence (6.60) and if j$\in\mathcal{C}_j$ then we have $0 \leq x_{k+1} \leq \bar{\delta}_{k+1}^{\,j}$ hence (6.61). A symmetric argument proves (4).

C. 8 Proof of Proposition 6.7

We prove the proposition by induction; (6.72)-(6.76) are trivially true for k = N by (6.79). Now suppose (6.72) - (6.78) hold at some time k + 1. That is, for all i

$$x_{k+1}^2 \; K_{k+1}^{LB}(i) \leq V_{k+1}(x_{k+1}, r_{k+1}=1) \leq x_{k+1}^2 \; K_{k+1}^{UB}(i) \quad .$$

Then for any $j \in \underline{M}$

$$x_{k+1}^2 \left[\sum_{i \in \underline{M}} p(j,i;x_{k+1}) \left[\begin{array}{c} K_{k+1}^{LB}(i) \\ + \\ Q(i) \end{array} \right] \right] \leq \sum_{i \in \underline{M}} p(j,i;x_{k+1}) \left[\begin{array}{c} x_{k+1}^2 \, Q(i) \\ + \\ V_{k+1}(x_{k+1}, r_{k+1}=i) \end{array} \right]$$

$$\leq x_{k+1}^2 \sum_{i \in \underline{M}} p(j,i;x_{k+1}) \left[\begin{array}{c} K_{k+1}^{UB}(i) \\ + \\ Q(i) \end{array} \right] \quad .$$

From the definitions of $\hat{K}_{k+1}^{LB}(j)$ and $\hat{K}_{k+1}^{UB}(j)$ in (6.77) - (6.78) we thus have

$$x_{k+1}^2 \; \hat{K}_{k+1}^{LB}(j) \leq \sum_{i \in \underline{M}} p(j,i;x_{k+1}) \left[\begin{array}{c} x_{k+1}^2 \, Q(i) \\ + \\ V_{k+1}(x_{k+1}, r_{k+1}=i) \end{array} \right] \leq x_{k+1}^2 \; \hat{K}_{k+1}^{UB}(j).$$

Now define

$$V_k^{LB}(x_k,j) \triangleq \min_{u_k} \left\{ u_k^2 R(j) + x_{k+1}^2 \hat{K}_{k+1}^{LB}(j) \right\}$$

$$V_k^{UB}(x_k,j) \triangleq \min_{u_k} \left\{ u_k^2 R(j) + x_{k+1}^2 \hat{K}_{k+1}^{UB}(j) \right\} \quad .$$

Recall that

$$V_k(x_k,r_k=j) = \min_{u_k} \left\{ u_k^2 R(j) + \sum_{i \in M} p(j,i:x_{k+1}) \left[\begin{array}{l} x_{k+1}^2 Q(i) \\ + \\ V_{k+1}(x_{k+1},r_{k+1}=i) \end{array} \right] \right\}$$

Thus

$$V_k^{LB}(x_k,r_k=j) \leq V_k(x_k,r_k=j) \leq V_k^{UB}(x_k,r_k=i) \quad . \qquad \text{(C.8.1)}$$

Solving for each of the costs in (C.8.1) we directly obtain (6.73) - (6.76). Thus (C.72) - (C.78) holds for k, which completes the proof. □

C.9 Proof of Proposition 6.8

From (6.80), if we define $\overline{K}_k(j)$ (for each $j \in \underline{M}$) by the recursive equation

$$\overline{K}_k(j) = \frac{a^2(j)\, R(j) \left[\sum_{i \in \mathcal{C}_j} p_{ji} \overline{K}_{k+1}(i) + Q(i)) \right]}{R_{(j)} + b^2(j) \left[\sum_{i \in \mathcal{C}_j} p_{ji} \left(\overline{K}_{k+1}(i) + Q(i) \right) \right]} \tag{C.9.1}$$

where

$$\overline{K}_N(j) = K_T(j)$$

then at each time k

$$K_K^{UB}(j) \leq \overline{K}_k(j)$$

(in all $j \in \underline{M}$). Similarly with the p_{ji} definition of (6.83) if we define $\underline{K}_k(j)$ by

$$\underline{K}_k(j) = \frac{a^2(j)\, R(j) \left[\sum_{i \in \mathcal{C}_j} p_{ji} \left(\underline{K}_{k+1}(i) + Q(i) \right) \right]}{R(j) + b^2(j) \left[\sum_{i \in \mathcal{C}_j} p_{ji} \left(\underline{K}_{k+1}(i) + Q(i) \right) \right]} \tag{C.9.2}$$

$$\underline{K}_N(i) = K_T(j)$$

then at each time k

$$\underline{K}_k(j) \leq K_k^{LB}(j) \quad .$$

A direct application of Proposition 3.2 to (C.9.1) yields (6.82), and to (C.9.2) yields (6.85). Hence (6.86) - (6.87). □

C.10 Proof of Proposition 6.11

We have already shown that for $\hat{K}_N(2) < \hat{K}_N(1) \equiv \hat{K}_N(3)$ the expected cost-to-go has a single minimum. For the second case of

$$\hat{K}_N(2) > \hat{K}_N(1) \equiv \hat{K}_N(3) \quad ,$$

$V_{N-1}(x_{N-1}, r_{n\_1}=1)$ can have local minima if and only if

$$\min_{x_{N-1}} \quad V_{N-1}^{1,R} < \delta_{N-1}(2)$$

$$\min_{x_{N-1}} \quad V^{3,L} > \delta_{N-1}(3)$$

or equivalently, if

$$\left.\frac{\partial V_{N-1}^{1,R}}{\partial x_{N-1}}\right|_{x_{N-1} = \delta_{N-1}(2)} > 0$$

$$\left.\frac{\partial V_{N-1}^{3,L}}{\partial x_{N-1}}\right|_{x_{N-1} = \delta_{N-1}(3)} < 0$$

(since the other candidate cost functions $V_{N-1}^{1,U}$, $V_{N-1}^{2,U}$, $V_{N-1}^{3,U}$ all are minimal at zero). The minimizing x_{N-1} for $V_{N-1}^{1,R}$ and $V_{N-1}^{3,L}$ are clearly given by (6.162) with values (6.163). From appendix C.1 we have that

$$\frac{\partial V_{N-1}^{1,R}}{\partial x_{N-1}} = \frac{2a(1)\ R(1)}{b^2(1)} \left(a(1)\ x_{N-1} + \alpha\right). \qquad \text{(C.10.1)}$$

Substitution of $x_{N-1} = \delta_{N-1}(2)$ in (C.10.1) gives

$$\frac{2a(1)\ R(1)}{b^2(1)}\ (a(1)\ \delta_{N-1}(2) + \alpha) > 0$$

which yields (6.161) directly.

C.11 Proof of Fact 7.2

The evolution of $K_k(1:2)$ as N-k increases is specified by (6.96):

$$K_k(1:2) = \frac{a^2(2)\, R(2)[K_{k+1}(1:2) + Q(2)]}{R(2) + b^2(2)[K_{k+1}(1:2) + Q(2)]} \qquad \text{(C.11.1)}$$

Claim: $K_{k-1}(1:2) > K_k(1:2)$ if and only if $K_{k-2}(1:2) > K_{k-1}(1:2)$.

To see this we use (C.11.1) as follows:

$$K_{k-2}(1:2) > K_{k-1}(1:2)$$

$$\Longleftrightarrow \frac{a^2(2)\, R(2)[K_{k-1}(1:2) + Q(2)]}{R(2) + b^2(2)[K_{k-1}(1:2) + Q(2)]} > \frac{a^2(2)\, R(2)[K_k(1:2) + Q(2)]}{R(2) + b^2(2)[K_k(1:2) + Q(2)]}$$

$$\Longleftrightarrow [K_{k-1}(1:2) + Q(2)]\left[\begin{array}{l} R(2) \\ + \\ b^2(2)[K_k(1:2) + Q(2)] \end{array}\right]$$

$$> [K_k(1:2) + Q(2)]\left[\begin{array}{l} R(2) \\ + \\ b^2(2)[K_{k-1}(1:2) + Q(2)] \end{array}\right]$$

$$\Longleftrightarrow K_{k-1}(1:2) > K_k(1:2)$$

as claimed. Consequently since condition (7.12) guarantees that $K_{N-1}(1:2) > K_N(1:2) = K_T(2)$ we have (1) of Fact 7.2 by induction.

From the recursive equation for $K_k^{LM}(1)$ (i.e. (6.105)), similar algebraic manipulations to those above show that if $K_k^{LM}(1) > K_{k+1}^{LM}(1)$ for some specified k then since $K_k(1:2) > K_{k+1}(1:2)$ by (1) we

have $\hat{K}_k^{LM}(1) > \hat{K}_{k+1}^{LM}(1)$, hence $K_{k-1}^{LM}(1) > K_k^{LM}(1)$. Condition (7.13) with i = 1 guarantees that $K_{N-1}^{LM}(1) > K_N^{LM}(1)$, hence (2) of Fact 7.2 follows by induction. Similarly we obtain (3) of fact 7.2 from (6.104) and (7.23) with i = 2. □

C.12 Proof of Fact 7.3

This fact is proved by induction in each of the two cases. Recall the equations for the endpiece, middlepiece, upper bound and lower bound parameters:

$$K_k^{Re}(1) \equiv K_k^{Le}(1) = \frac{a^2(1)\, R(1)\, \hat{K}_{k+1}^{Le}(1)}{R(1) + b^2(1)\, \hat{K}_{k+1}^{Le}(1)} \qquad \text{(C.12.1)}$$

$$\hat{K}_{k+1}^{Le}(1) = (1 - \omega_2)(K_{k+1}^{Le}(1) + Q(1)) + \omega_2(K_{k+1}(1{:}2) + Q(2))$$

$$K_N^{Le}(1) = K_N^{Re}(1) = K_T(1) \qquad \text{(C.12.2)}$$

and

$$K_k^{LM}(1) \equiv K_k^{RM}(1) = \frac{a^2(1)\, R(1)\, \hat{K}_{k+1}^{LM}(1)}{R(1) + b^2(1)\, \hat{K}_{k+1}^{LM}(1)} \qquad \text{(C.12.3)}$$

$$\hat{K}_{k+1}^{LM}(1) = (1 = \omega_1)(K_{k+1}^{LM}(1) + Q(1) + \omega_1(K_{k+1}(1{:}2) + Q(2)) \qquad \text{(C.12.4)}$$

$$K_N^{LM}(1) = K_T(1)$$

and

$$K_k^{UB}(1) = \frac{a^2(1)\, R(1)\, \hat{K}_{k+1}^{UB}(1)}{R(1) + b^2(1)\, \hat{K}_{k+1}^{UB}(1)} \qquad \text{(C.12.5)}$$

$$\hat{K}^{UB}_{k+1}(1) = \max_{t=1,..,\psi^1_{k+1}} \sum_{i=1,2} \lambda_{1i}\,(\ell^{1i}_t)\,[K^{UB}_{k+1}(i) + Q(i)] \qquad \text{(C.12.6)}$$

$$K^{UB}_N(1) = K_T(1)$$

and

$$K^{LB}_k(1) = \frac{a^2(1)\,R(1)\,\hat{K}^{LB}_{k+1}(1)}{R(1) + b^2(1)\,\hat{K}^{LB}_{k+1}(1)} \qquad \text{(C.12.7)}$$

$$\hat{K}^{LB}_{k+1}(1) = \min_{t=1,..,\psi^1_{k+1}} \sum_{i=1,2} \lambda_{1i}(\ell^{1i}_t)\,[K^{LB}_{k+1}(1) + Q(i)^{\frac{1}{2}} \qquad \text{(C.12.8)}$$

$$K^{LB}_N(1) = K_T(1) \quad .$$

At all times k, $K^{LB}_k(2) = K^{UB}_k(2) = K_k(1{:}2)$, where $K_k(1{:}2)$ is given by (6.96) $\equiv$(C.11.1).

Suppose $\omega_2 > \omega_1$ as in (1) of Fact 7.3.γ Assume that $K^{Le}_{k+1}(1) = K^{UB}_{k+1}(1)$ at some time k+1. Then by Facts 7.1 and 7.2, $\hat{K}^{UB}_{k+1}(1)$ in (C.12.6) becomes

$$\hat{K}^{UB}_{k+1}(1) = (1 - \omega_2)(K^{UB}_{k+1}(1) + Q(1)) + \omega_2(K_{k+1}(1{:}2) + Q(2))$$

$$= K^{Le}_{k+1}(1) \qquad \text{by (C.12.2)} \quad \bullet$$

Hence by (C.12.1), (C.12.5) we have that

$$K^{Le}_{k+1}(1) = K^{UB}_{k+1}(1) \quad \text{implies} \quad K^{Le}_{k}(1) = K^{UB}_{k}(1) \ .$$

At time K = N, $K^{Le}_{N}(1) = K^{UB}_{N}(1)$, hence $K^{Le}_{k}(1) \equiv K^{UB}_{k}(1)$ at all times k, by induction.

Analogous arguments show that $K^{LM}_{k}(1) \equiv K^{LB}_{k}(1)$ at all times k (when $\omega_2 > \omega_1$). The two claims in part (2) of Fact 7.3 (where $\omega_1 > \omega_2$) are proved in the same manner: by comparison of (C.12.7) - (C.12.8) and induction. □

C.13 Commensurate Goals Problem Derivation - Part I

We are considering the following problem class:

$$\min_{u_o,\ldots,u_{N-1}} E\left\{\sum_{K=k_o}^{N-1}\left[u_K^2\, R(r_K) + x_{u+1}^2\, Q(r_{K+1})\right] + x_N^2\, K_T(r_N)\right\} \tag{C.13.1}$$

where

$$x_{K+1} = a(r_K)\, x_K + b(r_K)\, a_K \tag{C.13.2}$$

$$r_K \in \{1,2\}$$

$$p(1,2{:}x) = \begin{cases} \omega_1 & \text{if } |x| < \alpha \\ \omega_2 & \text{if } |x| > \alpha \end{cases} \qquad 0 < \alpha \tag{C.13.3}$$

$$p(1,1{:}x) = 1 - p(1,2{:}x) \qquad p(2,1) = 0 \qquad p(2,2) = 1$$

where

$$0 \leq K_T(1) \leq K_T(2)$$

$$0 < a(1) \leq a(2) \tag{C.13.4}$$

$$0 < \omega_1, \omega_2 < 1$$

$$0 < \alpha, R(1), R(2)$$

$$b(1), b(2) \neq 0$$

We assume

$$\frac{a^2(1)}{a^2(2)} \leq \frac{b^2(1)/R(1)}{b^2(2)/R(2)} \tag{C.13.5}$$

hence

$$\begin{pmatrix} x_k^2\, Q(2) \\ + \\ V_k(x_k, r_k=2) \end{pmatrix} \geq x_k^2 \begin{pmatrix} Q(1) \\ + \\ K_k^{UB}(1) \end{pmatrix}$$

by Fact 7.1.

We assume that $0 \leq K_T(2)$.

$$< \frac{\left[\begin{matrix} R(2)[a^2(2) - 1] \\ -b^2(2)\, Q(2) \end{matrix}\right] + \sqrt{\left(\begin{matrix} R(2)[a^2(2)-1] \\ -b^2(2)\, Q(2) \end{matrix}\right)^2 + 4b^2(2)a^2(2)R(2)Q(2)}}{2b^2(2)} \qquad \text{(C.13.6)}$$

and $0 \leq K_T(1)$

$$< \frac{\left[\begin{matrix} -\{R(1)(1-a^2(1)(1-\omega_i))+b^2(1)[Q(1)+\omega_i(K_T(2)+Q(2)\neq Q(1))]\} \\ + \sqrt{\{R(1)(1-a^2(1)(1-\omega_i))+b^2(1)[Q(1)+\omega_i(K_T(2)+Q(2)-Q(1))]\}^2 + 4a^2(1)R(1)b^2(1)(1-\omega_i)[Q(1)+\omega_i(K_T(2)+Q(2)-Q(1))]} \end{matrix}\right]}{2b^2(1)\ (1 - \omega_i)} \qquad \text{(C.13.7)}$$

for $i = 1,2$

hence, by Fact 7.2, $K_k^{LM}(1)$, $K_k^{Re}(1)$ and $K_k(1{:}2)$ are monotone increasing sequences as $(N - k)$ increases. We also assume that

$$\omega_2 > \omega_1 \qquad \text{(C.13.8)}$$

hence, by Fact 7.3 we have that

- the endpieces $V_k^{Le}(1) \equiv V_k^{Re}(1)$ are given by the same function of x_k as the upper bound $V_k^{UB}(1)$
- The middlepiece $V_k^{LM}(1) \equiv V_k^{RM}(1)$ is given by the same function of x_k as the lower bound $V_k^{LB}(1)$

In addition we assume that

$$a(1) < 1 + \frac{b^2(1)}{R(1)} \left[(1-\omega_1) \begin{pmatrix} K_T(1) \\ + \\ Q(1) \end{pmatrix} + \omega_1 \begin{pmatrix} K_T(2) \\ + \\ Q(2) \end{pmatrix} \right]$$

$$= 1 + \frac{b^2(1)}{R(1)} \hat{K}_N(2) \qquad \text{(C.13.9)}$$

hence we have "situation (1)" as in (7.22) and figures 7.11(a), 7.14(d). In section 6.6 we obtained the complete solution for this problem at time $k = N-1$: (6.112) - (6.118), (6.121) - (6.142) (that is, fact 6.9). We can show that

$$K_{N-1}(3:1) < K_{N-1}(1:1) = K_{N-1}(5:1) < K_{N-1}(2:1) = K_{N-1}(4:1) \qquad \text{(C.13.10)}$$

(as in figure 7.14(c)) by the following lemma:

Lemma C.13.1:

For finite $K_1 > K_2 > 0$, $R > 0$ and a^2, b^2 we have the following:

(1) $K_1 > K_2$ if and only if $\dfrac{a^2 R K_1}{R + b^2 K_1} > \dfrac{a^2 R K_2}{R + b^2 K_2}$ (C.13.11)

(2) For any finite K, $\dfrac{a^2 R}{b^2} > \dfrac{a^2 R K}{R + b^2 K}$. (C.13.12)

Proof: For (1), note the following equivalences:

$$\frac{a^2 R K_1}{R + b^2 K_1} > \frac{a^2 R K_2}{R + b^2 K_2}$$

$$\Longleftrightarrow \begin{pmatrix} a^2 R^2 K_1 \\ + \\ a^2 R b^2 K_1 K_2 \end{pmatrix} > \begin{pmatrix} a^2 R^2 K_2 \\ + \\ a^2 R b^2 K_1 K_2 \end{pmatrix}$$

$$\Longleftrightarrow a^2 R^2 K_1 > a^2 R^2 K_2 \Longleftrightarrow K_1 > K_2 \quad .$$

Now note that

$$\lim_{K\to\infty}\left(\frac{a^2 R K}{R+b^2}\right) = \lim_{K\to\infty}\left(\frac{a^2 R}{R/K + b^2}\right) = \frac{a^2 R}{b^2}$$

hence (2) follows from (1). □

Since in case 1 we have

$$\hat{K}_N(1) \equiv \hat{K}_N(3) > \hat{K}_N(2) \quad ,$$

(1) of Lemma C.13.1 and (6.128), (6.136) yield

$$K_{N-1}(1{:}1) = K_{N-1}(5{:}1) > K_{N-1}(3{:}1) \qquad \text{(C.13.13)}$$

and (2) of Lemma C.13.1 yields

$$K_{N-1}(2{:}1) = K_{N-1}(4{:}1) > K_{N-1}(1{:}1) \quad \bullet \qquad \text{(C.13.14)}$$

Since $V_{N-1}(2:1) = V_{N-1}^{2,L}$ and $V_{N-1}(3:1) = V_{N-1}^{2,U}$ we have

$$V_{N-1}(2:1) = \left(\begin{array}{l} x_{N-1}^2 \; K_{N-1}(2:1) \\ \quad + \\ x_{N-1} \; H_{N-1}(2:1) \\ \quad + \\ G_{N-1}(2:1) \end{array} \right) > x_{N-1}^2 \; K_{N-1}(3:1) = V_{N-1}(3:1) \qquad \text{(C.13.15)}$$

except for equality at $x_{N-1} = \delta_{N-1}(2)$.

Let us now consider time $k = N-2$. Among the eligible[1] candidate cost-to-go functions for $V_{N-2}(x_{N-2}, r_{N-2}=1)$ are:

$$V_{N-2}^{t,U}(x_{N-2},1) = x_{N-2}^2 \; {}_{N-2}(t) + x_{N-2} \; H_{N-2}(t) + G_{N-2}(t) \qquad \text{(C.13.16)}$$

for

$$\frac{\theta_{N-2}(t)}{a(1)} \leq x_{N-2} \leq \frac{\Theta_{N-2}(t)}{a(1)}$$

$$t = 1,\ldots,7$$

where (see appendix C.1) we have

$$K_{N-2}(t) = \frac{a^2(1)\; R(1)\; \hat{K}_{N-1}(t)}{R(1) + b^2(1)\; \hat{K}_{N-1}(t)} \qquad t = 1,\ldots,7 \qquad \text{(C.13.17)}$$

$$H_{N-2}(1) = H_{N-2}(3) = H_{N-2}(4) = H_{N-2}(5) = H_{N-2}(7) = 0$$

$$H_{N-2}(2) = \frac{a(1)\; R(1)\; \hat{H}_{N-1}(2)}{R(1) + b^2(1)\; \hat{K}_{N-1}(2)} = -H_{N-2}(6) \qquad \text{(C.13.18)}$$

---

[1] In the sense of section 7.2

$$G_{N-2}(1) = G_{N-2}(3) = G_{N-2}(4) = G_{N-2}(5) = G_{N-2}(7) = 0$$

$$G_{N-2}(2) = \hat{G}_{N-1}(2) - \frac{b^2(1)\ [\hat{H}_{N-1}(2)]^2}{4[R(1)+b^2(1)\hat{K}_{N-1}(2)]} = G_{N-2}(6) \qquad \text{(C.13.19)}$$

with

$$\hat{K}_{N-1}(t) = (1-\omega_2)\begin{bmatrix} Q(1) \\ + \\ K_{N-1}(t:1) \end{bmatrix} + \omega_2\begin{bmatrix} Q(12) \\ + \\ K_{N-1}(1:2) \end{bmatrix} \qquad t=1,2,3$$

$$\hat{K}_{N-1}(4) = (1-\omega_1)\begin{bmatrix} Q(1) \\ + \\ K_{N-1}(3:1) \end{bmatrix} + \omega_1\begin{bmatrix} Q(2) \\ + \\ K_{N-1}(1:2) \end{bmatrix}$$

$$\hat{K}_{N-1}(t) = (1-\omega_2)\begin{bmatrix} K_{N-1}(t-2:1) \\ + \\ Q(1) \end{bmatrix} + \omega_2\begin{bmatrix} K_{N-1}(1:2) \\ + \\ Q(2) \end{bmatrix} \qquad t = 5,6,7$$

(C.13.20)

$$\hat{H}_{N-1}(t) = 0 \quad t=1,3,4,5,7$$

$$\hat{H}_{N-1}(2) = (1-\omega_2)\ H_{N-1}(2:1) = \frac{(1-\omega_2)2a(1)\ R(1)\alpha}{b^2(1)} = -\hat{H}_{N-1}(6)$$

(C.13.21)

$$\hat{G}_{N-1}(t) = 0 \quad t=1,3,4,5,7$$

$$\hat{G}_{N-1}(2) = (1-\omega_2)\ G_{N-1}(2:1) = \frac{(1-\omega_2)\alpha^2(R(1) + b^2(1)\ \hat{K}_N\ (2))}{b^2(1)}$$

$$= \hat{G}_{N-1}(6)$$

and

$$\theta_{N-2}(t) = \gamma_{N-1}(t-1)\left[1 + \frac{b^2(1)\,\hat{K}_{N-1}(t)}{R(1)}\right] + \frac{b^2(1)}{2R(1)}\,\hat{H}_{N-1}(t) \qquad (C.13.22)$$

$$t=2,3,\ldots,7$$

$$\Theta_{N-2}(t) = \gamma_{N-1}(t)\left[1 + \frac{b^2(1)\,\hat{K}_{N-1}(t)}{R(1)}\right] + \frac{b^2(1)}{2R(1)}\,\hat{H}_{N-1}(t) \qquad (C.13.23)$$

$$t=1,2,\ldots,6$$

where

$$\gamma_{N-1}(1) = \delta_{N-1}(1) \qquad \gamma_{N-1}(3) = -\alpha \qquad \gamma_{N-1}(5) = \delta_{N-1}(3)$$

$$\gamma_{N-1}(2) = \delta_{N-1}(2) \qquad \gamma_{N-1}(4) = \alpha \qquad \gamma_{N-1}(6) = \delta_{N-1}(4)$$

Given (C.13.10), $\omega_1 < \omega_2$ and $K^{UB}_{N-1} < K_{N-1}(1:2)$

we have

$$> \hat{K}_{N-1}(1) \equiv \hat{K}_{N-1}(7) > \hat{K}_{N-1}(3) \equiv \hat{K}_{N-1}(5) > \hat{K}_{N-1}(4) \qquad (C.13.24)$$

by Lemma C.13.1, and thus

$$V^{4,U}_{N-2} < V^{3,U}_{N-2} \equiv V^{5,U}_{N-2} < V^{7,U}_{N-2} \equiv V^{1,U}_{N-2} \quad \text{at all } x_{N-2} \qquad (C.13.25)$$ •

By (C.13.15) we also have

$$V^{2,U}_{N-2} > V^{3,U}_{N-2} \quad \text{except at equality at} \quad x_{N-2} = \frac{\theta_{N-2}(3)}{a(1)} \qquad (C.13.26)$$

$$V^{6,U}_{N-2} > V^{5,U}_{N-2} \quad \text{except equality at} \quad x_{N-2} = \frac{\theta_{N-2}(6)}{a(1)}$$

Note that (C.13.24) - (C.13.26) are the same as (7.26) - (7.28).

In addition to the $V_{N-2}^{t,U}$ (t=1,...,7), the other two eligible candidate functions for $V_{N-2}(x_{N-2},r_{N-2}=1)$ are

$$V_{N-2}^{4,L}(x_{N-2},r_{N-2}=1) = x_{N-2}^2 \tilde{K}_{N-2} + x_{N-2} \tilde{H}_{N-2}(3) + \hat{G}_{N-2}(3,4)$$

$$V_{N-2}^{4,R}(x_{N-2},r_{N-2}=1) = x_{N-2}^2 \tilde{K}_{N-2} + x_{N-2} \tilde{H}_{N-2}(4) + \tilde{G}_{N-2}(4,4)$$

where [1]

$$\tilde{K}_{N-2} = a^2(1)\, R(1)/b^2(1) \qquad \text{(C.13.26)}$$

$$\tilde{H}_{N-2}(3) = 2a(1)\, R(1)\, \alpha/b^2(1) \qquad \text{(C.13.27)}$$

$$\tilde{H}_{N-2}(4) = -2a(1)\, R(1)\, \alpha/b^2(1) \qquad \text{(C.13.28)}$$

$$\tilde{G}_{N-2}(3,4) = \alpha^2 \left[\hat{K}_{N-1}(4) + \frac{R(1)}{b^2(1)}\right] = \tilde{G}_{N-2}(4,4) \qquad \text{(C.13.29)}$$

The relationships (7.29) - (7.30) are by definition, and Lemma C.13.1 yields

$$\tilde{K}_{N-2} > K_{N-2}(2) > K_{N-2}(1) \quad . \qquad \text{(C.13.30)}$$

When the first situation for $V_{N-2}(x_{N-2},r_{N-2}=1)$ occurs (as shown in figure 7.16) we have

---

(1) From Appendix C.1.

$$V_{N-2}(i:1) = x_{N-2}^2 K_{N-2}(i:1) + x_{N-2} H_{N-2}(i:1) + G_{N-2}(i:1)$$

$$\text{for} \quad \delta_{N-2}(i-1) \leq x_{N-2} \leq \delta_{N-2}(i) \qquad \text{(C.13.31)}$$

with $\quad i=1,2,\ldots,m_{N-2}(1)$

where

$$m_{N-2}(1) = 9. \qquad \text{(C.13.32)}$$

Here

$$\begin{aligned}
K_{N-2}(i:1) &= K_{N-2}(i) \qquad i=1,2,3 \\
K_{N-2}(4:1) &= \tilde{K}_{N-2} = K_{N-2}(6:1) \\
K_{N-2}(5:1) &= K_{N-2}(4) \\
K_{N-2}(i:1) &= K_{N-2}(i-2) \qquad i=7,8,9 \\
H_{N-2}(i:1) &= G_{N-2}(i:1) = 0 \qquad i=1,3,5,7,9 \qquad \text{(C.13.33)} \\
H_{N-2}(2:1) &= H_{N-2}(2) = -H_{N-2}(6) = -H_{N-2}(8:1) \\
G_{N-2}(2:1) &= G_{N-2}(2) = G_{N-2}(6) = G_{N-2}(8:1) \\
H_{N-2}(4:1) &= \tilde{H}_{N-2}(3) = -\tilde{H}_{N-2}(4) = -H_{N-2}(6:1) \\
G_{N-2}(4:1) &= \tilde{G}_{N-2}(3,4) = \tilde{G}_{N-2}(4,4) = G_{N-2}(6:1)
\end{aligned}$$

with

$$\delta_{N-2}(0) \triangleq -\infty \qquad \delta_{N-2}(9) \triangleq +\infty$$

$$\delta_{N-2}(2) = \frac{\Theta_{N-2}(2)}{a(1)} = \frac{\theta_{N-2}(3)}{a(1)} \leq \frac{-\Theta_{N-2}(5)}{a(1)} = \frac{-\theta_{N-2}(6)}{a(1)} = -\delta_{N-2}(7)$$

$$\delta_{N-2}(4) = \frac{\theta_{N-2}(4)}{a(1)} = \frac{-\Theta_{N-2}(4)}{a(1)} = -\delta_{N-2}(5) \qquad \text{(C.13.34)}$$

and

$$\delta_{N-2}(3) = -\delta_{N-2}(6)$$

$$\delta_{N-2}(1) = -\delta_{N-2}(8) \quad \bullet$$

Joining point $\delta_{N-2}(1)$ occurs at the leftmost intersection of the functions $V_{N-2}^{1,U}$ and $V_{N-2}^{2,U}$. This is the least x_{N-2} such that

$$V_{N-2}^{2,U} - V_{N-2}^{1,U} = x_{N-2}^2 \left[K_{N-2}(2) - K_{N-2}(1)\right] + x_{N-2} H_{N-2}(2) + G_{N-2}(2) = 0 \bullet$$

From figure 7.15 we see that this intersection exists for all parameter values consistent with the assumptions of this section.

Using the quadratic formula we find this point to be

$$\delta_{N-1}(2) = \frac{-\alpha}{a^2(1)} \left(1 + \frac{b^2(1)}{R(1)} \hat{K}_N(1)\right)\left(1 + \frac{b^2(1)}{R(1)} \hat{K}_{N-1}(1)\right) \left(1 + \sqrt{1 - \chi_1}\right)$$

(C.13.35)

where

$$\chi_1 = \frac{[R(1)+b^2(1)\hat{K}_{M-1}(2)]}{[R(1) + b^2(1)\ \hat{K}_N(1)]\,[R(1) + b^2(1)\ \hat{K}_{N-1}(1)]} \left[\begin{array}{l} R(1) + b^2(1)\ \hat{K}_N(2) \\ -a^2(1)\ R^2(1)\,(1-\omega_2) \\ \hline R(1) + b^2(1)\ \hat{K}_{N-1}(2) \end{array} \right]$$

$$= \frac{\left\{ \begin{array}{l} [1 + \frac{b^2(1)}{R(1)}\ \hat{K}_N(2)]\ [1 + \frac{b^2(1)}{R(1)}\ \{(1-\omega_2)Q(1) + \omega_2(Q(2) + K_{N-1}(1:2))\}] \\ \quad + \frac{b^2(1)}{R(1)}\ \hat{K}_N(2)\ (1 - \omega_2)\ a^2(1) \end{array} \right\}}{[1 + \frac{b^2(1)}{R(1)}\ \hat{K}_N(1)]\ [1 + \frac{b^2(1)}{R(1)}\ \hat{K}_{N-1}(1)]} \qquad \text{(C.13.36)}$$

Joining point $\delta_{N-2}(3)$ occurs at the leftmost intersection of the functions $V^{3,U}_{N-2}$ and $V^{4,L}_{N-2}$. Using the quadratic formula, we find this to be

$$\delta_{N-2}(3) = \frac{-\alpha}{a(1)}\ (1 + \frac{b^2(1)}{R(1)}\ \hat{K}_{N-1}(3))\ \left[1 + \sqrt{1 - \frac{R(1) + b^2(1)\ \hat{K}_{N-1}(4)}{R(1) + b^2(1)\ \hat{K}_{N-1}(3)}}\right]. \qquad \text{(C.13.38)}$$

Since $\hat{K}_{N-1}(4) \leq \hat{K}_{N-1}(3)$, this intersection of $V^{3,U}_{N-2}$ and $V^{4,L}_{N-2}$ always exists (for the problems of this Section). This completes the derivation of $V_{N-2}(x_{N-2}, r_{N-2}=1)$ for the situation that is shown in figure 7.16.

Next let us consider the situation shown in figure 7.17. Here (C.13.31) holds with

$$\ell_{N-2}(1) = 7 \qquad \text{(C.13.39}$$

and

$$K_{N-2}(i:1) = K_{N-2}(i) \qquad i=1,2,6,7$$

$$K_{N-2}(4:1) = K_{N-2}(4) \qquad i=6,7$$

$$K_{N-2}(3:1) = \tilde{K}_{N-2} = K_{N-2}(5:1)$$

$$H_{N-2}(i:1) = G_{N-2}(i:1) = 0 \quad i=1,4,7 \qquad \text{(C.13.40)}$$

$$H_{N-2}(2:1) = H_{N-2}(2) = -H_{N-2}(6) = -H_{N-2}(6:1)$$

$$G_{N-2}(2:1) = G_{N-2}(2) = G_{N-2}(6) = G_{N-2}(6:1)$$

$$H_{N-2}(3:1) = \tilde{H}_{N-2}(3) = -\tilde{H}_{N-2}(4) = -H_{N-2}(5:1)$$

$$G_{N-2}(3:1) = \tilde{G}_{N-2}(3,4) = \tilde{G}_{N-2}(4,4) = G_{N-2}(5:1)$$

with

$$\delta_{N-2}(0) \triangleq -\infty \qquad \delta_{N-2}(7) \triangleq +\infty$$

$$\delta_{N-2}(3) = \frac{\theta_{N-2}(4)}{a(1)} = \frac{-\Theta_{N-2}(4)}{a(1)} = -\delta_{N-2}(4) \qquad \text{(C.13.41)}$$

and

$$\delta_{N-2}(1) = -\delta_{N-2}(6) \triangleq +\infty \qquad \text{(C.13.42)}$$

$$\delta_{N-2}(2) = -\delta_{N-2}(5)$$

Jointing point $\delta_{N-2}(1)$ occurs at the leftmost intersection of the functions $V_{N-2}^{1,U}$ and $V_{N-2}^{2,u}$, which we have already computed in (C.13.35).

Joining point $\delta_{N-2}(2)$ is the leftmost intersection [1] of $V_{N-2}^{4,L}$ and $V_{N-2}^{2,U}$.

[1] This intersection must exist for the situation of figure 7.17 to occur.

That is, it is the least x_{N-2} such that

$$V^{4,L}_{N-2} - V^{2,U}_{N-2} = x^2_{N-2}\,[\tilde{K}_{N-2} - K_{N-2}(2)] + K_{N-2}\,[\tilde{H}_{N-2}(3) - H_{N-2}(2)]$$

$$+ [\tilde{G}_{N-2}(3,4) - G_{N-2}(2)] = 0 \quad .$$

Using the quadratic formula we find that

$$\delta_{N-1}(2) = \frac{-\alpha}{a(1)}\left[1 + \frac{b^2(1)}{R(1)}\left\{\begin{matrix}(1-\omega_2)Q(1) \\ + \omega_2(Q(2) + K_{N-1}(1:2))\end{matrix}\right\}\right]\left[1 + \sqrt{1 - X_2}\right] \qquad \text{(C.13.43)}$$

where

$$X_2 = (1 - \omega_2)\left[\left(1 + \frac{b^2(1)}{R(1)}\ \hat{K}_N(2)\left(1 + \frac{b^2(1)}{R(1)}\left[\begin{matrix}1-\omega_2\ Q(1) \\ + \omega_2(Q(2) + K_{N-1}(1:2))\end{matrix}\right]\right)\right.\right.$$

$$\left.\left. + \frac{b^2(1)}{R(1)} K_N(2)(1 - \omega_2)a^2(1)\right]\right.$$

$$\cdot \qquad \left.\frac{}{\left[1 + \frac{b^2(1)}{R(1)}\left\{(1- \omega_2)Q(1) + \omega_2(Q(2) + K_{N-1}(1:2))\right]^2}\right] \qquad \text{(C.13.44)}$$

We note in passing that, in general, there need not be any intersection of the functions $V^{4,L}_{N-2}(x_{N-2})$ and $V^{2,U}_{N-2}(x_{N-2})$. That is, we can have $X_2 \geq 1$. The condition $X_2 < 1$ is necessary for the situation of figure 7.17 to occur.

Now let us consider the situation shown in figure 7.18. Here (C.13.31) holds with

$$m_{N-2}(1) = 5 \tag{C.13.45}$$

and

$$K_{N-2}(1:1) = K_{N-2}(1)$$

$$K_{N-2}(2:1) = \tilde{K}_{N-2} = K_{N-2}(4:1)$$

$$K_{N-2}(3:1) = K_{N-2}(4)$$

$$K_{N-2}(5:1) = K_{N-2}(7)$$

$$H_{N-2}(i:1) = G_{N-2}(i:1) = 0 \qquad i=1,3,5 \tag{C.13.46}$$

$$H_{N-2}(2:1) = \tilde{H}_{N-2}(3) = -\tilde{H}_{N-2}(4) = -H_{N-2}(4:1)$$

$$G_{N-2}(2:1) = \tilde{G}_{N-2}(3,4) = \tilde{G}_{N-2}(4,4) = G_{N-2}(4:1)$$

with

$$\delta_{N-2}(0) \triangleq -\infty \qquad \delta_{N-2}(5) \triangleq +\infty$$

$$\delta_{N-2}(2) = \frac{\theta_{N-2}(4)}{a(1)} = \frac{-\theta_{N-2}(4)}{a(1)} = -\delta_{N-2}(3) \tag{C.13.47}$$

and

$$\delta_{N-2}(1) = -\delta_{N-2}(4) \qquad \bullet$$

Joining point $\delta_{N-2}(1)$ is the leftmost intersection of $V_{N-2}^{4,L}$ and $V_{N-2}^{1,U}$. That is, the least x_{N-2} such that

$$V_{N-2}^{4,L} - V_{N-2}^{1,U} = x_{N-2}^2 [\tilde{K}_{N-2} - K_{N-2}(1)] + x_{N-2} \tilde{H}_{N-2}(3)) + \tilde{G}_{N-2}(3,4) = 0$$

Using the quadratic formula we find that

$$\delta_{N-2}(1) = \frac{-\alpha}{a(1)} (1 + \frac{b^2(1)}{R(1)} \hat{K}_{N-1}(\cdot)) \left(1 + \sqrt{1 - \frac{R(1) + b^2(1)\, \hat{K}_{N-1}(4)}{R(1) + b^2(1)\, K_{N-1}(1)}}\right). \quad \text{(C.13.48)}$$

Since $\hat{K}_{N-1}(4) \leq \hat{K}_{N-1}(1)$, this intersection of $V_{N-2}^{4,L}$ and $V_{N-2}^{1,U}$ always exists (for the problems of this section).

In fact 7.4 we list several graphical conditions on the candidate expected costs-to-go for $V_{N-2}(x_{N-2}, r_{N-2}=1)$ that relate to the three situations described above. In particular

$$\left(\begin{array}{l}\text{situation (1)} \\ \text{(C.13.31) - (C.13.38)} \\ \text{figure 7.16}\end{array}\right) \Longleftrightarrow \left(\begin{array}{l}\text{Leftmost intersection of} \\ V_{N-2}^{4,L} \text{ and } V_{N-2}^{3,U} \text{ to the right} \\ \text{of } \theta_{N-2}(3)/a(1)\end{array}\right) \quad \text{(C.13.49)}$$

$$\left(\begin{array}{l}\text{situation (3)} \\ \text{(C.13.31), (C.13.45) -} \\ \text{(C.13.48)}\end{array}\right) \Longleftrightarrow \left(\begin{array}{l}\text{Leftmost intersection of} \\ V_{N-2}^{4,L} \text{ and } V_{N-2}^{1,U} \text{ to the left of} \\ \text{(or at) leftmost intersection} \\ \text{of } V_{N-2}^{2,U} \text{ and } V_{N-2}^{1,U}\end{array}\right) \quad \text{(C.13.50)}$$

Now from (C.13.22) and (C.13.38), the right hand side of (C.13.49) becomes (7.32). Since the denominator of (7.32) is grater than one, any a(1) satisfying (7.32) will be consistent with our assumption (C.13.9). Note that

$$1 < 1 + \sqrt{1 - \frac{R(1) + b^2(1)\,\hat{K}_{N-1}(4)}{R(1) + b^2(1)\,\hat{K}_{N-1}(3)}} < 2$$

(since $\hat{K}_{N-1}(4) < \hat{K}_{N-1}(3)$). Thus we have that (7.32) holds if (7.35) holds.

We can obtain the less conservative, sufficient conditions (7.34), (7.36) substituting in (7.32) (7.33 the values

$$\hat{K}_{N-1}(4) = (1-\omega_1)(K_{N-1}(3:1) + Q(1)) + \omega_1 (K_{N-1}(1:2) + Q(2))$$

$$\hat{K}_{N-1}(3) = (1-\omega_2)(K_{N-1}(3:1) + Q(1)) + \omega_2 (K_{N-1}(1:2) + Q(2))$$

$$\hat{K}_{N-1}(1) = (1-\omega_2)(K_{N-1}(1:1) + Q(1)) + \omega_2 (K_{N-1}(1:2) + Q(2))$$

Since, by facts 7.1 - 7.3,

$$K_T(1) \leq K_{N-1}(3:1) \leq K_{N-1}(1:1) < K_{N-1}(1:2) \qquad \text{(C.13.51)}$$

we have

(C.13.52)

$$\frac{\frac{b^2(1)}{R(1)}(\omega_2-\omega_1)\{(Q(2) - Q(1))\}}{1+\frac{b^2(1)}{R(1)}(K_{N-1}(1:2) + (1-\omega_2)\,Q(1) + \omega_2\,Q(2))} < \left(1 - \frac{R(1) + b^2(1)\,\hat{K}_{N-1}(4)}{R(1) + b^2(1)\,\hat{K}_{N-1}(3)}\right)$$

$$< \frac{\frac{b^2(1)}{R(1)}(\omega_2-\omega_1)\{(K_{N-1}(1:2) + Q(2) - Q(1) - K_T(1)}{1 + \frac{b^2(1)}{R(1)}((1-\omega_2)(K_T(1) + Q(1) + \omega_2(K_{N-1}(1:2) + Q(2)))} \bullet$$

From (7.32) and the right two terms of (C.13.52) we get (7.34). From (7.32) and the left two terms of (C.13.52) we obtain (7.37).

From (C.13.35) and (C.13.48) the right hand side of (C.13.50) becomes (7.33). Using (C.13.51), we can derive the inequalities

$$\frac{b^2(1)(\omega_2-\omega_1)(Q(2) - Q(1)}{R(1) + b^2(1)\left\{K_{N-1}(1:2) + 1-\omega_2)(Q(1) +\omega_2\ Q(2)\right\}} < 1 - \frac{R(1) + b^2(1)\ K_{N-1}(4)}{R(1) + b^2(1)\ K_{N-1}(1)}$$

$$< b^2(1)\left[(\omega_2-\omega_1)\begin{pmatrix} K_{N-1}(1:2) + Q(2) \\ -K_T(1) - Q(1) \end{pmatrix} + \right.$$

$$\left. \frac{+(1-\omega_2)\left(K_N(1) - \hat{K}_N(2)\right)\left(R(1) + b^2(1)\ \hat{K}_N(2)\right)^2}{R(1) + b^2(1)\ K_N(1))(R(1) + b^2(1)\ \hat{K}_N(1)} \right]$$

$$\frac{}{R(1) + b^2(1)\left\{(1-\omega_2)(Q(1) + K_T(1) +\omega_2(Q(2) + K_{N-1}(1:2)\right\}}$$

(C.13.53)

C.14 Proof of Proposition 7.7

Proposition 7.7 is proved inductively for decreasing values of (N-k). From Fact 6.9 we see that the proposition holds at time (N-1). In appendix C.13 it is shown that Proposition 7.7 holds at time (N-2). We prove that Proposition 7.7 holds at all times (N-ℓ) by an induction on ℓ, beginning with $\ell = 2$.

Suppose that Proposition 7.7 holds at time (N-ℓ+1). We will show that it holds at N-ℓ as well.

We first show that Proposition 7.7(4) holds; that is, the grid points in the composite partition of x_{N-k+1} obey (7.44) for $k = \ell$. This is clearly true if we have

$$\delta_{N-\ell+1}(2\ell-2) < -\alpha \qquad \text{(C.14.1)}$$

and

$$\alpha < \delta_{N-\ell+1}(2\ell - 1) \qquad \text{(C.14.2)}$$

From Proposition 7.7(4) (for $k = \ell-1$) we have

$$\delta_{N-\ell+1}(2\ell-2) = -\delta_{N-\ell+1}(2\ell-1)$$

Thus we need only verify (C.14.1) to prove that Proposition 7.7(4) holds for $k=\ell$.

We have assumed (by 7.12) and Fact 7.6(1)) that

$$a(1) < 1 + \frac{b^2(1)}{R(1)} \hat{K}_N(2)$$

and since $\hat{K}_N(2) \equiv \hat{K}_N^{LM}$ and $\{\hat{K}_{N-k}^{LM}\}$

increases with (N-k), we have

$$a(1) < 1 + \frac{b^2(1)}{R(1)} \hat{K}_{N-k+1}^{LM} \quad \text{, for all } k .$$

Since (7.44) and Proposition 7.7(5) hold for $k = \ell-1$, we have

$$\hat{K}^{LM}_{N-\ell+1} = \hat{K}_{N-\ell+1}(2\ell)$$

hence

$$a(1) < 1 + \frac{b^2(1)}{R(1)} \hat{K}_{N-\ell+1}(2\ell) \quad .$$

Therefore we have[1]

$$\frac{-\alpha}{a(1)} \left(1 + \frac{b^2(1)}{R(1)} \hat{K}_{N-\ell+1}(2\ell) < -\alpha \right) \quad . \qquad \text{(C.14.3)}$$

By (7.68) the left-hand side of (C.14.3) is $\delta_{N-\ell+1}(2\ell-2)$. Thus (C.14.1) holds, so we have verified Proposition 7.7(4) for $k = \ell$.

The composite $x_{N-\ell+1}$ partition and the eligible condidate cost-to-go functions for $V_{N-\ell}(x_{N-\ell}, r_{N-\ell}=1)$ are shown in figure C.14.1. The formulas for the parameters of each of these candidate cost functions and associated control laws are given in Appendices C.1 - C.4.

Using the fact that Proposition 7.7(4) is true for $\ell = k$ (verified above) and that Proposition 7.7(9-10) are true for $\ell = k-1$ (by assumption) we can simultaneously verify items 1-3 and 5-8 of Proposition 7.7 for $\ell = k$. Then we will prove that Proposition 7.7(9,10), hold for $\ell=k$, to complete the inductive step.

Given the composite $x_{N-\ell+1}$ partition of (7.44), we can use Proposition 5.2 to list the eligible candidate costs:

$V^{t,U}_{N-\ell}$ $\qquad t = 1,\ldots,4\ell-1$

$V^{2\ell,L}_{N-\ell}$

$V^{2\ell,R}_{N-\ell}$

[1] $\alpha > 0$.

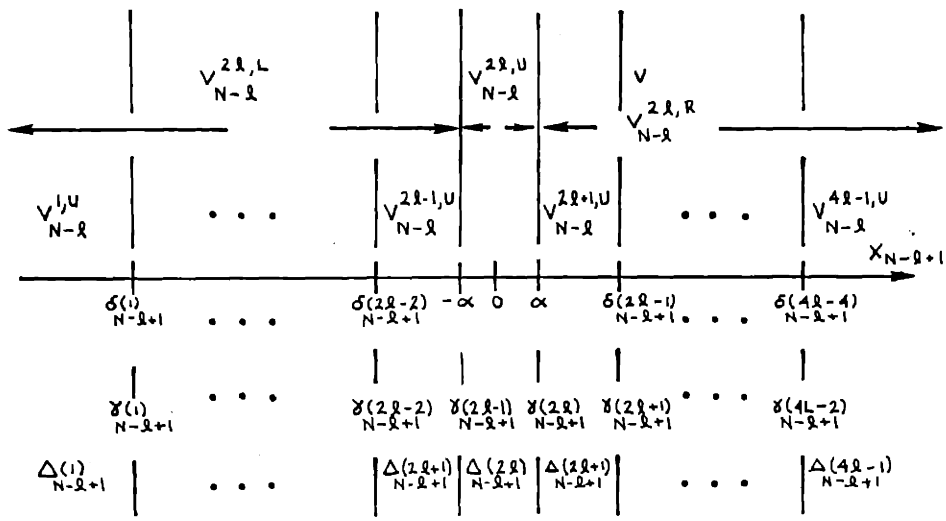

Figure C.14.1 Composite x-Partition Grid Points and Intervals.

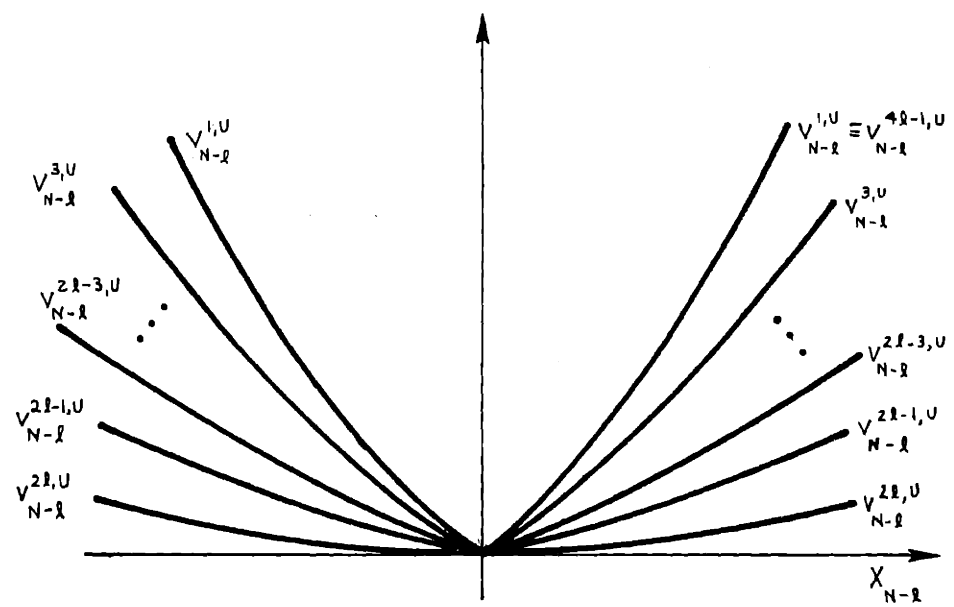

Figure C.14.2: Ordering of Candidate Cost Functions

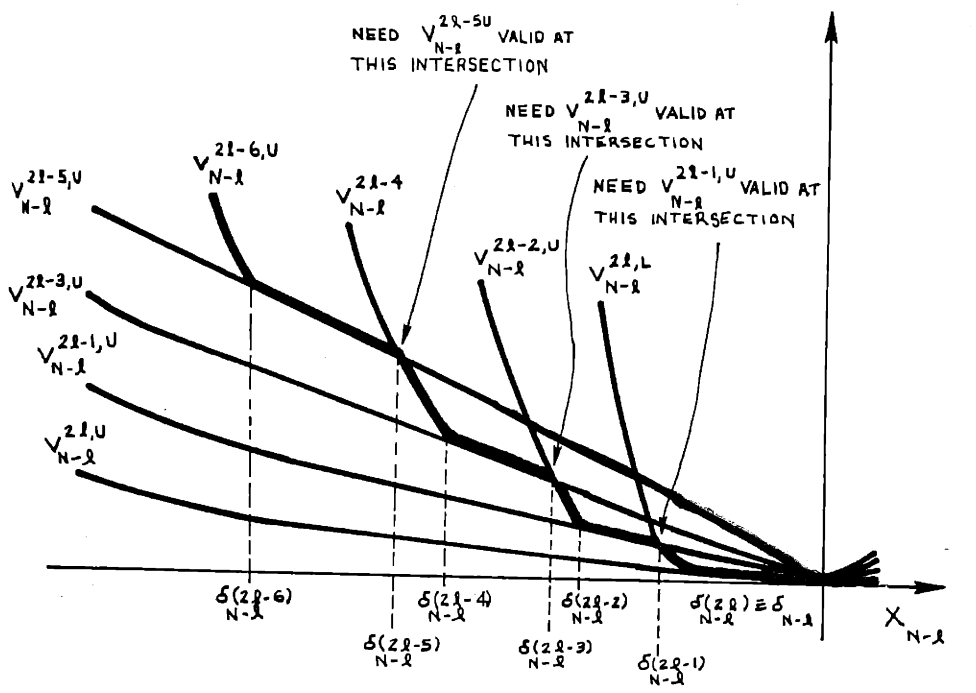

Figure C.14.3: Finding the Optimal Cost for negative x values, moving leftwards from zero.

Formulas for the parameters of these cost functions are given in Appendices C.1 - C.4. Now given that Proposition 7.7(9) is true at $k = \ell-1$ we have

$$V_{N-\ell}^{2\ell,U} < V_{N-\ell}^{2\ell-1,U} < V_{N-\ell}^{2\ell-3,U} < \ldots < V_{N-\ell}^{3,U} < V_{N-\ell}^{1,U} \quad , \qquad (C.14.4)$$

as shown in figure C.14.2.

From Facts 7.1 - 7.3 we know the formulas for the controller end-pieces

$$V_{N-\ell}^{Le}(1) = V_{N-\ell}^{1,U} = V_{N-\ell}(1:1)$$

$$V_{N-\ell}^{Re}(1) = V_{N-\ell}^{4\ell-1,U} = V_{N-\ell}(m_{N-\ell}(1):1)$$

and the middlepiece

$$V_{N-\ell}^{LM}(1) = V_{N-\ell}(m_{N-\ell}(1)/2 + 1:1) = V_{N-\ell}^{2\ell,U} \quad . \qquad (C.14.5)$$

Since the middlepiece cost function in (C.14.5) is also the lower bound cost function

$$V_{N-\ell}^{LB}(1) \equiv V_{N-1}^{LM}(1) \equiv V_{N-\ell}^{2\ell,U}$$

(by Facts 7.1 - 7.3), it is optimal over its entire region of validity:

$$\underline{\delta}_{N-\ell}(1) = \frac{-\alpha}{a(1)}\left(1 + \frac{b^2(1)}{R(1)}\hat{K}_{N-\ell+1}(2\ell)\right) < x_{N-\ell} < \frac{\alpha}{a(1)}\left(1 + \frac{b^2(1)}{R(1)}\hat{K}_{N-\ell+1}(2\ell)\right) \triangleq \tilde{\delta}_{N-\ell}(1).$$

Now let us consider $V_{N-\ell}(x_{N-\ell}, r_{N-\ell}=1)$ from $x_{N-\ell}=0$ leftwards (for increasingly negative $x_{N-\ell}$). Since $V_{N-\ell}^{2\ell,L}$ intersects $V_{N-\ell}^{2\ell,U}$ at $\underline{\delta}_{N-\ell}(1)$, it is clearly optimal immediately to the left of $\underline{\delta}_{N-\ell}(1)$, as shown in figure C.14.3.

$V_{N-\ell}^{2\ell,L}$ will remain optimal as we consider increasingly negative $x_{N-\ell}$ in figure C.14.3, until it intersects another valid eligible[1] candidate cost-to-go function. As shown in figure C.14.3, this next optimal piece of $V_{N-2}(x_{N-2}, r_{N-2}=1)$ will coincide with $V_{N-2}^{2\ell-1,U}$ if $V_{N-2}^{2\ell-1,U}$ is valid immediately to the left of its intersection with $V_{N-2}^{2\ell,L}$. If this is the case then this intersection is a joining point of $V_{N-2}(x_{N-2}, r_{N-2}=1)$ and $V_{N-2}^{2\ell-1,U}$ is optimal until $V_{N-2}^{2\ell-1,U}$ ceases to be valid, at

$$x_{N-\ell} = \frac{\Theta_{N-\ell}(2\ell-1)}{a(1)} = \delta_{N-\ell}^{(2\ell-2)} \quad \bullet \qquad \text{(C.14.6)}$$

To the left of this point, $V_{N-2}^{2\ell-2,U}$ will be valid until[2] it intersects another valid eligible candidate cost. The next (to the left) piece of $V_{N-2}(x_{N-2}, r_{N-2}=1)$ will be $V_{N-2}^{2\ell-3,U}$ if it is valid immediately to the left at its leftmost intersection with $V_{N-2}^{2\ell-3,U}$. This process continues until $V_{N-2}^{2,U}$ intersects $V_{N-2}^{1,U} = V_{N-2}^{Le}(1)$.

When the requirements of validity described above and shown in figure C.14.3 are met, then (1) - (3) and (5) - (8) of Proposition 7.7 hold for k = ℓ. That is, using (7.70) - (7.71) for k = ℓ we need

$$\delta_{N-\ell}(2i) < \delta_{N-\ell}(2i+1) \qquad \text{(C.14.7)}$$

$$\text{for } i = \ell-1, \ldots, 1$$

for (1) - (3) and (5) - (8) to be true.

---

[1] In the sense of section 7.2

[2] as $x_{N-\ell}$ decreases

Let us consider

$$\delta_{N-\ell}(2\ell-2) < \delta_{N-\ell}(2\ell-1) \quad . \tag{C.14.8}$$

We have, by (7.71) with k = ℓ :

$$\delta_{N-\ell}(2\ell-1) = \frac{-H_{N-\ell}(2\ell:1)}{2[K_{N-\ell}(2\ell:1) - K_{N-\ell}(2\ell-1:1)]} (1 + \sqrt{1-\chi}) \tag{C.149}$$

where

$$\chi = \frac{4[K_{N-\ell}(2\ell:1) - K_{N-\ell}(2\ell-1:1)]\ G_{N-\ell}(2\ell:1)}{H^2_{N-\ell}(2\ell:1)} \quad . \tag{C.14.10}$$

Now since

$$H_{N-\ell}(2\ell:1) = 2a(1)\ R(1)\ \alpha/b^2(1)$$

$$K_{N-\ell}(2\ell:1) - K_{N-\ell}(2\ell-1:1) = \frac{a^2(1)\ R^2(1)}{b^2(1)\ (R(1) + b^2(1)\ \hat{K}_{N-\ell+1}(2\ell-1)}$$

we have

$$\delta_{N-\ell}(2\ell-1) = \frac{-\alpha}{a(1)} (1 + \frac{b^2(1)}{R(1)} \hat{K}_{N-\ell+1}(2\ell-1)(1 + \sqrt{1-\chi}) \quad . \tag{C.14.11}$$

From (7.70) = (C.14.6) we have

$$\delta_{N-\ell}(2\ell-2) = \frac{-\alpha}{a^2(1)} (1 + \frac{b^2(1)}{R(1)} \hat{K}_{N-\ell+2}(2\ell-2))(1 + \frac{b^2(1)}{R(1)} \hat{K}_{N-\ell+1}(2\ell-1)) \tag{C.14.12}$$

From (C.14.11) and (C.14.12) we have that (C.14.8) holds if

$$a(1) < \frac{1 + \frac{b^2(1)}{R(1)} \hat{K}_{N-\ell+2}(2\ell-2)}{1 + \sqrt{1-\chi}} \quad . \tag{C.14.13}$$

But

$$\frac{1}{2} < \frac{1}{1 + \sqrt{1-\chi}} < 1$$

So (C.14.13) (hence (C.14.8)) holds if

$$a(1) < \frac{1}{2}\left(1 + \frac{b^2(1)}{R(1)} \hat{K}_{N-\ell+2}(2\ell-2)\right) . \tag{C.14.14}$$

Now

$$\hat{K}_{N-\ell+2}(2\ell-2) = \hat{K}^{LM}_{N-\ell+2}(1)$$

so we need

$$a(1) < \frac{1}{2}\left(1 + \frac{b^2(1)}{R(1)} \hat{K}^{LM}_{N-\ell+2}(1)\right). \tag{C.14.15}$$

This is guaranteed to be true, however, since by (7.35) we have assumed

$$a(1) < \frac{1}{2}\left(1 + \frac{b^2(1)}{R(1)} \hat{K}_N(2)\right)$$

$$= \frac{1}{2}\left(1 + \frac{b^2(1)}{R(1)} \hat{K}^{LM}_N(1)\right) \tag{C.14.16}$$

and (by Facts 7.1 - 7.3), $\{\hat{K}^{LM}_{N-k}\}$ increases monotonely as $(N-k) \to \infty$. So (C.14.7) holds for $i = \ell - 1$. For other values of i in (C.14.7) we need

$$\delta_{N-\ell}(2i) < \delta_{N-\ell}(2i+1) \qquad\qquad i = 1,2,\ldots,\ell-2$$

to hold which, by (7.70) - (7.71) (with $k = \ell$), requires that

$$\frac{-\alpha}{a(1)}\left(1 + \frac{b^2(1)}{R(1)} \hat{K}_{N-i+1}(2i)\right) \prod_{j=1}^{\ell-1}\left[1 + \frac{\frac{b^2(1)}{R(1)} \hat{K}_{N-\ell+j}(2i+1)}{a(1)}\right] <$$

$$< \frac{-H_{N-\ell}(2i+2:1)}{2[K_{N-\ell}(2i+2:1) - K_{N-\ell}(2i+1:1)]} \left(1 + \sqrt{1-\chi_i}\right) \tag{C.14.18}$$

where $0 < \chi_i < 1$. (C.14.19)

Substituting for the parameters in (C.14.17) yields the requirement

$$a(1) < \frac{(1 + \frac{b^2(1)}{R(1)} \hat{K}_{N-i+1}(2i))}{1 + \sqrt{1-\chi_i}} \qquad \text{(C.14.20)}$$

which is, by (C.14.19), guaranteed if

$$a(1) < \frac{1}{2} (1 + \frac{b^2(1)}{R(1)} \hat{K}_{N-i+1}(2i)) \quad . \qquad \text{(C.14.21)}$$

But $$\hat{K}_{N-i+1}(2i) = \hat{K}^{LM}_{N-i+1}(1) < \hat{K}^{LM}_{N}(1)$$

so (C.14.15) guarantees that (C.14.21) holds for i = 1,2,..., ℓ-2. Thus condition (7.35) $\equiv$ (C.14.16) results in the situation of figure C.14.2 That is, (1) - (8) of Proposition 7.7 hold for k = ℓ .

Given (1) - (8), it is easily verified that (9) - (10) of Proposition 7.7 hold,using Lemma C.13.1. This completes the inductive step (on ℓ), and the proof of Proposition 7.7.

□

C.15 Conflicting Goals Problem Derivation

We are considering problems of the class (C.13.1) - (C.13.7) where, instead of (C.13.8) we have

$$\omega_1 > \omega_2 \tag{C.15.1}$$

hence, by Fact 7.3 it follows that:

- the endpieces $V_k^{Le}(1) \equiv V_k^{Re}(1)$ are given are given by the same function of x_k as the lower bound $V_k^{LB}(1)$
- the middlepiece $V_k^{LM}(1) \equiv V_k^{RM}(1)$ is given by the same function of x_k as the upper bound $V_k^{UB}(1)$.

That is, we have the opposite of the situation in section 7.5 and Appendix C.13.

We will also assume that (7.14) holds:

$$a(1) < \left(1 + \frac{b^2(1)}{R(1)} \hat{K}_N(2)\right)\left(1 - \sqrt{1 - \frac{R(1) + b^2(1)\, \hat{K}_N(1)}{R(1) + b^2(1)\, \hat{K}_N(2)}}\right) \tag{C.15.2}$$

hence we have "situation (1)" of table 7.2 and figure 7.23(d) applies.

In section 6.6 we obtained the complete solution for this problem at $k = N-1$; it is specified by (6.112) - (6.116), (6.119) - (6.120), (6.147) - (6.154) and figures 6.14 - 6.16. Using lemma C.13.1 we can show that, as in figure 7.23(c):

$$K_{N-1}(2:1) = K_{N-1}(4:1) > K_{N-1}(3:1) > K_{N-1}(1:1) = K_{N-1}(5:1). \tag{C.15.3}$$

This is done as follows: since we have

$$\hat{K}_N(2) < \hat{K}_N(1) = \hat{K}_N(3) \ ,$$

then (1) of Lemma C.13.1 and (6.128), (6.130) yield

$$K_{N-1}(1:1) \equiv K_{N-1}(5:1) < K_{N-1}(3:1) \quad .$$

The other inequality in (C.15.3) is obtained using (2) of Lemma C.13.1. Since $V_{N-1}(2:1) = V_{N-1}^{1,R}$ and $V_{N-1}(1:1) = V_{N-1}^{1,U}$ we have

$$V_{N-1}(2:1) = \left(\begin{array}{l} x_{N-1}^2 \; K_{N-1}(2:1) \\ \quad + \\ x_N \; H_{N-1}(2:1) \\ \quad + \\ G_{N-1}(2:1) \end{array} \right) > x_{N-1}^2 \; K_{N-1}(1:1) = V_{N-1}(1:1) \qquad \text{(C.15.4)}$$

except for equality at $x_{N-1} = \delta_{N-1}(1)$.

Now let us consider time K = N-2 for this problem. Among the eligible candidate cost-to-go functions for $V_{N-2}(x_{N-2} | r_{N-2}=1)$ are

$$V_{N-2}^{t,U}(x_{N-2,1}) = x_{N-2}^2 \; K_{N-2}(t) + x_{N-2} \; H_{N-2}(t) + G_{N-2}(t) \qquad \text{(C.15.5)}$$

for

$$\frac{\theta_{N-2}(t)}{a(1)} \leq x_{N-2} \leq \frac{\Theta_{N-2}(t)}{a(1)} \qquad \text{for } t = 1,2,\ldots,7$$

where (see appendix C.1) we have the parameters in (C.15.5) as given by (C.13.17) - (C.13.23).

Given (C.15.3), $\omega_2 > \omega_1$ and $K_{N-1}^{UB}(1) < K_{N-1}(1:2)$ we have

$$\hat{K}_{N-1}(1) = \hat{K}_{N-1}(7) < \hat{K}_{N-1}(3) = \hat{K}_{N-1}(5) < \hat{K}_{N-1}(4) \qquad \text{(C.15.6)}$$

by Lemma C.13.1(1) and thus

$$V^{4,U}_{N-2} > V^{3,U}_{N-2} = V^{5,U}_{N-2} > V^{7,U}_{N-2} = V^{1,U}_{N-2} \quad \text{at all } x_{N-2} \tag{C.15.7}$$

By (C.15.6) we also have

$$V^{2,U}_{N-2} > V^{1,U}_{N-2} \qquad \text{except equality at } x_{N-2} = \theta_{N-2}(2)/a(1)$$

$$V^{6,U}_{N-2} > V^{7,U}_{N-2} \qquad \text{except equality at } x_{N-2} = \theta_{N-2}(7)/a(1)$$

That is, we have verified (7.106) - (7.108) and figure 7.24.

In addition to the $V^{t,U}_{N-2}(t=1,\ldots,7)$ the other two eligible candidate functions for $V_{N-2}(x_{N-2},r_{N-2}=1)$ are

$$V^{3,U}_{N-2}(x_{N-2},r_{N-2}=1) = x^2_{N-2}\,\tilde{\tilde{K}}_{N-2} + x_{N-2}\,\tilde{\tilde{H}}_{N-2}(3) + \tilde{\tilde{G}}_{N-2}(3,3)$$

$$V^{5,L}_{N-2}(x_{N-2},r_{N-2}=1) = x^2_{N-2}\,\tilde{\tilde{K}}_{N-2} + x_{N-2}\,\tilde{\tilde{H}}_{N-2}(4) + \tilde{\tilde{G}}_{N-2}(4,5)$$

where $\tilde{\tilde{K}}_{N-2}$, $\tilde{\tilde{H}}_{N-2}(3)$ and $\tilde{\tilde{H}}_{N-2}(4)$ are given by (C.13.26) - (C.13.28) and

$$\tilde{\tilde{G}}_{N-2}(3,3) = \alpha^2\left[\hat{K}_{N-1}(3) + \frac{R(1)}{b^2(1)}\right] = \tilde{\tilde{G}}_{N-2}(4,5)\ .$$

When the first situation for $V_{N-2}(x_{N-2},r_{N-2}=1)$ occurs (as shown in figure 7.25) we have

$$V_{N-2}(i{:}1) = x^2_{N-2}\,K_{N-2}(i{:}1) + x_{N-2}\,H_{N-2}(i{:}1) + G_{N-2}(i{:}1)$$

$$\text{for} \quad \delta_{N-2}(i{:}1) \le x_{N-2} \le \delta_{N-2}(i) \tag{C.15.8}$$

$$\text{with} \quad i = 1,2,\ldots,m_{N-2}(1)$$

where

$$m_{N-2}(1) = 9 \tag{C.15.9}$$

Here

$$K_{N-2}(i:1) = K_{N-2}(i) \qquad i = 1,2,3$$

$$K_{N-2}(4:1) = \tilde{K}_{N-2} = K_{N-2}(6:1)$$

$$K_{N-2}(5:1) = K_{N-2}(4)$$

$$K_{N-2}(i;1) = K_{N-2}(i-2) \qquad i = 7,8,9$$

$$H_{N-2}(i:1) = G_{N-2}(i:1) = 0 \qquad i = 1,3,5,7,9$$

$$H_{N-2}(2:1) = H_{N-2}(2) = -H_{N-2}(6) = -H_{N-2}(8:1) \qquad \text{(C.15.10)}$$

$$G_{N-2}(2:1) = G_{N-2}(2) = G_{N-2}(6) = G_{N-2}(8:1)$$

$$H_{N-2}(4:1) = \tilde{H}_{N-2}(3) = -\tilde{H}_{N-2}(4) = -H_{N-2}(6:1)$$

$$G_{N-2}(4:1) = \tilde{\tilde{G}}_{N-2}(3,3) = \tilde{\tilde{G}}_{N-2}(4,4) = G_{N-2}(6:1)$$

with

$$\delta_{N-2}(0) \triangleq -\infty \qquad \delta_{N-2}(9) \triangleq +\infty$$

$$\delta_{N-2}(1) = \frac{\Theta_{N-2}(1)}{a(1)} = \frac{\theta_{N-2}(2)}{a(1)} = \frac{-\Theta_{N-2}(5)}{a(1)} = \frac{-\theta_{N-2}(7)}{a(1)} = -\delta_{N-2}(8)$$

$$\delta_{N-2}(3) = \frac{\Theta_{N-2}(3)}{a(1)} = \frac{-\theta_{N-2}(5)}{a(1)} = -\delta_{N-2}(6) \qquad \text{(C.15.11)}$$

and

$$\delta_{N-2}(2) = -\delta_{N-2}(7)$$

$$\delta_{N-2}(4) = -\delta_{N-2}(5)$$

Joining point $\delta_{N-2}(2)$ occurs at the rightmost intersection of the functions $V_{N-2}^{2,U}$ and $V_{N-2}^{3,U}$. This is the greatest x_{N-2} such that

$$V^{2,U}_{N-2} - V^{3,U}_{N-2} = x^2_{N-2}\left[K_{N-2}(2) - K_{N-2}(3)\right] + x_{N-2}H_{N-2}(2) +$$

$$+ G_{N-2}(2) = 0 \quad .$$

From figure 7.25 we see that this intersection exists for all parameter values consistent with the assumptions of this section. Using the quadratic formula we find this point to be

$$\delta_{N-2}(2) = \frac{-\alpha}{a^2(1)}\left(1 + \frac{b^2(1)}{R(1)}\hat{K}_N(2)\right)\left(1 + \frac{b^2}{R}\hat{K}_{N-1}(3)\right)\left(1 - \sqrt{1-\chi_3}\right) \qquad \text{(C.15.12)}$$

where

$$\chi_3 = \frac{\left(1 + \frac{b^2(1)}{R(1)}\hat{K}_N(1)\right)\left(1 + \frac{b^2(1)}{R(1)}\hat{K}_{N-1}(2)\right) - (1-\omega_2)a^2(1)}{\left(1 + \frac{b^2(1)}{R(1)}\hat{K}_{N-1}(3)\right)\left(1 + \frac{b^2}{R(1)}\hat{K}_N(2)\right)} \quad . \qquad \text{(C.15.13)}$$

Joining point $\delta_{N-2}(4)$ occurs at the rightmost intersection of the functions $V^{3,R}_{N-2}$ and $V^{4,U}_{N-2}$. Using the quadratic formula, we find this intersection to be

$$\delta_{N-2}(4) = \frac{-\alpha}{a(1)}\left(1 + \frac{b^2(1)}{R(1)}\hat{K}_{N-1}(4)\right)\left(1 - \sqrt{1 - \frac{R(1) + b^2(1)\hat{K}_{N-1}(3)}{R + b^2(1)\hat{K}_{N-1}(4)}}\right). \qquad \text{(C.15.14)}$$

Since $\hat{K}_{N-1}(3) \leq \hat{K}_{N-1}(4)$ for this problem, this intersection of $V^{3,R}_{N-2}$ and $V^{4,U}_{N-2}$ always exists (for the problems of section 7.6). This completes the derivation of $V_{N-2}(x_{N-2}, r_{N-2}=1)$ for the situation that is shown in figure 7.25.

Next let us consider the situation shown in figure 7.26. Here (C.15.8)

holds with

$$m_{N-2}(1) = 7 \qquad \text{(C.15.15)}$$

and

$$\begin{aligned}
K_{N-2}(i:1) &= K_{N-2}(1) \qquad i=1,2,6,7 \\
K_{N-2}(4:1) &= K_{N-2}(4) \\
K_{N-2}(3:1) &= \tilde{K}_{N-2} = K_{N-2}(5:1) \\
H_{N-2}(i:1) &= G_{N-2}(i:1) \qquad i=1,4,7 \\
H_{N-2}(2:1) &= H_{N-2}(2) = -H_{N-2}(6) = -H_{N-2}(6:1) \\
G_{N-2}(2:1) &= G_{N-2}(2) = G_{N-2}(6) = G_{N-2}(6:1) \qquad \text{(C.15.16)} \\
H_{N-2}(3:1) &= \tilde{H}_{N-2}(3) = -\tilde{H}_{N-2}(4) = -H_{N-2}(5:1) \\
G_{N-2}(3:1) &= \tilde{G}_{N-2}(3,3) = \tilde{G}_{N-2}(4,5) = G_{N-2}(5:1)
\end{aligned}$$

with

$$\delta_{N-2}(0) \triangleq -\infty \qquad \delta_{N-2}(7) \triangleq +\infty$$

$$\delta_{N-2}(1) = \frac{\Theta_{N-2}(1)}{a(2)} = -\frac{\theta_{N-2}(7)}{a(1)} = -\delta_{N-2}(6) \qquad \text{(C.15.17)}$$

and

$$\begin{aligned}
\delta_{N-2}(2) &= -\delta_{N-2}(6) \\
\delta_{N-2}(3) &= -\delta_{N-2}(4) \qquad \text{(C.15.18)}
\end{aligned}$$

Joining point $\delta_{N-2}(2)$ occurs at the rightmost intersection of the functions $V_{N-2}^{2,U}$ and $V_{N-2}^{3,R}$. Using the quadratic formula we find that

$$\delta_{N-2}(2) = \frac{-\alpha}{a(1)}\left(1 - a(1)(1-\omega_2) + \frac{b^2(1)}{R(1)}\hat{K}_{N-1}(2)\right)\left(1 - \sqrt{1-\chi_4}\right) \qquad \text{(C.15.19)}$$

where

$$\chi_4 = \frac{\left[\begin{array}{l} (1 + \frac{b^2(1)}{R(1)} \hat{K}_{N-1}(2))\left[1 + \frac{b^2(1)}{R(1)} \hat{K}_{N-1}(3) - (1-\omega_2)(1 + \frac{b^2(1)}{R(1)} \hat{K}_N(1)\right] \\ \\ + a^2(1)(1 - \omega_2)^2 \end{array} \right]}{[1 + \frac{b^2(1)}{R(1)} \hat{K}_{N-1}(2) - a(1)(1 - N_2)]^2} \qquad \text{(C.15.20)}$$

In general, there need not be any intersection of the functions $V_{N-2}^{2,U}$ and $V_{N-2}^{3,R}$. That is, we may have $\chi_4 > 1$ in (C.15.20). The condition $\chi_4 \leq 1$ is necessary for the situation of figure 7.26 to occur.

Joining point $\delta_{N-2}(3)$ occurs at the rightmost intersection of the functions $V_{N-2}^{3,R}$ and $V_{N-2}^{4,U}$, which we have already computed in (C.15.14).

Now let consider the situation shown in figure 7.27. Here (C.15.8) holds with

$$m_{N-2}(1) = 5 \qquad \text{(C.15.21)}$$

and

$$\begin{aligned} K_{N-2}(i:1) &= K_{N-2}(i) && i = 1,2 \\ K_{N-2}(3:1) &= K_{N-2}(4) \\ K_{N-2}(i:1) &= K_{N-2}(i+2) && i = 4,5 \\ H_{N-2}(i:1) &= G_{N-2}(i:1) = 0 && i = 1,3,5 \\ H_{N-2}(2:1) &= H_{N-2}(2) = -H_{N-2}(6) = -H_{N-2}(4:1) \\ G_{N-2}(2:1) &= G_{N-2}(2) = G_{N-2}(6) = G_{N-2}(4:1) \end{aligned} \qquad \text{(C.15.22)}$$

with

$$\delta_{N-2}(0) \triangleq -\infty \qquad \delta_{N-2}(5) \triangleq +\infty$$

$$\delta_{N-2}(1) = \frac{\Theta_{N-2}(1)}{a(1)} = -\frac{\Theta_{N-2}(7)}{a(1)} = \delta_{N-2}(4) \tag{C.15.23}$$

and

$$\delta_{N-2}(2) = -\delta_{N-2}(3) \quad . \tag{C.15.24}$$

Joining point $\delta_{N-2}(2)$ occurs at the rightmost intersection of the functions $V^{2,}_{N-2}$ and $V^{4,U}_{N-2}$. Using the quadratic formula we find this intersection to be

$$\delta_{N-2}(2) = \frac{-\alpha(1-\omega_2)(R(1) + b^2(1)\,\hat{K}_{N-1}(4)}{b^2(1)(\hat{K}_{N-1}(2) - \hat{K}_{N-1}(4)} \left(1 - \sqrt{1 - \chi_5}\right) \tag{C.15.25}$$

$$= \frac{-\alpha}{a^2(1)} (1-\omega_2)\left(1 + \frac{b^2(1)}{R(1)}\,\hat{K}_N(2)\right)\left(1 + \frac{b^2(1)}{R(1)}\,\hat{K}_{N-1}(4)\right)\chi_6 \left(1-\sqrt{1-\chi_5}\right) \tag{C.15.26}$$

where

$$\chi_5 = \frac{b^2(1)(\hat{K}_{N-1}(2)-\hat{K}_{N-1}(4))\left[\left(1+\frac{b^2(1)}{R(1)}\,\hat{K}_N(1)\right)\left(1+\frac{b^2(1)}{R(1)}\,\hat{K}_{N-1}(2)\right)-(1-\omega_2)a^2(1)\right]}{\left(R + b^2(1)\,\hat{K}_{N-1}(4)\right)a^2(1)(1-\omega_2)} \tag{C.15.27}$$

and

$$\chi_6 = 1 + (\omega_1 - \omega_2)(1 + b^2(1))(R(1) + b^2(1)\,\hat{K}_N(2))(Q(1) - Q(2) - K_{N-1}(1:2)) \tag{C.15.28}$$

Since $V^{2,U}_{N-2}$ and $V^{4,U}_{N-2}$ must have two intersections to the left of $x_{N-2} = 0$, (C.15.26) implies that

$$\hat{K}_{N-1}(2) > \hat{K}_{N-1}(4) \quad . \tag{C.15.29}$$

In fact 7.9 we list several graphical conditions on the candidate expected costs-to-go for $V_{N-2}, r_{N-2}=1)$ that relate to the possible situations described above. In particular,

$$\left(\begin{array}{l}\text{situation (1)}\\ \text{(C.15.9) - (C.15.14)}\\ \text{figure 7.25}\end{array}\right) \iff \left(\begin{array}{l}\text{rightmost intersection}\\ \text{of } V_{N-2}^{2,U} \text{ and } V_{N-2}^{3,U} \text{ is}\\ \text{to the } \underline{\text{left}} \text{ of}\\ \Theta_{N-2}(3)/a(1)\end{array}\right) \tag{C.15.30}$$

$$\left(\begin{array}{l}\text{situation (3)}\\ \text{(C.15.21) - (C.15.26)}\\ \text{figure 7.27}\end{array}\right) \iff \left(\begin{array}{l}\text{rightmost intersection of}\\ V_{N-2}^{2,U} \text{ and } V_{N-2}^{4,U} \text{ to the right}\\ \text{(or at) rightmost intersection}\\ \text{of } V_{N-2}^{3,R} \text{ and } V_{N-2}^{4,U}\end{array}\right). \tag{C.15.31}$$

From (C.15.12) and (C.15.22), the right-hand side of (C.15.30) becomes (7.113). From (C.15.14) and (C.15.25), the right-hand side of (C.15.31) becomes (7.114).

Using the fact that

$$K_{N-1}(2:1) = a^2(1)\ R(1)/b^2(1)$$

we can rewrite (C.15.13) as

$$\chi_3 = \frac{\left\{\left(1 + \frac{b^2(1)}{R(1)}\hat{K}_N(1)\right)\left(1 + \frac{b^2(1)}{R(1)}[(1-\omega_2)Q(1) + \omega_2(K_{N-1}(1:2) + Q(2))]\right) + (1-\omega_2)\,a^2(1)\,\frac{b^2(1)}{R(1)}\hat{K}_N(1)\right\}}{\left(1 + \frac{b^2(1)}{R(1)}\hat{K}_N(2)\right)\left(1 + \frac{b^2(1)}{R(1)}\left[\begin{array}{l}(1-\omega_2)(K_{N-1}(3:1) + Q(1))\\ + \omega_2(K_{N-1}(1:2) + Q(2))\end{array}\right]\right)} \tag{C.15.32}$$

which leads to the bound

$$\lambda_3 > \frac{\left(1 + \frac{b^2(1)}{R(1)} \hat{K}_N(1)\right)\left(1 + \frac{b^2(1)}{R(1)} \begin{bmatrix} (1-\omega_2)\, Q(1) \\ + \omega_2 (K_{N-1}(1:2) + Q(2)) \end{bmatrix}\right)}{\left(1 + \frac{b^2(1)}{R(1)} \hat{K}_N(2)\right)\left(1 + \frac{b^2(1)}{R(1)} \begin{bmatrix} (1-\omega_2)\, Q(1) \\ +\omega_2\, Q(2) + K_{N-1}(1:2) \end{bmatrix}\right)} \tag{C.15.33}$$

which yields (7.115) of fact 7.11 directly. To obtain (7.116), we note from (C.15.13) that

$$\lambda_3 > \frac{1 + \frac{b^2(1)}{R(1)} \hat{K}_N(1)}{1 + \frac{b^2(1)}{R(1)} \hat{K}_N(2)} \tag{C.15.34}$$

Since $\hat{K}_{N-1}(2) > \hat{K}_{N-1}(3)$. Thus since

$$\hat{K}_N(2) = \hat{K}_N^{LM}(1) > \hat{K}_\infty^{LM}(1)$$

(by Fact 7.3), (C.15.34) yields (7.116). □

C. 16 Proof of Proposition 7.12

Proposition 7.12 is proved inductively, for decreasing values of (N-k). From fact 6.10, we see that the proposition holds at time (N-1). In appendix C.15, it is shown that Proposition 7.12 holds at all times (N-ℓ) by an induction on ℓ, beginning with ℓ= 2.

Suppose that Proposition 7.12 holds at time (N-ℓ) + 1. We will show that it holds at time N-ℓ as well.

We first show that Proposition 7.12(4) holds; that is, the grid points in the composite partition of x_{N-k+1} obey (7.122) for k = ℓ. Following the argument for proving Proposition 7.7(4) in Appendix C.14, we need only verify that

$$\delta_{N-\ell+1}(2\ell-2) < -\alpha \quad . \tag{C.16.1}$$

Using the expression for $\delta_{N-\ell+1}(2\ell-2)$ given in (7.128), we have that (C.16.1) holds if

$$a(1) < \left(1 + \frac{b^2(1)}{R(1)} \hat{K}_{N-\ell+2}(2\ell-2)\right)\left(1 - \sqrt{1 - \frac{R(1) + b^2(1)\, \hat{K}_{N-\ell+2}(2\ell-3)}{R(1) + b^2(1)\, \hat{K}_{N-\ell+2}(2\ell-2)}}\right) . \tag{C.16.2}$$

But (C.16.2) is implied by assumption (7.117). To see this, note that (C.16.2) can be rewritten as

$$a(1) < \left(1 + \frac{b^2(1)}{R(1)} \hat{K}^{LM}_{N-\ell+2}(1)\right)\left(1 - \sqrt{\frac{b^2(1)(\omega_2-\omega_1)[Q(2)-Q(1)+K_{N-\ell+2}(1:2)K^{LM}_{N-\ell+2}(1)}{R(1) + b^2(1)\, \hat{K}^{LM}_{N-\ell+2}(1)}}\right) \tag{C.16.3}$$

and (7.117) can be rewritten as

$$a(1) < \left(1 + \frac{b^2(1)}{R(1)} \hat{K}_N^{LM}(1)\right)\left(1 - \sqrt{\frac{b^2(1)(\omega_2-\omega_1)[Q(2)-Q(1)+K_\infty(1:2)-K_T(1)]}{R(1) + b^2(1)\,\hat{K}_N^{LM}(1)}}\right)$$

(C.16.4)

Since, by Facts 7.1 - 7.3, the sequences $\{K_k(1:2)\}$, $\{K_k^{LM}(1)\}$ and $\{\hat{K}_k^{LM}(1)\}$ increase with decreasing k, (C.16.4) ≡ (7.117) is more restrictive than (C.16.3) ≡ (C.16.2). Thus (C.16.1) holds, and we have shown that Proposition 7.12(4) holds for $k = \ell$.

The composite $x_{N-\ell+1}$ partition and the eligible candidate cost-to-go functions for $V_{N-\ell}(x_{N-\ell}, r_{N-\ell}=1)$ are shown in figure C.16.1 The formulas for the parameters of each of these candidate cost functions and associated control laws are given in Appendices C.1.- C.4. Note that $V_{N-\ell}^{2\ell+1,L}$ is eligible and valid for $x_{N-\ell+1} \leq 0$; we can exclude its eligibility in the interval $(0,\alpha)$ because $V_{N-\ell}^{2\ell,R}$ is eligible here and $V_{N-\ell}^{2\ell,R}$ and $V_{N-\ell}^{2\ell+1,L}$ cross at $x_{N-\ell+1} = 0$.

Using the fact that Proposition 7.12(4) is true for $\ell = k$ (as verified above) and that Proposition 7.12 (10-11) are true for $\ell - k-1$ (by assumption) we can simultaneously verify items (1) - (3) and (5) - (9) of Proposition 7.12 for $\ell = k$. Then we will prove that Proposition 7.12 (10,11) holds for $\ell = k$, to complete the inductive step.

Given the composite $x_{N-\ell+1}$ partition of (7.122), we can use Proposition 5.2 to list the eligible candidate costs:

$V_{N-\ell}^{t,U}$ $\quad t = 1,\ldots,4\ell - 1$

$V_{N-\ell}^{2\ell-1,R}$

$V_{N-\ell}^{2\ell+1,L}$

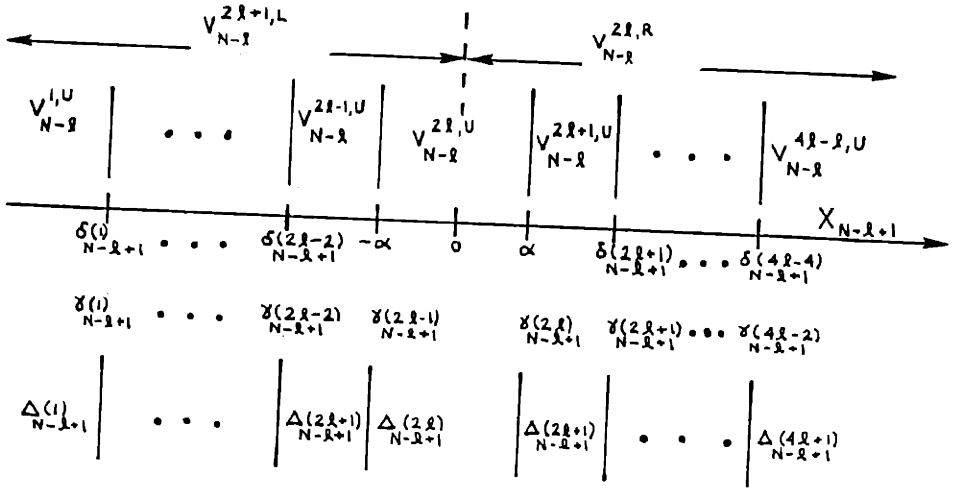

Figure C.16.1: Composite x-Partition Grid Points and Intervals

Now given that (7.134) of Preposition 7.12 is true at $k = \ell-1$, we have

$$V_{N-\ell}^{1,U} < V_{N-\ell}^{3,U} < \ldots < V_{N-\ell}^{2\ell-1,U} < V_{N-\ell}^{2\ell,U} \qquad \text{(C.16.5)}$$

as shown in figure C.16.2.

From Facts 7.1 - 7.3 we know the formula for the controller endpieces

$$V_{N-\ell}^{Le}(1) = V_{N-\ell}^{1,U} = V_{N-\ell}(1:1)$$

$$V_{N-\ell}^{Re}(1) = V_{N-\ell}^{4\ell-1,U} = V_{N-\ell}(m_{N-\ell}(1):1)$$

and the middlepiece

$$V_{N-\ell}^{LM}(1) = V_{N-\ell}\left(\frac{m_{N-\ell}(1)}{2} + 1:1\right) = V_{N-\ell}^{2\ell,U}$$

From figures C.16.1-2 we see that $V_{N-\ell}^{2\ell,U}$ is optimal over some interval about zero because at $x_{N-\ell} = 0$, $V_{N-\ell}^{2\ell,U}$ is less than the other two candidates ($V_{N-\ell}^{2\ell+1,L}$ and $V_{N-\ell}^{2\ell,R}$) .

The endpiece functions $V_{N-\ell}^{1,U} = V_{N-\ell}^{4\ell-1,U}$ are the same as the <u>lower bound</u> function $V_{N-\ell}^{LB}(1)$ for this problem. Thus these functions are <u>optimal</u> over their entire regions of validity:

$$V_{N-\ell}(x_{N-\ell}, r_{N-\ell}=1) = V_{N-\ell}^{1,U} \qquad \text{for } x_{N-\ell} \leq \frac{\theta_{N-\ell}(1)}{a(1)}$$

$$V_{N-\ell}(x_{N-\ell}, r_{N-\ell}=1) = V_{N-\ell}^{4\ell-1,U} \qquad \text{for } x_{N-\ell} \geq \frac{\theta_{N-\ell}(4\ell-1)}{a(1)}$$

Now let us consider $V_{N-\ell}(x_{N-\ell}, r_{N-\ell}=1)$ as we sweep rightwards from $x_{N-\ell} = -\infty$. To the immediate right of

$$\delta_{N-\ell}(1) = \frac{\theta_{N-\ell}(1)}{a(1)} \quad ,$$

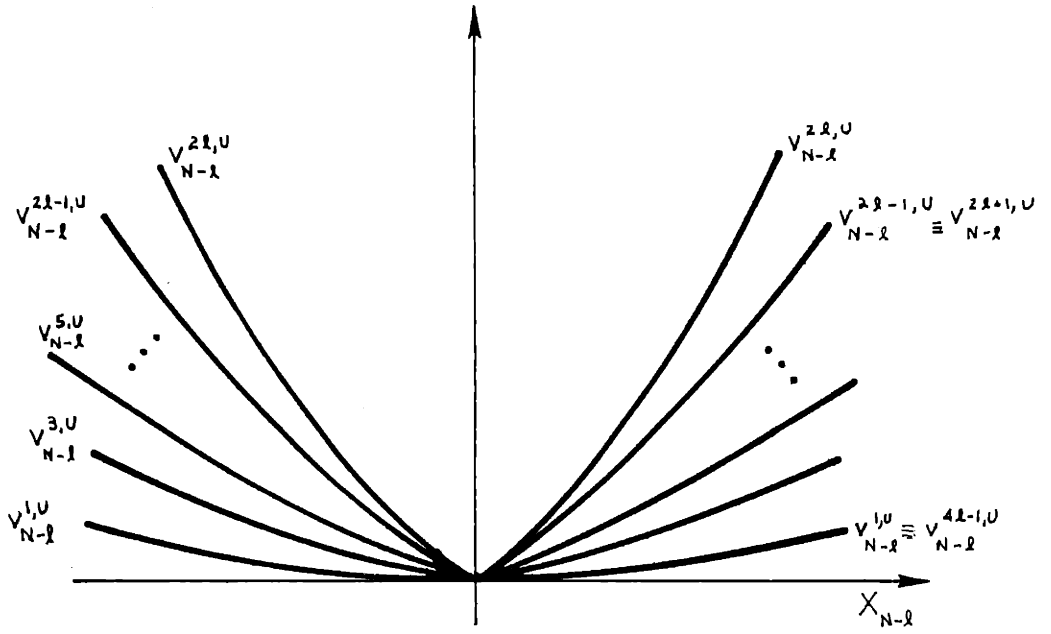

Figure C.16.2: Ordering of Candidate Cost Functions

$V_{N-\ell}^{2,U}$ is optimal. It will remain optimal as $x_{N-\ell}$ increases, until it intersects another eligible valid candidate cost. This next optimal cost will be $V_{N-\ell}^{3,U}$, unless $V_{N-\ell}^{3,U}$ is not valid to the right of the $V_{N-\ell}^{2,U}$ and $V_{N-\ell}^{3,U}$ intersection (see figure C.16.3). If $V_{N-\ell}^{3,U}$ is valid immediately to the right of this intersection, then this intersection is joining point $\delta_{N-\ell}(2)$. $V_{N-\ell}^{3,U}$ will then be optimal (to the left of $\delta_{N-\ell}(2)$) until

$$\delta_{N-\ell}(3) = \Theta_{N-\ell}(3)/a(1) ,$$

where $V_{N-\ell}^{3,U}$ ceases to be valid and $V_{N-\ell}^{4,U}$ becomes optimal (for $\ell \geq 3$). Then next joining point will be at the intersection of $V_{N-\ell}^{4,U}$ and $V_{N-\ell}^{5,U}$ (for $\ell \geq 3$), if $V_{N-\ell}^{5,U}$ is valid here.

This pattern continues (if the validity requirements shown in figure C.16.3 are met) until, at

$$\delta_{N-\ell}(2\ell-1) = \Theta_{N-\ell}(2\ell-1)/a(1),$$

the optimal cost becomes $V_{N-\ell}^{2\ell-1,R}$. $V_{N-\ell}^{2\ell-1,R}$ is then optimal until it intersects $V_{N-\ell}^{2\ell,U}$ (the middlepiece).

When the requirements of validity that are described above and shown in figure C.16.3 are met, then (1) - (3) and (5) - (9) of Proposition 7.12 hold for $k = \ell$. That is, using (7.129) - (7.130) for $k = \ell$ we need

$$\delta_{N-\ell}(2i) < \delta_{N-\ell}(2i + 1) \qquad \text{for } i = 1,\ldots, \ell-1 \qquad \text{(C.16.6)}$$

for (1) - (3) and (5) - (9) to be true.

From (7.129) - (7.130) we can rewrite (C.16.6) as

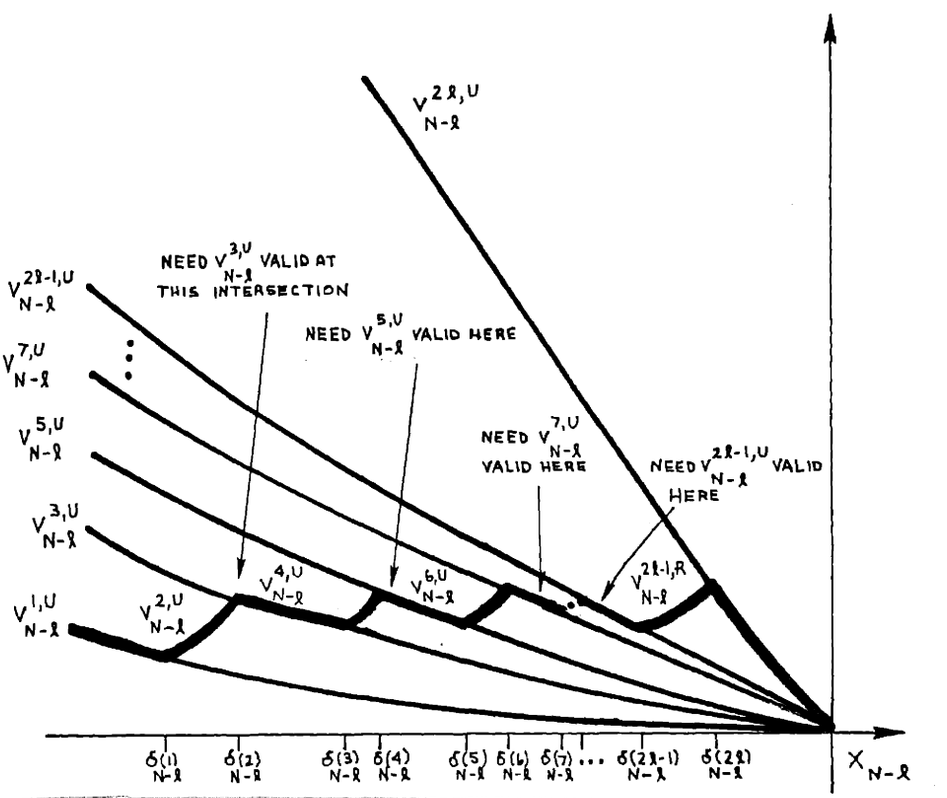

Figure c.16.3: Finding the Optimal Cost for negative x, moving leftwards from zero.

$$a(1) < \left(1 + \frac{b^2(1)}{R(1)} \hat{K}_{N-i+1}(2i)\right)\left(1 - \sqrt{1 - \chi_\ell(i)}\right) \qquad \text{(C.16.7)}$$

where

$$\chi_\ell(i) = \frac{1}{R(1) + b^2(1)\,\hat{K}_{N-i+1}(2i)} \prod_{\rho=1}^{\ell-1} \frac{R(1)+b^2(1)\hat{K}_{N-\ell+\rho}(2i)}{R(1) + b^2(1)\hat{K}_{N-\ell+\rho}(2i+1)}$$

$$\cdot \left([R(1) + b^2(1)\,\hat{K}_{N-i+1}(2i-1)] - \sum_{s=1}^{\ell-i} \frac{[a^2(1)\,R^2(1)(1-\omega_2)]^s}{[R(1) + b^2(1)\,\hat{K}_{N-i-s+1}(2i)]} \prod_{q=1}^{s-1} \left[R(1)+b^2(1)\hat{K}_{N-i-q+1}(2i)\right]^2 \right) \cdot \qquad \text{(C.16.8)}$$

If (C.16.7) holds at each $i = 1,2,\ldots,\ell - 1$ then so does (C.16.6) and, consequently, (1) - (3) and (5) - (9) of Proposition 7.12 holds for $k = \ell$. Now

$$\hat{K}_{N-i+1}(2i) = \hat{K}^{LM}_{N-i+1}(1) \qquad \text{(C.16.9)}$$

so, by Facts 7.1 - 7.3,

$$\left(1 + \frac{b^2(1)}{R(1)} \hat{K}_{N-i+1}(2i)\right) > \left(1 + \frac{b^2(1)}{R(1)} \hat{K}_N(2)\right) \cdot \qquad \text{(C.16.10)}$$

From (C.16.8) we see that for each $i = 1,\ldots, \ell-1$,

$$\chi_\ell(i) > \frac{R(1) + b^2(1)\,\hat{K}_{N-i+1}(2i-1)}{R(1) + b^2(1)\,\hat{K}_{N-i+1}(2i)} \qquad \text{(C.16.11)}$$

(since $\hat{K}_{N-\ell+\rho}(2i) > \hat{K}_{N-\ell+\rho+1}(2i)$ by (10) of Proposition (7.12). From (C.16.9) and (C.16.11) we obtain

$$\chi_\ell(i) > \frac{R(1) + b^2(1)\,\hat{K}_N(1)}{R(1) + b^2(1)\,\hat{K}^{LM}_\infty(1)} \qquad \text{(C.16.12)}$$

since the middlepiece parameter sequence $\{K^{LM}_{N-k}(1)\}$ increases with (N-k). From (C.16.7), (C.16.10) and (C.16.12) we have that if

$$a(1) < \left(1 + \frac{b^2(1)}{R(1)} \hat{K}_N(2)\right)\left(1 - \sqrt{1 - \frac{R(1) + b^2(1)\ \hat{K}_N(1)}{R(1) + b^2(1)\ \hat{K}^{LM}_{\infty}(1)}}\right) \qquad \text{(C.16.13)}$$

then (C.16.6) holds. But we have assumed (C.16.13) to be true, since it is identical to (7.116) of fact 7.11.

Given that (1) - (9) of Proposition 7.12 hold for $k = \ell$, it is easily verified that (10) - (11) are also true (using Lemma C.13.1). This completes the inductive step (on ℓ), and therefore the proof of Proposition 7.12. □

C.17 Proof of Proposition 7.14

Consider first a commensurate goals problem satisfying the assumptions of Proposition 7.7. Applying the controller described in (1) of Proposition 7.14, we obtain expected cost-to-go $\tilde{V}_{N-k}(x_{N-k}, r_{N-k}=1)$ for $(N-k) \leq (N-p)$. Since the controller that we are applying is suboptimal, we have

$$V_{N-k}(x_{N-k}, r_{N-k}=1) \leq \tilde{V}_{N-k}(x_{N-k}, r_{N-k}=1)$$

at each x_{N-k} value. From fact 7.3(1), we have that the endpiece cost function is an upperbound:

$$V_{N-k}(x_{N-k}, r_{N-k}=1) < V^{Le}_{N-k}(1) \equiv V^{Re}_{N-k}(1) \equiv V^{UB}_{N-k}(1) \equiv x^2_{N-k} K_{N-k}(1:1) \quad .$$

From (9) of Proposition 7.7 we have that

$$x^2_{N-k} K_{N-k}(2(k-p+1)+1:1) \leq V_{N-k}(x_{N-k}, r_{N-k}=1)$$

for each $k \leq p$, at all x_{N-k} not in $(\delta_{N-k}(2(k-p)), \delta_{N-k}(2(k+p)+1))$. To prove (7.145) it remains to be shown that for these x_{N-k} we have

$$V_{N-k}(x_{N-k}, r_{N-k}=1) \leq x^2_{N-k} K_{N-k}(1:1) \qquad \text{(C.17.1)}$$

For $x_{N-k} > \delta_{N-k}(4k)$ and $x_{N-k} < \delta_{N-k}(1)$, the optimal expected cost-to go and the suboptimal controller's expected cost-to-go coincide; that is, equality holds in (C.17.1). For any x_{N-k} satisfying

$$\delta_{N-k}(2(k+p)+1) < x_{N-k} < \delta_{N-k}(4k)$$

or

$$\delta_{N-k}(1) < x_{N-k} < \delta_{N-k}(2(k-p)),$$

the approximate controller applies the endpiece laws[1]

$u_{N-k}(1:1),\ldots,u_{N-k+d-1}(1:1)$ (or $u_{N-k}(4k+1:1),\ldots,u_{N=k+d-1}(4(k-d)+1:1))$
$+1$

until, at some time (N-k+d), it drives x_{N-k+d} inside the interval

$$(\delta_{N-k+d}(2(k-d-p)),\ \delta_{N-k+d}(2(k-d+p)+1)). \qquad \text{(C.17.2)}$$

Then, starting with u_{N-k+d}, the suboptimal controller uses true optimal control laws. That is, the expected cost-to-go of the suboptimal controller once x is inside (C.17.2) is the optimal expected cost-to-go. Since this cost, $V_{N-k+d}(x_{N-k}, r_{N-k}=1)$, is bounded above by $x^2_{N-k+d}\ K_{N-k+d}(1:1)$, we have (C.17.1) and thus (7.145) holds.

For conflicting goals problems satisfying the assumptions of Proposition 7.12, an analogous argument holds, using fact 7.3(2) and (10) of the Proposition 7.12. Part (3) of Proposition 7.14 follows directly from (2).

□

---

[1] unless the system jumps to form r=2

C. 18 Proof of Proposition 7.16:

Consider a JLQ problem specified by (5.1) - (5.6) when the sub-optimal controller of Proposition 7.16(1) is applied. Clearly at all $x_{N-k} \in \mathbb{R}$,

$$V_{N-k}(x_{N-k}, r_{N-k}=j) \leq \tilde{V}_{N-k}(x_{N-k}, r_{N-k}=j) \tag{C.18.1}$$

for each $j \in \bar{}$, since the applied controller is not optimal. Recall that the optimal JLQ controller minimizes, for $k \geq 1$:

$$V_{N-k}(x_{N-k}, r_{N-k}) = \min_{u_{N-k}, \ldots, u_{N-1}} E \left\{ \sum_{\ell=0}^{N-1} \left[x_{N-k+\ell+1}^2 \, Q(r_{N-k+\ell+1}) + x_{N-k+\ell+1} \, S(r_{N-k+\ell+1}) + P(r_{N-k+\ell+1}) + u_{N-k+\ell}^2 \, R(r_{N-k+\ell}) + \right] + V_N(x_N, r_N) \right\} \tag{C.18.2}$$

where

$$V_N(x,r) = x^2 \, K_T(r) + x \, H_T(r) + G_T(r) \quad . \tag{C.18.3}$$

From (7.151) we see that $V^{L,p}(x_{N-k}, r_{N-k})$ corresponds to the problem in (C.18.2) if no costs are incurred after time $(N-p)$. That is, if $V_{N-p}(x_{N-p}, r_{N-p}) = 0$. Consequently

$$V^{L,p}(x_{N-k}, r_{N-k}=j) \leq V_{N-k}(x_{N-k}, r_{N-k}=j) \tag{C.18.4}$$

for each $x_{N-k} \in \mathbb{R}$, at each $j \in \underline{M}$. From (7.152) - (7.153), we see that $V^{U,p}_{N-k}(x_{N-k},r_{N-k})$ solves the problem in (C.18.2) if we have the additional constraints

$$x_{N-k+\ell} = 0 \qquad \ell = p,p+1,\ldots,k \quad \bullet$$

Thus at each time (N-k),

$$V_{N-k}(x_{N-k},r_{N-k}=j) \leq V^{U,p}_{N-k}(x_{N-k},r_{N-k}) \tag{C.18.5}$$

for all (x_{N-k},r_{N-k}). Combining (C.18.1) - (C.18.5), it is clear that (7.150) is true if

$$\tilde{V}_{N-k}(x_{N-k},r_{N-k}) \leq V^{U,p}_{N-k}(x_{N-k},r_{N-k}) \tag{C.18.6}$$

for all (x_{N-k},r_{N-k}). We can verify (C.18.6) by noting that $\tilde{V}_{N-k}(x_{N-k},r_{N-k})$ is the cost achieved by the optimal controller for the problem (C.18.7) (for (N-k) < (N-p)):

$$\tilde{V}_{N-k}(x_{N-k},r_{N-k}) = \min_{u_{N-k},\ldots,u_{N-k+p-1}} E \left\{ \sum_{\ell=0}^{p-1} \left[x^2_{N-k+\ell+1} Q(r_{N-k+\ell+1}) + x_{N-k+\ell+1} S(r_{N-k+\ell+1}) + P(r_{N-k+\ell+1}) + u^2_{N-k+\ell} R(r_{N-k+\ell}) \right] + V_N(x_{N-k+p}, r_{N-k+p}) \right\} \quad \bullet \tag{C.18.7}$$

Comparing (C.18.7) with the problem (7.152) that $V^{U,p}_{N-k}(x_{N-k},r_{N-k})$ solves, we see that (C.18.6) is true. Thus Proposition 7.16(2) holds; Proposition 7.16(3) follows immediately.

□

D. APPENDICES TO PART IV

D.1 One-Step Solution Equations (for Proposition 8.1)

For $t = 1,2,\ldots,\psi^j_{k+1}$ let

ℓ^{ji}_t be the index of $\lambda_{ji}(\cdot)$ valid in (8.3) when

$$x_{k+1} \in \Delta^j_{k+1}(t)$$

ξ^{ji}_t be the index of the piece of $V_{k+1}(x_{k+1}, t_{k+1}=i)$

valid when $x_{k+1} \in \Delta^j_{k+1}(t)$,

ς^{ji}_t be The index of the x-cost

$Q(x_{k+1}, r_{k+1}=i)$ valid when

$$x_{k+1} \in \Delta^j_{k+1}(t)$$

and in proof step 1 of Proposition 8.1.

Define the conditional cost parameters in (8.39) by

$$\hat{K}^j_{k+1}(t) = \sum_{i=1}^{M} \lambda_{ji}(\ell^{ji}_t)\,[K_{k+1}(\xi^{ji}_t; i) + Q^i(\varsigma^{ji}_t)] \tag{D.1.1}$$

$$\hat{H}^j_{k+1}(t) = \sum_{i=1}^{M} \lambda_{ji}(\ell^{ji}_t)\,[H_{k+1}(\xi^{ji}_t; i) + S^i(\varsigma^{ji}_t)] \tag{D.1.2}$$

$$\hat{G}^j_{k+1}(t) = \sum_{i=1}^{M} \lambda_{ji}(\ell^{ji}_t)\,[G_{k+1}(\xi^{ji}_t; i) + P^i(\varsigma^{ji}_t)] \tag{D.1.3}$$

Suppose that $b(j) \neq 0$. Then let

$$\theta_k^j\ (\psi_{k+1}^j) = \gamma_{k+1}^j\ (\psi_{k+1}^j - 1)\ \left[1 + \frac{b^2(j)\ \hat{K}_{k+1}^j\ (\psi_{k+1}^j)}{R(j)}\right] + \frac{b^2(j)}{2R(j)}\ \hat{H}_{k+1}\ (\psi_{k+1}^j) \tag{D.1.4}$$

$$\Theta_k^j(1) = \gamma_{k+1}^j(1)\ \left[1 + \frac{b^2(j)\hat{K}_{k+1}^j(1)}{R(j)}\right] + \frac{b^2(j)}{2R(j)}\ \hat{H}_{k+1}^j(1) \bullet \tag{D.1.5}$$

For $t = 2,\ldots,\psi_{k+1}^j - 1$ if

$$\hat{K}_{k+1}^j(t) > \frac{-R(j)}{b^2(j)} \bullet \tag{D.1.6}$$

then let

$$\theta_k^j(t) = \gamma_{k+1}^j(t-1)\ \left[1 + \frac{b^2(j)\ \hat{K}_{k+1}^j(t)}{R(j)}\right] + \frac{b^2(j)}{2R(j)}\ \hat{H}_{k+1}^j(t) \tag{D.1.7}$$

$$\Theta_k^j(t) = \gamma_{k+1}^j(t)\ \left[1 + \frac{b^2(j)\ \hat{K}_{k+1}^j(t)}{R(j)}\right] + \frac{b^2(j)}{2R(j)}\ \hat{H}_{k+1}^j(t) \tag{D.1.8}$$

For $t = 2,\ldots,\psi_{k+1}^j - 1$, if

$$\hat{K}_{k+1}^j(t) < \frac{-R(j)}{b^2(j)} \tag{D.1.9}$$

then let

$$\theta_k^j(t) = \Theta_k^j(t) = \frac{[\gamma_{k+1}^j(t) + \gamma_{k+1}^j(t-1)]\ [R(j) + b^2(j)\ \hat{K}_{k+1}^j(t)] + b^2(j)\hat{H}_{k+1}^j(t)}{2R(j)} \bullet \tag{D.1.10}$$

For $t = 2,\ldots,\psi_{k+1}^j - 1$, if

$$\frac{-R(j)}{b^2(j)} = \hat{K}_{k+1}^j(t) \tag{D.1.11}$$

then let

$$\Theta_k^j(t) = \theta_k^j(t) = \frac{b^2(j)}{2R(j)}\ \hat{H}_{k+1}^j(t) \bullet \tag{D.1.12}$$

Note that (D.1.12) is consistent with (D.1.7), (D.1.8) and (D.1.10) when (D.1.11) holds.

The candidate costs-to-go in (8.44) and corresponding optimal control laws in (8.45), and the optimal $x_{k+1} \in \Delta^j_{k+1}(t)$ values achieved by these controls are:

$$V^{t,L}_k(x_k,j) = x_k^2 \tilde{K}^j_k + x_k \tilde{H}^j_k(t-1) + \tilde{G}^j_k(t-1,t) \tag{D.1.13}$$

$$u^{t,L}_k(x_k,j) = -\tilde{L}^j_k x_k + \tilde{F}^j_k(t-1) \tag{D.1.14}$$

$$x^{t,L}_{k+1}(x_k,j) = \gamma^t_{k+1}(t-1) \tag{D.1.15}$$

$$\text{for } t = 2,3,\ldots,\psi^j_{k+1} \quad \text{if}$$

$$a(j)\, x_k \leq \theta^j_k(t)$$

and

$$V^{t,R}_k(x_k,j) = x_k^2 \tilde{K}^j_k + x_k \tilde{H}^j_k(t) + \tilde{G}^j_k(t,t) \tag{D.1.16}$$

$$u^{t,R}_k(x_k,j) = -\tilde{L}^j_k x_k + \tilde{F}^j_k(t) \tag{D.1.17}$$

$$x^{t,R}_{k+1}(x_k,j) = \gamma^-_{k+1}(t) \tag{D.1.18}$$

$$\text{for } t = 1,2,\ldots,\psi^j_{k+1} - 1 \quad \text{if}$$

$$\theta^j_k(t) \leq a(j)\, x_k .$$

For $t = 1$, $t = \psi^j_{k+1}$, and for $t = 2,\ldots,\psi^j_{k+1} - 1$ if (D.1.6) holds, we have

$$V_k^{t,U}(x_k,j) = x_k^2\, K_k^j(t) + x_k\, H_k^j(t) + G_k^j(t) \tag{D.1.19}$$

$$u_k^{t,U}(x_k,j) = -L_k^j(t)\, x_k + F_k^j(t) \tag{D.1.20}$$

$$x_{k+1}^{t,U}(x_k,j) + [a(j) - b(j)\, L_k^j(t)]x_k + b(j)\, F_k^j(t) \tag{D.1.21}$$

if

$$\theta_k^j(t) < a(j)\, x_k < \Theta_k^j(t) \quad \bullet$$

In (D.1.13) - (D.1.14) and (D.1.16) - (D.1.17) we have

$$\tilde{K}_k^j = \frac{a^2(j)\, R(j)}{b^2(j)} \tag{D.1.22}$$

$$\tilde{H}_k^j(t) = \frac{-2a(j)\, R(j)\, \gamma_{k+1}^j(t)}{b^2(j)}$$

$$\text{for } t = 1,\ldots,\psi_{k+1}^j - 1 \tag{D.1.23}$$

$$\tilde{G}_k^j(s,t) = \left\{ \begin{array}{l} \hat{G}_{k+1}^j(t) + \gamma_{k+1}^j(s)\, \hat{H}_{k+1}^j(t) \\ + [\gamma_{k+1}^j(s)]^2 \left[\hat{K}_{k+1}^j(t) + \dfrac{R(j)}{b^2(j)}\right] \end{array} \right\} \tag{D.1.24}$$

defined for

$$s = t \quad \text{for } t = 1,\ldots,\psi_{k+1}^j - 1$$

and $\quad s = t-1 \text{ for } t = 2,\ldots,\psi_{k+1}^j$,

and

$$\tilde{L}_k^j = a(j)/b(j) \tag{D.1.25}$$

$$\tilde{F}_k^j(t) = \gamma_{k+1}^j(t)/b(j) \tag{D.1.26}$$

$$\text{for } t = 1,\ldots,\psi_{k+1}^j - 1$$

In (D.1.19) - (D.1.21) we have

$$K_N^j(t) = K_T(j)$$

$$K_k^j(t) = \frac{a^2(j)\ R(j)\ \hat{K}_{k+1}^j(t)}{R(j) + b^2(j)\ \hat{K}_{K+1}^j(t)} \tag{D.1.27}$$

$$H_N^j(t) = H_T(j)$$

$$H_k^j(t) = \frac{a(j)\ R(j)\ \hat{H}_{k+1}^j(t)}{R(j) + b^2(j)\ \hat{K}_{k+1}^j(t)} \tag{D.1.28}$$

$$G_N^j(t) = G_T(j) \tag{D.1.29}$$

$$G_k^j(t) = \hat{G}_{k+1}^j(t) - \frac{b^2(j)\ [\hat{H}_{k+1}^j(t)]^2}{4[R(j) + b^2(j)\ \hat{K}_{k+1}^j(t)]} \tag{D.1.30}$$

and

$$L_k^j(t) = \frac{a(j)\ b(j)\ \hat{K}_{k+1}^j(t)}{R(j) + b^2(j)\ \hat{K}_{k+1}^j(t)} \tag{D.1.31}$$

$$F_k^j(t) = \frac{-b(j)\ \hat{H}_{k+1}^j(t)}{2[R(j) + b^2(j)\ \hat{K}_{k+1}^j(t)]} \tag{D.1.32}$$

The values of $m_k(j)$, $\{\delta_k^j(t) : t=1,\ldots,m_k(j) - 1\}$, $K_k(t:j)$, $H_k(t:j)$, $G_k(t:j)$, $L_k(t:j)$ and $F_k(t:j)$ are assigned, for each $j \in \underline{M}$, by performing the minimization indicated in (8.49). The procedure for doing this is given in section 8.5. The derivation of (D.1.4) - (D.1.32) is done in the next appendix section.

If $b(j) = 0$ then the optimal control is

$$u_k(x_k, r_k=j) = 0 \tag{D.1.33}$$

with

$$x_{k+1} = a(j)\, x_k \tag{D.1.34}$$

and cost

$$V_k(x_k, r_k=j) = a^2(j)\, \hat{K}^j_{k+1}(t)\, x_k^2 + a(j)\, \hat{H}^j_{k+1}(t)\, x_k + \hat{G}^j_{k+1}(t) \tag{D.1.35}$$

where the index t is determined by which region $\Delta^j_{k+1}(t)$ the x_{k+1} value is in (for each x_k value).

When $b(j) = 0$, (D.1.33) - (D.1.35) are the same as (D.1.13) - (D.1.15) with $\theta^j_k(t)$ and $\Theta^j_k(t)$ as in (D.1.4) - (D.1.8).

D.2 Derivation of (D.1.4) - (D.1.32)

From (8.42) and (D.1.1) - (D.1.3) we have that

$$V_k[x_k, r_k=j \mid t] = \min_{\substack{u_k \\ \text{s.t.} \\ x_{k+1} \in \Delta^j_{k+1}(t)}} \left\{ \begin{array}{l} u_k^2 R(j) \\ \quad + \\ x_{k+1}^2 \hat{K}^j_{k+1}(t) + \hat{H}^j_{k+1}(t)\, x_{k+1} \\ \quad + \\ \hat{G}^j_{k+1}(t) \end{array} \right\} . \qquad \text{(D.2.1)}$$

From (8.1) we have (for $b(j) \neq 0$) that

$$u_k = \frac{x_{k+1} - a(j)\, x_k}{b(j)} \qquad (b)j) \neq 0 . \qquad \text{(D.2.2)}$$

Thus (D.2.1) becomes

$$V_k[x_k, r_k=j \mid t] = \min_{x_{k+1} \in \Delta^j_{k+1}(t)} \left| \begin{array}{l} x_{k+1}^2 [\hat{K}^j_{k+1}(t) + \frac{R(j)}{b^2(j)} \\ \quad + \\ x_{k+1} [\hat{H}^j_{k+1}(t) - \frac{2a(j)\, R(j)\, x_k}{b^2(j)}] \\ \quad [\hat{G}^j_{k+1}(t) + \frac{a^2(j)\, R(j)\, x_k^2}{b^2(j)}] \end{array} \right| . \qquad \text{(D.2.3)}$$

Suppose that $b(j) \neq 0$ and

$$\frac{\delta 2 V_k[x_k, r_k=j \mid t]}{(\delta x_{k+1})^2} = 2[\frac{R(j)}{b^2(j)} + \hat{K}^j_{k+1}(t)] > 0 . \qquad \text{(D.2.4)}$$

Then we can minimize (D.2.3) by differentiating with respect to x_{k+1}

and setting to zero. We find that the optimal x_{k+1} is then

$$x_{k+1} = \frac{2a(j)\ R(j)\ x_k - b^2(j)\ \hat{H}^j_{k+1}(t)}{2[R(j) + b^2(j)\ \hat{K}^j_{k+1}(t)]} \qquad \text{(D.2.5)}$$

if this x_{k+1} is, in fact, in $\Delta^j_{k+1}(t)$.

For $t = 1$ and $t = \psi^j_{k+1}$, (D.2.4) is always true. For t=1, $x_{k+1} \in \Delta^j_{k+1}(1)$ if and only if

$$a(j)x_k \leq \frac{\left[\gamma^j_{k+1}(t)\ [R(j) + b^2(j)\ \hat{K}^j_{k+1}(t)] + \frac{b^2(j)}{2}\ \hat{H}^j_{k+1}(t)\right]}{R(j)} \bullet \qquad \text{(D.2.6)}$$

We define the right side of (D.2.6) to be $\Theta^j_k(1)$, as in (D.1.5). For $t = \psi^j_{k+1}$, $x_{k+1} \in \Delta^j_{k+1}(\psi^j_{k+1})$ if and only if

$$\frac{\left[\gamma^j_{k+1}(t\text{-}1)\ [R(j) + b^2(j)\ \hat{K}^j_{k+1}(t)] + \frac{b^2(j)}{2}\ \hat{H}^j_{k+1}(t)\right]}{R(j)} \leq a(j)\ x_k \bullet \qquad \text{(D.2.7)}$$

We define the left side of (D.2.7) to be $\Theta^j_k(\psi^j_{k+1})$, as in (D.1.4). For $t = 2,\ldots,\psi^j_{k+1}-1$ with (D.2.4) holding, $x_{k+1} \in \Delta^j_{k+1}(t)$ if and only if

$$\frac{\left[\gamma^{j}_{k+1}(t-1)[R(j) + b^2(j)\hat{K}^{j}_{k+1}(t)] + \frac{b^2(j)}{2}\hat{H}^{j}_{k+1}(t)\right]}{R(j)} < a(j)\,x_k < \frac{\left[\gamma^{j}_{k+1}(t)[R(j) + b^2(j)\hat{K}^{j}_{k+1}(t)] + \frac{b^2(j)}{2}\hat{H}^{j}_{k+1}(t)\right]}{R(j)} \tag{D.2.8}$$

The left and right sides of (D.2.8) are defined to be $\theta^{j}_{k}(t)$ and $\Theta^{j}_{k}(t)$ respectively, as in (D.1.7)-(D.1.8)(D.2.) yields (D.1.19) - (D.1.21) and (D.1.27) - (D.1.32).

Now if $b(j) \neq 0$ and (D.2.4) holds but

$$a(j)x_k \leq \theta^{j}_{k}(t) \quad ,$$

(D.2.4) implies that the best we can do is to drive x_{k+1} to $\gamma^{j+}_{k+1}(t-1)$, the left boundary of $\Delta^{j}_{k+1}(t)$. Thus from (D.2.2)

$$u^{t,L}(x_{k+1},j) = -\frac{a(j)\,x_k + \gamma^{j}_{k+1}(t-1)}{b(j)} \tag{D.2.9a}$$

which yields (D.1.13) - (D.1.15) with (D.1.22) - (D.1.26).

Similarly, if

$$a(j)x_k \geq \theta^{j}_{k}(t)$$

the best we can do is drive x_{k+1} to $\gamma^{j}_{k+1}(t)$, the right boundary of $\Delta^{j}_{k+1}(t)$. We then obtain

$$u^{t,R}(x_{k+1},j) = \frac{-a(j)x_k + \gamma^{j}_{k+1}(t)}{b(j)} \tag{D.2.9b}$$

which yields (D.1.16) - (D.1.18) with (D.1.22) - (D.1.26).

If $b(j) \neq 0$ and we have

$$\frac{\partial^2 V_k[x_k, r_k=j|t]}{(\partial x_{k+1})^2} < 0 \qquad \text{(D.2.11)}$$

then the optimal x_{k+1} is at one of the boundaries of $\Delta^j_{k+1}(t)$. We drive x_{k+1} to the left boundary, $\gamma^{j+}_{k+1}(t-1)$, if

$$\left[\begin{array}{l}[\gamma^j_{k+1}(t-1)]^2\ \hat{K}^j_{k+1}(t) \\ \quad + \\ \hat{H}^j_{k+1}(t)\ \gamma^j_{k+1}(t-1) \\ \quad + \\ \hat{G}^j_{k+1}(t) \\ \quad + \\ \left(\dfrac{\gamma^j_{k+1}(t-1) - a(j)x_k}{b(j)}\right)^2 R(j)\end{array}\right] \leq \left[\begin{array}{l}[\gamma^j_{k+1}(t)]^2\ \hat{K}^j_{k+1}(t) \\ \quad + \\ \hat{H}^j_{k+1}(t)\ \gamma^j_{k+1}(t) \\ \quad + \\ \hat{G}^j_{k+1}(t) \\ \quad + \\ \left(\dfrac{\gamma^j_{k+1}(t) - a(j)x_k}{b(j)}\right)^2 R(j)\end{array}\right], \qquad \text{(D.2.11)}$$

and to the right boundary, $\gamma^j_{k+1}(t)$, otherwise. We can rewrite (D.2.11)

$$a(j)x_k \leq \frac{[b^2(j)\ \hat{K}^j_{k+1}(t) + R(j)][\gamma^j_{k+1}(t) + \gamma^j_{k+1}(t-1)] + b^2(j)\ \hat{H}^j_{k+1}(t)}{2R(j)} . \qquad \text{(D.2.12)}$$

The right side of (D.2.11) is defined to be $\theta^j_k(t) = \Theta^j_k(t)$ when $b(j) \neq 0$ and (D.2.10) holds, as in (D.1.10).

If $b(j) \neq 0$ and we have

$$\frac{\partial^2 V_k[x_k, r_k=j|t]}{(\delta x_{k+1})^2} = 2\left[\frac{R(j)}{b^2(j)} + \hat{K}^j_{k+1}(t)\right] = 0 \qquad \text{(D.2.13)}$$

then for each x_k value, the quantity that is to be minimized in (D.2.3) is a linear function of x_{k+1}. When we have

$$\frac{\delta V_k}{\delta x_{k+1}}[x_k, r_k=j|t] = \hat{H}^j_{k+1}(t) - \frac{2a(j)\ R(j)}{b^2(j)}\ x_k > 0 \qquad \text{(D.2.14)}$$

then the best x_{k+1} value in $\Delta^j_{k+1}(t)$ is the left boundary, $\gamma^j_{k+1}(t-1)$, since the cost to be minimized in (D.2.3) increases with x_{k+1} (for fixed x_k). When we have

$$\frac{\partial V_k}{\partial x_{k+1}}[x_k, r_k=j|t] = \hat{H}^j_{k+1}(t) - \frac{2a(j)\ R(j)}{b^2(j)}\ x_k < 0 \qquad \text{(D.2.15)}$$

the best $x_{k+1} \in \Delta^j_{k+1}(t)$ is $\gamma^j_{k+1}(t)$. For

$$\hat{H}^j_{k+1}(t) - \frac{2a(j)\ R(j)}{b^2(j)}\ x_k = 0\ , \qquad \text{(D.2.16)}$$

any $x_{k+1} \in \Delta^j_{k+1}(t)$ yields the same result in (D.2.3) (for fixed x_k). From (D.2.13) - (D.2.16) we thus get (D.1.11) - D.1.12). □

D.3 Proof of Proposition 8.2:

We first note that relationships (C.3.1) - (C.3.3) of Lemma C.3.1 hold when both

$$\hat{K}^j_{k+1}(t) > -\frac{R(j)}{b^2(j)} \tag{D.3.1}$$

$$\hat{K}^j_{k+1}(\ell) > \frac{-R(j)}{b^2(j)} \text{ ,} \tag{D.3.2}$$

since the θ's and Θ's are defined by (D.1.4) - (D.1.8) (which are the same as (C.1.4) - (C.1.6)).

Let us assume that $\hat{V}_{k+1}(x_{k+1}|r_k=j)$ is continuous at $\gamma^j_{k+1}(t)$ and that (D.3.1) - (D.3.2) hold for t and $\ell = t+1$. By continuity

$$V_k^{t,R}(x_k,j) = V_k^{t+1,L}(x_k,j) \tag{D.3.3}$$

since we are driving to the same x_{k+1} value in each, with the same cost. Hence from (D.1.4)

$$\tilde{G}^j_k(t,t) = \tilde{G}^j_k(t,t+1) \text{ .} \tag{D.3.4}$$

Suppose that we also have

$$\left.\frac{\partial}{\partial x_{k+1}} \hat{V}_{k+1}(x_{k+1}|r_k=j)\right|_{x_{k+1}=(\gamma^j_{k+1}(t))^+} \leq \left.\frac{\partial}{\partial x_{k+1}} \hat{V}_{k+1}(x_{k+1}|r_k=j)\right|_{x_{k+1}=[\gamma^j_{k+1}(t)]^-} \text{ .} \tag{D.3.5}$$

That is

$$\begin{pmatrix} 2\,\hat{K}^j_{k+1}(t+1)\ \gamma^j_{k+1}(t) \\ + \\ \hat{H}^j_{k+1}(t+1) \end{pmatrix} \leq \begin{pmatrix} 2\,\hat{K}^j_{k+1}(t)\ \gamma^j_{k+1}(t) \\ + \\ \hat{H}^j_{k+1}(t) \end{pmatrix} . \tag{D.3.6}$$

Then by Lemma C.3.1 we have

$$\theta^j_k(t+1) \leq \theta^j_k(t) \quad . \tag{D.3.7}$$

Now (D.3.3) and (D.3.7) are together sufficient to guarantee that neither $V_k^{t,R}(x_k,j)$ nor $V_k^{t+1,L}(x_k,j)$ can be optimal for any x_k, since

$$V_k^{t,R}(x_k,j) \geq V_k^{t,U}(x_k,j)$$

$$V_k^{t+1,L}(x_k,j) \geq V_k^{t+1,U}(x_k,j)$$

for all x_k. Thus for each $\gamma^j_{k+1}(t)$ at which $\hat{V}_{k+1}(x_k|r_k=j)$ is continuous, with (D.3.1) - (C.3.2) holding for t and ℓ = t+1 and with (D.3.6) holding:

$$\min\{V_k^{t,U}(x_k,j),\ V_k^{t,R}(x_k,j),\ V_k^{t+1,L}(x_k,j),\ V_k^{t+1,U}(x_k,j)\}$$

$$= V_k^{t,U}(x_k,j) \quad \text{or} \quad V_k^{t+1,U}(x_k,j) \quad . \tag{D.3.8}$$

for each x_k

This verifies (i) of Proposition 8.2.

Suppose that (D.3.1) - (D.3.2) hold for t and $\ell = t+1$ and $\hat{V}_{k+1}(x_{k+1}|r_k=j)$ is continuous at $\gamma^j_{k+1}(t)$ <u>but</u>

$$\frac{\partial}{\partial x_{k+1}} \hat{V}_{k+1}(x_{k+1}|r_k=j) \quad > \quad \frac{\partial}{\partial x_{k+1}} \hat{V}_{k+1}(x_k \Big| r_{k+1}=j) \Big|_{x_{k+1}=(\gamma^j_{k+1}(t))^+} \quad \text{(D.3.9)}$$

That is,

$$\begin{pmatrix} 2\hat{K}^j_{k+1}(t+1)\gamma^j_{k+1}(t) \\ + \\ \hat{H}^j_{k+1}(t+1) \end{pmatrix} > \begin{pmatrix} 2\hat{K}^j_{k+1}(t)\ \gamma^j_{k+1}(t) \\ + \\ \hat{H}^j_{k+1}(t) \end{pmatrix} \quad \text{(D.3.10)}$$

Then by Lemma C.3.1 we have

$$\theta^j_k(t+1) > \Theta^j_k(t) \quad \text{(D.3.11)}$$

From (D.3.3), (D.3.11) we have that

$$V^{t,R}_k(x_k,j) \equiv V^{t+1,L}_k(x_k,j)$$

<u>may</u> be optimal for

$$\theta^j_k(t) < a(j)\ x_k < \theta^j_k(t+1)$$

Hence we have (8.53) in (i) of Proposition 8.2

If
$$\hat{K}^j_{k+1}(t) < \frac{-R(j)}{b^2(j)} \quad \text{(D.3.12)}$$

then
$$\theta^j_k(t) = \Theta^j_k(t)\ , \quad \text{(D.3.13)}$$

as given by (D1.10). Here

$$V_k^{t+1,U} \quad \text{is } \underline{\text{never}} \text{ valid}$$

hence (ii) of Proposition 8.2

Now suppose that $\hat{V}_{k+1}(x_{k+1}|r_k=j)$ is <u>not</u> continuous at $\gamma_{k+1}^j(t)$. Suppose that

$$\hat{V}_{k+1}([\gamma_{k+1}^j(t)]^-|j) < \hat{V}_{k+1}([\gamma_{k+1}^j(t)]^+|j) \tag{D.3.14}$$

That is, $\hat{V}_{k+1}(x_{k+1}|r_k=j)$ has a discontinuous <u>increase</u> at $\gamma_{k+1}^j(t)$. This can happen only if $\gamma_{k+1}^j(t)$ is a form transition probability $\nu_{ji}(\ell)$, $\ell \in \{1,\ldots,\overline{\nu}_{ji-1}\}$, or an x-cost discontinuity $\mu_i(n)$, $n \in \{1,\ldots,\overline{\mu}_i-1\}$, for some $i \in \mathcal{C}_j$.

Then clearly

$$V_k^{t,R}(x_k,j) < V_k^{t+1,L}(x_k,j) \tag{D.3.15}$$

So in this case $V_k^{t+1,L}(x_k,j)$ <u>cannot</u> be optimal for any x_k. However, $V_k^{t,R}(x_k,j)$ may be. Similarly, if

$$\hat{V}_{k+1}([\gamma_{k+1}^j(t)]^-|j) > \hat{V}_{k+1}([\gamma_{k+1}^j(t)]^+|j) \tag{D.3.16}$$

(which implies that $\gamma_{k+1}^{j(i)}$ is a form transition probability discontinuity or x-cost discontinuity, then

$$V_k^{t+1,L}(x_k,j) < V_k^{t,R}(x_k,j) \tag{D.3.17}$$

hence $V_k^{t,R}(x_k,j)$ cannot be optimal. Thus we need consider only the candidate costs-to-go listed in the statement of Proposition 8.2.□

D.4 JLPC One-Step Solution Details (for Proposition 9.1)

In this section we provide details for the computations in steps 3 and 4 of the constructive proof of Proposition 9.1.

Obtaining the z_{k+1} grid (in step 3):

It is straightforward to verify that for each $s = 1,\ldots,\bar{\sigma}$, and $t = 1,\ldots,\psi^j_{k+1}$ in (9.101) we have

$$\min[\sigma(s),\ \max[\gamma^j_{k+1}(t)-z_{k+1},\sigma(s-1)]] = \max[\sigma(s-1),\ \min[\gamma^j_{k+1}(t) - z_{k+1},\sigma(s)]]$$
$$\triangleq L^j(s,t), \qquad \text{(D.4.1)}$$

where the numerical value of each integration limit $L^j(s,t)$ depends upon z_{k+1} as follows:

$$L^j(s,t) = \begin{cases} \sigma(s) & \text{if} \quad z_{k+1} \leq A^j(s,t) \triangleq \gamma^j_{k+1}(t) - \sigma(s) \\ \gamma^j_{k+1}(t) - z_{k+1} & \text{if} \quad A^j(s,t) \leq z_{k+1} \leq B^j(s,t) \\ \sigma(s-1) & \text{if} \quad z_{k+1} \geq B^j(s,t) \triangleq \gamma^j_{k+1}(t) - \sigma(s-1) \end{cases} \qquad \text{(D.4.2)}$$

The values of $\{A^j(s,t),\ B^j(s+1,t)\colon s = 1,\ldots\bar{\sigma}-1;\ t=1,\ldots,\psi^j_{k+1}-1\}$ in (D.4.2) comprise a tentative partition of z_{k+1}. Given the grid points $\{\gamma^j_{k+1}(t)\}$ and $\{\sigma(s)\}$ we obtain the tentative partition

$$\{\tilde{\Delta}(\ell) = (\tilde{\gamma}(\ell-1),\ \tilde{\gamma}(\ell)) \qquad \ell = 1,\ldots,\tilde{\psi}\}\ ,$$

where the $\tilde{\psi}$-1 grid points are distinct elements of the set

$$\{\gamma^j_{k+1}(t) - \sigma(s) \ :\ t=1,\ldots,\psi^j_{k+1}-1;\ \ s = 1,\ldots,\bar{\sigma}-1 \qquad \text{(D.4.3)}$$

and are ordered as follows:

$$-\infty \triangleq \tilde{\gamma}(0) < \tilde{\gamma}(1) < \ldots < \tilde{\gamma}(\tilde{\psi}-1) < \tilde{\gamma}(\tilde{\psi}) \triangleq \infty \quad .$$

To obtain the z_{k+1} partition $\{\hat{\Delta}^j_{k+1}(t) : t=1,\ldots,\hat{\psi}^j_{k+1}\}$ of (9.97) - (9.98) we must make the evaluation indicated in (9.102), and add extra grid points to (D.4.3) as needed.

Using (D.4.1) - (D.4.2) we can determine the limits of integration in (9.101) over each z_{k+1} interval in (D.4.3). We can then evaluate $\hat{V}_{k+1}(z_{k+1}|r_k=j)$ over each of these intervals $\tilde{\Delta}(\ell)$, by (9.101). An efficient way to carry out these computations is to do them for $z_{k+1} \in \tilde{\Delta}(1)$, and then to successively calculate $\hat{V}_{k+1}(z_{k+1}|r_k=j)$ over $\tilde{\Delta}(\ell+1)$ from $\hat{V}_{k+1}(z_{k+1}|r_k=j)$ over $\tilde{\Delta}(\ell)$ by adding or subtracting (as appropriate) those integrals in (9.101) whose limits change when we move from $\tilde{\Delta}(\ell)$ to $\tilde{\Delta}(\ell+1)$.

That is:

1. Compute $\hat{\hat{V}}_{k+1}(z_{k+1}|r_k=j)$ over $\tilde{\Delta}(1)$. By (D.4.2), the integration limits $\prec^j(s,t)$ are all equal to $\sigma(s)$. Thus for all $z_{k+1} \in \tilde{\Delta}(1)$, (9.101) becomes

$$\hat{\hat{V}}_{k+1}\left(z_{k+1}\,\middle|\,\begin{matrix} r_k=j \\ z_{k+1}\in\tilde{\Delta}(1)\end{matrix}\right) = \sum_{s=1}^{\bar{\sigma}} \int_{\sigma(s-1)}^{\sigma(s)} \omega(v;s)\hat{V}^j_{k+1}(z_{k+1}+v;1)dv \quad . \tag{D.4.4}$$

2. Compute $\hat{\hat{V}}_{k+1}(z_{k+1}|r_k=j\ ,\ z_{k+1} \in \tilde{\Delta}(\ell+1))$ from $\hat{\hat{V}}_{k+1}(z_{k+1}|r_k=j,\ \ z_{k+1} \in \tilde{\Delta}(\ell)$ as follows:

- if $\tilde{\gamma}^j_{k+1}(\ell) = A^j(s^*,t^*)$ for some s^*,t^* in (D.4.2), then the limit $L^j(s^*,t^*)$ in (D.4.1) - (D.4.2) becomes $\gamma^j_{k+1}(t^*) - z_{k+1}$ instead of $\sigma(s^*)$; consequently we add

$$\int_{\gamma^j_{k+1}(t^*)-z_{k+1}}^{\sigma(s^*)} \omega(v;s^*)[\hat{V}^j_{k+1}(z_{k+1}+v;t^*+1) - \hat{V}^j_{k+1}(z_{k+1}+v;t^*)]\,dV \qquad \text{(D.4.5)}$$

to $\hat{\hat{V}}_{k+1}(z_{k+1}|r_k=j,\ z_{k+1} \in \tilde{\Delta}(\ell)$.

- if $\tilde{\gamma}^j_{k+1}(\ell) = B^j(s^*,t^*)$ for some s^*,t^* in (D.4.2), then the limit $L^j(s^*,t^*)$ in (D.4.1) - (D.4.2) becomes $\sigma(s^*-1)$ instead of $\gamma^j_{k+1}(t^*) - z_{k+1}$; consequently we add

$$\int_{\gamma^j_{k+1}(t^*)-z_{k+1}}^{\sigma(s^*-1)} \omega(v;s^*)[\hat{V}^j_{k+1}(z_{k+1}+v;t^*) - \hat{V}_{k+1}(z_{k+1}+v;t^*+1)]\,dV \qquad \text{(D.4.6)}$$

to $\hat{\hat{V}}_{k+1}(z_{k+1}|r_k=j,\ z_{k+1} \in \tilde{\Delta}(\ell))$.

Adding the integrals specified by (D.4.5) - (D.4.6) to $\hat{\hat{V}}_{k+1}(z_{k+1}|r_k=j,\ \ z_{k+1} \in \tilde{\Delta}(\ell))$ yields $\hat{\hat{V}}_{k+1}(z_{k+1}|r_k=j,\ z_{k+1} \in \tilde{\Delta}(\ell+1))$. This is done sequentially until $\hat{\hat{V}}_{k+1}(z_{k+1}|r_k=j,\ z_{k+1} \in \tilde{\Delta}(\tilde{\psi}))$ is obtained.[1]

---

[1] If, however, the JLPC control problem is completely symmetric about zero, we need only follow this procedure for z_{k+1} intervals to the left of zero.

3. Now we differentiate each $\hat{\hat{V}}_{k+1}(z_{k+1}|r_k=j,\ z_{k+1} \in \tilde{\Delta}(\ell))$ twice with respect to z_{k+1}. Based upon the second derivative

, we break up $\tilde{\Delta}(\ell)$ into disjoint intervals such that $\hat{\hat{V}}_{k+1}(z_{k+1}|r_k=j)$ is convex or concave over each.

Following the three steps, we obtain the z_{k+1} partition and $\hat{\hat{V}}_{k+1}(z_{k+1}|r_k=j)$ pieces described by (9.97) - (9.98).

Solving the constrained-in-z_{k+1} subproblems (in step 4):

The $\tilde{\psi}^j_{k+1}$ subproblems in (9.103) are solved as follows:

1. If $\dfrac{\partial^2 V_k(x_k, r_k=j|t)}{(\partial z_{k+1})^2}$ in (9.111) is nonpositive over $\hat{\Delta}^j_{k+1}(t)$ then the optimal subproblem cost $V_k(x_k, r_k=j|t)$ in (9.103) has the two-point structure of (9.107). From (9.108) - (9.109), the joining point in (9.107) is given by

$$\theta^j_k(t) = \Theta^j_k(t) = \frac{1}{2}\left[\hat{\gamma}_{k+1}(t-1) + \hat{\gamma}^j_{k+1}(t) + \frac{b^2(j)\left[\hat{\hat{V}}^j_{k+1}(z_{k+1};t)\Big|_{z_{k+1}=\hat{\gamma}^j_{k+1}(t-1)} - \hat{\hat{V}}^j_{k+1}(z_{k+1};t)\Big|_{z_{k+1}=\hat{\gamma}^j_{k+1}(t)}\right]}{R(j)\,[\hat{\gamma}^j_{k+1}(t-1) - \hat{\gamma}^j_{k+1}(t)]}\right] \quad \text{(D.4.7)}$$

2. If $\dfrac{\partial^2 V_k(x_k, r_k - j \mid t)}{(\partial z_{k+1})^2}$ in (9.111) is positive over $\hat{\Delta}^j_{k+1}(t)$

then we must solve (9.110) to obtain the z_{k+1} (as a function of x_k) which minimizes (9.103). It is the optimal $z^{t,U}_{k+1}$ (resulting in cost $V^{t,U}_k(x_k, j)$ in (9.106)) for those x_k values such that this z_{k+1} is in $\hat{\Delta}^j_{k+1}(t)$ (if any such x_k values exist).

Solving (9.110) to obtain $z^{t,U}_{k+1}$ and computing the joining points $\theta^j_k(t)$, $\Theta^j_k(t)$ in (9.106) may be quite difficult to do analytically (depending upon the form of the function $\hat{\hat{V}}^j_{k+1}(z_{k+1}; t)$).

D.5 Proof of Proposition 9.2

We begin by verifying 4(i) - (ii). We are considering the solution of (9.113), subject to (9.114). The cost $V_k(x_k, r_k=j\ t)$ can be written as a function of z_{k+1}, as in (9.103). To find the optimal z_{k+1} in $\hat{\Delta}^j_{k+1}(t)$ we differentiate (9.103) twice with respect to z_{k+1}, as in (9.110) - (9.111). If for a given x_k the first derivative is zero (i.e. (9.110) is satisfied) for some $z_{k+1} = z^*$ then we have (9.126) - (9.128) directly (with $z_{k+1} = z^*$). This z^* is the unconstrained optimal if the second derivative is positive (i.e. (9.111) is satisfied) and if z^* is, in fact, in $\hat{\Delta}^j_{k+1}(t)$. Condition (9.125) results in the satisfaction of (9.111). The definitions for $\theta^j_k(t)$ and $\Theta^j_k(t)$ in (9.129) - (9.130) correspond to $z^{t,U}_{k+1}(x_k, j) = z^*$ of (9.127) inside the interval $\hat{\Delta}^j_{k+1}(t)$. Since we have chosen the z_{k+1} partition so that (9.111) is satisfied throughout $\hat{\Delta}^j_{k+1}(t)$ or not at all, the "inactive constraint" solution $z^{t,U}_{k+1}(x_k, j)$ in (9.127) is unique. To verify that $\theta^j_k(t) < \Theta^j_k(t)$ for each $t=1,\ldots,\hat{\psi}^j_{k+1}$ in (9.131) we note that

$$\begin{bmatrix} \hat{\gamma}^j_{k+1}(t) \\ -\hat{\gamma}^j_{k+1}(t-1) \end{bmatrix} > \frac{b^2(j)}{2R(j)} \left[\left. \frac{\partial \hat{V}^j_{k+1}(z;t)}{\partial z} \right|_{z=[\hat{\gamma}^j_{k+1}(t-1)]^+} - \left. \frac{\partial \hat{V}^j_{k+1}(z;t)}{\partial z} \right|_{z=[\hat{\gamma}^j_{k+1}(t)]^-} \right] \tag{D.5.1}$$

since by (9.111)

$$\frac{\partial^2 \hat{V}^j_{k+1}(z:t)}{\partial z^2} + \frac{2R(j)}{b^2(j)} > 0 \qquad \text{for all } z \in (\hat{\gamma}^j_{k+1}(t-1), \hat{\gamma}^j_{k+1}(t)) \tag{D.5.2}$$

This completes verification of 4(i) - (ii).

We next establish items (1) - (3) of Proposition 9.2. Suppose that (9.111) is satisfied for all $z \in \hat{\Delta}^j_{k+1}(t)$ (i.e., the second derivative is positive), but that for a given x_k the value of z_{k+1} satisfying (9.110) is less than $\hat{\gamma}^j_{k+1}(t-1)$. Then then best (lowest cost) z_{k+1} in $\hat{\Delta}^j_{k+1}(t)$ is on the left boundary as in (9.116), which is obtained with control (9.115) and results in cost (9.117). If, however, the z_{k+1} value satisfying (9.110) for a given x_k is greater than $\hat{\gamma}^j_{k+1}(t)$, then (9.118) - (9.120) apply. Here the values of $\theta^j_k(t)$ and/or $\Theta^j_k(t)$ are given by (9.129) - (9.130). Now suppose that (9.111) is <u>not</u> satisfied as in (9.121). Then the solution to (9.110) is not a minimum; the only choices of z_{k+1} in $\hat{\Delta}^j_{k+1}(t)$ are the boundaries $\hat{\gamma}^j_{k+1}(t-1)$ and $\hat{\gamma}^j_{k+1}(t)$. In this case the values of $\theta^j_k(t)$ and/or $\Theta^j_k(t)$ in (1) - (2) are specified by the intersection of $V^{t,L}_k(x_k, r_k=j)$ and $v^{t,R}_k(x_k, j)$. This yields (9.122) - (9.124) directly. Thus we have established (1) - (3) of Proposition 9.2.

Items 4(iii) and 4(iv) of the proposition follow immediately. Item 4(v) is a direct consequence of the relationship

$$\frac{\partial^2 V_k^{t,U}(x_k,j)}{\partial x_k^2} = a^2(j) \left.\frac{\partial^2 \hat{V}_{k+1}^{j}(z_{k+1};t)}{(\partial z_{k+1})^2}\right|_{z_{k+1}=z_{k+1}^{t,U}} \quad \text{(D.5.3)}$$

For $t=1$ and $t=\hat{\psi}_{k+1}^{j}$, if

$$\frac{\partial^2 \hat{V}_{k+1}^{j}(z_{k+1};t)}{(\partial z_{k+1})^2} < 0 \qquad \text{then as} \quad |z_{k+1}| \to \infty$$

we will have $\hat{\hat{V}}_{k+1}^{j}(z_{k+1};t) < 0$, which violates the requirements on $\hat{\hat{V}}_{k+1}(z_{k+1}|r_k=j)$.

D.6 Proof of Proposition 9.3

To prove this proposition we first establish the following relationship between $\theta_k^j(t)$, $\Theta_k^j(t)$ and the slopes of $\hat{\hat{V}}_{k+1}(z_{k+1}|r_k=j)$ at the points $\{\hat{\gamma}_{k+1}^{j}(t)\}$ for those t where $v_k^{t,U}$ exists.

Lemma D.6.1

For t and ℓ such that

$$\frac{\partial^2 \hat{V}_{k+1}^{j}(z_{k+1};t)}{(\partial z_{k+1})^2} + \frac{2\,R(j)}{b^2(j)} > 0 \quad \text{(D.6.1)}$$

$$\frac{\partial^2 \hat{V}_{k+1}^{j}(z_{k+1};\ell)}{(\partial z_{k+1})^2} + \frac{2\,R(j)}{b^2(j)} > 0 \quad \text{(D.6.2)}$$

the following relationships hold:

1. $\theta_k^j(t) > \theta_k^j(\ell)$ if and only if

$$\left.\frac{\partial \hat{\hat{V}}_{k+1}^j(z_{k+1};t)}{\partial z_{k+1}}\right|_{z_{k+1}=\hat{\gamma}_{k+1}^j(t-1)} - \left.\frac{\partial \hat{\hat{V}}_{k+1}^j(z_{k+1};t)}{\partial z_{k+1}}\right|_{z_{k+1}=\hat{\gamma}_{k+1}^j(\ell-1)} > \frac{2\,R(j)}{b^2(j)}\begin{bmatrix}\hat{\gamma}_{k+1}^j(\ell-1)\\ -\hat{\gamma}_{K+1}^j(t-1)\end{bmatrix}. \tag{D.6.3}$$

2. $\Theta_k^j(t) > \Theta_k^j(\ell)$ if and only if

$$\left.\frac{\partial \hat{\hat{V}}_{k+1}^j(z_{k+1};t)}{\partial z_{k+1}}\right|_{z_{k+1}=\hat{\gamma}_{k+1}^j(t)} - \left.\frac{\partial \hat{\hat{V}}_{k+1}^j(z_{k+1};\ell)}{\partial z_{k+1}}\right|_{z_{k+1}=\hat{\gamma}_{k+1}^j(\ell)} > \frac{2\,R(j)}{b^2(j)}\begin{bmatrix}\hat{\gamma}_{k+1}^j(\ell)\\ -\hat{\gamma}_{k+1}^j(t)\end{bmatrix}. \tag{D.6.4}$$

3. $\Theta_k^j(t) > \theta_k^j(\ell)$ if and only if

$$\left.\frac{\partial \hat{\hat{V}}_{k+1}^j(z_{k+1};t)}{\partial z_{k+1}}\right|_{z_{k+1}=\hat{\gamma}_{k+1}^j(t)} - \left.\frac{\partial \hat{\hat{V}}_{k+1}^j(z_{k+1};\ell)}{\partial z_{k+1}}\right|_{z_{k+1}=\hat{\gamma}_{k+1}^j(\ell-1)} > \frac{2\,R(j)}{b^2(j)}\begin{bmatrix}\hat{\gamma}_{k+1}^j(\ell-1)\\ -\hat{\gamma}_{k+1}^j(t)\end{bmatrix}. \tag{D.6.5}$$

This lemma follows directly from (9.129) - (9.130). It is a generalization of Lemma C.3.1. □

Proof of Proposition 9.3, continued:

Suppose that $\hat{\hat{V}}_{k+1}(z_{k+1}|r_k=j)$ is continuous at $\hat{\gamma}^j_{k+1}(t)$. Then by (9.117), (9.120) we have

$$V_k^{t,R}(x_k;j) = V_k^{t+1}(x_k,j) \quad , \tag{D.6.6}$$

since

$$\hat{\hat{V}}^j_{k+1}(\hat{\gamma}^j_{k+1}(t);t) = \hat{\hat{V}}^j_{k+1}(\hat{\gamma}^j_{k+1}(t);t+1) \quad .$$

Now suppose that we also have

$$\left.\frac{\partial \hat{\hat{V}}^j_{k+1}(z_{k+1};t+1)}{\partial z_{k+1}}\right|_{z_{k+1}=\hat{\gamma}^j_{k+1}(t)} \leq \left.\frac{\partial \hat{\hat{V}}^j_{k+1}(z_{k+1};t)}{\partial z_{k+1}}\right|_{z_{k+1}=\hat{\gamma}^j_{k+1}(t)} \tag{D.6.7}$$

as in (i) of Proposition 9.3.

Then by Lemma D.6.1 we have

$$\theta^j_k(t+1) \leq \Theta^j_k(t) \quad . \tag{D.6.8}$$

Now (D.6.6) and (D.6.8) are together sufficient to guarantee that neither $V_k^{t,R}(x_k,j)$ nor $V_k^{t+1,L}(x_k,j)$ can be optimal for any x_k, since

$$V_k^{t,R}(x_k,j) \geq V_k^{t,U}(x_k,j)$$

$$V_k^{t+1,L}(x_k,j) \geq V_k^{t+1,U}(x_k,j)$$

for all x_k (with equality only at $\frac{\theta_k^j(t)}{a(j)}$ and $\frac{\theta_k^j(t)}{a(j)}$, respectively).

Thus for each $z_{k+1} = \hat{\gamma}_{k+1}^j(t)$ at which $\hat{\hat{V}}_{k+1}(z_{k+1}|r_k=j)$ is continuous with (D.6.1), (D.6.2), (D.6.7) holding for t and $\ell = t+1$;

$$\min \left\{ \begin{matrix} V_k^{t,U}(x_k,j), & V_k^{t,R}(x_k,j), \\ V_k^{t+1,L}(x_k,j), & V_k^{t+1,U}(x_k,j) \end{matrix} \right\} = \begin{matrix} V_k^{t,U}(x_k,j) \quad \text{or} \\ V_k^{t+1,U}(x_k,j) \end{matrix} \qquad \text{(D.6.9)}$$

for each x_k. This verifies (i) of Proposition 9.3.

Suppose that (D.6.1) - (D.6.2) hold for t and $\ell = t+1$ and $\hat{\hat{V}}_{k+1}(z_{k+1}|r_k=j)$ is continuous at $\hat{\gamma}_{k+1}(t)$ but (D.6.7) does not hold. Then by Lemma D.6.1 we have

$$\theta_k^j(t+1) > \theta_k^j(t) \qquad \text{(D.6.10)}$$

From (D.6.6), (D.6.10) we have that

$$V_k^{t,R}(x_k,j) \equiv V_k^{t+1,L}(x_k,j)$$

<u>may</u> be optimal for

$$\theta_k^j(t) < a(j)\, x_k < \theta_k^j(t+1) \quad .$$

Therefore we have verified (i) of Proposition 9.3.

Proposition 9.3(ii) follows directly from Proposition 9.2(3). Now consider Proposition 9.3(iii) - (iv): if $\hat{\hat{V}}_{k+1}(z_{k+1}|r_k=j)$ is

discontinuous at $\hat{\gamma}^j_{k+1}(t)$ with (9.141) holding then clearly (from (9.117), (9.120)) we have $V_k^{t,R}(x_k,j) < V_k^{t+1,L}(x_k,j)$. So in this case $V_k^{t+1,L}(x_k,j)$ cannot be optimal for any x_k. However, $V_k^{t,R}(x_k,j)$ may be. This verifies Proposition 9.3(iii); (iv) follows analogously.

Thus we need only consider the candidate costs-to-go listed in the statement of Proposition 9.3. □

D.7 Proof of Proposition 9.6:

1. Differentiation of $V_k^{t,L}(x_k,j)$ in (9.117) and $V_k^{t,R}(x_k,j)$ in (9.120) with respect to x_k yields (9.144) - (9.145) for any x_k where these actively-constrained costs are optimal.

   For any x_k from which some $v_k^{t,U}(x_k,j)$ is optimal, Proposition 9.2(4) and

$$\frac{\partial V_k^{t,U}}{\partial x_k} = a(j) \left. \frac{\partial \hat{V}^j_{k+1}(z_{k+1};t)}{\partial z_{k+1}} \right|_{z_{k+1} = z^{t,U}_{k+1}}$$

   yields (9.144) - (9.145).

2. At joining points $\delta = x_k$ where $V_k(x_k,r_k=j)$ is differentiable, $u_k(x_k,r_k=j)$ and $z_{k+1}(x_k,r_k=j)$ are clearly continuous, from (1).

3. At a joining point $x_k = \delta$ where the slope of $V_k(x_k, r_k=j)$ decreases discontinuously, (9.144), (9.145) yield (i) and (ii) directly.

4. From 3(ii) we have that the mapping

$$x_k \mapsto z_{k+1}(x_k, r_k=j)$$

increases discontinuously at joining points where $V_k(x_k, r_k=j)$ is not differentiable, and from (2), the mapping is continuous at other joining points.

Now between joining points, if the optimal cost corresponds to hedging-to-a-point then clearly the mapping is constant. If the optimal cost does not correspond to hedging-to-a-point, then in such a region

$$V_k(x_k, r_k=j) = V_k^{t,U}(x_k, j)$$

for some $t \in \{1, \ldots, \hat{\psi}_{k+1}^j\}$. Thus

$$z_{k+1}(x_k, r_k=j) = a(j)x_k - \frac{b^2(j)}{2a(j)R(j)} \frac{\partial V_k(x_k, r_k=j)}{\partial x_k}$$

$$= z_{k+1}^{t,U}(x_k, t_k=j) = a(j)x_k - \frac{b^2(j)}{2a(j)R(j)} \frac{\partial \hat{V}_{k+1}^j(z_{k+1}; t)}{\partial z_{k+1}} \Bigg|_{z_{k+1}=z_{k+1}^{t,U}(z_k, j)} \cdot$$

(D.7.1)

Differentiating (D.7.1),

$$\frac{\partial z_{k+1}^{t,U}(x_k,j)}{\partial x_k} = a(j) - \frac{b^2(j)}{2R(j)} \left. \frac{\partial^2 \hat{V}_{k+1}^{j}(z_{k+1};t)}{(\partial^2 z_{k+1})^2} \right|_{z_{k+1}=z_{k+1}^{t,U}(x_k,j)} \cdot \frac{\partial z_{k+1}^{t,U}(x_k,j)}{\partial x_k} \tag{D.7.2}$$

which yields

$$\frac{\partial z_{k+1}^{t,U}(x_k,j)}{\partial x_k} = \frac{a(j)}{\left[1 + \frac{b^2(j)}{2R(j)} \left. \frac{\partial^2 \hat{\hat{V}}_{k+1}^{j}(z_{k+1};t)}{(\partial z_{k+1})^2} \right|_{z_{k+1}=z_{k+1}^{t,U}(x_k,j)}\right]} . \tag{D.7.3}$$

Now by (9.125) of Proposition 9.2, $V_k^{t,U}$ only exists when

$$\left. \frac{\partial^2 \hat{V}_{k+1}^{j}(z_{k+1};t)}{(\partial z_{k+1})^2} \right|_{z_{k+1}=z_{k+1}^{t,U}(x_k,j)} + \frac{2R(j)}{b^2(j)} > 0 \tag{D.7.4}$$

hence

$$\frac{b^2(j)}{2R(j)} \left. \frac{\partial^2 \hat{V}_{k+1}^{j}(z_{k+1};t)}{(\partial z_{k+1})^2} \right|_{z_{k+1}=z_{k+1}^{t,U}(x_k,j)} + 1 > 0 \quad . \tag{D.7.5}$$

From (D.7.5) and (D.7.3) we have

$$\frac{\partial z_{k+1}^{t,U}(x_k, j)}{\partial x_k} > 0 \qquad \text{if } a(j) > 0$$

$$\frac{\partial z_{k+1}^{t,U}(x_k, j)}{\partial x_k} < 0 \qquad \text{if } a(j) < 0.$$

Thus we have 4(i),(ii).

5. Item (5) follows directly from the monotonicity of the mapping

$$x_k \longmapsto z_{k+1}(x_k, r_k=j)$$

in 4(i), since each candidate cost corresponds to driving z_{k+1} into a different region of values; if a certain candidate were optimal over two disconnected intervals of x_k values then the monotonicity of the mapping would be violated.

□

References

1. R.B. Asher, et.al. (1976): Bibliography on Adaptive Control Systems, Proc. of the IEEE, Vol. 64, No. 8, pp. 1226-1240.

2. M. Athans (1972): ed, Special Issue on the Linear Quadratic Gaussian Problem, IEEE Trans. Automatic Control, AC-16, No.6, Dec.

3. M. Athans and P. Varaiya (1975): A Survey of Adaptive Stochastic Control Methods, in ERDA Report CONF-780867, Systems Engineering for Power: Status and Prospects (L.H. Fink and K Carlsen, eds.) pp. 356-366. October.

4. M. Athans, W.S. Levine and A.H. Levis (1967): Proceedings of the Fifth Congress of AICA, Lausane, Switz, p.1

5. A. Aviženis (1978): ed., Special Issue on Fault-Tolerant Digital Systems, Proc. IEEE, Vol. 66, No. 10.

6. R. E. Barlow and F. Proschan (1965), Mathematical Theory of Reliability, John Wiley, New York.

7. R.E. Barlow and F. Proschan (1975): Statistical Theory of Reliability and Life Testing, Holt, Rinehart and Winston, New York

8. I. Bazovsky (1961): Reliability Theory and Practice, Prentice-Hall, Englewood Cliffs, New Jersey.

9. R.V. Beard (1971): Failure Accommodation in Linear Systems Through Self-Reorganization, Rpt. MVL-71-1, Man-Vehicle Lab., MIT, Cambridge, Mass.

10. R. Bellman (1957): Dynamic Programming, Princeton Univeristy Press, Princeton, N.J.

11. D.P. Bertsekas (1976): Dynamic Programming and Stochastic Control, Academic Press, New York.

12. J.D. Birdwell (1978): On Reliable Control System Designs, Ph.D.Thesis, Dept. of Elec. Eng. and Computer Sci., MIT, (Rpt. ESL-TH-821), Cambridge, MA.

13. J.D. Birdwell and M. Athans (1977): On the Relationship Between Reliability and Linear Quadratic Optimal Control, Proc. 1977 Conf. on Decision and Control, pp. 129-134.

14. J.D. Birdwell, D. Castañon, and M. Athans (1979): On Reliable Control System Designs With and Without Feedback Reconfiguration, Proc.1978 IEEE Conf. on Decision and Control.

15. H.W. Bode (1945): Network Analysis and Feedback Amplifier Design, Van Nostrand, Princeton, N.J.

16. R. Boel (1974): Optimal Control of Jump Processes, Ph.D. Thesis, Dept. of Elec. Eng. and Computer Sci., Univ. of Calif. Berkeley.

17. R. Boel and P. Varaiya (1975): Optimal Control of Markovian Jump Processes, Proc. 1975 IEEE Conf. on Decision and Control, pp. 153-156.

18. R. Boel, P. Varaiya and E. Wong (1975): Martingales on Jump Processes I: Representation Results and II: Applications, SIAM J. Control 13, 999-1061, Aug.

19. S.R. Calabro (1962): Reliability Principles and Practices, Mc-Graw-Hill, New York.

20. M.H.A. Davis (1976): The Representation of Martingales of Jump Processes, SIAM J. Control 14, 623-638.

21. M.H.A. Davis (1979): Martingale Methods in Stochastic Control, LIDS-P-874, MIT, Cambridge, Mass.

22. E.J. Davison (1974): Automatica, Vol. 10, pp. 309.

23. J. Endrenyi (1978): Reliability Modeling in Electric Power Systems, John Wiley and Sons, New York.

24. A.A. Feldbaum (1960;1961): Theory of Dual Control I-IV, Automation and Remote Control, No. 9,11 (1961); No.1,2 (1962).

25. P.M. Fishman and D.L. Snyder (1976): The Statistical Analysis of Space-Time Point Processes, IEEE Trans. Inf. Theory, IT-22, May, pp. 257-276.

26. I.I. Gihman and A.V. Skorokod (1972): Stochastic Differential Equations, Springer Verlag, New York.

27. B.V. Gnedenko, Yu.K. Belyayev and A.D. Solovyev (1969): Mathematical Methods of Reliability Theory, Academic Press, New York.

28. A.S. Goldman and T.B. Slattery (1964): Maintainability, Wiley, New York.

29. A.E. Greene and A.J. Bourne (1972): Reliability Technology, Wiley-Interscience, London.

30. I.M. Horowitz, (1963): Synthesis of Feedback Systems, New York, Academic Press.

31. I.M. Horowitz and M.S. Sidi (1972): Synthesis of Feedback Systems with Large Plant Ignorance for Prescribed Time-Domain Tolerances, Int. J. Control, Vol. 16, No. 2, pp. 287-309.

32. L. Isaksen and H.J. Payne (1973): IEEE Trans. Automatic Control, Vol. 18, p.210.

33. I.N. Kovalenko (1977): Limit Theorems for Reliability Theory, Kibernetika, No. 6, pp. 106-116, Nov.-Dec.

34. N.N. Krasovskii and E.A. Lidskii (1961): Analytical Design of Controllers in Systems with Random Attributes I, II, III, Automation and Remote Control, Vol. 22, pp. 1021-1025, 1141-1146, 1289-1294.

35. E. Kreindler (1968): On the Definition and Application of the Sensitivity Function, J. Franklin Inst., Vol. 285, No.1, pp. 26-36.

36. H.J. Kushner (1971): Introduction to Stochastic Control, Holt, Rinehart and Winston, New York.

37. H.J. Kushner and DiMasi(1978): Approximations for Functionals and Optimal Control Problems on Jump Diffusion Processes, J.Math. Anal. Appl., Vol. 63, pp. 772-800.

38. H. Kwakernaak and R. Sivan (1972): Linear Optimal Control Systems, J. Wiley and Sons, New York.

39. H. Lampert (1975): Measures of Importance of Events in Cut Sets and Fault Trees, in Reliability and Fault Tree Analysis: Theoretical and Applied Aspects of System Reliability and Safety Assessment, Philadelphia, pp. 77-100.

40. I.D. Landau (1977): A Survey of Model Reference Adaptive Techniques (Theory and Applications), Automatica, Vol. 10, pp. 353-380.

41. N.A. Lehtomaki (1981): Practical Robustness Measures in Multivariable Control System Analysis, PH.D. Thesis, MIT,Dept.of E.E.& C.S.,Cambridge,Ma.

42. S.I. Marcus (1978): Modeling and Analysis of Stochastic Differential Equations Driven by Point Processes, IEEE Trans. Inf. Theory, IT-24, No.2, March, pp. 164-172.

43. E.F. Moore and C.E. Shannon (1956): J. Franklin Inst., 262,171:262,281.

44. I.D. Murchland (1975): Fundamental Concepts and Relations for Reliability Analysis of Multistate Systems, in Reliability and Fault Analysis, Philadelphia, pp. 581-618.

45. B.D. Pierce and D.D. Sworder (1971):Bayes and Minimal Controllers for a Linear Systems with Stochastic Jump Parameters, IEEE Trans. Automatic Control, Vol. AC-16, No.4, pp. 300-306.

46. E. Pieruschka (1963): Principles of Reliability, Prentice-Hall, Englewood Cliffs, New Jersey.

47. R.S. Ratner and D.G. Luenberger (1969): Performance Adaptive Renewal Policies for Linear Systems, IEEE Trans. Automatic Control, AC-14, pp. 344-351.

48. R.W. Rishel (1972): Optimality of Controls for Systems with Jump Markov Disturbances, In Optimization Techniques, ed. A.V. Balakrishnan, Academic Press, New York.

49. R.W. Rishel (1974: 1975): A Minimum Principle for Controlled Jump Processes, Proc. Internat. Symp. on Control, Numer., Methods and Computer Syst. Modelling, IRIA, June 1974: Springer Lecture Notes in Econ. and Math. Syst. 107,Springer Verlag, New York.

50. R.W. Rishel (1975): Control of Systems with Jump Markov Disturbances IEEE Trans. Automatic Control, AC-20, pp. 241-244.

51. R.W. Rishel (1975): Dynamic Programming and Minimum Principles for Systems with Jump Markov Distrubances, SIAM J. Control 13, 338-371.

52. N.H. Roberts (1964): Mathematical Methods in Reliability Engineering, McGraw-Hill, New York.

53. V.G. Robinson and D.D. Sworder (1974): A Computational Algorithm for Design of Regulators for Linear Jump Parameter Systems, IEEE Trans. Automatic Control, AC-19, Feb. pp. 47-49.

54. G.H. Sandler (1963): System Reliability Engineering, Prentice-Hall Englewood Cliffs, New Jersey.

55. M.G. Safonov and M. Athans (1976): Gain and Phase Margins for Multiloop LQG Regulatros, Proc. 1976 IEEE Conf. on Decision and Control.

56. M.G. Safonov (1977): Robustness and Stability Aspects of Stochastic Multivariable Feedback System Design, Ph.D. Thesis, Dept. of Elec. Eng. and Computer Sci., MIT, Cambridge, MA.

57. M.G. Safonov and M. Athans (1978): Robustness and Computational Aspects of Nonlinear Stochastic Estimators and Regulators, IEEE Trans. Automatic Control, AC-23, Aug., 717-725.

58. M.L. Shooman (1968): Probabilistic Reliability: An Engineering Approach, McGraw-Hill, New York.

59. D.D. Šiljak (1972): IEEE Trans Syst. Man. Cybernetics, 2, pp.657.

60. D.D. Šiljak (1978): Large-Scale Dynamic Systems: Stability and Structure, North-Holland Elsevier, New York.

61. D.D. Šiljak (1980):Reliable Control Using Multiple Control Systems, Int. J. Control, Vol. 31, No.2, pp. 303-329.

62. D.L. Snyder (1975): Random Point Processes, Wiley, New York.

63. D.D. Sworder (1969) Feedback Control of a Class of Linear Systems with Jump Parameters, IEEE Trans. Automatic Control, AC-14, No.1, Feb. , pp.9-14.

64. D.D. Sworder(1970): Uniform Performance-Adaptive Renewal Policies for Linear Systems, IEEE Trans. Automatic Control AC-15, No.5, Oct., pp. 581-583.

65. D.D. Sworder (1972): Baye's Controllers with Memory for a Linear System With Jump Parameters, IEEE Trans. Automatic Control, Vol.AC-17, No.2, pp. 119-121.

66. D.D. Sworder (1972): Control of Jump Parameter Systems with Discontinuous State Trajectories, IEEE Trans. Automatic Control, AC-17, Oct., 740-741.

67. D.D. Sworder (1976): Control of Systems Subject to Sudden Changes in Character, Proc. of IEEE, Vol. 64, No.8, pp. 1219-1225.

68. D.D. Sworder (1977): A Simplified Algorithm for Computing Stationary Cost Variances for a Class of Optimally Controlled Jump Parameter Systems, IEEE Trans. Automatic Control, Vol. AC-22, pp. 236-239.

69. D.D. Sworder and L.L. Choi (1976): Stationary Cost Densities for Optimally Controlled Stochastic Systems, IEEE Trans. Automatic Control, Vo. AC-21, No.4, pp. 492-499.

70. D.D. Sworder and V.G. Robinson (1974): Feedback Regulators for Jump Parameeter Systems with State and Control Dependent Transition Rates, IEEE Trans. Automatic Control AC-18, No.4, Aug., pp. 355-360.

71. P. Varaiya (1975): The Martingale Theory of Jump Processes, IEEE Trans. on Automatic Control AC-20, No.1, Feb., 34-42.

72. W.H. von Alven (1964): ed. Reliability Engineering, Prentice-Hall Englewood Cliffs, New Jersey.

73. J. Von Neuman (1966): Automata Studies, ed. E.E. Shannon and E.F. Moore, Annals of Math. Studies, No. 34, (Princeton, N.J. Princeton Univ. Press) p. 43.

74. A.S. Willsky (1976): A Survey of Design Methods for Failure Detection in Dynamic Systems, Automatica, Vol. 12, pp. 601-611.

75. A.S. Willsky, et.al.(1979): Stochastic Stability Rsearch For Complex Power Systems, Interim Report for DOE Contract No. ET-76-C-01-2295.

76. W.M. Wonham (1970): Random Differential Equations in Control Theory, in Probabilitistic Methods in Applied Mathematics, Vol. 2, A.T. Bharucha-Reid, ed. Acadmic Press, New York, pp.131-213.

77. P.K. Wong (1975): On the Interaction Structure of Linear Multi-Input Feedback Control Systems, M.S. Thesis, MIT.,Cambridge, Mass.

78. P.K. Wong and M. Athans (1977): Closed-Loop Structural Stability for Linear-Quadratic Optimal Systems, IEEE Trans. on Automatic Control, Vol. AC-22, No.1, pp. 94-99.

79. G. Zames (1966): On the Input-Output Stability of Time-Varying Non-Linear Feedback Systems - Part I: Conditions Using Concepts of Loop Gain, Conicity and Positivity, IEEE Trans. on Automatic Control, Vol. AC-11, No. 34, pp. 228-238.

80. G. Zames (1966): On the Input-Output Stability of Time-Varying Non-linear Feedback Systems - Part II: Conditions Involving Circles in the Frequency Place and Sector Nonlinearities, IEEE Trans. on Automatic Control, Vol. AC-11, No.3, pp. 465-476.

81. N. Zelen (1963): Statistical Theory of Reliability (ed). Univ. of Wisconsin Press, Madison, Wisc.